THE MATHEMATICAL THEORY OF COSMIC STRINGS

Cosmic Strings in the Wire Approximation

M R ANDERSON

IoP

THE MATHEMATICAL THEORY OF COSMIC STRINGS
COSMIC STRINGS IN THE WIRE APPROXIMATION

Series in High Energy Physics, Cosmology and Gravitation

Other books in the series

THE MATHEMATICAL THEORY OF COSMIC STRINGS

COSMIC STRINGS IN THE WIRE APPROXIMATION

Malcolm R Anderson

*Department of Mathematics,
Universiti Brunei, Darussalam*

IoP

Contents

Introduction

The existence of cosmic strings was first proposed in 1976 by Tom Kibble, who drew on the theory of line vortices in superconductors to predict the formation of similar structures in the Universe at large as it expanded and cooled during the early phases of the Big Bang. The critical assumption is that the strong and electroweak forces were first isolated by a symmetry-breaking phase transition which converted the energy of the Higgs field into the masses of fermions and vector bosons. Under certain conditions, it is possible that some of the Higgs field energy remained in thin tubes which stretched across the early Universe. These are cosmic strings.

The masses and dimensions of cosmic strings are largely determined by the energy scale at which the relevant phase transition occurred. The grand unification (GUT) energy scale is at present estimated to be about 10^{15} GeV, which indicates that the GUT phase transition took place some 10^{-37}–10^{-35} s after the Big Bang, when the temperature of the Universe was of the order of 10^{28} K. The thickness of a cosmic string is typically comparable to the Compton wavelength of a particle with GUT mass or about 10^{-29} cm. This distance is so much smaller than the length scales important to astrophysics and cosmology that cosmic strings are usually idealized to have zero thickness.

The mass per unit length of such a string, conventionally denoted μ, is proportional to the square of the energy scale, and in the GUT case has a value of about 10^{21} g cm^{-1}. There is no restriction on the length of a cosmic string, although in the simplest theories a string can have no free ends and so must either be infinite or form a closed loop. A GUT string long enough to cross the observable Universe would have a mass within the horizon of about 10^{16} $M_{\odot}$, which is no greater than the mass of a large cluster of galaxies.

Interest in cosmic strings intensified in 1980–81, when Yakov Zel'dovich and Alexander Vilenkin independently showed that the density perturbations generated in the protogalactic medium by GUT strings would have been large enough to account for the formation of galaxies. Galaxy formation was then (and remains now) one of the most vexing unsolved problems facing cosmologists. The extreme isotropy of the microwave background indicates that the early Universe was very smooth. Yet structure has somehow developed on all scales from the planets to clusters and superclusters of galaxies. Such structure cannot be

adequately explained by random fluctuations in the density of the protogalactic medium unless additional *ad hoc* assumptions about the process of galaxy formation are made.

Cosmic strings, which would appear spontaneously at a time well before the epoch of galaxy formation, therefore provided an attractive alternative mechanism for the seeding of galaxies. The first detailed investigations of the string-seeded model were based on the assumption that the initial string network quickly evolved towards a 'scaling solution', dominated by a hierarchy of closed loops which formed as a by-product of the collision and self-intersection of long (horizon-sized) strings, and whose energy scaled as a constant fraction of the total energy density of the early, radiation-dominated Universe. With the additional assumption that each loop was responsible for the formation of a single object, the model could readily account for the numbers and masses of the galaxies, and could also explain the observed filamentary distribution of galaxy clusters across the sky.

Despite its initial promise, however, this rather naive model later fell into disfavour. More recent high-resolution simulations of the evolution of the string network have suggested that a scaling solution does not form: that in fact loop production occurs predominantly on very small scales, resulting in an excess of small, high-velocity loops which do not stay in the one place long enough to act as effective accretion seeds. Furthermore, the expected traces of cosmic strings have not yet been found in either the microwave or gravitational radiation backgrounds. As a result, work on the accretion of protogalactic material onto string loops has largely been abandoned, although some work continues on the fragmentation of planar wakes trailing behind long strings.

Nonetheless, research into the properties and behaviour of cosmic strings continues and remains of pressing interest. All numerical simulations of the string network to date have neglected the self-gravity of the string loops, and it is difficult to estimate what effect such neglect has on the evolution of the network. Indeed, the gravitational properties of cosmic strings are as yet only poorly understood, and very little progress has been made in developing a self-consistent treatment of the dynamics of cosmic strings in the presence of self-gravity.

Even if it proves impossible ever to resurrect a string-seeded cosmology, the self-gravity and dynamics of cosmic strings will remain an important field of study, for a number of reasons. On the practical level, cosmic strings may have played an important role in the development of the early Universe, whether or not they can single-handedly explain the formation of galaxies. More abstractly, cosmic strings are natural higher-dimensional analogues of black holes and their gravitational properties are proving to be just as rich and counter-intuitive. Cosmic string theory has already thrown some light on the structure of closed timelike loops and the dynamics of particles in $2 + 1$ gravity.

A cosmic string is, strictly speaking, a vortex solution of the Abelian Higgs equations, which couple a complex scalar and real vector field under the action of

a scalar potential. However, as was first shown by Dietrich Förster in 1974, the action of an Abelian Higgs vortex can be adequately approximated by the Nambu action[1] if the vortex itself is very nearly straight. To leading order in its curvature, therefore, a cosmic string can be idealized as a line singularity, independently of the detailed structure of the Higgs potential. To describe a cosmic string in terms of the Nambu action is to reduce it to a more fundamental geometrical object, predating the cosmic string and known to researchers in the early 1970s as the 'relativistic string'. Nowadays, the dichotomy is perceived to lie not so much between vortex strings and relativistic strings as between cosmic strings (vortex strings treated as relativistic strings) and superstrings (the supersymmetric counterparts of relativistic strings).

In this volume I have attempted to summarize all that is at present known about the dynamics and gravitational properties of individual cosmic strings in the zero-thickness or 'wire' approximation. Chapter 1 is devoted to a summary of the field-theoretic aspects of strings, starting from a description of the role of the Higgs mechanism in electroweak unification and ending with a justification of the wire approximation for the Abelian Higgs string, on which the Nambu action is based. Throughout the rest of the book I treat cosmic strings as idealized line singularities, and make very few references to the underlying field theory. Nor do I give any space to the cosmological ramifications of cosmic strings (other than what appears here and in chapter 1), the structure and evolution of string networks, or to the theory of related topological defects such as global strings, superconducting strings, monopoles, domain walls or textures. Any reader interested in these topics would do best to consult 'Cosmic strings and domain walls' by Alexander Vilenkin, *Physics Reports*, **121**, pp 263–315 (1985), 'The birth and early evolution of our universe' by Alexander Vilenkin, *Physica Scripta* **T36**, pp 114–66 (1990), *Cosmic Strings and Other Topological Defects* by Alexander Vilenkin and Paul Shellard (Cambridge University Press, 1994) or 'Cosmic strings' by Mark Hindmarsh and Tom Kibble, *Reports on Progress in Physics*, **58**, 477 (1995).

In chapter 2 I give an outline of the dynamics of zero-thickness strings in a general background spacetime, including an introduction to pathological features such as cusps and kinks. Chapter 3 concentrates on the dynamics of cosmic strings in a Minkowski background, whose symmetries admit a wide range of conservation laws. A catalogue of many of the known exact string solutions in Minkowski spacetime is presented in chapter 4. Although possibly rather dry, this chapter is an important source of reference, as most of the solutions it describes are mentioned in earlier or later sections. Chapter 5 examines the more limited work that has been done on the dynamics of cosmic strings in non-flat spacetimes, principally the Friedmann–Robertson–Walker, Schwarzschild, Kerr and plane-fronted (pp) gravitational wave metrics.

---

[1] The action of a two-dimensional relativistic sheet. It was first derived, independently, by Yoichiro Nambu in 1970 and Tetsuo Goto in 1971.

From chapter 6 onwards, the focus of the book shifts from the dynamics to the gravitational effects of zero-thickness cosmic strings. Chapter 6 itself takes an extensive look at the gravitational effects of cosmic strings in the weak-field approximation. In chapter 7 the exact strong-field metric about an infinite straight cosmic string is analysed in some detail. Although one of the simplest non-trivial solutions of the Einstein equations, this metric has a number of unexpected properties. Chapter 8 examines systems of infinite straight cosmic strings, their relationship to $2 + 1$ gravity, and the proper status of the Letelier–Gal'tsov 'crossed-string' metric. Chapter 9 describes some of the known variations on the standard straight-string metric, including travelling-wave solutions, strings through black holes, strings embedded in radiating cylindrical spacetimes, and snapping string metrics. Finally, chapter 10 collects together a miscellany of results relating to strong-field gravity outside non-straight cosmic strings, an area of study which remains very poorly understood.

The early stages of writing this book were unfortunately marred by personal tragedy. For their support during a time of great distress I would like to thank Tony and Helen Edwards, Bernice Anderson, Michael Hall, Jane Cotter, Ann Hunt, Lyn Sleator and George Tripp. Above all, I would like to dedicate this book to the memory of Antonia Reardon, who took her own life on 12 May 1994 without ever finishing dinner at the homesick restaurant.

Malcolm Anderson
Brunei, June 2002

Chapter 1

Cosmic strings and broken gauge symmetries

One of the most striking successes of modern science has been to reduce the complex panoply of dynamical phenomena we observe in the world around us— from the build-up of rust on a car bumper to the destructive effects of cyclonic winds—to the action of only four fundamental forces: gravity, electromagnetism, and the strong and weak nuclear forces. This simple picture of four fundamental forces, which became evident only after the isolation of the strong and weak nuclear forces in the 1930s, was simplified even further when Steven Weinberg in 1967 and Abdus Salam in 1968 independently predicted that the electromagnetic and weak forces would merge at high temperatures to form a single *electroweak* force.

The Weinberg–Salam model of electroweak unification was the first practical realization of the Higgs mechanism, a theoretical device whereby a system of initially massless particles and fields can be given a spectrum of masses by coupling it to a massive scalar field. The model has been extremely successful not only in describing the known weak reactions to high accuracy, but also in predicting the masses of the carriers of the weak force, the $W^{\pm}$ and Z^0 bosons, which were experimentally confirmed on their discovery in 1982–83.

A natural extension of the Weinberg–Salam model is to incorporate the Higgs mechanism into a unified theory of the strong and the electroweak forces, giving rise to a so-called *grand unification theory* or GUT. A multitude of candidate GUTs have been proposed over the last 30 years, but unfortunately the enormous energies involved preclude any experimental testing of them for many decades to come. Another implication of electroweak unification is the possibility that a host of exotic and previously undreamt-of objects may have formed in the early, high-temperature, phase of the Universe, as condensates of the massive scalar field which forms the basis of the Higgs mechanism. These objects include pointlike condensates (monopoles), two-dimensional sheets (domain walls) and, in particular, long filamentary structures called *cosmic strings*.

1

   Most of this book is devoted to a mathematical description of the dynamics and gravitational properties of cosmic strings, based on the simplifying assumption that the strings are infinitely thin, an idealization often referred to as the *wire approximation*. As a consequence, there will be very little discussion of the field-theoretic properties of cosmic strings. However, in order to appreciate how cosmic strings might have condensed out of the intense fireball that marked the birth of the Universe it is helpful to first understand the concept of spontaneous symmetry-breaking that underpins the Higgs mechanism.

   In this introductory chapter I, therefore, sketch the line of theoretical development that leads from gauge field theory to the classical equations of motion of a cosmic string, starting from a gauge description of the electromagnetic field in section 1.1 and continuing through an account of electroweak symmetry-breaking in section 1.2 to an analysis of the Nielsen–Olesen vortex string in section 1.3 and finally a derivation of the Nambu action in section 1.5. The description is confined to the semi-classical level only, and the reader is assumed to have no more than a passing familiarity with Maxwell's equations, the Dirac and Klein–Gordon equations, and elementary tensor analysis.

   The detailed treatment of electroweak unification in section 1.2 lies well outside the main subject matter of this book and could easily be skipped on a first reading. Nonetheless, it should be remembered that cosmic strings are regarded as realistic ingredients of cosmological models solely because of the role of the Higgs mechanism in electroweak unification. Most accounts of the formation of cosmic strings offer only a heuristic explanation of the mechanism or illustrations from condensed matter physics, while the mathematics of electroweak unification is rarely found outside textbooks on quantum field theory. Hence the inclusion of what I hope is an accessible (if simplified) mathematical description of the Weinberg–Salam model.

   In this and all later chapters most calculations will be performed in *Planck units*, in which the speed of light c, Newton's gravitational constant G and Planck's constant $\hbar$ are all equal to 1. This means that the basic units of distance, mass and time are the Planck length $\ell_{\mathrm{Pl}} = (G\hbar/c^3)^{1/2} \approx 1.6 \times 10^{-35}$ m, the Planck mass $m_{\mathrm{Pl}} = (c\hbar/G)^{1/2} \approx 2.2 \times 10^{-8}$ kg and the Planck time $t_{\mathrm{Pl}} = (G\hbar/c^5)^{1/2} \approx 1.7 \times 10^{-43}$ s respectively. Two derived units that are important in the context of cosmic string theory are the Planck energy $E_{\mathrm{Pl}} = (c^5\hbar/G)^{1/2} \approx 1.9 \times 10^8$ J and the Planck mass per unit length $m_{\mathrm{Pl}}/\ell_{\mathrm{Pl}} \approx 1.4 \times 10^{27}$ kg m^{-1}, which measures the gravitational field strength of a cosmic string. More familiar SI units will be restored when needed.

   Some additional units that will be used occasionally are the electronvolt, 1 eV $\approx 1.6 \times 10^{-19}$ J, the solar mass, $1 M_\odot \approx 2.0 \times 10^{30}$ kg, the solar radius, $1 R_\odot \approx 7.0 \times 10^8$ m, the solar luminosity $1 L_\odot \approx 3.9 \times 10^{26}$ J s^{-1} and the light year, 1 l.y.$\approx 9.5 \times 10^{15}$ m. The electronvolt is a particularly versatile unit for particle physicists, as it is used to measure not only energies but masses $m = E/c^2$ and temperatures $T = E/k_{\mathrm{B}}$, where k_{B} is Boltzmann's constant. Thus 1 eV is equivalent to a mass of about 1.8×10^{-36} kg or $8.2 \times 10^{-29} m_{\mathrm{Pl}}$, and equivalent to

a temperature of about 1.2×10^4 K. (As a basis for comparison, the rest mass of the electron in electronvolt units is 0.511 MeV, while the temperature at the centre of the Sun is only about 1 keV.)

Throughout this book, spacetime is assumed to be described by a four-dimensional metric tensor with signature -2, so that timelike vectors have positive norm and spacelike vectors have negative norm. If the background is flat the metric tensor is denoted by $\eta_{\mu\nu}$, whereas if the spacetime is curved it is denoted by $g_{\mu\nu}$. Greek indices $\mu, \nu, \ldots$ run from 0 to 3 (with x^0 usually the timelike coordinate), lower-case roman indices $i, j, k, \ldots$ from either 1 to 3 or 2 to 3 as indicated in the relevant sections, and upper-case roman indices $A, B, \ldots$ from 0 to 1. Also, round brackets around spacetime indices denote symmetrization, and square brackets, anti-symmetrization, so that for example $S_{(\mu\nu)} = \frac{1}{2}(S_{\mu\nu} + S_{\nu\mu})$ and $S_{[\mu\nu]} = \frac{1}{2}(S_{\mu\nu} - S_{\nu\mu})$ for a general 2-tensor $S_{\mu\nu}$. Unless otherwise stated, the Einstein summation convention holds, so that repeated upper and lower indices are summed over their range.

Because sections 1.1 and 1.2 review material that is long established and familiar to most theoretical particle physicists, I have included no references to individual books or papers. Anyone interested in studying gauge theories or electroweak unification in more detail should consult a standard textbook on quantum field theory. Examples include *Quantum Field Theory* by Claude Itzykson and Jean-Bernard Zuber (McGraw-Hill, Singapore, 1985); *Quantum Field Theory* by Franz Mandl and Graham Shaw (Wiley-Interscience, Chichester, 1984); and, for the more mathematically minded, *Quantum Field Theory and Topology* by Albert Schwarz (Springer, Berlin, 1993). Similarly, an expanded treatment of the discussion in sections 1.3 and 1.4 of the Nielsen–Olesen vortex string and defect formation, in general, can be found in the review article 'Cosmic strings' by Mark Hindmarsh and Tom Kibble, *Reports on Progress in Physics*, **58**, 477 (1995).

1.1   Electromagnetism as a local gauge theory

The first unified description of electricity and magnetism was developed by James Clerk Maxwell as long ago as the 1860s. Recall that Maxwell's equations relating the electric field $\mathbf{E}$ and magnetic flux density $\mathbf{B}$ in the presence of a prescribed charge density ρ and current density $\mathbf{j}$ have the form

$$\nabla \cdot \mathbf{B} = 0 \qquad \nabla \times \mathbf{E} + \frac{\partial}{\partial t}\mathbf{B} = \mathbf{0} \qquad (1.1)$$

and

$$\nabla \cdot \mathbf{E} = \rho \qquad \nabla \times \mathbf{B} - \frac{\partial}{\partial t}\mathbf{E} = \mathbf{j}. \qquad (1.2)$$

Here, for the sake of simplicity, the electric and magnetic field strengths are measured in Heaviside units (in which the permeability and permittivity of free space are 4π and $1/4\pi$ respectively), with a factor of 4π absorbed into ρ and $\mathbf{j}$.

Maxwell's equations can be recast in a more compact and elegant form by passing over to spacetime notation. Here and in the next section, points in spacetime will be identified by their Minkowski coordinates $x^\mu = [t, x, y, z] \equiv [t, \mathbf{r}]$, which are distinguished by the fact that the line element $ds^2 = dt^2 - d\mathbf{r}^2 \equiv \eta_{\mu\nu} \, dx^\mu \, dx^\nu$ is invariant under Lorentz transformations, where $\eta_{\mu\nu} = \mathrm{diag}(1, -1, -1, -1)$ is the 4×4 metric tensor. In general, spacetime indices on vectors or tensors are lowered or raised using the metric tensor $\eta_{\mu\nu}$ or its inverse $\eta^{\mu\nu} = (\eta_{\mu\nu})^{-1} = \mathrm{diag}(1, -1, -1, -1)$, so that for example $A^\mu = \eta^{\mu\nu} A_\nu$ for any vector field A^μ. In particular, $\eta^{\mu\lambda} \eta_{\lambda\nu} = \delta^\mu_\nu$, the 4×4 identity tensor (that is, $\delta^\mu_\nu = 1$ if $\mu = \nu$ and 0 if $\mu \neq \nu$).

Maxwell's equations can be rewritten in spacetime notation by defining a 4-current density $j^\mu = [\rho, \mathbf{j}]$ and a 4-potential $A^\mu = [A^0, \mathbf{A}]$, in terms of which

$$\mathbf{E} = -\nabla A^0 - \frac{\partial}{\partial t}\mathbf{A} \qquad \text{and} \qquad \mathbf{B} = \nabla \times \mathbf{A}. \tag{1.3}$$

The homogeneous equations (1.1) are then automatically satisfied, while the inhomogeneous equations (1.2) reduce to

$$\Box A^\mu - \partial^\mu(\partial_\nu A^\nu) = j^\mu \tag{1.4}$$

where $\partial_\mu = \partial/\partial x^\mu \equiv [\partial/\partial t, \nabla]$ and $\partial^\mu = [\partial/\partial t, -\nabla]$ are the covariant and contravariant spacetime derivative operators and $\Box = \partial_\mu \partial^\mu \equiv \partial^2/\partial t^2 - \nabla^2$ is the d'Alembertian.

One of the interesting features of the 4-vector equation (1.4) is that the potential A^μ corresponding to a given current density j^μ is not unique. For suppose that $A^\mu = A^\mu_0$ is a solution to (1.4). Then if Λ is any sufficiently smooth function of the spacetime coordinates the potential $A^\mu = A^\mu_0 + \partial^\mu \Lambda$ is also a solution. Note, however, that the electric and magnetic flux densities $\mathbf{E}$ and $\mathbf{B}$ are unaffected by the addition of a spacetime gradient $\partial^\mu \Lambda$ to A^μ. This is one of the simplest examples of what is known as *gauge invariance*, where the formal content of a field theory is preserved under a transformation of the dynamical degrees of freedom (in this case, the components of the 4-potential A^μ, which is the archetype of what is known as a *gauge field*). Gauge invariance might seem like little more than a mathematical curiosity but it turns out to have important consequences when a field theory comes to be quantized. In particular, electromagnetic gauge invariance implies the existence of a massless spin-1 particle, the photon.

Although the details of field quantization lie outside the scope of this book, it is instructive to examine the leading step in the quantization process, which is the construction of a field action I of the form

$$I = \int \mathcal{L} \, d^4 x. \tag{1.5}$$

Here the Lagrange density or 'lagrangian' $\mathcal{L}$ is a functional of the field variables and their first derivatives, and is chosen so that the value of I is stationary

whenever the corresponding field equations are satisfied. In the electromagnetic case, $\mathcal{L}$ should depend on A_μ and $\partial_\nu A_\mu$. The value of I is then stationary whenever A_μ satisfies the Euler–Lagrange equation

$$\frac{\partial \mathcal{L}}{\partial A_\mu} - \partial_\nu \left(\frac{\partial \mathcal{L}}{\partial [\partial_\nu A_\mu]} \right) = 0 \tag{1.6}$$

which reduces to the electromagnetic field equation (1.4) if $\mathcal{L}$ has the form

$$\mathcal{L} = -\tfrac{1}{4} F_{\mu\nu} F^{\mu\nu} - j^\mu A_\mu \tag{1.7}$$

with $F_{\mu\nu} = \partial_\mu A_\nu - \partial_\nu A_\mu$. Strictly speaking, (1.7) is just one of a large family of possible solutions for the lagrangian, as the addition of the divergence of an arbitrary 4-vector functional of A_μ, j^μ and the coordinates x^μ to $\mathcal{L}$ leaves the Euler–Lagrange equation (1.6) unchanged.

A notable feature of the lagrangian (1.7) is that it is not gauge-invariant, for if A_μ is replaced with $A_\mu + \partial_\mu \Lambda$ then $\mathcal{L}$ transforms to $\mathcal{L} - j^\mu \partial_\mu \Lambda$. In view of the equation $\partial_\mu j^\mu = 0$ of local charge conservation—which is generated by taking the 4-divergence of (1.4)—the gauge-dependent term $j^\mu \partial_\mu \Lambda \equiv \partial_\mu (j^\mu \Lambda)$ is a pure divergence and the field equations remain gauge-invariant as before. However, the gauge dependence of $\mathcal{L}$ does reflect the important fact that the 4-current j^μ has not been incorporated into the theory in a self-consistent manner. In general, the material charges and currents that act as sources for the electromagnetic field will change in response to that field, and so should be treated as independent dynamical variables in their own right.

This can be done, in principle, by adding to the lagrangian (1.7) a further component describing the free propagation of all the matter sources present—be they charged leptons (electrons, muons or tauons), charged hadrons (mesons such as the pion, or baryons such as the proton) or more exotic species of charged particles—and replacing j^μ with the corresponding superposition of 4-currents. In some cases, however, it is necessary to make a correction to j^μ to account for the interaction of the matter fields with the electromagnetic field.

As a simple example, a free electron field can be described by a bispinor ψ (a complex 4-component vector in the Dirac representation) which satisfies the Dirac equation

$$i\gamma^\mu \partial_\mu \psi - m\psi = 0 \tag{1.8}$$

where m is the mass of the electron and $\gamma^\mu = [\gamma^0, \gamma^1, \gamma^2, \gamma^3]$ are the four fundamental 4×4 Dirac matrices. Since γ^0 is a Hermitian matrix ($\gamma^{0\dagger} = \gamma^0$) while the other three Dirac matrices are anti-Hermitian ($\gamma^{k\dagger} = -\gamma^k$ for $k = 1, 2$ or 3) with $\gamma^0 \gamma^k = -\gamma^k \gamma^0$, the Hermitian conjugate of (1.8) can be written as

$$i\partial_\mu \overline{\psi} \gamma^\mu + \overline{\psi} m = 0 \tag{1.9}$$

where $\overline{\psi} = \psi^\dagger \gamma^0$. Both the Dirac equation (1.8) and its conjugate (1.9) are generated from the lagrangian

$$\mathcal{L}_{\text{el}} = i\overline{\psi} \gamma^\mu (\partial_\mu \psi) - m\overline{\psi} \psi. \tag{1.10}$$

By adding $\overline{\psi}\times$(1.8) to (1.9)$\times\psi$ it is evident that $\partial_\mu(\overline{\psi}\gamma^\mu\psi) = 0$. The free electron 4-current j^μ_{el} is, therefore, proportional to $\overline{\psi}\gamma^\mu\psi$, and can be written as

$$j^\mu_{\text{el}} = e\overline{\psi}\gamma^\mu\psi \tag{1.11}$$

where the coupling constant e must be real, as $\overline{\psi}\gamma^\mu\psi$ is Hermitian, and can be identified with the electron charge. It is, therefore, possible to couple the electromagnetic field and the electron field together through the lagrangian:

$$\begin{aligned}\mathcal{L} &= -\tfrac{1}{4}F_{\mu\nu}F^{\mu\nu} - j^\mu_{\text{el}}A_\mu + \mathcal{L}_{\text{el}} \\ &\equiv -\tfrac{1}{4}F_{\mu\nu}F^{\mu\nu} - e\overline{\psi}\gamma^\mu A_\mu\psi + i\overline{\psi}\gamma^\mu(\partial_\mu\psi) - m\overline{\psi}\psi.\end{aligned} \tag{1.12}$$

Here, the presence of the interaction term $j^\mu_{\text{el}}A_\mu$ in $\mathcal{L}$ modifies the Euler–Lagrange equations for $\overline{\psi}$ and ψ to give the electromagnetically-coupled Dirac equations

$$i\gamma^\mu\partial_\mu\psi - m\psi = e\gamma^\mu A_\mu\psi \quad\text{and}\quad i\partial_\mu\overline{\psi}\gamma^\mu + m\overline{\psi} = -e\overline{\psi}\gamma^\mu A_\mu \tag{1.13}$$

which replace (1.8) and (1.9) respectively. However, as is evident from (1.13), it is still true that $\partial_\mu(\overline{\psi}\gamma^\mu\psi) = 0$, so j^μ_{el} remains a conserved 4-current and there is no need to make any further corrections to $\mathcal{L}$.

It is often convenient to write the lagrangian (1.12) in the form

$$\mathcal{L} = -\tfrac{1}{4}F_{\mu\nu}F^{\mu\nu} + i\overline{\psi}\gamma^\mu(D_\mu\psi) - m\overline{\psi}\psi \tag{1.14}$$

where $D_\mu = \partial_\mu + ieA_\mu$ is the electromagnetic covariant derivative. Because the electromagnetic and Dirac fields interact only through the derivative D_μ, they are said to be *minimally coupled*. One advantage of introducing the operator D_μ is that the effect of a gauge transformation of the potential A_μ is easily seen. For if A_μ is replaced by $A_\mu + \partial_\mu\Lambda$ then D_μ is transformed to $D_\mu + ie\partial_\mu\Lambda$. The lagrangian (1.14) will, therefore, remain invariant if ψ is replaced by $\psi e^{-ie\Lambda}$ and $\overline{\psi}$ by $\overline{\psi}e^{ie\Lambda}$. Thus $\mathcal{L}$ is gauge-invariant if the components of the Dirac bispinor ψ are suitably rotated in the complex plane. It is for this reason that the electromagnetic field is characterized as having a *local $U(1)$ symmetry*, $U(1)$ being the group of complex rotations and the qualifier 'local' referring to the fact that the rotation angle $e\Lambda$ can vary from point to point in spacetime. (By contrast, a theory which is invariant under the action of group elements that are constant throughout spacetime is said to have a 'global' symmetry.)

Coupling other charged leptonic species to an electromagnetic field can be achieved in exactly the same way, although, of course, the mass m is typically different for each species. The same is, in principle, true of hadronic coupling, as all hadrons can be decomposed into two or more quarks, which (like the electron) are spin-$\tfrac{1}{2}$ fermions. However, because quarks are always bound together in pairs or triples by the strong nuclear force there is little value in coupling quarks to an electromagnetic field except as part of a more general theory which includes the

strong interaction. (Of course, protons and other spin-$\frac{1}{2}$ baryons can also, as a first approximation, be coupled to the electromagnetic field in the same way as leptons.)

Another type of matter field which turns out to be a crucial ingredient of electroweak unification is a complex scalar field (or multiplet of scalar fields) ϕ which satisfies the Klein–Gordon equation:

$$(\Box + m^2)\phi = 0 \tag{1.15}$$

and, at a quantum level, describes charged spin-0 bosons of mass m. The corresponding lagrangian is:

$$\mathcal{L}_{\text{sc}} = (\partial_\mu \phi^\dagger)(\partial^\mu \phi) - m^2 \phi^\dagger \phi. \tag{1.16}$$

It is easily seen that (1.15) gives rise to a conserved current

$$j_{\text{sc}}^\mu = ie'[\phi^\dagger(\partial^\mu \phi) - (\partial^\mu \phi^\dagger)\phi] \tag{1.17}$$

where e' is a coupling constant, the scalar charge. (Note, in particular, that if ϕ is real then j_{sc}^μ vanishes and the corresponding spin-0 bosons are uncharged.)

Adding $\mathcal{L}_{\text{sc}}$ to the bare electromagnetic lagrangian (1.7) and replacing j^μ with j_{sc}^μ then gives a tentative lagrangian of the form

$$\mathcal{L} = -\tfrac{1}{4} F_{\mu\nu} F^{\mu\nu} - ie' A_\mu [\phi^\dagger(\partial^\mu \phi) - (\partial^\mu \phi^\dagger)\phi] + (\partial_\mu \phi^\dagger)(\partial^\mu \phi) - m^2 \phi^\dagger \phi. \tag{1.18}$$

However, the presence of the interaction introduces an inhomogeneous source term on the right of the Klein–Gordon equation, which now reads:

$$(\Box + m^2)\phi = -ie'[A_\mu \partial^\mu \phi + \partial^\mu (A_\mu \phi)] \tag{1.19}$$

and j_{sc}^μ is no longer conserved, as

$$\partial_\mu j_{\text{sc}}^\mu = 2e'^2 \partial_\mu (A^\mu \phi^\dagger \phi). \tag{1.20}$$

It is, therefore, necessary to add a correction term $\Delta\mathcal{L}$ to the lagrangian constructed so that the divergence of the new 4-current is zero under the action of the corrected field equations. In general, if $\mathcal{L}$ is a lagrangian depending on an electromagnetic potential A_μ coupled to one or more matter fields then the associated 4-current is $j^\mu = -\partial\mathcal{L}/\partial A_\mu$. Hence, if $\Delta\mathcal{L}$ is assumed to be a functional of $\phi^\dagger$, ϕ and the electromagnetic variables only, the condition $\partial_\mu j^\mu = 0$ reduces to

$$2e'^2 \partial_\mu (A^\mu \phi^\dagger \phi) - \partial_\mu \left(\frac{\partial \Delta\mathcal{L}}{\partial A_\mu} \right) + ie' \left(\phi^\dagger \frac{\partial \Delta\mathcal{L}}{\partial \phi^\dagger} - \phi \frac{\partial \Delta\mathcal{L}}{\partial \phi} \right) = 0. \tag{1.21}$$

This has an obvious solution $\Delta\mathcal{L} = e'^2 A_\mu A^\mu \phi^\dagger \phi$, with a corresponding 4-current $j^\mu = j_{\text{sc}}^\mu - 2e'^2 A^\mu \phi^\dagger \phi$. Adding $\Delta\mathcal{L}$ to the right of (1.18) gives a lagrangian which is again minimally coupled, as it can be cast in the form

$$\mathcal{L} = -\tfrac{1}{4} F_{\mu\nu} F^{\mu\nu} + (D_\mu^* \phi^\dagger)(D^\mu \phi) - m^2 \phi^\dagger \phi \tag{1.22}$$

where now $D_\mu = \partial_\mu + ie'A_\mu$. As in the fermionic case, the lagrangian is invariant under the $U(1)$ gauge transformation $A_\mu \rightarrow A_\mu + \partial_\mu\Lambda$, $\phi \rightarrow \phi e^{-ie'\Lambda}$ and $\phi^\dagger \rightarrow \phi^\dagger e^{ie'\Lambda}$.

Finally, mention should be made of the possibility of massive gauge fields. If W_μ is a vector potential (possibly complex) whose spin-1 carrier particles on quantization have mass m_W, then the simplest generalization of the electromagnetic 4-vector equation (1.4) in the absence of sources j^μ is the *Proca equation*:

$$\Box W^\mu - \partial^\mu(\partial_\nu W^\nu) + m_W^2 W^\mu = 0. \tag{1.23}$$

The corresponding lagrangian is

$$\mathcal{L}_W = -\tfrac{1}{2}W_{\mu\nu}(W^{\mu\nu})^* + m_W^2 W^\mu W_\mu^* \tag{1.24}$$

where $W_{\mu\nu} = \partial_\mu W_\nu - \partial_\nu W_\mu$. If W_μ is complex, the carrier particles are charged, whereas if W_μ is real they are neutral. Note, however, that $\mathcal{L}_W$ is not invariant under gauge transformations of the form $W_\mu \rightarrow W_\mu + \partial_\mu\Lambda$. It is the search for a gauge-invariant description of massive gauge fields that leads ultimately to electroweak unification.

1.2 Electroweak unification

The existence of the weak interaction was first suggested by Wolfgang Pauli in 1930 as a way of explaining certain short-range nuclear reactions that seemed to violate energy and momentum conservation. The most famous example is beta decay, in which a neutron decays to form a proton and an electron. The simplest explanation is that the production of the electron is accompanied by the emission of a light (possibly massless) uncharged spin-$\tfrac{1}{2}$ lepton, the neutrino, which carries off the missing energy and momentum. Thus the electron bispinor ψ_e is paired with a second complex bispinor ψ_{ν_e} which describes the electron neutrino field, and it turns out that there are similar bispinor fields ψ_{ν_μ} and ψ_{ν_τ} describing the muon and tauon neutrinos (although the latter is a relatively recent addition to electroweak theory, as the tauon itself was only discovered in 1975).

Another important ingredient of electroweak theory was added in 1957 with the discovery that weak interactions fail to conserve parity (or space-reflection symmetry). For example, in beta decay the electron can, in principle, emerge with its spin either parallel or anti-parallel to its direction of motion, and is said to have either *positive* or *negative helicity* in the respective cases. If parity were conserved, electrons with positive helicity would be observed just as often as those with negative helicity. However, the electrons produced in beta decay almost always have negative helicity.

Now, any Dirac bispinor ψ can be decomposed as a sum $\psi^L + \psi^R$ of left-handed and right-handed fields:

$$\psi^L = \tfrac{1}{2}(1 - \gamma_5)\psi \qquad \text{and} \qquad \psi^R = \tfrac{1}{2}(1 + \gamma_5)\psi \tag{1.25}$$

where the Hermitian matrix $\gamma_5 = i\gamma^0\gamma^1\gamma^2\gamma^3$ satisfies the identity $\gamma_5^2 = 1$, and so $P_\pm = \frac{1}{2}(1 \pm \gamma_5)$ are both projection operators (that is, $P_\pm^2 = P_\pm$). For massless fermions, ψ^L and ψ^R are negative- and positive-helicity eigenstates respectively (hence the names 'left-handed' and 'right-handed'). For massive leptons, ψ^L and ψ^R remain good approximations to helicity eigenstates, particularly at high energies.

The crucial feature of weak parity-violation is that only left-handed leptons (and right-handed anti-leptons) are ever involved in weak reactions. In fact, each of the lepton helicity states can be assigned a number analogous to the ordinary electric charge, called the *weak isospin charge*, which measures its strength in certain weak interactions. In suitable units, the weak isospin charge of ψ^L is equal to $-\frac{1}{2}$ for electrons, muons and tauons, and equal to $+\frac{1}{2}$ for neutrinos, while the weak isospin charge of ψ^R is zero for all leptons. Like photons, the carriers of the weak interaction are themselves (weakly) uncharged.

However, weak interactions are observed to come in two types: those like the electron–neutrino scattering process $\nu_\mu + e^- \rightarrow \nu_\mu + e^-$ which involve no exchange of electric charge, and those like inverse muon decay $\nu_\mu + e^- \rightarrow \nu_e + \mu^-$ in which there is an exchange of electric charge (in this case, from the electron to the muon fields). This suggests that the weak interaction is described by not one but three gauge fields to allow for exchange particles with positive, negative and zero electric charge.

The above considerations lead to the following procedure for constructing a lagrangian $\mathcal{L}$ for the weak interaction. In analogy with the free-electron lagrangian (1.10), the lagrangian for the free-lepton fields has the form

$$\mathcal{L}_{\text{lep}} = i\overline{\psi}_e\gamma^\mu(\partial_\mu\psi_e) + i\overline{\psi}_{\nu_e}\gamma^\mu(\partial_\mu\psi_{\nu_e}) + \cdots \tag{1.26}$$

where the ellipsis (...) denotes equivalent terms for the muon and tauon fields and their neutrinos. Mass terms like $m_e\overline{\psi}_e\psi_e$ have been omitted for reasons that will become clear later. Since $\gamma_5\gamma^\mu = -\gamma^\mu\gamma_5$ for all Dirac matrices γ^μ it follows that $P_+^\dagger\gamma^0\gamma^\mu P_- = P_-^\dagger\gamma^0\gamma^\mu P_+ = 0$ and so $\overline{\psi}^R\gamma^\mu\partial_\mu\psi^L = \overline{\psi}^L\gamma^\mu\partial_\mu\psi^R = 0$ for any fermion field ψ.

Thus the lagrangian (1.26) can be expanded as

$$\mathcal{L}_{\text{lep}} = i[\overline{\psi}_e^L\gamma^\mu(\partial_\mu\psi_e^L) + \overline{\psi}_e^R\gamma^\mu(\partial_\mu\psi_e^R) + \overline{\psi}_{\nu_e}^L\gamma^\mu(\partial_\mu\psi_{\nu_e}^L) + \overline{\psi}_{\nu_e}^R\gamma^\mu(\partial_\mu\psi_{\nu_e}^R)] + \cdots . \tag{1.27}$$

Here, since the right-handed neutrino field $\psi_{\nu_e}^R$ has neither weak nor electric charge it can be discarded. Also, the two left-handed fields ψ_e^L and $\psi_{\nu_e}^L$ can be combined into a 'two-component' vector field $\Psi_e^L = (\psi_{\nu_e}^L, \psi_e^L)^\intercal$. The free-lepton lagrangian then becomes

$$\mathcal{L}_{\text{lep}} = i[\overline{\Psi}_e^L\gamma^\mu(\partial_\mu\Psi_e^L) + \overline{\psi}_e^R\gamma^\mu(\partial_\mu\psi_e^R)] + \cdots \tag{1.28}$$

where, of course, $\overline{\Psi}_e^L = (\overline{\psi}_{\nu_e}^L, \overline{\psi}_e^L)$.

The example of the electromagnetic field suggests that the interaction between the lepton fields and the weak field can be described by minimally coupling three gauge fields $A_{k\mu}$ (where $k = 1, 2, 3$) to the left-handed terms in $\mathcal{L}_{\text{lep}}$. Furthermore, if the resulting lagrangian is to be invariant under transformations of $A_{k\mu}$ and $\Psi_{\text{e}}^{\text{L}}$ which, in some way, generalize the gauge transformations $A_\mu \to A_\mu + \partial_\mu \Lambda$ and $\psi \to \psi \text{e}^{-ie\Lambda}$ of the electromagnetic and Dirac fields, it is necessary to find a continuous three-parameter group which acts on the components of the complex two-component field $\Psi_{\text{e}}^{\text{L}}$.

A suitable candidate for this group is $SU(2)$, the group of unitary complex 2×2 matrices with determinant 1, which is generated by the three Hermitian matrices

$$\boldsymbol{\tau}^1 = \begin{pmatrix} 0 & 1 \\ 1 & 0 \end{pmatrix} \qquad \boldsymbol{\tau}^2 = \begin{pmatrix} 0 & -i \\ i & 0 \end{pmatrix} \qquad \text{and} \qquad \boldsymbol{\tau}^3 = \begin{pmatrix} 1 & 0 \\ 0 & -1 \end{pmatrix}. \quad (1.29)$$

(That is, $\mathbf{U}$ is an element of $SU(2)$ if and only if $\mathbf{U} = \text{e}^{i\mathbf{M}}$ for some real linear combination $\mathbf{M}$ of $\boldsymbol{\tau}^1$, $\boldsymbol{\tau}^2$ and $\boldsymbol{\tau}^3$.) The gauge fields $A_{k\mu}$ can, therefore, be mapped linearly to a single Hermitian matrix operator:

$$\mathbf{A}_\mu = \boldsymbol{\tau}^k A_{k\mu} \quad (1.30)$$

and coupled to the lepton fields by replacing ∂_μ with $D_\mu = \partial_\mu + \frac{1}{2} ig\mathbf{A}_\mu$ in the left-handed terms in $\mathcal{L}_{\text{lep}}$, where g is the weak isospin coupling constant. (The constant $\frac{1}{2}$ is included here as a measure of the weak isospin of the left-handed fields, which strictly speaking is the charge conserved under the action of $\boldsymbol{\tau}^3$ only, and hence has opposing signs for the electron and neutrino components.)

The corresponding gauge transformations of $\mathbf{A}_\mu$ are then specified by demanding that the resulting lagrangian remain invariant when $\Psi^{\text{L}} \to \mathbf{U}^{-1}\Psi^{\text{L}}$ and $\overline{\Psi}^{\text{L}} \to \overline{\Psi}^{\text{L}}\mathbf{U}$ for each of the lepton species, where $\mathbf{U}$ is any element of $SU(2)$. If $\mathbf{A}_\mu$ is assumed to transform to $\mathbf{A}_\mu + \delta\mathbf{A}_\mu$ then $\overline{\Psi}^{\text{L}}\gamma^\mu(D_\mu\Psi^{\text{L}})$ remains invariant if

$$\delta\mathbf{A}_\mu = -(\partial_\mu\mathbf{U}^{-1})\mathbf{U}/(\tfrac{1}{2}ig) + \mathbf{U}^{-1}\mathbf{A}_\mu\mathbf{U} - \mathbf{A}_\mu. \quad (1.31)$$

The connection with the rule for $U(1)$ gauge transformations becomes clearer if $\mathbf{U}$ is expressed as $\text{e}^{\frac{1}{2}ig\mathbf{\Lambda}}$, where $\mathbf{\Lambda}$ is a real linear combination of the generators $\boldsymbol{\tau}^1$, $\boldsymbol{\tau}^2$ and $\boldsymbol{\tau}^3$. Then $\mathbf{U}^{\pm 1} \approx \mathbf{I} \pm \frac{1}{2}ig\mathbf{\Lambda}$ for small values of $\mathbf{\Lambda}$, and the limiting form of $\delta\mathbf{A}_\mu$ is:

$$\delta\mathbf{A}_\mu \approx \partial_\mu\mathbf{\Lambda} + \tfrac{1}{2}ig[\mathbf{A}_\mu, \mathbf{\Lambda}] \quad (1.32)$$

where $[\mathbf{A}_\mu, \mathbf{\Lambda}] \equiv \mathbf{A}_\mu\mathbf{\Lambda} - \mathbf{\Lambda}\mathbf{A}_\mu$.

The next step is to generalize the electromagnetic field energy term $-\frac{1}{4}F_{\mu\nu}F^{\mu\nu}$ to the case of the three $SU(2)$ gauge fields $A_{k\mu}$. One obvious possibility is to add

$$-\tfrac{1}{4}(f_{1\mu\nu}f_1^{\mu\nu} + f_{2\mu\nu}f_2^{\mu\nu} + f_{3\mu\nu}f_3^{\mu\nu}) \equiv -\tfrac{1}{8}\text{Tr}(\mathbf{f}_{\mu\nu}\mathbf{f}^{\mu\nu}) \quad (1.33)$$

to the lepton lagrangian, where $f_{k\mu\nu} = \partial_\mu A_{k\nu} - \partial_\nu A_{k\mu}$ and $\mathbf{f}_{\mu\nu} = \partial_\mu \mathbf{A}_\nu - \partial_\nu \mathbf{A}_\mu$. (The right-hand side of (1.33) follows from the fact that $\mathrm{Tr}(\boldsymbol{\tau}^j \boldsymbol{\tau}^k) = 2\delta^{jk}$ for the three generating matrices $\boldsymbol{\tau}^k$.) However, such a term is not locally $SU(2)$-invariant, as

$$\mathbf{f}_{\mu\nu} \rightarrow \mathbf{U}^{-1}\mathbf{f}_{\mu\nu}\mathbf{U} + 2(\partial_{[\mu}\mathbf{U}^{-1})\mathbf{A}_{\nu]}\mathbf{U} + 2\mathbf{U}^{-1}\mathbf{A}_{[\nu}(\partial_{\mu]}\mathbf{U}) + 2(\partial_{[\mu}\mathbf{U}^{-1})(\partial_{\nu]}\mathbf{U})/(\tfrac{1}{2}ig) \tag{1.34}$$

if $\mathbf{A}_\mu \rightarrow \mathbf{A}_\mu + \delta\mathbf{A}_\mu$ with $\delta\mathbf{A}_\mu$ given by (1.31).

This problem can be eliminated by simply replacing ∂_μ in $\mathbf{f}_{\mu\nu}$ with the coupled derivative D_μ, so that the field energy term becomes $-\tfrac{1}{8}\,\mathrm{Tr}(\mathbf{F}_{\mu\nu}\mathbf{F}^{\mu\nu})$, where

$$\mathbf{F}_{\mu\nu} = D_\mu\mathbf{A}_\nu - D_\nu\mathbf{A}_\mu \equiv \partial_\mu\mathbf{A}_\nu - \partial_\nu\mathbf{A}_\mu + \tfrac{1}{2}ig[\mathbf{A}_\mu, \mathbf{A}_\nu]. \tag{1.35}$$

Then, under the transformation $\mathbf{A}_\mu \rightarrow \mathbf{A}_\mu + \delta\mathbf{A}_\mu$,

$$\begin{aligned}
\mathbf{F}_{\mu\nu} \rightarrow &[\partial_\mu - (\partial_\mu\mathbf{U}^{-1})\mathbf{U} + \tfrac{1}{2}ig\mathbf{U}^{-1}\mathbf{A}_\mu\mathbf{U}][-(\partial_\nu\mathbf{U}^{-1})\mathbf{U}/(\tfrac{1}{2}ig) + \mathbf{U}^{-1}\mathbf{A}_\nu\mathbf{U}] \\
&- [\partial_\nu - (\partial_\nu\mathbf{U}^{-1})\mathbf{U} + \tfrac{1}{2}ig\mathbf{U}^{-1}\mathbf{A}_\nu\mathbf{U}][-(\partial_\mu\mathbf{U}^{-1})\mathbf{U}/(\tfrac{1}{2}ig) + \mathbf{U}^{-1}\mathbf{A}_\mu\mathbf{U}] \\
= &\ \mathbf{U}^{-1}\mathbf{F}_{\mu\nu}\mathbf{U} \tag{1.36}
\end{aligned}$$

where the last line follows after expanding and invoking the identity $(\partial_\mu\mathbf{U}^{-1})\mathbf{U} = -\mathbf{U}^{-1}(\partial_\mu\mathbf{U})$. Hence,

$$\mathrm{Tr}(\mathbf{F}_{\mu\nu}\mathbf{F}^{\mu\nu}) \rightarrow \mathrm{Tr}(\mathbf{U}^{-1}\mathbf{F}_{\mu\nu}\mathbf{F}^{\mu\nu}\mathbf{U}) = \mathrm{Tr}(\mathbf{F}_{\mu\nu}\mathbf{F}^{\mu\nu}) \tag{1.37}$$

and is locally $SU(2)$-invariant as claimed.

A candidate lagrangian for the coupled weak and lepton fields is therefore:

$$\mathcal{L}_{SU(2)} = -\tfrac{1}{8}\,\mathrm{Tr}(\mathbf{F}_{\mu\nu}\mathbf{F}^{\mu\nu}) + i\overline{\Psi}_\mathrm{e}^\mathrm{L}\gamma^\mu(\partial_\mu + \tfrac{1}{2}ig\mathbf{A}_\mu)\Psi_\mathrm{e}^\mathrm{L} + i\overline{\psi}_\mathrm{e}^\mathrm{R}\gamma^\mu\partial_\mu\psi_\mathrm{e}^\mathrm{R} + \cdots. \tag{1.38}$$

It turns out that the corresponding quantized field theory is renormalizable (that is, finite to all orders in perturbation theory). However, it suffers from the serious defect that the lepton fields and the bosons carrying the gauge fields $\mathbf{A}_\mu$ are all massless. This is contrary to the observed fact that at least three of the leptons (the electron, muon and tauon) are massive, while the extremely short range of the weak force indicates that the gauge bosons must be massive as well. It might seem possible to manually insert the lepton masses by adding mass terms like $m_\mathrm{e}\overline{\psi}_\mathrm{e}\psi_\mathrm{e}$ to the lagrangian, but

$$\overline{\psi}_\mathrm{e}\psi_\mathrm{e} \equiv \overline{\psi}_\mathrm{e}^\mathrm{L}\psi_\mathrm{e}^\mathrm{R} + \overline{\psi}_\mathrm{e}^\mathrm{R}\psi_\mathrm{e}^\mathrm{L} \tag{1.39}$$

is clearly not $SU(2)$-invariant, and adding terms of this type destroys the renormalizability of the theory.

The solution to this quandary is to construct a lagrangian which jointly describes the weak and electromagnetic fields by adding a fourth, $U(1)$-invariant,

gauge field B_μ, and then coupling the entire system to a pair of complex scalar fields $\phi = (\phi_1, \phi_2)^\mathsf{T}$ whose uncoupled lagrangian

$$\mathcal{L}_{\text{sc}} = (\partial_\mu \phi^\dagger)(\partial^\mu \phi) - V(\phi^\dagger \phi) \tag{1.40}$$

is a generalization of the Klein–Gordon lagrangian (1.16), containing as it does a general scalar potential V in place of the Klein–Gordon mass term $m^2 \phi^\dagger \phi$.

The scalar fields will be discussed in more detail shortly. First, the gauge field B_μ is incorporated into the lagrangian by minimally coupling it to both the left-handed and right-handed fields Ψ^L and ψ^R, with coupling constants $-\frac{1}{2}g'$ and $-g'$ in the two cases. The coefficients $-\frac{1}{2}$ and -1 outside g' here measure what is called the *weak hypercharge* of the lepton fields, which is defined to be the difference between the electric charge (in units of $|e|$) and the weak isospin charge of the particle. Thus the left-handed electron $(-1+\frac{1}{2})$ and neutrino $(0-\frac{1}{2})$ fields both have a weak hypercharge of $-\frac{1}{2}$, while the right-handed electron field $(-1 + 0)$ has weak hypercharge -1. It is the weak hypercharge rather than the electric charge by which B_μ is coupled to the lepton fields because, as will become evident later, B_μ combines parts of the electromagnetic and uncharged weak fields.

If the field energy contribution of B_μ is assumed to have the standard electromagnetic form $-\frac{1}{4}G_{\mu\nu}G^{\mu\nu}$, where $G_{\mu\nu} = \partial_\mu B_v - \partial_v B_\mu$, the electroweak lagrangian becomes

$$\mathcal{L}_{\text{ew}} = -\tfrac{1}{8}\operatorname{Tr}(\mathbf{F}_{\mu\nu}\mathbf{F}^{\mu\nu}) - \tfrac{1}{4}G_{\mu\nu}G^{\mu\nu} + i\overline{\psi}_{\text{e}}^{\text{R}}\gamma^\mu(\partial_\mu - ig'B_\mu)\psi_{\text{e}}^{\text{R}}$$
$$+ i\overline{\Psi}_{\text{e}}^{\text{L}}\gamma^\mu(\partial_\mu + \tfrac{1}{2}ig\mathbf{A}_\mu - \tfrac{1}{2}ig'B_\mu)\Psi_{\text{e}}^{\text{L}} + \cdots. \tag{1.41}$$

This lagrangian is invariant under both the local $SU(2)$ transformations $\mathbf{A}_\mu \to \mathbf{A}_\mu + \delta\mathbf{A}_\mu$ and $\Psi^L \to \mathbf{U}^{-1}\Psi^L$ and the local $U(1)$ transformations $B_\mu \to B_\mu + \partial_\mu\Lambda$, $\Psi^L \to \Psi^L e^{-\frac{1}{2}ig'\Lambda}$ and $\psi^R \to \psi^R e^{-ig'\Lambda}$, and so is said to have $SU(2) \times U(1)$ symmetry.

Turning now to the contribution of the complex scalar fields $\phi = (\phi_1, \phi_2)^\mathsf{T}$, the scalar potential V can assume a wide variety of forms but one simple assumption is to truncate V after the first three terms in its Maclaurin expansion to give

$$V(\phi^\dagger \phi) = V_0 + \alpha^2 \phi^\dagger \phi + \beta^2 (\phi^\dagger \phi)^2 \tag{1.42}$$

where the constant V_0 is chosen so as to normalize V to zero in the ground state. Note that α^2 need not be positive: it is common to write the leading coefficient as a square in analogy with the mass term $m^2 \phi^\dagger \phi$ in (1.16). However, β^2 must be positive to ensure that V is bounded below, since otherwise the theory is unstable to the production of scalar particles with arbitrarily high energies.

If the scalar doublet ϕ is assumed to transform like Ψ^L under $SU(2)$ gauge transformations then its upper component ϕ_1 has weak isospin charge $+\frac{1}{2}$ and its lower component ϕ_2 has weak isospin charge $-\frac{1}{2}$. In situations where ϕ has

a non-zero expectation value it is conventional to use the $SU(2)$ gauge freedom to transform ϕ_1 to 0, leaving ϕ_2 as the only physical component. To ensure that this field has zero electric charge, ϕ is assigned a weak hypercharge $+\frac{1}{2}$, and so if it is minimally coupled to the interaction fields the full electroweak lagrangian becomes

$$\mathcal{L} = \mathcal{L}_{ew} + (\partial_\mu \phi + \tfrac{1}{2} ig\mathbf{A}_\mu \phi + \tfrac{1}{2} ig' B_\mu \phi)^\dagger (\partial^\mu \phi + \tfrac{1}{2} ig\mathbf{A}_\mu \phi + \tfrac{1}{2} ig' B_\mu \phi)$$
$$- V_0 - \alpha^2 \phi^\dagger \phi - \beta^2 (\phi^\dagger \phi)^2 - g_e(\overline{\Psi}_e^L \psi_e^R \phi + \phi^\dagger \overline{\psi}_e^R \Psi_e^L) - \cdots. \quad (1.43)$$

The last (or Yukawa) term in (1.43), which models the interaction between the scalar and electron fields, is the only possible $SU(2)$-invariant combination of the electron fields and ϕ which is quadratic in the first and linear in the second. Of course, similar terms describing the interaction of ϕ with the muon and tauon fields are included as well, although the values of the associated coupling constants g_e, g_μ and g_τ are, in general, all different.

The crucial feature of the lagrangian (1.43) is that the global minimum of V occurs when $\phi^\dagger \phi = -\frac{1}{2}\alpha^2/\beta^2$. Thus if $\alpha^2 > 0$ the vacuum expectation value of ϕ is $\langle \phi \rangle = (0,0)^\mathsf{T}$, and the scalar fields are effectively decoupled from the gauge and lepton fields in (1.43). This means that the electroweak exchange particles and the leptons remain massless, while the charged spin-0 bosons described by ϕ have mass α.

However, if $\alpha^2 < 0$ the vacuum expectation value of ϕ is non-zero:

$$\langle \phi \rangle = (\tfrac{1}{\sqrt{2}} |\alpha|/\beta) \varphi \equiv \lambda \varphi \quad (1.44)$$

where φ is some scalar doublet with $\varphi^\dagger \varphi = 1$. Since the electroweak lagrangian (1.43) remains invariant under a local $SU(2)$ transformation if $\phi \to \mathbf{U}^{-1}\phi$, and $SU(2)$ is a three-parameter group, it is always possible to choose $\mathbf{U}$ so that ϕ is transformed into the canonical form $\phi = (0, \phi_2)^\mathsf{T}$ where ϕ_2 is now real at all points in spacetime. In particular, $\langle \phi \rangle = (0, \lambda)^\mathsf{T}$ and if ϕ_2 is expanded about its vacuum value in the form $\phi_2 = \lambda + \sigma$, where σ is real, then to leading order in σ the Weinberg–Salam lagrangian (1.43) reads

$$\mathcal{L} = \mathcal{L}_{ew} + \tfrac{1}{4}[(g'B^\mu - gA_3^\mu)(g'B_\mu - gA_{3\mu}) + g^2(A_1^\mu A_{\mu 1} + A_2^\mu A_{2\mu})](\lambda + \sigma)^2$$
$$+ \partial_\mu \sigma \partial^\mu \sigma - 4\beta^2 \lambda^2 \sigma^2 - g_e(\overline{\psi}_e^L \psi_e^R + \overline{\psi}_e^R \psi_e^L)(\lambda + \sigma) + \cdots \quad (1.45)$$

plus terms cubic and quartic in σ. (Here, V_0 has been set equal to $\beta^2 \lambda^4$ so that $V = 0$ when $\sigma = 0$.)

The lagrangian can be further simplified by recalling that $\overline{\psi}_e^L \psi_e^R + \overline{\psi}_e^R \psi_e^L = \overline{\psi}_e \psi_e$ and introducing the normalized fields

$$Z_\mu = (g^2 + g'^2)^{-1/2}(g'B_\mu - gA_{3\mu}) \qquad A_\mu = (g^2 + g'^2)^{-1/2}(gB_\mu + g'A_{3\mu})$$

and

$$W_\mu = \tfrac{1}{\sqrt{2}}(A_{1\mu} + iA_{2\mu}) \quad (1.46)$$

in terms of which

$$\mathcal{L} = \mathcal{L}_{\text{ew}} + \partial_\mu \sigma \partial^\mu \sigma + \tfrac{1}{4}[(g^2 + g'^2)Z^\mu Z_\mu + 2g^2 W^\mu W_\mu^*](\lambda + \sigma)^2$$
$$- 4\beta^2 \lambda^2 \sigma^2 - g_e \bar{\psi}_e \psi_e (\lambda + \sigma) + \cdots . \tag{1.47}$$

Here, in view of the fact that $\bar{\psi}_e^L \gamma^\mu \psi_e^L + \bar{\psi}_e^R \gamma^\mu \psi_e^R = \overline{\psi}_e \gamma^\mu \psi_e$,

$$\mathcal{L}_{\text{ew}} = -\tfrac{1}{8}\text{Tr}(\mathbf{F}_{\mu\nu}\mathbf{F}^{\mu\nu}) - \tfrac{1}{4}G_{\mu\nu}G^{\mu\nu} + i\bar{\psi}_e \gamma^\mu [\partial_\mu - i(g^2 + g'^2)^{-1/2}gg'A_\mu]\psi_e$$
$$+ \tfrac{1}{2}(g^2 + g'^2)^{-1/2}Z_\mu[(g'^2 - g^2)\overline{\psi}_e^L \gamma^\mu \psi_e^L + 2gg'\overline{\psi}_e^R \gamma^\mu \psi_e^R]$$
$$+ i\overline{\psi}_{\nu_e}^L \gamma^\mu \partial_\mu \psi_{\nu_e}^L + \tfrac{1}{2}(g^2 + g'^2)^{1/2}\overline{\psi}_{\nu_e}^L \gamma^\mu Z_\mu \psi_{\nu_e}^L$$
$$+ \tfrac{1}{\sqrt{2}}g(\overline{\psi}_{\nu_e}^L \gamma^\mu W_\mu^* \psi_e^L + \overline{\psi}_e^L \gamma^\mu W_\mu \psi_{\nu_e}^L) + \cdots \tag{1.48}$$

with

$$-\tfrac{1}{8}\text{Tr}(\mathbf{F}_{\mu\nu}\mathbf{F}^{\mu\nu}) - \tfrac{1}{4}G_{\mu\nu}G^{\mu\nu} = -\tfrac{1}{2}W_{\mu\nu}(W^{\mu\nu})^* - \tfrac{1}{4}Z_{\mu\nu}Z^{\mu\nu} - \tfrac{1}{4}F_{\mu\nu}F^{\mu\nu} \tag{1.49}$$

(where $W_{\mu\nu} = \partial_\mu W_\nu - \partial_\mu W_\nu$, $Z_{\mu\nu} = \partial_\mu Z_\nu - \partial_\mu Z_\nu$ and $F_{\mu\nu} = \partial_\mu A_\nu - \partial_\mu A_\nu$), plus a host of third- and fourth-order cross terms describing the interactions of the W_μ, Z_μ and A_μ fields.

The physical content of the theory when $\alpha^2 < 0$ can be read directly from (1.47), (1.48) and (1.49). The first line of (1.48) indicates that the electron field is minimally coupled to the electromagnetic field A_μ and has electric charge $e = -(g^2 + g'^2)^{-1/2}gg'$. From the second line of (1.47) the mass of the electron field is $m_e = \lambda g_e$. The neutrino field remains massless and uncoupled to the electromagnetic field but both it and the electron field are coupled to the charged field W_μ and the neutral field Z_μ. Furthermore, the quadratic field terms in the first line of (1.47) indicate that the spin-1 carriers of these fields (the $W^\pm$ and Z^0 bosons) are massive, with

$$m_W^2 = \tfrac{1}{2}g^2\lambda^2 \qquad \text{and} \qquad m_Z^2 = \tfrac{1}{2}(g^2 + g'^2)\lambda^2. \tag{1.50}$$

Finally, the real scalar field σ describes a neutral spin-0 particle (the Higgs boson) with mass

$$m_H^2 = 4\beta^2\lambda^2 \equiv -2\alpha^2. \tag{1.51}$$

Because the ground state $\phi = (0, \lambda)^\mathsf{T}$ of the Higgs field ϕ is not invariant under the action of the gauge group $SU(2)$ when $\alpha^2 < 0$, but the theory retains a local $U(1)$ symmetry associated with the electromagnetic field A_μ, the $SU(2)$ symmetry is said to be *spontaneously broken*. Thus the leptons and the carriers of the weak fields, which are massless in the unbroken phase ($\alpha^2 > 0$), borrow mass from the scalar boson fields in the broken phase. (Although the neutrinos remain massless in the simplest versions of the Weinberg–Salam model, non-zero neutrino masses are easily incorporated by restoring the right-handed neutrino fields ψ_ν^R.)

Furthermore, knowledge of the electron charge e and the muon decay lifetime, together with data from neutrino scattering experiments, allow the values of the constants g, g' and λ to be determined with reasonable accuracy. The corresponding predicted values of the masses of the $W^{\pm}$ and Z^0 bosons are $m_W \approx 80$ GeV and $m_Z \approx 90$ GeV, which have been experimentally confirmed. Unfortunately, there is no direct evidence relating to the mass m_H of the Higgs boson (a particle which has not yet been observed), although it is almost certainly greater than about 65 GeV and could be as high as 1000 GeV.

The $SU(2)$ symmetry which underlies electroweak unification is clearly broken at everyday low temperatures. However, it is expected that the symmetry would be restored at temperatures above about 10^{15} K (or 100 GeV, the approximate energy of the $W^{\pm}$ and Z^0 bosons), which are thought to have prevailed during the first 10^{-11} s after the Big Bang. The reason for the restoration of the symmetry is that, at non-zero temperatures, the scalar potential V in (1.40) should be replaced by an effective potential V_T which is calculated by quantizing the full electroweak lagrangian and adding the 1-loop radiative corrections.
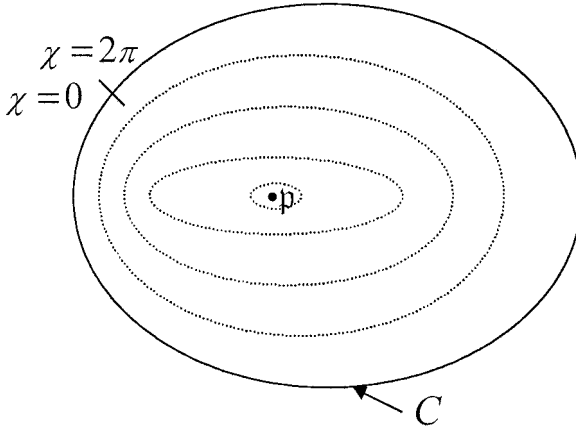
At high temperatures T this effective potential has the form

$$V_T = V(\phi^{\dagger}\phi) + AT^2\phi^{\dagger}\phi + O(T) \tag{1.52}$$
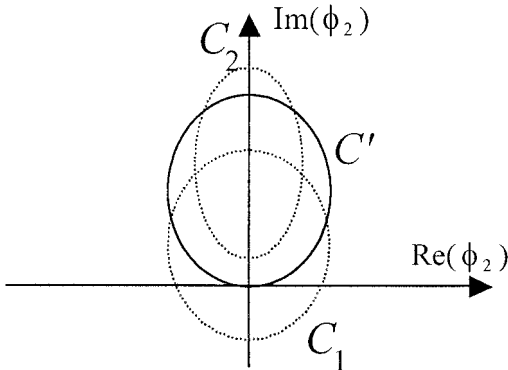
where A is a positive constant, plus temperature-dependent terms which do not involve ϕ. The coefficient of $\phi^{\dagger}\phi$ in V_T is, therefore, $\alpha^2 + AT^2$ and (if $\alpha^2 < 0$) is negative for $T < T_c$ and positive for $T > T_c$, where $T_c = (-\alpha^2/A)^{1/2}$. Thus the transition from the unbroken to the broken phase should occur as the temperature drops below a critical temperature T_c of roughly the same order as the Higgs mass m_H. However, the term of order T in V_T, which is only poorly understood, may (if non-negligible) delay the onset of the phase transition to temperatures well below the critical temperature, leading to a phase of supercooling followed by bubble nucleation, in which Planck-sized bubbles with non-zero $\langle\phi\rangle$ appear randomly and then expand until they fill the Universe.

1.3   The Nielsen–Olesen vortex string

To appreciate the connection between electroweak unification and the formation of cosmic strings, consider once again the Weinberg–Salam lagrangian (1.43) in the broken case $\alpha^2 < 0$, and suppose that the Higgs field ϕ has the form $\phi = \phi_0 e^{i\chi}(0, 1)^{\mathsf{T}}$ at all points in spacetime, where $\phi_0 \geq 0$ and χ are both real functions. If the Higgs field is close to equilibrium then it is to be expected that $\phi_0 \approx \lambda$ almost everywhere. However, it is possible that around some simple closed curve C the value of χ changes by 2π (or any other non-zero multiple $2\pi n$ of 2π). If the curve C is continuously deformed to a point $\mathfrak{p}$, as illustrated in figure 1.1, then either $\phi_0 = 0$ at $\mathfrak{p}$ or, since χ must have a unique value at $\mathfrak{p}$ if $\phi_0 \neq 0$, the net change in χ jumps from 2π to 0 on some member C' of the sequence of curves linking C to $\mathfrak{p}$. Since ϕ must be a continuous function of the

Figure 1.1. Deformation of the closed curve C to a point.

Figure 1.2. The net change in χ jumps from 2π to 0 on C'.

spatial coordinates, the second case is possible only if $\phi_0 = 0$ at at least one point on C'.

An example of a jump of this kind is sketched in figure 1.2, which shows the variations in the real and imaginary components of $\phi_2 = \phi_0 e^{i\chi}$ along three curves C_1, C' and C_2. The curve C_1 is assumed to sit just outside C', and the change in χ along it is 2π. By contrast, the value of χ on the curve C_2 (assumed to sit just inside C') lies entirely in the range $(0, \pi)$, and its net change is 0. Clearly, a necessary condition for this particular jump to occur is that C' pass through $\phi_2 = 0$.

The state $\phi = (0, 0)^\mathsf{T}$ is often called the *false vacuum*, as it coincides with the vacuum expectation value of ϕ in the unbroken phase ($\alpha^2 > 0$). If the symmetry is broken, the potential energy V of the false vacuum is larger

than that of the true vacuum $\phi = \lambda\varphi$, and so any point with $\phi = (0, 0)^\mathsf{T}$ (as well as neighbouring points) will have a higher energy than the ambient vacuum. Furthermore, it is evident from the deformation argument outlined earlier that a point with $\phi = (0, 0)^\mathsf{T}$ must occur on every smooth 2-surface which has C as its boundary, and that these points must form one or more continuous curves or filaments in space. Such a filament of non-zero Higgs field energy is called a *string* (or more specifically, if it arises from the lagrangian (1.43), an *electroweak string*).

More formally, the word 'string' denotes a general class of topological defects that may form when a quantum field theory possesses a set $\mathcal{M}$ of vacuum states whose first homotopy group (that is, the group of equivalence classes of loops in $\mathcal{M}$, two loops being equivalent if they can be smoothly deformed into each other without leaving $\mathcal{M}$) is non-trivial. In the case of electroweak strings, the set of vacuum states of the form $\lambda e^{i\chi}(0, 1)^\mathsf{T}$ is in one-to-one correspondence with $U(1)$, and the class of loops in $U(1)$ with no net change in the phase angle χ is clearly inequivalent to the class of loops on which χ changes by 2π (or any other non-zero multiple of 2π, hence the first homotopy group is $\mathbb{Z}$). Other possible types of topological defects include two-dimensional sheets or *domain walls* (which typically form when $\mathcal{M}$ itself is disconnected) and point defects or *monopoles* (which form when $\mathcal{M}$ contains inequivalent classes of closed surfaces rather than loops).

However, the example of the electroweak string cited earlier is somewhat misleading, as the full vacuum manifold $\mathcal{M}$ in the broken phase is the set of scalar doublets of the form $\lambda\varphi$, where $\varphi^\dagger\varphi = 1$, rather than $\lambda e^{i\chi}(0, 1)^\mathsf{T}$. In component form the condition $\varphi^\dagger\varphi = 1$ reads $|\varphi_1|^2 + |\varphi_2|^2 = 1$, so $\mathcal{M}$ is in one-to-one correspondence with $\mathbb{S}^3$, the surface of the unit sphere in four (Euclidean) dimensions. As in the more familiar case of the unit sphere $\mathbb{S}^2$ in 3 dimensions, any closed loop in $\mathbb{S}^3$ can always be deformed continuously to a point, so the first homotopy group of $\mathcal{M}$ is trivial. This means that an electroweak string with $\phi = \phi_0 e^{i\chi}(0, 1)^\mathsf{T}$, where the net change in χ on some set of closed curves is non-zero, can, in principle, 'unwind' to a pure vacuum state $\lambda\varphi$ everywhere by evolving through states with a non-zero upper component ϕ_1.

Whether such an unwinding is energetically favoured can only be determined by perturbation analysis. It turns out that electroweak strings are stable in some parts of the parameter space defined by the values of the constants g, g' and β, and unstable in other parts. The experimentally-determined value of m_W corresponds to a region in parameter space where electroweak strings are definitely *unstable*, but they can be stabilized by only minor modifications to the theory. Stable strings also arise in a host of more elaborate particle theories, some of which will be discussed later, in section 1.4.

The canonical example of a local gauge field theory that gives rise to stable strings is the *Abelian Higgs model*, which is constructed by coupling a single complex scalar field ϕ to a locally $U(1)$-invariant gauge field B_μ. The

corresponding lagrangian is:

$$\mathcal{L} = -\tfrac{1}{4}G_{\mu\nu}G^{\mu\nu} + (\partial_\mu\phi + ieB_\mu\phi)^*(\partial^\mu\phi + ieB^\mu\phi) - V_0 - \alpha^2\phi^*\phi - \beta^2(\phi^*\phi)^2 \tag{1.53}$$

where $G_{\mu\nu} = \partial_\mu B_\nu - \partial_\nu B_\mu$ as before, and e plays the role of the electroweak coupling constant $\tfrac{1}{2}g'$. On quantization the Abelian Higgs model retains the essential phenomenological features of the bosonic sector of the electroweak model. In the unbroken phase ($\alpha^2 > 0$) the gauge field describes massless neutral spin-1 bosons and the scalar field ϕ describes charged spin-0 bosons with mass α. In the broken phase ($\alpha^2 < 0$) the lagrangian decouples to describe neutral spin-0 particles (the Higgs bosons) with mass $m_H = 2\beta\lambda$ and neutral spin-1 particles (the analogues of the Z^0 bosons) with mass $m_V = \sqrt{2}|e|\lambda$, where $\lambda = \tfrac{1}{\sqrt{2}}|\alpha|/\beta$ as before.

For present purposes the most interesting feature of the Abelian Higgs model is the structure of the strings that can appear in the broken phase. Strings of this type, called *local $U(1)$ strings*, arise because the set $\mathcal{M}$ of true vacuum states $\phi = \lambda e^{i\chi}$ is in one-to-one correspondence with $U(1)$, just like the vacuum states $\lambda e^{i\chi}(0, 1)^\mathsf{T}$ of the electroweak string. However, unlike electroweak strings, the vacuum states of local $U(1)$ strings do not form part of a larger manifold of vacuum states with a trivial homotopy group. So local $U(1)$ strings cannot spontaneously unwind and evaporate.

Now, the Euler–Lagrange equations for the fields B_μ and ϕ read as

$$\Box B_\mu - \partial_\mu\partial_\nu B^\nu = ie(\phi^*\partial_\mu\phi - \phi\partial_\mu\phi^*) - 2e^2\phi^*\phi B_\mu \tag{1.54}$$

and

$$\Box\phi + ie(2B^\mu\partial_\mu\phi + \phi\partial_\mu B^\mu) - e^2B_\mu B^\mu\phi = 2\beta^2(\lambda^2 - \phi^*\phi)\phi \tag{1.55}$$

respectively. At a classical level, much of the research on the dynamics of cosmic strings has centred on generating exact or approximate filamentary solutions to these two equations. The simplest assumption, first systematically explored by Holger Nielsen and Poul Olesen in 1973 [NO73], is that the solution is static and cylindrically symmetric. This means that, if r and θ are standard polar coordinates, defined so that $x = r\cos\theta$ and $y = r\sin\theta$, then

$$B_\mu = B(r)\partial_\mu\theta \qquad \text{and} \qquad \phi = \Phi(r)e^{i\chi(\theta)} \tag{1.56}$$

for some choice of functions B, Φ and χ.

A single string centred on the z-axis will have $\Phi(0) = 0$ and $\Phi(r) \approx \lambda$ for large r. Since the azimuthal vector $\partial_\mu\theta$ is undefined at $r = 0$, it must also be the case that $B(0) = 0$. From (1.55) it is evident that a possible dimensionless radial coordinate is $\rho = 2\beta\lambda r \equiv m_H r$. Furthermore, χ will change by some non-zero integer multiple $2\pi n$ of 2π as the angle θ increases from 0 to 2π. Since the Higgs lagrangian (1.53) is locally $U(1)$-invariant, it is always possible to apply the gauge

transformation $B_\mu \to B_\mu + \partial_\mu \Lambda$ and $\phi \to \phi e^{-ie\Lambda}$, where $\Lambda = e^{-1}(\chi - n\theta)$, to reduce χ to $n\theta$. This absorbs χ into B_μ, and without loss of generality (provided that $e \neq 0$) the field variables can be rescaled in the form:

$$B_\mu = e^{-1}[P(\rho) - n]\partial_\mu \theta \qquad \text{and} \qquad \phi = \lambda Q(\rho)e^{in\theta} \qquad (1.57)$$

for some functions P and Q.

In view of the cylindrical symmetry of the problem, much of the analysis that follows is simplified by converting from Minkowski coordinates $x^\mu = [t, x, y, z]$ to cylindrical coordinates $x^\mu = [t, r, \theta, z]$. The metric tensor is then $\eta_{\mu\nu} = \text{diag}(1, -1, -r^2, -1)$, and, since, in particular, $G_{r\theta} = -G_{\theta r} = m_H P'/e$, the lagrangian becomes

$$\mathcal{L}/(m_H^2 \lambda^2) = -b^{-1}\rho^{-2}P'^2 - Q'^2 - \rho^{-2}P^2 Q^2 - \tfrac{1}{4}(1 - Q^2)^2 \qquad (1.58)$$

where a prime denotes $d/d\rho$ and $b = \tfrac{1}{2}e^2/\beta^2 \equiv m_V^2/m_H^2$ is the so-called Bogomol'nyi parameter.

Furthermore, in a general curvilinear coordinate system the action integral is

$$I = \int \mathcal{L}\eta^{1/2}\, d^4x \qquad (1.59)$$

where $\eta \equiv -\det(\eta_{\mu\nu})$ is the norm of the determinant of the metric tensor. In cylindrical coordinates $\eta = r^2$ and so the Euler–Lagrange equations become

$$r\frac{\partial \mathcal{L}}{\partial X} - \partial_\mu \left(r\frac{\partial \mathcal{L}}{\partial [\partial_\mu X]}\right) = 0 \qquad (1.60)$$

where X denotes any of the field variables in the lagrangian.

The Euler–Lagrange equations for the rescaled functions P and Q therefore read:

$$P'' - \rho^{-1}P' = bQ^2 P \qquad (1.61)$$
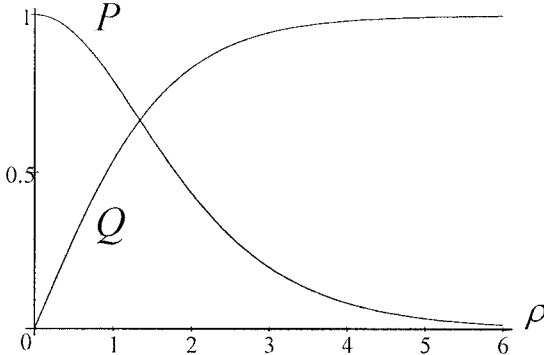
and

$$Q'' + \rho^{-1}Q' - \rho^{-2}P^2 Q = \tfrac{1}{2}(Q^2 - 1)Q. \qquad (1.62)$$

These equations need to be solved subject to the boundary conditions $P(0) = n$, $Q(0) = 0$ and $\lim_{\rho\to\infty} Q(\rho) = 1$. Since $Q \approx 1$ for large ρ, (1.61) reduces to a modified Bessel equation for P in this limit, and thus P can be expressed as a linear combination of an exponentially growing and an exponentially decaying function of ρ for large ρ. The exponentially growing solution is incompatible with (1.62), and so $\lim_{\rho\to\infty} P(\rho) = 0$.

In general, equations (1.61) and (1.62) cannot be integrated exactly, although simplifications do occur if $b = 0$ or 1. Nonetheless, it is relatively straightforward to show that, with $s \equiv \text{sgn}(n)$,

$$sP \approx |n| - p_0\rho^2 + \frac{bq_0^2}{4(|n| + 1)}\rho^{2|n|+2}$$

$$Q \approx q_0\rho^{|n|} - q_0\frac{(1 + 4|n|p_0)}{8(|n| + 1)}\rho^{|n|+2} \qquad (1.63)$$

Figure 1.3. Variation of P and Q as functions of ρ in the case $b = 1$ and $n = 1$.

for small ρ, and that if $b > \frac{1}{4}$

$$sP \approx p_\infty \rho^{1/2} e^{-\sqrt{b}\rho} \qquad \text{and} \qquad Q \approx 1 - q_\infty \rho^{-1/2} e^{-\rho} \qquad (1.64)$$

for large ρ, where p_0, q_0, p_∞ and q_∞ are positive constants to be determined.

Thus (recalling that $\rho = m_H r$) the Higgs field falls off exponentially with a characteristic length scale $1/m_H$, while the vector field has a characteristic decay scale $1/(\sqrt{b}m_H) \equiv 1/m_V$. The larger of these two length scales defines the radius of the Nielsen–Olesen vortex. (Note, however, that if $b = \frac{1}{4}$ then $1 - Q$ falls off as $e^{-\rho}$ rather than $\rho^{-1/2}e^{-\rho}$, while if $b < \frac{1}{4}$ it falls off as $\rho^{-1}e^{-2\sqrt{b}\rho}$.)

In the special case $b = 1$ (which occurs when $m_V = m_H$) the differential equations (1.61) and (1.62) can be rewritten as

$$X' = -\rho^{-1}QY \qquad \text{and} \qquad Y' = -\rho^{-1}sPY - \rho QX \qquad (1.65)$$

respectively, where $X = \rho^{-1}sP' - \frac{1}{2}(Q^2 - 1)$ and $Y = \rho Q' - sPQ$. The trivial solution $X = Y = 0$ is consistent with the known behaviour of P and Q in the limits of small and large ρ (with $p_0 = \frac{1}{4}$ and $p_\infty = q_\infty$) and so two first integrals of the field equations are

$$sP' = \frac{1}{2}\rho(Q^2 - 1) \qquad \text{and} \qquad Q' = \rho^{-1}sPQ. \qquad (1.66)$$

Figure 1.3 shows the variation of the rescaled vector field P and the rescaled Higgs field Q with ρ in the case where $b = 1$ and $n = 1$. The value of q_0 in this solution is determined (iteratively) to be about 0.60, while $p_\infty = q_\infty \approx 2.2$.

If $b = 0$ (or, equivalently, $e = 0$) the first of the field equations (1.61) can be integrated exactly. However, the Higgs field ϕ and the gauge field B_μ decouple in the Abelian Higgs lagrangian when $e = 0$, and the local $U(1)$ gauge transformation that led to the rescaling equations (1.57) breaks down. The equations for P and Q are, therefore, invalid. In fact, because the lagrangian

(1.53) possesses only *global* $U(1)$ invariance when $e = 0$, it is not possible to transform away the complex argument χ and the theory retains an extra degree of freedom that is reflected by the fact that in the broken phase it gives rise to *massless* spin-0 particles (the Goldstone bosons) as well as Higgs bosons. Strings that form in the broken phase of the Goldstone model are called *global strings*. Unlike local strings, global strings have a divergent mass per unit length and so are more difficult to incorporate into cosmological models.

At a classical level, the stress–energy content of a system of fields with lagrangian $\mathcal{L}$ can be described by a symmetric 4×4 stress–energy tensor $T^{\mu\nu}$ whose covariant components

$$T_{\mu\nu} = -2\frac{\partial\mathcal{L}}{\partial\eta^{\mu\nu}} - \eta_{\mu\nu}\mathcal{L} \tag{1.67}$$

are constructed by varying the action integral I with respect to $\eta^{\mu\nu}$. (See [Wei72, pp 360–1], for a detailed derivation. Note, however, that a sign reversal is necessary here, as Weinberg chooses to work with a spacetime metric with signature $+2$.) In the case of the Abelian Higgs lagrangian (1.53), each raised spacetime index marks the presence of one factor of $\eta^{\mu\nu}$, and so

$$T_{\mu\nu} = G_{\mu\lambda}G_{\nu}^{;\lambda} - 2(\partial_{(\mu}\phi^* - ieB_{(\mu}\phi^*)(\partial_{\nu)}\phi + ieB_{\nu)}\phi) - \eta_{\mu\nu}\mathcal{L} \tag{1.68}$$

In particular, for a static, cylindrically-symmetric solution of the form (1.57) the stress–energy tensor is diagonal, with $T_t^t = \varepsilon$ the energy density of the vortex and $T_k^j = -\operatorname{diag}(p_r, p_\theta, p_z)$ its pressure tensor. Clearly,

$$\varepsilon = -p_z = -\mathcal{L} \equiv m_H^2\lambda^2[b^{-1}\rho^{-2}P'^2 + Q'^2 + \rho^{-2}P^2Q^2 + \tfrac{1}{4}(1 - Q^2)^2] \tag{1.69}$$

while after some manipulation it can be seen that the radial and azimuthal pressures take the forms

$$p_r = m_H^2\lambda^2[b^{-1}\rho^{-2}P'^2 + Q'^2 - \rho^{-2}P^2Q^2 - \tfrac{1}{4}(1 - Q^2)^2] \tag{1.70}$$
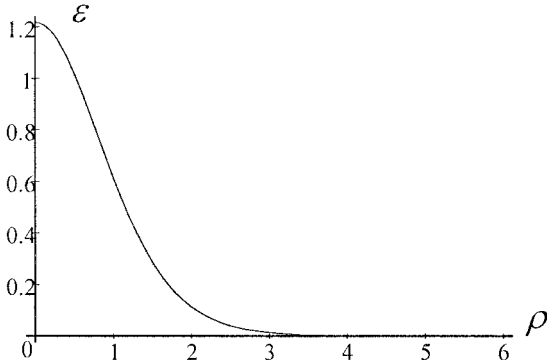
and

$$p_\theta = m_H^2\lambda^2[b^{-1}\rho^{-2}P'^2 - Q'^2 + \rho^{-2}P^2Q^2 - \tfrac{1}{4}(1 - Q^2)^2]. \tag{1.71}$$

Thus the energy density of the vortex is everywhere positive, while the longitudinal pressure p_z is negative and should more properly be referred to as a longitudinal *tension*. The constitutive relation $p_z = -\varepsilon$, which holds for all Nielsen–Olesen vortex strings, is one of the defining features of a canonical cosmic string. In the particular case $b = 1$,

$$\varepsilon = -p_z = m_H^2\lambda^2[\tfrac{1}{4}(1 - Q^2)^2 + 2\rho^{-2}P^2Q^2 + \tfrac{1}{4}(1 - Q^2)^2] \tag{1.72}$$

while $p_r = p_\theta = 0$. The scaled energy density $\varepsilon/(m_H^2\lambda^2)$ in this case is plotted against ρ for the $n = 1$ solution in figure 1.4.

Figure 1.4. The energy density ε (in units of $m_H^2 \lambda^2$) as a function of ρ in the case $b = 1$ and $n = 1$.

Since the speed of light c has the value 1 in Planck units, the total energy per unit length of any of the vortex solutions is equivalent to its mass per unit length, which is conventionally denoted by μ and is given by

$$\mu = 2\pi \int_0^\infty \varepsilon r \, dr \tag{1.73}$$

When $b = 1$, this integral reduces to

$$\mu = 2\pi \lambda^2 \int_0^\infty [\tfrac{1}{2}(1 - Q^2)^2 + 2\rho^{-2} P^2 Q^2] \rho \, d\rho$$
$$= 2\pi \lambda^2 \int_0^\infty [(\rho^{-1} P')' P + (\rho Q')' Q - s P'] \, d\rho \tag{1.74}$$

where the second line follows by combining (1.61), (1.62) and the first equation of (1.66). Thus

$$\mu = 2\pi \lambda^2 [\rho^{-1} P P' + \rho Q Q' - s P]_0^\infty - 2\pi \eta^2 \int_0^\infty (\rho^{-1} P'^2 + \rho Q'^2) \, d\rho$$
$$= 2\pi \lambda^2 (2q_0 + 1) - \tfrac{1}{2}\mu \tag{1.75}$$

and since $q_0 = \tfrac{1}{4}$ in this case, the mass per unit length μ is just $2\pi \lambda^2 \equiv m_V^2 / e^2$. More generally, $\mu = 2\pi \lambda^2 \bar{\mu}(b)$ for some function $\bar{\mu}$. Numerical studies indicate that $\bar{\mu}$ diverges as $|\ln b|$ as $b \to 0$ from above, which is consistent with the known behaviour of global strings.

Two other quantities of interest are the integrated in-plane pressures in the general case $b \neq 1$. Since the stress–energy tensor T_ν^μ by construction satisfies

the conservation equation $\partial_\mu T^\mu_\nu = 0^1$, and all t and z derivatives are zero, it follows that $\partial_x T^x_\nu + \partial_y T^y_\nu = 0$. Hence,

$$
\begin{aligned}
0 &= \int x(\partial_x T^x_\nu + \partial_y T^y_\nu)\,\mathrm{d}x\,\mathrm{d}y \\
&= \int [x T^x_\nu]^{x=\infty}_{x=-\infty}\,\mathrm{d}y + \int [x T^y_\nu]^{y=\infty}_{y=-\infty}\,\mathrm{d}x - \int T^x_\nu\,\mathrm{d}x\,\mathrm{d}y \qquad (1.76)
\end{aligned}
$$

and since the components of the stress–energy tensor fall off exponentially at infinity, $\int T^x_\nu\,\mathrm{d}x\,\mathrm{d}y = 0$. Similarly, $\int T^y_\nu\,\mathrm{d}x\,\mathrm{d}y = 0$.

Thus the integrated in-plane pressures $\int p_x\,\mathrm{d}x\,\mathrm{d}y$ and $\int p_y\,\mathrm{d}x\,\mathrm{d}y$ are in all cases zero. This result is not peculiar to Nielsen–Olesen strings, but is true of any material system whose stress–energy tensor is independent of t and z and falls off more rapidly than r^{-1} at infinity. However, it does indicate that Nielsen–Olesen strings have a particularly simple integrated stress–energy tensor

$$
\int T^\mu_\nu\,\mathrm{d}x\,\mathrm{d}y = \mu\,\mathrm{diag}(1, 0, 0 - 1). \qquad (1.77)
$$

Finally, it should be noted that Nielsen–Olesen strings also carry a magnetic flux

$$
M = \lim_{r\to\infty}\int_0^{2\pi}(-B_\theta B^\theta)^{1/2} r\,\mathrm{d}\theta = \lim_{\rho\to\infty}\int_0^{2\pi} e^{-1}|P(\rho) - n|\,\mathrm{d}\theta = 2\pi|n|/e \qquad (1.78)
$$

and so a string with winding number n carries $|n|$ units of the elementary magnetic flux $2\pi/e$. It was mentioned earlier that the topology of the Higgs field prevents local $U(1)$ strings from unwinding. However, it is possible for a Nielsen–Olesen string with winding number n to break up into $|n|$ strings, each carrying an elementary magnetic flux.

In fact, a perturbation analysis carried out by Bogomol'nyi [Bog76] indicates that Nielsen–Olesen strings with $|n| > 1$ are unstable to a break-up of this type if $b < 1$ (that is, if $m_V < m_H$) but remain stable if $b > 1$ (or $m_V > m_H$). At a physical level, this instability can be explained by the fact that magnetic flux lines repel one another and so the gauge field B_μ acts to disrupt the vortex, whereas the effect of the Higgs field ϕ is to confine the vortex so as to minimize the volume in which $|\phi| \neq \lambda$. The strengths of the two competing fields are proportional to the ranges $1/m_V$ and $1/m_H$ of their carrier particles, and so the gauge field wins out if $m_V < m_H$.

---

[1] See, for example, Weinberg [Wei72, pp 362–3], where it is shown that any stress–energy tensor $T_{\mu\nu}$ generated as a functional derivative of an action integral is conserved, provided that the lagrangian $\mathcal{L}$ is invariant under general coordinate transformations. Alternatively, the identity $\partial_\mu T^\mu_\nu = 0$ can be verified directly by taking the divergence of (1.68) and invoking the Euler–Lagrange equations (1.54) and (1.55).

1.4   Strings as relics of the Big Bang

The success of the Weinberg–Salam model in unifying the electromagnetic and weak forces has naturally led to a concerted effort to combine the electroweak and strong forces in a similar way. The strong force, which acts on the quark constituents of hadrons and is mediated by carrier particles called gluons, is accurately described by the theory of quantum chromodynamics (or QCD), which is based on the eight-parameter gauge group $SU(3)$. It is relatively straightforward to combine the electroweak and QCD lagrangians to give a single lagrangian with $SU(3) \times SU(2) \times U(1)$ symmetry which describes what is known as the *standard model*. However, it is tempting to hope that the standard model can be reformulated as the broken phase of a GUT described by a single gauge group whose symmetries are restored at high temperatures.

One of the advantages of such a theory is that it would depend on only one coupling constant rather than the three (g, g' and the strong coupling constant g_s) that appear in the standard model. The temperature at which grand unification might occur can be estimated by extrapolating the effective (that is, finite-temperature) values of these three coupling constants to a point where they are roughly equal. The resulting GUT temperature is about 10^{28}–10^{29} K (or 10^{15}–10^{16} GeV), which is only three or four magnitudes smaller than the Planck temperature $E_{Pl}/k_B \approx 10^{32}$ K and is well beyond the range of current or conceivable future particle accelerator technology.

Because the energies involved in grand unification are almost completely inaccessible to experiment, the range of possible GUTs is constrained only by the requirements of mathematical consistency The simplest gauge group that can break to produce $SU(3) \times SU(2) \times U(1)$ is $SU(5)$ but theories based on $SU(5)$ unification do not give rise to stable strings. The smallest group consistent with the standard model that does allow for stable strings is $SO(10)$, which can be broken in a variety of ways. The versions of $SO(10)$ unification that are most interesting from the viewpoint of cosmology (because they give rise to the longest-lived strings) involve supersymmetry (invariance under boson–fermion interchange), which has been postulated to operate at high energies but has not yet been observed. Also, the fact that the extrapolated values of the strong and electroweak coupling constants do not all converge at the same temperature suggests that grand unification might involve two (or more) phase transitions, which opens even more possibilities.

Ever since the observational confirmation of the cosmological expansion of the Universe in the 1950s and the discovery of the cosmic microwave background in 1964 it has been evident that at some time in the distant past, between about 10×10^9 and 15×10^9 years ago, the Universe formed a dense soup of particles and radiation with a temperature of the order of the Planck temperature. This state, known nowadays as the Big Bang, effectively marks the earliest time in the history of the Universe that could conceivably be described by the equations of classical cosmology. However, it should be stressed that it is not possible

to directly observe conditions in the Universe before about 300 000 years after the Big Bang, as it was only then, at a temperature of about 3000–4000 K, that the opaque electron–proton plasma filling the Universe recombined to form an effectively transparent hydrogen gas.

As the Universe expanded and cooled from its initial ultra-hot state it presumably underwent one or more grand unification phase transitions as the temperature dropped below 10^{28}–10^{29} K, around 10^{-39}–10^{-37} s after the Big Bang, and a further electroweak phase transition at a temperature of about 10^{15} K, some 10^{-11} s after the Big Bang. In both cases stable strings could possibly have formed. In the simplest models, the expectation value of the Higgs field ϕ slowly moves away from zero as the temperature drops below the critical temperature $T_c \sim m_H$. If the manifold of true vacuum states is $U(1)$, the phase factor χ will, in general, assume different values in different regions in space. It is expected that the values of χ will be correlated on length scales of the order of $1/m_H$, but that the difference in values between widely separated points will be randomly distributed. Whenever the net change in χ around a closed curve is non-zero, a string must condense somewhere in the interior of the curve. The overall effect, as confirmed by numerical simulations, is the appearance of a tangled network of strings with a structure much like spaghetti.

In the immediate aftermath of the phase transition, when the temperature is still close to T_c, the string tension remains small and the motion of the strings is heavily damped by the frictional effects of the surrounding high-density medium. However, once the temperature has dropped sufficiently far (to about 10^{25} K some 10^{-31} s after the Big Bang in the case of GUT strings) the string tension approaches its zero-temperature value $\mu \sim m_H^2$ and the motion of the strings is effectively decoupled from the surrounding medium. Henceforth, the strings move at relativistic speeds, and the evolution of the string network is driven principally by the gradual radiative decay of closed loops of string which break off from the network as a result of self-intersections of long (horizon-sized) strings. The dominant mechanism of energy loss from loops of GUT-scale string is gravitational radiation, but in the case of the much lighter electroweak strings the emission of Higgs and vector particles is more important.

Since $m_H \sim (10^{-4}$–$10^{-3})m_{Pl}$ for a GUT string, the mass per unit length of such a string would be $\mu \sim 10^{-8}$–10^{-6} in Planck units or, equivalently, 10^{19}–10^{21} kg m^{-1}. Thus, a loop of GUT string of length 10^5 light years (or 10^{21} m), which is the typical size of a galaxy, would have a total mass of 10^{40}–10^{42} kg or 10^{10}–$10^{12}M_\odot$, which is also the typical mass range of a galaxy. By contrast, an electroweak string has $m_H \sim 10^{-17}m_{Pl}$ and so a mass per unit length of $\mu \sim 10^{-34}$ or approximately 10^{-7} kg m^{-1}. A galaxy-sized loop of electroweak string would, therefore, have a mass of only 10^{14} kg, which is roughly the mass of a 3-km asteroid. Also, the thickness $1/m_H$ of a GUT string would be 10^3–10^4 Planck lengths, or 10^{-32}–10^{-31} m, whereas the thickness of an electroweak string would be about 10^{-18} m, which is only three orders of magnitude smaller than the electron radius.

From these estimates it is evident that the gravitational effects of GUT strings would be strong enough to have potentially important consequences for cosmology, but the gravitational effects of electroweak strings would not. The formation of gravitationally-bound clumps of baryonic matter, the precursors of today's galaxies or galaxy clusters, was not feasible until the Universe cooled sufficiently to allow hydrogen to recombine, and the radiation and matter fields to decouple, about 300 000 years after the Big Bang. The current distribution of baryonic matter in the Universe should be traceable directly to the collapse of such clumps. This constraint, as well as the observed inhomogeneities in the cosmic microwave background (which effectively consists of photons that were last scattered just before recombination), indicates that perturbations in the density of the protogalactic medium at the time of recombination must have been about 10^{-5} of the mean density.

One of the enduring unsolved problems in modern cosmology is to explain how density perturbations of this size might have arisen in the early Universe. Cosmic strings were first seriously considered as ingredients of cosmological models in the early 1980s because a stationary loop of GUT string with mass per unit length $\mu \sim 10^{-6}$ would act naturally as a seed for density perturbations of the required size. However, as mentioned in the Introduction, the initial promise of a string-seeded cosmology was not borne out in numerical simulations, primarily because the loops that broke off from the primordial string network typically moved at relativistic speeds and were unable to act as effective accretion seeds. Nonetheless, the fact that cosmic strings provide localized sources of mass and energy in an otherwise homogeneous Universe remains an attractive feature, and research into their potential cosmological effects will undoubtedly continue in the absence of a convincing alternative mechanism of structure formation.

There are, of course, many other possible types of topological defect that may have appeared in the early Universe. In particular, the complete absence of information about conditions in the early Universe between the breaking of the GUT symmetry at 10^{-39}–10^{-37} s and the electroweak phase transition at 10^{-11} s gives ample scope for numerous extra phase transitions. One that has been explored in some detail is the postulated breaking of the Peccei–Quinn symmetry, which rotates the phases of left-handed and right-handed fermions in opposite directions, at a temperature of 10^9–10^{11} GeV. This could give rise to both domain walls and axion strings (a special type of global string).

Another possibility is the formation of monopoles, which appear whenever a large gauge group spontaneously breaks down to a subgroup containing $U(1)$. Monopoles are an inevitable consequence of a GUT phase transition (although not an electroweak one), and since GUT monopoles have very large masses (about 10^{16} GeV or 10^{-8} g) their presence would imply an unacceptably high matter density for the Universe. One way to resolve this problem is to assume that the GUT phase transition proceeded by bubble nucleation, with all parts of the Universe that are currently observable expanding exponentially from a single Planck-sized bubble for a period of about 10^{-37}–10^{-35} s. The effect of this

process, known as *inflation*, would have been to dilute the monopole density to an acceptably low level. Once inflation ended, the Universe would have reheated to the critical temperature T_c and expansion and cooling would have continued normally. Inflation poses a problem for the formation of cosmic strings, as any GUT strings would usually be inflated away with the monopoles. However, it is possible to fine-tune the model so that the Universe passes through the GUT phase transition a second time—allowing GUT strings to recondense—at the end of the inflationary epoch.

Further possibilities include hybrid defects, such as monopoles joined by strings or domain walls bounded by strings. Finally, by adding extra scalar or spinor fields to the Higgs lagrangian it is possible to form cosmic strings which carry bosonic or fermionic currents. Provided that these currents are not too large, they will propagate along the string without dissipation, causing the string to behave like a superconducting wire. It turns out that the current on a superconducting string loop can potentially stabilize the loop, allowing it to persist almost indefinitely. GUT-scale superconducting loops would then survive to the present epoch with the same catastrophic densities as undiluted monopoles. However, electroweak superconducting strings would be more benign and could interact strongly with cosmic magnetic fields and plasmas.

In what follows I will be considering in detail the dynamics and gravitational effects of individual non-superconducting local strings only. Thus there will be little mention of the evolution of the primordial string network or its implications for the formation of large-scale structure in the Universe. Although the actual value of the mass per unit length μ of a string is not crucial to an analysis of its motion or gravitational field, it will normally be assumed to take on its GUT value of about 10^{-6}. Furthermore, for reasons explained shortly, the strings will almost everywhere be treated as zero-thickness lines, which effectively involves ignoring most of the field structure of the underlying vortices. In the few cases where the field-theoretic properties of the strings are important, reference will be made to the simple local $U(1)$ string described in section 1.3.

1.5   The Nambu action

The local $U(1)$ string has been extensively studied since 1973, and is now well understood at a semi-classical level. Furthermore, as will be seen in chapters 7 and 9, the Nielsen–Olesen vortex can be coupled to the Einstein equations to produce an exact (although numerically generated) self-gravitating solution, and this exact solution persists even after the addition of a certain class of gravitational disturbances known as travelling waves. However, all known field-theoretic solutions retain a high degree of spacetime symmetry that is unlikely to be a feature of realistic cosmological strings, whether they condensed at electroweak or GUT energy scales.

Even in the absence of gravity, there is little prospect that an exact solution to

the Abelian Higgs field equations (1.54) and (1.55) will ever be found describing
a curved or oscillating string, if only because non-trivial string solutions would
radiate field energy and therefore be dissipative. Hence, in order to study the
dynamics of general string configurations it is necessary to simplify the problem
by removing some of the degrees of freedom. Since the thickness of a GUT string
is only a few orders of magnitude larger than the Planck length, one obvious
simplification is to assume that the string actually has zero thickness. This was
first done by Nielsen and Olesen, who suggested that in the zero-thickness limit
non-straight vortex strings should behave like Nambu strings, a class of two-
dimensional mathematical objects that had earlier (in 1970) been proposed by
Yoichiro Nambu to explain the observed hadron particle spectrum. A rigorous
derivation of this result was published by Dietrich Förster [För74] in 1974.

   In the case of the standard Nielsen–Olesen vortex, the rescaled field variables
P and $1 - Q$ assume their false vacuum values (n and 1 respectively) on the axis
of symmetry, and fall off exponentially with the cylindrical radius ρ. The centre
of the string is, therefore, the set of points $\{x = y = 0\}$, which form a two-
dimensional surface **T** spanned by the unit vectors in the t- and z-directions. The
surface **T** is called the *world sheet* of the string. In parametric form, the world
sheet of the Nielsen–Olesen vortex has the equation $x^\mu = [\tau, 0, 0, \sigma]$, where τ
and σ are arbitrary independent variables. More generally, the world sheet of a
curved or moving string can be expressed in the form
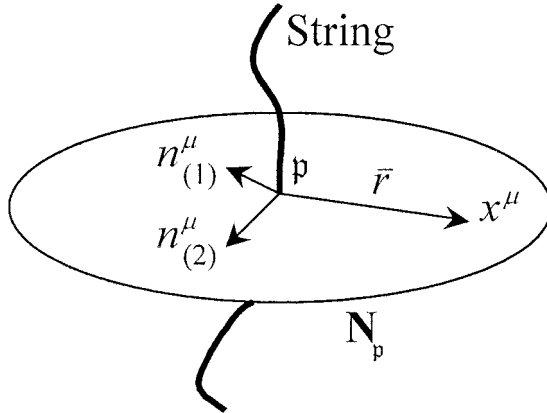
$$x^\mu = X^\mu(\zeta^A) \tag{1.79}$$

for some differentiable 4-vector function X^μ of two parameters $\zeta^A = (\zeta^0, \zeta^1)$.

   At each point on a parametrized 2-surface such as (1.79) the choice of world-
sheet coordinates ζ^A induces a natural pair of tangent vectors $\{t_A^\mu = X^\mu_{,A}\}$,
where '$,_A$' denotes partial differentiation with respect to ζ^A. Furthermore,
provided that the tangent vectors t_A^μ are everywhere linearly independent and not
both spacelike, there is a unique spacelike normal plane $\mathbf{N_p}$ through each point
$\mathfrak{p}$ on **T**. Let $\{n^\mu_{(j)}\}$ be a pair of orthonormal spacelike vector fields that span $\mathbf{N_p}$
at each point $\mathfrak{p}$ (see figure 1.5), with j ranging from 2 to 3 in this case. Thus
$n_{(j)} \cdot n_{(k)} = -\delta_{jk}$ at all points on the world sheet. (The dot product here denotes
the inner or metric product, so that $n_{(j)} \cdot n_{(k)} \equiv \eta_{\mu\nu} n^\mu_{(j)} n^\nu_{(k)}$.) In general there is
no unique or even preferred choice of normals $n^\mu_{(j)}$, as the defining features of the
normals are preserved under spatial rotations of the form $\mathbf{n}^\mu \to R\mathbf{n}^\mu$, where R is
any point-wise defined 2×2 rotation matrix. However, it will here be assumed
that the normals $n^\mu_{(j)}$ are at least once differentiable functions of the parameters
ζ^A.

   Once the parametrization (1.79) and the normal vector fields have been
specified, it is possible to transform from the original Minkowski coordinate
system $x^\mu = [t, x, y, z]$ to a system of spacetime coordinates $\bar{x}^\mu = [\zeta^0, \zeta^1, \chi^2, \chi^3]$ tailored to the geometry of the world sheet **T** by setting

$$x^\mu = X^\mu(\zeta^A) + n^\mu_{(k)}(\zeta^A)\chi^k. \tag{1.80}$$

Figure 1.5. The normal plane $\mathbf{N_p}$.

That is, given a general spacetime point x^μ its coordinates ζ^A are the world-sheet coordinates of the point $\mathfrak{p}$ at which the normal surface $\mathbf{N_p}$ through x^μ intersects $\mathbf{T}$, while $\bar{r} = (\delta_{jk}\chi^j\chi^k)^{1/2}$ is the geodesic distance from x^μ to the world sheet along $\mathbf{N_p}$ (refer again to figure 1.5 for an illustration). The action for a zero-thickness string centred on $\mathbf{T}$ is generated by rewriting the Higgs lagrangian (1.53) in terms of the tailored coordinates $\bar{x}^\mu$ and expanding it in powers of $\bar{r}$.

To do this, it is necessary first of all to transform the metric tensor from its Minkowski form $\eta_{\mu\nu} = \text{diag}(1, -1, -1, -1)$ to its tailored form $\bar{\eta}_{\mu\nu} = \eta_{\kappa\lambda}\Lambda^\kappa_\mu\Lambda^\lambda_\nu$, where $\Lambda^\kappa_\mu = \partial x^\kappa / \partial\bar{x}^\mu$. Thus $\Lambda^\mu_j = n^\mu_{(j)}$ and

$$\Lambda^\mu_A = t^\mu_A + n^\mu_{(k),A}\chi^k \equiv (\delta^B_A + K^B_{(j)A}\chi^j)t^\mu_B - \omega_A n^\mu_{(j)}\varepsilon^j_k\chi^k \tag{1.81}$$

where $K_{(j)AB} = n_{(j),A} \cdot t_B$ are the *extrinsic curvature tensors* and $\omega_A = n_{(2)} \cdot n_{(3),A}$ is the *twist vector* of the world sheet, while ε_{jk} is the 2×2 alternating tensor (with $\varepsilon_{23} = -\varepsilon_{32} = 1$ and $\varepsilon_{22} = \varepsilon_{33} = 0$) and $\varepsilon^j_k \equiv \delta^{jm}\varepsilon_{mk}$.

Upper-case indices are everywhere lowered and raised using the first fundamental form or *intrinsic 2-metric* of the world sheet $\gamma_{AB} = t_A \cdot t_B$ and its inverse $\gamma^{AB} = (\gamma_{AB})^{-1}$. Note also that because $n_{(2)} \cdot n_{(3)} = 0$ and $n_{(j)} \cdot t_A = 0$ the twist vector ω_A can alternatively be written as $-n_{(3)} \cdot n_{(2),A}$ and the extrinsic curvature tensors $K_{(j)AB}$ as $-n_{(j)} \cdot t_{A,B} \equiv -n_{(j)} \cdot X_{,AB}$, which incidentally demonstrates that $K_{(j)AB}$ is symmetric in A and B. The components of $\bar{\eta}_{\mu\nu}$ can, therefore, be expanded in the form:

$$\bar{\eta}_{AB} = \gamma_{AB} + 2K_{(j)AB}\chi^j + K^C_{(j)A}K_{(k)BC}\chi^j\chi^k - \omega_A\omega_B\bar{r}^2$$

$$\bar{\eta}_{Aj} = \omega_A\varepsilon_{jk}\chi^k \quad \text{and} \quad \bar{\eta}_{jk} = -\delta_{jk}. \tag{1.82}$$

Now, the coordinates $\bar{x}^\mu$ are uniquely defined only out to the local radius of curvature of the world sheet, where neighbouring normal planes first begin to

cross. More precisely, the coordinates $\bar{x}^\mu$ become degenerate when the coordinate basis vectors $\{\Lambda_A^\mu, \Lambda_k^\mu\}$ cease to be linearly independent, which, in turn, occurs when the matrix $\delta_A^B + K_{(j)A}^B \chi^j$ in (1.81) has vanishing determinant. Thus the tailored coordinate system breaks down at points χ^j on the family of ellipses

$$1 + K_{(j)A}^A \chi^j + \tfrac{1}{2}(K_{(j)A}^A K_{(k)B}^B - K_{(j)B}^A K_{(k)A}^B)\chi^j \chi^k = 0. \tag{1.83}$$

The 'radius of curvature' of the world sheet, therefore, depends not only on the choice of normal surface $\mathbf{N_p}$ but also on the choice of radial direction on $\mathbf{N_p}$. Let κ^{-1} be a typical value of this local radius of curvature. In general, for strings that are locally straight on Planck length scales, it is to be expected that κ^{-1} will be much larger than the exponential decay scale $1/m_H$ of the Higgs field (and, of course, $\kappa^{-1} \to \infty$ in the limiting case of a Nielsen–Olesen vortex). The dimensionless parameter $\epsilon = \kappa/m_H$ is, therefore, very small and forms a natural expansion parameter when studying the structure of non-straight strings.

The crucial assumption behind the expansion method is that the string fields B_μ and ϕ vary on length scales of order κ^{-1} in the tangential directions and of order $1/m_H$ in the normal directions. That is, if the fields are treated as functions of the dimensionless variables

$$\sigma^A = \kappa \zeta^A \qquad \text{and} \qquad \rho^j = m_H \chi^j \tag{1.84}$$

then their gradients with respect to σ^A and ρ^j are of comparable magnitude.

Furthermore, it is evident from (1.83) that κ is, by definition, a characteristic magnitude of the curvature tensors $K_{(j)B}^A$, while the twist vector $\omega_A = n_{(2)} \cdot n_{(3),A}$ also has the same dimensions as κ. Thus if $\hat{K}_{(j)AB} = \kappa^{-1} K_{(j)AB}$ and $\hat{\omega}_A = \kappa^{-1} \omega_A$ the tailored metric tensor $\bar{\eta}_{\mu\nu}$ can be rewritten in the dimensionless form

$$\bar{\eta}_{AB} = \gamma_{AB} + 2\epsilon \hat{K}_{(j)AB}\rho^j + \epsilon^2 (\hat{K}_{(j)A}^C \hat{K}_{(k)BC}\rho^j \rho^k - \hat{\omega}_A \hat{\omega}_B \hat{\rho}^2)$$

$$\bar{\eta}_{Aj} = \epsilon \hat{\omega}_A \varepsilon_{jk}\rho^k \qquad \text{and} \qquad \bar{\eta}_{jk} = -\delta_{jk} \tag{1.85}$$

where $\hat{\rho} = m_H \bar{r}$.

As was the case with the Nielsen–Olesen vortex, it is always possible to use a $U(1)$ gauge transformation to reduce the string fields to the form

$$B_\mu = e^{-1}(P_\mu - n\partial_\mu \bar{\theta}) \qquad \text{and} \qquad \phi = \lambda Q e^{in\bar{\theta}} \tag{1.86}$$

where $\bar{\theta}$ is the polar angle on each of the normal planes (so that $\chi^2 = \bar{r}\cos\bar{\theta}$ and $\chi^3 = \bar{r}\sin\bar{\theta}$) and $n \neq 0$ is the winding number of the string around the world sheet $\mathbf{T}$, but the vector field P_μ is now not necessarily parallel to $\partial_\mu \bar{\theta}$. Note also that if $\hat{\partial}_\mu$ denotes partial differentiation with respect to the dimensionless variables σ^A and ρ^j then $\partial_\mu \bar{\theta} = m_H \hat{\partial}_\mu \bar{\theta}$. The covariant vector field P_μ has the same transformation properties as ∂_μ and can therefore be recast in dimensionless form by writing $P_A = \kappa \hat{P}_A$ and $P_j = m_H \hat{P}_j$.

If the dynamical variables $\hat{P}_\mu$ and Q are expanded in powers of ϵ:

$$\hat{P}_\mu = \hat{P}_{0\mu} + \epsilon \hat{P}_{1\mu} + \epsilon^2 \hat{P}_{2\mu} + \cdots \qquad \text{and} \qquad Q = Q_0 + \epsilon Q_1 + \epsilon^2 Q_2 + \cdots \quad (1.87)$$

and the metric tensor $\bar{\eta}^{\mu\nu}$ expanded similarly by inverting (1.85) to give

$$\bar{\eta}^{AB} = \gamma^{AB} - 2\epsilon \hat{K}^{AB}_{(j)} \rho^j + 3\epsilon^2 \hat{K}^{AC}_{(j)} \hat{K}^{B}_{(k)C} \rho^j \rho^k + \cdots$$

$$\bar{\eta}^{Aj} = \epsilon \hat{\omega}^A \varepsilon^j_k \rho^k - 2\epsilon^2 \hat{\omega}^B \hat{K}^A_{(m)B} \rho^m \varepsilon^j_k \rho^k + \cdots$$

and

$$\bar{\eta}^{jk} = -\delta^{jk} + \epsilon^2 \hat{\omega}_A \hat{\omega}^A \varepsilon^j_m \varepsilon^k_n \rho^m \rho^n + \cdots \qquad (1.88)$$

then the Higgs lagrangian (1.53) can also be formally expanded in powers of ϵ. The functions appearing in the expansions of $\hat{P}_\mu$ and Q are then found by solving the Euler–Lagrange equations at successive orders in ϵ.

In the tailored coordinate system the action integral for the vortex reads:

$$I = \int \mathcal{L} \bar{\eta}^{1/2} \, \mathrm{d}^4 \bar{x} \qquad (1.89)$$

where

$$\bar{\eta} \equiv -\det(\bar{\eta}_{\mu\nu}) = \gamma [1 + \epsilon \hat{K}^A_{(j)A} \rho^j + \tfrac{1}{2} \epsilon^2 (\hat{K}^A_{(j)A} \hat{K}^B_{(k)B} - \hat{K}^A_{(j)B} \hat{K}^B_{(k)A}) \rho^j \rho^k] \qquad (1.90)$$

with $\gamma \equiv -\det(\gamma_{AB})$. Thus, at order ϵ^0,

$$\mathcal{L}_0 \bar{\eta}_0^{1/2} = m_H^2 \lambda^2 \gamma^{1/2} [-\tfrac{1}{4} b^{-1} \delta^{jm} \delta^{kn} G_{0jk} G_{0mn}$$
$$- \delta^{jk} (\partial_j Q_0 \partial_k Q_0 + Q_0^2 \hat{P}_{0j} \hat{P}_{0k}) - \tfrac{1}{4} (Q_0^2 - 1)^2] \qquad (1.91)$$

where $G_{0jk} = \partial_j \hat{P}_{0k} - \partial_k \hat{P}_{0j}$. The corresponding Euler–Lagrange equations read

$$\tfrac{1}{2} \delta^{jm} \partial_j (\partial_m \hat{P}_{0k} - \partial_k \hat{P}_{0m}) = b Q_0^2 \hat{P}_{0k} \qquad (1.92)$$

and

$$\delta^{jk} (\partial_j \partial_k Q_0 - Q_0^2 \hat{P}_{0j} \hat{P}_{0k}) = \tfrac{1}{2} Q_0 (Q_0^2 - 1) \qquad (1.93)$$

which are just the non-axisymmetric generalizations of the Nielsen–Olesen equations (1.61) and (1.62). Because $\hat{P}_{0j}$ and Q_0 satisfy the same boundary conditions as the Nielsen–Olesen functions $P_j = P \partial_j \theta$ and Q, it follows that $\hat{P}_{0j}$ and Q_0 must be axisymmetric and their dependence on $\hat{\rho}$ the same as the dependence of P_j and Q on ρ.

Thus, to leading order in ϵ the action integral I for a general vortex string is

$$I_0 = \int \mathcal{L}_0 \bar{\eta}_0^{1/2} \, \mathrm{d}^4 \bar{x}$$
$$= m_H^2 \lambda^2 \int \gamma^{1/2} \, \mathrm{d}^2 \zeta \int [-\tfrac{1}{4} b^{-1} \delta^{jm} \delta^{kn} G_{0jk} G_{0mn}$$
$$- \delta^{jk} (\partial_j Q_0 \partial_k Q_0 + Q_0^2 \hat{P}_{0j} \hat{P}_{0k}) - \tfrac{1}{4} (Q_0^2 - 1)^2] \, \mathrm{d}^2 \chi \qquad (1.94)$$

or, in view of (1.72) and (1.73),

$$I_0 = -\mu \int \gamma^{1/2} \, d^2\zeta \tag{1.95}$$

where μ is the constant mass per unit length of the string as before. The expression on the right of this equation is called the *Nambu action*. It contains information about the dynamics of the string world sheet by virtue of the fact that $\gamma = \det(t_A \cdot t_B)$ is a functional of the world-sheet tangent vectors $t_A^\mu = X^\mu{}_{,A}$.

If the components X^μ of the position vector of the world sheet are treated as dynamical variables in their own right then, since any parametric variation $\delta\gamma_{AB}$ in the 2-metric γ_{AB} will induce a corresponding variation $\delta\gamma^{1/2} = \frac{1}{2}\gamma^{1/2}\gamma^{AB}\delta\gamma_{AB}$ in $\gamma^{1/2}$, the Euler–Lagrange equations for X^μ become

$$(\gamma^{1/2}\gamma^{AB}X^\mu{}_{,A})_{,B} = 0. \tag{1.96}$$

This is the equation of motion for a zero-thickness cosmic string in a Minkowski background. At a heuristic level, (1.96) describes the vibrations of a perfectly elastic string whose sound propagation speed is equal to the speed of light c. It, and its generalization to non-flat background spacetimes, will be discussed in some detail in chapters 2 to 5.

Before exploring the extremely rich world of string dynamics in this, the wire approximation, it is instructive to briefly examine the possible effects on the equation of motion of higher-order terms in the Higgs lagrangian. Expanding $\mathcal{L}\bar{\eta}^{1/2}$ in powers of ϵ is algebraically very tedious, and only the final conclusions will be outlined here. A complete derivation of these results can be found in [And99b] and [ABGS97].

One feature to note about the expansion of $\mathcal{L}\bar{\eta}^{1/2}$ is that the first-order perturbations $\hat{P}_{1j}$ and Q_1 appear only linearly at order ϵ, in the form

$$\epsilon\gamma^{1/2}\left\{\frac{\partial\mathcal{L}_0}{\partial\hat{P}_{0j}}\hat{P}_{1j} + \frac{\partial\mathcal{L}_0}{\partial[\hat{\partial}_j\hat{P}_{0k}]}\hat{\partial}_j\hat{P}_{1k} + \frac{\partial\mathcal{L}_0}{\partial Q_0}Q_1 + \frac{\partial\mathcal{L}_0}{\partial[\hat{\partial}_j Q_0]}\hat{\partial}_j Q_1\right\}. \tag{1.97}$$

The resulting Euler–Lagrange equations are just the leading-order equations (1.92) and (1.93) for $\hat{P}_{0j}$ and Q_0 and no new information is obtained. Furthermore, the leading tangential components $\hat{P}_{0A}$ of $\hat{P}_\mu$ do not appear until order ϵ^2. The first-order corrections to $\mathcal{L}\bar{\eta}^{1/2}$ are, therefore, all metric terms linear in the normal coordinates ρ^j, and by symmetry they make no net contribution to the action integral I.

At order ϵ^2 there are three non-trivial Euler–Lagrange equations, namely two coupled linear inhomogeneous equations for $\hat{P}_{1j}$ and Q_1 and an uncoupled linear inhomogeneous equation for $\hat{P}_{0A}$. The driving terms in the coupled equations are both proportional to the *mean curvature* $K^A_{(j)A}$ of the world sheet. Now, taking the normal projection of the equation of motion (1.96) gives:

$$0 = n_{(i)} \cdot (\gamma^{1/2}\gamma^{AB}X_{,A})_{,B}$$
$$= (\gamma^{1/2}\gamma^{AB})_{,B}\, n_{(i)} \cdot t_A + \gamma^{1/2}\gamma^{AB}n_{(i)} \cdot X_{,AB} = -\gamma^{1/2}K^A_{(j)A} \tag{1.98}$$

and so the world sheet of a zero-thickness string has zero mean curvature. The equations for $\hat{P}_{1j}$ and Q_1 are, therefore, strictly homogeneous, and $\hat{P}_{1j} = Q_1 = 0$. Also, the equation for $\hat{P}_{0A}$ is easily solved, giving

$$\hat{P}_{0A} = \hat{\omega}_A \rho^j \varepsilon^k{}_j \hat{P}_{0k}. \tag{1.99}$$

The corresponding corrected action integral turns out to be

$$I_0 + \epsilon^2 I_2 = -\int \gamma^{1/2}[\mu + \epsilon^2 \alpha_1 \delta^{jk} \hat{K}^A_{(j)B} \hat{K}^B_{(k)A}] \, \mathrm{d}^2\zeta \tag{1.100}$$

where $\alpha_1 = -\int \bar{r}^2 \mathcal{L}_0 \, \mathrm{d}^2\chi$ is a positive constant. However, it turns out that the presence of I_2 adds no extra terms to the Euler–Lagrange equations for the position vector X^μ, and so the second-order corrections make only a trivial contribution to the action. This result follows because $\delta^{jk} \hat{K}^A_{(j)B} \hat{K}^B_{(k)A} = -\tilde{R}$, the intrinsic scalar curvature of the world sheet, and $\int \gamma^{1/2} \tilde{R} \, \mathrm{d}^2\zeta$ is a topological invariant (that is, $\gamma^{1/2}\tilde{R}$ can be expressed as a pure divergence: see [Sto89, p 141]).

At order ϵ^3 the corrections to $\mathcal{L}\bar{\eta}^{1/2}$ are again all odd functions of the normal coordinates ρ^j and so make no net contribution to I. It is only at order ϵ^4, where the Euler–Lagrange equations involve $\hat{P}_{2j}$, Q_2 and $\hat{P}_{1A}$, that non-trivial corrections to the action appear. The corrections to the action integral are then

$$\epsilon^4 I_4 = -\epsilon^4 \int \gamma^{1/2}[\alpha_2 (\delta^{jk} \hat{K}^A_{(j)B} \hat{K}^B_{(k)A})^2$$
$$+ \alpha_3 \delta^{jk} \delta^{mn} \hat{K}^A_{(j)B} \hat{K}^B_{(k)C} \hat{K}^C_{(m)D} \hat{K}^D_{(n)A}] \, \mathrm{d}^2\zeta \tag{1.101}$$

where the constants α_2 and α_3 are complicated integrals of the field variables. Numerical investigation indicates that α_2 can be either positive or negative, depending on the value of the Bogomol'nyi parameter b, while α_3 is a negative definite function of b.

The most important question relating to the correction terms in (1.101) is the effect they have on the rigidity of the string. A string is said to be *rigid* if its corrected motion leads to smaller world-sheet curvature than would be predicted on the basis of the Nambu equations of motion, and *anti-rigid* if the correction terms act to enhance the curvature of the world sheet. Numerical simulation of the collapse of a circular loop of string under the action of the Euler–Lagrange equations generated by the corrected action (1.101) indicates that the string in this case is anti-rigid (meaning that the string collapses to a point faster than a Nambu string would: see [ABGS97] for more detail).

However, in the case of an infinite string in the shape of an oscillating helix, the effect of the corrections is to increase the curvature at some points on the world sheet and reduce it at others. A string of this type therefore seems to exhibit the characteristics of both rigidity and anti-rigidity at different times. Nonetheless, oscillating helical strings are always anti-rigid at the moment of maximum

curvature, and there are further theoretical grounds for believing that anti-rigidity is, in general, more common than rigidity. This gives a qualified assurance that high-curvature features predicted on the basis of the wire approximation will not be suppressed by string rigidity. And, as will be seen later, it is in situations of high curvature that the dynamical and gravitational behaviour of Nambu strings is richest and most intriguing.

Chapter 2

The elements of string dynamics

2.1 Describing a zero-thickness cosmic string

As was explained in the concluding sections of the last chapter, a cosmic string
is essentially a long, thin filament of Higgs field energy, with a thickness smaller
than the radius of an electron and a length that could, in principle, stretch across
the 10^{10} or more light years to the edge of the visible Universe. In the wire
approximation, such a string is most easily visualized as a line of particles, each
with infinitesimal mass, interacting by means of a strong elastic tension. The
string can either be open (that is, infinite) or form a closed loop. Under the
action of its elastic tension the string can vibrate, oscillate or rotate at high speeds
and support a variety of transient, semi-permanent or permanent structures. The
resulting range of possible string trajectories will be examined in detail in this and
the next three chapters.

In the language of relativistic physics, the background spacetime through
which the string moves will be assumed to be a smooth four-dimensional
Lorentzian manifold equipped with a metric tensor $g_{\mu\nu}$. In elementary terms,
a four-dimensional manifold is a set of points $\mathbf{M}$ together with a collection of
subsets $\{U_\alpha\}$ covering $\mathbf{M}$ and a set of one-to-one functions $\{\phi_\alpha\}$ which each
map the corresponding subset U_α to an open subset of $\mathbb{R}^4$. The functions ϕ_α
are smooth in the sense that if S is in the intersection of U_α and U_β then they
induce a smooth map from $\phi_\alpha(S)$ to $\phi_\beta(S)$ (which are both subsets of $\mathbb{R}^4$). A
general point $\mathfrak{p}$ in $\mathbf{M}$ is identified by its local coordinates $x^\mu = [x^0, x^1, x^2, x^3]$ in
$\mathbb{R}^4$ (which may vary from one coordinate patch to another), and the *invariant* or
proper distance ds between two neighbouring points x^μ and $x^\mu + dx^\mu$ is given
by $ds^2 = g_{\mu\nu} dx^\mu dx^\nu$. Furthermore, at each point $\mathfrak{p}$ it is always possible to
find a smooth transformation of the coordinates x^μ near $\mathfrak{p}$ that reduces $g_{\mu\nu}$ to the
Minkowski form diag$(1, -1, -1, -1)$ at $\mathfrak{p}$.

For present purposes the metric tensor $g_{\mu\nu}$ (which may or may not be flat)
is considered to be fixed *ab initio*. The effect of assuming a fixed background
is to neglect the gravitational field of the string itself, and, therefore, the back-

reaction of this field on the string's dynamics. The problem of self-consistently coupling the gravitational field to the string's motion is one of the most difficult in string dynamics, and little progress has yet been made towards finding a complete solution. A comprehensive discussion of the problem, in both the weak-field approximation and the strong-field limit, will be given in chapters 6 and 10.

In the wire approximation, the trajectory of a cosmic string is represented as a two-dimensional surface **T**, or world sheet, embedded in the manifold **M**. The zero-thickness string is, therefore, a higher-dimensional analogue of the idealized (point) particle, which can be characterized as tracing out a one-dimensional surface (or curve) on **M**. Indeed, the term 'world sheet' was coined in analogy with the standard expression 'world line' used to describe the trajectory of a particle. The topology of the world sheet will depend on the type of string it describes. For an infinite string **T** has the topology of a plane, while for a closed loop **T** has the topology of a cylinder. More complicated topologies are possible if the string intersects itself (or another string) and breaks up into two or more daughter loops.

As was the case with the core of a local $U(1)$ string in section 1.5, the equation of the world sheet can be written parametrically in the form

$$x^\mu = X^\mu(\zeta^0, \zeta^1) \tag{2.1}$$

where the variables ζ^0 and ζ^1 are usually referred to as *world-sheet* or *gauge* coordinates and the X^μ are (usually) twice-differentiable functions constrained by an equation of motion (see section 2.2). However, if the string supports a certain type of discontinuity known as a *kink*, the requirement that the X^μ be twice differentiable can be relaxed slightly. Kinks will be discussed at greater length in section 2.7.

For a straight string lying along the z-axis in Minkowski spacetime the world sheet has an obvious parametrization $X^\mu = [\tau, 0, 0, \sigma]$, where $\tau \equiv \zeta^0$ and $\sigma \equiv \zeta^1$. However, there is, in general, no preferred choice of gauge coordinates ζ^0 and ζ^1, and the only conditions that will for the present be placed on the choice of coordinates is that they preserve the differentiability properties of the functions X^μ, and that the first partial derivatives of X^μ are nowhere zero. A set of coordinates of this type will be referred to as a *regular gauge*.

As was seen in section 1.5, the choice of parametrization specifies two tangent vector fields $t_A^\mu = X^\mu{}_{,A}$ which span the tangent space at each point on **T**. (As before, the index A runs from 0 to 1.) In a regular gauge in the absence of kinks, the tangent vectors are everywhere continuous, differentiable and non-zero. The corresponding 2-metric γ_{AB} induced on the world sheet by the spacetime metric $g_{\mu\nu}$ is

$$\gamma_{AB} = g_{\mu\nu} t_A^\mu t_B^\nu. \tag{2.2}$$

In all standard treatments of string dynamics, the string material is assumed to be non-tachyonic. This means that at almost all points on the world sheet **T** the tangent space is spanned by one timelike and one spacelike vector, and

so the 2-metric γ_{AB} has signature 0 (that is, has one positive and one negative eigenvalue). It is possible, however, for the tangent space to become degenerate and collapse into a null line at certain points on the world sheet, at which the 2-metric is singular. Such points are called *cusps*. For the moment I will ignore the possibility of cusps and resume discussion of them in section 2.6.

Ideally, any description of a cosmic string should be invariant under transformations of both the spacetime and gauge coordinates. Depending on the context, therefore, the quantity t_A^μ can be regarded as either a set of two spacetime vectors or a set of four gauge vectors. Furthermore, by introducing the connections generated separately by $g_{\mu\nu}$ and γ_{AB}:

$$\Gamma^\mu_{\kappa\lambda} = \tfrac{1}{2} g^{\mu\nu}(g_{\nu\kappa,\lambda} + g_{\nu\lambda,\kappa} - g_{\kappa\lambda,\nu}) \tag{2.3}$$

and

$$\Gamma^C_{AB} = \tfrac{1}{2}\gamma^{CD}(\gamma_{DA,B} + \gamma_{DB,A} - \gamma_{AB,D}) \tag{2.4}$$

it is possible to define a world-sheet derivative of t_A^μ:

$$D_B t_A^\mu = t_A^\mu{}_{,B} + \Gamma^\mu_{\kappa\lambda} t_A^\kappa t_B^\lambda - \Gamma^C_{AB} t_C^\mu \tag{2.5}$$

which behaves as a contravariant tensor under spacetime transformations and as a covariant tensor under gauge transformations[1]. The derivative operator D_B can be generalized in the natural way to apply to mixed spacetime/gauge tensors of arbitrary rank[2].

Both t_A^μ and its world-sheet derivatives are, of course, defined only on the world sheet. However, whereas the tangent vectors lie along the world sheet, the gauge components of $D_B t_A^\mu$ (regarded as spacetime vectors) are all orthogonal to the world sheet:

$$t_C \cdot D_B t_A = 0. \tag{2.6}$$

This last result follows from the identity $\Gamma^C_{AB} = \gamma^{CE}(t_{A,B} \cdot t_E + \Gamma_{\mu\nu\lambda} t_A^\mu t_B^\nu t_E^\lambda)$, which can be verified by expanding (2.4), and is a useful auxiliary to the equation of motion, as will be seen shortly.

Another important quantity is the *scalar curvature* of the world sheet. If X^μ is three-times differentiable the commutator of the second covariant derivatives of t_A^μ is

$$D_B D_C t_A^\mu - D_C D_B t_A^\mu = R^\mu{}_{\kappa\lambda\nu} t_A^\kappa t_C^\lambda t_B^\nu - \tilde{R}^E{}_{ACB} t_E^\mu \tag{2.7}$$

---

[1] From here onwards, partial differentiation with respect to spacetime coordinates x^μ will be denoted by a subscripted index '$,\mu$' rather than the operator ∂_μ.

[2] Specifically, for a general tensor S,

$$D_C S^{\mu_1...\mu_m A_1...A_p}_{\nu_1...\nu_n B_1...B_q} = S^{\mu_1...\mu_m A_1...A_p}_{\nu_1...\nu_n B_1...B_q}{}_{,C}$$

plus one factor of $\Gamma^{\mu_k}_{\kappa\lambda} t_C^\kappa$ contracted with S for each upper spacetime index μ_k, plus one factor of $\Gamma^{A_k}_{CD}$ contracted with S for each upper gauge index A_k, minus one factor of $\Gamma^\lambda_{\kappa\nu_k} t_C^\kappa$ contracted with S for each lower gauge index ν_k, and minus one factor of $\Gamma^D_{B_k C}$ contracted with S for each lower gauge index B_k.

where $R^\mu{}_{\kappa\lambda\nu}$ and $\tilde{R}^E{}_{ACB}$ are the curvature tensors of the background spacetime **M** and the world sheet **T**, respectively.[3] After projecting equation (2.7) onto the world sheet and contracting over the gauge indices, the scalar curvature $\tilde{R}$ of **T** can be expressed in the form:

$$\tilde{R} = \gamma^{AB}\gamma^{CD}(R_{\mu\kappa\lambda\nu}t_A^\kappa t_B^\nu t_C^\lambda t_D^\mu + D_C t_A \cdot D_B t_D - D_B t_A \cdot D_C t_D) \qquad (2.8)$$

where the second covariant derivatives of t_A^μ have been eliminated in favour of first derivatives through the use of the orthogonality relation (2.6). Since the world sheet is two-dimensional, the curvature tensor $\tilde{R}^E{}_{ACB}$ has the simple form

$$\tilde{R}^E{}_{ACB} = \tfrac{1}{2}\tilde{R}(\delta_C^E\gamma_{AB} - \delta_B^E\gamma_{AC}) \qquad (2.9)$$

and so can easily be reconstructed once $\tilde{R}$ is known.

2.2   The equation of motion

The process by which the lagrangian for a local $U(1)$ vortex string can be reduced to a simple action integral over the string's world sheet in the zero-thickness limit was described in some detail in section 1.5. Strictly speaking, the analysis given there applies only to a string moving in a flat background, but the generalization to a curved background is straightforward.

An alternative, and much more direct, derivation follows the line of reasoning used by Yoichiro Nambu when he first formulated the theory of relativistic strings. Nambu assumed that the action integral I that generates the string equation of motion must be a functional of $g_{\mu\nu}$ and the unknown functions X^μ which

(i)   is invariant with respect to both spacetime and gauge transformations; and
(ii)   involves no higher derivatives of X^μ than the first.

The unique solution (up to a constant scaling factor) is the Nambu action [Nam71, Got71]:

$$I = -\mu \int \gamma^{1/2}\, \mathrm{d}^2\zeta \qquad (2.10)$$

where μ is the (constant) mass per unit length of the string, and $\gamma = -\det(\gamma_{AB})$ as before.

It should be noted that the Nambu action is not the only possible action integral for a two-dimensional surface. More general classical models exist involving lagrangians that depend on the extrinsic curvature or twist of the

---

[3] Here, the convention assumed for the Riemann tensor is that

$$R^\mu{}_{\kappa\lambda\nu} = \Gamma^\mu{}_{\kappa\lambda,\nu} - \Gamma^\mu{}_{\kappa\nu,\lambda} + \Gamma^\mu{}_{\nu\rho}\Gamma^\rho{}_{\kappa\lambda} - \Gamma^\mu{}_{\lambda\rho}\Gamma^\rho{}_{\kappa\nu}$$

and similarly for $\tilde{R}^E{}_{ACB}$.

world sheet [Pol86, LRvN87, And99b] and, therefore, violate condition (ii). As mentioned in section 1.5, the reason for including higher-order terms in the lagrangian is to correct for the curvature of the string but their effects on the dynamics of the string are usually significant only in the neighbourhood of a cusp or a kink [CGZ86, ABGS97].

The essential difference between the action integral (2.10) and the formally identical expression for the zero-thickness action I_0 of section 1.5 is that, in the general case of a non-flat spacetime, the lagrangian $\gamma^{1/2}$ depends non-trivially on the functions X^μ through the dependence of the metric tensor $g_{\mu\nu}$ on the spacetime coordinates.

If the action of equation (2.10) is integrated between two fixed non-intersecting spacelike curves in **M**, then the functions X^μ which extremize I (and thus the area of the world sheet between the curves) satisfy the usual Euler–Lagrange equations:

$$\frac{\partial}{\partial \zeta^A}\left(\frac{\partial \gamma^{1/2}}{\partial X^\mu,_A}\right) - \frac{\partial \gamma^{1/2}}{\partial X^\mu} = 0. \tag{2.11}$$

This equation can be expanded by recalling that $\delta\gamma^{1/2} = \frac{1}{2}\gamma^{1/2}\gamma^{AB}\delta\gamma_{AB}$ and $\gamma_{AB} = g_{\mu\nu}X^\mu,_A X^\nu,_B$, so that

$$(\gamma^{1/2}\gamma^{AB}g_{\lambda\mu}X^\lambda,_A),_B - \tfrac{1}{2}\gamma^{1/2}\gamma^{AB}g_{\kappa\lambda,\mu}X^\kappa,_A X^\lambda,_B = 0 \tag{2.12}$$

or, since $\gamma^{AB},_B = -\gamma^{AC}\gamma^{BD}\gamma_{CD},_B$ and $X^\mu,_A = t^\mu_A$,

$$0 = \gamma^{1/2}[g_{\lambda\mu}(\gamma^{AB}t^\lambda_A,_B - \gamma^{AC}\gamma^{BD}\gamma_{CD},_B t^\lambda_A + \tfrac{1}{2}\gamma^{CD}\gamma_{CD},_B t^\lambda_A)$$
$$+ \gamma^{AB}(g_{\lambda\mu,\kappa} - \tfrac{1}{2}g_{\kappa\lambda,\mu})t^\kappa_A t^\lambda_B]. \tag{2.13}$$

In view of the definitions (2.3) and (2.4) of the connections and (2.5) this equation reads simply:

$$\gamma^{AB}D_B t^\mu_A = 0. \tag{2.14}$$

On the face of it, the equation of motion (2.14) has four independent components. However, the orthogonality result (2.6) indicates that the components of (2.14) tangent to the world sheet are identically zero, and so only two of the components are non-trivial. The *projection operators $p_{\mu\nu}$ and $q_{\mu\nu}$* parallel and normal to the world sheet, respectively, are defined to be

$$p_{\mu\nu} = g_{\mu\kappa}g_{\nu\lambda}\gamma^{CD}t^\kappa_C t^\lambda_D \tag{2.15}$$

and

$$q_{\mu\nu} = g_{\mu\nu} - p_{\mu\nu}. \tag{2.16}$$

In terms of the projection operators, the non-trivial components of the equation of motion can be rewritten in the form

$$q_{\mu\nu}\gamma^{AB}X^\nu,_{AB} = -q_{\mu\nu}\Gamma^\nu_{\rho\sigma}p^{\rho\sigma} \tag{2.17}$$

where the right-hand side is a known function of X^μ and its first partial derivatives alone.

Since the determinant of γ_{AB} is negative, equation (2.17) is a hyperbolic partial differential equation. The characteristics of this equation (that is, the curves along which the initial data propagates) are curves on the world sheet whose tangent vectors τ^A are orthogonal to the vector solutions n_A of the equation $\gamma^{AB} n_A n_B = 0$. The constraint $\tau^A n_A = 0$ is obviously satisfied if $\tau^A = \gamma^{AB} n_B$, and so it is evident that the tangent vectors τ^A are null with respect to the induced 2-metric:

$$\gamma_{AB} \tau^A \tau^B = 0. \tag{2.18}$$

In other words, the characteristics are the level curves of the null tangent vectors that span the tangent space at each point on $\mathbf{T}$. It is therefore possible to reconstruct a string's trajectory from a knowledge of the coordinates X^μ and the tangent vectors $X^\mu{}_{,A}$ on any one spacelike cross section of the world sheet. The fact that (2.17) constitutes a system of only two equations for the four unknown functions X^μ indicates that two degrees of freedom, corresponding to arbitrary transformations of the gauge coordinates, still remain once the initial data have been specified.

In view of the equation of motion (2.14), the expression (2.8) derived earlier for the scalar curvature $\tilde{R}$ of the world sheet simplifies to give

$$\tilde{R} = R_{\kappa\lambda\mu\nu} p^{\kappa\mu} p^{\lambda\nu} + \gamma^{AB} \gamma^{CD} D_C t_A \cdot D_B t_D. \tag{2.19}$$

Hence, $\tilde{R}$ splits naturally into two parts, one a linear combination of the components of the background curvature tensor tangent to $\mathbf{T}$ and the other dependent on the local dynamics of the string.

An alternative way of expressing the equation of motion (2.14) is in terms of the extrinsic curvature of the world sheet. If $n^\mu_{(2)}$ and $n^\mu_{(3)}$ are orthonormal vector fields which at each point on world sheet form a basis for the subspace of $\mathbf{M}$ orthogonal to $\mathbf{T}$, as described in section 1.5, then the extrinsic curvature tensors $K_{(2)AB}$ and $K_{(3)AB}$ of the world sheet $\mathbf{T}$ in a general non-flat spacetime are defined to be

$$K_{(j)AB} = t^\mu_B D_A n_{(j)\mu} \equiv -n_{(j)\mu} D_A t^\mu_B \tag{2.20}$$

where the second identity follows because $n_{(j)} \cdot t_B = 0$ everywhere. In particular, since $D_A t^\mu_B$ is orthogonal to the world sheet, and $g^{\mu\nu} = \gamma^{EF} t^\mu_E t^\nu_F - \delta^{jk} n^\mu_{(j)} n^\nu_{(k)}$, the expression (2.19) for the scalar curvature $\tilde{R}$ becomes

$$\tilde{R} = R_{\kappa\lambda\mu\nu} p^{\kappa\mu} p^{\lambda\nu} - \delta^{jk} K^A_{(j)B} K^B_{(k)A}. \tag{2.21}$$

Now, in view of (2.20), the mean curvature of the world sheet is

$$K^A_{(j)A} = -n_{(j)\mu} \gamma^{AB} D_A t^\mu_B \tag{2.22}$$

which vanishes by virtue of the equation of motion (2.14). Thus, as was demonstrated previously in the case of a flat background, the equation of motion is equivalent to the two curvature constraints $K^A_{(j)A} = 0$.

2.3   Gauge conditions, periodicity and causal structure

The equation of motion (2.14) for a relativistic string can be greatly simplified by an appropriate choice of gauge coordinates ζ^0 and ζ^1. A fundamental result of differential equation theory (see [Eis40, p 151]) states that it is always possible to choose two real coordinates σ_+ and σ_- on a surface with an indefinite 2-metric so that the line element has the form

$$ds^2 = f_1(\sigma_+, \sigma_-) \, d\sigma_+ \, d\sigma_- \qquad (2.23)$$

and so the diagonal elements of γ_{AB} are zero. The coordinate net defined by σ_+ and σ_- is identical to the family of null characteristics of the equation of motion described in the previous section. For this reason, I will refer to any choice of gauge coordinates that reduces the line element to the form (2.23) as a *light-cone gauge*. (It should be noted that, historically, the term 'light-cone gauge' has been used in a slightly different sense: see section 3.2.)

Clearly, γ_{AB} is conformally flat (that is, $\gamma_{AB} = f_1 \eta_{AB}$, where η_{AB} is some flat 2-metric) in any light-cone gauge. Since $\gamma^{AB}\Gamma^C_{AB}$ is identically zero for any conformally-flat 2-metric, the equation of motion (2.14) reduces to

$$\frac{\partial}{\partial\sigma_-}t^\mu_+ + \frac{\partial}{\partial\sigma_+}t^\mu_- + 2\Gamma^\mu_{\kappa\lambda}t^\kappa_+ t^\lambda_- = 0 \qquad (2.24)$$

or, equivalently,

$$X^\mu_{;+-} = 0 \qquad (2.25)$$

where the subscripted symbol '; $\pm$' is shorthand for the first covariant derivative $X^\nu_\pm D_\nu$ along the world sheet, with $X^\nu_\pm = \partial X^\nu/\partial\sigma_\pm$ and D_ν the four-dimensional covariant derivative as before.

Equation (2.25) needs to be supplemented by the gauge conditions

$$X_+ \cdot X_+ = X_- \cdot X_- = 0 \qquad (2.26)$$

which ensure that the diagonal elements of γ_{AB} are zero. Note that there is no unique choice of light-cone coordinates, as any differentiable reparametrization of the form

$$\sigma_+ \to \overline{\sigma}_+(\sigma_+) \qquad \text{and} \qquad \sigma_- \to \overline{\sigma}_-(\sigma_-) \qquad (2.27)$$

will preserve the gauge condition (2.26) and so the general form (2.23) of the line element on **T**.

Since any physical spacetime **M** is time-orientable, the parameters σ_+ and σ_- can always be chosen to be future-directed, meaning that if u^μ is any future-directed timelike vector field then $u \cdot X_+$ and $u \cdot X_-$ are positive everywhere. Corresponding to each light-cone gauge of this type it is possible to define a future-directed timelike coordinate

$$\tau = \tfrac{1}{2}(\sigma_+ + \sigma_-) \qquad (2.28)$$

and an orthogonal spacelike coordinate

$$\sigma = \tfrac{1}{2}(\sigma_+ - \sigma_-) \qquad (2.29)$$

which convert the line element on $\mathbf{T}$ into the diagonal form

$$ds^2 = f_2(\tau, \sigma)(d\tau^2 - d\sigma^2). \qquad (2.30)$$

In this, what I will refer to as the *standard gauge*[4], the equation of motion becomes

$$X^\mu{}_{;\tau\tau} = X^\mu{}_{;\sigma\sigma} \qquad (2.31)$$

subject to the gauge conditions

$$X_\tau^2 + X_\sigma^2 = 0 \qquad \text{and} \qquad X_\tau \cdot X_\sigma = 0. \qquad (2.32)$$

Here, the subscripted derivatives '; τ' and '; σ' are defined analogously to '; $\pm$' (with the semi-colon omitted in the case of the first derivative).

As mentioned earlier, the topology of the world sheet will vary according to the type of string being described. If the string is infinite, $\mathbf{T}$ is non-compact and it is always possible to choose the gauge coordinates (whether standard or light-cone) to have range $\mathbb{R}^2$. However, if the string forms a closed loop then $\mathbf{T}$ has cylindrical topology and the gauge coordinates will typically be discontinuous across a particular timelike curve Γ on the world sheet.

To be definite, let Γ be the line $\sigma = 0$. If $\mathfrak{p}$ denotes any point on Γ then $\mathfrak{p}$ has light-cone coordinates $\sigma_+ = \sigma_- = \tau$. Since $\mathbf{T}$ is spacelike-compact, there exists a second point $\mathfrak{p}^*$ on $\mathbf{T}$ with gauge coordinates

$$\sigma_+ = \tau + L_+ \qquad \text{and} \qquad \sigma_- = \tau - L_- \qquad (2.33)$$

(which is spacelike-separated from $\mathfrak{p}$ in $\mathbf{T}$ provided that L_+ and L_- are both positive) for which

$$X^\mu(\mathfrak{p}^*) = X^\mu(\mathfrak{p}). \qquad (2.34)$$

In principle, the gauge periods L_+ and L_- could be functions of τ. However, the requirement that the tangent vector X_τ^μ also be continuous[5] across Γ translates directly into the equation

$$(L'_+ - L'_-)X_\tau^\mu(\mathfrak{p}) + (L'_+ + L'_-)X_\sigma^\mu(\mathfrak{p}) = 0 \qquad (2.35)$$

where a prime denotes differentiation with respect to τ. From (2.35) and the linear independence of X_τ^μ and X_σ^μ it follows that L'_+ and L'_- are separately zero, and

---

[4] The standard gauge is sometimes called the *conformal gauge*, as γ_{AB} is conformally flat. Of course, the light-cone gauge is just as much a conformal gauge. Another common name for the standard gauge is the *orthonormal gauge*.

[5] This condition ensures that the local velocity of the string is continuous across Γ. If it were violated, the string would normally break apart, which is precisely what happens at a fragmentation event. The only situation in which the continuity condition can be violated without fragmentation is at a kink (see section 2.7).

thus the gauge periods are both constant.[6] It is always possible to rescale σ_+ and σ_- so that L_+ and L_- are equal (with their value denoted by L). The periodicity condition (2.34) then becomes, in the new standard gauge,

$$X^\mu(\tau, 0) = X^\mu(\tau, L). \qquad (2.36)$$

It should be stressed that the gauge periods L_+ and L_- are constants only if **T** has strict cylindrical topology. Analogous but more complicated results can apply in other cases. For example, if a single loop fragments into two (so that the world sheet has a 'trousers' topology) then the gauge periods have different values on each of the three loops. For a more detailed discussion, see [Tho88] and [And90].
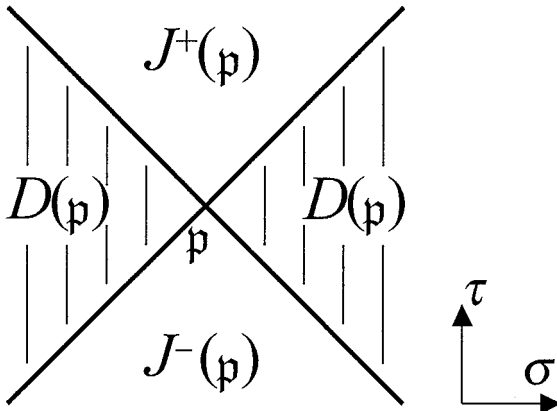
Henceforth, when discussing closed loops, I will assume that the light-cone coordinates have been chosen so that $L_+ = L_-$ and thus the lines of constant τ form closed loops on **T** (with gauge period L). This restriction is not in itself sufficient to determine a unique choice of standard or light-cone gauge. However, the residual gauge freedom can be removed in a natural way in Minkowski spacetime. The resulting gauge will be discussed in more detail in section 3.1.

Before turning to discuss the role of conservation laws in string dynamics, it is instructive to briefly examine the causal structure of the world sheet viewed as a self-contained two-dimensional manifold. If $\mathfrak{p}$ is any point on **T**, the *causal future* $J^+(\mathfrak{p})$ of $\mathfrak{p}$ is defined to be the set of points $\mathfrak{q}$ on **T** for which there is a future-directed causal curve in **T** from $\mathfrak{p}$ to $\mathfrak{q}$. (A causal curve is a curve whose tangent vector u^μ is everywhere timelike or null, so that $u \cdot u \geq 0$.) Similarly, the *causal past* $J^-(\mathfrak{p})$ of $\mathfrak{p}$ is the set of points $\mathfrak{q}$ on **T** for which there is a future-directed causal curve in **T** from $\mathfrak{q}$ to $\mathfrak{p}$. A designation which may be less familiar but is equally important in the context of cosmic strings is the set $D(\mathfrak{p})$ of points causally disconnected from $\mathfrak{p}$ in **T** but connected to it by one or more spacelike curves, defined by

$$D(\mathfrak{p}) = [J^+(J^-(\mathfrak{p})) - J^-(\mathfrak{p})] \cap [J^-(J^+(\mathfrak{p})) - J^+(\mathfrak{p})]. \qquad (2.37)$$

The boundaries of $J^+(\mathfrak{p})$, $J^-(\mathfrak{p})$ and $D(\mathfrak{p})$ are segments of the integral curves of the null tangent vectors on **T** or, equivalently, lines of constant σ_+ and σ_- in any light-cone gauge. Any spacelike curve on **T** through $\mathfrak{p}$ lies entirely in $D(\mathfrak{p})$ (except at $\mathfrak{p}$ itself). It is clear that any point in $J^+(\mathfrak{p})$ lies inside the causal future of $\mathfrak{p}$ as defined on the full background spacetime **M**, and that a similar result holds for $J^-(\mathfrak{p})$. However, a point in $D(\mathfrak{p})$ need not be causally disconnected from $\mathfrak{p}$ in **M**.

---

[6] Equation (2.35) will not hold if the point $\mathfrak{p}$ lies on a kink, and so, in principle, L_+ and L_- need only be piecewise constant on a kinked loop. However, L_+ and L_- must be continuous functions of τ, since otherwise there will be connected segments of the world sheet which map to the same spacetime point X^μ, contradicting the requirement that the gauge be regular. A similar argument indicates that L_+ and L_- will remain constant even if Γ passes through a cusp (see section 2.6), where the tangent vectors, although continuous, are parallel.
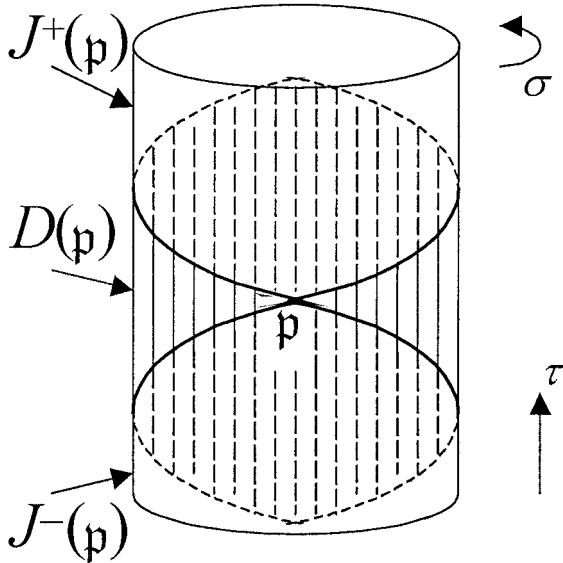
Figure 2.1. Causal structure of an infinite string.

If the world sheet has the topology of $\mathbb{R}^2$ then its causal structure is identical to that of two-dimensional Minkowski spacetime with $J^+(\mathfrak{p})$, $J^-(\mathfrak{p})$ and $D(\mathfrak{p})$ as shown in figure 2.1. A more interesting causal structure obtains if the world sheet has strict cylindrical topology. The causally-disconnected set $D(\mathfrak{p})$ is then compact, as shown in figure 2.2. Even more complicated situations arise in cases of string intersection or fragmentation. In particular, if a string breaks into two and $\mathfrak{p}$ is any point on one of the daughter loops, points on the second daughter loop, although causally disconnected from $\mathfrak{p}$, typically do not lie in $D(\mathfrak{p})$. Thus, the union of $J^+(\mathfrak{p})$, $J^-(\mathfrak{p})$ and $D(\mathfrak{p})$ does not generally cover the world sheet $\mathbf{T}$ (see [And90]).

2.4   Conservation laws in symmetric spacetimes

Although cosmic strings are most elegantly described in terms of a two-dimensional world sheet, in astrophysical or cosmological problems it is often more natural to visualize them as one-dimensional objects (line singularities) in space. A question which then arises is whether a cosmic string can be assigned well-defined properties such as length, mass, energy, momentum, angular momentum and so forth. Typically, an *infinite* string cannot be meaningfully described in this way but if the underlying spacetime admits certain types of isometries a string loop will have simple analogues of some or all of the Newtonian macroscopic properties.

Of course, even in the absence of isometries it is possible to write down a formal expression for the stress–energy tensor $T^{\mu\nu}$ of a general string configuration directly from the action integral (2.10). The relevant procedure is

Figure 2.2. Causal structure of a loop.

outlined in [Wei72], and in the present case gives[7]

$$T^{\mu\nu}(x) = 2\mu g^{-1/2} \int \frac{\partial}{\partial g_{\mu\nu}}(\gamma^{1/2})\delta^4(x - X)\,\mathrm{d}^2\zeta$$

$$= \mu g^{-1/2} \int \gamma^{1/2}\gamma^{AB} X^\mu{}_{,A} X^\nu{}_{,B}\,\delta^4(x - X)\,\mathrm{d}^2\zeta \qquad (2.38)$$

where $g = -\det(g_{\mu\nu})$ and the integral is taken over the entire world sheet. In the standard gauge, the stress–energy tensor takes the somewhat simpler form

$$T^{\mu\nu}(x) = \mu g^{-1/2} \int (X^\mu_\tau X^\nu_\tau - X^\mu_\sigma X^\nu_\sigma)\delta^4(x - X)\,\mathrm{d}^2\zeta \qquad (2.39)$$

from which it can be seen that the relativistic string is characterized by a distributional energy density $T^{\tau\tau} \equiv t^\tau_\mu t^\tau_\nu T^{\mu\nu}$ which integrates out to give an energy per unit length μ, and a longitudinal tension $-T^{\sigma\sigma} \equiv -t^\sigma_\mu t^\sigma_\nu T^{\mu\nu}$ of the same magnitude.

By virtue of the equation of motion (2.14), the stress–energy tensor satisfies the conservation equation

$$D_\nu T^{\mu\nu} = 0. \qquad (2.40)$$

If the background spacetime admits a Killing vector field k_μ then the corresponding momentum current $k_\mu T^{\mu\nu}$ is divergence-free, and a conserved

[7] Again, a sign reversal is necessary here, as Weinberg chooses to work with a spacetime metric with signature $+2$.

macroscopic property can be constructed by taking an appropriate volume integral. However, this method of formulating conservation laws for a cosmic string is rather unwieldy not least because the definition of the stress–energy tensor (2.38) itself involves a double integral over the world sheet.

An equivalent but simpler approach is to work directly from the equation of motion. If k_μ is a Killing vector field then

$$\gamma^{AB} D_B (k \cdot X_{,A}) = k_\mu (\gamma^{AB} D_B X^\mu_{,A}) + \gamma^{AB} X^\mu_{,A} X^\nu_{,B} D_\nu k_\mu = 0 \quad (2.41)$$

where the first term on the right vanishes because of (2.14) and the second through the Killing equation $D_{(\nu}k_{\mu)} = 0$. At this point it proves useful to introduce the world-sheet momentum currents P^A_μ, which are the canonical conjugates of the world-sheet tangent vectors:

$$P^A_\mu = \mu \frac{\partial}{\partial X^\mu_{,A}} (\gamma^{1/2}) = \mu \gamma^{1/2} \gamma^{AB} g_{\mu\nu} X^\nu_{,B}. \quad (2.42)$$

If the left-hand side of (2.41) is converted to an ordinary divergence and written in terms of P^A_μ, the result is the very simple conservation equation

$$(k \cdot P^A)_{,A} = 0. \quad (2.43)$$

One important consequence of (2.43) is that if S is a closed subset of the world sheet with boundary $\partial\mathsf{S} = \{\zeta^A(s)\}$ then, from Stokes' theorem,

$$0 = \int_{\mathsf{S}} (k \cdot P^A)_{,A} \, d^2\zeta = \oint_{\partial\mathsf{S}} \gamma^{-1/2} k \cdot P^A n_A \, d\ell \quad (2.44)$$
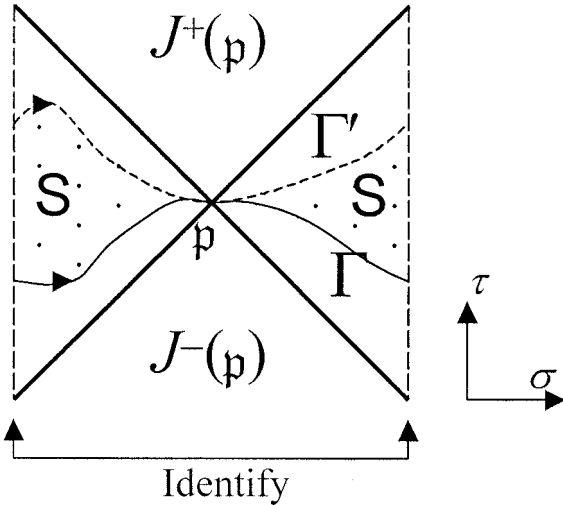
where

$$n_A = \gamma^{1/2} |\gamma_{CD} \dot{\zeta}^C \dot{\zeta}^D|^{-1/2} \varepsilon_{AB} \dot{\zeta}^B \quad (2.45)$$

is the outward unit normal on $\partial\mathsf{S}$ and

$$d\ell = |\gamma_{CD} \dot{\zeta}^C \dot{\zeta}^D|^{1/2} \, ds. \quad (2.46)$$

(Here, as before, ε_{AB} is the flat-space alternating tensor, with $\varepsilon_{01} = -\varepsilon_{10} = 1$ and $\varepsilon_{00} = \varepsilon_{11} = 0$; and an overdot denotes d/ds.) In particular, if S is bounded by two spacelike slices of the world sheet then the line integrals of $\gamma^{-1/2} k \cdot P^A$ along each of the slices will yield the same value.

The local conservation laws embodied in equation (2.43) and its integral version (2.44) are applicable to any string in a symmetric spacetime, irrespective of the topology of its world sheet. If the string is infinite, however, the line integral of a momentum current along a spacelike section of the world sheet will not generally converge, and so a global statement of conservation is usually not possible. This reflects the fact that an infinite string will typically have an infinite energy and momentum. In the case of a string loop, by contrast, macroscopic laws do exist and can often be useful in analysing the dynamics of the string.

Figure 2.3. The subset S.

In particular, if the world sheet **T** of the string has strictly cylindrical topology then there is a conserved integral $C(k)$ corresponding to each Killing vector field k_μ given by:

$$C(k) = \oint_\Gamma \gamma^{-1/2} k \cdot P^A n_A \, d\ell \equiv \mu \oint_\Gamma \gamma^{1/2} \gamma^{AB} k \cdot X_{,A} \, \varepsilon_{BC} \dot\zeta^C \, ds \qquad (2.47)$$

where Γ is any closed spacelike curve on **T** with winding number 1. To see that the choice of Γ is immaterial (and so $C(k)$ is conserved), note that if $\mathfrak{p}$ is any point on Γ, and Γ' is a second closed curve through the set $D(\mathfrak{p})$ with winding number 1 and the same orientation as Γ, then $\Gamma - \Gamma'$ bounds a closed subset S of the world sheet, as shown in figure 2.3. In view of equation (2.44), the line integral of $\gamma^{-1/2} k \cdot P^A$ along Γ' also has the value $C(k)$. By iterating this procedure as many times as necessary, the result can be extended to any closed spacelike curve Γ' on **T** to the past or future of Γ.

Strictly speaking, the requirement that the curve Γ be spacelike in the definition of $C(k)$ is not essential if **T** has cylindrical topology. Any closed curve with winding number 1 will generate the same conserved quantity. However, in more complicated cases involving string collisions or fragmentation the mechanics of stress–energy conservation can be obscured unless attention is restricted to spacelike slices through the world sheet. For example, if a single string loop intersects itself and breaks into two daughter loops then any spacelike slice that lies to the past of the fragmentation event will generate a single conserved integral $C_0(k)$; whereas a spacelike slice that passes to the future of the fragmentation event will induce two closed curves on **T** and, therefore,

two conserved integrals $C_1(k)$ and $C_2(k)$, which separately characterize the two daughter loops[8]. It is clear from the discussion following (2.47) that $C_1(k) + C_2(k) = C_0(k)$.

For a general string loop, the conserved quantity $C(k)$ is often most easily evaluated by choosing Γ to be a curve of constant τ in the standard gauge, for then (2.47) becomes

$$C(k) = \mu \int_0^L k \cdot X_\tau \, d\sigma. \tag{2.48}$$

If the Killing vector field k_μ is timelike then $C(k)$ can be interpreted as an energy integral for the string; whereas if k_μ is spacelike then $C(k)$ is a momentum integral. In the special case where the orbits of k_μ are closed spacelike curves, $C(k)$ will be an angular momentum integral. Minkowski spacetime is, of course, maximally symmetric, and so the full range of conservation laws are available for a string loop if the background spacetime is flat. These laws will be discussed at greater length in section 3.3.

2.5 Invariant length

In the absence of any underlying symmetry, it is not possible to characterize the trajectory of a string loop in terms of conserved energy or momentum integrals. Nonetheless, there do exist integrals defined on appropriate subsets of the world sheet which, although not normally conserved, can be recognized as natural extensions of familiar conserved scalar functionals in Minkowski spacetime.

The simplest integral invariant of this type is what is called the *invariant length* of a string loop, which is closely related to its energy. Consider, first of all, a spacelike section of the loop represented by a closed curve $\Gamma = \{\zeta^A(s)\}$ on **T** with winding number 1. The length of this section is just the proper distance along Γ:

$$\ell(\Gamma) = \oint_\Gamma |\gamma_{AB} \dot{\zeta}^A \dot{\zeta}^B|^{1/2} \, ds \tag{2.49}$$

where an overdot denotes d/ds as before.

In general, the length $\ell(\Gamma)$ varies from one spacelike section of the string to another. This feature is not particular surprising, as even in Minkowski spacetime different inertial observers would be expected to measure different lengths for an extended object like a cosmic string. In a general spacetime, moreover, there is typically no spacelike surface that a freely-falling observer would regard as his or her instantaneous rest frame. It would, therefore, be useful to be able to assign to a string loop a length which is not observer-dependent. (Recall that this can be done for rigid rods in Minkowski spacetime. The proper length of a rigid rod is a strict upper bound for the length of the rod as measured by any inertial observer.)

---

[8] The mechanics of string fragmentation is discussed in more detail in section 2.7.

Given any point $\mathfrak{p}$ on the world sheet of a string loop, the invariant length of the loop at $\mathfrak{p}$ is defined to be [And90]

$$\ell_I(\mathfrak{p}) = 2\sqrt{A(\mathfrak{p})} \tag{2.50}$$

where

$$A(\mathfrak{p}) = \int_{D(\mathfrak{p})} \gamma^{1/2}\,d^2\zeta \tag{2.51}$$

is the area of the subset $D(\mathfrak{p})$ whose interior is causally disconnected from $\mathfrak{p}$. Note that ℓ_I is invariant with respect to both spacetime and gauge transformations and although it typically varies from point to point on the world sheet $\mathbf{T}$, it does not rely on any particular slicing of $\mathbf{T}$. The factor of two appears in (2.50) so as to ensure that ℓ_I coincides with the standard formulation of invariant length in Minkowski spacetime (see section 3.3).

The invariant length possesses a number of useful features in Minkowski spacetime [And90]. It is conserved (provided that the world sheet retains strict cylindrical topology), and it constitutes an upper bound for any measurement of the length of the string. Furthermore, the quantity $\mu\ell_I$ can be shown to be a lower bound for any measurement of the energy of the string. If a single loop breaks into two, the invariant length is no longer conserved on the full world sheet but assumes a constant value ℓ_0 at points sufficiently far to the past of the fragmentation event, and constant values ℓ_1 and ℓ_2 at points on the daughter loops to the future of the fragmentation event. The length ℓ_0 is always strictly greater than $\ell_1 + \ell_2$, with the difference $\ell_0 - (\ell_1 + \ell_2)$ corresponding to the kinetic energy of the relative motion of the daughter loops.

In a general spacetime, however, the invariant length is typically not conserved nor is it possible to interpret $\ell_I(\mathfrak{p})$ as an upper bound for the length $\ell(\Gamma)$ of the loop as measured along any spacelike curve Γ through $\mathfrak{p}$.

2.6 Cusps and curvature singularities

So far the analysis of string dynamics has proceeded on the assumption that the first fundamental form γ_{AB} of the world sheet is non-degenerate. However, analytic studies of solutions to the equation of motion (2.14) in a Minkowski background suggest that it is very common for the 2-metric γ_{AB} to become non-degenerate at isolated points on the world sheet (see section 3.6). Points of this type, which are known as *cusps*, have important consequences for the evolution of a string network, as the flux of gravitational radiation from a string loop is typically dominated by the radiation from its cusps (see chapter 6). The possibility of cusplike behaviour was first recognized by Neil Turok in 1984 [Tur84].

A point of degeneracy of γ_{AB} occurs whenever the determinant γ vanishes or, equivalently, whenever the tangent vectors t_A^μ are linearly dependent. Since the tangent space is normally spanned by a spacelike and a timelike vector, the vectors t_A^μ are both null at an isolated cusp, and the tangent space collapses to

a null line there. Of course, a point of degeneracy need not be isolated and solutions are known to exist in a Minkowski background with lines of cusps which divide the world sheet into two or more disjoint regions. Since a cusp is an ordinary point of the standard-gauge equation of motion (2.31), there is, in principle, no obstacle to continuing a solution through a line of cusps. Whether such a continued solution is physically meaningful is open to question, however, as the gravitational field of a string diverges at a cusp, and non-isolated cusps are typically prone to gravitational collapse. Examples of strings with non-isolated cusps are examined in sections 4.2.1 and 4.2.2.

The dynamics of a string in the neighbourhood of an isolated cusp is easily analysed in a general background metric. Suppose that an isolated cusp occurs at a point $\mathfrak{p}$ on the world sheet, and choose the spacetime coordinates x^μ to be locally inertial at $\mathfrak{p}$, so that $g_{\mu\nu} = \eta_{\mu\nu} + O(|x - X(\mathfrak{p})|^2)$, where $\eta_{\mu\nu}$ is the Minkowski tensor. If we adopt a regular light-cone gauge and identify $\mathfrak{p}$ with the point $\sigma_+ = \sigma_- = 0$ then in some neighbourhood of $\mathfrak{p}$ the tangent vectors have the form

$$X^\mu_+ = \lambda_+ n^\mu + a^\mu \sigma_+ + b^\mu \sigma_- + o(\sigma_+, \sigma_-) \qquad (2.52)$$

and

$$X^\mu_- = \lambda_- n^\mu + b^\mu \sigma_+ + c^\mu \sigma_- + o(\sigma_+, \sigma_-) \qquad (2.53)$$

where the vectors n^μ, a^μ, b^μ, and c^μ and the scalars $\lambda_+ > 0$ and $\lambda_- > 0$ are all constant, n^μ is future-directed null and the other three vectors satisfy the gauge constraints

$$a \cdot n = b \cdot n = c \cdot n = 0. \qquad (2.54)$$

As a result, the components of the world-sheet metric tensor

$$\gamma_{AB} = \gamma^{1/2} \begin{pmatrix} 0 & 1 \\ 1 & 0 \end{pmatrix} \qquad (2.55)$$

tend to zero as $\gamma^{1/2} = X_+ \cdot X_- = o(\sigma_+, \sigma_-)$ at $\mathfrak{p}$.

Since the spacetime connection $\Gamma^\mu_{\kappa\lambda}$ is of order $|X - X(\mathfrak{p})|$ near $\mathfrak{p}$, the equation of motion
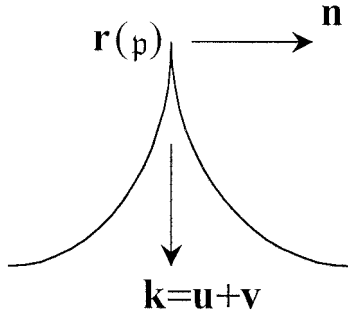
$$\gamma^{AB} X^\mu{}_{,AB} = -\gamma^{AB} \Gamma^\mu_{\kappa\lambda} X^\kappa_A X^\lambda_B \qquad (2.56)$$

reads simply as $X^\mu{}_{,+-} = 0$ to leading order or, equivalently, $b^\mu = 0$. Hence, the parametric equation of the string near the cusp is

$$X^\mu(\sigma_+, \sigma_-) = X^\mu(\mathfrak{p}) + (\lambda_+\sigma_+ + \lambda_-\sigma_-)n^\mu + \tfrac{1}{2}a^\mu\sigma_+^2 + \tfrac{1}{2}c^\mu\sigma_-^2 + o(\sigma_+^2, \sigma_+\sigma_-, \sigma_-^2). \qquad (2.57)$$

In particular, the constant-time slice $x^0 = 0$ through $\mathfrak{p}$ intersects the world sheet along a parametric curve with the equation

$$(\lambda_+\sigma_+ + \lambda_-\sigma_-)n^0 + \tfrac{1}{2}a^0\sigma_+^2 + \tfrac{1}{2}c^0\sigma_-^2 = 0 \qquad (2.58)$$

Figure 2.4. A generic cusp.

to leading order in σ_+ and σ_- (where $n^\mu = [n^0, \mathbf{n}]$ and similar conventions apply to a^μ and c^μ), and so the projection of the world sheet onto this 3-surface near the cusp has the vector form

$$\mathbf{r}_0(\sigma) = \mathbf{r}(\mathfrak{p}) + (\mathbf{u} + \mathbf{v})\sigma^2 + o(\sigma^2) \tag{2.59}$$

where

$$\mathbf{u} = \frac{1}{8(n^0)^3}\lambda_+^{-2}(n^0\mathbf{a} - a^0\mathbf{n}) \qquad \mathbf{v} = \frac{1}{8(n^0)^3}\lambda_-^{-2}(n^0\mathbf{c} - c^0\mathbf{n}) \tag{2.60}$$

and

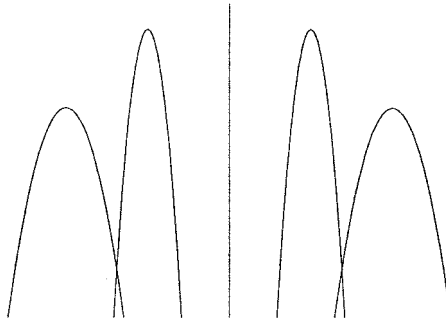$$\sigma = (\lambda_+\sigma_+ - \lambda_-\sigma_-)n^0.$$

Geometrically, this means that the projection of the string onto any spacelike 3-surface through $\mathfrak{p}$ does indeed exhibit a cusplike singularity, with the cusp directed anti-parallel to the vector $\mathbf{k} = \mathbf{u} + \mathbf{v}$, as shown in figure 2.4. Furthermore, since $a \cdot n = c \cdot n = 0$ the vector $\mathbf{n}$ which defines the direction of the string's null 4-velocity at the cusp is orthogonal to both $\mathbf{u}$ and $\mathbf{v}$, and so is orthogonal to the apex of the cusp. The rate at which the two branches of the projection open out from the cusp depends on the higher-order terms in equation (2.57). If, as is usually the case, the position function X^μ is three-times differentiable at $\mathfrak{p}$ then the next lowest term in (2.59) will be of order σ^3 and the projection of the string will trace out a curve with equation $y \propto x^{2/3}$ relative to an appropriate choice of axes. This situation is examined in more detail in section 3.6.

The formation and dissolution of the cusp in the local Lorentz frame defined by the inertial coordinates x^μ can also be examined by introducing a local time coordinate

$$\tau = (\lambda_+\sigma_+ + \lambda_-\sigma_-)\, n^0 + \tfrac{1}{2}a^0\sigma_+^2 + \tfrac{1}{2}c^0\,\sigma_-^2. \tag{2.61}$$

In terms of τ and σ, the projection of the string's trajectory onto surfaces of constant τ near the cusp has the form

$$\mathbf{r}(\tau, \sigma) = \mathbf{r}(\mathfrak{p}) + \mathbf{n}\tau + \mathbf{u}(\tau + \sigma)^2 + \mathbf{v}(\tau - \sigma)^2 + o(\tau^2, \tau\sigma, \sigma^2) \tag{2.62}$$

Figure 2.5. The development of a generic cusp.

and the development of a generic cusp is shown schematically in figure 2.5. The plane in which the cusp forms is spanned by the vectors **u** and **v**. Note that the trajectory is time-symmetric about the cusp for small values of τ. The cusp itself is shown as a straight line, as nothing has been assumed about the higher-order terms in (2.57) responsible for the divergence of the two branches of the cusp.

Another important feature of a cusp is that the local stress–energy density of the string is divergent. To see this, recall from section 2.4 that the stress–energy tensor of the world sheet is

$$T^{\mu\nu}(x) = \mu g^{-1/2} \int \gamma^{1/2} \gamma^{AB} X^{\mu}{}_{,A} X^{\nu}{}_{,B}\, \delta^4(x - X)\, \mathrm{d}^2\zeta \tag{2.63}$$

and so, in the notation of (2.57),

$$T^{\mu\nu}(x) = \mu g^{-1/2} \int (X^{\mu}_{+} X^{\nu}_{-} + X^{\mu}_{-} X^{\nu}_{+}) \delta^4(x - X)\, \mathrm{d}\sigma_+ \,\mathrm{d}\sigma_-$$

$$\approx 2\mu\lambda_+\lambda_- n^{\mu} n^{\nu} \int \delta^4(x - X)\, \mathrm{d}\sigma_+ \,\mathrm{d}\sigma_- \tag{2.64}$$

near the cusp. Since the transformation between the gauge variables σ_+ and σ_- and physical spacetime coordinates tangent to the world sheet is singular at the cusp, the integral on the right of this expression diverges as the field point x^{μ} approaches $\mathfrak{p}$.

In fact, if x^{μ} is the point $[\tau, \mathbf{r}(\tau, \sigma) + \mathbf{x}]$, where τ, σ and $\mathbf{r}$ are defined as before, and $\mathbf{x} \cdot \mathbf{r}_{\sigma}(\tau, \sigma) = 0$ (so that $\mathbf{x}$ is normal to the world sheet), then for small values of τ, σ and $|\mathbf{x}|$,

$$\int \delta^4(x - X)\, \mathrm{d}\sigma_+ \,\mathrm{d}\sigma_- \approx [2\lambda_+\lambda_-(n^0)^2]^{-1} \int \delta(\tau - \tau')$$

$$\times \delta^3[\mathbf{r}(\tau, \sigma) + \mathbf{x} - \mathbf{r}(\tau', \sigma')]\, \mathrm{d}\tau' \,\mathrm{d}\sigma'$$

$$= [2\lambda_+\lambda_-(n^0)^2]^{-1} \int \delta^3[\mathbf{r}(\tau, \sigma) + \mathbf{x} - \mathbf{r}(\tau, \sigma')]\, \mathrm{d}\sigma'$$

$$= [2\lambda_+\lambda_-(n^0)^2]^{-1}\frac{\delta^2(\mathbf{x})}{|\mathbf{r}_\sigma(\tau,\sigma)|} \tag{2.65}$$

where

$$|\mathbf{r}_\sigma(\tau,\sigma)| = 2[(\mathbf{u}+\mathbf{v})^2\sigma^2 + 2(\mathbf{u}^2-\mathbf{v}^2)\sigma\tau + (\mathbf{u}-\mathbf{v})^2\tau^2]^{1/2}. \tag{2.66}$$

Hence,

$$T^{\mu\nu}(x) \approx 2\mu n^\mu n^\nu (n^0)^{-2}\frac{\delta^2(\mathbf{x})}{|\mathbf{r}_\sigma(\tau,\sigma)|} \tag{2.67}$$

near the cusp, and the stress–energy per unit length of string diverges as $|\mathbf{r}_\sigma(\tau,\sigma)|^{-1}$. In particular, on the spacelike surface $\tau = 0$ defined by the formation of the cusp,

$$T^{\mu\nu}(x) \approx \mu n^\mu n^\nu (n^0)^{-2}\frac{\delta^2(\mathbf{x})}{|\mathbf{u}+\mathbf{v}||\sigma|}. \tag{2.68}$$

The fact that the stress–energy of the world sheet diverges in this way was first recognized by Alexander Vilenkin (see [Vac87]).

   Given the pathological behaviour of the stress–energy tensor at a cusp, it is not surprising that cusps can also be identified with singularities of the scalar curvature function $\tilde{R}$. This can be seen by first referring to the expression (2.19) for $\tilde{R}$. If the background curvature is bounded and the world-sheet position function X^μ is twice differentiable then $\tilde{R}$ diverges only at points where the 2-metric γ_{AB} is non-invertible, which can occur only at a cusp in a regular gauge (and, therefore, in any gauge, as $\tilde{R}$ is, by definition, gauge-invariant).

   To demonstrate the converse result—namely that every isolated cusp is a singularity of $\tilde{R}$—it is most convenient to work in the light-cone gauge, as then

$$\begin{aligned}\tilde{R} &= 2\gamma^{-1}(\gamma^{1/2})_{,+-} - 2\gamma^{-3/2}(\gamma^{1/2})_{,+}(\gamma^{1/2})_{,-} \\ &= 2\gamma^{-1/2}(\ln\gamma^{1/2})_{,+-}\end{aligned} \tag{2.69}$$

where $\gamma^{1/2} = X_+ \cdot X_-$, and the subscripts denote partial derivatives with respect to σ_+ and σ_-, as before. Suppose that $\tilde{R}$ is bounded in some deleted neighbourhood N of an isolated cusp $\mathfrak{p}$. Then $(\ln\gamma^{1/2})_{,+-}$ is also bounded in N (as $\gamma^{1/2} = 0$ at $\mathfrak{p}$), and so

$$\ln\gamma^{1/2} = B(\sigma_+,\sigma_-) + f(\sigma_+) + g(\sigma_-) \tag{2.70}$$

where B is bounded in N but f and g need not be. Thus, $\gamma^{1/2}(\mathfrak{p}) = 0$ only if f or g diverges at $\mathfrak{p}$. However, if f (or g) diverges at $\mathfrak{p}$ then $\gamma^{1/2}$ must vanish on a curve of constant σ_+ (or σ_-) through $\mathfrak{p}$, and the cusp cannot be isolated. Hence, $\tilde{R}$ is necessarily unbounded in the neighbourhood of an isolated cusp.
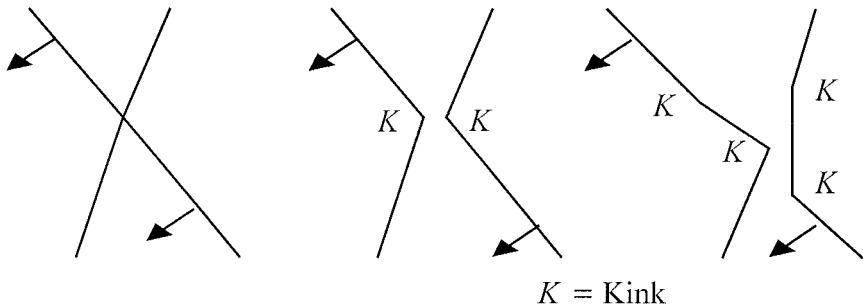
2.7 Intercommuting and kinks

The Nambu action (2.10) is, as was seen in section 1.5, only the lowest-order approximation to a large family of more complicated phenomenological models for a cosmic string. As such, its range of applicability does not extend to situations where the local geometry of the fields constituting the string differs appreciably from a gently curving vortex tube. A cusp, where the local curvature of the string is effectively infinite, is one example of a point on the world sheet where the Nambu approximation fails and it remains an open question whether field-theoretic effects would act to dampen or accentuate cusps.

The Nambu approximation also breaks down when two strings (or segments of the same string) are close enough to interact. The most common situation of this type occurs when two strings cross, and fortunately it is relatively straightforward to simulate the process of string intersection at the full field-theoretic level. This was first done in the case of colliding global $U(1)$ strings by Paul Shellard [She87]; and for the more pertinent case of local $U(1)$ strings (which were described in detail in section 1.5) by Moriarty *et al* [MMR88a, MMR88b], Shellard and Ruback [SR88], Shellard [She88] and Matzner and McCracken [MM88].
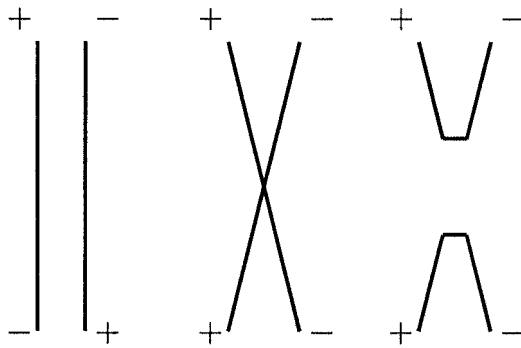
In general, collisions involving straight segments of local strings are modelled by taking two copies of the Nielsen–Olesen vortex string and translating, rotating and Lorentz boosting the field variables ϕ and B_μ until the transformed single-string solutions (ϕ_1, $B_{1\mu}$) and (ϕ_2, $B_{2\mu}$) are approaching one another at a given angle and with a given relative velocity. Provided that the cores of the two strings are initially far enough apart, the initial state of the composite two-string system can be adequately approximated by the fields $\phi = \phi_1\phi_2$ and $B_\mu = B_{1\mu} + B_{2\mu}$. The subsequent evolution of these fields is then studied by numerically integrating the Abelian Higgs equations of motion (1.54) and (1.55) forward in time.

The resulting numerical simulations predict that on colliding two pieces of string will not pass uneventfully through one another but rather will *intercommute* ('exchange partners') as shown in figure 2.6. This is true irrespective of the relative velocities of the two pieces or of the angle of collision (provided that the two segments are not exactly parallel). Indeed, for low relative velocities (less than about $0.4c$) the intercommuting event is effectively elastic, although a considerable amount of field energy can be radiated away from the collision if the velocity is of the order of $0.9c$ or greater.

To understand why intercommuting is an almost universal phenomenon (in collisions of global strings as well as of local strings), recall that the Nielsen–Olesen vortex string carries a magnetic flux proportional to its winding number n. If attention is restricted to the stable cases $n = \pm 1$, it is evident that the sign of n determines the orientation of the string relative to the background coordinate system. In fact, an $n = -1$ string (henceforth an *anti-string*) can be generated by reflecting an $n = +1$ string through the plane perpendicular to the string axis.
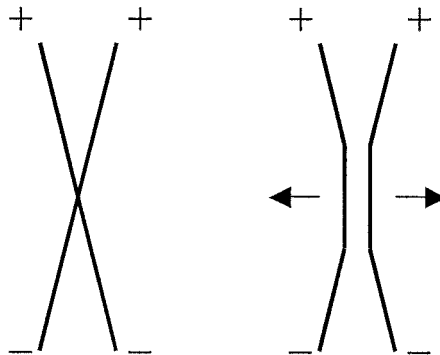
$K = \mathrm{Kink}$

Figure 2.6. The intercommuting of two straight strings.

Figure 2.7. The intercommuting of a string/anti-string pair.

If a string and a parallel anti-string pass close to one another, as shown in the first frame of figure 2.7, the total winding number about any loop which encloses both strings will be 0, and it is possible for the two vortices to unwind and evaporate. This is precisely what happens in simulations of head-on collisions of string/anti-string pairs at low to moderate velocities, although if the relative velocity is greater than about $0.9c$ a new string/anti-string pair, much less energetic than the original pair and moving in the reverse directions, appears in the aftermath of the annihilation [MMR88a]. For string/anti-string pairs that collide at small angles, as in the second frame of figure 2.7, it is expected that the overlapping sections will evaporate in a similar way, leaving the free ends of the two strings to reconnect as shown in the third frame of the figure. This is again confirmed by numerical simulations, although for collision velocities greater than about $0.9c$ the situation is complicated by the appearance of a residual loop of string enclosing the point of intersection, which subsequently collapses and evaporates [MM88].

In the case of collisions between straight-string segments that are aligned in roughly the same direction, the mechanics of intercommuting is slightly different.

Figure 2.8. The intercommuting of almost-parallel strings.

Peter Ruback [Rub88] has shown that, in the critical case where the Bogomol'nyi parameter b is equal to 1 (and the radial forces due to the Higgs field ϕ and the gauge field B_μ cancel one another exactly), the low-velocity collision of two parallel strings can be treated analytically and that the strings involved in such a collision will scatter at right angles. This rather surprising prediction has since been confirmed numerically for a wide range of values of the collision velocity and the Bogomol'nyi parameter b, although once again complications (in the form of the appearance of an additional weak string/anti-string pair) can occur at ultra-relativistic velocities [She88].

When two strings that are almost parallel collide, it is to be expected that the overlapping sections will also scatter at right angles. An illustration is given in figure 2.8, where the two strings are initially moving in directions perpendicular to the plane of the diagram. The scattered segments therefore emerge from the point of intersection moving left and right across the plane of the diagram. This means that the scattered segments can only reconnect with the two left-hand or right-hand halves, causing the strings to intercommute as shown.

The importance of intercommuting for the dynamics of the Nambu string lies in the fact that the collision fragments typically contain points where the tangent plane to the world sheet is discontinuous, and so the fragments themselves are *kinked*. In figure 2.6, both daughter strings support a kink (in fact, a coincident pair of kinks, one moving up the string and the other down it) at the point of intersection. Kinks are not temporary features like isolated cusps, and indeed at the level of the Nambu approximation they can propagate indefinitely around the world sheet without dissipation.

In order to describe the evolution of a kink, suppose that in standard-gauge coordinates the trajectory of the kink—which is just a line of discontinuity of the tangent plane—has the equation $\sigma = \sigma_k(\tau)$. In the vicinity of the kink, the

position function X^μ has the general form

$$X^\mu(\tau, \sigma) = \begin{cases} V^\mu(\tau, \sigma) & \text{if } \sigma \leq \sigma_k(\tau) \\ W^\mu(\tau, \sigma) & \text{if } \sigma \geq \sigma_k(\tau) \end{cases} \qquad (2.71)$$

where the vector functions V^μ and W^μ are twice differentiable, and $W^\mu(\tau, \sigma_k(\tau)) = V^\mu(\tau, \sigma_k(\tau))$. The tangent vectors $t_A^\mu = X^\mu{}_{,A}$ are, therefore, piecewise continuous across the kink, with a discontinuity of the form $\Delta_A^\mu H(\sigma - \sigma_k)$, where

$$\Delta_A^\mu(\tau) = W_A^\mu(\tau, \sigma_k(\tau)) - V_A^\mu(\tau, \sigma_k(\tau)) \qquad (2.72)$$

and H is the Heaviside step function.

If we now impose the equation of motion (2.31) it is easily seen that V^μ and W^μ both satisfy the equation $X^\mu{}_{;\tau\tau} = X^\mu{}_{;\sigma\sigma}$ away from the kink, while the step-function discontinuity gives rise to the further constraint:

$$(\Delta_{\tau\tau}^\mu - \Delta_{\sigma\sigma}^\mu) H(\sigma - \sigma_k) - (\sigma_k' \Delta_\tau^\mu + \Delta_\sigma^\mu)\delta(\sigma - \sigma_k) = 0 \qquad (2.73)$$

where

$$\Delta_{AB}^\mu(\tau) = W^\mu{}_{;AB}(\tau, \sigma_k(\tau)) - V^\mu{}_{;AB}(\tau, \sigma_k(\tau)). \qquad (2.74)$$

The term proportional to H in (2.73) vanishes by virtue of the differentiability properties of V^μ and W^μ, and so the equation of motion imposes the single constraint

$$\sigma_k' \Delta_\tau^\mu + \Delta_\sigma^\mu = 0. \qquad (2.75)$$

Furthermore, the string will break apart at the kink unless

$$\frac{d}{d\tau} W^\mu(\tau, \sigma_k(\tau)) = \frac{d}{d\tau} V^\mu(\tau, \sigma_k(\tau)) \qquad (2.76)$$

or, equivalently,

$$\Delta_\tau^\mu + \sigma_k' \Delta_\sigma^\mu = 0. \qquad (2.77)$$

Combining the constraints (2.75) and (2.77) gives $\sigma_k'^2 = 1$. That is, a kink can only propagate along lines of constant $\tau + \sigma$ or $\tau - \sigma$, and since the four-velocity

$$\frac{d}{d\tau} X^\mu(\tau, \sigma_k(\tau)) = X_\tau^\mu \pm X_\sigma^\mu \qquad (2.78)$$

of the kink is a null vector by virtue of the gauge conditions (2.32), it will always move at the speed of light relative to the background spacetime. This result is simply a restatement of the fact that the characteristics of the equation of motion are null curves.

Although kinks propagate at the speed of light, the local velocity of the string itself in the neighbourhood of a kink, while discontinuous, is, in general, subluminal on both sides of the kink (see chapter 4). Furthermore, kinks are distinguished from cusps in that the scalar curvature function $\tilde{R}$ is bounded in a deleted neighbourhood of a kink, although the discontinuity in $\tilde{R}$ on the locus of

the kink itself is unbounded. This can be seen by calculating $\tilde{R}$ explicitly. If the discontinuity in γ across the kink is represented in the form

$$\gamma = \gamma_1 + (\gamma_2 - \gamma_1)H(\sigma_\pm) \tag{2.79}$$

where γ_1 and γ_2 are smooth functions, it follows from equation (2.69) that

$$\tilde{R} = \tilde{R}_1 + (\tilde{R}_2 - \tilde{R}_1)H(\sigma_\pm) + [\gamma_1^{-3/2} + (\gamma_2^{-3/2} - \gamma_1^{-3/2})H(\sigma_\pm)]$$
$$\times [\gamma_1^{1/2}(\gamma_2^{1/2}),_\mp - \gamma_2^{1/2}(\gamma_1^{1/2}),_\mp]\delta(\sigma_\pm). \tag{2.80}$$

Here, $\tilde{R}_1$ and $\tilde{R}_2$ are the (smooth) curvature functions generated separately by γ_1 and γ_2. The discontinuity in $\tilde{R}$, therefore, includes a delta-function-like singularity, although strictly speaking the presence of the product $H(\sigma_\pm)\delta(\sigma_\pm)$ on the right-hand side of (2.80) places the singularity outside the framework of conventional distribution theory.

However, this description applies only to idealized (zero-thickness) kinks. A more realistic version of a kink is a narrow segment of the string where the gradients of the tangent vectors are large but bounded. All the relevant dynamical quantities (including the scalar curvature) are then continuous across the kink, although the local curvature is typically very large. If two kinks of this type cross, an extremely narrow cusp known as a *microcusp* forms. These will be discussed in more detail in section 3.6.

Chapter 3

String dynamics in flat space

The Minkowski spacetime is the only background metric of cosmological interest in which the string equation of motion (2.14) can be integrated exactly. It is, therefore, not surprising that most work on string dynamics has been done in the Minkowski background, and that string dynamics in flat space is reasonably well understood. Only the Robertson–Walker background is of comparable importance and there little can be done without resort to approximations or numerical techniques (see section 5.1).

In this chapter the Minkowski version of the string equation of motion will be examined in some detail. The various laws relating to conservation of momentum, angular momentum and invariant length will be formulated explicitly and the inter-relationship between the kinks, cusps and self-intersections of a string loop will be analysed with the aid of a particular representation known as the Kibble–Turok sphere. In addition, a number of methods for generating exact periodic solutions will be presented.

3.1 The aligned standard gauge

In what follows, it is assumed that the Minkowski metric tensor $\eta_{\mu\nu}$ has its Cartesian form $\mathrm{diag}(1, -1, -1, -1)$ and that the parametrization $x^\mu = X^\mu(\tau, \sigma)$ of the world sheet has been chosen so that τ and σ are standard-gauge coordinates (see section 2.3). As mentioned in the previous chapter, there is no unique choice for the gauge coordinates in the standard gauge. One simple way to eliminate the residual gauge freedom is to identify τ with the Minkowski time coordinate $x^0 = t$. I will call this choice the *aligned standard gauge*.

Whichever form of the standard gauge is prescribed, the equation of motion (2.31) in a Minkowski background reads:

$$X^\mu{}_{,\tau\tau} = X^\mu{}_{,\sigma\sigma} \tag{3.1}$$

subject to the gauge conditions

$$X_\tau^2 + X_\sigma^2 = 0 \qquad \text{and} \qquad X_\tau \cdot X_\sigma = 0. \tag{3.2}$$

The general solution to (3.1) is

$$X^\mu(\tau, \sigma) = A^\mu(\tau + \sigma) + B^\mu(\tau - \sigma) \qquad (3.3)$$

where A^μ and B^μ are arbitrary functions of their arguments, save for the gauge constraints

$$A'^2 = B'^2 = 0 \qquad (3.4)$$

where a prime here denotes the derivative with respect to the relevant argument. The trajectory $X^\mu(\tau, \sigma)$ is thus a linear superposition of left- and right-moving modes which propagate along the string at the speed of light.

If the gauge coordinates (τ, σ) are not initially aligned with the time coordinate t, this can easily be achieved by defining a new pair of standard-gauge coordinates $(\overline{\tau}, \overline{\sigma})$ which satisfy the equations

$$A^0(\tau + \sigma) = \tfrac{1}{2}(\overline{\tau} + \overline{\sigma}) \qquad \text{and} \qquad B^0(\tau - \sigma) = \tfrac{1}{2}(\overline{\tau} - \overline{\sigma}). \qquad (3.5)$$

Then, after dropping the bars, the general solution (3.3) becomes

$$X^\mu(\tau, \sigma) = [\tau, \tfrac{1}{2}\mathbf{a}(\tau + \sigma) + \tfrac{1}{2}\mathbf{b}(\tau - \sigma)] \qquad (3.6)$$

where $\mathbf{a}$ and $\mathbf{b}$ are 3-vector functions with the property that

$$\mathbf{a}'^2 = \mathbf{b}'^2 = 1. \qquad (3.7)$$

The functions $\mathbf{a}'$ and $\mathbf{b}'$, therefore, lie on the surface of a unit sphere, first introduced by Tom Kibble and Neil Turok in 1982 [KT82] and as a result often referred to as the *Kibble–Turok sphere*[1]. The implications of the Kibble–Turok sphere for the dynamics of a string loop will be considered in more detail in sections 3.6–3.9.

If the string is closed and contains only one connected component (so that the world sheet $\mathbf{T}$ has strict cylindrical topology), then in the aligned standard gauge lines of constant τ form closed loops on $\mathbf{T}$. The function $X^\mu(\tau, \sigma)$ is, therefore, periodic in σ with some constant gauge period L, so that

$$X^\mu(\tau, 0) = X^\mu(\tau, L) \qquad (3.8)$$

for all values of τ. In terms of the mode functions $\mathbf{a}$ and $\mathbf{b}$, the periodicity condition (3.8) reads:

$$\mathbf{a}(\tau) + \mathbf{b}(\tau) = \mathbf{a}(\tau + L) + \mathbf{b}(\tau - L). \qquad (3.9)$$

---

[1] It should be mentioned that many authors have chosen to use a gauge convention in which $\mathbf{a}$ is a function of $\sigma - \tau$ and $\mathbf{b}$ a function of $\sigma + \tau$. The principal drawback of this convention is that cusps occur when $\mathbf{a}'$ and $\mathbf{b}'$ are anti-parallel rather than parallel, which, in turn, complicates discussion of the Kibble–Turok representation. In what follows, I will adhere to the convention of (3.6) throughout, transforming previously published solutions into this form where necessary.

Since the tangent vector X_σ^μ is also a periodic function of σ, it follows that

$$\mathbf{a}'(\tau) - \mathbf{b}'(\tau) = \mathbf{a}'(\tau + L) - \mathbf{b}'(\tau - L) \tag{3.10}$$

as well. The most general solution of these two equations is

$$\mathbf{a}(\tau) = \widehat{\mathbf{a}}(\tau) + \mathbf{V}\tau \qquad \text{and} \qquad \mathbf{b}(\tau) = \widehat{\mathbf{b}}(\tau) + \mathbf{V}\tau \tag{3.11}$$

where $\mathbf{V}$ is a constant vector, and $\widehat{\mathbf{a}}$ and $\widehat{\mathbf{b}}$ are periodic functions with period L satisfying the relations

$$(\widehat{\mathbf{a}}' + \mathbf{V})^2 = (\widehat{\mathbf{b}}' + \mathbf{V})^2 = 1. \tag{3.12}$$

As will be seen shortly, the vector $\mathbf{V}$ can be interpreted as the bulk velocity of the string loop, while the gauge period L is related to the energy of the loop.

In terms of the periodic mode functions $\widehat{\mathbf{a}}$ and $\widehat{\mathbf{b}}$, the string trajectory takes the form

$$X^\mu(\tau, \sigma) = [\tau, \tfrac{1}{2}\widehat{\mathbf{a}}(\tau + \sigma) + \tfrac{1}{2}\widehat{\mathbf{b}}(\tau - \sigma) + \mathbf{V}\tau]. \tag{3.13}$$

Although the functions $\widehat{\mathbf{a}}$ and $\widehat{\mathbf{b}}$ each have period L, the entire trajectory, in fact, has period $L/2$, as was first pointed out by Kibble and Turok [KT82]. To see this, note that

$$\begin{aligned}
X^\mu(\tau &+ L/2, \sigma + L/2) \\
&= [\tau + L/2, \tfrac{1}{2}\widehat{\mathbf{a}}(\tau + \sigma + L) + \tfrac{1}{2}\widehat{\mathbf{b}}(\tau - \sigma) + \mathbf{V}(\tau + L/2)] \\
&= [\tau + L/2, \tfrac{1}{2}\widehat{\mathbf{a}}(\tau + \sigma) + \tfrac{1}{2}\widehat{\mathbf{b}}(\tau - \sigma) + \mathbf{V}(\tau + L/2)] \tag{3.14}
\end{aligned}$$

which is simply the original configuration (3.13) translated by an amount $L\mathbf{V}/2$.

3.2 The GGRT gauge

An alternative method of fixing a choice of standard gauge, first formulated by Goddard, Goldstone, Rebbi and Thorn in 1973 [GGRT73], is to choose a constant timelike or null vector u^μ and define

$$\tau = \frac{u \cdot X}{2u \cdot P} \tag{3.15}$$

where P^μ is the constant total 4-momentum of the string. If u^μ is timelike, the effect is to set τ equal to $\frac{1}{2E'}t'$, where t' is the time coordinate and E' the energy of the string in a frame with 4-velocity parallel to u^μ. Goddard *et al* [GGRT73] themselves preferred a gauge choice in which u^μ is null, as this leads to some simplifications when quantizing the relativistic string, which was their primary concern. The resulting gauge is what was originally meant by the term 'light-cone gauge' or (less commonly) 'light-front gauge'. I will refer to it simply as the *GGRT gauge*.

Since the total 4-momentum P^μ of an infinite string is undefined, it is often preferable to replace the factor $2u \cdot P$ in (3.15) with some fixed constant. Following Christopher Thompson [Tho88], who revived the GGRT gauge in 1988, I will replace $2u \cdot P$ with 1 and make the choice

$$u^\mu = [1, 0, 0, -1] \tag{3.16}$$

so that

$$\tau = t + z \tag{3.17}$$

where z is the third spatial component of X^μ.

As in the aligned standard gauge, the general solution (3.3) to the equation of motion consists of a linear superposition of left- and right-moving modes, which in the present case will be written as

$$X^\mu(\tau, \sigma) = [t_L(\tau + \sigma) + t_R(\tau - \sigma), \mathbf{p}(\tau + \sigma) + \mathbf{q}(\tau - \sigma), z_L(\tau + \sigma) + z_R(\tau - \sigma)] \tag{3.18}$$

where $\mathbf{p}$ and $\mathbf{q}$ are 2-vector functions. The GGRT gauge choice $\tau = t + z$ implies that

$$t_L' + z_L' = \tfrac{1}{2} \qquad \text{and} \qquad t_R' + z_R' = \tfrac{1}{2} \tag{3.19}$$

and so, after some algebraic manipulation, the gauge constraints (3.2) read:

$$t_L' - z_L' = 2\mathbf{p}'^2 \qquad \text{and} \qquad t_R' - z_R' = 2\mathbf{q}'^2. \tag{3.20}$$

Solving the last two sets of equations simultaneously gives

$$t_L' = \tfrac{1}{4} + \mathbf{p}'^2 \qquad t_R' = \tfrac{1}{4} + \mathbf{q}'^2$$

and

$$z_L' = \tfrac{1}{4} - \mathbf{p}'^2 \qquad z_R' = \tfrac{1}{4} - \mathbf{q}'^2. \tag{3.21}$$

These restrictions, which take the place of the constraints $\mathbf{a}'^2 = \mathbf{b}'^2 = 1$ in the aligned standard gauge, have the specific advantage of being linear in the t–z mode functions. Thus, for example, a solution containing only a finite number of harmonics in $\sigma_\pm = \tau \pm \sigma$ can be generated by simply choosing the functions $\mathbf{p}$ and $\mathbf{q}$ to be finite harmonic series and integrating (3.21). The corresponding procedure in the aligned standard gauge is far more complicated (see section 3.5).

However, if the string forms a closed loop then the equations (3.21) need to be supplemented by the condition

$$\int_0^L (t_L' - t_R') \, d\sigma = \int_0^L (z_L' - z_R') \, d\sigma = 0 \tag{3.22}$$

or, equivalently,

$$\int_0^L \mathbf{p}'^2 \, d\sigma_+ = \int_0^L \mathbf{q}'^2 \, d\sigma_- \tag{3.23}$$

which, to a large extent, vitiates the advantage of the GGRT gauge in generating finite-harmonic solutions.

Another disadvantage of the GGRT gauge is that the coordinates τ and σ are singular at a cusp if the cusp velocity is parallel to u^μ (as $u \cdot X_\tau = 1$ everywhere but $u \cdot X_\tau = 0$ at a cusp in any non-singular gauge). Furthermore, solutions in the GGRT gauge trace out curves on the surface of the paraboloid $t - x^2 - y^2 = \frac{1}{4}$ rather than on the unit sphere. The resulting geometric description is typically harder to visualize and so has less heuristic value than the Kibble–Turok sphere.

Finally, it should be noted that for any particular choice of u^μ the GGRT gauge is incompatible with all standard-gauge solutions (3.3) in which either $u \cdot A$ or $u \cdot B$ is identically zero, as in such cases there is no reparametrization $\{\overline{\sigma}_+(\sigma_+), \overline{\sigma}_-(\sigma_-)\}$ that can transform $u \cdot X$ into a function of $\overline{\tau}$ alone. Since A'^μ and B'^μ are both null vectors the (unwelcome) possibility that either $u \cdot A = 0$ or $u \cdot B = 0$ is consistent with the gauge conditions if u^μ is null but not if u^μ is timelike. An example of this problem will be encountered in section 5.6.

Despite these caveats, the use of the GGRT gauge has helped to generate a number of simple solutions that would otherwise have remained undiscovered (see [Tho88]).

3.3   Conservation laws in flat space

Because the Minkowski spacetime has maximal symmetry, the components of the world-sheet momentum currents P_μ^A defined in section 2.4 are all separately conserved. The contravariant components of the momentum currents are

$$P^{\mu A} = \mu \gamma^{1/2} \gamma^{AB} X^\mu_{,B} \tag{3.24}$$

where, in the aligned standard gauge,

$$X_\tau^\mu = [1, \tfrac{1}{2}\mathbf{a}' + \tfrac{1}{2}\mathbf{b}'] \qquad X_\sigma^\mu = [0, \tfrac{1}{2}\mathbf{a}' - \tfrac{1}{2}\mathbf{b}'] \tag{3.25}$$

$$\gamma^{1/2} = X_\tau^2 = \tfrac{1}{2}(1 - \mathbf{a}' \cdot \mathbf{b}') \tag{3.26}$$

and

$$\gamma^{AB} = \gamma^{-1/2} \operatorname{diag}(1, -1). \tag{3.27}$$

The local Lorentz factor of the string is $\lambda = \gamma^{-1/4}$, which diverges (and so indicates the formation of a cusp) whenever $\mathbf{a}' \cdot \mathbf{b}' = 1$.

An observer at rest with respect to the spacetime coordinates would measure the local 4-momentum at any point on the string to be

$$p^\mu = \lambda \mu X_\tau^\mu = \gamma^{-1/4} \mu [1, \tfrac{1}{2}\mathbf{a}' + \tfrac{1}{2}\mathbf{b}'] \tag{3.28}$$

and the element of proper distance along the string as

$$d\ell = (-X_\sigma^2)^{1/2} \, d\sigma = \gamma^{1/4} \, d\sigma. \tag{3.29}$$

Hence, the total energy ΔE and momentum $\Delta \mathbf{p}$ of a segment of the string covering the parameter range σ to $\sigma + \Delta \sigma$ as measured by such an observer are

$$\Delta E = \int p^0 d\ell = \mu \Delta \sigma \qquad \text{and} \qquad \Delta \mathbf{p} = \int \mathbf{p} \, d\ell = \tfrac{1}{2}\mu(\Delta \mathbf{a} - \Delta \mathbf{b}). \quad (3.30)$$

Note, in particular, that the local energy content of the string is proportional to σ in the aligned standard gauge.

The total 4-momentum P^μ of a string loop with parametric period L is most conveniently calculated by integrating $P^{\mu A}$ around a curve of constant τ, as in equation (2.48), so that

$$P^\mu = \mu \int_0^L X_\tau^\mu \, d\sigma = \mu \int_0^L [1, \tfrac{1}{2}\widehat{\mathbf{a}}'(\tau + \sigma) + \tfrac{1}{2}\widehat{\mathbf{b}}'(\tau - \sigma) + \mathbf{V}] \, d\sigma. \quad (3.31)$$

Since the mode functions $\widehat{\mathbf{a}}$ and $\widehat{\mathbf{b}}$ are periodic with period L, they make no contribution to P^μ, and so

$$P^\mu = \mu L[1, \mathbf{V}]. \tag{3.32}$$

Hence, μL is the total energy of the string as expected, and $\mathbf{V}$ can be interpreted as its bulk velocity.

A similar conclusion can be drawn from the dynamics of the centre-of-mass 4-vector $\bar{X}^\mu$ of the loop, which is defined by

$$\bar{X}^\mu(\tau) = L^{-1} \int_0^L X^\mu \, d\sigma = L^{-1} \int_0^L [\tau, \tfrac{1}{2}\widehat{\mathbf{a}}(\tau + \sigma) + \tfrac{1}{2}\widehat{\mathbf{b}}(\tau - \sigma) + \mathbf{V}\tau] \, d\sigma. \quad (3.33)$$

In view of the periodicity of $\widehat{\mathbf{a}}$ and $\widehat{\mathbf{b}}$, this equation can be expressed more compactly as

$$\bar{X}^\mu(\tau) = [\tau, \bar{\mathbf{X}}_0 + \mathbf{V}\tau] \tag{3.34}$$

where

$$\bar{\mathbf{X}}_0 = L^{-1} \int_0^L [\tfrac{1}{2}\widehat{\mathbf{a}}(\sigma) + \tfrac{1}{2}\widehat{\mathbf{b}}(-\sigma)] \, d\sigma \tag{3.35}$$

is the spatial centre-of-mass at time $\tau = 0$. Thus the centre-of-mass of the loop follows an inertial trajectory with 3-velocity $\mathbf{V}$.

An additional result, due to Tom Kibble [Kib85], is that the root mean square velocity of a string loop in its centre-of-momentum frame, averaged over a period of oscillation, is $\frac{1}{\sqrt{2}}$. This follows from the fact that, if $\mathbf{r}(\tau, \sigma)$ is the spatial position vector of the string, then

$$\mathbf{r},_{\tau\tau} = \mathbf{r},_{\sigma\sigma} \qquad \text{and} \qquad \mathbf{r}_\sigma^2 = 1 - \mathbf{r}_\tau^2 \tag{3.36}$$

and so the period mean of $\mathbf{r}_\tau^2$ in a general Lorentz frame is

$$\langle \mathbf{r}_\tau^2 \rangle \equiv \frac{1}{L^2} \int_0^L \int_0^L \mathbf{r}_\tau^2 \, d\sigma \, d\tau = \frac{1}{L} \int_0^L \mathbf{V} \cdot \mathbf{r}_\tau \, d\sigma - \frac{1}{L^2} \int_0^L \int_0^L \mathbf{r} \cdot \mathbf{r},_{\tau\tau} \, d\sigma \, d\tau$$

$$= \mathbf{V}^2 - \frac{1}{L^2} \int_0^L \int_0^L \mathbf{r} \cdot \mathbf{r}_{,\sigma\sigma} \, d\sigma \, d\tau = \mathbf{V}^2 + \frac{1}{L^2} \int_0^L \int_0^L \mathbf{r}_\sigma^2 \, d\sigma \, d\tau$$

$$= \mathbf{V}^2 + \langle 1 - \mathbf{r}_\tau^2 \rangle. \tag{3.37}$$

Hence, $\langle \mathbf{r}_\tau^2 \rangle = \frac{1}{2}(1 + \mathbf{V}^2)$ and so, in particular, $\langle \mathbf{r}_\tau^2 \rangle = \frac{1}{2}$ in the centre-of-momentum frame. Since $\langle \mathbf{r}_\tau \rangle = \mathbf{V}$, the mean square deviation of $\mathbf{r}_\tau$ from the bulk velocity $\mathbf{V}$ in a more general frame is

$$\langle (\mathbf{r}_\tau - \mathbf{V})^2 \rangle = \frac{1}{2}(1 - \mathbf{V}^2). \tag{3.38}$$

However, it should be pointed out that the integrals over σ in (3.37) are mass-weighted averages rather than ordinary spatial averages, as it is $\gamma^{1/4} \, d\sigma$ rather than $d\sigma$ that is the proper distance element. This is evident also from the calculation of the total 4-momentum P^μ, which indicates that the bulk velocity $\langle \mathbf{r}_\tau \rangle = \mathbf{V}$ is mass-weighted. As a result, the value of $\langle \mathbf{r}_\tau^2 \rangle$ is weighted towards segments of the loop with high Lorentz factor and so, in a sense, overstates the actual mean square velocity.

Another useful conserved quantity is the total angular momentum of a string loop [Tur84]. This can be calculated in two ways. If $\mathbf{n}$ is any unit 3-vector then the rotational Killing vector about $\mathbf{n}$ is

$$k_\mu = [0, \mathbf{n} \times \mathbf{r}] \tag{3.39}$$

where $\mathbf{r}$ is again the spatial position vector. The total angular momentum of the string about $\mathbf{n}$ is, therefore,

$$J(\mathbf{n}) = \mu \int_0^L k \cdot X_\tau \, d\sigma = \frac{1}{4}\mu\mathbf{n} \cdot \int_0^L (\mathbf{a} + \mathbf{b}) \times (\mathbf{a}' + \mathbf{b}') \, d\sigma. \tag{3.40}$$

Now, in terms of the periodic mode functions $\widehat{\mathbf{a}}$ and $\widehat{\mathbf{b}}$,

$$(\mathbf{a} + \mathbf{b}) \times (\mathbf{a}' + \mathbf{b}') = \widehat{\mathbf{a}} \times \widehat{\mathbf{a}}' + \widehat{\mathbf{b}} \times \widehat{\mathbf{b}}' + \widehat{\mathbf{a}} \times \widehat{\mathbf{b}}' + \widehat{\mathbf{b}} \times \widehat{\mathbf{a}}'$$
$$+ 2\tau\mathbf{V} \times (\widehat{\mathbf{a}}' + \widehat{\mathbf{b}}') + 2(\widehat{\mathbf{a}} + \widehat{\mathbf{b}}) \times \mathbf{V} \tag{3.41}$$

where, since

$$\frac{d}{d\sigma}[\widehat{\mathbf{b}}(\tau - \sigma) \times \widehat{\mathbf{a}}(\tau + \sigma)] = \widehat{\mathbf{b}}(\tau - \sigma) \times \widehat{\mathbf{a}}'(\tau + \sigma) + \widehat{\mathbf{a}}(\tau + \sigma) \times \widehat{\mathbf{b}}'(\tau - \sigma) \tag{3.42}$$

the third, fourth and fifth terms on the right of (3.41) all vanish on integration. Hence,

$$J(\mathbf{n}) = \frac{1}{4}\mu\mathbf{n} \cdot \int_0^L (\widehat{\mathbf{a}} \times \widehat{\mathbf{a}}' + \widehat{\mathbf{b}} \times \widehat{\mathbf{b}}') \, d\sigma + \mathbf{n} \cdot (\mathbf{M} \times \mathbf{V}) \tag{3.43}$$

where

$$\mathbf{M} = \frac{1}{2}\mu \int_0^L (\widehat{\mathbf{a}} + \widehat{\mathbf{b}}) \, d\sigma \equiv \frac{1}{2}\mu L \bar{\mathbf{X}}_0 \tag{3.44}$$

is the mass moment of the loop. The angular momentum vector measured by an observer at rest with respect to the coordinate system is, therefore,

$$\mathbf{J} = \tfrac{1}{4}\mu \int_0^L (\widehat{\mathbf{a}} \times \widehat{\mathbf{a}}' + \widehat{\mathbf{b}} \times \widehat{\mathbf{b}}') \, d\sigma + \mathbf{M} \times \mathbf{V}. \tag{3.45}$$

Note, in particular, that the left- and right-moving modes contribute separately to $\mathbf{J}$.

In the rest frame of the loop, $\widehat{\mathbf{a}}'$ and $\widehat{\mathbf{b}}'$ are both unit vectors, and so $\widehat{\mathbf{a}}$ and $\widehat{\mathbf{b}}$ trace out closed curves each of length L in $\mathbb{R}^3$. Suppose that $\widehat{\mathbf{a}}$ traces a planar curve which does not intersect itself. Then

$$\mathbf{A}_a = \tfrac{1}{2} \int_0^L \widehat{\mathbf{a}} \times \widehat{\mathbf{a}}' \, d\sigma \tag{3.46}$$

is a vector normal to the plane with magnitude equal to the area enclosed by the curve. In the more general case where the curve does intersect itself, $\mathbf{A}_a$ can be found by breaking the curve up into non-intersecting closed segments and adding the corresponding vector areas. Furthermore, if the curve is not planar, it is always possible to project $\widehat{\mathbf{a}}$ onto a plane normal to the direction of $\mathbf{A}_a$ and so generate a closed planar curve with length strictly less than L; the magnitude of $\mathbf{A}_a$ is then the area enclosed by this curve.

Since the area enclosed by a curve of fixed length is maximal when the curve is a circle, $|\mathbf{A}_a|$ is bounded above by $L^2/(4\pi)$. A similar argument applies to the contribution of the $\widehat{\mathbf{b}}$ mode to the angular momentum vector $\mathbf{J}$, and so

$$|\mathbf{J}| \le \frac{1}{4\pi}\mu L^2 \tag{3.47}$$

for any loop configuration [SQSP90]. Equality holds in (3.47) if and only if the mode functions $\widehat{\mathbf{a}}$ and $\widehat{\mathbf{b}}$ trace out co-planar circles with the same orientation. This corresponds to a trajectory in the form of a rotating doubled straight line whose ends are moving at the speed of light (see section 4.2.2).

An alternative way to characterize the angular momentum of a loop is to first construct the angular momentum currents

$$M_A^{\mu\nu} = \mu(X^\mu X^\nu{}_{,A} - X^\nu X^\mu{}_{,A}). \tag{3.48}$$

By virtue of the flat-space equation of motion $\gamma^{AB} X^\mu{}_{,AB} = 0$, these satisfy the conservation equation

$$\gamma^{AB} M_A^{\mu\nu}{}_{,B} = \mu(X^\mu \gamma^{AB} X^\nu{}_{,AB} - X^\nu \gamma^{AB} X^\mu{}_{,AB}) = 0. \tag{3.49}$$

Hence, the conserved total angular momentum tensor of the loop is

$$M^{\mu\nu} = \int_0^L M_\tau^{\mu\nu} \, d\sigma = \begin{pmatrix} 0 & -M_x & -M_y & -M_y \\ M_x & 0 & J_z & -J_y \\ M_y & -J_z & 0 & J_x \\ M_z & J_y & -J_x & 0 \end{pmatrix} \tag{3.50}$$

and so can be used to reconstruct the components of both **M** and **J** in any Lorentz frame.

A further macroscopic property of interest is the invariant length of a closed loop. The parametric period L in an aligned standard gauge typically has different values in different reference frames. The minimum possible value of the parametric period occurs in the rest frame of the loop, and is

$$L_{\min} = (1 - \mathbf{V}^2)^{1/2} L \qquad (3.51)$$

where L and $\mathbf{V}$ are the parametric period and bulk velocity of the loop in an arbitrary frame. Since the quantity $\mu L_{\min}$ is the magnitude of the 4-momentum P^μ (equation (3.32)), it is natural to interpret $L_{\min}$ as, in some sense, the rest length of the string. It was first identified by Tanmay Vachaspati and Alexander Vilenkin [VV85] in 1985, and called by them the *invariant length* of the loop.

As previously mentioned (section 2.5), the invariant length $\ell_I(\mathfrak{p})$ of a string loop in an arbitrary background spacetime is defined to be twice the square root of the area of the subset $D(\mathfrak{p})$ whose interior is causally disconnected from the point $\mathfrak{p}$. This definition is motivated by the fact that $\ell_I(\mathfrak{p})$ is a natural world-sheet scalar and reduces to the invariant length $L_{\min}$ at all points on the world sheet when the background is Minkowski. To see this, it is most convenient to calculate ℓ_I in the light-cone coordinates $\sigma_\pm = \tau \pm \sigma$ corresponding to an arbitrary aligned standard gauge (τ, σ). Then

$$\ell_I(\sigma_+, \sigma_-) = 2\left(\int_{\sigma_- - L}^{\sigma_-} \int_{\sigma_+}^{\sigma_+ + L} X_+ \cdot X_- \, d\sigma_+ \, d\sigma_- \right)^{1/2}$$

$$= \left[\int_{\sigma_- - L}^{\sigma_-} \int_{\sigma_+}^{\sigma_+ + L} (1 - \mathbf{a}' \cdot \mathbf{b}') \, d\sigma_+ \, d\sigma_- \right]^{1/2} \qquad (3.52)$$

where, in terms of the periodic mode functions $\widehat{\mathbf{a}}(\sigma_+)$ and $\widehat{\mathbf{b}}(\sigma_-)$,

$$1 - \mathbf{a}' \cdot \mathbf{b}' = 1 - \widehat{\mathbf{a}}' \cdot \widehat{\mathbf{b}}' - (\widehat{\mathbf{a}}' + \widehat{\mathbf{b}}') \cdot \mathbf{V} - \mathbf{V}^2. \qquad (3.53)$$

Hence,

$$\ell_I(\sigma_+, \sigma_-) = \left[\int_{\sigma_- - L}^{\sigma_-} \int_{\sigma_+}^{\sigma_+ + L} (1 - \mathbf{V}^2) \, d\sigma_+ \, d\sigma_- \right]^{1/2} = (1 - \mathbf{V}^2)^{1/2} L \quad (3.54)$$

as claimed.

As well as comprising a strict lower bound for the parametric period L, the invariant length $L_{\min}$ has the useful property that it forms an upper bound for the proper length of the string loop as measured in any Lorentz frame. The length ℓ of the loop on a cross-sectional surface of constant τ in the aligned standard gauge is

$$\ell(\tau) = \int_0^L (-X_\sigma^2)^{1/2} \, d\sigma \leq \left[L \int_0^L (-X_\sigma^2) \, d\sigma \right]^{1/2} \qquad (3.55)$$

where the second term on the right follows from Schwarz's inequality. Now,

$$-X_\sigma^2 = \tfrac{1}{4}(\widehat{\mathbf{a}}'^2 + \widehat{\mathbf{b}}'^2 - 2\widehat{\mathbf{a}}' \cdot \widehat{\mathbf{b}}') \le \tfrac{1}{4}(\widehat{\mathbf{a}}'^2 + \widehat{\mathbf{b}}'^2 + 2|\widehat{\mathbf{a}}'||\widehat{\mathbf{b}}'|) \qquad (3.56)$$

and so, again by virtue of Schwarz's inequality,

$$\int_0^L (-X_\sigma^2)\,\mathrm{d}\sigma \le \tfrac{1}{4}\int_0^L \widehat{\mathbf{a}}'^2\,\mathrm{d}\sigma + \tfrac{1}{4}\int_0^L \widehat{\mathbf{b}}'^2\,\mathrm{d}\sigma$$
$$+ \tfrac{1}{2}\left(\int_0^L \widehat{\mathbf{a}}'^2\,\mathrm{d}\sigma\right)^{1/2}\left(\int_0^L \widehat{\mathbf{b}}'^2\,\mathrm{d}\sigma\right)^{1/2}. \qquad (3.57)$$

Finally, in view of the gauge conditions (3.12) on the periodic mode functions $\widehat{\mathbf{a}}$ and $\widehat{\mathbf{b}}$,

$$\widehat{\mathbf{a}}'^2 = 1 - 2\widehat{\mathbf{a}}' \cdot \mathbf{V} - \mathbf{V}^2 \qquad \text{and} \qquad \widehat{\mathbf{b}}'^2 = 1 - 2\widehat{\mathbf{b}}' \cdot \mathbf{V} - \mathbf{V}^2 \qquad (3.58)$$

and, therefore,

$$\ell(\tau) \le (1 - \mathbf{V}^2)^{1/2} L = L_{\min}. \qquad (3.59)$$

Note that this upper bound is achievable whenever $\widehat{\mathbf{a}}'$ and $\widehat{\mathbf{b}}'$ are anti-parallel and X_σ^2 is constant at all points on the surface of constant τ. This will occur if and only if the periodic mode functions have the form

$$\widehat{\mathbf{a}}(\tau + \sigma) = (1 - \mathbf{V}^2)^{1/2}\,\widehat{\mathbf{u}}(\sigma + \tau - \tau_0) \qquad (3.60)$$

and

$$\widehat{\mathbf{b}}(\tau - \sigma) = (1 - \mathbf{V}^2)^{1/2}\,\widehat{\mathbf{u}}(\sigma + \tau_0 - \tau) \qquad (3.61)$$

where τ_0 is a constant, and $\widehat{\mathbf{u}}$ is a periodic function with period L and satisfies the constraints

$$\widehat{\mathbf{u}}'^2 = 1 \qquad \text{and} \qquad \widehat{\mathbf{u}}' \cdot \mathbf{V} = 0. \qquad (3.62)$$

In particular, the measured length will be equal to the invariant length $L_{\min}$ in the rest frame of the string loop whenever the loop is momentarily stationary.

3.4   Initial-value formulation for a string loop

A considerable amount of effort has been invested by a number of authors in generating simple yet interesting solutions which satisfy the periodicity condition (3.8), largely for the purpose of estimating the flux of gravitational radiation from realistic string loops (see section 6.5). A common method is to decompose the trajectory into Fourier components and then impose the constraints $\mathbf{a}'^2 = \mathbf{b}'^2 = 1$, a procedure which can be simplified considerably by using a spinorial representation (see section 3.5). However, a method which has more direct physical appeal is to reconstruct a trajectory from its initial data on a surface of constant Minkowski time t.

Suppose then that on an initial surface $t = 0$ a string loop has position vector $\mathbf{r}_0(\theta)$ and velocity $\mathbf{v}_0(\theta)$, where θ is a parametric variable with range 0 to θ^*, and $\mathbf{r}_0$ and $\mathbf{v}_0$ are periodic functions of θ so that

$$\mathbf{r}_0(0) = \mathbf{r}_0(\theta^*) \qquad \text{and} \qquad \mathbf{v}_0(0) = \mathbf{v}_0(\theta^*). \tag{3.63}$$

If the trajectory of the loop is described using the aligned standard gauge, θ must be a function of the spacelike gauge coordinate σ on the initial surface, and so at $\tau = 0$ the world-sheet tangent vectors have the form

$$X_\tau^\mu = [1, \mathbf{v}_0] \tag{3.64}$$

and

$$X_\sigma^\mu = \left[0, \mathbf{r}_0' \frac{d\theta}{d\sigma}\right]. \tag{3.65}$$

The gauge constraint $X_\tau \cdot X_\sigma = 0$ then requires that $\mathbf{v}_0 \cdot \mathbf{r}_0' = 0$, so the initial velocity of the loop must be chosen to be everywhere orthogonal to $\mathbf{r}_0'$. This restriction is simply a reflection of the fact that a string is locally invariant with respect to boosts parallel to the world sheet, and so any longitudinal component in the string's velocity is undetectable. In view of the second gauge constraint

$$0 = X_\tau^2 + X_\sigma^2 = 1 - \mathbf{r}_0'^2 \left(\frac{d\theta}{d\sigma}\right)^2 - \mathbf{v}_0^2 \tag{3.66}$$

the parameter θ and the gauge coordinate σ are related by the equation

$$\frac{d\theta}{d\sigma} = |\mathbf{r}_0'|^{-1} \sqrt{1 - \mathbf{v}_0^2}. \tag{3.67}$$

Since according to equation (3.6), the tangent vectors on the initial surface $\tau = 0$ are just

$$X_\tau^\mu(0, \sigma) = [1, \tfrac{1}{2}\mathbf{a}'(\sigma) + \tfrac{1}{2}\mathbf{b}'(-\sigma)] \tag{3.68}$$

and

$$X_\sigma^\mu(0, \sigma) = [0, \tfrac{1}{2}\mathbf{a}'(\sigma) - \tfrac{1}{2}\mathbf{b}'(-\sigma)] \tag{3.69}$$

it follows immediately that, if $\theta(0) = 0$,

$$\mathbf{a}(\tau + \sigma) = \mathbf{r}_0(\theta(\sigma + \tau)) + \int_0^{\theta(\sigma+\tau)} \mathbf{v}_0 \frac{d\sigma}{d\theta} d\theta \tag{3.70}$$

and

$$\mathbf{b}(\tau - \sigma) = \mathbf{r}_0(\theta(\sigma - \tau)) - \int_0^{\theta(\sigma-\tau)} \mathbf{v}_0 \frac{d\sigma}{d\theta} d\theta. \tag{3.71}$$

In particular, if the loop is initially motionless then the full trajectory is

$$X^\mu(\tau, \sigma) = [\tau, \tfrac{1}{2}\mathbf{r}_0(\theta(\sigma + \tau)) + \tfrac{1}{2}\mathbf{r}_0(\theta(\sigma - \tau))] \tag{3.72}$$

where the function $\theta(\sigma)$ is determined implicitly by the equation

$$\frac{d\sigma}{d\theta} = |\mathbf{r}'_0|. \tag{3.73}$$

In the more general case of non-static initial data, the parametric period L of the loop is given by

$$L = \int_0^{\theta^*} (1 - \mathbf{v}_0^2)^{-1/2} |\mathbf{r}'_0| \, d\theta \tag{3.74}$$

while the bulk velocity of the loop is

$$\mathbf{V} = L^{-1} \int_0^{\theta^*} (1 - \mathbf{v}_0^2)^{-1/2} |\mathbf{r}'_0| \mathbf{v}_0 \, d\theta. \tag{3.75}$$

Examples of solutions generated using this method will be given in section 4.6.

3.5   Periodic solutions in the spinor representation

Even though the general solution (3.6) to the string equation of motion in a Minkowski background is extremely simple, the problem of constructing periodic solutions which satisfy the gauge condition $\mathbf{a}'^2 = \mathbf{b}'^2 = 1$ is not entirely trivial. As mentioned earlier, one possible method is to begin with periodic initial data, although the integrals (3.70) and (3.71) which then result are usually very complicated. An alternative is to expand the mode functions $\mathbf{a}'$ and $\mathbf{b}'$ as a finite series of harmonics in $\sigma_+ = \tau + \sigma$ and $\sigma_- = \tau - \sigma$, respectively.

For example, if $\mathbf{a}'$ contains only zero- and first-order harmonics then it has the general form

$$\mathbf{a}' = \mathbf{V} + \mathbf{C}\cos(2\pi\sigma_+/L) + \mathbf{S}\sin(2\pi\sigma_+/L) \tag{3.76}$$

where $\mathbf{C}$ and $\mathbf{S}$ are constant vectors. The gauge condition $\mathbf{a}'^2 = 1$ then implies that

$$\mathbf{C} \cdot \mathbf{V} = \mathbf{S} \cdot \mathbf{V} = \mathbf{C} \cdot \mathbf{S} = 0 \qquad \mathbf{C}^2 = \mathbf{S}^2 \qquad \text{and} \qquad \mathbf{V}^2 + \mathbf{C}^2 = 1 \tag{3.77}$$

so that the general solution for $\mathbf{a}'$ reads:

$$\mathbf{a}' = (\mathbf{n}_1 \times \mathbf{n}_2)\cos\phi + \mathbf{n}_1 \sin\phi \cos(2\pi\sigma_+/L) + \mathbf{n}_2 \sin\phi \sin(2\pi\sigma_+/L) \tag{3.78}$$

where $\mathbf{n}_1$ and $\mathbf{n}_2$ are any two orthogonal unit vectors and ϕ is an arbitrary constant. A similar first-order solution exists for $\mathbf{b}'$.

Finding periodic solutions in this way rapidly becomes unworkable as the number of harmonics increases. If $\mathbf{a}'$ contains all harmonics up to order N, so that

$$\mathbf{a}' = \mathbf{V} + \sum_{n=1}^{N} \mathbf{C}_n \cos(2\pi n\sigma_+/L) + \sum_{n=1}^{N} \mathbf{S}_n \sin(2\pi n\sigma_+/L) \tag{3.79}$$

then the gauge condition $\mathbf{a}'^2 = 1$ is equivalent to $4N + 1$ separate conditions on $2N + 1$ vectors. Fortunately, it is possible to generate solutions containing all harmonics up to an arbitrary order relatively easily by working in a spinor representation due to Robert Brown, Eric Rains and Cyrus Taylor [BRT91], which, in turn, expands on earlier work by Brown and David DeLaney [BD89].

The first step is to represent the components of $\mathbf{a}'$ as the complex 2×2 matrix

$$\mathbf{P} = \begin{pmatrix} 1 + a'_z & a'_x - \mathrm{i}a'_y \\ a'_x + \mathrm{i}a'_y & 1 - a'_z \end{pmatrix}. \tag{3.80}$$

The gauge condition $\mathbf{a}'^2 = 1$ then becomes $\det \mathbf{P} = 0$. Because of this constraint, $\mathbf{P}$ can always decomposed as the product of a complex two-spinor $\mathbf{\Psi}$ and its Hermitian conjugate:

$$\mathbf{P} = \mathbf{\Psi}\mathbf{\Psi}^\dagger. \tag{3.81}$$

The only condition that needs to be imposed on $\mathbf{\Psi}$ *a priori* is that $\mathbf{\Psi}^\dagger\mathbf{\Psi} = 2$, as $\mathrm{Tr}\,\mathbf{P} = 2$. As an example, one very simple choice for $\mathbf{\Psi}$ is:

$$\mathbf{\Psi} = \begin{pmatrix} \sqrt{2} \\ 0 \end{pmatrix} \tag{3.82}$$

which corresponds to

$$\mathbf{P} = \begin{pmatrix} 2 & 0 \\ 0 & 0 \end{pmatrix} \text{ or, equivalently, to } \mathbf{a}' = [0, 0, 1]. \tag{3.83}$$

The general solution containing all harmonics up to order N can be constructed by simply choosing

$$\Psi = \prod_{n=N}^{1} \mathbf{Q}_n(\xi_+)\, \mathbf{\Psi}_0 \tag{3.84}$$

where $\mathbf{\Psi}_0$ is any constant two-spinor satisfying the constraint $\mathbf{\Psi}_0^\dagger\mathbf{\Psi}_0 = 2$, the variable ξ_+ is shorthand for $2\pi\sigma_+/L$, and

$$\mathbf{Q}_n(\xi_+) = \begin{pmatrix} \mathrm{e}^{-\mathrm{i}\xi_+/2} & 0 \\ 0 & \mathrm{e}^{\mathrm{i}\xi_+/2} \end{pmatrix} \begin{pmatrix} \cos\tfrac{1}{2}\phi_n & -\mathrm{i}\sin\tfrac{1}{2}\phi_n\mathrm{e}^{\mathrm{i}\theta_n} \\ -\mathrm{i}\sin\tfrac{1}{2}\phi_n\mathrm{e}^{-\mathrm{i}\theta_n} & \cos\tfrac{1}{2}\phi_n \end{pmatrix} \tag{3.85}$$

(with ϕ_n, θ_n arbitrary) is the most general rotation matrix containing first-order harmonics in $\xi_+/2$. Because $\mathbf{Q}_n$ is unitary, the trace condition $\mathbf{\Psi}^\dagger\mathbf{\Psi} = 2$ is automatically preserved.

Although $\mathbf{\Psi}_0$ is, in principle, arbitrary, all the harmonic solutions will be generated (up to a spatial rotation) if $\mathbf{\Psi}_0$ is chosen to have the simple form (3.82). The effect of this is to align the highest-order harmonics along the x–y plane. As an illustration, the family of 01-harmonic solutions generated by this method is

$$\mathbf{a}' = \sin(\xi_+ - \theta_1)\sin\phi_1\widehat{\mathbf{x}} - \cos(\xi_+ - \theta_1)\sin\phi_1\widehat{\mathbf{y}} + \cos\phi_1\widehat{\mathbf{z}} \tag{3.86}$$

while the family of 012-harmonic solutions is

$$
\begin{aligned}
\mathbf{a}' = {} & [\sin\phi_1 \sin^2(\phi_2/2) \sin(2\theta_2 - \theta_1) + \cos\phi_1 \sin\phi_2 \sin(\xi_+ - \theta_2) \\
& + \sin\phi_1 \cos^2(\phi_2/2) \sin(2\xi_+ - \theta_1)]\hat{\mathbf{x}} + [\sin\phi_1 \sin^2(\phi_2/2) \cos(2\theta_2 - \theta_1) \\
& - \cos\phi_1 \sin\phi_2 \cos(\xi_+ - \theta_2) - \sin\phi_1 \cos^2(\phi_2/2) \cos(2\xi_+ - \theta_1)]\hat{\mathbf{y}} \\
& + [\cos\phi_1 \cos\phi_2 - \sin\phi_1 \sin\phi_2 \cos(\xi_+ + \theta_2 - \theta_1)]\hat{\mathbf{z}}. \quad (3.87)
\end{aligned}
$$

String trajectories involving both types of mode function will be examined in more detail in section 4.4.1.

A more generic use of the spinor formalism, which predates the method of Brown *et al* and is applicable to any standard gauge rather than just the aligned standard gauge, was first developed by Hughston and Shaw [HS88]. Recall that in the standard gauge the general solution to the equation of motion is

$$
X^\mu(\tau, \sigma) = A^\mu(\sigma_+) + B^\mu(\sigma_-) \quad (3.88)
$$

where A'_μ and B'_μ are both null vectors. On writing

$$
\mathbf{P} = \begin{pmatrix} A'_t + A'_z & A'_x - \mathrm{i}A'_y \\ A'_x + \mathrm{i}A'_y & A'_t - A'_z \end{pmatrix} \quad (3.89)
$$

the gauge constraint $A'^2 = 0$ becomes $\det\mathbf{P} = 0$ and so $\mathbf{P}$ can again be decomposed as the product of a complex two-spinor $\mathbf{\Psi} = [\psi_1, \psi_2]^\top$ and its Hermitian conjugate. However, the decomposition is not unique, as any rotation in the phases of ψ_1 and ψ_2 which leaves $\psi_1\bar\psi_2$ invariant also leaves $\mathbf{P}$ invariant. Hughston and Shaw chose to scale $\mathbf{\Psi}$ so that

$$
\psi_1\psi_2' - \psi_2\psi_1' = 1 \quad (3.90)
$$

almost everywhere, from which it follows that $\psi_1\psi_2'' - \psi_2\psi_1'' = 0$ and, therefore, that

$$
\mathbf{\Psi}'' = U(\sigma_+)\mathbf{\Psi} \quad (3.91)
$$

for some scalar function U.

It is thus possible to generate periodic solutions of the equation of motion by substituting a suitable periodic function U into equation (3.91) and solving for $\mathbf{\Psi}$. It is readily seen that if U is real then the orbit of A'_μ is planar, whereas if U is complex it is non-planar. Although this method can generate additional solutions in those cases where (3.91) is tractable, it is difficult to control the gauge in which the solution appears. Furthermore, because there is no simple relationship between the form of U and the form of $\mathbf{\Psi}$, it is not a convenient method for generating solutions with a finite number of harmonics. Brown *et al* [BRT91] have shown that in the aligned standard gauge the 01-harmonic solutions correspond to the simple choice $U = \text{constant}$ (in fact $U = -\pi^2/L^2$ in the notation used here) but that for the family of 012 solutions U is a forbiddingly complicated function of σ_+.
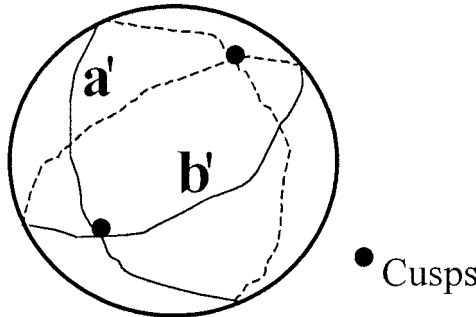
Figure 3.1. The Kibble–Turok sphere.

3.6 The Kibble–Turok sphere and cusps and kinks in flat space

In the aligned standard gauge, as we have seen, the position vector $X^\mu(\tau, \sigma)$ of a string loop can be characterized by two vector functions $\mathbf{a}(\sigma_+)$ and $\mathbf{b}(\sigma_-)$ whose derivatives trace out a pair of curves on the surface of the Kibble–Turok sphere, as shown in figure 3.1. Furthermore, in the centre-of-momentum frame of the loop, $\mathbf{a}$ and $\mathbf{b}$ are strictly periodic functions of their arguments with period L, and so

$$\int_0^L \mathbf{a}'(\sigma_+)\,\mathrm{d}\sigma_+ = \int_0^L \mathbf{b}'(\sigma_-)\,\mathrm{d}\sigma_- = \mathbf{0}. \tag{3.92}$$

That is, the centroids of both the $\mathbf{a}'$ and $\mathbf{b}'$ curves lie at the centre of the sphere. In particular, this means that neither curve can lie wholly inside a single hemisphere.

The Kibble–Turok representation, although simple, has provided a number of valuable insights into the dynamics and evolution of strings in flat space. Consider, first of all, a string loop without kinks in its centre-of-momentum frame. The $\mathbf{a}'$ and $\mathbf{b}'$ curves are then closed and continuous and since neither can lie wholly inside a hemisphere it requires some work to prevent the curves from crossing. Furthermore, if the curves do cross, they must do so an even number of times (if points of cotangency are excluded). Now, it was seen in section 3.3 that a cusp appears whenever $\mathbf{a}' \cdot \mathbf{b}' = 1$ or, equivalently, whenever the $\mathbf{a}'$ and $\mathbf{b}'$ curves cross. Thus it can be seen that cusps are, in some sense, generic to kinkless loops and necessarily occur in pairs.

In fact, following Thompson [Tho88] it is possible to divide cusps into two classes depending on the relative orientation of the $\mathbf{a}'$ and $\mathbf{b}'$ curves. The tangent vectors to the two curves are proportional to $\mathbf{a}''$ and $\mathbf{b}''$ respectively, and so at a cusp the vector $\mathbf{a}'' \times \mathbf{b}''$ is normal to the surface of the Kibble–Turok sphere. If this vector is directed out of the sphere, so that $(\mathbf{a}'' \times \mathbf{b}'') \cdot \mathbf{a}' > 0$, the cusp is said to be a *procusp* (or simply a cusp). However, if the vector is directed into the sphere, so that $(\mathbf{a}'' \times \mathbf{b}'') \cdot \mathbf{a}' < 0$, the cusp is referred to as an *anti-cusp*. It is clear

from the geometry of the Kibble–Turok sphere that for kinkless loops the number of cusps and anti-cusps is equal and that cusps and anti-cusps occur alternately along the $\mathbf{a}'$ and $\mathbf{b}'$ curves.

In order to examine the structure of a general cusp in more detail, it is conventional to assume that the position vector $X^\mu(\tau, \sigma)$ is an analytic function of the standard-gauge coordinates σ and τ at the cusp. Then in a neighbourhood of the cusp (here taken to be at $\tau = \sigma = 0$)

$$\mathbf{a}' = \mathbf{v}_c + \mathbf{a}''_c \sigma_+ + \tfrac{1}{2}\mathbf{a}'''_c \sigma_+^2 + O(\sigma_+^3) \tag{3.93}$$

and

$$\mathbf{b}' = \mathbf{v}_c + \mathbf{b}''_c \sigma_- + \tfrac{1}{2}\mathbf{b}'''_c \sigma_-^2 + O(\sigma_-^3) \tag{3.94}$$

where $\sigma_\pm = \tau \pm \sigma$ as before and $\mathbf{v}_c$ is a unit vector, the instantaneous velocity of the cusp. (In terms of the somewhat more general analysis of a cusp given in section 2.6, the vectors $\mathbf{v}_c$, $\mathbf{a}''_c$ and $\mathbf{b}''_c$ are just $\mathbf{n}$, $4\mathbf{u}$ and $4\mathbf{v}$ respectively.)

In view of the gauge conditions $\mathbf{a}'^2 = \mathbf{b}'^2 = 1$, the coefficient vectors satisfy the constraints

$$\mathbf{v}_c \cdot \mathbf{a}''_c = \mathbf{v}_c \cdot \mathbf{b}''_c = 0 \qquad \text{and} \qquad \mathbf{v}_c \cdot \mathbf{a}'''_c + |\mathbf{a}''_c|^2 = \mathbf{v}_c \cdot \mathbf{b}'''_c + |\mathbf{b}''_c|^2 = 0 \tag{3.95}$$

and so on the face of it it would appear that once the direction of $\mathbf{v}_c$ is specified the structure of the cusp to third order is fixed by seven parameters: the magnitudes of $\mathbf{a}''_c$ and $\mathbf{b}''_c$, the angle between $\mathbf{a}''_c$ and $\mathbf{b}''_c$, and the components of $\mathbf{a}'''_c$ and $\mathbf{b}'''_c$ normal to $\mathbf{v}_c$. In particular, the tangent vector $\mathbf{t}_c = \tfrac{1}{2}(\mathbf{a}''_c + \mathbf{b}''_c)$ to the cusp and the direction $\mathbf{s}_c = \tfrac{1}{2}(\mathbf{a}'''_c - \mathbf{b}'''_c)$ of the spreading of the string (see figure 3.2) satisfy

$$\mathbf{v}_c \cdot \mathbf{t}_c = 0 \qquad \text{and} \qquad \mathbf{v}_c \cdot \mathbf{s}_c = \tfrac{1}{2}(|\mathbf{b}''_c|^2 - |\mathbf{a}''_c|^2). \tag{3.96}$$

Note that at $\tau = 0$ the circumcusp region is described parametrically by the equation

$$\mathbf{r}(0, \sigma) = \tfrac{1}{2}\mathbf{t}_c \sigma^2 + \tfrac{1}{6}\mathbf{s}_c \sigma^3 + O(\sigma^4) \tag{3.97}$$

and so unless $\mathbf{t}_c$ and $\mathbf{s}_c$ are linearly dependent the cusp locally has the characteristic $y \propto x^{2/3}$ shape mentioned in section 2.6.
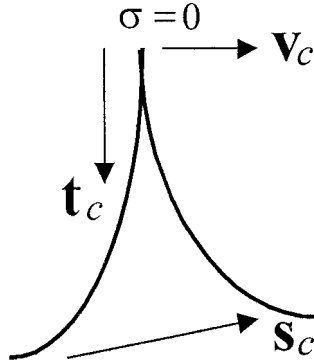
José Blanco-Pillado and Ken Olum have recently shown [BPO99] that it is possible to reduce the number of independent third-order parameters at a cusp to four by invoking a suitable Lorentz transformation. To see this, note first that under a Lorentz boost to a frame with velocity $\mathbf{v}_0$ the null vectors

$$A'^\mu = [1, \mathbf{a}'] \qquad \text{and} \qquad B'^\mu = [1, \mathbf{b}'] \tag{3.98}$$

transform to give

$$A'^{\overline{\mu}} = [\lambda_0(1 - \mathbf{a}' \cdot \mathbf{v}_0), \mathbf{A}] \qquad \text{and} \qquad B'^{\overline{\mu}} = [\lambda_0(1 - \mathbf{b}' \cdot \mathbf{v}_0), \mathbf{B}] \tag{3.99}$$

where $\lambda_0 = (1 - |\mathbf{v}_0^2|)^{-1/2}$ and $\mathbf{A}$ and $\mathbf{B}$ are vector functions of σ_+ and σ_- respectively. In the boosted frame the role of the mode functions $\mathbf{a}'$ and $\mathbf{b}'$ is

Figure 3.2. The vectors $\mathbf{v}_c$, $\mathbf{t}_c$ and $\mathbf{s}_c$.

assumed by two new functions $\widetilde{\mathbf{a}}'$ and $\widetilde{\mathbf{b}}'$ of the corresponding aligned gauge coordinates $\widetilde{\sigma}_+$ and $\widetilde{\sigma}_-$ and the analogues of the vectors A'^μ and B'^μ are:

$$\widetilde{A}'^{\overline{\mu}} \equiv [1, \widetilde{\mathbf{a}}'] = f_\mathbf{a} A'^{\overline{\mu}} \qquad \text{and} \qquad \widetilde{B}'^{\overline{\mu}} \equiv [1, \widetilde{\mathbf{b}}'] = f_\mathbf{b} B'^{\overline{\mu}} \qquad (3.100)$$

where

$$f_\mathbf{a} = \lambda_0^{-1}(1 - \mathbf{a}' \cdot \mathbf{v}_0)^{-1} \qquad \text{and} \qquad f_\mathbf{b} = \lambda_0^{-1}(1 - \mathbf{b}' \cdot \mathbf{v}_0)^{-1}. \qquad (3.101)$$

Similarly, the world-sheet derivative operators $D_\pm = \partial/\partial\sigma_\pm$ and $\widetilde{D}_\pm = \partial/\partial\widetilde{\sigma}_\pm$ are related by

$$\widetilde{D}_+ = f_\mathbf{a} D_+ \qquad \text{and} \qquad \widetilde{D}_- = f_\mathbf{b} D_- \qquad (3.102)$$

and so the higher derivatives of $\widetilde{\mathbf{a}}'$ and $\widetilde{\mathbf{b}}'$ can be calculated from the identities

$$[0, \widetilde{\mathbf{a}}''] = \widetilde{D}_+ \widetilde{A}'^{\overline{\mu}} = f_\mathbf{a} D_+(f_\mathbf{a} A'^{\overline{\mu}}) = f_\mathbf{a}^2 D_+ A'^{\overline{\mu}} + A'^{\overline{\mu}} f_\mathbf{a} D_+ f_\mathbf{a} \qquad (3.103)$$

$$[0, \widetilde{\mathbf{b}}''] = \widetilde{D}_- \widetilde{B}'^{\overline{\mu}} = f_\mathbf{b} D_-(f_\mathbf{b} B'^{\overline{\mu}}) = f_\mathbf{b}^2 D_- B'^{\overline{\mu}} + B'^{\overline{\mu}} f_\mathbf{b} D_- f_\mathbf{b} \qquad (3.104)$$

$$[0, \widetilde{\mathbf{a}}'''] = \widetilde{D}_+^2 \widetilde{A}'^{\overline{\mu}} = f_\mathbf{a}^3 D_+^2 A'^{\overline{\mu}} + 3 f_\mathbf{a}^2 D_+ f_\mathbf{a} D_+ A'^{\overline{\mu}}$$
$$+ [f_\mathbf{a}^2 D_+^2 f_\mathbf{a} + f_\mathbf{a}(D_+ f_\mathbf{a})^2] A'^{\overline{\mu}} \qquad (3.105)$$

and

$$[0, \widetilde{\mathbf{b}}'''] = \widetilde{D}_-^2 \widetilde{B}'^{\overline{\mu}} = f_\mathbf{b}^3 D_-^2 B'^{\overline{\mu}} + 3 f_\mathbf{b}^2 D_- f_\mathbf{b} D_- B'^{\overline{\mu}}$$
$$+ [f_\mathbf{b}^2 D_-^2 f_\mathbf{b} + f_\mathbf{b}(D_- f_\mathbf{b})^2] B'^{\overline{\mu}}. \qquad (3.106)$$

At a cusp, the null vectors $A'^{\overline{\mu}}$ and $B'^{\overline{\mu}}$ are equal and orthogonal to both $D_+ A'^{\overline{\mu}}$ and $D_- B'^{\overline{\mu}}$, while

$$f_\mathbf{a} = f_\mathbf{b} = f \equiv \lambda_0^{-1}(1 - \mathbf{v}_c \cdot \mathbf{v}_0)^{-1} \qquad (3.107)$$

and

$$D_+ f_{\mathbf{a}} = \lambda_0 \, f^2 \mathbf{a}_{\mathrm{c}}'' \cdot \mathbf{v}_0 \qquad \text{and} \qquad D_- f_{\mathbf{b}} = \lambda_0 f^2 \mathbf{b}_{\mathrm{c}}'' \cdot \mathbf{v}_0. \qquad (3.108)$$

Hence, in view of (3.95) the dot products of various pairwise combinations of (3.103)–(3.106) give:

$$|\widetilde{\mathbf{a}}_{\mathrm{c}}''|^2 = f^4 |\mathbf{a}_{\mathrm{c}}''|^2 \qquad |\widetilde{\mathbf{b}}_{\mathrm{c}}''|^2 = f^4 |\mathbf{b}_{\mathrm{c}}''|^2 \qquad \text{and} \qquad \widetilde{\mathbf{a}}_{\mathrm{c}}'' \cdot \widetilde{\mathbf{b}}_{\mathrm{c}}'' = f^4 \mathbf{a}_{\mathrm{c}}'' \cdot \mathbf{b}_{\mathrm{c}}'' \tag{3.109}$$

$$\widetilde{\mathbf{a}}_{\mathrm{c}}'' \cdot \widetilde{\mathbf{a}}_{\mathrm{c}}''' = f^5 (\mathbf{a}_{\mathrm{c}}'' \cdot \mathbf{a}_{\mathrm{c}}''' + 2\lambda_0 f |\mathbf{a}_{\mathrm{c}}''|^2 \mathbf{a}_{\mathrm{c}}'' \cdot \mathbf{v}_0) \tag{3.110}$$

$$\widetilde{\mathbf{b}}_{\mathrm{c}}'' \cdot \widetilde{\mathbf{b}}_{\mathrm{c}}''' = f^5 (\mathbf{b}_{\mathrm{c}}'' \cdot \mathbf{b}_{\mathrm{c}}''' + 2\lambda_0 f |\mathbf{b}_{\mathrm{c}}''|^2 \mathbf{b}_{\mathrm{c}}'' \cdot \mathbf{v}_0) \tag{3.111}$$

$$\widetilde{\mathbf{a}}_{\mathrm{c}}'' \cdot \widetilde{\mathbf{b}}_{\mathrm{c}}''' = f^5 \{\mathbf{a}_{\mathrm{c}}'' \cdot \mathbf{b}_{\mathrm{c}}''' + \lambda_0 f [3(\mathbf{a}_{\mathrm{c}}'' \cdot \mathbf{b}_{\mathrm{c}}'')\mathbf{b}_{\mathrm{c}}'' \cdot \mathbf{v}_0 - |\mathbf{a}_{\mathrm{c}}''|^2 \mathbf{b}_{\mathrm{c}}'' \cdot \mathbf{v}_0]\} \tag{3.112}$$
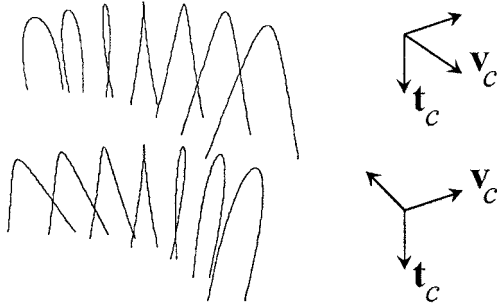
and

$$\widetilde{\mathbf{b}}_{\mathrm{c}}'' \cdot \widetilde{\mathbf{a}}_{\mathrm{c}}''' = f^5 \{\mathbf{b}_{\mathrm{c}}'' \cdot \mathbf{a}_{\mathrm{c}}''' + \lambda_0 f [3(\mathbf{a}_{\mathrm{c}}'' \cdot \mathbf{b}_{\mathrm{c}}'')\mathbf{a}_{\mathrm{c}}'' \cdot \mathbf{v}_0 - |\mathbf{b}_{\mathrm{c}}''|^2 \mathbf{a}_{\mathrm{c}}'' \cdot \mathbf{v}_0]\}. \tag{3.113}$$

The first three equations indicate that the vectors $\mathbf{a}_{\mathrm{c}}''$ and $\mathbf{b}_{\mathrm{c}}''$ are rescaled by a factor of f^2, and possibly rotated about the direction of $\mathbf{v}_{\mathrm{c}}$ (to which they must remain orthogonal), but are otherwise unchanged by the Lorentz boost. Altogether, the seven equations contain three free parameters (the components of the boost velocity $\mathbf{v}_0$), and can be used to impose a variety of possible coordinate conditions at the cusp.

For example, if $\mathbf{a}_{\mathrm{c}}''$ and $\mathbf{b}_{\mathrm{c}}''$ are non-parallel the tangent vector $\mathbf{t}_{\mathrm{c}} = \frac{1}{2}(\mathbf{a}_{\mathrm{c}}'' + \mathbf{b}_{\mathrm{c}}'')$ can be rescaled to a unit vector by choosing f appropriately. It is then possible to fix $\mathbf{a}_{\mathrm{c}}'' \cdot \mathbf{v}_0$ and $\mathbf{b}_{\mathrm{c}}'' \cdot \mathbf{v}_0$ so that $\mathbf{a}_{\mathrm{c}}'' \cdot \mathbf{s}_{\mathrm{c}} = \mathbf{b}_{\mathrm{c}}'' \cdot \mathbf{s}_{\mathrm{c}} = 0$, and, therefore, that the direction of spread $\mathbf{s}_{\mathrm{c}}$ is parallel to the cusp velocity $\mathbf{v}_{\mathrm{c}}$. As a result, the cusp can be characterized by only four independent parameters: the relative magnitude of $\mathbf{a}_{\mathrm{c}}''$ and $\mathbf{b}_{\mathrm{c}}''$, the angle between $\mathbf{a}_{\mathrm{c}}''$ and $\mathbf{b}_{\mathrm{c}}''$, and the components of $\mathbf{a}_{\mathrm{c}}'''$ normal to $\mathbf{v}_{\mathrm{c}}$. Note that, in view of equations (3.96) and (3.109), it is never possible to find a Lorentz boost which makes $\mathbf{v}_{\mathrm{c}}$ and $\mathbf{s}_{\mathrm{c}}$ orthogonal if they are initially non-orthogonal.

Figure 3.3 illustrates the time development of a generic cusp in the frame where $|\mathbf{t}_{\mathrm{c}}| = 1$ and $\mathbf{v}_{\mathrm{c}}$ and $\mathbf{s}_{\mathrm{c}}$ are parallel. The four free cusp parameters, which have been randomly generated, are $|\mathbf{a}_{\mathrm{c}}''|/|\mathbf{b}_{\mathrm{c}}''| = 0.4456$, $\angle(\mathbf{a}_{\mathrm{c}}'', \mathbf{b}_{\mathrm{c}}'') = 0.9422$, $\mathbf{a}_{\mathrm{c}}''' \cdot \mathbf{t}_{\mathrm{c}} = 0.9882$ and $\mathbf{a}_{\mathrm{c}}''' \cdot (\mathbf{t}_{\mathrm{c}} \times \mathbf{v}_{\mathrm{c}}) = -0.3164$. Unfortunately the projections of the near-cusp region onto the planes spanned by $\mathbf{t}_{\mathrm{c}}$ and $\mathbf{v}_{\mathrm{c}}$ and by $\mathbf{t}_{\mathrm{c}}$ and $\mathbf{t}_{\mathrm{c}} \times \mathbf{v}_{\mathrm{c}}$ contain swallow-tail caustics which obscure the structure of the cusp itself, so the figure shows the projections after rotating these planes by $\pi/4$. In each row the time coordinate τ ranges from -0.3 (left) to 0.3 (right) at intervals of 0.1, while $|\sigma - \sigma_a|$ ranges from -0.6 to 0.6, where σ_a is the value of σ at the apex of the arc. Varying the values of the free parameters has little effect on the overall geometry of the near-cusp region, except in certain critical cases that will be discussed in more detail in section 3.9.

Figure 3.3. Time development of a generic cusp.

To second order in τ and σ the local Lorentz factor $\lambda = (X_\tau^2)^{-1/2}$ in the vicinity of a cusp is given by

$$\lambda^{-2} = \tfrac{1}{2}(1 - \mathbf{a}' \cdot \mathbf{b}') \approx \tfrac{1}{4}(|\mathbf{a}_c''|^2 \sigma_+^2 - 2\mathbf{a}_c'' \cdot \mathbf{b}_c'' \sigma_+ \sigma_- + |\mathbf{b}_c''|^2 \sigma_-^2) \qquad (3.114)$$

and the subset of the world sheet on which λ is greater than some value $\lambda_{\min}$ is (in the limit of large λ) the interior of an ellipse in τ–σ parameter space with semi-major and semi-minor axes $s_\pm$ satisfying

$$s_\pm^2 = 2\lambda_{\min}^{-2}\left[|\mathbf{a}_c''|^2 + |\mathbf{b}_c''|^2 \pm \sqrt{(|\mathbf{a}_c''|^2 + |\mathbf{b}_c''|^2)^2 - 4|\mathbf{a}_c'' \times \mathbf{b}_c''|^2}\right]/|\mathbf{a}_c'' \times \mathbf{b}_c''|^2.$$
$$(3.115)$$

In particular, the *duration* of the cusp (the time during which $\lambda > \lambda_{\min}$ somewhere on the string) is given by

$$|\tau| < \lambda_{\min}^{-1}\rho_\tau \qquad (3.116)$$

while the equivalent inequality for the spacelike gauge coordinate σ is

$$|\sigma| < \lambda_{\min}^{-1}\rho_\sigma \qquad (3.117)$$

where

$$\rho_\tau = |\mathbf{a}_c'' \times \mathbf{b}_c''|^{-1}|\mathbf{a}_c'' + \mathbf{b}_c''| \qquad \text{and} \qquad \rho_\sigma = |\mathbf{a}_c'' \times \mathbf{b}_c''|^{-1}|\mathbf{a}_c'' - \mathbf{b}_c''| \quad (3.118)$$

are characteristic length scales associated with the cusp.

Of course, the physical radius ρ of the region in which the local Lorentz factor is greater than $\lambda_{\min}$ is proportional not to σ but rather to σ^2 (see section 2.6). At the moment at which the cusp forms (i.e. at $\tau = 0$), it follows from equations (3.6), (3.93), (3.94) and (3.114) that the physical radius is

$$\rho = \lambda_{\min}^{-2}\rho_c \qquad \text{where} \qquad \rho_c \equiv |\mathbf{a}_c'' + \mathbf{b}_c''|^{-1} = \tfrac{1}{2}|\mathbf{t}_c|^{-1}. \qquad (3.119)$$

Moreover, it is easily seen that $\rho_\sigma \geq 4\rho_c$, and so the physical radius satisfies the inequality

$$\rho \leq \tfrac{1}{4}\lambda_{\min}^{-2}\rho_\sigma. \tag{3.120}$$

In the rest frame of the string the vectors $\mathbf{a}''$ and $\mathbf{b}''$ typically have magnitudes of order L^{-1}, and so the length scales ρ_τ, ρ_σ and ρ_c are normally of order L. However, ρ_c can be substantially smaller than L at a microcusp (see below), and in the most extreme cases could be as small as the thickness of the string. For a GUT string, this core thickness would be about 10^{-29} cm, and could be as small as $10^{-50}L$ for a string of cosmological size. Another scale factor which turns out to be an important determinant of the magnitude of gravitational effects near a cusp is

$$R_c = (|\mathbf{a}_c''|^2 + |\mathbf{b}_c''|^2)^{-1/2}. \tag{3.121}$$

It is clear that $R_c \leq \rho_c$, and R_c and ρ_c are almost always of the same order. Furthermore, all four length scales dilate as $f^{-2} = \lambda_0^2(1 - \mathbf{v}_c \cdot \mathbf{v}_0)^2$ under a Lorentz boost, and so are not Lorentz-invariant.

In the case of a string loop confined to a plane, the Kibble–Turok representation consists simply of two coincident great circles on the unit sphere. Cusps are, therefore, inevitable on a planar loop without kinks. Moreover, the fact that the $\mathbf{a}'$ and $\mathbf{b}'$ curves are coincident everywhere means that the cusps are extended rather than isolated and form a closed curve with a non-trivial homotopy on the world sheet. The cusps are, therefore, either persistent features of the string, as in the example to be discussed in section 4.2.2, or occur simultaneously along a segment of the string which has momentarily been compressed to a point, as in the case of the circular loop analysed in section 4.2.1. Even more complicated behaviour is possible if the loop supports kinks, as these can both emit and absorb long-lived cusps. Examples will be given in sections 4.2.4 and 4.6.

Incidentally, if a cusp does occur as a persistent feature on a string world sheet, then (like a kink) it must propagate with the speed of light relative to the background spacetime. To see this, suppose that the trajectory of the cusp is $\sigma = \sigma_c(\tau)$ for some differentiable function σ_c. Then the cusp traces out the spatial curve
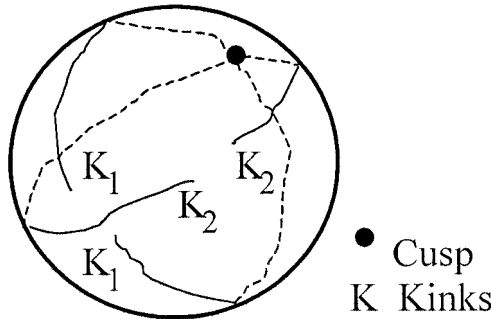
$$\mathbf{r}_c(\tau) = \tfrac{1}{2}[\mathbf{a}(\tau + \sigma_c(\tau)) + \mathbf{b}(\tau - \sigma_c(\tau))] \tag{3.122}$$

with instantaneous speed

$$|\mathbf{r}_c'(\tau)| = \tfrac{1}{2}[(1 + \sigma_c')^2 + 2(1 - \sigma_c'^2)\mathbf{a}' \cdot \mathbf{b}' + (1 - \sigma_c')^2]^{1/2} = 1 \tag{3.123}$$

as the unit vectors $\mathbf{a}'$ and $\mathbf{b}'$ are, by definition, parallel at all points on the cusp's trajectory.

So far this analysis of the Kibble–Turok sphere has focused on loops without kinks. The effect of including loops with kinks is simply to relax the requirement that the $\mathbf{a}'$ and $\mathbf{b}'$ curves be continuous. A kink corresponds to each break in either of the two curves. An example of the Kibble–Turok representation of a loop with

Figure 3.4. Kibble–Turok sphere of a loop with two kinks and one cusp.
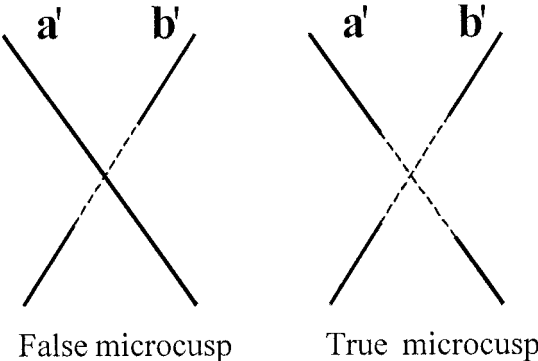
two kinks, one left-moving and one right-moving, is shown in figure 3.4. One immediate consequence of the Kibble–Turok representation is that it is clear that a loop can support any number of kinks, and there is no necessary correlation between the number of left-moving and the number of right-moving kinks.

Furthermore, as is evident from figure 3.4, once a loop develops kinks the number of cusps need no longer be even, as the $\mathbf{a}'$ and $\mathbf{b}'$ curves need not cross an even number of times. This result is slightly deceptive, however. As was indicated in section 2.7, kinks on a real string would not be true discontinuities in the tangent vectors, but narrow segments where the gradients of the tangent vectors are large but bounded. (In fact, the fields constituting a string typically do not vary on length scales smaller than the radius of the vortex, which as has been mentioned is about 10^{-29} cm for a GUT string.) As a result, a kink does not represent a real break in either the $\mathbf{a}'$ or $\mathbf{b}'$ curves, and the ends of any break are effectively joined by a segment on which either $\mathbf{a}''$ or $\mathbf{b}''$ is very large.

Since the physical dimensions of the joining segment are of the order of the Planck length, the segment is unlikely to have any detailed structure and can be represented by the great circle which joins the two ends of the kink. If a segment of this type crosses the other curve on the Kibble–Turok sphere then a special class of cusp known as a *microcusp* forms. Indeed, there are two possible types of microcusp: one where the break in one curve crosses a continuous segment of the other; and one where two breaks cross, as shown in figure 3.5.

In the first case, $\mathbf{a}''$ is very large at the microcusp but $\mathbf{b}''$ is not (or *vice versa*), and so the length scales ρ_τ and ρ_σ are, in general, not particularly small. Hence, the duration of such a microcusp is typically no smaller than that of an ordinary cusp, although the cusp radii ρ_c and R_c are much smaller than the macroscopic length scale L. This type of microcusp is a *false microcusp*.

In the second case, by contrast, both $\mathbf{a}''$ and $\mathbf{b}''$ are very large at the microcusp and both the duration and radius of the microcusp are consequently, very small. This is a *true microcusp*. In both cases, the magnitude of the separation vector $\mathbf{s}_c = \frac{1}{2}(\mathbf{a}_c''' - \mathbf{b}_c''')$ will be considerably larger than L^{-2}. As will be seen shortly,

Figure 3.5. False and true microcusps.

the energy content E_c of a cusp scales roughly as $|\mathbf{v}_c \cdot \mathbf{s}_c|^{-1/2}$ and so the energy of a microcusp is typically much smaller than that of a standard cusp. Like cusps, microcusps can be divided into two further classes (pro-microcusps and anti-microcusps) according to the relative orientation of the $\mathbf{a}'$ and $\mathbf{b}'$ curves at the point of intersection.

Examples of loops with both true and false microcusps are examined in section 4.3.

3.7   Field reconnection at a cusp

The importance of cusps for the secular evolution of a string trajectory lies in the fact that radiation from cusps is almost certainly the dominant form of energy loss for the string. A cusp typically radiates both gravitational and Higgs field energy. A more detailed discussion of gravitational radiation from cusps is given in chapter 6. The field-theoretical aspects of Higgs vortex strings lies somewhat outside the subject matter of this book but it is possible on the basis of the simple dynamical considerations outlined earlier to give an order-of-magnitude estimate of the power radiated by a cusp.

Naively, a realistic cosmic string can be visualized as a cylindrical wire with a small but non-zero radius r. Near a cusp the wire doubles back on itself and so for a brief period of time the two branches of the cylinder will overlap. It is to be expected that microphysical forces will become important in the overlapping region, and lead to the emission of particles with some characteristic total energy E_c. To estimate the size of this region, note that the separation of the two branches of the string at time $\tau = 0$ (the moment of formation of the cusp) at a given value of $|\sigma|$ is

$$|\mathbf{r}(0, \sigma) - \mathbf{r}(0, -\sigma)| \approx \tfrac{1}{6}|\mathbf{s}_c|\sigma^3 \qquad (3.124)$$

where $\mathbf{s}_c = \tfrac{1}{2}(\mathbf{a}_c''' - \mathbf{b}_c''')$ as before. If this separation distance is set equal to $2r$

then the overlap region would seem to cover the parameter range

$$|\sigma| \leq \sigma_{\mathrm{ov}} \equiv (12r/|\mathbf{s}_{\mathrm{c}}|)^{1/3} \sim r^{1/3} L^{2/3} \tag{3.125}$$

and so have a physical radius of the order of $|\mathbf{t}_{\mathrm{c}}|\sigma_{\mathrm{ov}}^2 \sim r^{2/3} L^{1/3}$. This estimate was first published in 1987 by Robert Brandenburger [Bra87].

However, as Blanco-Pillado and Olum have rightly pointed out [BPO99], this derivation of σ_{ov} neglects the effect of Lorentz contraction on the cross-sectional shape of the wire. Since the string is travelling close to the speed of light near the cusp, the wire will be elliptical in cross section rather than circular, with semi-major axis r and semi-minor axis r/λ in the direction of $\mathbf{v}_{\mathrm{c}}$, where from (3.114) the local Lorentz factor has the form

$$\lambda^{-1} \approx |\mathbf{t}_{\mathrm{c}}|\sigma. \tag{3.126}$$

Equating the component of the separation vector $\frac{1}{6}\mathbf{s}_{\mathrm{c}}\sigma^3$ in the direction of $\mathbf{v}_{\mathrm{c}}$ with the minor axis $2r/\lambda$ then gives
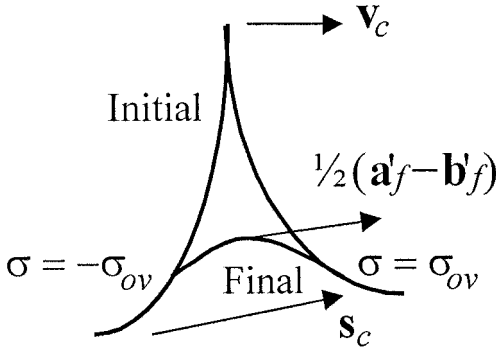
$$\sigma_{\mathrm{ov}} \approx (6r|\mathbf{t}_{\mathrm{c}}|/|\mathbf{v}_{\mathrm{c}} \cdot \mathbf{s}_{\mathrm{c}}|)^{1/2} = (6r/|\mathbf{a}_{\mathrm{c}}'' - \mathbf{b}_{\mathrm{c}}''|)^{1/2} \sim r^{1/2} L^{1/2}. \tag{3.127}$$

The corresponding physical radius $|\mathbf{t}_{\mathrm{c}}|\sigma_{\mathrm{ov}}^2$ is of order r, independently of the macroscopic length scale L. The total energy E_{c} available in the overlap region is of order $\mu\sigma_{\mathrm{ov}} \sim \mu r^{1/2} L^{1/2}$ and any particles emitted by the cusp will have Lorentz factors of the order of $|\mathbf{t}_{\mathrm{c}}|^{-1}\sigma_{\mathrm{ov}}^{-1} \sim (L/r)^{1/2}$.

The derivation of the estimate (3.127) for σ_{ov} has of course been very heuristic. A more careful analysis by Blanco-Pillado and Olum [BPO99] shows that because the velocity $\mathbf{v}$ of the string near the cusp deviates slightly from $\mathbf{v}_{\mathrm{c}}$, the minor axes of the two branches of the wire are rotated relative to $\mathbf{v}_{\mathrm{c}}$, and so the separation of the branches needs to be somewhat larger than r/λ. The corresponding value of σ_{ov} is also larger than that shown in (3.127) but nonetheless remains of order $r^{1/2} L^{1/2}$. Note that for a GUT string $r \sim 10^{-29}$ cm and $\mu \sim 10^{21}$ g/cm, and so a loop the size of a star cluster ($L \sim 10^{20}$ cm) would have $\sigma_{\mathrm{ov}} \sim 10^{-5}$ cm and a characteristic cusp energy $E_{\mathrm{c}} \sim 10^{38}$ erg, which is the mass-energy content of about 10^{17} g or, equivalently, the total energy output of the Sun over 6 h. The Lorentz factor at the boundary of the overlap region would be $\lambda_{\mathrm{min}} \sim L/\sigma_{\mathrm{ov}} \sim 10^{25}$, and the corresponding cusp duration $L/\lambda_{\mathrm{min}} \sim 10^{-16}$ s.

Provided that $r \ll L$, the field energy $E_{\mathrm{c}} \sim \mu r^{1/2} L^{1/2}$ radiated by an individual cusp will be negligibly small in comparison with the total energy μL of the string loop, and so should have minimal impact on the dynamics of the loop. For a long time it was thought that the effect of cusps on the secular evolution of a loop could be adequately approximated by assuming that the $\mathbf{a}'$ and $\mathbf{b}'$ curves would be slowly and continuously deformed by the energy loss at the cusps. This forms the basis for the 'adiabatic' approach to loop evolution, which is discussed in more detail in section 3.9.

Recently, however, Olum and Blanco-Pillado have suggested an alternative view of the dissipation of cusps that seems to have been vindicated by lattice

Figure 3.6. Reconnection at a cusp.

field theory simulations of Higgs vortex strings [OBP99]. According to the
'overlap' model, the field energy that can be released at a cusp is contained in the
circumcusp region $|\sigma| \leq \sigma_{ov}$ where the two branches of the string overlap. One
simple way to model this energy release is to assume that the entire circumcusp
region is excised from the string and replaced with a smooth segment joining the
two points $\mathbf{r}(0, -\sigma_{ov})$ and $\mathbf{r}(0, \sigma_{ov})$, as in figure 3.6. The modified trajectory
then evolves according to the usual Nambu–Goto equations of motion (3.1) until
another cusp appears and the process of excision and reconnection is repeated.
Although obviously an idealization, this routine provides a reasonable schematic
description of the mechanism of cusp dissipation in Olum and Blanco-Pillado's
simulations.

To generate a more precise description of the reconnection process, suppose
as before that the cusp appears at $\tau = \sigma = 0$, and let the mode functions
be $\mathbf{a}_i(\sigma_+)$ and $\mathbf{b}_i(\sigma_-)$ for $\tau < 0$, and $\mathbf{a}_f(\sigma_+)$ and $\mathbf{b}_f(\sigma_-)$ for $\tau > 0$. During
reconnection a smooth bridging segment appears to replace the branches of the
string that previously occupied the parameter range $|\sigma| \leq \sigma_{ov}$. The details of the
process of evaporation and reconnection will, of course, depend on field-theoretic
considerations that are outside the scope of the present analysis. However, it
is possible to sketch out the salient features of the process by making a few
simplifying assumptions.

First of all, since the evaporation of the circumcusp region presumably
proceeds from the cusp downwards, it seems reasonable to assume that each point
on this part of the string snaps back to the bridging segment under the action of the
unbalanced string tension, and so the position vector $\mathbf{r}_f$ of the bridging segment
satisfies

$$\mathbf{r}_f(\sigma) = \mathbf{r}_i(\sigma) + q(\sigma)\mathbf{r}_i'(\sigma) \tag{3.128}$$

where $\mathbf{r}_i$ is the position vector before reconnection, and q is some scalar function
with $q(\pm\sigma_{ov}) = 0$. Also, if it is assumed that the reconnection process is
minimally inelastic then the components of the velocity $\mathbf{v}_f$ of the bridging segment

transverse to the bridge will be the same as the corresponding components of the initial velocity $\mathbf{v}_i$, and so

$$\mathbf{v}_f(\sigma) = \mathbf{v}_i(\sigma) - [\mathbf{v}_i(\sigma) \cdot \mathbf{r}_f'(\sigma)]|\mathbf{r}_f'(\sigma)|^{-2}\mathbf{r}_f'(\sigma). \tag{3.129}$$

Now, the original gauge coordinate σ will not, in general, retain its role as an aligned standard gauge coordinate on the bridging segment. In fact, according to (3.67) the new spacelike coordinate $\overline{\sigma}$ in the aligned standard gauge is given by

$$\frac{d\overline{\sigma}}{d\sigma} = |\mathbf{r}_f'|/\sqrt{1 - |\mathbf{v}_f|^2} \equiv |\mathbf{r}_f'|^2[|\mathbf{r}_i'|^2|\mathbf{r}_f'|^2 + q^2(\mathbf{v}_i \cdot \mathbf{r}_i'')^2]^{-1/2} \tag{3.130}$$

where all terms on the right are understood to be functions of σ, and

$$|\mathbf{r}_f'|^2 = (1 + q')^2|\mathbf{r}_i'|^2 + 2q(1 + q')(\mathbf{r}_i \cdot \mathbf{r}_i'') + q^2|\mathbf{r}_i''|^2. \tag{3.131}$$

In particular, the total energy of the bridging segment is

$$\Delta E_f = \mu \Delta\overline{\sigma} = \mu \int_{-\sigma_{ov}}^{\sigma_{ov}} |\mathbf{r}_f'|^2[|\mathbf{r}_i'|^2|\mathbf{r}_f'|^2 + q^2(\mathbf{v}_i \cdot \mathbf{r}_i'')^2]^{-1/2} \, d\sigma \tag{3.132}$$

while from (3.70) and (3.71) the reconnected mode functions are

$$\mathbf{a}_f'(\overline{\sigma}) = \mathbf{v}_i + |\mathbf{r}_f'|^{-2}\{[|\mathbf{r}_i'|^2|\mathbf{r}_f'|^2 + q^2(\mathbf{v}_i \cdot \mathbf{r}_i'')^2]^{1/2} - q(\mathbf{v}_i \cdot \mathbf{r}_i'')\}\mathbf{r}_f' \tag{3.133}$$

and

$$\mathbf{b}_f'(-\overline{\sigma}) = \mathbf{v}_i - |\mathbf{r}_f'|^{-2}\{[|\mathbf{r}_i'|^2|\mathbf{r}_f'|^2 + q^2(\mathbf{v}_i \cdot \mathbf{r}_i'')^2]^{1/2} + q(\mathbf{v}_i \cdot \mathbf{r}_i'')\}\mathbf{r}_f'. \tag{3.134}$$

The undetermined function q can be fixed by minimizing the total energy ΔE_f. It is evident from (3.130) that the bridging segment which minimizes ΔE_f is likely to approximate closely a straight-line segment from $\mathbf{r}_i(-\sigma_{ov})$ to $\mathbf{r}_i(\sigma_{ov})$, as this minimizes the physical distance $\int |\mathbf{r}_f'| \, d\sigma$. In fact, if the near-cusp expansions

$$\mathbf{r}_i(\sigma) \approx \tfrac{1}{2}\mathbf{t}_c\sigma^2 + \tfrac{1}{6}\mathbf{s}_c\sigma^3 \tag{3.135}$$

and

$$\mathbf{v}_i(\sigma) \approx \mathbf{v}_c + \mathbf{u}_c\sigma \qquad (\text{with } \mathbf{u}_c \equiv \tfrac{1}{2}(\mathbf{a}_c'' - \mathbf{b}_c'')) \tag{3.136}$$

are inserted into (3.132) then, to leading order in $\sigma_{ov}/L \sim (r/L)^{1/2}$,

$$\Delta E_f = \mu \int_{-\sigma_{ov}}^{\sigma_{ov}} [(1 + q')\sigma + q]^2\{\sigma^2[(1 + q')\sigma + q]^2 + \kappa^2\sigma^2q^2\}^{-1/2} \, d\sigma \tag{3.137}$$

where $\kappa = \tfrac{1}{2}(\mathbf{s}_c \cdot \mathbf{v}_c)/|\mathbf{t}_c|^2$ is a dimensionless parameter. It is clear that at this level of approximation ΔE_f will be minimized if $(1 + q')\sigma + q = 0$, which, in turn, gives

$$q(\sigma) = \tfrac{1}{2}(\sigma_{ov}^2 - \sigma^2)/\sigma. \tag{3.138}$$

From (3.128) it can be seen that the corresponding bridging segment has the form

$$\mathbf{r}_f(\sigma) = \tfrac{1}{2}\mathbf{t}_c\,\sigma_{ov}^2 + \tfrac{1}{4}\mathbf{s}_c(\sigma_{ov}^2 - \tfrac{1}{3}\sigma^2)\sigma \qquad (3.139)$$

and so is geometrically straight as suggested.

In the lattice field theory simulation published by Olum and Blanco-Pillado [OBP99] the bridging segment is indeed approximately straight over the middle two-thirds of its length but bends over near the boundary of the overlap region to match smoothly onto the exterior string trajectory. Since the length $\tfrac{1}{6}|\mathbf{s}_c|\sigma_{ov}^3$ of the bridging segment is, by definition, of roughly the same size as the boosted string thickness r/λ at the boundary of the overlap region, the smoothing effects of the non-zero string thickness are presumably independent of the ratio L/r (which for reasons of limited resolution is set at only 15 in the simulation). Thus the straight-line approximation (3.139) is a fairly crude one, although it is probably the best that can be offered in the absence of additional assumptions about the nature of the underlying fields.

If the bridging segment is assumed to be straight then the new spacelike coordinate $\overline{\sigma}$ is given by

$$\overline{\sigma} = \int \tfrac{1}{4}|\mathbf{v}_c \cdot \mathbf{s}_c|^{-1}|\mathbf{s}_c|^2(\sigma_{ov}^2 - \sigma^2)\,\mathrm{d}\sigma = \tfrac{1}{4}|\mathbf{v}_c \cdot \mathbf{s}_c|^{-1}|\mathbf{s}_c|^2(\sigma_{ov}^2 - \tfrac{1}{3}\sigma^2)\sigma \quad (3.140)$$

and, in particular, the total energy of the bridge is

$$\Delta E_f = \mu\Delta\overline{\sigma} = \tfrac{\mu}{3}|\mathbf{v}_c \cdot \mathbf{s}_c|^{-1}|\mathbf{s}_c|^2\sigma_{ov}^3. \qquad (3.141)$$

Note here that $\Delta E_f \sim \mu r(r/L)^{1/2}$ is for a cosmological string a negligible fraction of the original cusp energy $E_c \sim \mu r(L/r)^{1/2}$.

Also, at this level of approximation the new mode functions $\mathbf{a}_f'$ and $\mathbf{b}_f'$ are extremely simple, as

$$\mathbf{a}_f' \approx \mathbf{v}_c + (|\mathbf{v}_c \cdot \mathbf{s}_c| - \mathbf{v}_c \cdot \mathbf{s}_c)|\mathbf{s}_c|^{-2}\mathbf{s}_c \qquad (3.142)$$
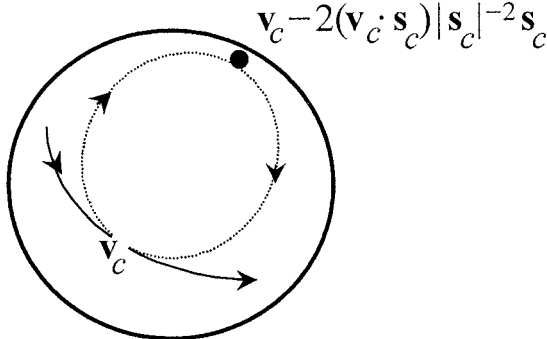
and

$$\mathbf{b}_f' \approx \mathbf{v}_c - (|\mathbf{v}_c \cdot \mathbf{s}_c| + \mathbf{v}_c \cdot \mathbf{s}_c)|\mathbf{s}_c|^{-2}\mathbf{s}_c. \qquad (3.143)$$

It was seen in (3.96) that $\mathbf{v}_c \cdot \mathbf{s}_c = \tfrac{1}{2}(|\mathbf{b}_c''|^2 - |\mathbf{a}_c''|^2)$, and so if $|\mathbf{b}_c''| > |\mathbf{a}_c''|$ the mode functions reconnect over the range $|\sigma| < \sigma_{ov}$ with

$$\mathbf{a}_f' \approx \mathbf{v}_c \qquad \text{and} \qquad \mathbf{b}_f' \approx \mathbf{v}_c - 2|\mathbf{v}_c \cdot \mathbf{s}_c||\mathbf{s}_c|^{-2}\mathbf{s}_c. \qquad (3.144)$$

That is, the mode function $\mathbf{a}'$ is essentially unchanged on the bridging segment but the mode function $\mathbf{b}'$ jumps from the neighbourhood of $\mathbf{v}_c$ at $\sigma = -\sigma_{ov}$ to the point $\mathbf{v}_c - 2(\mathbf{v}_c \cdot \mathbf{s}_c)|\mathbf{s}_c|^{-2}\mathbf{s}_c$ on the Kibble–Turok sphere and then back to $\mathbf{v}_c$ at $\sigma = \sigma_{ov}$, as shown in figure 3.7. In particular, if the cusp is boosted into a frame in which $\mathbf{s}_c$ is parallel to $\mathbf{v}_c$ then (since $\mathbf{v}_c \cdot \mathbf{s}_c > 0$ by assumption) $\mathbf{b}'$ jumps from $\mathbf{v}_c$ to the antipodal point $-\mathbf{v}_c$ and back again. If, on the other hand,

Figure 3.7. Reconnection on the Kibble–Turok sphere.

$|\mathbf{b}_c''| < |\mathbf{a}_c''|$ then the mode function $\mathbf{b}'$ remains unchanged and it is the mode function $\mathbf{a}'$ that reconnects through the point $\mathbf{v}_c - 2(\mathbf{v}_c \cdot \mathbf{s}_c)|\mathbf{s}_c|^{-2}\mathbf{s}_c$.

In physical terms this means that the cusp evaporates to leave a pair of co-moving kinks separated by such a small gauge distance $\Delta\bar{\sigma} \sim (\sigma_{ov}/L)^3$ that they are effectively indistinguishable and together constitute a fundamentally new feature: a *reversing segment* propagating around the string at the speed of light. The new parametric period $L' = L + \Delta\bar{\sigma} - 2\sigma_{ov}$ will, of course, be negligibly smaller than L if the string is cosmological, and at intervals of $L'/2$ the reversing segment will develop into a cusplike feature with a maximum Lorentz factor $|\mathbf{t}_c|^{-1}\sigma_{ov}^{-1} \sim (L/r)^{1/2}$. It was seen earlier that $(L/r)^{1/2}$ could easily be as high as 10^{25} for a cosmological string, so this *truncated cusp* retains many of the extreme conditions characteristic of a true cusp, although it is much less energetic and is presumably stable to the emission of Higgs field energy.

Finally, mention should be made of the effects of cusp evaporation on the total momentum of the string. To leading order in σ_{ov}/L the momentum of the excised segment is

$$\Delta\mathbf{p}_i \approx 2\mu\mathbf{v}_c\sigma_{ov} \tag{3.145}$$

whereas the momentum of the bridging segment is

$$\Delta\mathbf{p}_f \approx \tfrac{\mu}{3}|\mathbf{s}_c \cdot \mathbf{v}_c|^{-1}[|\mathbf{s}_c|^2\mathbf{v}_c - (\mathbf{v}_c \cdot \mathbf{s}_c)\mathbf{s}_c]\sigma_{ov}^3. \tag{3.146}$$

The difference $\Delta\mathbf{p}_i - \Delta\mathbf{p}_f$ is the momentum of the radiated cusp energy, which for a cosmological string is effectively just $\Delta\mathbf{p}_i$. Thus, not surprisingly, the evaporation of the cusp boosts the loop in the direction of $-\mathbf{v}_c$.

3.8 Self-intersection of a string loop

Another property of a string loop which is potentially just as important for the evolution of a cosmological string network as the number of cusps or kinks is

the number of times the loop intersects itself during an oscillation period. It was mentioned in section 2.7 that when two segments of a string cross they almost invariably intercommute. A loop with a large number of self-intersections would, therefore, quickly disintegrate into a profusion of daughter loops, many of them moving at high bulk velocities relative to the centre-of-momentum frame of the original loop. It is through this mechanism that numerical simulations of primordial string networks rapidly become dominated by small, high-velocity loops.

In the aligned standard gauge, a string loop intersects itself whenever the position function $\mathbf{r}(\tau, \sigma)$ coincides for two separate values of σ; that is, whenever

$$\mathbf{a}(\tau + \sigma_1) + \mathbf{b}(\tau - \sigma_1) = \mathbf{a}(\tau + \sigma_2) + \mathbf{b}(\tau - \sigma_2) \qquad (3.147)$$

for distinct values σ_1 and σ_2 (modulo the parametric period L). If the loop then intercommutes, it will break into two daughter loops, one with parametric range $\sigma_+ \in [\tau + \sigma_1, \tau + \sigma_2]$ and $\sigma_- \in [\tau - \sigma_2, \tau - \sigma_1]$ and the other with parametric range $\sigma_+ \in [\tau + \sigma_2, \tau + \sigma_1]$ and $\sigma_- \in [\tau - \sigma_1, \tau - \sigma_2]$ (all modulo L). In terms of the Kibble–Turok representation, the $\mathbf{a}'$ and $\mathbf{b}'$ curves of the original loop are each broken into two segments, and the two daughter loops each inherit one segment from each curve. Clearly, both daughter loops support at least one left-moving and one right-moving kink, corresponding to the ends of the two inherited segments.

The total 4-momenta of the two daughter loops in the original loop's centre-of-momentum frame are easily calculated and (if $\sigma_2 > \sigma_1$) reduce to

$$P_{(1)}^\mu = \mu[\sigma_2 - \sigma_1, \mathbf{a}(\tau + \sigma_2) - \mathbf{a}(\tau + \sigma_1)] \qquad (3.148)$$

and
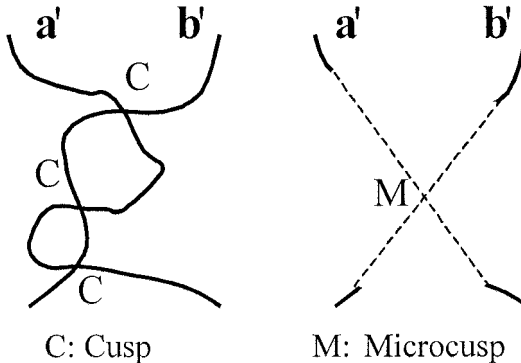
$$P_{(2)}^\mu = \mu[L - (\sigma_2 - \sigma_1), -\mathbf{a}(\tau + \sigma_2) + \mathbf{a}(\tau + \sigma_1)]. \qquad (3.149)$$

Thus, although the spatial components of the momenta balance exactly, the energies of the two daughter loops emerge in the ratio $L - (\sigma_2 - \sigma_1) : \sigma_2 - \sigma_1$, and are by no means necessarily equal. Similarly, the bulk velocities of the daughter loops are

$$\mathbf{V}_{(1)} = \frac{\mathbf{a}(\tau + \sigma_2) - \mathbf{a}(\tau + \sigma_1)}{\sigma_2 - \sigma_1} \qquad \text{and} \qquad \mathbf{V}_{(2)} = \frac{-\mathbf{a}(\tau + \sigma_2) + \mathbf{a}(\tau + \sigma_1)}{L - (\sigma_2 - \sigma_1)}$$
$$(3.150)$$

and although they are guaranteed by the mean-value theorem to be subluminal, they do not, in general, add to zero. In particular, if $\sigma_2 - \sigma_1 \ll L$ then one of the daughter loops is slow moving and retains most of the energy of the original loop, while the other is small and moves off at near-light speed.

The fact that the Kibble–Turok representation of a daughter loop after self-intersection consists simply of segments from the two curves on the parent Kibble–Turok sphere indicates that new cusps cannot be created by self-intersection. If a particular cusp is inherited by one of the daughter loops, it will not appear on the other daughter. Indeed, if two segments which cross
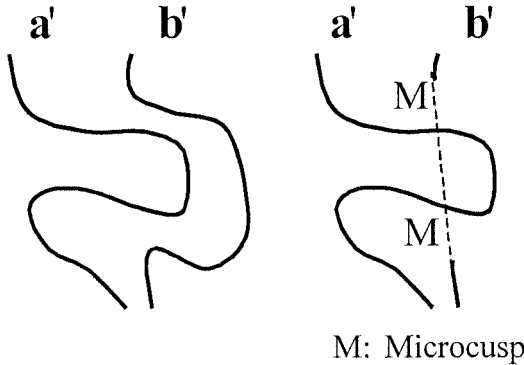
Figure 3.8. Three cusps replaced by a microcusp.

on the parent sphere are inherited separately by the two daughter loops, the corresponding cusp will disappear altogether. Since a similar argument also applies to the intersection of segments from different loops, it might seem that the process of intercommuting would act to quickly destroy any cusps that were originally supported by the string network.

However, it must be remembered that each cusp that disappears during an intersection event is typically replaced by a microcusp on *both* daughter loops, as the gaps in the curves on the Kibble–Turok spheres of the daughter loops are not true discontinuities. Similarly, if a cusp is inherited by one of the daughter loops, a corresponding microcusp is inherited by the other. As a result, the total number of cusps *and* microcusps generally doubles with each generation of daughter loops [Gar88]. The doubling need not be exact, however, as there is no strict correspondence between excised cusps and the microcusps that replace them. For example, if two tangled segments of the $\mathbf{a}'$ and $\mathbf{b}'$ curves which intersect one another a number of times are replaced by kinks, the resulting great circle segments can intersect one another (and so form a microscusp) at most once (see figure 3.8). Conversely, if the $\mathbf{a}'$ and $\mathbf{b}'$ curves contain neighbouring convoluted segments which do not cross, and one of the segments is replaced by a kink, it is possible that two or more false microcusps will be created (see figure 3.9). Nonetheless, even if the total number of cusps and microcusps on the daughter loop differs from that of the parent loop, the difference is always an even integer.

The inclusion of gravitational back-reaction from string loops is thought to complicate the relationship between cusps and microcusps even further. It was seen earlier that the curvature of the world sheet is extremely high on the locus of a kink. It is believed that gravitational radiation from a string loop would be driven preferentially by regions of high curvature, and would, therefore, act to broaden any kinks (in the sense that the local magnitude of $\mathbf{a}''$ or $\mathbf{b}''$ would gradually be reduced to its characteristic value L^{-1}: see section 6.11 for a more detailed discussion). As a consequence, any microcusps on a loop would also be

M: Microcusp

Figure 3.9. Creation of a pair of microcusps.

broadened by gravitational dissipation, and would eventually become true cusps, which, in turn, would quickly evaporate to form truncated cusps. Overall, it seems likely that, in the words of David Garfinkle, 'kinkless loops with cusps' would be more generic than 'cuspless kinky loops' [Gar88]. (However, numerical solutions have, to date, been more supportive of the converse view: see section 6.9.2.)

Since the occurrence of a self-intersection is determined by the properties of the functions **a** and **b** rather than their derivatives, the Kibble–Turok sphere is of itself little help in analysing the dynamics of self-intersection. However, Andreas Albrecht and Thomas York have devised a simple extension of the Kibble–Turok formalism which is particularly adapted to the question of whether a given loop intersects itself [AY88]. Given any solution of the equation of motion and a positive constant $\Delta < L$, we can define

$$\mathbf{a}_\Delta(\sigma_+) = \frac{1}{\Delta}[\mathbf{a}(\sigma_+ + \Delta) - \mathbf{a}(\sigma_+)] \tag{3.151}$$

and

$$\mathbf{b}_\Delta(\sigma_-) = \frac{1}{\Delta}[\mathbf{b}(\sigma_-) - \mathbf{b}(\sigma_- - \Delta)]. \tag{3.152}$$

Note that $|\mathbf{a}_\Delta|$ and $|\mathbf{b}_\Delta|$ are bounded above by 1. Hence, as σ_+ and σ_- vary from 0 to L the functions $\mathbf{a}_\Delta$ and $\mathbf{b}_\Delta$ trace out closed curves inside the Kibble–Turok sphere. Furthermore, as Δ tends to 0, $\mathbf{a}_\Delta \to \mathbf{a}'$ and $\mathbf{b}_\Delta \to \mathbf{b}'$, while as Δ tends to L, the curves defined by $\mathbf{a}_\Delta$ and $\mathbf{b}_\Delta$ both shrink to the origin of the sphere[2]. Thus, as Δ varies from 0 to L, the curves traced out by $\mathbf{a}_\Delta$ and $\mathbf{b}_\Delta$ generate two surfaces which stretch across the Kibble–Turok sphere and are bounded by the $\mathbf{a}'$ and $\mathbf{b}'$ curves respectively. I will call these surfaces $\mathfrak{A}$ and $\mathfrak{B}$, and the sub-surfaces interior to $\mathbf{a}_\Delta$ and $\mathbf{b}_\Delta$ will be denoted $\mathfrak{A}_\Delta$ and $\mathfrak{B}_\Delta$.

---

[2] Strictly speaking, this is true only in the centre-of-momentum frame of the loop. In a more general frame, the $\mathbf{a}_\Delta$ and $\mathbf{b}_\Delta$ curves shrink to the point inside the sphere which corresponds to the bulk velocity **V**, as can be seen from (3.11).

A self-intersection of a string loop occurs whenever $\mathbf{a}_\Delta(\sigma_+) = \mathbf{b}_\Delta(\sigma_-)$ for some combination of the values of σ_+, σ_- and Δ. At a geometric level, each self-intersection corresponds to a point where the $\mathbf{a}_\Delta$ and $\mathbf{b}_\Delta$ curves cross for some value of Δ. By virtue of the periodicity of the mode functions $\mathbf{a}$ and $\mathbf{b}$ (in the centre-of-momentum frame), the functions $\mathbf{a}_\Delta$ and $\mathbf{b}_\Delta$ satisfy the complementarity relations

$$\Delta\mathbf{a}_\Delta(\sigma_+) = -(L - \Delta)\mathbf{a}_{L-\Delta}(\sigma_+ + \Delta) \qquad (3.153)$$

and

$$\Delta\mathbf{b}_\Delta(\sigma_-) = -(L - \Delta)\mathbf{b}_{L-\Delta}(\sigma_- - \Delta). \qquad (3.154)$$

Hence, whenever the curves $\mathbf{a}_\Delta$ and $\mathbf{b}_\Delta$ cross, the complementary curves $\mathbf{a}_{L-\Delta}$ and $\mathbf{b}_{L-\Delta}$ also cross. This is a reflection of the fact that if the loop breaks into two at a self-intersection, one of the daughter loops will have a parametric period Δ and the other a parametric period $L - \Delta$. Furthermore, as was seen earlier, the bulk velocities of the two daughter loops are just $\mathbf{a}_\Delta(\sigma_+)$ and $\mathbf{a}_{L-\Delta}(\sigma_+ + \Delta)$, respectively.

For the purposes of the following analysis, it is convenient to assume for the moment that a loop does not fragment when it intersects itself. In principle, therefore, a given loop can intersect itself any number of times during the course of an oscillation period. The total number of self-intersections is calculated by simply counting the number of times the $\mathbf{a}_\Delta$ and $\mathbf{b}_\Delta$ curves cross as Δ varies from 0 to $L/2$. This number, in turn, is related to the linking number $Y(\Delta)$ of the $\mathbf{a}_\Delta$ and $\mathbf{b}_\Delta$ curves. The linking number of $\mathbf{a}_\Delta$ and $\mathbf{b}_\Delta$ is the number of times the curve $\mathbf{b}_\Delta$ passes through the sub-surface $\mathfrak{A}_\Delta$ in the direction of the outward normal to $\mathfrak{A}_\Delta$ minus the number of times $\mathbf{b}_\Delta$ passes through $\mathfrak{A}_\Delta$ in the opposite direction, where the outward normal on $\mathfrak{A}_\Delta$ is defined relative to the orientation of the curve $\mathbf{a}_\Delta$ that bounds $\mathfrak{A}_\Delta$. At values of Δ which correspond to a self-intersection of the string loop, the linking number Y is discontinuous, and jumps by 1.

Just as cusps and microcusps can be assigned a polarity, the concept of linking number allows self-intersections to be divided into two classes according to whether Y jumps by $+1$ or -1 as Δ increases through its value at the self-intersection. The change in Y at the jump will be referred to as the *polarity* h_{si} of the self-intersection. As will be seen shortly, self-intersections do not always occur in pairs like cusps but they can be created and destroyed in pairs.

For small values of Δ, the value of the linking number on a kinkless loop is determined solely by the properties of the cusps. This is because $\mathbf{a}_\Delta$ and $\mathbf{b}_\Delta$ tend to $\mathbf{a}'$ and $\mathbf{b}'$ as $\Delta \to 0$, and so the curve $\mathbf{b}_\Delta$ can only pass through the surface $\mathfrak{A}_\Delta$ in the neighbourhood of a point where the curves $\mathbf{a}'$ and $\mathbf{b}'$ cross. From the expansions (3.93) and (3.94) of the mode functions near a cusp, it follows that

$$\mathbf{a}_\Delta \approx \mathbf{v}_c + \tfrac{1}{2}\mathbf{a}_c''\Delta + \tfrac{1}{6}\mathbf{a}_c'''\Delta^2 \qquad \text{and} \qquad \mathbf{b}_\Delta \approx \mathbf{v}_c - \tfrac{1}{2}\mathbf{b}_c''\Delta + \tfrac{1}{6}\mathbf{b}_c'''\Delta^2 \quad (3.155)$$

for small values of Δ, and so

$$|\mathbf{a}_\Delta|^2 \approx 1 - \tfrac{1}{12}|\mathbf{a}_c''|^2\Delta^2 \qquad \text{and} \qquad |\mathbf{b}_\Delta|^2 \approx 1 - \tfrac{1}{12}|\mathbf{b}_c''|^2\Delta^2. \qquad (3.156)$$

Hence, the curve $\mathbf{b}_\Delta$ passes inside $\mathbf{a}_\Delta$, and so passes through $\mathfrak{A}_\Delta$, only if $|\mathbf{b}_c''| > |\mathbf{a}_c''|$. Furthermore, it is easily verified that if $\mathbf{b}_\Delta$ does pass through $\mathfrak{A}_\Delta$ it passes through in the direction of the outward normal if $(\mathbf{a}_c'' \times \mathbf{b}_c'') \cdot \mathbf{a}_c' > 0$, and in the opposite direction otherwise. As a result, the linking number for small Δ is

$$Y(0^+) = \sum_{\text{cusps}} f_c g_c \qquad (3.157)$$

where

$$f_c = \begin{cases} 1 & \text{if } |\mathbf{b}_c''| > |\mathbf{a}_c''| \\ 0 & \text{if } |\mathbf{b}_c''| < |\mathbf{a}_c''| \end{cases} \qquad (3.158)$$

and the factor g_c is equal to $+1$ at a cusp and -1 at an anti-cusp.

If the loop supports kinks, equation (3.157) needs to be generalized to include microcusps. In the limit as $\Delta \to 0$, the curves $\mathbf{a}_\Delta$ and $\mathbf{b}_\Delta$ do not tend to segments of great circles at a kink but rather to straight-line segments which join the two ends of the kink and pass through the interior of the unit sphere. If $\delta\mathbf{a}'$ and $\delta\mathbf{b}'$ denote the jump in $\mathbf{a}'$ or $\mathbf{b}'$ across a kink, a straight-line segment on $\mathbf{b}_\Delta$ will pass inside a straight-line segment on $\mathbf{a}_\Delta$ at a true microcusp only if $|\delta\mathbf{b}'| > |\delta\mathbf{a}'|$. At a false microcusp, only one of the two curves is discontinuous but if $\delta\mathbf{a}'$ or $\delta\mathbf{b}'$ is defined to be zero on the continuous curve, it is again the case that $\mathbf{b}_\Delta$ passes inside $\mathbf{a}_\Delta$ if $|\delta\mathbf{b}'| > |\delta\mathbf{a}'|$. Hence, equation (3.157) can be extended to loops with kinks by summing over all microcusps as well as cusps, and setting

$$f_c = \begin{cases} 1 & \text{if } |\delta\mathbf{b}_c'| > |\delta\mathbf{a}_c'| \\ 0 & \text{if } |\delta\mathbf{b}_c'| < |\delta\mathbf{a}_c'| \end{cases} \qquad (3.159)$$

at each microcusp. As for cusps, the factor g_c is equal to $+1$ at a microcusp and -1 at an anti-microcusp.

Consider now the second limit $\Delta = L/2$. According to the complementarity relations (3.153) and (3.154),

$$\mathbf{a}_{L/2}(\sigma_+) = -\mathbf{a}_{L/2}(\sigma_+ + L/2) \qquad \text{and} \qquad \mathbf{b}_{L/2}(\sigma_-) = -\mathbf{b}_{L/2}(\sigma_- - L/2) \qquad (3.160)$$

and so the curves $\mathbf{a}_{L/2}$ and $\mathbf{b}_{L/2}$ are symmetric about the origin. This means that each time $\mathbf{b}_{L/2}$ passes through the surface $\mathfrak{A}_{L/2}$ in one direction, it will pass through it in the opposite direction half a period later, and, therefore, that $Y(L/2) = 0$. Consequently, as Δ increases from 0 to $L/2$, the linking number Y varies from the value $Y(0^+)$ to 0. Since each jump in Y corresponds to a self-intersection, and Y need not be a monotonic function of Δ (as the curves $\mathbf{a}_\Delta$ and $\mathbf{b}_\Delta$ can cross any even number of times as Δ varies from 0 to $L/2$ without

affecting the net change in Y, provided that the total polarity of the corresponding self-intersections is zero), it follows that

$$\text{total number of self-intersections} = \left| \sum_{\text{cusps}} f_c g_c \right| + 2N \qquad (3.161)$$

where N is a non-negative integer. An equivalent restatement of this result is that the sum of the polarities of the self-intersections satisfies

$$\sum_{\text{self-intersections}} h_{si} = - \sum_{\text{cusps}} f_c \, g_c. \qquad (3.162)$$

If a loop does break into two at a self-intersection, this analysis can in principle be repeated to determine whether either of the daughter loops will intersect itself. Since the Kibble–Turok representation of each daughter loop consists of segments from the $\mathbf{a}'$ and $\mathbf{b}'$ curves on the parent Kibble–Turok sphere, the functions $\mathbf{a}_\Delta$ and $\mathbf{b}_\Delta$ on the daughter loops are closely related to their analogues on the parent loop. One difference is that as the increment Δ approaches the parametric period of the daughter loop, the corresponding $\mathbf{a}_\Delta$ and $\mathbf{b}_\Delta$ curves shrink to the point $\mathbf{V}$ representing the bulk velocity of the daughter loop rather than to the origin but this does not materially affect the analysis.

To be definite, suppose that a self-intersection occurs at the points $\tau = \sigma = 0$ and $\tau = 0$, $\sigma = \Delta^*$ on the parent loop, and consider the daughter loop that inherits the segments $\sigma_+ \in [0, \Delta^*]$ and $\sigma_- \in [-\Delta^*, 0]$. If $\overline{\mathbf{a}}_\Delta$ and $\overline{\mathbf{b}}_\Delta$ denote the anologues of the functions $\mathbf{a}_\Delta$ and $\mathbf{b}_\Delta$ on the daughter loop then

$$\overline{\mathbf{a}}_\Delta(\sigma_+) = \begin{cases} \mathbf{a}_\Delta(\sigma_+) \\ \Delta^{-1}[\mathbf{a}(\sigma_+ + \Delta - \Delta^*) - \mathbf{a}(\sigma_+) + \mathbf{a}(\Delta^*) - \mathbf{a}(0)] \end{cases} \qquad (3.163)$$

for $0 < \sigma_+ < \Delta^* - \Delta$ and $\Delta^* - \Delta < \sigma_+ < \Delta^*$ respectively; and

$$\overline{\mathbf{b}}_\Delta(\sigma_+) = \begin{cases} \mathbf{b}_\Delta(\sigma_-) \\ \Delta^{-1}[\mathbf{b}(\sigma_-) - \mathbf{b}(\sigma_- + \Delta^* - \Delta) + \mathbf{b}(0) - \mathbf{b}(-\Delta^*)] \end{cases} \qquad (3.164)$$

for $\Delta - \Delta^* < \sigma_- < 0$ and $-\Delta^* < \sigma_- < \Delta - \Delta^*$ respectively. Note that the loop remains connected at the kink points $\sigma_+ = 0, \Delta^*$ and $\sigma_- = -\Delta^*, 0$, as $\mathbf{b}(0) - \mathbf{b}(-\Delta^*) = \mathbf{a}(\Delta^*) - \mathbf{a}(0)$.

A self-intersection can, therefore, appear on the daughter loop in one of two ways: either (i) $\mathbf{a}_\Delta(\sigma_+) = \mathbf{b}_\Delta(\sigma_-)$ for some choice of $\sigma_+ \in [0, \Delta^* - \Delta]$ and $\sigma_- \in [\Delta - \Delta^*, 0]$; or (ii)

$$\mathbf{a}(\sigma_+ + \Delta) - \mathbf{a}(\sigma_+) = \mathbf{b}(\sigma_-) - \mathbf{b}(\sigma_- + \Delta^* - \Delta) + \mathbf{b}(0) - \mathbf{b}(-\Delta^*) \quad (3.165)$$

for some choice of $\sigma_+ \epsilon [0, \Delta^* - \Delta]$ and $\sigma_- \epsilon [-\Delta^*, \Delta - \Delta^*]$. In the first case, the daughter loop inherits a self-intersection from its parent, in the sense that if the parent loop had not fragmented at time $\tau = 0$ the segment constituting the

daughter loop would, in any case, have intersected itself before $\tau = \Delta^*/2$ (the time required for the two kinks to each propagate halfway around the segment). The second case corresponds to an entirely new self-intersection.
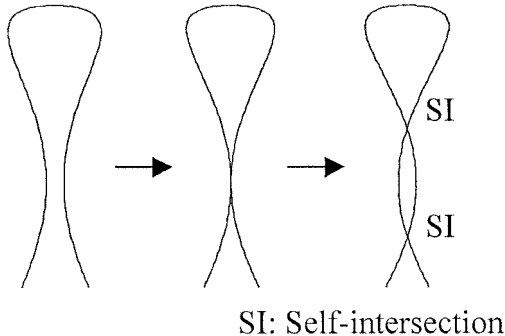
An alternative way of exploring the connection between the number of self-intersections on a parent loop and its daughter loops is to compare the boundary linking numbers $Y(0^+)$. Any cusps or microcusps that are inherited directly from the parent loop would make an unchanged contribution to $Y(0^+)$ on the daughter loop. However, the segments excised from the $\mathbf{a}'$ and $\mathbf{b}'$ curves as a result of the fragmentation are replaced by one or more microcusps on the daughter loop, and there seems to be no general rule governing the change this induces in $Y(0^+)$. Sample solutions indicate that the value of $Y(0^+)$ on a daughter loop can be larger or smaller than, or equal to, the boundary linking number on the parent loop. Similarly, there is no obvious rule relating the sum of $Y(0^+)$ over all daughter loops to the value of $Y(0^+)$ on the parent loop.

3.9   Secular evolution of a string loop
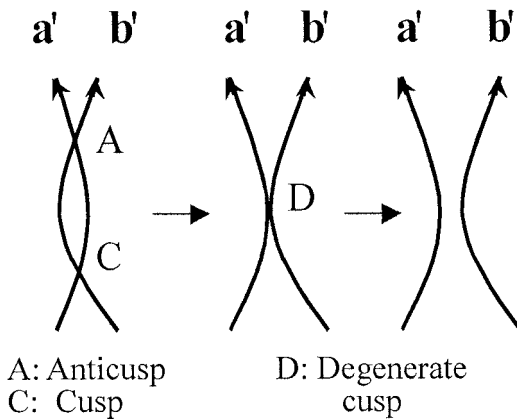
A loop of cosmic string in a cosmological background or in the vicinity of a gravitating object will not move according to the flat-space solution (3.6) but will, in general, be subject to more complicated dynamics (see chapter 5). However, if the external perturbation is sufficiently weak the Kibble–Turok formalism and its extension to self-intersections can be used to place constraints on the possible evolution of the loop. The critical assumption is that the background metric is close to flat and the evolution of the loop can be represented by continuous deformations of the $\mathbf{a}'$ and $\mathbf{b}'$ curves on the surface of the Kibble–Turok sphere. It was seen in section 3.7 that this assumption breaks down whenever a cusp evaporates but if it is understood that any cusps on a string loop would, in reality, be truncated and presumably stable to the emission of Higgs field energy then the assumption remains reasonable until such time as the loop intersects itself or strays close enough to intersect another string.

The single most important tool for analysing the secular evolution of a string loop is the Albrecht–York formula (3.162), which relates the number of cusps of various types (which for present purposes will include microcusps as well as ordinary cusps) to the number of self-intersections on the loop. As Albrecht and York were the first to realize, there are three basic ways in which cusps and self-intersections can be created, altered or destroyed [AY88].

The simplest of these occurs when a pair of self-intersections with opposite polarities h_{si} spontaneously appears and bifurcates or merges and annihilates. (In practice, of course, it is only the creation of self-intersections that is relevant, as any pre-existing self-intersections will have long ago fragmented the string into daughter loops.) The mechanics of the creation of a pair of self-intersections is illustrated in figure 3.10, which shows a slowly-evolving loop at essentially the same parametric time during three successive oscillation periods.

SI: Self-intersection

Figure 3.10. Creation of a pair of self-intersections.

A: Anticusp   D: Degenerate
C: Cusp   cusp

Figure 3.11. Cusp–anti-cusp annihilation.

The second process of interest involves the spontaneous creation or annihilation of a pair of cusps. It is clear from the geometry of the Kibble–Turok sphere that the number of cusps and microcusps on a loop must be even, and that cusps (of all types) can only be created or destroyed in pairs. An example of cusp annihilation is shown in figure 3.11. It is evident that two cusps can coalesce only if they constitute a cusp–anti-cusp pair and furthermore, that at the moment of annihilation both cusps will share the same second-order structure vectors $\mathbf{a}_c''$ and $\mathbf{b}_c''$ and, therefore, the same value of f_c. The same is true of cusp creation. Thus, in both cases $\sum f_c g_c = 0$ for the cusp–anti-cusp pair, and the process of cusp creation or annihilation can be seen to have no effect on the number or type of self-intersections.

The point at which the two cusps coincide in figure 3.11 is sometimes referred to as a *degenerate cusp*. At a degenerate cusp the vectors $\mathbf{a}_c''$ and $\mathbf{b}_c''$ are parallel (although generally of different magnitudes). As a result, the

characteristic cusp length scales ρ_τ and ρ_σ introduced in section 3.6 are divergent. This is just an indication that the near-cusp expansion performed in equations (3.93) and (3.94) contains too few terms to describe a cusp of this type adequately.

At a degenerate cusp $\mathbf{a}_c'' = \alpha\mathbf{q}$ and $\mathbf{b}_c'' = \beta\mathbf{q}$, where $\mathbf{q}$ is a unit vector orthogonal to the vector $\mathbf{v}_c$ which defines the direction of the null 4-velocity at the cusp. If the second-order expansions (3.93) and (3.94) for $\mathbf{a}'$ and $\mathbf{b}'$ at the cusp are extended to fourth order in σ_+ and σ_- as follows:

$$\mathbf{a}' = \mathbf{v}_c + \alpha\mathbf{q}\sigma_+ + \tfrac{1}{2}\mathbf{a}_c'''\sigma_+^2 + \tfrac{1}{6}\mathbf{a}_c^{(4)}\sigma_+^3 + \tfrac{1}{24}\mathbf{a}_c^{(5)}\sigma_+^4 + O(\sigma_+^5) \qquad (3.166)$$

and

$$\mathbf{b}' = \mathbf{v}_c + \beta\mathbf{q}\sigma_- + \tfrac{1}{2}\mathbf{b}_c'''\sigma_-^2 + \tfrac{1}{6}\mathbf{b}_c^{(4)}\sigma_-^3 + \tfrac{1}{24}\mathbf{b}_c^{(5)}\sigma_-^4 + O(\sigma_-^5) \qquad (3.167)$$

then the local Lorentz factor λ has the form:

$$\begin{aligned}
\lambda^{-2} = &\tfrac{1}{4}(\alpha\sigma_+ - \beta\sigma_-)(\alpha\sigma_+ - \beta\sigma_- + \mathbf{q}\cdot\mathbf{a}_c'''\sigma_+^2 \\
&- \mathbf{q}\cdot\mathbf{b}_c'''\sigma_-^2 + \tfrac{1}{3}\mathbf{q}\cdot\mathbf{a}_c^{(4)}\sigma_+^3 - \tfrac{1}{3}\mathbf{q}\cdot\mathbf{b}_c^{(4)}\sigma_-^3) \\
&+ \tfrac{1}{16}(|\mathbf{a}_c'''|^2\sigma_+^4 - 2\mathbf{a}_c'''\cdot\mathbf{b}_c'''\sigma_+^2\sigma_-^2 + |\mathbf{b}_c'''|^2\sigma_-^4) + \cdots. \quad (3.168)
\end{aligned}$$

The boundary of the subset of the world sheet on which the Lorentz factor is greater than some minimum value $\lambda_{\min}$ is evidently quite complicated but reasonable approximations for the maximum cusp size and duration can be found by setting $\alpha\sigma_+ - \beta\sigma_- = 0$. Then

$$\sigma_+\sigma_- = 4\alpha\beta|\beta^2\mathbf{a}_c''' - \alpha^2\mathbf{b}_c'''|^{-1}\lambda_{\min}^{-1} \qquad (3.169)$$
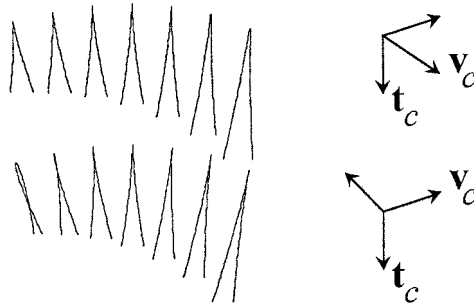
and the duration of the cusp is given by

$$|\tau| = |\alpha + \beta||\beta^2\mathbf{a}_c''' - \alpha^2\mathbf{b}_c'''|^{-1/2}\lambda_{\min}^{-1/2} \qquad (3.170)$$

while the (parametric) cusp size is

$$|\sigma| = |\alpha - \beta||\beta^2\mathbf{a}_c''' - \alpha^2\mathbf{b}_c'''|^{-1/2}\lambda_{\min}^{-1/2}. \qquad (3.171)$$

Note here that unlike an ordinary cusp, whose size and duration scale as $L/\lambda_{\min}$, a degenerate cusp scales as $L/\lambda_{\min}^{1/2}$ and is, therefore, typically larger and longer-lasting. In particular if $\lambda_{\min} \sim (L/r)^{1/2}$, as is the case for the boundary of an evaporating cusp or the apex of a truncated cusp, then the duration of a degenerate cusp is of order $L^{3/4}r^{1/4}$ rather than $L^{1/2}r^{1/2}$. For a cosmological string with $r \sim 10^{-29}$ cm and $L \sim 10^{20}$ cm the duration of a degenerate cusp would, therefore, be about 10^{-3} s as opposed to the 10^{-16} s calculated for an ordinary cusp in section 3.7. The physical size of a degenerate cusp would similarly be magnified by a factor of order $(L/r)^{1/4}$, although the size of the overlap region and its energy content E_c are unchanged as they depend on the
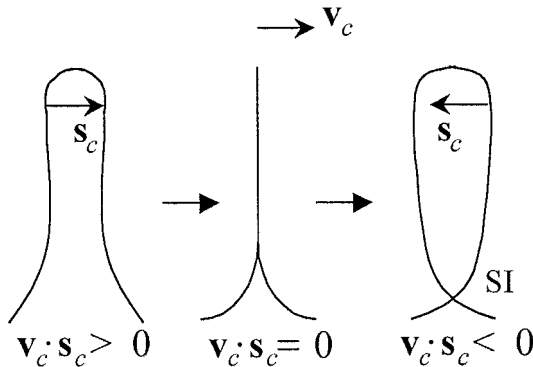
Figure 3.12. Time development of a degenerate cusp.

bridging vector $\mathbf{s}_c$, which has no special properties at a degenerate cusp. The time development of a degenerate cusp is shown in figure 3.12. The cusp parameters, time intervals and viewing angles for the cusp are the same as for the ordinary cusp depicted in figure 3.3 (except that the angle between the vectors $\mathbf{a}_c''$ and $\mathbf{b}_c''$ has been set to zero), so the two diagrams are directly comparable. Note here that, although the cusp itself appears only momentarily at $\tau = 0$, a cusplike geometry persists for much longer than in the generic case.
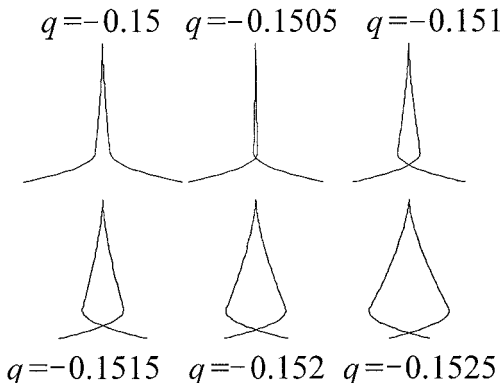
The last of the three evolutionary processes consistent with the Albrecht–York formula (3.162) involves the creation or destruction of a self-intersection by a cusp. It is topologically impossible for an isolated cusp to change its cusp type g_c under continuous deformations but there is no obstacle to a change in the cusp factor f_c of an individual cusp. Such a change corresponds to a reversal in the sign of the quantity $|\mathbf{b}_c''| - |\mathbf{a}_c''|$ which signals the rate at which the two mode functions move away from the crossover point $\mathbf{v}_c$. If the cusp factor f_c changes from 1 to 0 (or *vice versa*) then according to (3.162) the quantity $\sum h_{si}$ must change by ± 1, and so the cusp creates or destroys a self-intersection of the required polarity. (As before, only the process of creation will be considered physically admissible.)

At a physical level, in view of the gauge condition $\mathbf{v}_c \cdot \mathbf{s}_c = \frac{1}{2}(|\mathbf{b}_c''|^2 - |\mathbf{a}_c''|^2)$, the cusp factor f_c changes whenever the relative orientation of the bridging vector $\mathbf{s}_c$ and the cusp velocity $\mathbf{v}_c$ reverses. Thus a continuous deformation of the mode functions which leads to a change in the cusp factor corresponds to a bulk twisting of the near-cusp region as shown schematically in figure 3.13. It is, therefore, not very surprising that a self-intersection forms—although it is perhaps surprising that it forms as soon as $|\mathbf{b}_c''| - |\mathbf{a}_c''|$ vanishes, and that the process must always involve a cusp.

Contrary to the claims of Albrecht and York [AY88], a self-intersection created in this way need not appear at the location of the cusp itself. The linking number formula (3.162) only requires that the sum of h_{si} over all self-intersections change by ± 1, and, in principle, this can be accomplished by the crossover of the $\mathbf{a}_\Delta$ and $\mathbf{b}_\Delta$ curves at any value of Δ. This is illustrated in
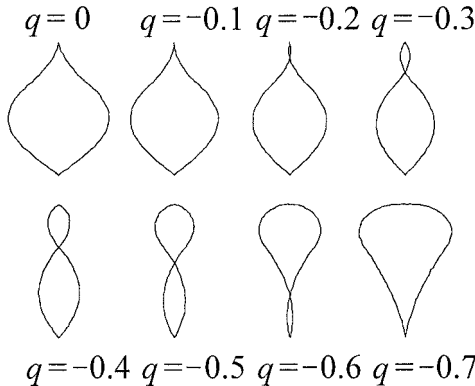
Figure 3.13. Appearance of a self-intersection as a result of cusp twisting.

Figure 3.14. Self-intersections on a continuous sequence of loops.

figure 3.14, which depicts the appearance of a self-intersection in a continuous sequence of string trajectories belonging to a 4-parameter family of strings—the 'balloon' strings—that will be discussed in more detail in section 4.3. In the notation of that section the sequence shown has the parameter values $(\frac{1}{2}\pi, -1; \frac{\pi}{6}, q)$, where q ranges from -0.15 to -0.1525 at intervals of -0.0005. The top sixth of the string ($|\sigma/L| \leq 0.074$) is plotted, in projection, at the moment of cusp formation, with the cusp at the apex (where $\sigma = 0$). For convenience, the horizontal scale is magnified by a factor of about 250. The cusp factor f_c changes from 0 to 1 at $q = -0.15\,039$ and a self-intersection appears not at the cusp itself but some way down the string (in fact at $\sigma/L = \pm 0.065\,54$).

As the magnitude of the parameter q continues to increase, the locus of the self-intersection moves down the string as shown in figure 3.15, which now depicts the whole string at the moment of cusp formation, with the horizontal magnification set at about 2 to 1. At the south pole of the string there is a (true)

$q=0$ $q=-0.1$ $q=-0.2$ $q=-0.3$

$q=-0.4$ $q=-0.5$ $q=-0.6$ $q=-0.7$

Figure 3.15. Migration of a self-intersection down a sequence of loops.

microcusp, and the magnitudes of the jumps in the two mode functions at the microcusp are equal when $q = -2/3$. At this value of q the self-intersection merges with the microcusp and disappears.

In the absence of detailed simulations of the secular evolution of a cosmic string under the action of its own or other sources of gravity, it is difficult to judge whether the three basic types of interaction sketched out in figures 3.10, 3.11 and 3.13 are commonplace or exceptional processes or whether their overall effect would be to multiply or attenuate the number of cusps and self-intersections. What is clear, however, is that the inclusion of cusp evaporation complicates the situation considerably. In particular, if the locus of a cusp can drift along the mode functions as envisaged in figure 3.11, cusp evaporation will be a recurrent process, with each cusp leaving behind a trail of reversing segments as it migrates and radiates. The resulting Kibble–Turok representation would be extraordinarily convoluted, to say the least.

Another example of the problems posed by truncated cusps lies in the mechanics of the process of cusp twisting depicted in figure 3.13. For a true (singular) cusp a continuous deformation of the mode functions which reverses the sign of $|\mathbf{b}_c''| - |\mathbf{a}_c''|$ essentially involves perturbations localized around the crossover point $\mathbf{v}_c$, and would seem to entail few drastic consequences for the string other than the apearance of a self-intersection. The corresponding transition for a truncated cusp is more awkward, as a reversal in the direction of the bridging vector $\mathbf{s}_c$ is necessarily coupled with the exchange of a reversing segment between the two mode functions. Thus if it is the $\mathbf{b}'$ mode that initially reconnects to the point $\mathbf{v}_c - 2(\mathbf{v}_c \cdot \mathbf{s}_c)|\mathbf{s}_c|^{-2}\mathbf{s}_c$ at a truncated cusp, any continuous deformation leading to a reversal in the sign of $\mathbf{v}_c \cdot \mathbf{s}_c$ will push the reconnection point back to $\mathbf{v}_c$, where, in principle, it could now be transferred to the $\mathbf{a}'$ mode. However, once the reconnection point returns to $\mathbf{v}_c$ a true cusp will appear, and this will presumably radiate Higgs field energy and evaporate immediately, creating a new

reconnection whose structure (since $\mathbf{v}_c \cdot \mathbf{s}_c = 0$) depends on higher-order terms in the cusp expansion. In this case, therefore, the appearance of a self-intersection will probably be circumvented.

Chapter 4

A bestiary of exact solutions

In this chapter I will describe a number of exact solutions to the string equations of motion in Minkowski spacetime. The purpose of this is not only to illustrate the richness and complexity of string dynamics but also to introduce some of the standard trajectories that have been used in benchmark calculations of the gravitational back-reaction and radiation fluxes from a cosmic string (a topic to be discussed in some detail in chapter 6). Each of the solutions examined here will be written in the aligned standard gauge. Unless otherwise stated, each trajectory is described in its centre-of-momentum frame. Where applicable, all the cusps, kinks and self-intersections supported by the string are identified and the angular momentum vector $\mathbf{J}$ is given if finite and non-zero. In all examples involving loops, the parameter L denotes the invariant length of the string, so that the total energy in the centre-of-momentum frame is μL.

4.1 Infinite strings

4.1.1 The infinite straight string

The simplest of all string configurations in Minkowski spacetime is the infinite straight string. In the rest frame of the string the equation of the world sheet is

$$X^{\mu} = [\tau, 0, 0, \sigma] \tag{4.1}$$

where the spatial coordinates have been chosen so that the string is aligned with the z-axis. In fact, the spatial projections of the trajectory are just straight lines along the z-axis, and the world sheet of the string is intrinsically flat. The infinite straight string is the only possible static configuration in the absence of external forces.

If the string is boosted so that it has a velocity $\mathbf{V} = V_x \hat{\mathbf{x}} + V_y \hat{\mathbf{y}}$ normal to the world sheet then the equation of the world sheet in the aligned standard gauge becomes

$$X^{\mu} = [\tau, V_x \tau, V_y \tau, (1 - \mathbf{V}^2)^{1/2} \sigma]. \tag{4.2}$$

In this case, the mode decomposition of the trajectory reads:

$$\mathbf{a}(\sigma_+) = \sigma_+ \mathbf{V} + (1 - \mathbf{V}^2)^{1/2} \sigma_+ \widehat{\mathbf{z}} \qquad (4.3)$$

and

$$\mathbf{b}(\sigma_-) = \sigma_- \mathbf{V} - (1 - \mathbf{V}^2)^{1/2} \sigma_- \widehat{\mathbf{z}} \qquad (4.4)$$

and, in particular, $\mathbf{a}' \cdot \mathbf{b}' = 2\mathbf{V}^2 - 1$ everywhere.

4.1.2   Travelling-wave solutions

Another important class of solutions supported by infinite strings are travelling waves. These are constructed by taking a straight string and superposing a single left- or right-moving mode. For example, if the underlying straight string is at rest and aligned with the z-axis then travelling-wave solutions which propagate up the string have the general form

$$X^\mu = [\tau, 0, 0, \sigma] + [0, x(\tau - \sigma), y(\tau - \sigma), z_-(\tau - \sigma)] \qquad (4.5)$$

where, in view of the gauge condition $X_\tau^2 + X_\sigma^2 = 1$,

$$z_-(\sigma_-) = \tfrac{1}{2}\sigma_- \pm \tfrac{1}{2} \int_0^{\sigma_-} \sqrt{1 - 4x'^2(u) - 4y'^2(u)} \, du \qquad (4.6)$$

and the functions x and y satisfy the inequality $x'^2 + y'^2 \le \tfrac{1}{4}$ but are otherwise arbitrary. The minus sign in equation (4.6) corresponds to trajectories on which the spacelike tangent vector X_σ^μ is inclined at less than $\tfrac{1}{4}\pi$ to the vertical ('shallow' waves), and the plus sign to trajectories on which X_σ^μ is inclined at between $\tfrac{1}{4}\pi$ and $\tfrac{1}{2}\pi$ to the vertical ('steep' waves).

    The analogous equation for travelling waves which propagate down the string is

$$X^\mu = [\tau, 0, 0, \sigma] + [0, x(\tau + \sigma), y(\tau + \sigma), z_+(\tau + \sigma)] \qquad (4.7)$$
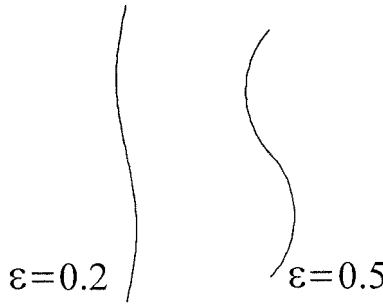
with

$$z_+(\sigma_+) = -\tfrac{1}{2}\sigma_+ \pm \tfrac{1}{2} \int_0^{\sigma_+} \sqrt{1 - 4x'^2(u) - 4y'^2(u)} \, du. \qquad (4.8)$$

    Travelling waves propagate along a string with a fixed shape and a pattern speed equal to the speed of light. However, the local velocity of the string is not directed along the z-axis nor is it generally lightlike. In fact,

$$X_\tau^2 = \tfrac{1}{2}\left[1 \mp \sqrt{1 - 4x'^2 - 4y'^2}\right] = \cos^2\theta \qquad (4.9)$$

where θ is the angle between the spacelike tangent vector and the vertical. In particular, for shallow waves the local Lorentz factor $\lambda = |X_\tau|^{-1}$ is bounded above by $\sqrt{2}$, while for steep waves $\lambda \ge \sqrt{2}$.

$\varepsilon = 0.2$ $\varepsilon = 0.5$

Figure 4.1. Profiles of two shallow travelling sine waves.

If the local speed of the string is small compared to c then the profile of the travelling wave can be read off directly from the coordinate functions x and y but for relativistic speeds the shape of the wave is significantly distorted. For example, if the coordinate functions describe a sine wave in the x–z plane, so that $x(\sigma_-) = \varepsilon \sin \sigma_-$ and $y(\sigma_-) = 0$, then for shallow-wave solutions the vertical coordinate $z = \sigma + z_-$, which has the explicit form

$$z(\tau, \sigma) = \tfrac{1}{2}\sigma_+ - \tfrac{1}{2} \int_0^{\sigma_-} \sqrt{1 - 4\varepsilon^2 \cos^2(u)}\, du \qquad (4.10)$$

is just $\sigma + O(\varepsilon^2)$ for small values of ε, and (because $x = \varepsilon \sin \sigma_-$ is of order ε) the profile of the shallow-wave solution has a recognizably sinusoidal shape. However, if ε takes on its limiting value of $\tfrac{1}{2}$ then for shallow waves

$$z(\tau, \sigma) = \tfrac{1}{2}\sigma_+ + \tfrac{1}{2}(\cos \sigma_- - 1)\, \mathrm{sgn}(\sigma_-) \qquad (4.11)$$

and the profile of the trajectory becomes a train of cycloids with a noticeably narrower base (see figure 4.1, which compares the cases $\varepsilon = 0.2$ and $\varepsilon = 0.5$).
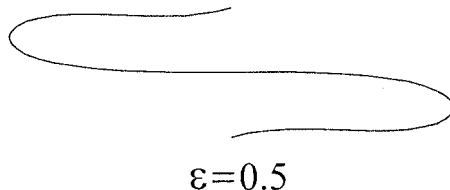
The distortion is even more extreme for *steep-wave* solutions, as can be seen in figure 4.2, which shows the profile of the steep travelling sine wave with $\varepsilon = 0.5$. As the value of ε decreases, the vertical compression of the steep-wave solutions becomes ever more severe, and in the limit of small ε

$$z(\tau, \sigma) \approx \tau - \tfrac{1}{2}\varepsilon^2(\sigma_- + \sin \sigma_- \cos \sigma_-). \qquad (4.12)$$
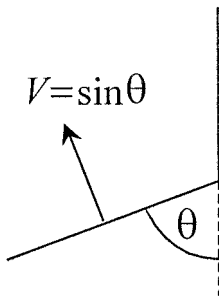
In this limit, the string consists of a ladder of short, straight, almost horizontal segments (with length 2ε) moving in the z-direction at near-light speed.

One of the simplest travelling-wave solutions is a piecewise-straight string which supports a single kink, as in figure 4.3. If the upper branch of the string is at rest, and the angle between the lower branch and the vertical is θ, then for an upward-moving kink

$$X^\mu = \begin{cases} [\tau, 0, 0, \sigma] & \text{for } \sigma \geq \tau \\ [\tau, -(\tau - \sigma)\sin\theta\cos\theta, 0, \sigma + (\tau - \sigma)\sin^2\theta] & \text{for } \sigma \leq \tau \end{cases} \qquad (4.13)$$

$$\varepsilon=0.5$$

Figure 4.2. Profile of a steep travelling sine wave.

$V=\sin\theta$

θ
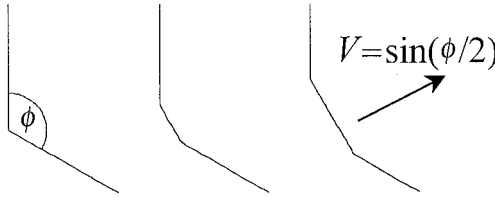
Figure 4.3. A straight string with a single kink.

where the spacelike coordinates have been chosen so that the branches span the x–z plane. Note that although the kink propagates directly up the string at the speed of light, the lower branch of the string moves obliquely with a speed $V = \sin\theta$. The velocity of the moving branch can be reversed by replacing $\tau - \sigma$ with $-(\tau + \sigma)$ in (4.13) and breaking the configuration at $\sigma = -\tau$ rather than at $\sigma = \tau$.

Strictly speaking, equation (4.13) applies only if the angle of inclination θ of the moving branch is less than $\frac{1}{2}\pi$. Kinks with junction angles $\theta \geq \frac{1}{2}\pi$ are not viable, as they require the moving branch to travel either at light speed (if $\theta = \frac{1}{2}\pi$) or at superluminal speeds (if $\theta > \frac{1}{2}\pi$). The effect of continuing θ to values beyond $\frac{1}{2}\pi$ in (4.13) is not to increase the junction angle but simply to reflect the moving branch from the left side to the right side of figure 4.3. However, the prohibition on junction angles $\theta \geq \frac{1}{2}\pi$ holds only if one of the branches is stationary. If both branches are allowed to move then kinks with any value of θ are possible, as is evident from many of the solutions examined later in this chapter.

4.1.3   Strings with paired kinks

The kinked solutions described in the previous section are non-static but maintain a constant profile. By contrast, a string that is initially at rest and has the same kinked spacelike cross section as before will decompose into a pair of kinks

Figure 4.4. A string with paired kinks.

moving in opposite directions. If ϕ denotes the initial angle between the two branches, the equation of the trajectory reads:

$$X^\mu = \begin{cases} [\tau, 0, 0, \sigma] & \text{for } \sigma \geq \tau \\ [\tau, \frac{1}{2}(\tau - \sigma)\sin\phi, 0, \frac{1}{2}(\tau + \sigma) - \frac{1}{2}(\tau - \sigma)\cos\phi] & \text{for } |\sigma| \leq \tau \\ [\tau, -\sigma\sin\phi, 0, \sigma\cos\phi] & \text{for } \sigma \leq -\tau. \end{cases}$$
(4.14)

The evolution of the trajectory is shown in figure 4.4. The two kinks propagate along their respective branches at the speed of light, with the straight-line segment joining the kinks moving in the direction midway between the branches at a speed $V = \sin(\phi/2)$.

In practice, kinks would normally form on a string as a result of intercommuting events associated with self-intersections or intersections with other strings. As a simple example of an intercommuting event, consider two infinite straight strings, one at rest aligned with the z-axis and one parallel to the x-axis and moving with speed V in the y-direction. If the strings cross at the origin at time $t = 0$ then the trajectories of the reconnected fragments are:

$$X^\mu_{(1)} = \begin{cases} [\tau, 0, 0, \sigma] & \text{for } \sigma \geq \tau \\ [\tau, -\frac{1}{2}(1 - V^2)^{1/2}(\tau - \sigma), \frac{1}{2}V(\tau - \sigma), \frac{1}{2}(\tau + \sigma)] & \text{for } |\sigma| \leq \tau \\ [\tau, (1 - V^2)^{1/2}\sigma, V\tau, 0] & \text{for } \sigma \leq -\tau \end{cases}$$
(4.15)
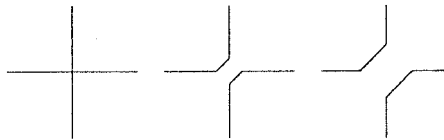
and

$$X^\mu_{(2)} = \begin{cases} [\tau, (1 - V^2)^{1/2}\sigma, V\tau, 0] & \text{for } \sigma \geq \tau \\ [\tau, \frac{1}{2}(1 - V^2)^{1/2}(\tau + \sigma), \frac{1}{2}V(\tau + \sigma), -\frac{1}{2}(\tau - \sigma)] & \text{for } |\sigma| \leq \tau \\ [\tau, 0, 0, \sigma] & \text{for } \sigma \leq -\tau. \end{cases}$$
(4.16)
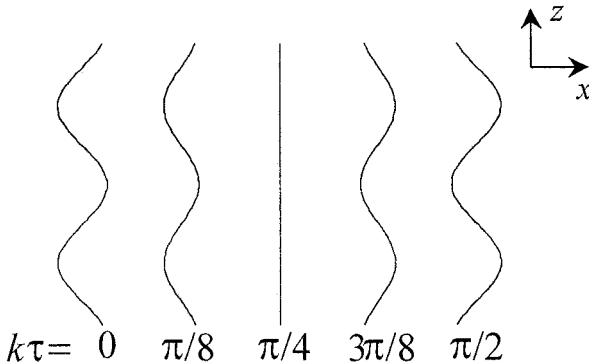
The projection of the trajectories onto the x–z plane for $\tau \geq 0$ is shown in figure 4.5. The straight-line segments linking each pair of intercommuted branches move in opposite directions with speed $1/\sqrt{2}$, independently of the intersection speed V.

4.1.4 Helical strings

As a final example of a solution of the equations of motion supported by an infinite string, consider a string in the shape of a helix with radius R and pitch angle α. If

Figure 4.5. The intercommuting of two straight strings.

Figure 4.6. A helical string in breathing mode.

the string is initially at rest, the equation of the trajectory reads:
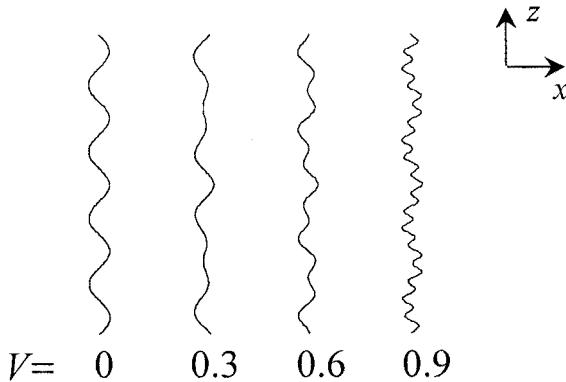
$$X^\mu = [\tau,\, R\cos(k\tau)\cos(k\sigma),\, R\cos(k\tau)\sin(k\sigma),\, \sigma\sin\alpha] \qquad (4.17)$$

where $k = R^{-1}\cos\alpha$. The projection of the trajectory onto the x–z plane is shown in figure 4.6 for a pitch angle $\alpha = \frac{1}{4}\pi$; the projection onto the y–z plane is identical, except for a displacement of $\pi R \tan\alpha/2$ (one quarter period) along the z-axis. The helix first contracts laterally under the action of the string tension and degenerates into a (non-static) straight line along the z-axis at $k\tau = \frac{1}{2}\pi$. It then re-expands until it reaches its maximum radius R again at $k\tau = \pi$, when it once more has its original helical shape, although rotated by an angle π about the z-axis. The pattern is, of course, periodic with a period $2\pi/k$ in τ.

This particular trajectory is often referred to as a helical string in 'breathing mode', as the helix does not propagate along the string. The local Lorentz factor of the string is

$$\lambda = [1 - \cos^2\alpha\,\sin^2(k\tau)]^{-1/2} \qquad (4.18)$$

and so assumes a maximum value of $\sec\alpha$ when the helix has momentarily degenerated into a straight line at $k\tau = \frac{1}{2}\pi$. For $0 < \alpha < \frac{1}{2}\pi$ the Lorentz factor is finite everywhere, and the string does not support any cusps. For $\alpha = \frac{1}{2}\pi$ the trajectory is just a static straight line, while in the limit as $\alpha \to 0$ the helix becomes a cylindrical shell with an infinite surface density. Although the trajectory in the latter case is unphysical, its projection onto the x–y plane

Figure 4.7. Profiles of boosted helical strings.

is mathematically equivalent to the collapsing circular loop to be examined in section 4.2.1.

If the breathing-mode solution (4.17) is boosted by a speed V along the z-axis, the result is a helix whose profile propagates along the axis:

$$X^\mu = [\tau, \tfrac{1}{2}R\cos(k_+\sigma_+) + \tfrac{1}{2}R\cos(k_-\sigma_-), \tfrac{1}{2}R\sin(k_+\sigma_+)$$
$$- \tfrac{1}{2}R\sin(k_-\sigma_-), z(\tau, \sigma)] \qquad (4.19)$$

where

$$k_\pm = R^{-1}(1 - V^2)^{1/2}(1 \pm V\sin\alpha)^{-1}\cos\alpha \qquad (4.20)$$

and
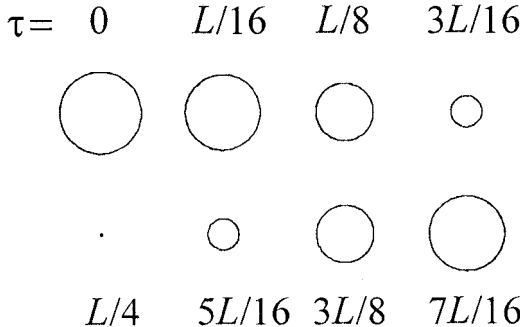
$$z(\tau, \sigma) = (1 - V^2\sin^2\alpha)^{-1}[(1 - V^2)\sigma\sin\alpha + V\tau\cos^2\alpha]. \qquad (4.21)$$

Note here that although the speed of the helical pattern up the axis is V, the local speed of the string itself has a vertical component $(1 - V^2\sin^2\alpha)^{-1}V\cos^2\alpha$ strictly smaller than V, a discrepancy which illustrates the fact that boosts parallel to the string are undetectable. The profile of the helix is also significantly distorted for relativistic values of V, as can be seen from figure 4.7, which shows the x–z projection of a helix with pitch angle $\alpha = \tfrac{1}{4}\pi$ at time $\tau = 0$ boosted vertically with $V = 0, 0.3, 0.6$ and 0.9.

4.2 Some simple planar loops

4.2.1 The collapsing circular loop

A string loop in the shape of a circle which is initially at rest will accelerate inwards under the action of its own tension and ultimately collapse to a point. If

$$\tau = \quad 0 \qquad L/16 \quad L/8 \quad 3L/16$$

$$L/4 \quad 5L/16 \quad 3L/8 \quad 7L/16$$

Figure 4.8. Collapse and re-expansion of a circular loop.

the loop lies in the $x{-}y$ plane and has invariant length L then the equation of the trajectory is

$$X^{\mu} = [\tau,\, R\cos(\tau/R)\cos(\sigma/R),\, R\cos(\tau/R)\sin(\sigma/R),\, 0] \tag{4.22}$$

where $R = L/2\pi$. The loop collapses to a point at $\tau = L/4$. The local Lorentz factor of the string is

$$\lambda = \sec(2\pi\tau/L) \tag{4.23}$$

and so diverges at $\tau = L/4$. Thus the entire string is concentrated into a single cusp at the moment of collapse.

The fate of the loop once it has collapsed to a point will be discussed in more detail in later chapters. However, it should be noted that if the solution (4.22) is taken seriously then the loop re-emerges from the collapse point and expands until it reaches its maximum radius $L/2\pi$ again at $\tau = L/2$, as shown in figure 4.8. The cycle of collapse and re-expansion then repeats indefinitely.

The collapsing circular loop also has a high degree of spatial symmetry and, for this reason, its gravitational field has been studied more extensively than any other non-trivial solution of the equations of motion (see chapter 10).

4.2.2 The doubled rotating rod

A planar loop solution that is mathematically very similar to the collapsing circular loop is the doubled rotating rod, whose equation is

$$X^{\mu} = [\tau,\, R\cos(\tau/R)\cos(\sigma/R),\, R\sin(\tau/R)\cos(\sigma/R),\, 0] \tag{4.24}$$

where $R = L/2\pi$ again. This differs from the circular loop trajectory (4.22) only in that the parameters τ and σ have been interchanged in the x- and y-components. The shape of the doubled rotating rod is that of a straight line of length L/π that rotates about its midpoint with a period L. The local Lorentz factor of the string is

$$\lambda = \sec(2\pi\sigma/L) \tag{4.25}$$

and so the two endpoints of the rod (at $\sigma = L/4$ and $\sigma = 3L/4$) are permanent cusps travelling at the speed of light.

It is important to note that the full parameter range of $[0, L]$ in σ covers the length of the rod twice, and so the rest mass per unit length at any point on the rod is 2μ rather than μ. The discrepancy between the invariant length L and the actual length $2L/\pi$ of stringlike material in the rod is due to relativistic length contraction.

Unlike the collapsing circular loop, the doubled rotating rod has a non-zero angular momentum vector

$$\mathbf{J} = \frac{1}{4\pi}\mu L^2 \widehat{\mathbf{z}}. \tag{4.26}$$

In fact, as was seen in section 3.3, the rotating rod has the largest angular momentum of all solutions with the same values of μ and L.

4.2.3   The degenerate kinked cuspless loop

The Kibble–Turok representations of both the collapsing circular loop and the doubled rotating rod consist of pairs of unit circles in the x–y plane. It is evident from the geometry of the Kibble–Turok sphere that a planar loop will be free of cusps only if at least one of the mode curves is discontinuous. The most extreme case of this type occurs when both mode curves degenerate into a pair of antipodal points, so that the equation of the trajectory becomes

$$X^{\mu} = [\tau, \tfrac{1}{2}\mathbf{a}(\tau + \sigma) + \tfrac{1}{2}\mathbf{b}(\tau - \sigma)] \tag{4.27}$$

where

$$\mathbf{a}(\sigma_+) = \begin{cases} (\sigma_+ - L/4)\widehat{\mathbf{a}} & \text{for } 0 \leq \sigma_+ \leq L/2 \\ (3L/4 - \sigma_+)\widehat{\mathbf{a}} & \text{for } L/2 \leq \sigma_+ \leq L \end{cases} \tag{4.28}$$

and
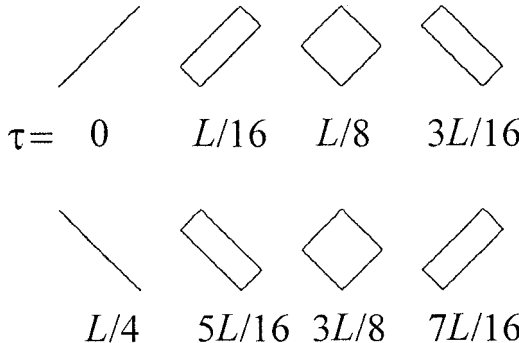
$$\mathbf{b}(\sigma_-) = \begin{cases} (\sigma_- - L/4)\widehat{\mathbf{b}} & \text{for } 0 \leq \sigma_- \leq L/2 \\ (3L/4 - \sigma_-)\widehat{\mathbf{b}} & \text{for } L/2 \leq \sigma_- \leq L \end{cases} \tag{4.29}$$

and $\widehat{\mathbf{a}}$ and $\widehat{\mathbf{b}}$ are linearly independent unit vectors.
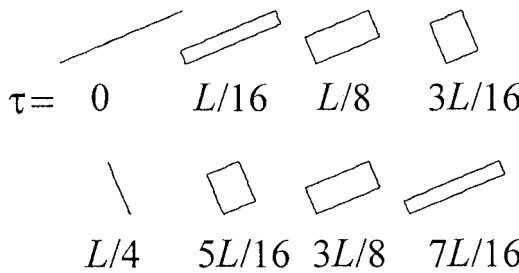
The resulting solution is cuspless but supports two right-moving kinks at $\sigma_+ = 0$ and $L/2$, and two left-moving kinks at $\sigma_- = 0$ and $L/2$. The loop itself has the shape of a rectangle with sides oriented in the directions of $\widehat{\mathbf{a}}+\widehat{\mathbf{b}}$ and $\widehat{\mathbf{a}}-\widehat{\mathbf{b}}$, and a total perimeter length which varies from $\alpha_- L$ to $\alpha_+ L$, where

$$\alpha_{\pm} = \frac{1}{\sqrt{2}}(1 \pm \widehat{\mathbf{a}} \cdot \widehat{\mathbf{b}})^{1/2}. \tag{4.30}$$

The rectangle periodically collapses to form a doubled straight line when the kinks cross. The evolution of the trajectory for the choice $\widehat{\mathbf{a}} = \widehat{\mathbf{x}}$ and $\widehat{\mathbf{b}} = \widehat{\mathbf{y}}$ is illustrated for a full period ($0 \leq \tau < L/2$) in figure 4.9 and in the case $\widehat{\mathbf{a}} = \widehat{\mathbf{x}}$ and $\widehat{\mathbf{b}} = (\widehat{\mathbf{x}} + \widehat{\mathbf{y}})/\sqrt{2}$ in figure 4.10.

Figure 4.9. A degenerate kinked cuspless loop with orthogonal branches.

Figure 4.10. A degenerate kinked cuspless loop with branches at 45°.

The local speed of the branches on a degenerate kinked cuspless loop is $\alpha_\pm$, where the choice of sign depends on the orientation of the branch. If $\widehat{\mathbf{a}}$ and $\widehat{\mathbf{b}}$ are orthogonal (as in figure 4.9) then the local speed is everywhere $1/\sqrt{2}$. Although the solutions described here do not support macrocusps, they do support (true) microcusps whenever two kinks cross, as at $\tau = 0$ and $L/4$ in figures 4.9 and 4.10.

4.2.4   Cat's-eye strings

Cat's-eye strings are planar solutions of the equations of motion that are intermediate between the kinked cuspless loops of the previous section and the collapsing circular loop or doubled rotating rod. The Kibble–Turok representation of a cat's-eye string consists of one continuous mode curve and one discontinuous mode curve, so that the loop supports kinks moving in one direction only. As an example, consider the case where the discontinuous mode curve traces out two quarter circles on the Kibble–Turok sphere. There are then two possible configurations, depending on whether the mode curves have the same or opposite orientations.

If the orientations are the same, the resulting trajectory is a *spinning cat's-eye* described by the mode functions

$$\mathbf{a}(\sigma_+) = \frac{L}{2\pi}[\cos(2\pi\sigma_+/L)\widehat{\mathbf{x}} + \sin(2\pi\sigma_+/L)\widehat{\mathbf{y}}] \tag{4.31}$$

and

$$\mathbf{b}(\sigma_-) = \begin{cases} \dfrac{L}{\pi}[\cos(\pi\sigma_-/L)\widehat{\mathbf{x}} + \sin(\pi\sigma_-/L)\widehat{\mathbf{y}}] & \text{for } 0 \leq \sigma_- \leq L/2 \\[2mm] \dfrac{L}{\pi}[\{1 - \sin(\pi\sigma_-/L)\}\widehat{\mathbf{x}} + \{1 + \cos(\pi\sigma_-/L)\}\widehat{\mathbf{y}}] & \text{for } L/2 \leq \sigma_- \leq L \end{cases} \tag{4.32}$$

where **b** is (of course) assumed to be periodic with period L in σ_-. The evolution of the trajectory is shown in figure 4.11. The loop supports two kinks moving in an anti-clockwise direction around the string, and two semi-permanent cusps moving in the opposite direction. The local Lorentz factor of the string is

$$\lambda = \begin{cases} 2^{1/2}[1 - \cos\{\pi(\tau + 3\sigma)/L + \phi\}]^{-1/2} & \text{for } 0 < \sigma_- < L/2 \\ 2^{1/2}[1 - \sin\{\pi(\tau + 3\sigma)/L + \phi\}]^{-1/2} & \text{for } L/2 < \sigma_- < L \end{cases} \tag{4.33}$$

where the phase factor ϕ is equal to 0 if σ_-/L lies in $(0, 1)$ modulo 2 and $\phi = \pi$ otherwise. The cusps, therefore, move along the paths $\sigma = L/3 - \tau/3$ and $\sigma = 5L/6 - \tau/3$ for $0 < \tau < 3L/8$.

At $\tau = 0$ the cusps appear at the positions of the kinks together with a pair of self-intersections. The self-intersections subsequently move towards the middle of the string and can just be seen in the second frame of figure 4.11. When $\tau/L \approx 0.1112$ (shortly before frame 3) the self-intersections meet in the middle of the string and annihilate. The kinks and cusps continue to propagate around the string until $\tau = 3L/16$, at which moment the kinks (at the obtuse angles of the diamond) form false microcusps. The loop then shrinks laterally until its opposite sides cross and create a new pair of self-intersections at $\tau/L \approx 0.2638$. When $\tau = 3L/8$ the cusps and self-intersections merge with the kinks, which continue to propagate freely until $\tau = L/2$. The loop is then back in its original configuration, and the cycle is repeated indefinitely.
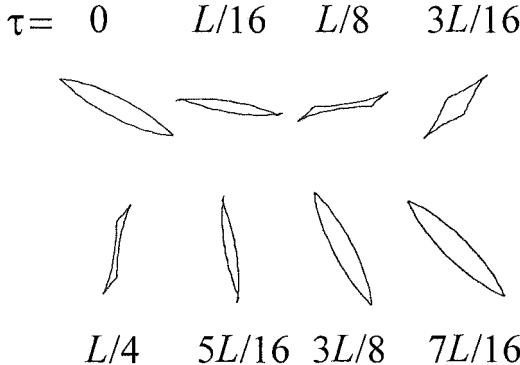
As its name suggests, the spinning cat's-eye string carries a significant angular momentum. In fact, its total angular momentum vector is

$$\mathbf{J} = \left(\frac{3}{8\pi} - \frac{1}{2\pi^2}\right)\mu L^2\widehat{\mathbf{z}} \tag{4.34}$$

and the magnitude of $\mathbf{J}$ is 86% of the angular momentum of a doubled rotating rod with the same values of μ and L.

When the two mode curves have opposing orientations, the resulting solution describes an *oscillating cat's-eye*. This can be constructed by taking

$$\mathbf{a}(\sigma_+) = \frac{L}{2\pi}[\cos(2\pi\sigma_+/L)\widehat{\mathbf{x}} - \sin(2\pi\sigma_+/L)\widehat{\mathbf{y}}] \tag{4.35}$$

$$\tau = \quad 0 \qquad L/16 \quad L/8 \quad 3L/16$$

$$L/4 \quad 5L/16 \quad 3L/8 \quad 7L/16$$

Figure 4.11. The spinning cat's-eye string.

and leaving the **b** mode function in the form given by equation (4.32). The evolution of the corresponding trajectory is shown in figure 4.12. In comparison with the spinning cat's-eye, the oscillating cat's-eye is more nearly circular and its motion is largely radial rather than rotational. The oscillating cat's-eye does support a pair of kinks and a pair of cusps moving in the opposite direction but the persistence time of the cusps is relatively brief. The local Lorentz factor of the string is

$$\lambda = \begin{cases} 2^{1/2}[1 + \cos\{\pi(3\tau + \sigma)/L + \phi\}]^{-1/2} & \text{for } 0 < \sigma_- < L/2 \\ 2^{1/2}[1 - \sin\{\pi(3\tau + \sigma)/L + \phi\}]^{-1/2} & \text{for } L/2 < \sigma_- < L \end{cases} \qquad (4.36)$$

where the phase factor ϕ is defined as before.
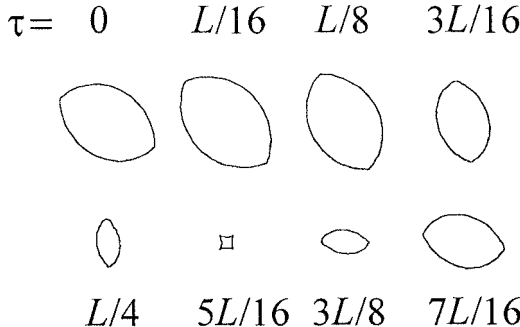
The cusps are, therefore, present only between $\tau = L/4$ and $\tau = 3L/8$, moving along the paths $\sigma = 3L/2 - 3\tau$ and $\sigma = L - 3\tau$. Note that the kinks and cusps coincide at $\tau = L/4$ and $\tau = 3L/8$ in figure 4.12 but are separately visible at $\tau = 5L/16$, when the string traces out a four-pointed star. At this moment (false) microcusps also appear at the locations of the kinks but the string is otherwise free of both macrocusps and microcusps.

The angular momentum vector of the oscillating cat's-eye is

$$\mathbf{J} = \left(\frac{1}{8\pi} - \frac{1}{2\pi^2} \right) \mu L^2 \hat{\mathbf{z}} \qquad (4.37)$$

and has a magnitude only 14% of the angular momentum of a rotating rod with the same values of μ and L.

If the discontinuous mode curve on the Kibble–Turok sphere is dilated so that it more nearly approaches a full circle, the spinning and oscillating cat's-eye strings more closely resemble the rotating rod and circular loop, respectively. At the other extreme, if the discontinuous mode curve degenerates into a pair of antipodal points the result is a *degenerate cat's-eye* string with mode functions of

$$\tau = \quad 0 \qquad L/16 \quad L/8 \quad 3L/16$$

$$L/4 \quad 5L/16 \quad 3L/8 \quad 7L/16$$

Figure 4.12. The oscillating cat's-eye string.

the general form

$$\mathbf{a}(\sigma_+) = \frac{L}{2\pi}[\cos(2\pi\sigma_+/L)\widehat{\mathbf{x}} + \sin(2\pi\sigma_+/L)\widehat{\mathbf{y}}] \tag{4.38}$$

and

$$\mathbf{b}(\sigma_-) = \begin{cases} (\sigma_- - L/4)\widehat{\mathbf{x}} & \text{for } 0 \le \sigma_- \le L/2 \\ (3L/4 - \sigma_-)\widehat{\mathbf{x}} & \text{for } L/2 \le \sigma_- \le L \end{cases} \tag{4.39}$$

where, of course, $\widehat{\mathbf{x}}$ could be replaced by any unit vector in the x–y plane.
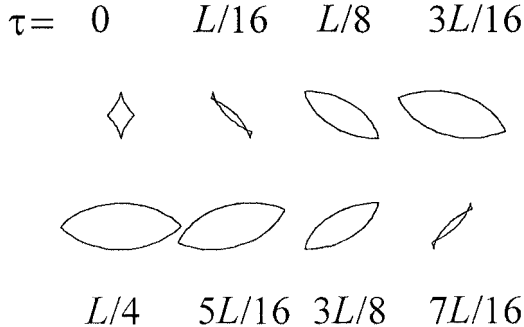
The trajectory of the degenerate cat's-eye is shown in figure 4.13. The local Lorentz factor of the string is

$$\lambda = \begin{cases} 2^{1/2}[1 + \sin 2\pi(\tau + \sigma)/L]^{-1/2} & \text{for } 0 < \tau - \sigma < L/2 \\ 2^{1/2}[1 - \sin 2\pi(\tau + \sigma)/L]^{-1/2} & \text{for } L/2 < \tau - \sigma < L \end{cases} \tag{4.40}$$

and so as well as a pair of kinks the degenerate cat's-eye supports semi-permanent cusps moving along the paths $\sigma = L/4 - \tau$ and $\sigma = 3L/4 - \tau$ during the time interval $-L/8 < \tau < L/8$. At $\tau = 0$ in figure 4.13 the cusps can be seen at the top and bottom of the diamond, while the kinks are at the extreme right and extreme left. Initially the top left and bottom right branches of the string are moving outwards, while the other two branches are moving inwards and ultimately cross at the origin at $\tau/L = \frac{1}{8} - \frac{1}{4\pi} \approx 0.0454$. This event creates a pair of self-intersections which subsequently migrate along the string and can be seen near the extreme ends in the second frame of figure 4.13. Each cusp–kink pair coalesces with the corresponding self-intersection to form a (false) microcusp at $\tau = L/8$, leaving a kink which propagates freely around the loop until $\tau = 3L/8$. At this point the kinks each emit a cusp and a self-intersection and the sequence described earlier is reversed: the self-intersections move back towards the centre of the string until the branches unwind at $\tau/L = \frac{3}{8} + \frac{1}{4\pi} \approx 0.4546$.

It is readily seen that in the case of the degenerate cat's-eye only the mode function $\mathbf{a}$ carries angular momentum and so the angular momentum vector

$$\mathbf{J} = \frac{1}{8\pi}\mu L^2 \widehat{\mathbf{z}} \tag{4.41}$$

$$\tau = \quad 0 \qquad L/16 \quad L/8 \quad 3L/16$$

$$L/4 \quad 5L/16 \quad 3L/8 \quad 7L/16$$

Figure 4.13. The degenerate cat's-eye string.

has a magnitude equal to one-half the angular momentum of a rotating rod with the same values of μ and L.

4.3 Balloon strings

Balloon strings are a non-planar family of trajectories constructed principally to illustrate the process discussed in section 3.9 by which a self-intersection can be created as a result of cusp twisting. The mode functions $\mathbf{a}'$ and $\mathbf{b}'$ both trace out arcs of great circles on the Kibble–Turok sphere, in the x–z and y–z planes respectively. The mode functions cross at the north pole of the sphere, producing a cusp but both are generally broken in the vicinity of the south pole, creating one or more microcusps.

The defining feature of the mode functions is that they are piecewise harmonic functions of the light-cone coordinates $\sigma_{\pm}$, with a break in smoothness occurring at a single pair of points arranged symmetrically about the north pole of the Kibble–Turok sphere. Thus (with $\xi_+ = 2\pi\sigma_+/L$) the function $\mathbf{a}'$ has the general form:

$$\mathbf{a}'(\sigma_+) = \begin{cases} \sin(m\xi_+)\widehat{\mathbf{x}} + \cos(m\xi_+)\widehat{\mathbf{z}} & \text{for } |\xi_+| < \chi \\ \sin(n\xi_+ - ps_+)\widehat{\mathbf{x}} + \cos(n\xi_+ - ps_+)\widehat{\mathbf{z}} & \text{for } \chi < |\xi_+| < \pi \end{cases} \quad (4.42)$$

for some choice of constants m, n, p and $\chi \in (0, \pi)$, with $s_+ \equiv \text{sgn}(\xi_+)$. The continuity of the mode function at $|\xi_+| = \chi$ imposes the condition

$$p = (n - m)\chi \qquad (\text{modulo } 2\pi) \qquad (4.43)$$

while the string will be in its centre-of-momentum frame only if $\mathbf{a}'$ satisfies the moment condition $\int_{-L}^{L} \mathbf{a}' \, d\sigma_+ = \mathbf{0}$, which translates into the constraint

$$m^{-1}\sin(m\chi) + n^{-1}[\sin(n\pi - p) - \sin(n\chi - p)] = 0. \qquad (4.44)$$

If the function $\mathbf{a}'$ is required to map continuously onto a smooth great circle in the limit as $p \to 0$, the constraint equations (4.43) and (4.44) have the unique parametric solution:

$$m(\alpha, p) = \frac{\alpha}{\alpha + p} n(\alpha, p) \qquad \text{and} \qquad \chi(\alpha, p) = \frac{\alpha + p}{n(\alpha, p)} \qquad (4.45)$$

where

$$n(\alpha, p) = 2 + \pi^{-1} p - \pi^{-1} \sin^{-1}\left(\frac{p \sin \alpha}{\alpha}\right) - 2\pi^{-1} \cos^{-1}\left(\frac{p \sin \alpha}{\alpha}\right) \quad (4.46)$$

and $\alpha = n\chi - p$ is the co-latitude on the Kibble–Turok sphere of the transition points $|\xi_+| = \chi$.

Integrating (4.42) gives the contribution of $\mathbf{a}$ to the position vector of the string as

$$\mathbf{a}(\sigma_+) = \begin{cases} \dfrac{L}{2\pi m}[-\cos(m\xi_+)\widehat{\mathbf{x}} + \sin(m\xi_+)\widehat{\mathbf{z}}] \\[2ex] \dfrac{L}{2\pi n}[\{C - \cos(n\xi_+ - ps_+)\}\widehat{\mathbf{x}} + \{S + \sin(n\xi_+ - ps_+)\}\widehat{\mathbf{z}}] \end{cases} \quad (4.47)$$

for $|\xi_+| \le \chi$ and $\chi < |\xi_+| \le \pi$ respectively, with

$$C(\alpha, p) = -\frac{p \cos \alpha}{\alpha} \qquad \text{and} \qquad S(\alpha, p) = \frac{p \sin \alpha}{\alpha}. \qquad (4.48)$$

Repeating this analysis for the second mode function $\mathbf{b}'$ gives

$$\mathbf{b}(\sigma_-) = \begin{cases} \dfrac{L}{2\pi m}[-\cos(m\xi_-)\widehat{\mathbf{y}} + \sin(m\xi_+)\widehat{\mathbf{z}}] \\[2ex] \dfrac{L}{2\pi n}[\{C - \cos(n\xi_- - qs_-)\}\widehat{\mathbf{y}} + \{S + \sin(n\xi_- - qs_-)\}\widehat{\mathbf{z}}] \end{cases} \quad (4.49)$$

for $|\xi_-| \le \chi$ and $\chi < |\xi_-| \le \pi$ respectively, where $s_- = \text{sgn}(\xi_-)$ and m, n, χ, C and S are now functions of the parameter q and a second co-latitude angle β. The full trajectory is, therefore, characterized by the four adjustable parameters α, p, β and q, which henceforth will be referred to in the shorthand form $(\alpha, p; \beta, q)$. In what follows, I will assume that α and β lie in the range $(0, \pi)$, and that $|p/\alpha| < 1$ and $|q/\beta| < 1$ to ensure that m and n are well defined for both modes.

The arcs traced out by the mode functions $\mathbf{a}'$ and $\mathbf{b}'$ intersect at the north pole of the Kibble–Turok sphere, indicating the presence of a macrocusp at $\tau = \sigma = 0$, but are generally discontinuous at $|\xi_\pm| = \pi$. The jump points on the $\mathbf{a}'$ curve occur at a co-latitude $n(\alpha, p)\pi - p$ on the Kibble–Turok sphere, which is readily seen to be less than π if $p < 0$ and greater than π if $p > 0$. Similarly, the jump points on the $\mathbf{b}'$ curve occur at a co-latitude $n(\beta, q)\pi - q$ which is less than π if $q < 0$ and greater than π if $q > 0$. Thus if p and q are both negative the two mode

curves break before reaching the south pole of the Kibble–Turok sphere, and the resulting kinks in the two modes cross at the south pole, marking the appearance of a (true) microcusp at $(\tau, \sigma) = (0, L/2)$.

If one of p or q is positive the situation is more complicated, as then one of the mode curves crosses the south pole a total of three times, twice as part of a continuous segment and once on a kink. So if p is positive and q is negative (or *vice versa*), the south pole marks the appearance at different times of two false microcusps and one true microcusp. Furthermore, if p and q are both positive a total of nine cusps of various types (four macrocusps, four false microcusps and one true microcusp) appear as a result of mode-crossing at the south pole.

In terms of the parameters α, p, β and q, the condition $|\mathbf{a}_c''| = |\mathbf{b}_c''|$ for the creation or annihilation of a self-intersection as a result of the twisting of the cusp at $\sigma = 0$ becomes $m(\alpha, p) = m(\beta, q)$. As explained in section 3.9, a self-intersection created in this way does not generally appear at the cusp itself, and in the case of the balloon strings it occurs at the position of the first of the transition points $|\xi_\pm| = \chi$, so that

$$\sigma_{\mathrm{si}} = \pm \frac{L}{2\pi} \min[\chi(\alpha, p), \chi(\beta, q)]. \tag{4.50}$$

The microcusp at $\sigma = L/2$ can also absorb or emit a self-intersection, although in this instance the self-intersection always appears or disappears at the position of the microcusp. The microcusp will emit or absorb a self-intersection whenever the jumps at $|\zeta_\pm| = \pi$ in the two mode functions have the same magnitude or, equivalently, when

$$n(\alpha, p)\pi - p = n(\beta, q)\pi - q. \tag{4.51}$$
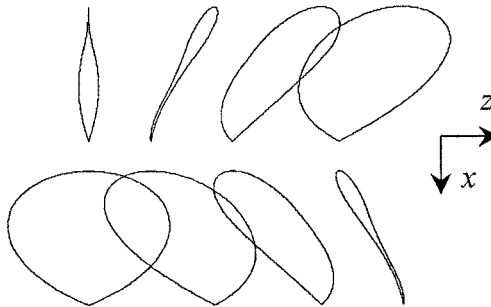
Figures 4.14 and 4.15 show the x–z and y–z projections of the $(\frac{1}{2}\pi, -1; \frac{1}{6}\pi, -0.15)$ balloon string, which was seen in section 3.9 to be close to self-intersection at $\sigma/L = \pm 0.06554$ when $\tau = 0$. As in figures 4.8–4.13, the projections of the loop are depicted at times $\tau = 0$, $L/16$, $L/8$ and $3L/16$ (top row) and $\tau = L/4$, $5L/16$, $3L/8$ and $7L/16$ (bottom row). The two kinks can be seen separately at the bottom-most point in the x–z projection and near the centre of the lower horizontal segment at $\tau = 3L/16$, $L/4$ and $5L/16$ in the y–z projection. (The other apparent kinks in figure 4.15 are just projection caustics.)

4.4   Harmonic loop solutions
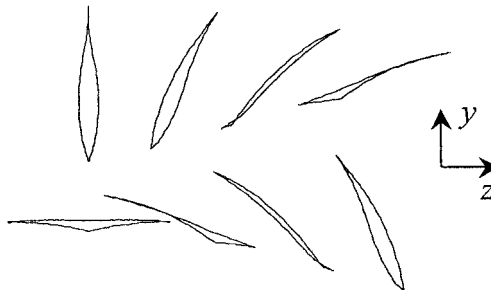
4.4.1   Loops with one harmonic

It was shown in section 3.5 that the most general mode function containing only zero- and first-order harmonics in $\xi_+ = 2\pi\sigma_+/L$ has

$$\mathbf{a}'(\sigma_+) = \sin(\xi_+ - \theta_1)\sin\phi_1\widehat{\mathbf{x}} - \cos(\xi_+ - \theta_1)\sin\phi_1\widehat{\mathbf{y}} + \cos\phi_1\widehat{\mathbf{z}} \tag{4.52}$$

Figure 4.14. The $(\frac{1}{2}\pi, -1; \frac{1}{6}\pi, -0.15)$ balloon string in the x–z projection.

Figure 4.15. The $(\frac{1}{2}\pi, -1; \frac{1}{6}\pi, -0.15)$ balloon string in the y–z projection.

where the coordinates have been chosen so that the zero-order harmonic is aligned with the z-axis. Note that if the solution describes a loop in its centre-of-momentum frame then $\cos\phi_1$ must be zero. Furthermore, it is always possible to rezero the parameters τ and σ so that $\theta_1 = 0$ or π. The mode function **a** can, therefore, be written in the form

$$\mathbf{a}(\sigma_+) = \frac{L}{2\pi}[\cos(2\pi\sigma_+/L)\hat{\mathbf{x}} + \sin(2\pi\sigma_+/L)\hat{\mathbf{y}}]. \tag{4.53}$$
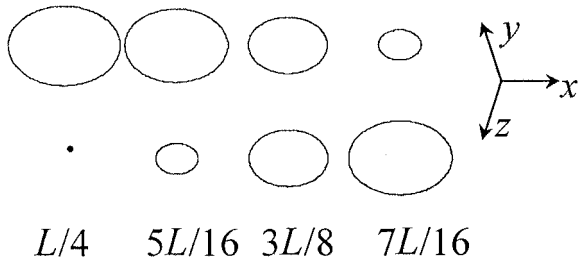
A similar argument can be applied to the mode function **b**, giving

$$\mathbf{b}(\sigma_-) = \frac{L}{2\pi}[\cos(2\pi\sigma_-/L)\hat{\mathbf{u}} + \sin(2\pi\sigma_-/L)\hat{\mathbf{v}}] \tag{4.54}$$

where $\hat{\mathbf{u}}$ and $\hat{\mathbf{v}}$ are any two orthogonal unit vectors.
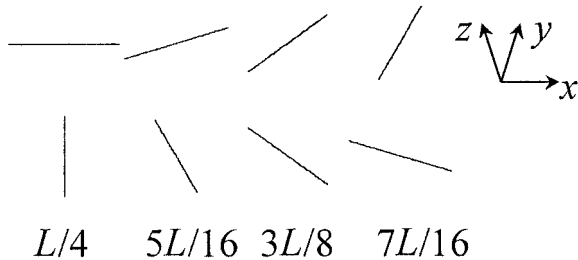
In the case where $\hat{\mathbf{u}}$ and $\hat{\mathbf{v}}$ span the x–y plane the solution describes either the collapsing circular loop or the doubled rotating rod examined in sections 4.2.1 and 4.2.2, depending on the relative orientation of the mode curves on the Kibble–Turok sphere. However, if either $\hat{\mathbf{u}}$ or $\hat{\mathbf{v}}$ has a non-zero z-component then the loop is non-planar. For example, if $\hat{\mathbf{u}} = \hat{\mathbf{x}}$ and $\hat{\mathbf{v}} = \hat{\mathbf{z}}$ the trajectory oscillates back and

Figure 4.16. A non-planar 1-harmonic string projected onto the plane spanned by $\widehat{\mathbf{x}}$ and $\widehat{\mathbf{y}} - \widehat{\mathbf{z}}$.

Figure 4.17. The same string projected onto the plane spanned by $\widehat{\mathbf{x}}$ and $\widehat{\mathbf{y}} + \widehat{\mathbf{z}}$.

forth between an ellipse of semi-major axis of length $L/2\pi$ in the $\widehat{\mathbf{x}}$ direction and semi-minor axis of length $(L/2\pi)/\sqrt{2}$ in the $\widehat{\mathbf{y}} - \widehat{\mathbf{z}}$ direction, and a doubled rod of length $(L/2\pi)/\sqrt{2}$ parallel to $\widehat{\mathbf{y}} + \widehat{\mathbf{z}}$, as demonstrated in figures 4.16 (which shows the projection onto the plane spanned by $\widehat{\mathbf{x}}$ and $\widehat{\mathbf{y}} - \widehat{\mathbf{z}}$) and 4.17 (the projection onto the plane spanned by $\widehat{\mathbf{x}}$ and $\widehat{\mathbf{y}} + \widehat{\mathbf{z}}$). The local Lorentz factor of the string in this case is

$$\lambda = 2^{1/2}[\cos^2(2\pi\tau/L) + \sin^2(2\pi\sigma/L)]^{-1/2} \tag{4.55}$$

and so cusps appear momentarily at $\tau = L/4$, at the extreme points $\sigma = 0$ and $L/2$ of the doubled rod, as would be expected. Also, the angular momentum of the loop

$$\mathbf{J} = \frac{1}{8\pi}\mu L^2(\widehat{\mathbf{z}} - \widehat{\mathbf{y}}) \tag{4.56}$$

and so has a magnitude $1/\sqrt{2} = 71\%$ of the angular momentum of a rotating rod with the same energy μL and invariant length L.

In general, the 1-harmonic solutions described by the mode functions (4.53) and (4.54) are all very similar to the trajectory illustrated in figures 4.16 and 4.17. They pass through a sequence of ellipses before degenerating into a doubled rod, with cusps appearing momentarily at the ends of the rod. If ψ denotes the angle between the plane spanned by the vectors $\widehat{\mathbf{u}}$ and $\widehat{\mathbf{v}}$ and the $x-y$ plane then, without loss of generality, the mode function $\mathbf{b}$ can be cast in the form

$$\mathbf{b}(\sigma_-) = \frac{L}{2\pi}[\cos(2\pi\sigma_-/L)\widehat{\mathbf{x}} + \sin(2\pi\sigma_-/L)(\cos\psi\widehat{\mathbf{y}} + \sin\psi\widehat{\mathbf{z}})] \qquad (4.57)$$

as the remaining freedom to rotate $\widehat{\mathbf{u}}$ and $\widehat{\mathbf{v}}$ about the z-axis can be eliminated by rotating the $x-y$ plane through the same angle and then rezeroing σ_+. The collapsing circular and rotating rod solutions are recovered when $\psi = \pi$ and $\psi = 0$ respectively.

In terms of ψ, the local Lorentz factor of the general non-planar 1-harmonic loop solution is:

$$\lambda = 2^{1/2}[(1 - \cos\psi)\cos^2(2\pi\tau/L) + (1 + \cos\psi)\sin^2(2\pi\sigma/L)]^{-1/2} \quad (4.58)$$

and so provided that $|\cos\psi| < 1$ the rod (together with its associated cusps) forms momentarily at $\tau = L/4$, aligned in the direction of the vector $(1 + \cos\psi)\widehat{\mathbf{y}} + \sin\psi\widehat{\mathbf{z}}$. The total length of this rod is $2^{-1/2}(1 + \cos\psi)^{1/2}L/\pi$. Also, the angular momentum vector of the loop

$$\mathbf{J} = \frac{1}{8\pi}\mu L^2[(1 + \cos\psi)\widehat{\mathbf{z}} - \sin\psi\widehat{\mathbf{y}}] \qquad (4.59)$$

and has magnitude

$$|\mathbf{J}| = \frac{1}{4\pi}2^{-1/2}(1 + \cos\psi)^{1/2}\mu L^2. \qquad (4.60)$$

4.4.2   Loops with two unmixed harmonics

One of the easiest way of constructing loop solutions involving two different harmonics is to allocate a single harmonic to each of the mode functions $\mathbf{a}$ and $\mathbf{b}$. In analogy with equations (4.53) and (4.54) the mode functions then have the general form

$$\mathbf{a}(\sigma_+) = \frac{L}{2\pi p}[\cos(p\xi_+)\widehat{\mathbf{x}} + \sin(p\xi_+)\widehat{\mathbf{y}}] \qquad (4.61)$$

and

$$\mathbf{b}(\sigma_-) = \frac{L}{2\pi q}[\cos(q\xi_-)\widehat{\mathbf{u}} + \sin(q\xi_-)\widehat{\mathbf{v}}] \qquad (4.62)$$

where p and q are any two non-zero integers, $\xi_\pm = 2\pi\sigma_\pm/L$ and $\widehat{\mathbf{u}}$ and $\widehat{\mathbf{v}}$ are orthogonal unit vectors as before. I will refer to these as p/q *harmonic solutions*. They were first examined in detail by Conrad Burden and Lindsay Tassie [BT84, Bur85].

Without loss of generality it can be assumed that p and q are relatively prime, since otherwise the full range $[0, L)$ of the parameter σ will cover the string more than once. In particular, all solutions with $|p| = |q|$ will be excluded, as they have already been discussed in section 4.4.1. The total angular momentum of a p/q harmonic string is

$$\mathbf{J} = \frac{1}{8\pi}\mu L^2(p^{-1}\widehat{\mathbf{z}}+q^{-1}\widehat{\mathbf{u}}\times\widehat{\mathbf{v}}) \qquad (4.63)$$

and so the **a** and **b** modes separately contribute an angular momentum vector proportional to that of the corresponding 1-harmonic solution but scaled as p^{-1} or q^{-1}.

The simplest p/q harmonic solutions are planar loops, which can be generated by setting $\widehat{\mathbf{u}} = \widehat{\mathbf{x}}$ and $\widehat{\mathbf{v}} = \widehat{\mathbf{y}}$. (As before, a rotation of $\widehat{\mathbf{u}}$ and $\widehat{\mathbf{v}}$ about the z-axis does not yield any new solutions, as it just corresponds to a spatial rotation and a translation in the zero point of σ_+.) Solutions of this type have angular momentum

$$\mathbf{J} = \frac{p + q}{4\pi pq}\mu L^2\widehat{\mathbf{z}} \qquad (4.64)$$

while their local Lorentz factor is

$$\lambda = 2^{1/2}[1 - \cos(p\xi_+ - q\xi_-)]^{-1/2}. \qquad (4.65)$$

The loops, therefore, support permanent cusps with trajectories of the form

$$\sigma = \frac{q - p}{q + p}\tau + \frac{n}{q + p}L \qquad (4.66)$$

where n is some integer. Given that the solutions are periodic with period L in σ, the total number of cusps is $|p + q|$. The cusps trace out a fixed circle in the background spacetime, as the distance of each cusp from the origin is

$$|\mathbf{r}_c| = \frac{L}{4\pi}\left|\frac{p+q}{pq}\right|. \qquad (4.67)$$

Furthermore, if the position vector of the planar p/q harmonic solutions is rewritten in the form

$$\mathbf{r}(\tau, \sigma) = \frac{1}{2}\left[\frac{p + q}{pq}\cos\chi\,(\cos\phi\widehat{\mathbf{x}} + \sin\phi\widehat{\mathbf{y}}) + \frac{p - q}{pq}\sin\chi\,(\sin\phi\widehat{\mathbf{x}} - \cos\phi\widehat{\mathbf{y}})\right] \qquad (4.68)$$

where

$$\phi = \frac{\pi}{L}[(p+q)\tau+(p-q)\sigma] \quad \text{and} \quad \chi = \frac{\pi}{L}[(p-q)\tau+(p+q)\sigma] \quad (4.69)$$

then it is evident that the solutions are rigidly rotating. To see this, consider the set of points with $\chi = \chi_0$ for some constant χ_0. These all lie on a circle centred on the origin, with phase angle

$$\phi = \frac{4\pi pq}{L(p + q)}\tau + \frac{p - q}{p + q}\chi_0. \qquad (4.70)$$

Since $d\phi/d\tau$ is constant and independent of the choice of χ_0, the entire configuration traced out by the string is rotating with a uniform pattern speed:

$$\omega = \frac{4\pi|pq|}{L|p+q|}. \tag{4.71}$$
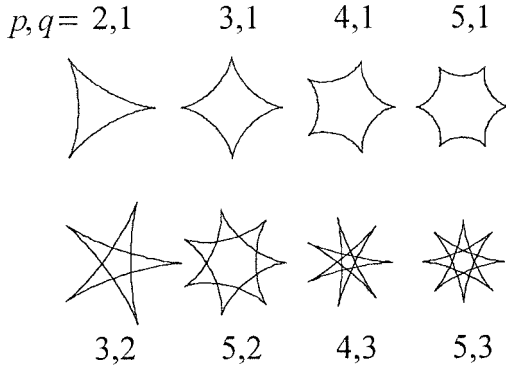
The formula for the pattern speed also follows directly from the expression (4.67) for $|\mathbf{r}_c|$, as it was seen in section 3.6 that persistent cusps always propagate at the speed of light. Franz Embacher [Emb92] has shown that the planar p/q harmonic solutions are the only planar loops in flat space that rotate rigidly. This result will be explored in more detail in section 4.5.

Comparison of (4.64) and (4.71) reveals an unexpected and somewhat counter-intuitive feature of the planar p/q harmonic solutions, namely that the pattern speed ω is *inversely* proportional to the magnitude $|\mathbf{J}|$ of the angular momentum vector. The contrast between ω and $|\mathbf{J}|$ is starkest when $p = N + 1$ and $q = -N$ with N large, as then $\omega \approx 4\pi N^2/L$ but $|\mathbf{J}| \approx \mu L^2/(4\pi N^2)$. In the limit as $N \to \infty$ the angular momentum of the string goes to zero but the pattern speed is infinite. The string in this limit traces out a circle (with an infinite winding number) which is static and, of course, rotationally symmetric. There is thus no inconsistency in the relationship between ω and $|\mathbf{J}|$, although it is important to recognize that the pattern speed is not at all indicative of the string's rotational energy.
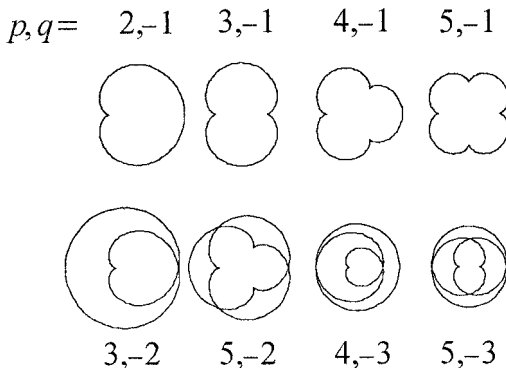
In addition to being stationary, the planar p/q harmonic solutions possess discrete rotational symmetry. At a fixed value of τ the functions $\cos\chi$ and $\sin\chi$ in (4.68) assume any particular pair of values $[\cos\chi_0, \sin\chi_0]$ or their antipodes $[-\cos\chi_0, -\sin\chi_0]$ a total of $|p+q|$ times as σ ranges from 0 to L. The corresponding pattern, therefore, has $|p+q|$-fold rotational symmetry, as would be expected given that the string is known to support $|p+q|$ permanent cusps.

One final property of the planar p/q harmonic strings that is helpful in visualizing the trajectory is the winding number of the pattern. From (4.61) and (4.62) it is clear that if $|p| < |q|$ then the mode function $\mathbf{a}$ has the dominant amplitude, whereas if $|p| > |q|$ then $\mathbf{b}$ is dominant. The winding number of the entire pattern is just the winding number of the dominant mode, and so is equal to the smaller of $|p|$ and $|q|$.

Figures 4.18 and 4.19 each show the patterns traced out by the eight planar p/q harmonic strings with the smallest available values of $|p|$ and $|q|$, with $q > 0$ in figure 4.18 and $q < 0$ in figure 4.19. Note that as $|p|$ and $|q|$ increase the diameter of the pattern generally shrinks if the invariant length L remains fixed. To illustrate fully the details of the smaller patterns, the second row in both figures has been magnified by a factor of two. Note also that a given solution with $q > 0$ has substantially more rotational energy than the corresponding solution with $q < 0$. The configurations in figure 4.18 thus have, on average, smaller pattern speeds than those in figure 4.19. The pattern frequencies $L\omega/(2\pi)$ in figure 4.18 range from $4/3$ for the $2/1$ string to $15/4$ for the $5/3$ string, whereas in figure 4.19 the frequencies range from $5/2$ for the $5/-1$ string to 24 for the $4/-3$ string.

$p, q = 2,1$ $3,1$ $4,1$ $5,1$

$3,2$ $5,2$ $4,3$ $5,3$

Figure 4.18. Planar p/q harmonic strings with $pq > 0$.

$p, q =$ $2,-1$ $3,-1$ $4,-1$ $5,-1$

$3,-2$ $5,-2$ $4,-3$ $5,-3$

Figure 4.19. Planar p/q harmonic strings with $pq < 0$.

As was the case with the 1-harmonic strings, the family of non-planar p/q harmonic strings can be fully described by the introduction of a third parameter ψ which measures the angle between the planes spanned by the position vectors of the **a** and **b** modes. The equation for the **b** mode then reads:
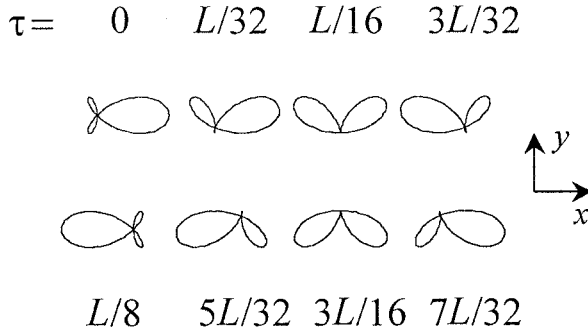
$$\mathbf{b}(\sigma_-) = \frac{L}{2\pi q}[\cos(q\xi_-)\widehat{\mathbf{x}} + \sin(q\xi_-)(\cos\psi\widehat{\mathbf{y}} + \sin\psi\widehat{\mathbf{z}})] \qquad (4.72)$$

and the local Lorentz factor of the corresponding loop is

$$\lambda = 2^{1/2}[1 - \sin(p\xi_+)\sin(q\xi_-) - \cos\psi\cos(p\xi_+)\cos(q\xi_-)]^{-1/2} \qquad (4.73)$$

while its net angular momentum is

$$|\mathbf{J}| = \frac{(p^2 + q^2 + 2pq\cos\psi)^{1/2}}{4\pi|pq|}\mu L^2. \qquad (4.74)$$

$$\tau = \quad 0 \quad L/32 \quad L/16 \quad 3L/32$$

$$L/8 \quad 5L/32 \quad 3L/16 \quad 7L/32$$

Figure 4.20. The 2/1 harmonic string with $\psi = \frac{1}{2}\pi$ in the x–y projection.

It follows after some algebraic manipulation of (4.73) that if $|\cos\psi| < 1$ then cusps occur only when $\sin(p\xi_+)\sin(q\xi_-) = 1$. With τ and σ both ranging over $[0, L)$ it would appear that, in general, a non-planar p/q harmonic string has a total of $4|pq|$ cusps (of the normal type), located at

$$\tau = (q + p + 4mq + 4np)\frac{L}{8pq} \qquad \sigma = (q - p + 4mq - 4np)\frac{L}{8pq} \quad (4.75)$$

and

$$\tau = (-p - q + 4mq + 4np)\frac{L}{8pq} \qquad \sigma = (p - q + 4mq - 4np)\frac{L}{8pq} \quad (4.76)$$
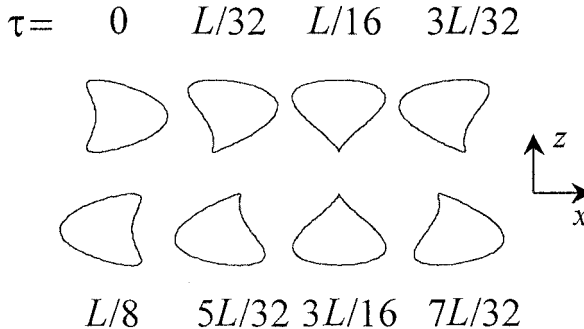
(all modulo L), where m and n are integers in $[1, 2|p|]$ and $[1, 2|q|]$ respectively.

However, any trajectory constructed from the p/q harmonic modes (4.61) and (4.62) is invariant under the translations

$$(\tau, \sigma) \rightarrow \left(\tau + \frac{L}{2|p|}, \sigma + \frac{L}{2|p|}\right) \qquad \text{and} \qquad (\tau, \sigma) \rightarrow \left(\tau + \frac{L}{2|q|}, \sigma - \frac{L}{2|q|}\right) \quad (4.77)$$

and so the fundamental period of the loop is not L but $T = \min\{\frac{L}{2|p|}, \frac{L}{2|q|}\}$. The number of distinct cusps appearing during a single period T in τ is, therefore, $2\min\{|q|, |p|\}$.

Figures 4.20 and 4.21 show the time development of the 2/1 harmonic loop with $\psi = \frac{1}{2}\pi$, in the x–y and x–z planes respectively, for τ between 0 and $\frac{7}{32}L$. This solution supports two cusps over a single period $T = \frac{1}{4}L$, at $(\tau/L, \sigma/L) = (\frac{1}{16}, \frac{5}{16})$ and $(\frac{3}{16}, \frac{15}{16})$. By comparison, the corresponding planar loop—illustrated in the first frame of figure 4.18—has three permanent cusps and rotates with a pattern speed $\frac{8\pi}{3L}$ consistent with threefold symmetry and a fundamental period of $\frac{1}{4}L$.

$$\tau = \quad 0 \qquad L/32 \quad L/16 \quad 3L/32$$

$$L/8 \quad 5L/32 \; 3L/16 \; 7L/32$$

Figure 4.21. The 2/1 harmonic string with $\psi = \frac{1}{2}\pi$ in the x–z projection.

4.4.3 Loops with two mixed harmonics

The equation for the most general 012-harmonic mode (modulo spatial rotations) was previewed in section 3.5. If the loop is in its centre-of-momentum frame, two of the four free parameters in that equation are constrained by the requirement that either $\sin\phi_1 = \cos\phi_2 = 0$ or $\cos\phi_1 = \sin(\phi_2/2) = 0$. In the first case, the mode function contains only first-order harmonics in ξ_+, while in the second case it contains only second-order harmonics. Thus a solution containing nothing other than first- and second-order harmonics must have one of the harmonics allocated to the mode function **a** and the other to **b**. This means that the (non-planar) 2/1 harmonic and $2/-1$ harmonic loops are the most general solutions containing only first-and second-order harmonics.

The analogous result is not true for solutions containing only first- and third-order harmonics, however. In this case, solutions can be found in which the two harmonics are mixed between the two modes. The most general solution of this type was first constructed by David DeLaney *et al* [DES90], building on earlier work by Kibble and Turok [KT82], Turok [Tur84] and Chen *et al* [CDH88]. Following DeLaney *et al* I will refer to this solution as the *1–3/1–3 harmonic loop*.

DeLaney *et al* derived the general expression for a 1–3 harmonic mode function **a**′ by taking a general 12-parameter 3-vector containing both harmonics and then solving the constraint $|\mathbf{a}'| = 1$ to eliminate seven of the parameters. A somewhat more elegant approach is to use the spinor method of section 3.5 to generate the six-parameter 0123-harmonic mode function and adjust the parameters so as to remove the 0- and 2-harmonics while retaining a mixture of the 1- and 3-harmonics. This gives

$$
\begin{aligned}
\mathbf{a}'(\sigma_+) = \; &\pm \{[\cos^2(\phi_2/2)\sin(3\xi_+ - \theta_1) - \sin^2(\phi_2/2)\sin(\xi_+ + \theta_1 - 2\theta_2)]\widehat{\mathbf{x}} \\
&+ [-\cos^2(\phi_2/2)\cos(3\xi_+ - \theta_1) + \sin^2(\phi_2/2)\cos(\xi_+ + \theta_1 - 2\theta_2)]\widehat{\mathbf{y}} \\
&- \sin(\phi_2)\cos(\xi_+ + \theta_2 - \theta_1)\widehat{\mathbf{z}}\}.
\end{aligned} \tag{4.78}
$$

The choice of sign in (4.78) can always be absorbed into ξ_+, while θ_1 and θ_2 can be reduced to a single parameter by rezeroing ξ_+ to eliminate θ_1 from the 3-harmonics and then defining $\theta = \theta_2 - 2\theta_1/3$. With an additional phase shift of $\frac{3}{2}\pi$ in ξ_+ (to conform with the conventions first used by Turok [Tur84][1]) the resulting mode function **a** is:

$$\mathbf{a}(\sigma_+) = \frac{L}{2\pi}\{[\tfrac{1}{3}\cos^2(\phi/2)\sin(3\xi_+) + \sin^2(\phi/2)\sin(\xi_+ - 2\theta)]\widehat{\mathbf{x}}$$
$$+ [-\tfrac{1}{3}\cos^2(\phi/2)\cos(3\xi_+) - \sin^2(\phi/2)\cos(\xi_+ - 2\theta)]\widehat{\mathbf{y}}$$
$$+ \sin\phi\cos(\xi_+ + \theta)\widehat{\mathbf{z}}\} \tag{4.79}$$

where the subscript has been dropped from ϕ_2. Similarly, the corresponding mode function **b** can be cast in the form

$$\mathbf{b}(\sigma_-) = \frac{L}{2\pi}\{[\tfrac{1}{3}\cos^2(\phi^*/2)\sin(3\xi_-) + \sin^2(\phi^*/2)\sin(\xi_- - 2\theta^*)]\widehat{\mathbf{x}}$$
$$+ [-\tfrac{1}{3}\cos^2(\phi^*/2)\cos(3\xi_-) - \sin^2(\phi^*/2)\cos(\xi_- - 2\theta^*)]\widehat{\mathbf{v}}$$
$$+ \sin\phi^*\cos(\xi_- + \theta^*)\widehat{\mathbf{w}}\} \tag{4.80}$$

with $\widehat{\mathbf{v}} = \cos\psi\,\widehat{\mathbf{y}} + \sin\psi\,\widehat{\mathbf{z}}$ and $\widehat{\mathbf{w}} = \cos\psi\,\widehat{\mathbf{z}} - \sin\psi\,\widehat{\mathbf{y}}$ for some choice of angle ψ.

The mode functions (4.79) and (4.80) together characterize the full five-parameter family of 1–3/1–3 harmonic solutions. The angular momentum of the solutions is:

$$\mathbf{J} = \frac{\mu L^2}{8\pi}\{[\sin^2(\phi/2)\sin\phi\sin\theta(4\cos^2\theta - 1)$$
$$+ \sin^2(\phi^*/2)\sin\phi^*\sin\theta^*(4\cos^2\theta^* - 1)]\widehat{\mathbf{x}}$$
$$+ [\sin^2(\phi/2)\sin\phi\cos\theta(4\cos^2\theta - 3) - \tfrac{1}{3}(1 - \cos\phi^* + \cos^2\phi^*)\sin\psi$$
$$+ \sin^2(\phi^*/2)\sin\phi^*\sin\theta^*(4\cos^2\theta^* - 3)\cos\psi]\widehat{\mathbf{y}}$$
$$+ [\tfrac{1}{3}(1 - \cos\phi + \cos^2\phi) + \tfrac{1}{3}(1 - \cos\phi^* + \cos^2\phi^*)\cos\psi$$
$$+ \sin^2(\phi^*/2)\sin\phi^*\sin\theta^*(4\cos^2\theta^* - 3)\sin\psi]\widehat{\mathbf{z}}\}. \tag{4.81}$$

The expression for the local Lorentz factor λ is too complicated to reproduce here and is of minimal value in identifying salient features such as cusps.

The 1–3/1–3 harmonic solutions have been studied extensively in [KT82, Tur84, CT86, CDH88, DES90], with a view primarily to identifying the subset of the parameter space where the loops self-intersect. A series of Monte Carlo simulations performed by Delaney *et al* [DES90] indicate that between 40% and 60% of the parameter space is occupied by self-intersecting loops, with the fraction more strongly dependent on the resolution of the simulation than on the measure assumed for the parameter space. An earlier study by Chen *et al*

---

[1] Note, however, that Turok takes **a** to be a function of $\sigma - \tau$ and **b** to be a function of $\sigma + \tau$. See section 3.1 for an explanation of the conventions used here.

[CDH88] examined the three-parameter sub-family of 1–3/1 harmonic solutions that results when $\phi^* = \pi$ and θ^* is set to zero[2]. In this case, between 30% and 40% of the parameter space generates self-intersecting loops. Self-intersection is least likely to occur when $\theta = 0$ (the 1- and 3-harmonics are in phase) and most likely to occur when $\phi = \frac{1}{2}\pi$ (the harmonics in $\mathbf{a}'$ have equal amplitudes).

An even smaller sub-family of solutions, first published by Neil Turok [Tur84] in 1984, can be recovered by setting $\phi^* = \pi$ and $\theta = \theta^* = 0$, so that

$$\mathbf{a}(\sigma_+) = \frac{L}{2\pi} \left\{ [\tfrac{1}{3}\alpha \sin(3\xi_+) + (1 - \alpha) \sin(\xi_+)]\widehat{\mathbf{x}} \right.$$
$$+ [-\tfrac{1}{3}\alpha \cos(3\xi_+) - (1 - \alpha) \cos(\xi_+)]\widehat{\mathbf{y}}$$
$$\left. - 2\sqrt{\alpha - \alpha^2} \cos(\xi_+)\widehat{\mathbf{z}} \right\} \tag{4.82}$$

and

$$\mathbf{b}(\sigma_-) = \tfrac{L}{2\pi}[\sin(\xi_-)\widehat{\mathbf{x}} - \cos(\xi_-)(\cos\psi\widehat{\mathbf{y}} + \sin\psi\widehat{\mathbf{z}})] \tag{4.83}$$

where $\alpha = \cos^2(\phi/2)$. Setting $\psi = 0$ in 4.83 gives the *Kibble–Turok solutions* [KT82], which were the earliest of the 1–3/1 harmonic loop solutions to be examined in any detail.
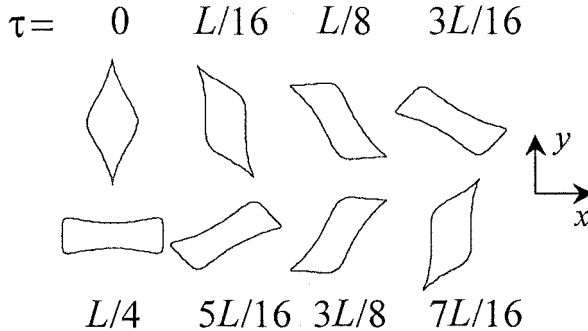
The Kibble–Turok solutions form a continuous one-parameter family of loops that ranges from the doubled rotating rod ($\alpha = 0$) to the planar 3/1 harmonic string ($\alpha = 1$). However, all solutions with $0 < \alpha < 1$ are non-planar and are free of self-intersections. The local Lorentz factor of the solutions is:

$$\lambda = 2^{1/2}[1 - \alpha \cos(4\pi\tau/L + 8\pi\sigma/L) - (1 - \alpha) \cos(4\pi\sigma/L)]^{-1/2} \tag{4.84}$$
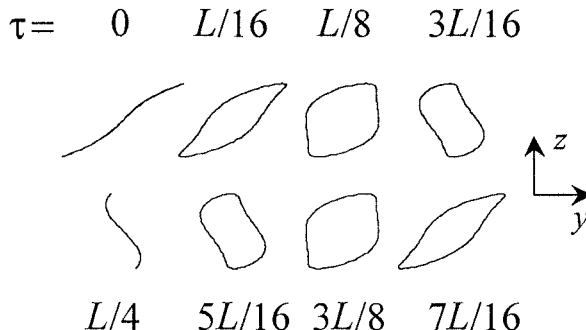
and so if $0 < \alpha < 1$ the solutions support just two, simultaneous, cusps (of the normal type) per oscillation period, at $(\tau, \sigma) = (0, 0)$ and $(0, L/2)$. Figures 4.22 and 4.23 give two views of the Kibble–Turok solution with $\alpha = 0.5$.

In a similar manner, the full two-parameter family of *Turok solutions* described by the mode functions (4.82) and (4.83) forms a bridge between the 1-harmonic solutions of section 4.4.1 and the general (non-planar) 3/1 harmonic strings. All Turok solutions with $0 < \alpha < 1$ support either two, four or six cusps, with two of the cusps always occurring at $(\tau, \sigma) = (0, 0)$ and $(0, L/2)$. Solutions with four cusps occur only when $\cos(\psi - \phi) = \pm 1$, with the two extra cusps appearing either at $\tau = 0$ or at $\tau = L/4$. Otherwise, the parameter space is evenly divided between the two- and six-cusp solutions, as shown in figure 4.24.

---

[2] The parameter ϕ used by Chen *et al* (CDH) is the same as the parameter I call ψ. However, the two remaining CDH parameters θ and η bear no simple relationship to the parameters ϕ and θ that appear in (4.79). The expression CDH derive for $\mathbf{a}'$ can be constructed from (4.78) by setting θ_1 equal to $\tan^{-1}(\frac{-\sin\theta\sin\eta}{\cos\theta+\cos\eta})$, $2\theta_2 - \theta_1$ to $\tan^{-1}(\frac{\cos\theta\cos\eta}{\cos\theta-\cos\eta})$ and $\cos\phi_2$ to $\cos\theta\cos\eta$, then translating ξ_+ by $\frac{3}{2}\pi$ and rotating the entire 3-vector by an angle θ about the *y*-axis. The equally complicated transformation from the CDH parameters to the parameter set used by DeLaney *et al* can be found in [DES90].

Figure 4.22. The Kibble–Turok string with $\alpha = 0.5$ in the x–y projection.
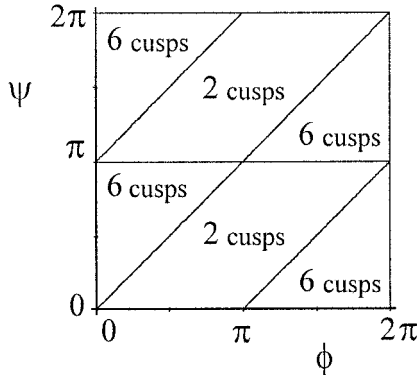
Figure 4.23. The same string in the y–z projection.

From (4.81), the angular momentum of the Turok solutions is:

$$\mathbf{J} = \frac{\mu L^2}{8\pi} \left\{ \left[-2(1 - \alpha)\sqrt{\alpha - \alpha^2} - \sin\psi \right] \hat{\mathbf{y}} + (\tfrac{4}{3}\alpha^2 - 2\alpha + 1 + \cos\psi)\hat{\mathbf{z}} \right\}. \tag{4.85}$$

The subset of the parameter space that corresponds to self-intersecting solutions has been discussed fully by Chen *et al* [CDH88].

Finally, mention should be made of the role played by the Turok solutions in estimates of the likelihood that a cosmic string will collapse to form a black hole. According to the 'hoop conjecture' (see [MTW73, pp 867–8]), an event horizon will form around a string loop if, at any moment, in the string's evolution it shrinks to a size small enough for it to fit inside a sphere with radius equal to the string's Schwarzschild radius $R_S = 2\mu L$. It is evident from (4.82) and (4.83) that all the Turok solutions are reflection-symmetric about the origin, as $\mathbf{r}(\tau, \sigma + L/2) = -\mathbf{r}(\tau, \sigma)$, and so the radius $R_{\min}$ of the smallest sphere that can enclose the string is found by maximizing $|\mathbf{r}(\tau, \sigma)|$ over σ with τ fixed and then minimizing over τ.

Figure 4.24. Cusp structure of the Turok solutions.

This particular problem was first examined in 1991 by Alexander Polnarev and Robert Zembowicz [PZ91], who claimed that the minimum radius occurs in all cases when $\tau = L/4$, and that

$$(2\pi R_{\min}/L)^2 = \left(\sqrt{\alpha - \alpha^2} - \sqrt{\beta - \beta^2}\right)^2 + (\tfrac{1}{3}\alpha - \beta)^2 \qquad (4.86)$$

where $\beta = \sin^2(\psi/2)$. A more recent analysis by Hansen *et al* [HCL00] indicates that (4.86) gives the correct formula for $R_{\min}$ only on a subset of the α–β parameter space. A full specification of $R_{\min}$ as a function of α and β is somewhat complicated but over much of the parameter space (including, in particular, a neighbourhood of the collapsing circular loop at $\alpha = \beta = 0$) the minimum radius occurs at either $\tau = 0$ or $\tau = L/4$ and according to Hansen *et al* is given by

$$(2\pi R_{\min}/L)^2 = \max\left\{4\alpha^2/9, \left(\sqrt{\alpha - \alpha^2} - \sqrt{\beta - \beta^2}\right)^2 + (\tfrac{1}{3}\alpha - \beta)^2\right\}.$$
$$(4.87)$$

However, formula (4.87) applies only if the parameter $\sin\psi$ appearing in (4.83) is positive, as in transforming from ψ to β Polnarev and Zembowicz have effectively lost that half of the parameter space in which $\sin\psi < 0$. If $\sin\psi$ is negative, the corresponding expression for the minimum radius (occurring again at $\tau = L/4$) is:

$$(2\pi R_{\min}/L)^2 = \left(\sqrt{\alpha - \alpha^2} + \sqrt{\beta - \beta^2}\right)^2 + (\tfrac{1}{3}\alpha - \beta)^2 \qquad (4.88)$$

which is always greater than or equal to $4\alpha^2/9$ for α and β in [0, 1].

A loop belonging to the Turok family will pass inside its Schwarzschild radius at least once per oscillation period if

$$(2\pi R_{\mathrm{min}}/L)^2 \leq 16\pi^2\mu^2. \tag{4.89}$$

For $\mu \ll 1$, Hansen *et al* [HCL00] have shown that if $\sin\psi > 0$ the subset of the α–β parameter space satisfying this constraint has a total area of about $2000\mu^{5/2}$ to leading order in μ, whereas if $\sin\psi < 0$ it is easily seen that the relevant subset has a total area of about $4000\mu^4$, again to leading order in μ. Thus, the estimate of $2000\mu^{5/2}$ that Hansen *et al* offer for the probability that a randomly-chosen Turok solution will collapse to form a black hole should strictly speaking be halved (to $1000\mu^{5/2} \approx 10^{-12}$ if $\mu \approx 10^{-6}$) but it relies on such a naive assumption about the appropriate probability measure on the α–β parameter space that its value is little more than heuristic anyway.

In connection with this result it should be mentioned that Robert Caldwell and Paul Casper [CC96] have examined an ensemble of 25 576 string loops generated by evolving a set of parent loops through successive fragmentation events until only stable daughter loops remain. They estimate that the fraction f of these loops that pass inside their Schwarzschild radius $2\mu L$ at least once during an oscillation period is:

$$f = 10^{4.9\pm0.2}\mu^{4.1\pm0.1} \tag{4.90}$$

which (although about 20 times larger) has a similar dependence on μ as the fraction of Turok solutions with $\sin\psi < 0$ that pass inside R_{S}. The corresponding probability of collapse for loops with $\mu \approx 10^{-6}$ is, therefore, $f \approx 10^{-20}$, which is considerably smaller than the estimate based on the full set of Turok loops.

4.4.4 Loops with three or more harmonics

The general method for constructing mode functions containing three or more harmonics should be clear from the preceding sections. The full family of 1–2–3/1–2–3 harmonic loops, for example, is described by mode functions with the same basic form as the 1–3 mode functions (4.79) and (4.80), save that the $\widehat{\mathbf{z}}$ and $\widehat{\mathbf{w}}$ components are second-order rather than first-order harmonics. Because the family is no longer invariant under rotations of $\mathbf{b}$ about the z-axis, the parameter space in this case is six-dimensional. Other families of multi-harmonic loops are just as complicated and, needless to say, none has yet been fully explored. However, two interesting sub-families of multi-harmonic solutions— discovered in circumstances that could perhaps be described as serendipitous— have been examined in connection with studies of gravitational radiation from cosmic strings.

The first of these is a modification of the Turok family (4.82)–(4.83) and was published by Tanmay Vachaspati and Alexander Vilenkin [VV85] in 1985.

Its construction relies on the identity

$$[-\alpha\cos(3\xi_+) + (1-\alpha)\cos(\xi_+)]^2 + [\alpha\sin(3\xi_+) + (1-\alpha)\sin(\xi_+)]^2$$
$$= 1 - 4(\alpha - \alpha^2)\cos^2(2\xi_+) \tag{4.91}$$

which indicates that the 3-harmonic mode function

$$\mathbf{a}(\sigma_+) = \frac{L}{2\pi}\left\{[-\tfrac{1}{3}\alpha\sin(3\xi_+) + (1-\alpha)\sin(\xi_+)]\widehat{\mathbf{x}} \right.$$
$$+ [-\tfrac{1}{3}\alpha\cos(3\xi_+) - (1-\alpha)\cos(\xi_+)]\widehat{\mathbf{y}}$$
$$\left. + \sqrt{\alpha - \alpha^2}\sin(2\xi_+)\widehat{\mathbf{z}}\right\} \tag{4.92}$$

satisfies the gauge constraint $|\mathbf{a}'| = 1$ as required. If the mode function (4.92) is combined with the standard 1-harmonic mode function

$$\mathbf{b}(\sigma_-) = \frac{L}{2\pi}[\sin(\xi_-)\widehat{\mathbf{x}} - \cos(\xi_-)(\cos\psi\widehat{\mathbf{y}} + \sin\psi\widehat{\mathbf{z}})] \tag{4.93}$$

then the result is the two-parameter family of *Vachaspati–Vilenkin solutions*.

Like the Turok solutions, the Vachaspati–Vilenkin solutions form a continuous link between the non-planar 1-harmonic loops ($\alpha = 0$) and the non-planar $3/-1$ harmonic loops ($\alpha = 1$). The total angular momentum

$$\mathbf{J} = \frac{\mu L^2}{8\pi}[-\sin\psi\widehat{\mathbf{y}} + (\tfrac{4}{3}\alpha^2 - 2\alpha + 1 + \cos\psi)\widehat{\mathbf{z}}] \tag{4.94}$$
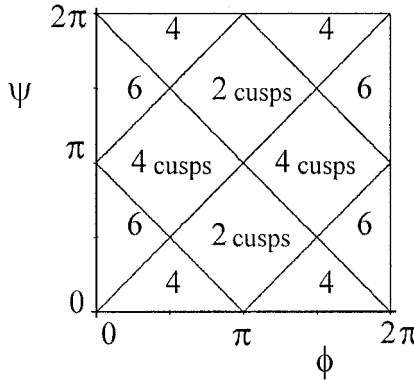
of the Vachaspati–Vilenkin solutions differs from the corresponding formula (4.85) for the Turok solutions only by the quantity $\mu L^2(1-\alpha)\sqrt{\alpha - \alpha^2}\widehat{\mathbf{y}}/(4\pi)$.

The cusp structure of the Vachaspati–Vilenkin solutions is somewhat more complicated than for the Turok solutions. In general, if $0 < \alpha < 1$ the solutions support either two, four or six cusps, with the parameter space partitioned as shown in figure 4.25, where the parameter ϕ is defined as before by $\alpha = \cos^2(\phi/2)$. However, if $\cos(\psi + \phi) = \pm 1$ or $\cos(\psi - \phi) = \pm 1$ the solution typically supports either three or five cusps. Solutions with $\psi = 0$ or $\psi = \pi$ support four cusps, appearing at $\tau = L/8$ and $3L/8$ or $\tau = 0$ respectively.
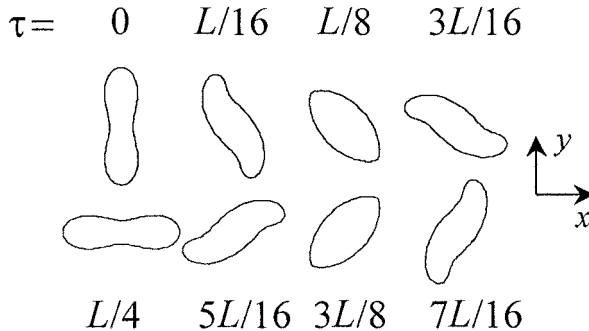
The time development of the Vachaspati–Vilenkin solution with $\alpha = 0.5$ and $\psi = 0$ is illustrated in figures 4.26 and 4.27. The parameters have been chosen so that a direct comparison with the corresponding Kibble–Turok solution, examined in the previous section, is possible. The four cusps occur, pairwise and equally spaced around the string, at $\tau = L/8$ and $\tau = 3L/8$.

The second family of multi-harmonic solutions is due to David Garfinkle and Tanmay Vachaspati [GV87a], and was discovered during a search for solutions free of both cusps and kinks. The mode functions describing the *Garfinkle–Vachaspati solutions* contain four different harmonics and have the form:

$$\mathbf{a}(\sigma_+) = \frac{-L}{2\pi(p^2 + 2)(2p^2 + 1)}\{[(p^2 + 1)^2\sin(2\xi_+) + \tfrac{1}{4}p^2\sin(4\xi_+)]\widehat{\mathbf{x}}$$

Figure 4.25. Cusp structure of the Vachaspati–Vilenkin solutions.

Figure 4.26. The Vachaspati–Vilenkin string with $\alpha = 0.5$ in the x–y projection.

$$+ 2\sqrt{2}p[(p^2 + 2)\cos\xi_+ + \tfrac{1}{3}\cos(3\xi_+)]\hat{\mathbf{y}}$$
$$+ [(p^4 + 2p^2 - 1)\cos(2\xi_+) + \tfrac{1}{4}p^2\cos(4\xi_+)]\hat{\mathbf{z}} \tag{4.95}$$
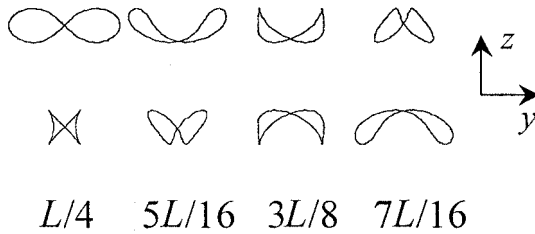
and

$$\mathbf{b}(\sigma_-) = \frac{L}{2\pi(p^2 + 2)(2p^2 + 1)}\{[(p^2 + 1)^2\sin(2\xi_-) + \tfrac{1}{4}p^2\sin(4\xi_-)]\hat{\mathbf{x}}$$
$$+ [(p^4 + 2p^2 - 1)\cos(2\xi_-) + \tfrac{1}{4}p^2\cos(4\xi_-)]\hat{\mathbf{y}}$$
$$+ 2\sqrt{2}p[(p^2 + 2)\cos\xi_- + \tfrac{1}{3}\cos(3\xi_-)]\hat{\mathbf{z}} \tag{4.96}$$

where p is a non-negative constant[3]. A method for generating these mode functions using rotation matrices is discussed in [BD89].

---

[3] Negative values of p can be ignored because reversing the sign of p is equivalent to replacing σ everywhere with $\pi - \sigma$ and then rotating the coordinate system by an angle π about the vector $\hat{\mathbf{y}} - \hat{\mathbf{z}}$.

$$\tau = \quad 0 \quad L/16 \quad L/8 \quad 3L/16$$

$$L/4 \quad 5L/16 \quad 3L/8 \quad 7L/16$$

Figure 4.27. The same string in the *y–z* projection.

When $p = 0$ and in the limit as $p \to \infty$ the Garfinkle–Vachaspati solutions degenerate into a standard 1-harmonic solution with angle $\psi = \frac{1}{2}\pi$ between the mode planes. The solutions typically support eight cusps per period but for a range of values of p between about 0.28 and 1.38 the loops are, in fact, cusp-free. The net angular momentum of the solutions is:
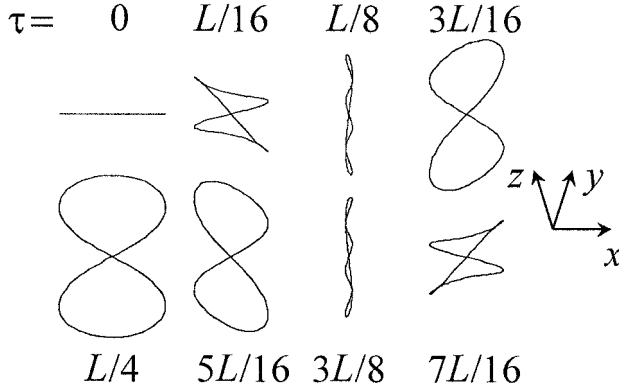
$$\mathbf{J} = \frac{\mu L^2}{8\pi} \frac{-2 + \frac{33}{4}p^4 + 8p^6 + 2p^8}{(p^2 + 2)^2(2p^2 + 1)^2}(\widehat{\mathbf{y}} - \widehat{\mathbf{z}}) \tag{4.97}$$

where the rational function of p preceding $\widehat{\mathbf{y}} - \widehat{\mathbf{z}}$ increases monotonically from $-\frac{1}{2}$ at $p = 0$ to $\frac{1}{2}$ in the limit as $p \to \infty$. The net angular momentum vanishes when $p \approx 0.6407$.
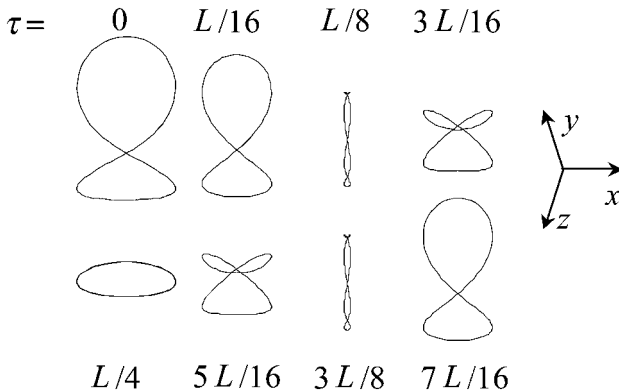
Figures 4.28 and 4.29 show the evolution of the $p = 1$ solution over the course of an oscillation period. In the first figure the loop is seen projected onto the plane orthogonal to the angular momentum vector $\mathbf{J} = \frac{65\mu L^2}{2592\pi}(\widehat{\mathbf{y}} - \widehat{\mathbf{z}})$, while the second figure shows the projection onto the plane containing $\widehat{\mathbf{x}}$ and $\mathbf{J}$, which points towards the top of the page. The solution is, of course, cusp-free, although the maximum local Lorentz factor, $\lambda \approx 4.6$, is still quite substantial.

4.5   Stationary rotating solutions

It was seen in section 4.4.2 that string solutions describing stationary rotating loops are easily generated by superposing left- and right-moving single-harmonic modes. In 1992 Franz Embacher [Emb92] showed that all stationary rotating planar string loops are members of the class of p/q harmonic solutions defined by (4.61)–(4.62), and also attempted to give a completely general characterization of the family of stationary rotating solutions, whether closed or not.

$$\tau = \quad 0 \quad\quad L/16 \quad\quad L/8 \quad\quad 3L/16$$

Figure 4.28. The Garfinkle–Vachaspati string with $p = 1$ projected along **J**.

$$\tau = \quad 0 \quad\quad L/16 \quad\quad L/8 \quad\quad 3L/16$$

Figure 4.29. The same string projected onto the plane of $\hat{\mathbf{x}}$ and **J**.

In Embacher's approach, the axis of rotation of the string is assumed without loss of generality to lie in the z-direction. The position vector of the string is then

$$
\mathbf{r}(\tau, \zeta) =
\begin{bmatrix}
\cos \omega\tau & \sin \omega\tau & 0 \\
-\sin \omega\tau & \cos \omega\tau & 0 \\
0 & 0 & 1
\end{bmatrix}
\begin{bmatrix}
\bar{x}(\zeta) \\
\bar{y}(\zeta) \\
\bar{z}(\zeta)
\end{bmatrix}
\tag{4.98}
$$

for some choice of pattern speed ω and functions $\bar{x}$, $\bar{y}$ and $\bar{z}$ of a coordinate $\zeta(\tau, \sigma)$ that for the moment remains unspecified. As a functional of τ and ζ the string action (2.10) is

$$
I = -\mu \int [(\mathbf{r}_{,\tau} \cdot \mathbf{r}_{,\zeta})^2 + \mathbf{r}_{,\zeta}^2 (1 - \mathbf{r}_{,\tau}^2)]^{1/2} \, d\zeta \, d\tau
\tag{4.99}
$$

and if (4.98) is substituted into (4.99) the action can be reduced to the form

$$\int \mathcal{L} \, d\zeta = \int [\overline{x}'^2 + \overline{y}'^2 + \overline{z}'^2 - \omega^2(\overline{x}\overline{x}' + \overline{y}\overline{y}')^2 - \omega^2(\overline{x}^2 + \overline{y}^2)\overline{z}'^2]^{1/2} \, d\zeta \quad (4.100)$$

where a prime denotes $d/d\zeta$.

As $\overline{z}$ is cyclic, the corresponding Euler–Lagrange equation integrates immediately to give

$$\overline{z}' \frac{1 - \omega^2(\overline{x}^2 + \overline{y}^2)}{\mathcal{L}} = K \quad (4.101)$$

where K is a constant. If $K = 0$ then either the solution is planar or $\omega^2(\overline{x}^2 + \overline{y}^2) = 1$; whereas if $K \neq 0$ the solution is non-planar. The possibility that $\omega^2(\overline{x}^2 + \overline{y}^2) = 1$, which Embacher missed, will be considered separately at the end of this section.

If $\omega^2(\overline{x}^2 + \overline{y}^2) \neq 1$ equation (4.101) suggests the gauge choice

$$\mathcal{L} = 1 - \omega^2(\overline{x}^2 + \overline{y}^2) \quad (4.102)$$

from which it follows that $\overline{z} = K\zeta$ (modulo translations in z). With the abbreviation $\overline{\mathbf{r}} = [\overline{x}, \overline{y}]$, the two remaining Euler–Lagrange equations read:

$$\frac{d}{d\zeta} \left[\frac{\overline{\mathbf{r}}' - \omega^2(\overline{\mathbf{r}} \cdot \overline{\mathbf{r}}')\overline{\mathbf{r}}}{\mathcal{L}} \right] + \frac{\omega^2 K^2 \overline{\mathbf{r}} + \omega^2(\overline{\mathbf{r}} \cdot \overline{\mathbf{r}}')\overline{\mathbf{r}}'}{\mathcal{L}} = 0. \quad (4.103)$$

Taking the dot product with $\overline{\mathbf{r}}$ and using the fact that $\overline{\mathbf{r}} \cdot [\overline{\mathbf{r}}' - \omega^2(\overline{\mathbf{r}} \cdot \overline{\mathbf{r}}')\overline{\mathbf{r}}] = \mathcal{L}\overline{\mathbf{r}} \cdot \overline{\mathbf{r}}'$ gives the equation

$$\frac{d}{d\zeta}(\overline{\mathbf{r}} \cdot \overline{\mathbf{r}}') + \frac{\omega^2 K^2 \overline{\mathbf{r}}^2 + 2\omega^2(\overline{\mathbf{r}} \cdot \overline{\mathbf{r}}')^2 - \overline{\mathbf{r}}'^2}{\mathcal{L}} = 0. \quad (4.104)$$

Furthermore, the square of (4.102) can be rearranged to read:

$$\omega^2 K^2 \overline{\mathbf{r}}^2 + \omega^2(\overline{\mathbf{r}} \cdot \overline{\mathbf{r}}')^2 - \overline{\mathbf{r}}'^2 = K^2 - (1 - \omega^2 \overline{\mathbf{r}}^2)^2 \quad (4.105)$$

and so in terms of $\mathcal{L} = 1 - \omega^2 \overline{\mathbf{r}}^2$ equation (4.104) becomes

$$\tfrac{1}{2}\mathcal{L}\mathcal{L}'' + \omega^2(\mathcal{L}^2 - K^2) - \tfrac{1}{4}\mathcal{L}'^2 = 0. \quad (4.106)$$

An immediate first integral of this equation is:

$$\mathcal{L}'^2 = -4\omega^2(\mathcal{L}^2 + \gamma\mathcal{L} + K^2) \quad (4.107)$$

where γ is an arbitrary constant. Note that $\mathcal{L}'^2$ will be non-negative and $\mathcal{L}'$ real only if $\gamma^2 \geq 4K^2$.

Integrating a second time gives

$$\mathcal{L} \equiv 1 - \omega^2 \overline{\mathbf{r}}^2 = A \cos^2 \omega\zeta + B \quad (4.108)$$

where

$$A = \pm(\gamma^2 - 4K^2)^{1/2} \qquad \text{and} \qquad B = -\tfrac{1}{2}\gamma \mp \tfrac{1}{2}(\gamma^2 - 4K^2)^{1/2} \qquad (4.109)$$

and an additive integration constant has been absorbed into ζ.

Finally, substitution of (4.108) into the Euler–Lagrange equations (4.103) results in a linear second-order equation for $\bar{\mathbf{r}}$:

$$(A \cos^2 \omega\zeta + B)\bar{\mathbf{r}}'' + (2A \sin \omega\zeta \cos \omega\zeta)\bar{\mathbf{r}}'$$
$$+ [A(K^2 - \gamma)\cos^2 \omega\zeta + B(K^2 - A)]\bar{\mathbf{r}} = 0 \qquad (4.110)$$

whose solution (modulo rotations in the plane) is

$$\bar{\mathbf{r}} = (B+1)^{1/2}\omega^{-1} \begin{bmatrix} k \cos \omega\zeta \cos \nu\omega\zeta + \sin \omega\zeta \sin \nu\omega\zeta \\ -k \cos \omega\zeta \sin \nu\omega\zeta + \sin \omega\zeta \cos \nu\omega\zeta \end{bmatrix} \qquad (4.111)$$

where

$$\nu^2 = 1 + K^2 - \gamma \qquad \text{and} \qquad k = \nu^{-1}(A + B + 1). \qquad (4.112)$$

Note here that the normalization constant $(B+1)^{1/2}\omega^{-1}$ in (4.111) is fixed by the integral constraint (4.108), and that the solution applies only if $\gamma < 1 + K^2$. The possibility of analytically continuing the solution to imaginary values of ν by converting $\cos \nu\omega\zeta$ and $\sin \nu\omega\zeta$ into the corresponding hyperbolic functions is precluded by (4.108), which ensures that $|\bar{\mathbf{r}}|$ is bounded.

The resulting solution to the string equations of motion—up to an arbitrary boost, rotation and/or translation—is, therefore,

$$\mathbf{r}(\tau, \zeta) = \begin{bmatrix} (B+1)^{1/2}\omega^{-1}[k \cos \omega\zeta \cos\{\omega(\nu\zeta + \tau)\} + \sin \omega\zeta \sin\{\omega(\nu\zeta + \tau)\}] \\ (B+1)^{1/2}\omega^{-1}[-k \cos \omega\zeta \sin\{\omega(\nu\zeta + \tau)\} + \sin \omega\zeta \cos\{\omega(\nu\zeta + \tau)\}] \\ K\zeta \end{bmatrix}. \qquad (4.113)$$

The solution can be rewritten in aligned standard gauge coordinates (τ, σ) by defining

$$\zeta = (\nu^2 - 1)^{-1}(\sigma - \nu\tau). \qquad (4.114)$$

The mode functions $\mathbf{a}$ and $\mathbf{b}$ then have the form

$$\mathbf{a}(\sigma_+) = \mathbf{f}_+(\sigma_+) \qquad \text{and} \qquad \mathbf{b}(\sigma_-) = \mathbf{f}_-(\sigma_-) \qquad (4.115)$$

where $\sigma_\pm = \tau \pm \sigma$ and

$$\mathbf{f}_\pm(\sigma_\pm) = \begin{bmatrix} (B+1)^{1/2}\omega^{-1}(k \pm 1)\cos\left(\dfrac{\omega\sigma_\pm}{\nu \pm 1}\right) \\ \mp(B+1)^{1/2}\omega^{-1}(k \pm 1)\sin\left(\dfrac{\omega\sigma_\pm}{\nu \pm 1}\right) \\ -K\dfrac{\sigma_\pm}{\nu \pm 1} \end{bmatrix}. \qquad (4.116)$$

It was mentioned earlier that the trajectory is non-planar if $K \neq 0$ and, in fact, the solution has the shape of a helicoid circling the z-axis in this case. Since the local Lorentz factor of the string is

$$\lambda = |\nu^2 - 1|[\tfrac{1}{4}(B+1)(\alpha^2 + \beta^2 - 2\alpha\beta\cos\theta) + K^2\nu^2]^{-1/2} \qquad (4.117)$$

where $\alpha = (k+1)(\nu-1)$, $\beta = (k-1)(\nu+1)$ and $\theta = 2\omega\zeta$, it is evident that the non-planar solutions are cusp-free.

In the planar limit, $\nu^2 = 1 - \gamma$ and either $(A, B, k) = (-\gamma, 0, \nu)$ or $(A, B, k) = (\gamma, -\gamma, \nu^{-1})$. As is evident from (4.108), the lagrangian reduces to $\mathcal{L} = -\gamma\cos^2\omega\zeta$ in the first case and to $\mathcal{L} = -\gamma\sin^2\omega\zeta$ in the second case. The choice of parameters, therefore, corresponds not to distinct sets of solutions but merely to a translation in the zero point of ζ. If attention is restricted to the case $(A, B, k) = (-\gamma, 0, \nu)$ then the local Lorentz factor is

$$\lambda = 2^{1/2}(1 - \cos\theta)^{-1/2} \qquad (4.118)$$

and permanent co-rotating cusps occur on the string wherever $\omega\zeta \equiv (\nu^2 - 1)^{-1}\omega(\sigma - \nu\tau)$ is an integer multiple of π.

In view of the mode function decomposition (4.116) it is clear that the trajectory will form a closed loop only if $K = 0$ and $\frac{\nu-1}{\nu+1}$ is rational. If $\frac{\nu-1}{\nu+1} = \frac{p}{q}$ with p and q relatively prime then the solution is a member of the p/q harmonic class (4.61)–(4.62) with $\widehat{\mathbf{u}} = \widehat{\mathbf{x}}$ and $\widehat{\mathbf{v}} = \widehat{\mathbf{y}}$. In particular, the invariant length is $L = 2\pi|p(\nu+1)|/\omega$ and the number of the cusps is $|p+q|$.

Turning now to the outstanding case $\omega^2(\overline{x}^2 + \overline{y}^2) = 1$, it is evident that a gauge choice consistent with this relation is

$$\overline{x}(\zeta) = \omega^{-1}\cos\kappa\zeta \qquad \text{and} \qquad \overline{y}(\zeta) = \omega^{-1}\sin\kappa\zeta \qquad (4.119)$$

where κ is some constant. The corresponding position vector of the string is

$$\mathbf{r}(\tau, \zeta) = [\,\omega^{-1}\cos(\omega\tau - \kappa\zeta), \quad -\omega^{-1}\sin(\omega\tau - \kappa\zeta), \quad \overline{z}(\zeta)\,] \qquad (4.120)$$

which, being a solution to the flat-space equations of motion, must have the form $\tfrac{1}{2}\mathbf{a}(\sigma_+) + \tfrac{1}{2}\mathbf{b}(\sigma_-)$. This, in turn, is possible only if $(\tfrac{1}{2}\omega - \kappa\zeta_+)(\tfrac{1}{2}\omega - \kappa\zeta_-) = 0$, as can be seen by setting $\overline{x}_{+-} = \overline{y}_{+-} = 0$. Assume without loss of generality that $\kappa\zeta_+ = \tfrac{1}{2}\omega$. Then

$$\omega\tau - \kappa\zeta = \tfrac{1}{2}\omega\sigma_- - \kappa\overline{\zeta}(\sigma_-) \qquad \text{and} \qquad \overline{z}(\zeta) = \overline{z}(\tfrac{1}{2}\kappa^{-1}\omega\sigma_+ + \overline{\zeta}(\sigma_-)) \quad (4.121)$$

for some function $\overline{\zeta}$.

The requirement that $\overline{z}$ be a sum of functions of σ_+ and σ_- entails that either $\overline{z}$ is linear or $\overline{\zeta}$ is constant. In either case, the gauge condition $\mathbf{a}'^2 = 1$ implies that $\overline{z}_+^2 = \tfrac{1}{4}$, while the possibility that $\overline{\zeta}' \neq 0$ turns out to be inconsistent with the constraint $\mathbf{b}'^2 = 1$. The most general solution with $\omega^2(\overline{x}^2 + \overline{y}^2) = 1$ is, therefore,

$$\mathbf{r}(\tau, \sigma) = [\,\omega^{-1}\cos(\tfrac{1}{2}\omega\sigma_- + \psi), \quad -\omega^{-1}\sin(\tfrac{1}{2}\omega\sigma_- + \psi), \quad z(\sigma_+)\,] \quad (4.122)$$

where ψ is an arbitrary phase factor, and $z'^2 = \frac{1}{4}$.

At first glance, it would appear that the only admissible choice for the z-component is $z(\sigma_+) = z_0 + \frac{1}{2}\sigma_+$, with z_0 a constant, and so (4.122) does no more than recover a particular family of travelling-wave solutions. However, the constraint $z'^2 = \frac{1}{4}$ can also be satisfied if z is only piecewise linear, with z' jumping from $\frac{1}{2}$ to $-\frac{1}{2}$ (or *vice versa*) any number of times. Each jump would, of course, correspond to a kink on the string, with each kink tracing out a horizontal circle of radius ω^{-1} with circular frequency equal to the pattern speed ω.

Furthermore, if $z(\sigma_+)$ is chosen to be a periodic function with period equal to the fundamental period $L = 4\pi/\omega$ of the circular mode then the string will form a closed loop. Solutions of this type are the only possible rigidly-rotating *non-planar* loops in flat space. Indeed, the simplest solution of this type, which supports two evenly-spaced kinks and has

$$z(\sigma_+) = z_0 + \begin{cases} \frac{1}{2}\sigma_+ & \text{if } 0 \le \sigma_+ < \frac{1}{2}L \\ \frac{1}{2}(L - \sigma_+) & \text{if } \frac{1}{2}L \le \sigma_+ < L \end{cases} \qquad (4.123)$$

is remarkable in that it radiates gravitational energy at the lowest rate known for any string loop (and so presumably is the most stable loop known). It will be examined in more detail in chapter 6.

4.6   Three toy solutions

4.6.1   The teardrop string

I will end this brief survey by considering three sample solutions that make use of the initial-value formulation of section 3.4. Recall that if the string is initially at rest with parametric position vector $\mathbf{r}_0(\theta)$ then the spacelike coordinate σ in the aligned standard gauge is just the arc length along the curve. For a string confined to the x–y plane, it is often convenient to identify the parameter θ with the polar angle, so that

$$\mathbf{r}_0(\theta) = r_0(\theta)(\cos\theta\widehat{\mathbf{x}} + \sin\theta\widehat{\mathbf{y}}) \qquad (4.124)$$

for some function r_0, and, therefore,
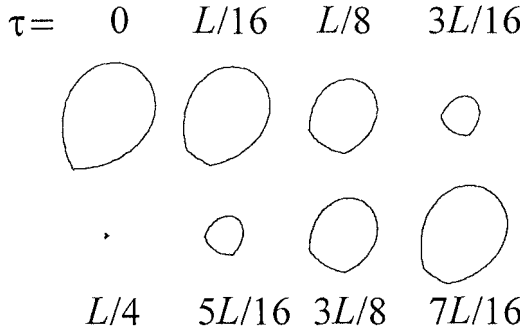
$$\sigma(\theta) = \int \sqrt{r_0^2(\theta) + r_0'^2(\theta)}\, d\theta. \qquad (4.125)$$

One simple class of closed curves in the plane admitting an explicit formula for $\sigma(\theta)$ is described by the family of second-order polynomials

$$r_0(\theta) = A(\theta - \tfrac{1}{2}\theta^2) \qquad (4.126)$$

where A is a positive constant and, to close the loop, θ ranges from 0 to 2. The corresponding spacelike gauge coordinate

$$\sigma = A(\theta - \tfrac{1}{2}\theta^2 + \tfrac{1}{6}\theta^3) \qquad (4.127)$$

$$\tau = \quad 0 \qquad L/16 \qquad L/8 \qquad 3L/16$$

$$L/4 \qquad 5L/16 \quad 3L/8 \quad 7L/16$$

Figure 4.30. The teardrop string.

ranges from 0 to $4A/3$, and so $A = 3L/4$, with L the invariant length as usual.

Solving for θ in terms of σ on the domain $[0, L)$ gives

$$\theta(\sigma) = \left[-2 + 4\sigma/L + \sqrt{5 - 16\sigma/L + 16(\sigma/L)^2} \right]^{1/3}$$
$$- \left[-2 + 4\sigma/L + \sqrt{5 - 16\sigma/L + 16(\sigma/L)^2} \right]^{-1/3} + 1 \quad (4.128)$$

and the full equation for the time development of the string is

$$\mathbf{r}(\tau, \sigma) = \frac{3L}{8} \begin{bmatrix} (\theta_+ - \frac{1}{2}\theta_+^2)\cos\theta_+ + (\theta_- - \frac{1}{2}\theta_-^2)\cos\theta_- \\ (\theta_+ - \frac{1}{2}\theta_+^2)\sin\theta_+ + (\theta_- - \frac{1}{2}\theta_-^2)\sin\theta_- \end{bmatrix} \quad (4.129)$$

with $\theta_\pm = \theta(\zeta_\pm)$, where $\zeta_\pm$ denotes $(\sigma \pm \tau)/L$ (modulo 1).

The evolution of the solution is illustrated for $0 \le \tau < L/2$ in figure 4.30. Initially the string loop has the shape of a 'teardrop', with a coincident pair of kinks forming the apex. The kinks propagate left and right around the string as the entire configuration begins to shrink. The local Lorentz factor of the solution can be expressed in the form
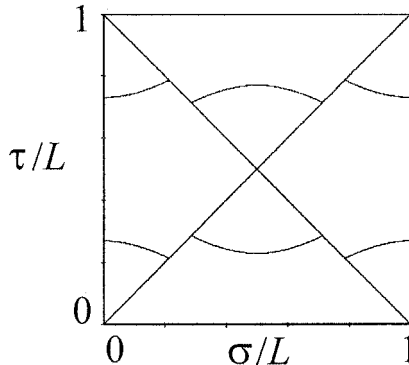
$$\lambda = (U^2 + V^2)^{1/2}/|U\cos V - V\sin V| \quad (4.130)$$

where

$$U = \frac{1}{2}[1 + \frac{1}{4}(\theta_+ + \theta_- - 2)^2 - \frac{1}{4}(\theta_+ - \theta_-)^2] \quad \text{and} \quad V = \frac{1}{2}(\theta_+ - \theta_-) \quad (4.131)$$

and so the loop supports semi-permanent cusps with the implicitly defined trajectories $U = V\tan V$.

The kinks themselves follow the curves $\theta_- = 0$ and $\theta_+ = 0$, and it is an easy matter to show that a cusp first appears at the location of each kink when θ_+ or θ_- is about 0.808, which corresponds to $\tau/L \approx 0.214$. The kinks and their daughter

Figure 4.31. World-sheet diagram for the teardrop string.
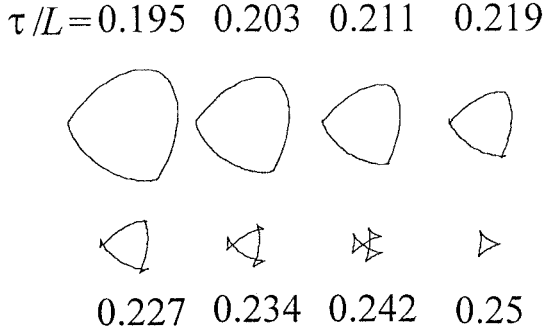
cusps, of course, propagate at light speed relative to the background spacetime but the cusps rapidly move ahead of the kinks on the world sheet, as can be seen from figure 4.31.

In this diagram, which shows the structure of the world sheet in terms of the standard-gauge coordinates σ and τ, the 45° lines represent the trajectories of the kinks and the curved lines trace out the paths of the cusps. It is evident not only that the cusps outrun the kinks but also that a second pair of semi-permanent cusps appears spontaneously at $\sigma = L/2$ shortly after the emission of the original pair. The creation of the second cusp pair corresponds to a double root in the equation $U = V \tan V$ at $(\theta_+, \theta_-) \approx (1.556, 0.444)$, with gauge time coordinate $\tau/L \approx 0.230$.

The shape of the loop in the last few moments before it shrinks to its minimum size at $\tau = L/4$ is shown in figure 4.32. In the first three frames the loop is still cusp-free, as the kinks each emit their daughter cusp (and a self-intersection) between frame 3 and frame 4. The second pair of cusps (and a third self-intersection) appears at the point furthest from the kinks between frame 5 and frame 6. At $\tau = L/4$ the loop degenerates into a three-pointed star, as shown in the last frame of figure 4.32. The points of the star consist of a pair of kinks (at the bottom left) and two pairs of cusps, with each pair coincident in the background spacetime but not in the τ–σ parameter space. The loop then re-expands, with the original pair of cusps colliding and annihilating at $\tau/L \approx 0.270$, and the second pair being absorbed by the kinks at $\tau/L \approx 0.286$. The original teardrop shape is restored at $\tau = L/2$.

4.6.2 The cardioid string

As a second simple application of the initial-value formulation, consider a string loop which is initially static and in the shape of a cardioid with the parametric

$$\tau/L = 0.195 \quad 0.203 \quad 0.211 \quad 0.219$$

$$0.227 \quad 0.234 \quad 0.242 \quad 0.25$$

Figure 4.32. The teardrop string for $0.195 \leq \tau/L \leq 0.25$.

equation

$$r_0(\theta) = A(1 - \cos\theta) \tag{4.132}$$

where A is a positive constant and θ ranges over $[0, 2\pi)$. From (4.125) the transformation from θ to the spacelike coordinate σ is given by

$$\sigma(\theta) = 8A \sin^2(\theta/4) \tag{4.133}$$

and so the invariant length of the loop is $L = 8A$.

In terms of σ the initial configuration has the form

$$\mathbf{r}_0(\theta(\sigma)) = L\{(\zeta - \zeta^2)[1 - 8(\zeta - \zeta^2)]\hat{\mathbf{x}} + 4(1 - 2\zeta)(\zeta - \zeta^2)^{3/2}\hat{\mathbf{y}}\} \tag{4.134}$$

with $\zeta = \sigma/L$, and so the equation for the full solution is

$$\mathbf{r}(\tau, \sigma) = L \left[\begin{matrix} (\zeta_+ - \zeta_+^2)[1 - 8(\zeta_+ - \zeta_+^2)] + (\zeta_- - \zeta_-^2)[1 - 8(\zeta_- - \zeta_-^2)] \\ 4(1 - 2\zeta_+)(\zeta_+ - \zeta_+^2)^{3/2} + 4(1 - 2\zeta_-)(\zeta_- - \zeta_-^2)^{3/2} \end{matrix} \right] \tag{4.135}$$
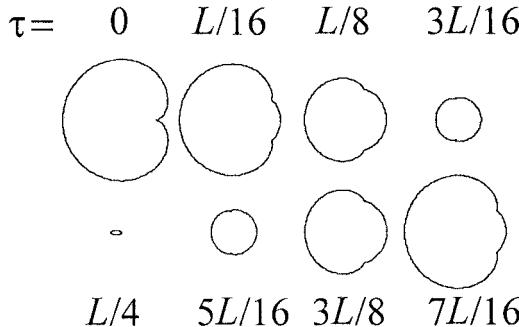
where $\zeta_\pm = (\sigma \pm \tau)/L$ (modulo 1) as before.

The time development of the solution over a single period of oscillation is shown in figure 4.33. The cleft in the cardioid at $\tau = 0$ is, of course, not a cusp but the superposition of two kinks, which subsequently propagate left and right around the string. The local Lorentz factor of the string is
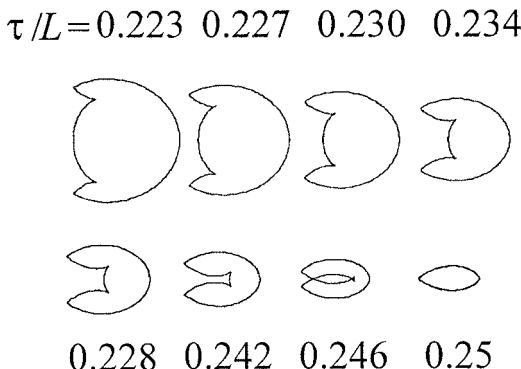
$$\lambda = 2^{1/2}[1 - (1 - 2\zeta_+)(1 - 16\Delta_+)(1 - 2\zeta_-)(1 - 16\Delta_-)$$
$$+ 4\Delta_+^{1/2}(3 - 16\Delta_+)\Delta_-^{1/2}(3 - 16\Delta_-)]^{-1/2} \tag{4.136}$$

where $\Delta_\pm = \zeta_\pm - \zeta_\pm^2$, and so, in particular, the Lorentz factor just forward of the kink travelling along the path $\tau = \sigma$ (where $\zeta_+ = 2\tau/L$ and $\zeta_- = 0$) is

$$\lambda = (1 - 2\tau/L)^{-1/2}|1 - 8\tau/L|^{-1} \qquad (0 \leq \tau < \tfrac{1}{2}L). \tag{4.137}$$

$\tau =$ 0   L/16   L/8   3L/16

L/4   5L/16   3L/8   7L/16

Figure 4.33. The cardioid string.

$\tau /L =$ 0.223   0.227   0.230   0.234

0.228   0.242   0.246   0.25
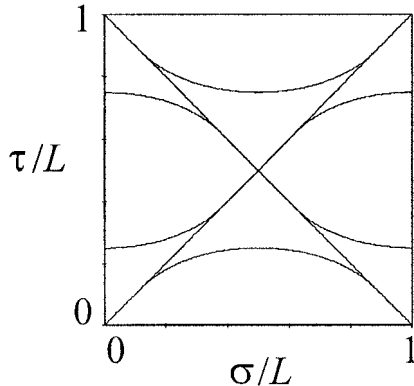
Figure 4.34. The cardioid string for $0.223 \le \tau/L \le 0.25$.

Thus a cusp appears at the location of the kink when $\tau = L/8$. The same is true of the second kink and as both cusps propagate around the world sheet faster than their progenitor kinks two characteristic 'fins' pointing in the direction of propagation develop on the loop, with a kink forming the tip of each fin and a cusp marking the base of the fin. The fins can only just be discerned in the $\tau = 3L/16$ frame of figure 4.33 but are shown clearly in figure 4.34, which contains snapshots of the loop during the last few moments before it contracts to its minimum size at $\tau = L/4$.

The trajectories of the cusps can be reconstructed by setting the denominator in the expression (4.136) for the local Lorentz factor to zero, isolating the term containing $\Delta_{\pm}^{1/2}$ and then squaring both sides. This gives the following necessary (but not sufficient) condition for the existence of a cusp:

$$(\zeta_+ + \zeta_- - 1)[1 + 8(\zeta_+ + \zeta_-) - 16\zeta_+\zeta_- + 16(\zeta_+^2 + \zeta_-^2)] = 0. \qquad (4.138)$$

It is easily checked that the first term here is spurious, while the second term

Figure 4.35. World-sheet diagram for the cardioid string.

defines a series of ellipses in τ–σ space, only segments of which correspond to the cusp trajectories. For τ in $[0, \frac{1}{4}L]$ the equation of the relevant segment is

$$16(\sigma/L)^2 - 16\sigma/L + 48(\tau/L)^2 + 1 = 0 \qquad (\tfrac{1}{8}L \le \tau \le \tfrac{1}{4}L). \qquad (4.139)$$

Figure 4.35 shows the world-sheet diagram for the cardioid string. As before, the 45° lines mark the kinks, while the curved lines trace the paths of the cusps. As was noted previously, both kinks emit a cusp at $\tau = L/8$. The cusps diverge from the kinks and propagate around the string at light speed, until they meet and annihilate at $\sigma = L/2$ when $\tau = L/4$. At the same instant, two new cusps emerge at $\sigma = 0$ and propagate backwards around the loop until they are absorbed by the kinks at $\tau = 3L/8$. The kinks continue their motion and recross at $\tau = L/2$, at which time the initial stationary configuration is restored. One surprising feature of the solution, evident from (4.137), is that the local speed of the string immediately ahead of the two kinks approaches the speed of light just before the kinks cross.

The most eventful phase of the loop's evolution occurs near the mid-point $\tau = L/4$ of the oscillation, when the string degenerates into the 'cigar' shape seen in the last frame of figure 4.31. Prior to this moment, the insides of the fins cross to create two self-intersections which move left and right along the string, as shown in the second-last frame of figure 4.34. The first appearance of the self-intersections occurs when $y(\tau, \sigma)$ and $y(\tau, \sigma),_\sigma$ are simultaneously zero, an event which numerical solution of the two equations places at $\sigma/L \approx 0.293$ and $\sigma/L \approx 0.707$ when $\tau/L \approx 0.244$. (This occurs between frames 6 and 7 in figure 4.34.)

At $\tau = L/4$ the left-hand self-intersection meets the two kinks, while the right-hand self-intersection simultaneously encompasses the annihilating pair of cusps at $\sigma = L/2$ and the newly-created cusp pair at $\sigma = 0$. Thus the left-hand end of the cigar is formed by the two kinks, coincident in the background

spacetime (but not in the τ–σ parameter space) and the right-hand end by the transfer of the cusps from $\sigma = L/2$ to $\sigma = 0$. The cigar itself is traced out twice by the string as σ ranges from 0 to L. For $\tau > L/4$ the process outlined earlier reverses, with the self-intersections travelling back towards the middle of the string, and colliding and disappearing at $\tau/L \approx 0.256$.

4.6.3   The figure-of-eight string

As was mentioned in section 4.4.3, it is not possible—in the standard gauge—to construct a mode function that contains first- and second-order harmonics only. It is, therefore, illuminating to study the evolution of a string loop that is initially stationary and traces out a curve $\mathbf{r}_0(\theta)$ generated from only first- and second-order harmonics in the parameter θ. One candidate curve of this type is

$$\mathbf{r}_0(\theta) = A(\cos\theta\widehat{\mathbf{x}} + u\sin\theta\widehat{\mathbf{y}} + v\sin 2\theta\widehat{\mathbf{z}}) \tag{4.140}$$

where A, u and v are constants, and θ ranges over $[0, 2\pi)$.

If v is chosen to have the form

$$v = \frac{1 - u^2}{4\sqrt{2}(1 + u^2)^{1/2}} \tag{4.141}$$

then $|\mathbf{r}'_0|^2$ is a degenerate quadratic in $\cos^2\theta$ and the standard-gauge coordinate σ satisfies the equation

$$\frac{d\sigma}{d\theta} = |\mathbf{r}'_0| = \frac{A}{2\sqrt{2}(1 + u^2)^{1/2}}[u^2 + 3 + 2(u^2 - 1)\cos^2\theta]. \tag{4.142}$$

Thus the invariant length of the loop is

$$L = \int_0^{2\pi} \frac{d\sigma}{d\theta}\,d\theta = \sqrt{2}A\pi(u^2 + 1)^{1/2}. \tag{4.143}$$
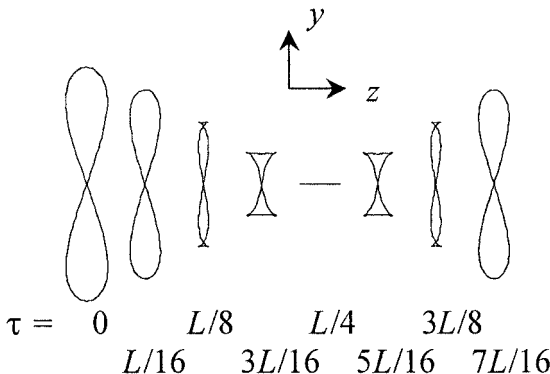
Eliminating A in favour of L and u in favour of a new parameter $w = \sqrt{2}\pi/(u^2 + 1)^{1/2}$ gives

$$\mathbf{r}_0(\theta(\sigma)) = \frac{L}{2\pi}\left[w\cos\theta\widehat{\mathbf{x}} + \sqrt{2 - w^2}\sin\theta\widehat{\mathbf{y}} + \tfrac{1}{4}(1 - w^2)\sin 2\theta\widehat{\mathbf{z}}\right] \tag{4.144}$$

where θ is related to σ through the equation

$$\sigma(\theta) = \frac{L}{2\pi}[\theta + \tfrac{1}{4}(1 - w^2)\sin 2\theta]. \tag{4.145}$$

Although (4.144) and (4.145) are well defined for all w in $[0, \sqrt{2}]$, it is evident that the transformation $\theta \to \theta + \tfrac{1}{2}\pi$ is equivalent to replacing w everywhere with

Figure 4.36. The figure-of-eight string.

$\sqrt{2 - w^2}$ and so only the range $0 \leq w \leq 1$ is relevant. The full time evolution of the solution is given by

$$\mathbf{r}(\tau, \sigma) = \frac{L}{4\pi} \left[w(\cos\theta_+ + \cos\theta_-)\hat{\mathbf{x}} + \sqrt{2 - w^2}(\sin\theta_+ + \sin\theta_-)\hat{\mathbf{y}} \right.$$
$$\left. + \tfrac{1}{4}(1 - w^2)(\sin 2\theta_+ + \sin 2\theta_-)\hat{\mathbf{z}} \right] \tag{4.146}$$

where $\theta_\pm = \theta(\sigma \pm \tau)$, with θ the unique inverse of (4.145).

All solutions with $0 < w < 1$ are non-planar and support two (ordinary) cusps per oscillation period, appearing at the points $(\theta_+, \theta_-) = (\tfrac{5}{4}\pi, \tfrac{1}{4}\pi)$ and $(\tfrac{7}{4}\pi, \tfrac{3}{4}\pi)$, which both have gauge time coordinate $\tau = L/4$. The $w = 1$ solution is simply the collapsing circular loop examined in section 4.2.1. Perhaps the most interesting member of the family is the $w = 0$ solution, which is planar and initially traces out the shape of a 'figure of eight'. The evolution of this loop is illustrated in figure 4.36. The segments of the string near the central cross-piece are very nearly straight, and experience little acceleration throughout the oscillation period. The outer segments of the loop, by contrast, are approximately circular, and quickly begin to collapse inwards at high speed.

The local Lorentz factor of the $w = 0$ solution is

$$\lambda = (1 + 2\cos^2\theta_+)^{1/2}(1 + 2\cos^2\theta_-)^{1/2}/|1 + 2\cos\theta_+ \cos\theta_-| \tag{4.147}$$

and so the loop supports two pairs of semi-permanent cusps with trajectories $\cos\theta_+ \cos\theta_- = -\tfrac{1}{2}$. Both pairs of cusps appear at $\tau/L = \tfrac{1}{8\pi}(\pi - 1) \approx 0.0852$, which is the moment the collapsing ends of the loop attain light speed[4]. A self-intersection is also created with each cusp pair, leading to the formation of a characteristic swallow-tail caustic at the two extreme ends of the string, as can

---

[4] In terms of (θ_+, θ_-) the cusp pairs first appear at $(\tfrac{3}{4}\pi, \tfrac{1}{4}\pi)$ and $(\tfrac{7}{4}\pi, \tfrac{5}{4}\pi)$, which correspond to $\sigma = L/4$ and $\sigma = 3L/4$ respectively.

be seen in the third frame of figure 4.36. The cusp pairs separate and travel in opposite directions around the loop while the self-intersections migrate towards the centre of the loop and annihilate at $\tau/L = \frac{1}{8\pi}(\pi + 1) \approx 0.1648$ (which occurs just before frame 4). The loop then continues to collapse and ultimately degenerates into a horizontal rod of length $\frac{L}{8\pi}$ at $\tau = L/4$, each end of the rod being marked by a pair of coincident cusps. The loop subsequently re-expands and returns to its initial configuration at $\tau = L/2$, with a pair of self-intersections appearing at the origin at $\tau/L \approx 0.3352$ and the two original cusp pairs merging and annihilating the self-intersections at $\tau/L \approx 0.4148$.

Chapter 5

String dynamics in non-flat backgrounds

In contrast to the plethora of known exact solutions to the string equation of motion in Minkowski spacetime, the dynamics of cosmic strings in other background metrics is relatively unexplored. In this chapter I examine the work that has been done on string dynamics in four standard non-flat backgrounds: the Robertson–Walker, Schwarzschild, Kerr and plane-fronted (pp)-wave spacetimes. In all cases it is most convenient to work in standard gauge coordinates τ and σ, in terms of which the equation of motion $X^{\mu}{}_{;\tau\tau} = X^{\mu}{}_{;\sigma\sigma}$ reads explicitly:

$$X^{\mu}{}_{,\tau\tau} + \Gamma^{\mu}_{\kappa\lambda} X^{\kappa}_{\tau} X^{\lambda}_{\tau} = X^{\mu}{}_{,\sigma\sigma} + \Gamma^{\mu}_{\kappa\lambda} X^{\kappa}_{\sigma} X^{\lambda}_{\sigma} \tag{5.1}$$

where the Christoffel components $\Gamma^{\mu}_{\kappa\lambda}$ are known functions of the position vector X^{μ}. The equation of motion is therefore a system of quasi-linear second-order hyperbolic partial differential equations (PDEs). As was seen in section 2.2, two first integrals of the equation are provided by the gauge conditions:

$$X_{\tau}^2 + X_{\sigma}^2 = 0 \qquad \text{and} \qquad X_{\tau} \cdot X_{\sigma} = 0 \tag{5.2}$$

and so (5.1) effectively comprises two linked second-order PDEs. It should not come as a surprise that very few exact solutions are known and that much of the work done in this area to date has focused on circular or static solutions.

5.1 Strings in Robertson–Walker spacetimes

From the viewpoint of classical cosmology, the most important non-flat background is the class of Robertson–Walker spacetimes, which have the general line element

$$\mathrm{d}s^2 = a^2(\eta) \left(\mathrm{d}\eta^2 - \frac{\mathrm{d}r^2}{1 - kr^2} - r^2 \mathrm{d}\theta^2 - r^2 \sin^2\theta \, \mathrm{d}\phi^2 \right) \tag{5.3}$$

where $k = 0$ or ± 1 and r, θ and ϕ are standard spherical polar coordinates. Since the $\eta = $ constant spacelike slices of Robertson–Walker spacetimes are

maximally symmetric, they possess six Killing vectors, any of which could be used to construct a conserved world-sheet integral along the lines of section 2.4.

For the purposes of generating the string equation of motion, only two of the Killing vectors are needed. The most convenient choices are:

$$k_\mu^{(1)} = a^2(1 - kr^2)^{-1/2}\cos\theta\,\delta_\mu^r - a^2(1 - kr^2)^{1/2}r\sin\theta\,\delta_\mu^\theta \tag{5.4}$$

and

$$k_\mu^{(2)} = a^2 r^2 \sin^2\theta\,\delta_\mu^\phi \tag{5.5}$$

With $X^\mu = (\eta, r, \theta, \phi)$ the corresponding conservation equations (2.43) then read:

$$[a^2(1 - kr^2)^{-1/2}\cos\theta r_{,\tau}]_{,\tau} - [a^2(1 - kr^2)^{1/2}r\sin\theta\theta_{,\tau}]_{,\tau}$$
$$= [a^2(1 - kr^2)^{-1/2}\cos\theta r_{,\sigma}]_{,\sigma} - [a^2(1 - kr^2)^{1/2}r\sin\theta\theta_{,\sigma}]_{,\sigma} \tag{5.6}$$

and

$$(a^2 r^2 \sin^2\theta\phi_{,\tau})_{,\tau} = (a^2 r^2 \sin^2\theta\phi_{,\sigma})_{,\sigma} \tag{5.7}$$

In addition, the gauge constraints (5.2) have the explicit form

$$(\eta_{,\tau})^2 + (\eta_{,\sigma})^2 - (1 - kr^2)^{-1}[(r_{,\tau})^2 + (r_{,\sigma})^2]$$
$$= r^2[(\theta_{,\tau})^2 + (\theta_{,\sigma})^2] + r^2\sin^2\theta[(\phi_{,\tau})^2 + (\phi_{,\sigma})^2] \tag{5.8}$$

and

$$\eta_{,\tau}\,\eta_{,\sigma} = (1 - kr^2)^{-1}r_{,\tau}\,r_{,\sigma} + r^2\theta_{,\tau}\,\theta_{,\sigma} + r^2\sin^2\theta\phi_{,\tau}\,\phi_{,\sigma}. \tag{5.9}$$

5.1.1 Straight string solutions

No general solution to equations (5.6)–(5.9) is, at present, known. However, it is relatively easy to integrate the equations if the string's trajectory has a high degree of symmetry. The simplest case occurs when the string is static and straight. Then it is always possible to transform the spatial coordinates in (5.3) so that the projection of the world sheet onto the surfaces of constant η is a straight line through $r = 0$. Thus θ and ϕ are constant, and with the gauge choice $\tau = \eta$ the constraint (5.9) reduces to $r_{,\tau} = 0$. Equation (5.8), which is now a first integral of (5.7), reads:

$$(1 - kr^2)^{-1}(r_{,\sigma})^2 = 1 \tag{5.10}$$

and so

$$r = |\sigma| \quad \sin|\sigma| \quad \text{or} \quad \sinh|\sigma| \tag{5.11}$$

depending on whether k is 0, 1 or -1 respectively. That is, the world-sheet parameter σ is just the proper conformal distance on the 3-surfaces of constant η.

Perturbations of this simple straight-line geometry were first considered by Alexander Vilenkin [Vil81a] in 1981. If θ and ϕ are assumed to have the form

$$\theta = \theta_0 + \varepsilon\,\theta_1(\tau, \sigma) \quad \text{and} \quad \phi = \phi_0 + \varepsilon\,\phi_1(\tau, \sigma) \tag{5.12}$$

where θ_0 and ϕ_0 are constants and ε is a small parameter, then to first order in ε the constraint equations (5.8) and (5.9) read:

$$(\eta,_\tau)^2 + (\eta,_\sigma)^2 = (s,_\tau)^2 + (s,_\sigma)^2 \qquad \text{and} \qquad \eta,_\tau \,\eta,_\sigma = s,_\tau \,s,_\sigma \qquad (5.13)$$

with

$$s(r) = \int_0^r (1 - ku^2)^{-1/2} \, du. \qquad (5.14)$$

equal to r, $\sin^{-1} r$ or $\sinh^{-1} r$.

If the gauge choice $\tau = \eta$ and $|\sigma| = s$ is retained, then to linear order in ε the equations (5.6) and (5.7) reduce to the PDEs

$$\theta_{1,\tau\tau} + \frac{2\dot{a}}{a}\theta_{1,\tau} = \theta_{1,\sigma\sigma} + 2r^{-1}r,_\sigma \,\theta_{1,\sigma} \qquad (5.15)$$

and

$$\phi_{1,\tau\tau} + \frac{2\dot{a}}{a}\phi_{1,\tau} = \phi_{1,\sigma\sigma} + 2r^{-1}r,_\sigma \,\phi_{1,\sigma} \qquad (5.16)$$

where $\dot{a}$ denotes $da/d\eta$.

To help solve these equations, first rotate the coordinates so that the unperturbed string lies in the equatorial plane (i.e. $\theta_0 = \pi/2$) along the line $\sin \phi_0 = 0$. Then in terms of the Cartesian coordinates $z = \varepsilon r \theta_1$ and $y = \varepsilon r \phi_1$ normal to the unperturbed trajectory, equations (5.15) and (5.16) read:

$$z,_{\tau\tau} + \frac{2\dot{a}}{a}z,_\tau = z,_{\sigma\sigma} + kz \qquad \text{and} \qquad y,_{\tau\tau} + \frac{2\dot{a}}{a}y,_\tau = y,_{\sigma\sigma} + ky. \qquad (5.17)$$

To proceed further, it is necessary to prescribe an explicit form for the conformal factor a. The two most common choices are $a(\eta) = A\eta$ and $a(\eta) = A\eta^2$ (with A a constant), which correspond to the early behaviour of radiation-dominated and matter-dominated Friedmann universes, respectively. If a is assumed to have a general power-law dependence on η:

$$a(\eta) = A\eta^q \qquad (5.18)$$

then the equation for z becomes

$$z,_{\tau\tau} + 2q\tau^{-1}z,_\tau = z,_{\sigma\sigma} + kz \qquad (5.19)$$

with a similar equation for y.

Hence, the linear modes of the string are generally of the form

$$y, z \propto \tau^{-(q-\frac{1}{2})} J_{\pm(q-\frac{1}{2})}[(\omega^2 - k)^{1/2}\tau]e^{i\omega\sigma} \qquad (5.20)$$

where J_ν is a Bessel function of the first kind, and ω is the mode frequency. For modes with $\omega^2 < k$ the Bessel functions J_ν in (5.20) should be replaced with the corresponding modified functions I_ν. Note that if the universe is closed ($k = 1$)

then σ ranges over $(-\pi, \pi]$, and so to ensure that the string is continuous ω must be an integer. Thus the only possible mode with $\omega^2 < k$ is a uniform translation of the string ($\omega = 0$) in a closed universe. In the degenerate case $\omega^2 - k = 0$ (which occurs only if $\omega = k = 0$ or $\omega = k = 1$) the mode functions are proportional to $e^{i\omega\sigma}$ and $\tau^{1-2q}e^{i\omega\sigma}$ (or $\ln \tau e^{i\omega\sigma}$ if $q = \frac{1}{2}$).

In the particular case of a radiation-dominated Friedmann universe ($q = 1$), the oscillatory modes are simply

$$\tau^{-1}\sin[(\omega^2 - k)^{1/2}\tau]e^{i\omega\sigma} \qquad \text{and} \qquad \tau^{-1}\cos[(\omega^2 - k)^{1/2}\tau]e^{i\omega\sigma}. \qquad (5.21)$$

Vilenkin [Vil81a] has argued that, when they form, cosmic strings are likely to be at rest with respect to the surrounding matter. Thus for τ small it is to be expected that $z_{,\tau}$ and $y_{,\tau}$ are both close to zero. This condition rules out modes of the second type in equation (5.21), and leaves only modes of the form

$$\tau^{-1}\sin[(\omega^2 - k)^{1/2}\tau]e^{i\omega\sigma}. \qquad (5.22)$$

Now, for modes with frequencies satisfying $\omega\tau \ll 1$ the time derivatives $z_{,\tau}$ and $y_{,\tau}$ are of order $\omega\tau$ and remain small, so the physical amplitudes ay and az of the perturbations increase linearly with $a \propto \tau \equiv \eta$. This means that perturbations with wavelengths $2\pi a/\omega$ larger than the horizon size $a\eta/2$ are amplified in tandem with the general expansion of the universe. However, for high-frequency modes with $\omega\tau \gg 1$ the physical amplitudes ay and az remain bounded and oscillatory, just as they would in a non-expanding universe. Similar conclusions apply in all other cases where the exponent q is positive, as $J_\nu(x) \sim x^\nu$ for x small and falls off as $x^{-1/2}$ for x large, so that bounded perturbations of the form (5.20) remain constant for small τ and fall off as $a^{-1} \propto \tau^{-q}$ at late times.

5.1.2 Ring solutions

A second class of trajectories that can be handled relatively easily are ring solutions. These are planar solutions whose projections onto surfaces of constant η are circles centred on $r = 0$. The coordinates r and η are, therefore, functions of τ only. If the ring lies in the plane $\sin\phi = 0$ then from the gauge condition (5.9) $\theta_{,\tau} = 0$. Equation (5.8) consequently reduces to

$$r^{-2}(\eta_{,\tau})^2 - (1 - kr^2)^{-1}r^{-2}(r_{,\tau})^2 = (\theta_{,\sigma})^2 \qquad (5.23)$$

which is possible only if $\theta_{,\sigma}$ is constant. With the gauge choice $\sigma = \theta$, equations (5.6) and (5.8) now read:

$$r_{,\tau\tau} + \frac{2\dot{a}}{a}\eta_{,\tau}r_{,\tau} + (1 - kr^2)^{-1}kr(r_{,\tau})^2 + (1 - kr^2)r = 0 \qquad (5.24)$$

and

$$(\eta_{,\tau})^2 = (1 - kr^2)^{-1}(r_{,\tau})^2 + r^2. \qquad (5.25)$$

Equations (5.24) and (5.25) have been integrated numerically in the case of a spatially-flat universe ($k = 0$) by Hector de Vega and Inigo Egusquiza [dVE94] for a variety of conformal functions a with the power-law form (5.18). However, solutions of this type give r only as an implicit function of the conformal time η. A more direct method is to use (5.25) and its derivative to replace τ with η as the independent variable in (5.24). The resulting equation is

$$\frac{(1 - kr^2)\ddot{r} + kr\dot{r}^2}{1 - \dot{r}^2 - kr^2} + \frac{2\dot{a}}{a}\dot{r} + r^{-1}(1 - kr^2) = 0 \qquad (5.26)$$

where an overdot again denotes $d/d\eta$. The corresponding equation in the flat case $k = 0$,

$$(1 - \dot{r}^2)^{-1}\ddot{r} + \frac{2\dot{a}}{a}\dot{r} + r^{-1} = 0 \qquad (5.27)$$

was first derived by Vilenkin [Vil81a].

With $a(\eta) = A\eta^q$ equation (5.26) can be rewritten as

$$\ddot{r} = -(1 - kr^2)^{-1}[kr\dot{r}^2 + 2q\eta^{-1}(1 - \dot{r}^2 - kr^2)\dot{r}] - (1 - \dot{r}^2 - kr^2)r^{-1} \quad (5.28)$$

For small values of η, this equation admits an analytic solution of the form

$$r(\eta) = r_0 + \dot{r}_0\eta + \tfrac{1}{2}\ddot{r}_0\eta^2 + \cdots \qquad (5.29)$$

provided that $\dot{r}_0 = 0$ or $\dot{r}_0^2 + kr_0^2 = 1$. The second possibility corresponds to luminal motion of the string and is unlikely to be of physical importance. If $\dot{r}_0 = 0$ then the initial acceleration of the loop is

$$\ddot{r}_0 = -(2q + 1)^{-1}r_0^{-1}(1 - kr_0^2). \qquad (5.30)$$
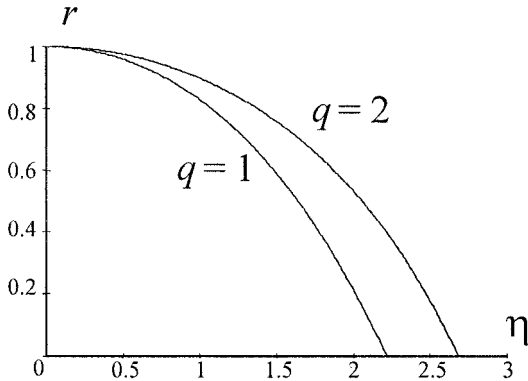
Thus, once the values of k and q have been prescribed, the analytic solutions of (5.28) are characterized by a single parameter, namely the initial radius r_0. Furthermore, if the spatial geometry is flat ($k = 0$) then the solution is scale-free, in the sense that if $r(\eta)$ is a solution then so is

$$\bar{r}(\eta) = \lambda r(\lambda^{-1}\eta) \qquad (5.31)$$
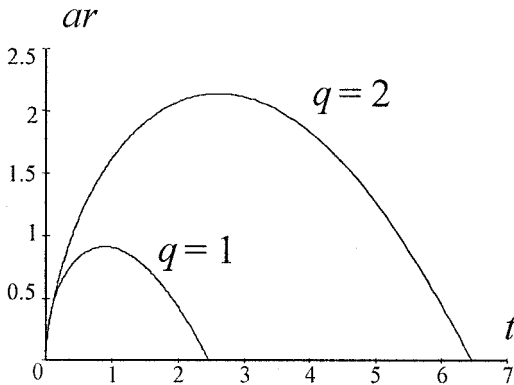
for any non-zero constant λ[1]. That is, the timescale for the collapse of any loop is proportional to its initial radius.

The shapes of the template solutions $r(\eta)$ for a radiation-dominated ($q = 1$) and a matter-dominated ($q = 2$) Friedmann universe with $k = 0$ are plotted in figure 5.1. The initial radius is $r_0 = 1$ in both cases. It is evident that the loop collapses more quickly in a radiation-dominated universe than in a matter-dominated universe. Figure 5.2 plots the physical radius ar of the ring, which is proportional to $\eta^q r(\eta)$, against the cosmological time $t = \int a\, d\eta$, which is

---

[1] This feature was first noted by de Vega and Egusquiza [dVE94].
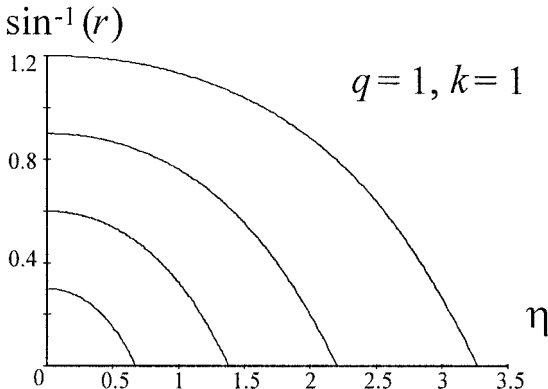
Figure 5.1. Coordinate radius r for ring solutions in two spatially-flat Friedmann universes.

Figure 5.2. Physical radius ar for ring solutions in two spatially-flat Friedmann universes.

proportional to $(q + 1)^{-1}\eta^{q+1}$. Note that for small values of η the conformal speed $\dot{r}$ remains close to zero and the loop participates in the general expansion of the universe. Eventually, however, the $q\eta^{-1}$ term in (5.28) ceases to dominate the dynamics of the loop, which then collapses at relativistic speed in a manner similar to the circular loop solutions of section 4.2.1. The transition between the regime of conformal expansion and the regime of relativistic collapse occurs when $\eta \approx r_0$.

Following de Vega and Egusquiza [dVE94], it is, in principle, possible to continue integrating the equations of motion through the point of collapse, allowing the loop to re-expand. The solution then oscillates with a period that falls off as η^{-q} and a physical amplitude that tends asymptotically to a fixed fraction of r_0. However, there are good reasons for believing that a collapsing circular loop of cosmic string would form a black hole rather than re-expand (see

Figure 5.3. Physical radius for ring solutions in a closed radiation-dominated Friedmann universe.

section 10.2), so the oscillating solutions are likely to be of little physical interest.
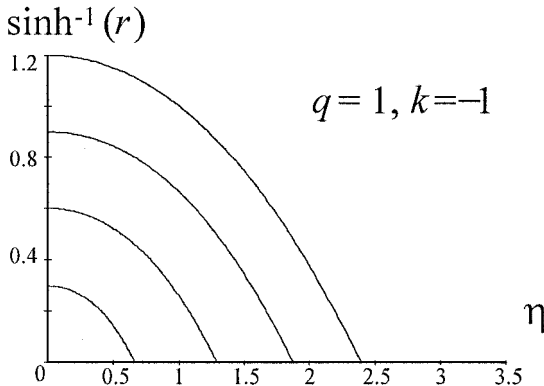
If $k \neq 0$, the non-trivial spatial geometry of the Robertson–Walker spacetimes for $r \sim 1$ and greater makes the dynamics of large rings more complicated. Some sample solutions in the cases $k = 1$ and $k = -1$ are shown in figures 5.3 and 5.4 for a radiation-dominated Friedmann universe. The dependent variable in the two diagrams is not the radial coordinate r but rather the physical conformal radius $\sin^{-1}(r)$ and $\sinh^{-1}(r)$ respectively. Note that in a closed universe ($k = 1$) the spatial curvature delays the collapse of large strings; in fact, a string loop with maximal radius, $r_0 = 1$, will, in principle, remain at $r = 1$ forever, although it is unstable to small perturbations. In the case of an open, hyperbolic universe ($k = -1$) the spatial curvature hastens the collapse of large strings. The results for a matter-dominated universe are similar.

De Vega and Egusquiza [dVE94] have integrated the ring equations of motion for a variety of Robertson–Walker metrics other than the standard Friedmann universes considered here. The backgrounds they have examined include the case $q = -3/4$; Myers' spacetime [Mye87], which is characterized by the expansion law $a(\eta) = e^{\eta}$; and Mueller's spacetime [Mue90].

Another background of cosmological interest is the de Sitter spacetime ($k = 0$, $q = -1$), which describes an exponentially inflating universe. Here, the evolution equations (5.6)–(5.9) are known to be integrable [dVS93], with the resulting conserved quantity in the case of the ring equations (5.24) and (5.25) being

$$C = \eta^{-1}\eta_{,\tau} - \eta^{-2}r\,r_{,\tau}\,. \tag{5.32}$$

All the ring solutions with r non-zero and analytic at $\eta = 0$ converge asymptotically to $r \approx \eta$ for large η. However, since $a(\eta) = A\eta^{-1}$ the relationship

Figure 5.4.   Physical radius for ring solutions in a hyperbolic radiation-dominated Friedmann universe.

between the conformal time η and the cosmological time t in this case is
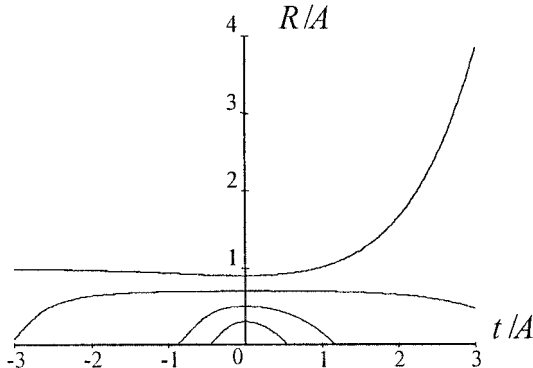
$$\eta = e^{-t/A} \tag{5.33}$$

and so the onset of inflation corresponds to η large—when the physical radius ar of all the ring solutions is approximately equal to the scaling constant A—while the inflationary epoch ends when η is close to zero, with $ar \sim e^{t/A}$.

Furthermore, the de Sitter universe is unique among the Robertson–Walker spacetimes with a power-law scaling of the form (5.18) in that the ring equation (5.27) can be written as an autonomous equation for the physical radius $R = ar$ as a function of the cosmological time t. In terms of the scaled variables $\bar{R} = R/A$ and $\bar{t} = t/A$ this equation reads simply:

$$\bar{R},_{\bar{t}\bar{t}} - \bar{R},_{\bar{t}} + [2(\bar{R},_{\bar{t}} - \bar{R}) + \bar{R}^{-1}][1 - (\bar{R},_{\bar{t}} - \bar{R})^2] = 0. \tag{5.34}$$

Equation (5.34) has an unstable solution $\bar{R} = 1/\sqrt{2}$ which divides the ring solutions into two distinct classes. Each ring solution can be characterized by the value $\bar{R}_0$ of $\bar{R}$ at which $\bar{R},_{\bar{t}} = 0$. If $\bar{R}_0 < 1/\sqrt{2}$ then the solution expands and recollapses in a finite proper time as illustrated by the three lower curves in figure 5.5 (which have $\bar{R}_0 = 0.3$, 0.5 and 0.7 respectively). However, if $1/\sqrt{2} < \bar{R}_0 < 1$ then the ring is eternal, with R asymptoting to A from below as $t \to -\infty$ and inflating away like $e^{t/A}$ as $t \to \infty$. (These are the solutions with $r \approx \eta$ for large η mentioned previously.) The upper curve in figure 5.5 is the solution for $\bar{R}_0 = 0.9$. Note that the zero point chosen for t in this diagram is the moment when $\bar{R} = \bar{R}_0$. The solution $\bar{R} = 1$ is unstable and luminal, while solutions with $\bar{R}_0 > 1$ are tachyonic.

Figure 5.5. Template ring solutions in the de Sitter universe.

5.2   Strings near a Schwarzschild black hole

Another background spacetime that has been studied extensively in the context of string dynamics is the exterior Schwarzschild metric, which in standard Schwarzschild coordinates has the form

$$ds^2 = \left(1 - \frac{2m}{r}\right) dt^2 - \left(1 - \frac{2m}{r}\right)^{-1} dr^2 - r^2\, d\theta^2 - r^2 \sin^2\theta\, d\phi^2 \quad (5.35)$$

where m is the mass of the source.

The line element (5.35) has four obvious Killing vectors:

$$k_\mu^{(1)} = \left(1 - \frac{2m}{r}\right)\delta_\mu^t \quad (5.36)$$

$$k_\mu^{(2)} = r^2 \sin^2\theta\, \delta_\mu^\phi \quad (5.37)$$

$$k_\mu^{(3)} = r^2(\sin\phi\, \delta_\mu^\theta + \sin\theta\cos\theta\cos\phi\, \delta_\mu^\phi) \quad (5.38)$$

and

$$k_\mu^{(4)} = r^2(\cos\phi\, \delta_\mu^\theta - \sin\theta\cos\theta\sin\phi\, \delta_\mu^\phi) \quad (5.39)$$

corresponding to time translations and infinitesimal spatial rotations.

For computational purposes, the most convenient set of evolution equations for an arbitrary string world sheet $X^\mu(\tau, \sigma)$ are the conservation equations generated by (5.36) and (5.37):

$$\left[\left(1 - \frac{2m}{r}\right) t_{,\tau}\right]_{,\tau} = \left[\left(1 - \frac{2m}{r}\right) t_{,\sigma}\right]_{,\sigma} \quad (5.40)$$

and

$$(r^2 \sin^2\theta\phi_{,\tau})_{,\tau} = (r^2 \sin^2\theta\phi_{,\sigma})_{,\sigma} \quad (5.41)$$

plus the gauge constraint

$$\left(1 - \frac{2m}{r}\right)[(t,_\tau)^2 + (t,_\sigma)^2] - \left(1 - \frac{2m}{r}\right)^{-1}[(r,_\tau)^2 + (r,_\sigma)^2]$$
$$= r^2[(\theta,_\tau)^2 + (\theta,_\sigma)^2] + r^2 \sin^2\theta[(\phi,_\tau)^2 + (\phi,_\sigma)^2] \qquad (5.42)$$

and the conservation equation

$$\sin\phi\,(k^{(3)} \cdot X^A),_A + \cos\phi\,(k^{(4)} \cdot X^A),_A = 0 \qquad (5.43)$$

which reads simply as

$$(r^2\theta,_\tau),_\tau - r^2 \sin\theta \cos\theta\,(\phi,_\tau)^2 = (r^2\theta,_\sigma),_\sigma - r^2 \sin\theta \cos\theta\,(\phi,_\sigma)^2. \qquad (5.44)$$

5.2.1 Ring solutions

One simple class of solutions, describing the collapse of a circular ring, can be generated by making the gauge choice $\sigma = \phi$ and assuming that t, r and θ are functions of the gauge time τ only. The non-trivial equations of motion (5.40), (5.42) and (5.44) then read:

$$\left[\left(1 - \frac{2m}{r}\right)t,_\tau\right],_\tau = 0 \qquad (5.45)$$

$$\left(1 - \frac{2m}{r}\right)(t,_\tau)^2 = \left(1 - \frac{2m}{r}\right)^{-1}(r,_\tau)^2 + r^2(\theta,_\tau)^2 + r^2 \sin^2\theta \qquad (5.46)$$

and

$$(r^2\theta,_\tau),_\tau + r^2 \sin\theta \cos\theta = 0. \qquad (5.47)$$

The first of these equations can be once integrated to give

$$\left(1 - \frac{2m}{r}\right)t,_\tau = K \qquad (5.48)$$

where, in view of the discussion on conservation laws in section 2.4, the conserved energy E of a ring with mass per unit length μ is equal to $2\pi\mu K$.

Substitution of (5.48) into the constraint equation (5.46) produces a quadratic invariant

$$K^2 = (r,_\tau)^2 + r(r - 2m)[(\theta,_\tau)^2 + \sin^2\theta] \qquad (5.49)$$

which when differentiated and combined with (5.47) gives the radial acceleration equation

$$r,_{\tau\tau} - (r - 3m)(\theta,_\tau)^2 + (r - m)\sin^2\theta = 0. \qquad (5.50)$$

This equation was first derived by de Vega and Egusquiza [dVE94]. One feature of (5.49) and (5.50) that should be noted is that once the ring has fallen inside the sphere $r = 3m$ collapse into the Schwarzschild singularity at $r = 0$ is inevitable

(although the ring itself may collapse to a point before it reaches $r = 0$), as $r_{,\tau\tau}$ is negative when $m < r < 3m$ and $r_{,\tau}$ cannot vanish if $0 < r < 2m$. The surface $r = 3m$ is therefore an effective horizon for all ring solutions[2].

Another quantity of interest is the proper time $s(\tau)$ in the rest frame of the ring, which is determined by the equation

$$\mathrm{d}s^2 = \left(1 - \frac{2m}{r}\right) \mathrm{d}t^2 - \left(1 - \frac{2m}{r}\right)^{-1} \mathrm{d}r^2 - r^2 \, \mathrm{d}\theta^2. \qquad (5.51)$$

In view of (5.46), therefore,

$$s_{,\tau} = r|\sin\theta|. \qquad (5.52)$$

The zero point of s will here be chosen to coincide with the instant at which the radial coordinate r attains its maximum value r_0. Then according to (5.49),

$$K^2 = r_0(r_0 - 2m)(\omega_0^2 + \sin^2\theta_0) \qquad (5.53)$$

where ω_0 is the value of $\theta_{,\tau}$ at $s = 0$. The dependence of r and θ on the proper time s can be found by integrating equations (5.49), (5.50) and (5.52) forward from $s = 0$.

In the case where the ring collapses inward along the equatorial plane $\theta = \pi/2$ the equations of motion can be solved exactly, to give

$$r(\tau) = m + (r_0 - m)\cos\tau \qquad (5.54)$$

and

$$s(\tau) = m\tau + (r_0 - m)\sin\tau. \qquad (5.55)$$

Note that the ring crosses the Schwarzschild horizon (at $r = 2m$) when

$$\tau = \cos^{-1}[m/(r_0 - m)] \qquad (5.56)$$

and falls into the singularity at $r = 0$ when
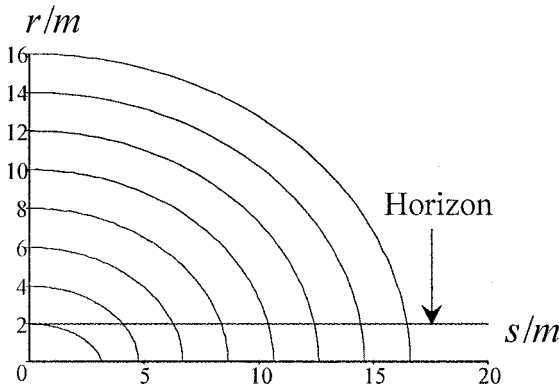
$$\tau = \pi - \cos^{-1}[m/(r_0 - m)]. \qquad (5.57)$$

If $r_0 \gg m$ these two events occur after a proper time $s \approx s^* - \frac{3}{2}m^2/r_0$ and $s \approx s^* + \frac{1}{2}m^2/r_0$ respectively, where

$$s^* = r_0 + \left(\frac{\pi}{2} - 1\right)m. \qquad (5.58)$$

Thus the time taken for the ring to fall from the horizon to the singularity is only $2m^2/r_0 \ll 2m$ in this limit. However, if $r_0 = 2m$ then the infall time is $s = m\pi$. The variation of r with s is shown for a selection of equatorial ring trajectories with r_0 ranging from $2m$ to $16m$ in figure 5.6.

---

[2] By way of comparison, the effective horizon for freely-moving *particles* is $r = 3\sqrt{3}m$.

Figure 5.6. Radius versus proper time for equatorial ring solutions in the Schwarzschild metric.

If $\theta \neq \pi/2$ the string describes a circle outside the equatorial plane but centred on the polar axis through the black hole. In this case the dynamics of the ring is complicated by the competition between the tension in the string, which induces a collapse towards the polar axis ($\theta = 0$ or π) and the inward radial acceleration due to the gravitational field of the hole. A variety of outcomes are possible, depending on the initial conditions on the trajectory.

Figure 5.7 shows r as a function of the proper time s for 11 solutions with $r_0 = 10m$, $\theta_0 = \pi/4$ and ω_0 ranging from 0 to 1. When $\omega_0 = 0, 0.1, 0.2$ or 0.3 the ring rapidly collapses onto the polar axis after relatively little radial infall. If $\omega_0 = 0.4, 0.5$ or 0.6 the ring remains open long enough to cross the black hole horizon and fall into the Schwarzschild singularity, while the solution with $\omega_0 = 0.7$ crosses the horizon but collapses to a point on the axis before reaching the singularity. In the remaining solutions, where $\omega_0 = 0.8, 0.9$ and 1, the ring falls across the equatorial plane and subsequently collapses to a point outside the south pole of the hole.

In order to visualize the geometry of the infall trajectories, it is instructive to write the line element on the spacelike hypersurfaces $t = $ constant in the conformally-flat form
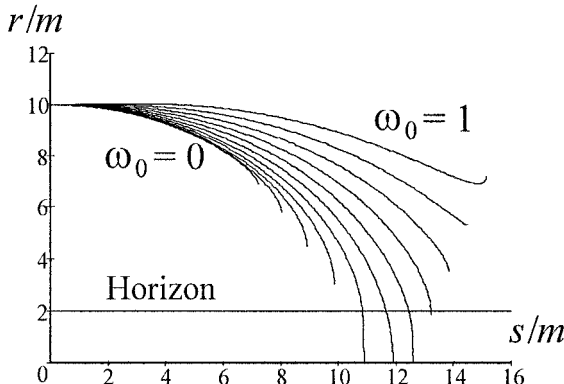
$$\mathrm{d}s^2 = -\left(1 + \frac{m}{2R}\right)^4 (\mathrm{d}R^2 + R^2\,\mathrm{d}\theta^2 + R^2 \sin^2\theta\,\mathrm{d}\phi^2) \tag{5.59}$$

where
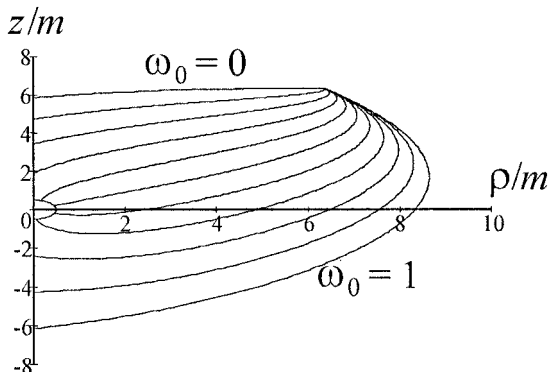
$$R = \tfrac{1}{2}(r - m) + \tfrac{1}{2}\sqrt{r^2 - 2mr}. \tag{5.60}$$

This transformation, which is well defined only for $r > 2m$, allows the trajectories to be expressed in terms of the horizontal and vertical coordinates

$$\rho = R \sin\theta \qquad \text{and} \qquad z = R\cos\theta \tag{5.61}$$

Figure 5.7. Radius versus proper time for non-equatorial ring solutions collapsing from $r_0 = 10m$, $\theta_0 = \pi/4$.

Figure 5.8. Trajectories of non-equatorial ring solutions collapsing from $r_0 = 10m$, $\theta_0 = \pi/4$.

respectively. Figure 5.8 plots z against ρ for the 11 solutions examined in figure 5.7.

As with the ring solutions in Robertson–Walker backgrounds, it is, in principle, possible to integrate the equations of motion through the point of collapse and so allow the ring to expand and recollapse any number of times. De Vega and Sanchez [dVE94] have done this for a range of ring solutions similar to the ones considered here. The resulting behaviour is surprisingly rich: in one solution the ring starts in the northern hemisphere, collapses on the south polar axis, re-expands and passes back over the hole to recollapse on the north polar axis with an oscillation amplitude larger than its initial amplitude. De Vega and Sanchez interpret this as a scattering-induced 'transmutation' of the string which

converts some of its bulk kinetic energy into oscillatory motion.

More recently, Andrei Frolov and Arne Larsen [FL99] have subjected the problem of the collapse and re-expansion of a circular string along the polar axis of a non-rotating black hole to a more detailed analysis. They divide the final state of the string into three classes: capture by the black hole, escape forward (from the northern hemisphere to the south pole) and escape with 'backscatter' (from the northern hemisphere back to the north pole). It turns out that all trajectories with $K \leq 4.37m$ end in capture, but that at higher energies the constant-K surfaces in the four-dimensional phase space generated by the initial values of r, $r_{,\tau}$, θ and $\theta_{,\tau}$ can show a complicated fractal structure. For $4.37m \leq K \leq 5.67m$ the boundaries between the regions of capture and the regions of escape remain regular but for $K \geq 5.67m$ the fractal dimension of the region boundaries on the two-dimensional slice of phase space defined by the initial condition $(r \cos \theta)_{,\tau} = 0$ rapidly rises from 1 to 1.6, and then more slowly to about 1.84, as K increases to $10^3 m$.

This fractal structure is of theoretical interest because, in the words of Frolov and Larsen [FL99], 'the system ... represents the simplest and most symmetric example of string dynamics in black hole spacetimes and therefore suggests quite generally that string dynamics in black hole spacetimes is chaotic'. Nonetheless, collapse and re-expansion solutions of this type are unlikely to be physical, for the reasons outlined in section 5.1.

5.2.2 Static equilibrium solutions

Another class of string solutions in a Schwarzschild background that can be constructed relatively easily are static equilibrium configurations. These describe infinite (open) strings in which the tension at each point exactly counters the gravitational attraction of the central mass, so that the string remains at rest with respect to the spatial coordinates. To generate a solution of this type, it is simplest to let $t = \tau$ and r, θ and ϕ be functions of σ only. The first of the equations of motion (5.40)–(5.44) is then satisfied identically, while the other three read:

$$(r^2 \sin^2 \theta \phi_{,\sigma}),_{\sigma} = 0 \qquad (5.62)$$

$$1 - \frac{2m}{r} = \left(1 - \frac{2m}{r}\right)^{-1} (r_{,\sigma})^2 + r^2(\theta_{,\sigma})^2 + r^2 \sin^2 \theta (\phi_{,\sigma})^2 \quad (5.63)$$

and

$$(r^2 \theta_{,\sigma}),_{\sigma} = r^2 \sin \theta \cos \theta (\phi_{,\sigma})^2. \qquad (5.64)$$

Note that if it were not for the presence of the term $2m/r$ on the left-hand side of (5.63), these would just be the equations of a subfamily of spacelike geodesics in the Schwarzschild metric. Furthermore, from equations (5.62) and (5.64) it is clear that the static equilibrium solutions are planar, and so it is possible without loss of generality to restrict attention to the equatorial plane. The equilibrium

equations then read:

$$\phi_{,\sigma} = J/r^2 \tag{5.65}$$

and

$$(r_{,\sigma})^2 = \left(1 - \frac{2m}{r}\right)^2 - J^2\left(1 - \frac{2m}{r}\right)/r^2 \tag{5.66}$$

where J is a constant.

In fact, if r_0 denotes the minimum value of r then $J^2 = r_0^2 - 2mr_0$, and on eliminating σ in favour of ϕ as the parametric variable the equilibrium conditions reduce to a single equation:

$$\left(\frac{dr}{d\phi}\right)^2 = (r^2 - 2mr)\left(\frac{r^2 - 2mr}{r_0^2 - 2mr_0} - 1\right) \tag{5.67}$$

with formal solution

$$\phi - \phi_0 = (r_0 - m)^{-1}(r_0^2 - 2mr_0)^{1/2}\{K[m/(r_0 - m)] - F[u, m/(r_0 - m)]\} \tag{5.68}$$

where $u = \sin^{-1}[(r_0 - m)/(r - m)]$,

$$F(u, k) = \int_0^u (1 - k^2 \sin^2 w)^{-1/2}\, dw \tag{5.69}$$

is the elliptical integral of the first kind, and $K(k) = F(\pi/2, k)$ is the corresponding complete integral.

In particular, the net angular deviation $\Delta\phi$ of the string from a straight line is

$$\Delta\phi \equiv \pi - 2\lim_{r\to\infty}(\phi - \phi_0) = \pi - 2(\bar{r} - 1)^{-1}(\bar{r}^2 - 2\bar{r})^{1/2}K[(\bar{r} - 1)^{-1}] \tag{5.70}$$
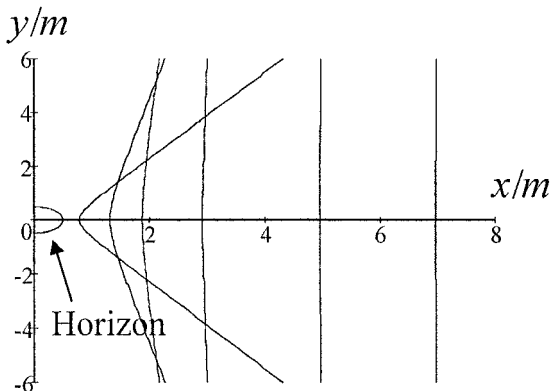
where $\bar{r} = r_0/m$. In the limit as the periastron point at $r = r_0$ approaches the black hole horizon, the angular deviation $\Delta\phi$ tends to π and the two branches of the static equilibrium solution collapse to a single radial line emanating from the horizon.

To better illustrate the distortion in the shape of the string induced by the presence of the central mass, figure 5.9 plots six sample static equilibrium solutions, with r_0/m equal to 8, 6, 4, 3, 2.5 and 2.1, in terms of the conformally-flat Cartesian coordinates $x = R\cos\phi$ and $y = R\sin\phi$, where R was defined previously in equation (5.60). In figure 5.10, the net angular deviation $\Delta\phi$ in the string is plotted against $\bar{r} = r_0/m$, with $\bar{r}$ ranging from 2 to 6. Note that for $\bar{r}$ close to 2,
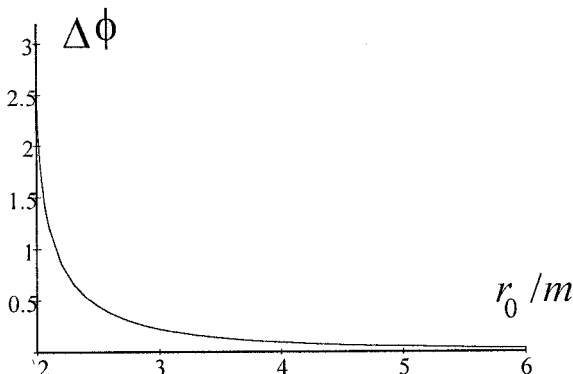
$$\Delta\phi \approx \pi + \sqrt{2}\varepsilon^{1/2}\ln\varepsilon \tag{5.71}$$

with $\varepsilon = \bar{r} - 2$, whereas, for large values of $\bar{r}$,

$$\Delta\phi \approx \frac{\pi}{4}m^2/r_0^2. \tag{5.72}$$

Figure 5.9. Six static equilibrium solutions in the Schwarzschild metric.

Figure 5.10. Angular deviation $\Delta\phi$ of a static string as a function of the periastron distance r_0.

5.3   Scattering and capture of a straight string by a Schwarzschild hole

Another class of string solutions in a Schwarzschild background that has received some attention recently describes the dynamical response of an infinite string, initially straight, as it passes by a non-rotating compact mass or black hole. The fully relativistic version of this problem can only be addressed numerically, and was first examined by Steven Lonsdale and Ian Moss in 1988 [LM88]. Unfortunately, Lonsdale and Moss gave very little mathematical detail of their calculations and more recent treatments of the problem by Jean-Pierre de Villiers and Valeri Frolov [VF98b, VF98a] and Don Page [Pag98] suggest substantially different conclusions.

The most convenient choice of coordinates for the Schwarzschild metric in this case is the isotropic form, which has the line element

$$ds^2 = (1 + \tfrac{1}{2}\psi)^{-2}(1 - \tfrac{1}{2}\psi)^2 \, dt^2 - (1 + \tfrac{1}{2}\psi)^4(dx^2 + dy^2 + dz^2) \qquad (5.73)$$

where $\psi = m/R$ is the equivalent Newtonian potential, and the conformal radial coordinate $R = (x^2 + y^2 + z^2)^{1/2}$ was introduced in (5.60). In the absence of a central mass, a straight string oriented parallel to the z-axis and travelling with uniform speed v in the x-direction has the standard-gauge trajectory

$$X_0^\mu(\sigma, \tau) \equiv [t_0, x_0, y_0, z_0] = [\gamma\tau, \gamma v\tau, b, \sigma] \qquad (5.74)$$

where $\gamma = (1 - v^2)^{-1/2}$ is the Lorentz factor and $b > 0$ the impact parameter of the string. In what follows, this flat-space trajectory will be imposed as the initial condition in the limit as $\tau \to -\infty$.

Broadly speaking, there are two possible fates in store for the string as it passes the central mass: either it remains entirely outside the black hole's event horizon at $R = \tfrac{1}{2}m$ and eventually recedes to infinity in an excited state, carrying off some of the hole's gravitational energy in the form of outward-moving oscillatory modes; or its near-equatorial section crosses the event horizon and is presumably crushed by the central singularity. De Villiers and Frolov [VF98b] refer to these two possibilities as *scattering* and *capture* respectively. The boundary between the two defines a critical curve in the two-dimensional parameter space generated by the speed v and impact parameter b of the initial trajectory.

It is possible to gain some analytic insight into the dynamical response of the string, and, in particular, the form of the critical curve, by expanding the string's trajectory in powers of the central mass m:

$$X^\mu(\sigma, \tau) = X_0^\mu + X_1^\mu + X_2^\mu + \cdots \qquad (5.75)$$

with X_k^μ proportional to m^k. To linear order in m the equation of motion (5.1) then reads:
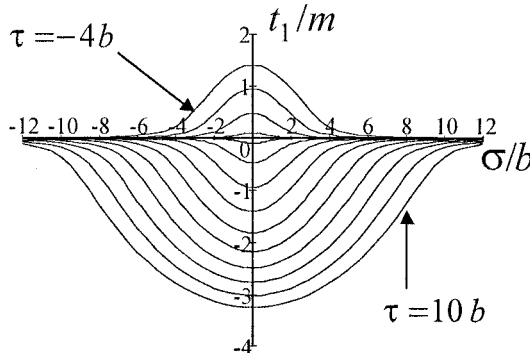
$$X_{1\ ,\tau\tau}^\mu - X_{1\ ,\sigma\sigma}^\mu = {}_1\Gamma_{\kappa\lambda}^\mu(X_0)(X_{0\ ,\sigma}^\kappa X_{0\ ,\sigma}^\lambda - X_{0\ ,\tau}^\kappa X_{0\ ,\tau}^\lambda) \qquad (5.76)$$

where ${}_1\Gamma_{\kappa\lambda}^\mu$ is the Christoffel symbol truncated at linear order in the potential ψ, so that

$${}_1\Gamma_{\kappa\lambda}^\mu(X_0)(X_{0\ ,\sigma}^\kappa X_{0\ ,\sigma}^\lambda - X_{0\ ,\tau}^\kappa X_{0\ ,\tau}^\lambda) = 2\gamma^2[v\psi_{,x}, 0, v^2\psi_{,y}, \psi_{,z}] \qquad (5.77)$$

with the right-hand expressions understood to be evaluated on the unperturbed trajectory $(x, y, z) = (\gamma v\tau, b, \sigma)$.

In order to recover the unperturbed trajectory in the limit as $\tau \to -\infty$, it is necessary to prescribe the initial data so that x_1, y_1 and z_1 are all zero in this limit. It turns out that t_1 diverges logarithmically in $|\tau|$ as $\tau \to -\infty$, and so it is

Figure 5.11. The perturbation t_1 as a function of τ and σ.

not possible to impose a similar condition on t_1. However, if t_1 is chosen to be zero at the moment of time symmetry $\tau = 0$ then t_1 remains everywhere small in comparison with $\gamma\tau$.

The resulting expression for the first-order perturbation in t is
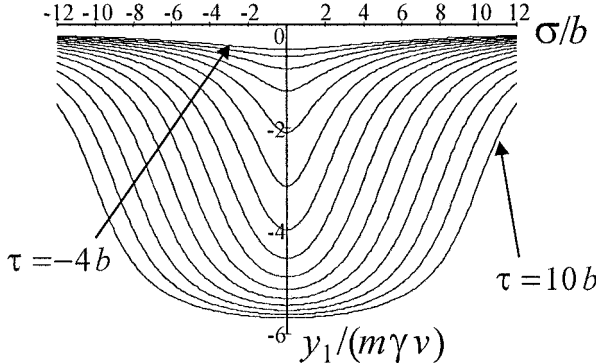
$$
\begin{aligned}
t_1 = & -m\gamma^3 v^2 \int_0^\tau \tau' \, d\tau' \int_{\sigma-(\tau-\tau')}^{\sigma+(\tau-\tau')} (\gamma^2 v^2 \tau'^2 + b^2 + \sigma'^2)^{-3/2} \, d\sigma' \\
= & \, m\{\ln[\gamma v^2 \tau - \gamma^{-1}\sigma + \alpha(\sigma, \tau)] + \ln[\gamma v^2 \tau + \gamma^{-1}\sigma + \alpha(\sigma, \tau)]\} \\
& + \tfrac{1}{2}m\gamma[\ln(\beta_+ - \sigma_+) - \ln(\beta_+ + \sigma_+) + \ln(\beta_- - \sigma_-) - \ln(\beta_- + \sigma_-)] \\
& - m[\ln(\beta_+ - \gamma^{-1}\sigma_+) + \ln(\beta_- - \gamma^{-1}\sigma_-)] \qquad\qquad (5.78)
\end{aligned}
$$

where $\alpha(\sigma, \tau) = \sqrt{\gamma^2 v^2 \tau^2 + b^2 + \sigma^2}$ and $\beta_\pm = \sqrt{b^2 + \sigma_\pm^2}$, with $\sigma_\pm = \tau \pm \sigma$ as before. The evolution of t_1 in the case $v = 0.5$ is shown in figure 5.11.
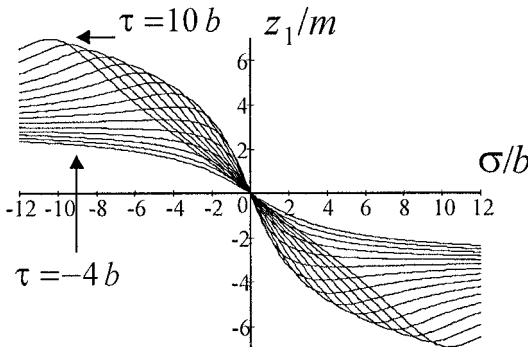
It is evident from the second component of the equation of motion that $x_1 = 0$, and so the perturbation of the trajectory in the direction of motion is zero to linear order in m. The perturbation y_1 in the direction of the black hole is given by

$$
\begin{aligned}
y_1 = & -m\gamma^2 v^2 b \int_{-\infty}^\tau d\tau' \int_{\sigma-(\tau-\tau')}^{\sigma+(\tau-\tau')} (\gamma^2 v^2 \tau'^2 + b^2 + \sigma'^2)^{-3/2} \, d\sigma' \\
= & -m\gamma v \left\{ \tan^{-1}\left[\frac{b^2 + \gamma^2 v^2 \tau\sigma_+}{b\gamma v\alpha(\sigma, \tau)}\right] + \tan^{-1}(v\sigma_+/b) \right\} \\
& - m\gamma v \left\{ \tan^{-1}\left[\frac{b^2 + \gamma^2 v^2 \tau\sigma_-}{b\gamma v\alpha(\sigma, \tau)}\right] + \tan^{-1}(v\sigma_-/b) \right\} \qquad (5.79)
\end{aligned}
$$

and is plotted in the case $v = 0.5$ in figure 5.12.

Figure 5.12. The perturbation y_1 as a function of τ and σ.

Figure 5.13. The perturbation z_1 as a function of τ and σ.

Finally, the longitudinal perturbation z_1, which essentially measures how the gauge parameter σ is changing at different values of z, is given by

$$
\begin{aligned}
z_1 = {}& -m\gamma^2 \int_{-\infty}^{\tau} d\tau' \int_{\sigma-(\tau-\tau')}^{\sigma+(\tau-\tau')} (\gamma^2 v^2 \tau'^2 + b^2 + \sigma'^2)^{-3/2} \sigma' \, d\sigma' \\
= {}& m\gamma \{ \ln[\gamma v^2 \tau - \gamma^{-1}\sigma + \alpha(\sigma,\tau)] - \ln[\gamma v^2 \tau + \gamma^{-1}\sigma + \alpha(\sigma,\tau)]\} \\
& - m\gamma[\ln(b^2 + v^2 \sigma_+^2) - \ln(b^2 + v^2 \sigma_-^2)]
\end{aligned} \tag{5.80}
$$

and is plotted in the case $v = 0.5$ in figure 5.13.

In the late-time limit all the non-zero perturbations t_1, y_1 and z_1 develop a pair of left- and right-moving kinks which propagate outwards at the speed of light. For the purposes of understanding the dynamics of the string, the most important of the perturbations is y_1, which in the limit as $\tau \to \infty$ has the form

$$
y_1 \approx -2m\gamma v \{\tan^{-1}[v(\tau + \sigma)/b] + \tan^{-1}[v(\tau - \sigma)/b]\}. \tag{5.81}
$$

Thus the kinks have an amplitude $\Delta y = -2\pi m\gamma v$, which is equal to the net deviation of the string in the y-direction to linear order in m, and have a spatial width of order b/v. The energy ΔE carried away by the kinks can be approximated to leading order in m as

$$\Delta E = \tfrac{1}{2}\mu \lim_{\tau \to \infty} \int_{-\infty}^{\infty} [(\partial y_1/\partial\sigma)^2 + (\partial y_1/\partial\tau)^2]\,\mathrm{d}\sigma$$
$$= 4\pi\mu m^2\gamma^2 v^3/b \tag{5.82}$$

where μ is the mass per unit length of the string.

Another feature of interest is the equation of the critical curve $b(v)$ dividing the scattering trajectories from those that are captured by the central mass. As is evident from figure 5.12, the point on the string that passes closest to the central mass in the linear approximation is the midpoint of the string at $\sigma = 0$. To linear order in m, the distance R_0 of this point from the central mass is given by

$$R_0^2(\tau) = \gamma^2 v^2\tau^2 + [b + y_1(0, \tau)]^2$$
$$\approx \gamma^2 v^2\tau^2 + b^2 - 4mb\gamma v \left[\tan^{-1}\left(\sqrt{\tau^2/b^2 + \gamma^{-2}v^{-2}}\right) + \tan^{-1}(v\tau/b)\right].$$
$$\tag{5.83}$$

The value $\tau_{\min}$ of τ which minimizes this expression satisfies the equation

$$0 = 2\gamma^2 v^2\tau_{\min} - \frac{4mb^2\gamma v^2}{b^2 + v^2\tau_{\min}^2}\left[1 + \frac{\tau_{\min}b}{\sqrt{\tau_{\min}^2 + b^2\gamma^{-2}v^{-2}}}\right]. \tag{5.84}$$

At this level of approximation $\tau_{\min} = 2m\gamma^{-1} + O(m^2)$, with
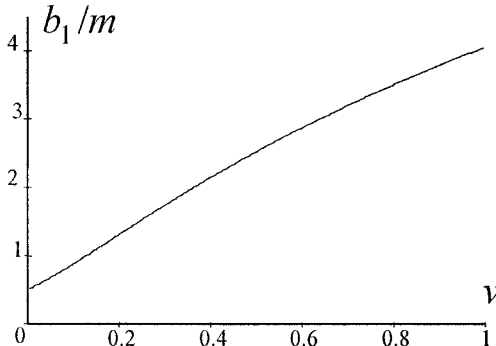
$$R_0^2(2m\gamma^{-1}) = b^2 - 4bm\gamma v \tan^{-1}(\gamma^{-1}v^{-1}) + O(m^2). \tag{5.85}$$

The critical value of b can now be calculated by setting $R_0^2(2m\gamma^{-1})$ equal to $m^2/4$, the square of the radius of the black hole's event horizon. To linear order in m, therefore, the critical value of b is

$$b_1(v) = \left[2\gamma v \tan^{-1}(\gamma^{-1}v^{-1}) + \tfrac{1}{2}\sqrt{1 + 16\gamma^2 v^2\{\tan^{-1}(\gamma^{-1}v^{-1})\}^2}\right] m \tag{5.86}$$

where the subscript 1 indicates the level of approximation.

The graph of b_1/m against v is shown in figure 5.14. Note that in the low-velocity limit $v \to 0$ the critical impact parameter b_1 approaches $\tfrac{1}{2}m$, whereas in the ultra-relativistic limit $v \to 1$ it tends to $(2 + \tfrac{1}{2}\sqrt{17})m \approx 4.062m$. The first of these limits can be understood by referring back to the static equilibrium solutions examined in section 5.2.2. There it was seen that for small values of m the bending angle $\Delta\phi$ of the string is of order m^2. Thus in the static limit the

Figure 5.14. The first-order approximation b_1 to the critical curve.

string does not bend at all to linear order in m, and the string propagates past the central mass with a constant impact parameter. (This can also be seen directly from the general expression (5.79) for y_1.)

However, it is clear on physical grounds that a string with a small initial velocity will eventually fall into the central mass unless its impact parameter is very large. In fact, as has been argued by Don Page [Pag98], the bending angle of a string moving at a low speed v should be of order $\Delta\phi \sim v/c$ (where c is the speed of light), as longitudinal disturbances will move with velocity c whereas the radial motion of the string is of order v. Given that $\Delta\phi$ is known to be of order m^2 in this limit, it must on dimensional grounds be proportional to m^2/b^2, and so the critical value of b should be of order $m/v^{1/2}$. Thus the linear approximation is extremely poor in the low-velocity limit.

Similarly, in the ultra-relativistic limit it is to be expected that, because perturbations in the string can propagate no faster than the speed of light, the elements of the string are essentially decoupled from one another and should behave like ultra-relativistic particles. The critical impact parameter for a freely-moving ultra-relativistic particle in the Schwarzschild metric is known to be $3\sqrt{3}m \approx 5.196m$, and so the linear approximation is accurate to no better than about 20% in this limit as well.

A more reliable approximation to the critical curve can be generated by solving the string equation of motion (5.1) to order m^2. Once the second-order perturbations $x_2(\sigma, \tau)$ and $y_2(\sigma, \tau)$ are known, the distance R_0 of the midpoint of the string from the central mass is given to order m^2 by

$$R_0^2(\tau) = [\gamma v\tau + x_2(0, \tau)]^2 + [b + y_1(0, \tau) + y_2(0, \tau)]^2. \qquad (5.87)$$

Since the time $\tau_{\min}$ of closest approach is of order m and x_2 and y_2 are of order m^2,

$$R_0^2(\tau_{\min}) = \gamma^2 v^2 \tau_{\min}^2 + b^2 - 4mb\gamma v \left[\tan^{-1}\left(\sqrt{\tau_{\min}^2/b^2 + \gamma^{-2}v^{-2}} \right) \right.$$

$$+ \tan^{-1}(v\tau_{\min}/b)\Big] + 2by_2(0,0) + O(m^3) \qquad (5.88)$$

from which it is evident that $\tau_{\min} = 2m\gamma^{-1} + O(m^2)$ as before. So the distance of closest approach is given by

$$R_0^2(2m\gamma^{-1}) = b^2 - 4bm\gamma v \tan^{-1}(\gamma^{-1}v^{-1}) + 4\gamma^2 v^2[\tan^{-1}(\gamma^{-1}v^{-1})]^2 m^2$$
$$- 4v^2 m^2 + 2by_2(0,0) + O(m^3) \qquad (5.89)$$

and can be calculated exactly to order m^2 from a knowledge of $y_2(0,0)$ alone.

Now, the equation for the perturbation y_2 reads:

$$y_{2,\tau\tau} - y_{2,\sigma\sigma} = 2\Gamma^y_{\kappa\lambda}(X_0)(X_{0,\sigma}^\kappa X_{0,\sigma}^\lambda - X_{0,\tau}^\kappa X_{0,\tau}^\lambda)$$
$$+ 2\,_1\Gamma^y_{\kappa\lambda}(X_0)(X_{1,\sigma}^\kappa X_{0,\sigma}^\lambda - X_{1,\tau}^\kappa X_{0,\tau}^\lambda)$$
$$+_1 \Gamma^y_{\kappa\lambda,\nu}(X_0)X_1^\nu(X_{0,\sigma}^\kappa X_{0,\sigma}^\lambda - X_{0,\tau}^\kappa X_{0,\tau}^\lambda) \qquad (5.90)$$

where $_2\Gamma^\mu_{\kappa\lambda}$ is the contribution to the Christoffel symbol quadratic in the potential ψ, and gives

$$_2\Gamma^y_{\kappa\lambda}(X_0)(X_{0,\sigma}^\kappa X_{0,\sigma}^\lambda - X_{0,\tau}^\kappa X_{0,\tau}^\lambda) = -\tfrac{1}{2}\gamma^2(7 + 2v^2)\psi\psi_{,y}. \qquad (5.91)$$

Also, after some algebraic manipulation it can be seen that

$$_1\Gamma^y_{\kappa\lambda,\nu}(X_0)X_1^\nu(X_{0,\sigma}^\kappa X_{0,\sigma}^\lambda - X_{0,\tau}^\kappa X_{0,\tau}^\lambda) = 2\gamma^2 v^2(\psi_{,yy}\, y_1 + \psi_{,yz}\, z_1) \quad (5.92)$$

and

$$2\,_1\Gamma^y_{\kappa\lambda}(X_0)(X_{1,\sigma}^\kappa X_{0,\sigma}^\lambda - X_{1,\tau}^\kappa X_{0,\tau}^\lambda)$$
$$= 2[(\gamma t_{1,\tau} - z_{1,\sigma})\psi_{,y} - \gamma v y_{1,\tau}\, \psi_{,x} + y_{1,\sigma}\, \psi_{,z}] \qquad (5.93)$$

where the first term on the right can be simplified by invoking the identity $\gamma t_{1,\tau} - z_{1,\sigma} = 2\gamma^2\psi$, which follows by expanding the gauge constraint $X_\tau^2 + X_\sigma^2 = 0$ to linear order in m.

Integration of (5.90), therefore, gives

$$y_2(0,0) = \int_{-\infty}^0 d\tau \int_\tau^{-\tau} [\tfrac{1}{4}\psi\psi_{,y} + \gamma^2 v^2(\psi_{,yy}\, y_1 + \psi_{,yz}\, z_1)$$
$$- \gamma v y_{1,\tau}\, \psi_{,x} + y_{1,\sigma}\, \psi_{,z}]\, d\sigma \qquad (5.94)$$

where as previously ψ and its derivatives are evaluated on the unperturbed trajectory $(x, y, z) = (\gamma v\tau, b, \sigma)$. In view of the rather forbidding expressions (5.79) and (5.80) for the perturbations y_1 and z_1 an exact expression for $y_2(0,0)$ might seem unlikely. However, after a considerable amount of mathematical reduction it turns out that

$$y_2(0,0) = m^2 b^{-1}\gamma v \left[\sin^{-1}(1 - 2\gamma^{-2}) - \frac{\pi}{2}\right] + 4m^2 b^{-1}\gamma^2 v^2 \ln\left(\frac{\gamma^2}{\gamma^2 - 1}\right)$$
$$- \tfrac{1}{4}m^2 b^{-1}\gamma^{-1}v^{-1}(1 + 8\gamma^2 v^2)\tan^{-1}(\gamma^{-1}v^{-1}). \qquad (5.95)$$

The critical value b_2 of the impact parameter can now be found by setting the formula for $R_0^2(2m\gamma^{-1})$ in (5.89) equal to the square $m^2/4$ of the horizon radius and solving for b, to give

$$b_2(v) = \left[2\gamma v \tan^{-1}(\gamma^{-1}v^{-1}) + \tfrac{1}{2}\sqrt{F(v)}\right] m \qquad (5.96)$$

where

$$F(v) = 1 + 16v^2 - 8\gamma v \left[\sin^{-1}(1 - 2\gamma^{-2}) - \frac{\pi}{2}\right] - 32\gamma^2 v^2 \ln\left(\frac{\gamma^2}{\gamma^2 - 1}\right)$$

$$+ 2\gamma^{-1}v^{-1}(1 + 8\gamma^2 v^2) \tan^{-1}(\gamma^{-1}v^{-1}). \qquad (5.97)$$

Note here that $b_2 \approx \frac{1}{\sqrt{2}}m/v^{1/2}$ in the low-velocity limit, in line with the expectations mentioned earlier; whereas in the ultra-relativistic limit ($v \to 1$) the value of b_2 tends to $(2 + \tfrac{1}{2}\sqrt{17})m$ and thus gives no improvement over the first-order approximation b_1.

De Villiers and Frolov [VF99] have integrated the full string equations of motion (5.1) for a wide range of initial velocities v and impact parameters b, and have constructed a numerical approximation to the critical curve $b = b_{\text{crit}}(v)$, as shown by the open circles in figure 5.15. Their results confirm that $b_{\text{crit}} \sim m/v^{1/2}$ for v close to 0 and that $b_{\text{crit}} \to 3\sqrt{3}m$ as $v \to 1$. The well-defined minimum of about 3.2 in b_{crit}, which occurs at $v \approx 0.25$, is due to the action of the string tension, which is almost inoperative at high velocities but lends the string sufficient rigidity at moderate velocities to allow it to escape the black hole's clutches down to relatively small impact parameters[3].

As can be seen from figure 5.15, the second-order expansion b_2 predicts the general shape of the critical curve quite well but consistently underestimates the values of b_{crit} by 10–20%. Page [Pag98] has predicted that b_{crit} should be a discontinuous function of v, particularly for ultra-relativistic string velocities, as he expects the string in this limit to wrap itself around the black hole a large number of times before being captured. However, de Villiers and Frolov [VF99] have seen no evidence in their numerical simulations of multiple wrappings of the string for their range of initial velocities, which extends up to $v = 0.995$.
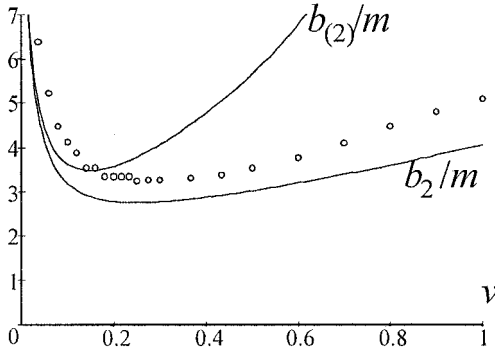
Both Page [Pag98] and de Villiers and Frolov [VF98a] make use of a somewhat cruder approximation than b_2 to estimate the critical impact parameter at order m^2 in the string trajectory. They do this by calculating the distance of the string plane from the equatorial plane at late times

$$y_\infty = b + \lim_{\tau \to \infty}[y_1(\sigma, \tau) + y_2(\sigma, \tau)] \qquad (5.98)$$

and then setting it equal to the black hole radius $m/2$. Since

$$\lim_{\tau \to \infty} y_1(\sigma, \tau) = -2\pi m\gamma v \qquad (5.99)$$

---

[3] By contrast, the earliest published analysis of string scattering by a Schwarzschild hole, due to Lonsdale and Moss [LM88], claimed that b_{crit} was a monotonically decreasing function of v and that $b_{\text{crit}} \sim v^{-1}$ for small v.

Figure 5.15. Two second-order approximations b_2 and $b_{(2)}$ for the critical curve plotted against the numerical results of de Villiers and Frolov.

and

$$
\begin{aligned}
\lim_{\tau \to \infty} y_2(\sigma, \tau) &= \int_{-\infty}^{\infty} d\tau \int_{-\infty}^{-\infty} [\tfrac{1}{4}\psi\psi_{,y} + \gamma^2 v^2 (\psi_{,yy}\, y_1 + \psi_{,yz}\, z_1) \\
&\quad - \gamma v y_{1,\tau}\, \psi_{,x} + y_{1,\sigma}\, \psi_{,z}\,]\, d\sigma \\
&= -\frac{\pi}{4} m^2 b^{-1} \gamma^{-1} v^{-1} (1 + 16\gamma^2 v^2)
\end{aligned}
\tag{5.100}
$$

this procedure leads to the approximate critical curve:

$$
b_{(2)} = \left[\tfrac{1}{4} + \pi \gamma v + \tfrac{1}{4}\sqrt{4\pi \gamma^{-1} v^{-1} + 1 + 72\pi \gamma v + 16\pi^2 \gamma^2 v^2} \right] m. \tag{5.101}
$$

The dependence of $b_{(2)}$ on v is also shown in figure 5.15. Note that for small values of v the value of $b_{(2)}$ diverges as $(\pi/4)^{1/2} m v^{-1/2}$, which is consistent with the numerical results, but that $b_{(2)}$ also diverges (as $2\pi\gamma$) in the ultra-relativistic limit.

5.4   Ring solutions in the Kerr metric

A natural extension of the analysis of the previous sections is to consider the motion of a cosmic string in the gravitational field of a rotating black hole. The relevant background spacetime is then the Kerr metric, which in Boyer–Lindquist coordinates (t, r, θ, ϕ) has the line element

$$
\begin{aligned}
ds^2 &= g_{tt}\, dt^2 + 2g_{t\phi}\, dt\, d\phi + g_{\phi\phi}\, d\phi^2 + g_{rr}\, dr^2 + g_{\theta\theta}\, d\theta^2 \\
&= \rho^{-2}[(r^2 - 2mr + a^2 \cos^2 \theta)\, dt^2 + 4mar \sin^2 \theta\, dt\, d\phi - \Sigma^2 \sin^2 \theta\, d\phi^2] \\
&\quad - \Delta^{-1} \rho^2\, dr^2 - \rho^2\, d\theta^2
\end{aligned}
\tag{5.102}
$$

where

$$\rho^2 = r^2 + a^2 \cos^2 \theta \qquad \Delta = r^2 - 2mr + a^2 \tag{5.103}$$

and

$$\Sigma^2 = (r^2 + a^2)^2 - a^2 \Delta \sin^2 \theta \tag{5.104}$$

and m and ma are the mass and angular momentum of the source, respectively. The zeroes of the function Δ correspond to the outer and inner event horizons of the black hole, while the surface $r^2 - 2mr + a^2 \cos^2 \theta = 0$ is the static limit of the hole (the boundary of the ergosphere): the minimum radius at which a test particle can remain at rest with respect to the angular coordinate ϕ.

The complexity of the Kerr metric makes it a daunting task to write down, let alone solve, the general string equations of motion but one case that is known to be exactly solvable is the collapse of a circular ring centred on the rotation axis of the hole. This particular problem is made tractable by the fact that the Kerr metric possesses two simple Killing vectors, one timelike

$$k_{\mu}^{(1)} = g_{tt}\delta_{\mu}^t + g_{t\phi}\delta_{\mu}^{\phi} \tag{5.105}$$

and one rotational

$$k_{\mu}^{(2)} = -(g_{\phi\phi}\delta_{\mu}^{\phi} + g_{t\phi}\delta_{\mu}^t). \tag{5.106}$$

The corresponding conservation equations read:

$$(g_{tt}t_{,\tau} + g_{t\phi}\phi_{,\tau}),_{\tau} = (g_{tt}t_{,\sigma} + g_{t\phi}\phi_{,\sigma}),_{\sigma} \tag{5.107}$$

and

$$-(g_{\phi\phi}\phi_{,\tau} + g_{t\phi}t_{,\tau}),_{\tau} = -(g_{\phi\phi}\phi_{,\sigma} + g_{t\phi}t_{,\sigma}),_{\sigma}. \tag{5.108}$$

In addition, the gauge constraints (5.2) have the form:

$$g_{tt}[(t_{,\tau})^2 + (t_{,\sigma})^2] + 2g_{t\phi}(t_{,\tau}\phi_{,\tau} + t_{,\sigma}\phi_{,\sigma}) + g_{\phi\phi}[(\phi_{,\tau})^2 + (\phi_{,\sigma})^2]$$
$$= -g_{rr}[(r_{,\tau})^2 + (r_{,\sigma})^2] - g_{\theta\theta}[(\theta_{,\tau})^2 + (\theta_{,\sigma})^2] \tag{5.109}$$

and

$$g_{tt}t_{,\tau}t_{,\sigma} + g_{t\phi}(t_{,\tau}\phi_{,\sigma} + t_{,\sigma}\phi_{,\tau}) + g_{\phi\phi}\phi_{,\tau}\phi_{,\sigma} + g_{rr}r_{,\tau}r_{,\sigma} + g_{\theta\theta}\theta_{,\tau}\theta_{,\sigma} = 0. \tag{5.110}$$

For a solution with circular geometry centred on the rotation axis, it is always possible to choose the gauge coordinates so that r and θ are functions of τ alone but because of the rotational frame-dragging induced by the spin of the black hole it is not necessarily true that t and ϕ will separately be functions of τ and σ only. However, the symmetry of the solution ensures that each element of the string will fall along a path of zero angular momentum, so that

$$-(g_{\phi\phi}\phi_{,\tau} + g_{t\phi}t_{,\tau}) = 0. \tag{5.111}$$

This condition allows equation (5.108) to be integrated once, giving

$$-(g_{\phi\phi}\phi,_\sigma +g_{t\phi}t,_\sigma) = F(\tau) \tag{5.112}$$

for some function F. Using equations (5.111) and (5.112) to eliminate $\phi,_\tau$ and $\phi,_\sigma$ from the second of the gauge constraint equations (5.110) then gives

$$(g_{tt} - g_{t\phi}^2/g_{\phi\phi})t,_\tau t,_\sigma = 0 \tag{5.113}$$

and so $t,_\sigma = 0$. By choosing $F(\tau) = -g_{\phi\phi}$, it is always possible to set $\phi,_\sigma = 1$, but it should be noted that $\phi,_\tau \neq 0$ in general.

As in the Schwarzschild case, the energy conservation equation (5.107) can now be integrated to give

$$g_{tt}t,_\tau +g_{t\phi}\phi,_\tau \equiv (g_{tt} - g_{t\phi}^2/g_{\phi\phi})t,_\tau = K \tag{5.114}$$

where $2\pi\mu K$ is the total energy of the string. This reduces the first of the gauge constraints, equation (5.109), to

$$(g_{tt} - g_{t\phi}^2/g_{\phi\phi})^{-1} K^2 + g_{\phi\phi} + g_{rr}(r,_\tau)^2 + g_{\theta\theta}(\theta,_\tau)^2 = 0. \tag{5.115}$$

Explicitly in terms of r and θ this equation reads:

$$(r,_\tau)^2 + \Delta(\theta,_\tau)^2 = [(r^2 + a^2)^2 - a^2\Delta \sin^2\theta]\rho^{-4}(K^2 - \Delta\sin^2\theta). \tag{5.116}$$

To close the equations of motion it is necessary to invoke a further equation for either $r,_\tau$ or $\theta,_\tau$. The Kerr metric is known to possess an additional symmetry, reflected in the existence of a Killing–Staeckel tensor which generates a further non-trivial constant of motion, that allows the geodesic equation $\dot{x}^\mu D_\mu \dot{x}^\nu = 0$ to be separated completely [Car77]. Unfortunately, this Killing–Staeckel tensor has only limited value when integrating the cosmic string equations of motion, and it is more convenient to use the θ component of the string equation (5.1) directly, which eventually reduces to the form

$$(\rho^2\theta,_\tau),_\tau +a^2\sin\theta\cos\theta\rho^{-2}K^2$$
$$= \sin\theta\cos\theta[a^2\sin^2\theta(\Delta - 2mr)\rho^{-2} - (r^2 + a^2)] \tag{5.117}$$

and is the generalization to the Kerr metric of equation (5.47).

An alternative form of the equation of motion can be generated by differentiating equation (5.116) and then using (5.117) to eliminate the terms involving $\theta,_{\tau\tau}$. After a considerable amount of algebraic manipulation, this gives the following generalization of the radial acceleration equation (5.50):

$$2\rho^{-2}a^2\sin\theta\cos\theta r,_\tau \theta,_\tau$$
$$= -\Sigma^{-2}(r^2 + a^2)[r^3 - 3mr^2 + a^2(r + m)](\theta,_\tau)^2 r,_{\tau\tau}$$
$$+ \Sigma^{-2}\rho^{-2}a^2[r^3 + 3mr^2 + a^2\cos^2\theta(r - m)](r,_\tau)^2 \sin^2\theta$$
$$+ (r - m)\sin^2\theta + \rho^{-4}a^2(r - m)(r^2 + 2mr + a^2\cos^2\theta)\sin^4\theta. \tag{5.118}$$

In particular, at any point where $r,_\tau = 0$,

$$
\begin{aligned}
r,_{\tau\tau} = & -(r-m)\sin^2\theta - \rho^{-4}a^2(r-m)(r^2+2mr+a^2\cos^2\theta)\sin^4\theta \\
& + \Sigma^{-2}(r^2+a^2)[r^3 - 3mr^2 + a^2(r+m)](\theta,_\tau)^2
\end{aligned}
\tag{5.119}
$$

and since the outer event horizon of a non-extreme Kerr black hole lies outside $r = m$ the effective horizon for circular string solutions occurs when

$$
r^3 - 3mr^2 + a^2(r+m) = 0. \tag{5.120}
$$

That is, the string will inevitably be captured by the hole if it falls inside the surface $r = r^*$, where

$$
r^* = m[1 + 2p^{1/6}\cos(q/3)] \tag{5.121}
$$

with

$$
p = 1 - j^2 + \tfrac{1}{3}j^4 - \tfrac{1}{27}j^6 \tag{5.122}
$$

and

$$
q = \tan^{-1}[j(1 - \tfrac{2}{3}j^2 - \tfrac{1}{27}j^4)^{1/2}/(1 - j^2)] \tag{5.123}
$$

where $j = a/m$. In the non-rotating limit $j = 0$, the standard Schwarzschild result $r^* = 3m$ is recovered; whereas in the extreme Kerr limit $j \to 1$ the radius r^* of the effective horizon tends to $(1 + \sqrt{2})m \approx 2.414m$. For intervening values of j, the effective horizon radius r^* is a monotonically-decreasing function of j.

Other than this (comparatively minor) shrinkage of the effective horizon, the dynamics of ring solutions aligned perpendicular to the spin axis of a Kerr hole is little different from the dynamics of ring solutions outside a Schwarzschild hole.

5.5 Static equilibrium configurations in the Kerr metric

It was seen previously that the Schwarzschild metric admits a simple family of static solutions to the string equation of motion (5.1). It should perhaps not come as a surprise that similar families of solutions exist in any stationary background spacetime, including, of course, the Kerr metric. What is more surprising is that the equations governing static string configurations in the Kerr metric are completely separable and therefore exactly integrable [FSZH89]. Brandon Carter and Valeri Frolov in 1989 described this particular result as 'the latest addition to the long list of what Chandrasekhar ... has referred to as the "miraculous" properties of the Kerr solution, of which the earliest ... was the separability of the simple geodesic Hamilton-Jacobi equation' [CF89].

For present purposes, the line element of a general stationary spacetime will be expressed in the form

$$
ds^2 = g_{tt}\,dt^2 + 2g_{ta}\,dt\,dx^a + g_{ab}\,dx^a\,dx^b \tag{5.124}
$$

where the indices a, b range from 1 to 3, and the metric components are all independent of the timelike coordinate t. In such a case, static equilibrium solutions of the string equation of motion are most naturally constructed by setting

$$x^a = x^a(\sigma) \qquad t,_\tau = 1 \qquad \text{and} \qquad t,_\sigma = -g_{ta}x^a,_\sigma / g_{tt}. \tag{5.125}$$

The gauge conditions (5.2) then reduce to the single constraint

$$(g_{tt}g_{ab} - g_{ta}g_{tb})x^a,_\sigma \, x^b,_\sigma = -g_{tt}^2 \tag{5.126}$$

while the timelike and spacelike components of the equation of motion (5.1) read:

$$-g_{tb}x^b,_{\sigma\sigma} + (g_{tt}\Gamma_{bc}^t - \Gamma_{tbc} + g_{bc}\Gamma_{tt}^t - 2g_{tb}\Gamma_{tc}^t + 2g_{tb}\Gamma_{ttc}/g_{tt})x^b,_\sigma \, x^c,_\sigma = 0 \tag{5.127}$$

and

$$g_{tt}g_{ab}x^b,_{\sigma\sigma} + (g_{tt}\Gamma_{abc} - 2g_{tc}\Gamma_{abt} + g_{bc}\Gamma_{att})x^b,_\sigma \, x^c,_\sigma = 0 \tag{5.128}$$

respectively. Note here that equation (5.127) is just the projection of (5.128) in the direction of g_{tb}.

In principle, all static string solutions can now be generated by introducing explicit expressions for the metric and Christoffel components and integrating the three components of (5.128). However, as was evident in the previous section, the algebra involved in manipulating the Christoffel symbols and related expressions in the Kerr metric is often prohibitive. A much more elegant technique for dealing with equation (5.128) has been developed by Frolov *et al* [FSZH89].

This takes as its starting point the Nambu action (2.10), which in a standard gauge reads:

$$I = -\mu \int [(g_{\mu\nu}x^\mu,_\tau \, x^\nu,_\sigma)^2 - (g_{\kappa\lambda}x^\kappa,_\tau \, x^\lambda,_\tau)(g_{\mu\nu}x^\mu,_\sigma \, x^\nu,_\sigma)]^{1/2} \, d\sigma \, d\tau. \tag{5.129}$$

If it is assumed that $t \equiv x^0 = \tau$ and $x^a = x^a(\sigma)$ then in a stationary background the Nambu action reduces to the one-dimensional action:

$$I = -\mu\tau \int (g_{ta}g_{tb}x^a,_\sigma \, x^b,_\sigma - g_{tt}g_{ab}x^a,_\sigma \, x^b,_\sigma)^{1/2} \, d\sigma \tag{5.130}$$

so the static solutions $x^a = x^a(\sigma)$ are effectively the geodesics of a 3-surface S with the metric

$$h_{ab} = g_{ta}g_{tb} - g_{tt}g_{ab}. \tag{5.131}$$

Now, the gauge choice that led to the reduced action (5.130) is not the same as that appearing in the full equation (5.128), and so, in particular, the spacelike gauge coordinate σ needs to be given different labels to distinguish the two cases. Henceforth I will refer to the reduced-action spacelike gauge coordinate as $\bar\sigma$. If

h_{ab} is positive definite and $\bar{\sigma}$ is normalized so that it corresponds with the measure of proper distance on the 3-surface S then

$$(g_{ta}\,g_{tb} - g_{tt}g_{ab})x^a{}_{,\bar{\sigma}}\,x^b{}_{,\bar{\sigma}} = 1. \tag{5.132}$$

Comparison with the gauge constraint (5.126) indicates that the relationship between σ and $\bar{\sigma}$ is:

$$\mathrm{d}\bar{\sigma} = g_{tt}\,\mathrm{d}\sigma. \tag{5.133}$$

Furthermore, the geodesic equation on S

$$h_{ab}x^b{}_{,\bar{\sigma}\bar{\sigma}} + \bar{\Gamma}_{abc}x^b{}_{,\bar{\sigma}}\,x^c{}_{,\bar{\sigma}} = 0 \tag{5.134}$$

can be reconstructed by adding (5.128) to g_{ta} times (5.127), so the two descriptions are entirely equivalent.

In the Kerr metric, the non-zero components of the 3-metric h_{ab} are:

$$h_{rr} = \Delta^{-1}(\Delta - a^2\sin^2\theta) \tag{5.135}$$
$$h_{\theta\theta} = \Delta - a^2\sin^2\theta \tag{5.136}$$

and

$$h_{\phi\phi} = \Delta\sin^2\theta \tag{5.137}$$

with $\Delta = r^2 - 2mr + a^2$ as before. Although h_{ab} is diagonal, it has a complicated causal structure. Outside the boundary of the ergosphere (where $\Delta = a^2\sin^2\theta$) the coordinates r, θ and ϕ are all spacelike but between the ergosphere boundary and the outer event horizon (i.e. for $0 < \Delta < a^2\sin^2\theta$) both r and θ are timelike. Further signature changes occur inside the outer event horizon.

To allow for the possibility of solutions with $h_{ab}x^a{}_{,\bar{\sigma}}\,x^b{}_{,\bar{\sigma}} < 0$ inside the ergosphere, the normalization condition (5.132) needs to be generalized to read:

$$h_{ab}x^a{}_{,\bar{\sigma}}\,x^b{}_{,\bar{\sigma}} = \kappa \tag{5.138}$$

where $\kappa = 0$ or ± 1. At a physical level, solutions with $\kappa = 0$ or $\kappa = -1$ correspond to static strings with zero or negative gravitational energy, respectively. They are string analogues of the familiar zero- and negative-energy orbits available to trapped massive particles inside the Kerr ergosphere.

Since $h_{ab,\phi} = 0$, the geodesic equation has an immediate first integral:

$$\phi_{,\bar{\sigma}} = \frac{J}{\Delta\sin^2\theta} \tag{5.139}$$

where J is a constant. Substituting this into the normalization condition (5.138) then gives a second integral of the motion:

$$(\Delta - a^2\sin^2\theta)[(r_{,\bar{\sigma}})^2 + \Delta(\theta_{,\bar{\sigma}})^2] = \kappa\Delta - \frac{J^2}{\sin^2\theta}. \tag{5.140}$$

One of the remarkable features of the Kerr metric alluded to earlier is that the geodesic equation describing static string equilibria possesses a third integral of the motion, which is reflected in the existence of a Killing–Staeckel tensor for the 3-metric h_{ab} [FSZH89]. A Killing–Staeckel tensor is a tensor field ξ_{ab} with the property that $\nabla_{(a}\xi_{bc)} = 0$, where the round brackets indicate symmetrization over all three indices. Given any Killing–Staeckel tensor ξ_{ab} the quadratic form $\xi_{ab}x^a,_{\bar\sigma}\,x^b,_{\bar\sigma}$ is a constant of the corresponding geodesic equations. In the case of the 3-metric (5.135)–(5.137), the required Killing–Staeckel tensor has the mixed components:

$$\xi_b^a = \text{diag}(a^2 \sin^2\theta,\, \Delta,\, \Delta + a^2 \sin^2\theta) \tag{5.141}$$

and so the third integral of the motion reads:

$$(\Delta - a^2 \sin^2\theta)[a^2 \sin^2\theta(r,_{\bar\sigma})^2 + \Delta^2(\theta,_{\bar\sigma})^2] = q\Delta - (\Delta + a^2 \sin^2\theta)\frac{J^2}{\sin^2\theta} \tag{5.142}$$

where q is a constant.

Solving equations (5.140) and (5.142) simultaneously for $r,_{\bar\sigma}$ and $\theta,_{\bar\sigma}$ then gives

$$(r,_{\bar\sigma})^2 = (\Delta - a^2 \sin^2\theta)^{-2}\Re(r) \tag{5.143}$$

and

$$(\theta,_{\bar\sigma})^2 = (\Delta - a^2 \sin^2\theta)^{-2}\Theta(\theta) \tag{5.144}$$

where

$$\Re(r) = \kappa\Delta^2 - q\Delta + a^2 J^2 \tag{5.145}$$

and

$$\Theta(\theta) = q - \kappa a^2 \sin^2\theta - J^2/\sin^2\theta. \tag{5.146}$$

It is evident from (5.143) and (5.144) that the equation for $r(\theta)$ separates completely:

$$\Re^{-1/2}\mathrm{d}r = \pm\Theta^{-1/2}\,\mathrm{d}\theta. \tag{5.147}$$

Furthermore, the equation for ϕ also separates, as (5.139) can be rewritten as

$$\phi,_{\bar\sigma} \equiv J\left[\frac{1}{\sin^2\theta(\Delta - a^2 \sin^2\theta)} - \frac{a^2}{\Delta(\Delta - a^2 \sin^2\theta)}\right]$$

$$= J\left[\frac{\pm\theta,_{\bar\sigma}}{\sin^2\theta\Theta^{1/2}} - \frac{\pm r,_{\bar\sigma}}{\Delta\Re^{1/2}}\right] \tag{5.148}$$

The full solution is therefore expressible, in principle, in terms of elliptic integrals.

One simple family of solutions, again due to Frolov *et al* [FSZH89], is found by fixing the value θ_0 of the co-latitude angle θ and setting $\kappa = 1$, $J^2 = a^2 \sin^4\theta_0$ and $q = 2a^2 \sin^2\theta_0$. Then $\Theta(\theta_0) = \Theta'(\theta_0) = 0$ and the geodesic equation for θ is automatically satisfied when the string lies wholly within the cone-like surface

$\theta = \theta_0$. Furthermore, $\Re(r) = (\Delta - a^2 \sin^2 \theta_0)^2$ and thus (5.143) gives $r = \pm \overline{\sigma}$, while (5.139) reduces to

$$\frac{d\phi}{dr} = \pm \frac{a}{r^2 - 2mr + a^2}. \tag{5.149}$$

Hence, if $0 < a^2 < m^2$,

$$\phi(r) = \phi_0 \pm \tfrac{1}{2} a(m^2 - a^2)^{-1/2} \ln\left(\frac{r - r_-}{r - r_+}\right) \tag{5.150}$$

where ϕ_0 is the asymptotic value of ϕ in the limit as $r \to \infty$, and $r_\pm = m \pm (m^2 - a^2)^{1/2}$ are the radii of the outer and inner event horizons. The string, therefore, spirals in towards the outer event horizon at $r = r_+$ but never quite reaches it. In the extreme Kerr metric (for which $a^2 = m^2$) the string traces out the Archimedean spiral $\phi(r) = \phi_0 \pm m/(r - m)$.

In general, any solution with $\theta = \theta_0$ must have positive energy, as it is not possible to choose J so that $\Theta'(\theta_0) = 0$ when $\kappa \leq 0$. The only exceptions occur in the equatorial plane. It is evident from (5.146) that if $\sin \theta_0 = 1$ then $\Theta(\theta_0) = \Theta'(\theta_0) = 0$ whenever $q = \kappa a^2 + J^2$ but there is no further constraint on the value of J^2/a^2. Thus, equatorial solutions possess an extra degree of freedom that is otherwise absent when $\theta_0 \neq \pi/2$, and, in principle, can have zero or negative energies in the ergosphere.

In the case of a static equilibrium configuration confined to the equatorial plane, the functional form of $\Re$ is:

$$\Re(r) = (\Delta - a^2)(\kappa \Delta - J^2) \tag{5.151}$$

and so (5.139) and (5.143) can be combined to give

$$\frac{d\phi}{dr} = \pm \Delta^{-1} \left(\frac{r^2 - 2mr}{\Delta \kappa / J^2 - 1}\right)^{1/2}. \tag{5.152}$$

Here, $\Delta = r^2 - 2mr + a^2$ is positive everywhere outside the outer event horizon, while $r^2 - 2mr$ is positive outside the ergosphere boundary (at $r = 2m$) and negative inside it. If $\kappa \neq 0$ the remaining term, $\Delta \kappa / J^2 - 1$, has zeroes at $r = m \pm (m^2 - a^2 + J^2/\kappa)^{1/2}$. Only if $\kappa = 1$ does the larger zero lie outside the outer event horizon, and then it lies outside the ergosphere boundary if $J^2 > a^2$ and inside the ergosphere if $J^2 < a^2$. In what follows, I will refer to the larger zero as r_{turn}. In all cases the smaller zero (if real and positive) is located inside the horizon.

The possible static equilibrium solutions in the equatorial plane can therefore be classified as follows (refer to figure 5.16 for illustrative examples). If $\kappa = 1$ and $J^2 < a^2$ solutions exist with $r \geq 2m$ and with $r_+ < r \leq r_{\text{turn}}$. In solutions with $r \geq 2m$, $d\phi/dr$ goes to zero like $(r - 2m)^{1/2}$ near $r = 2m$, and so

$r - 2m$ scales as $(\phi - \phi_e)^{2/3}$, where ϕ_e is the value of ϕ where the string touches the ergosphere boundary. The solution, therefore, has a cusplike feature on the ergosphere boundary but quickly asymptotes to a pair of radial lines, with the angle between the asymptotes increasing monotonically from 0 to $b \ln(r_+/r_-)$ as $|J|$ varies from 0 to $|a|$, where $b = |a|(m^2 - a^2)^{-1/2}$. (The maximum separation angle $b \ln(r_+/r_-)$ is zero when $a = 0$, and peaks at 2 radians in the extreme Kerr limit $|a| = m$.)

The second type of solution, which is confined to the ergosphere, passes smoothly through its point of maximum radius at $r = r_{\text{turn}}$ and spirals an infinite number of times in towards the outer event horizon, in both the clockwise and anti-clockwise directions. In the limit as $|J| \to 0$ the ergosphere solution vanishes, while the outer solution degenerates into a doubled straight line terminating at $r = 2m$. Solutions with $J^2 < a^2$ have no analogues in the Schwarzschild case.

If $\kappa = 1$ and $J^2 = a^2$, then the solution is just the equatorial member of the family of cone-embedded equilibria (5.150) examined earlier. Here, $r_{\text{turn}} = 2m$ and there is no singularity or turning point in $d\phi/dr$ at the ergosphere boundary. The string, therefore, passes smoothly through the ergosphere boundary and (if $a \neq 0$) spirals around the outer event horizon. In the Schwarzschild case, the corresponding solution is a straight string which terminates at the horizon.

If $\kappa = 1$ and $J^2 > a^2$, there are again separate inner and outer solutions. The outer solution has a smooth radial turning point at $r = r_{\text{turn}}$ and asymptotes to a pair of radial lines. The minimum radius r_{turn} ranges from $2m$ to ∞ and the separation angle of the asymptotes increases monotonically from $b \ln(r_+/r_-)$ to π^- as $|J|$ increases without bound. The ergosphere solution spirals around the outer event horizon (in both directions) in the usual manner but has a cusplike feature at the ergosphere boundary.
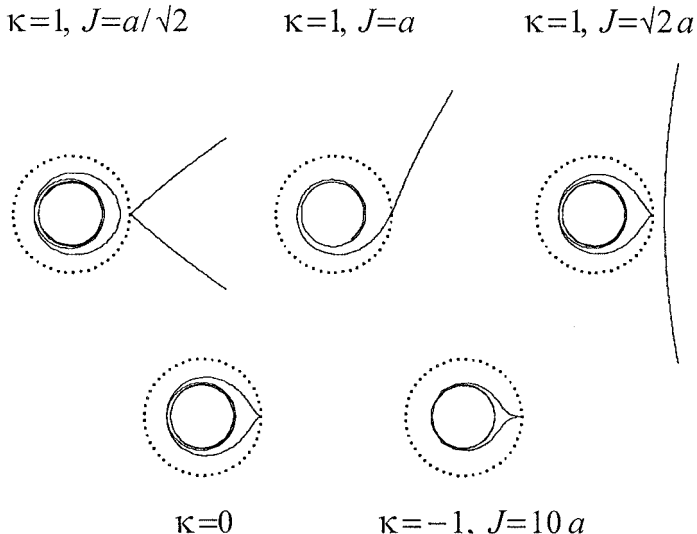
The case $\kappa = 0$ is mathematically equivalent to the limit $|J| \to \infty$. There is no solution outside the ergosphere, while the inner solution spirals inwards from a cusplike feature at the ergosphere boundary. This is one of the few cases where the analytic expression for ϕ is reasonably tractable. If $a^2 < m^2$ then

$$\pm[\phi(r) - \phi_e] = \cos^{-1}\left(\frac{r}{m} - 1\right)$$
$$+ \frac{j}{(1 - j^2)^{1/2}} \ln \left| \frac{(1+j)(r-m)+(m-\sqrt{2mr-r^2})\sqrt{1-j^2}}{(1+j)(r-m)-(m-\sqrt{2mr-r^2})\sqrt{1-j^2}} \right|^{1/2}$$
$$- \frac{j}{(1 - j^2)^{1/2}} \ln \left| \frac{(1-j)(r-m)+(m-\sqrt{2mr-r^2})\sqrt{1-j^2}}{(1-j)(r-m)-(m-\sqrt{2mr-r^2})\sqrt{1-j^2}} \right|^{1/2}$$

$$(5.153)$$

with $j = a/m$, while in the extreme Kerr metric

$$\pm[\phi(r) - \phi_e] = \cos^{-1}\left(\frac{r}{m} - 1\right) - \frac{(2mr - r^2)^{1/2}}{r - m}. \qquad (5.154)$$

Finally, if $\kappa = -1$ there is again no solution outside the ergosphere, while

$\kappa=1,\ J=a/\sqrt{2}$ $\kappa=1,\ J=a$ $\kappa=1,\ J=\sqrt{2}\,a$

$\kappa=0$ $\kappa=-1,\ J=10\,a$

Figure 5.16. Five examples of static equilibrium solutions in the extreme Kerr metric.

the ergosphere solution is qualitatively similar to the corresponding solution for $\kappa = 0$. The similarity between the $\kappa = -1$ and $\kappa = 0$ solutions is most pronounced at large values of $|J|$ but as $|J|$ decreases the cusplike feature at the ergsophere boundary sharpens in the $\kappa = -1$ solution, and the spirals become more tightly bound. In the limit as $|J| \to 0$ the solution degenerates into a doubled straight line stretching from the outer event horizon to the ergosphere boundary.

Figure 5.16 illustrates the sequence of equilibrium solutions described earlier in the case of the extreme Kerr metric ($a = m$). The solutions are plotted for five separate combinations of the parameters κ and J, with r the polar radius and ϕ the polar angle. In each frame the ergosphere boundary is shown as a dotted circle at $r = 2m$, while the outer event horizon at $r = r_+ = m$ is the limit set of the spirals. The extreme Kerr metric has been chosen because it has the largest possible ergosphere and so the salient features of the solutions can be seen most clearly. At smaller values of the spin parameter $|a|$ the distance between the ergosphere boundary and the outer event horizon contracts, and the spirals become more tightly bound; and, of course, the spirals disappear altogether in the limit as $|a| \to 0$.

Although the analysis here has been concerned almost exclusively with the Kerr metric, it is easily extended to other stationary background spacetimes with similar separability properties. Published examples include studies of string equilibria in the Kerr–Newman metric (which describes a charged rotating black hole) [FSZH89], the Kerr–de Sitter metric (which couples a Kerr black hole to

a cosmological constant) [CF89], and the NUT–Kerr–Newman spacetime (which describes a Kerr–Newman black hole immersed in an anisotropic cosmological background) [AB93]. In all cases the equilibrium solutions are qualitatively similar to the Kerr equilibria.

5.6 Strings in plane-fronted-wave spacetimes

A final example of a background metric in which string dynamics has been systematically examined is the general plane-fronted-wave (or *pp-wave*) spacetime, which has the line element:

$$ds^2 = du\, dv - dx^2 - dy^2 + F(u, x, y)\, du^2 \qquad (5.155)$$

where F is an arbitrary twice-differentiable function of its arguments. The coordinate v is null, and if $F \equiv 0$ the line element reduces to the standard Minkowski form with $u = t - z$ and $v = t + z$. When $F \neq 0$ the metric describes a train of gravitational waves with wavefronts parallel to the $x-y$ plane propagating up the z-axis. It can be shown that the pp-wave spacetime is a solution to the vacuum Einstein equations if and only if $F_{,xx} + F_{,yy} = 0$ but this constraint will not be imposed here.

Since the only non-zero components of the Christoffel symbol (modulo symmetries) are

$$\Gamma^x_{uu} = \tfrac{1}{2}F_{,x} \qquad \Gamma^y_{uu} = \tfrac{1}{2}F_{,y} \qquad \text{and} \qquad \Gamma^v_{u\mu} = F_{,\mu} \qquad (5.156)$$

the null vector field $k_\mu = D_\mu u$ is covariantly constant (that is, $D_\lambda k_\mu = 0$), and, in particular, k_μ is a Killing field. With $X^\mu = (u, v, x, y)$ denoting the position vector of a general string, the corresponding conservation equation (2.43) reads:

$$u_{,\tau\tau} = u_{,\sigma\sigma} \qquad (5.157)$$

and so the null coordinate u can be expressed as a sum of left- and right-moving modes.

Provided that u does contain modes of both types, the residual gauge freedom can be removed by setting $\tau = u$, in the same way that τ can be aligned with t in Minkowski spacetime (see section 3.1). The gauge choice $\tau = u$, which was first suggested by Gary Horowitz and Alan Steif [HS90], effectively extends the GGRT gauge of section 3.2 from the Minkowski metric to the pp-wave spacetime, and shares all the drawbacks of the GGRT gauge. In particular, as will be seen shortly, it misses a simple family of travelling-wave solutions.

With $\mathbf{r} = [x, y]$ and $\nabla = \partial/\partial\mathbf{r}$, the remaining components of the equation of motion in the GGRT gauge become

$$v_{,\tau\tau} - v_{,\sigma\sigma} + F_{,u} + 2\mathbf{r}_{,\tau} \cdot \nabla F = 0 \qquad (5.158)$$

and

$$\mathbf{r}_{,\tau\tau} - \mathbf{r}_{,\sigma\sigma} + \tfrac{1}{2}\nabla F = \mathbf{0}. \tag{5.159}$$

Two immediate first integrals are the gauge constraints $X_\tau^2 + X_\sigma^2 = 0$ and $X_\tau \cdot X_\sigma = 0$, which read:

$$v_{,\tau} = \mathbf{r}_{,\tau}^2 + \mathbf{r}_{,\sigma}^2 - F \qquad \text{and} \qquad v_{,\sigma} = 2\mathbf{r}_{,\tau} \cdot \mathbf{r}_{,\sigma} \tag{5.160}$$

respectively.   Since F is a function of τ and $\mathbf{r}$ only, (5.159) is a closed inhomogeneous wave equation which is typically nonlinear in $\mathbf{r}$. Once $\mathbf{r}(\tau, \sigma)$ is known, equations (5.160) can be integrated directly to give v.

    To proceed any further, it is necessary to first give a tighter prescription for the function F. Since F can always be removed by a coordinate transformation if it is linear in $\mathbf{r}$, the simplest non-trivial assumption is that F is a quadratic functional of x and y, so that

$$F(u, \mathbf{r}) = f(u)\mathbf{r}\mathbf{M}\mathbf{r}^{\mathrm{T}} \tag{5.161}$$

where $\mathbf{M}$ is a constant 2×2 symmetric matrix. The corresponding metric is called an *exact plane-wave* spacetime, and is a solution of the vacuum Einstein equations if $\mathrm{Tr}\,\mathbf{M} = 0$.

    The wave equation (5.159) for $\mathbf{r}$ can now be written as a pair of decoupled linear equations:

$$(\mathbf{e}_k \cdot \mathbf{r})_{,\tau\tau} - (\mathbf{e}_k \cdot \mathbf{r})_{,\sigma\sigma} + \lambda_k f(\tau)\mathbf{e}_k \cdot \mathbf{r} = 0 \qquad (k = 1, 2) \tag{5.162}$$

where $\mathbf{e}_1$ and $\mathbf{e}_2$ are orthonormal eigenvectors of $\mathbf{M}$, and λ_1 and λ_2 are the corresponding eigenvalues. If $\mathbf{e}_k \cdot \mathbf{r}$ is further decomposed as a sum of harmonic modes in σ:

$$\mathbf{e}_k \cdot \mathbf{r} = \sum_\omega R_k^{(\omega)}(\tau)e^{\mathrm{i}\omega\sigma} \tag{5.163}$$

then each of the mode functions $R_k^{(\omega)}$ satisfies the time-dependent oscillator equation [HS90]:

$$R_k^{(\omega)\prime\prime} + [\omega^2 + \lambda_k f(\tau)]R_k^{(\omega)} = 0. \tag{5.164}$$

    One simple situation in which (5.164) is tractable occurs when the gravitational wavefront is impulsive, so that $f(u) = f_0\delta(u)$ for some constant f_0. Then, for modes with $\omega \neq 0$,

$$R_k^{(\omega)}(\tau) = A_k(\omega)\cos(\omega\tau) + [B_k(\omega) - \omega^{-1}f_0\lambda_k A_k(\omega)H(\tau)]\sin(\omega\tau) \tag{5.165}$$

where A_k and B_k are arbitrary functions, and H is the Heaviside step function. The corresponding zero-mode solutions are

$$R_k^{(0)} = A_k + [B_k - f_0\lambda_k A_k H(\tau)]\tau. \tag{5.166}$$

In general, whatever the form of the mode functions, the equations (5.160) for v can be integrated to give:

$$v(\tau, \sigma) = 2 \sum_{k=1}^{2} \sum_{\omega, \varpi \neq -\omega} \frac{\varpi}{\omega + \varpi} R_k^{(\omega)'}(\tau) R_k^{(\varpi)}(\tau) e^{i(\omega + \varpi)\sigma}$$

$$- 2i\sigma \sum_{k=1}^{2} \sum_{\omega \neq 0} \omega R_k^{(\omega)'}(\tau) R_k^{(-\omega)}(\tau) + \sum_{k=1}^{2} R_k^{(0)'}(\tau) R_k^{(0)}(\tau).$$

$$(5.167)$$

Note however that if the wavefront is impulsive then the presence of F on the right-hand side of the source equation for $v,_\tau$ in (5.160) ensures that v is a discontinuous function of τ. This should come as no surprise, as the geodesics of the impulsive exact pp-wave spacetime are also known to be discontinuous [HS90], and the physical status of the spacetime is accordingly very uncertain.

In view of the geometry of the pp-wave spacetimes, it is natural to ask whether solutions exist which describe travelling waves propagating along a string in tandem with the plane-fronted gravitational waves. In a solution of this type the null coordinate u must be a function of σ_- (or σ_+) alone, and the GGRT gauge choice $\tau = u$ is unavailable. With u a function of σ_- the light-cone gauge conditions read:

$$X_+^2 = -|\mathbf{r},_+|^2 = 0 \qquad \text{and} \qquad X_-^2 = Fu'^2 + u'v,_- -|\mathbf{r},_-|^2 = 0 \quad (5.168)$$

and so $\mathbf{r}$ and $v,_-$ are also functions of σ_- only.

The remaining component of the equation of motion, $v,_{+-} = 0$, imposes no further constraints. Thus v is a sum of separate functions of σ_+ and σ_-, and for ease of comparison with the travelling-wave solutions of section 4.1.2 the gauge coordinates can be fixed so that

$$v(\sigma_+, \sigma_-) = \sigma_+ + z_-(\sigma_-) \qquad \text{and} \qquad u(\sigma_-) = \sigma_- - z_-(\sigma_-) \qquad (5.169)$$

for some function z_-. The second of the gauge conditions (5.168) then indicates that

$$z_-'(\sigma_-) = \frac{1 - 2F}{2(1 - F)} \pm \frac{1}{2(1 - F)} \sqrt{1 - 4(1 - F)|\mathbf{r}'|^2}. \qquad (5.170)$$

It is, therefore, evident that—like travelling waves in Minkowski spacetime—a travelling wave co-moving with a pp-wave can be either shallow or steep, and if $F < 1$ its planar projection $\mathbf{r}(\sigma_-)$ must satisfy the constraint $|\mathbf{r}'| \leq \frac{1}{2}(1 - F)^{-1/2}$.

However, because F is a functional of u and so of z_-, integrating (5.170) is, in general, very problematic. A more convenient gauge choice is $u = \sigma_-$, which allows the second of the gauge conditions (5.168) to be integrated directly to give

$$v(\sigma_+, \sigma_-) = \sigma_+ + \int_0^{\sigma_-} [|\mathbf{r}'(u)|^2 - F(u, \mathbf{r}(u))] \, du. \qquad (5.171)$$

In this gauge the planar projection $\mathbf{r}(\sigma_-)$ of the travelling wave can be any arbitrary differentiable curve. The corresponding string, of course, has a fixed pattern shape which propagates normal to the gravitational wavefronts at the speed of light, and since the element of proper distance induced on the world sheet is $\mathrm{d}s^2 = \mathrm{d}\sigma_+\,\mathrm{d}\sigma_-$ the world sheet is geometrically flat. The presence of the gravitational waves has no material effect on the travelling wave because the Riemann tidal force $R_{\kappa\lambda\mu\nu}X_\sigma^\kappa X_\tau^\lambda X_\sigma^\mu X_\tau^\nu$ on small segments of the string is identically zero, a feature not shared by disturbances propagating with any other speed or in any other direction.

Chapter 6

Cosmic strings in the weak-field approximation

A cosmic string, like any other concentration of mass and energy, acts as the source of a gravitational field. Because cosmic strings are extended objects, this gravitational field will affect not only the motion of nearby particles but also the trajectory of the string itself, and so calculating the gravitational field of even an isolated cosmic string in otherwise empty space can pose a complicated nonlinear problem. Nonetheless the gravitational field should not simply be ignored, as there are indications that it can have important effects on the dynamics and energetics of strings. For example, gravitational radiation is thought to be the dominant energy-loss mechanism for loops [Vil85], while it has been suggested that the radiation of momentum from an asymmetric loop could accelerate the loop to relativistic bulk velocities, giving rise to a so-called 'gravitational rocket effect' [VV85].

As was seen in section 2.4, the two-dimensional relativistic sheet that traces out the history of a zero-thickness string is characterized by a distributional stress–energy tensor of the form

$$T^{\mu\nu}(x) = \mu g^{-\frac{1}{2}} \int \gamma^{\frac{1}{2}} \gamma^{AB} X^{\mu}{}_{,A} \, X^{\nu}{}_{,B} \, \delta^4(x - X) \, \mathrm{d}^2\zeta \qquad (6.1)$$

where $x^{\mu} = X^{\mu}(\zeta^A)$ is the parametric equation of the world sheet and $\gamma_{AB} = g_{\mu\nu} X^{\mu}{}_{,A} X^{\nu}{}_{,B}$ is the induced 2-metric. It is the localized nature of $T^{\mu\nu}$ that is the most useful feature of the wire approximation, as it reduces the problem to one of solving only the *vacuum* Einstein equations outside the world sheet. Nonetheless, self-consistent solutions in which the world sheet satisfies the equation of motion imposed by its own gravitational field are still difficult to generate, and have to date been found only in cases with special symmetries. A common device is, therefore, to fix the trajectory of the world sheet in advance—usually by prescribing a solution to the flat-space equation of motion—and then calculate the resulting gravitational field.

The exact spacetime metric generated by an infinite *straight* string in the wire approximation will be examined in detail in chapter 7. One of its most striking features is that it is flat everywhere except on the world sheet of the string. This result should not be interpreted as implying that a straight cosmic string has no detectable gravitational field at all, as the presence of the string induces non-tidal spacetime distortions which can focus geodesics and cause gravitational lensing of the light from distant objects. In addition, any gravitating body passing close to a straight string would experience a self-gravitational acceleration of order $\mu m/r^2$ in the direction of the string, where m is the mass of the body and r the distance to the string (see section 7.6).

At a physical level, the absence of a gravitational field outside an isolated straight cosmic string is due to the invariance of the corresponding stress–energy tensor with respect to boosts along the string, a feature that is explored in more detail in section 7.2. By the same token, it is to be expected that a non-straight string would break this boost-invariance and generate a non-trivial exterior field. This is indeed what happens, although if the mass per unit length μ of the string is very much smaller than 1 (in Planck units) the exterior metric remains very nearly Minkowskian unless the local curvature of the world sheet is large. This fact makes the weak-field approximation an ideal tool for modelling the gravitational field outside realistic string configurations.

6.1 The weak-field formalism

In the weak-field approximation, the metric tensor

$$g_{\mu\nu} = \eta_{\mu\nu} + h_{\mu\nu} \tag{6.2}$$

is assumed to deviate from the Minkowski tensor $\eta_{\mu\nu} = \text{diag}(1, -1, -1, -1)$ by a perturbation $h_{\mu\nu}$ whose components are small in absolute value compared to 1. To linear order in $h_{\mu\nu}$ the Ricci tensor is

$$R_{\mu\nu} \approx \tfrac{1}{2}(\Box h_{\mu\nu} + h_{,\mu\nu} - h^{\lambda}_{\mu,\nu\lambda} - h^{\lambda}_{\nu,\mu\lambda}) \tag{6.3}$$

where, as previously, $\Box \equiv \partial_t^2 - \nabla^2$ is the flat-space d'Alembertian, h denotes h^{λ}_{λ}, and all indices are raised and lowered using $\eta_{\mu\nu}$.

If $h_{\mu\nu}$ is constrained to satisfy the harmonic gauge conditions $h^{\lambda}_{\mu,\lambda} = \tfrac{1}{2}h_{,\mu}$ then

$$R_{\mu\nu} \approx \tfrac{1}{2}\Box h_{\mu\nu} \tag{6.4}$$

and the Einstein equation $G_{\mu\nu} \equiv R_{\mu\nu} - \tfrac{1}{2}g_{\mu\nu}R = -8\pi T_{\mu\nu}$ becomes, to leading order,

$$\Box h_{\mu\nu} = -16\pi(T_{\mu\nu} - \tfrac{1}{2}\eta_{\mu\nu}T) \tag{6.5}$$

where $T_{\mu\nu}$ is the stress–energy tensor of the source, evaluated with $g_{\mu\nu} = \eta_{\mu\nu}$.

The standard retarded solution to equation (6.5) is

$$h_{\mu\nu}(t, \mathbf{x}) = -4 \int \frac{S_{\mu\nu}(t', \mathbf{x}')}{|\mathbf{x} - \mathbf{x}'|} \, d^3 x' \tag{6.6}$$

where $S_{\mu\nu} = T_{\mu\nu} - \frac{1}{2}\eta_{\mu\nu}T$ and t' denotes the retarded time $t - |\mathbf{x} - \mathbf{x}'|$. In physical terms, the source points $[t', \mathbf{x}']$ in the integral on the right of (6.6) range over all points on the past light cone of the field point $[t, \mathbf{x}]$ at which $S_{\mu\nu}$ is non-zero.

In the case of a cosmic string, the equation of the source (the world sheet) can be expressed in the form $x'^{\mu} = X^{\mu}(\tau, \sigma) = [\tau, \mathbf{r}(\tau, \sigma)]$, in keeping with the notation of section 3.3 for the aligned standard gauge in Minkowski spacetime. The stress–energy tensor (6.1) of the world sheet then reduces to

$$T_{\mu\nu}(t', \mathbf{x}') = \mu \int (V_{\mu}V_{\nu} - N_{\mu}N_{\nu}) \, \delta^{(3)}(\mathbf{x}' - \mathbf{r}(t', \sigma)) \, d\sigma \tag{6.7}$$

where $V^{\mu} = [1, \mathbf{r}_{\tau}]$, $N^{\mu} = [0, \mathbf{r}_{\sigma}]$, and it is understood that the retarded time t' and the parametric time τ are identical. Thus, the source term in (6.6) becomes

$$S_{\mu\nu}(t', \mathbf{x}') = \mu \int \Psi_{\mu\nu}(t', \sigma) \, \delta^{(3)}(\mathbf{x}' - \mathbf{r}(t', \sigma)) \, d\sigma \tag{6.8}$$

where

$$\Psi_{\mu\nu} = V_{\mu}V_{\nu} - N_{\mu}N_{\nu} - \frac{1}{2}\eta_{\mu\nu}(V^2 - N^2). \tag{6.9}$$

When (6.8) is substituted into the equation (6.6) for $h_{\mu\nu}$ the integration over d^3x' can be performed by first transforming from $\mathbf{x}'$ to $\mathbf{x}'' = \mathbf{x}' - \mathbf{r}(t', \sigma)$. The Jacobian of this transformation is:

$$|\partial\mathbf{x}'/\partial\mathbf{x}''| = |\partial\mathbf{x}''/\partial\mathbf{x}'|^{-1} = |1 - \mathbf{n}' \cdot \mathbf{r}_{\tau}(t', \sigma)|^{-1} \tag{6.10}$$

where $\mathbf{n}' = (\mathbf{x} - \mathbf{x}')/|\mathbf{x} - \mathbf{x}'|$ and so the solution to the weak-field equations becomes
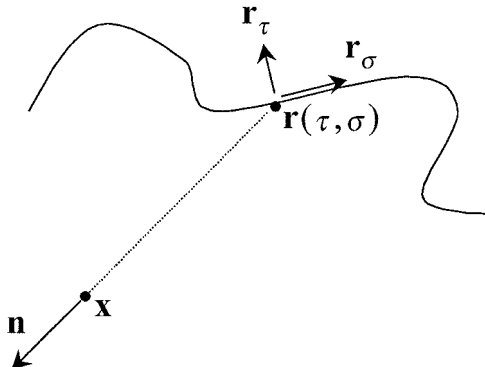
$$h_{\mu\nu}(t, \mathbf{x}) = -4\mu \int \frac{\Psi_{\mu\nu}(\tau, \sigma)}{|\mathbf{x} - \mathbf{r}(\tau, \sigma)|}[1 - \mathbf{n} \cdot \mathbf{r}_{\tau}(\tau, \sigma)]^{-1} \, d\sigma \tag{6.11}$$

where $\mathbf{n} = (\mathbf{x} - \mathbf{r}(\tau, \sigma))/|\mathbf{x} - \mathbf{r}(\tau, \sigma)|$ denotes the unit vector in the direction from the source point $\mathbf{r}$ to the field point $\mathbf{x}$ (see figure 6.1) and the parametric time τ is given implicitly by

$$\tau = t - |\mathbf{x} - \mathbf{r}(\tau, \sigma)|. \tag{6.12}$$

Equation (6.11), which expresses the gravitational field explicitly in terms of a line integral over the world sheet, was first derived by Neil Turok in 1984 [Tur84].

Turok has named the term $(1 - \mathbf{n} \cdot \mathbf{r}_{\tau})^{-1}$ in (6.11) the *beaming factor*. It diverges if the world sheet contains a cusp (where $|\mathbf{r}_{\tau}| = 1$) and the field point $\mathbf{x}$ lies on the future light cone of the cusp in the direction of $\mathbf{r}_{\tau}$. Thus, at the level of the weak-field approximation, a cusp emits a thin beam of gravitational energy in

Figure 6.1. Source and field points in weak-field calculations.

the direction of its own motion, much as a transonic aircraft emits a sonic boom. A more detailed treatment of the weak-field gravitational effects near a cusp will be given in section 6.2. Equation (6.11) also predicts non-trivial gravitational effects in the neighbourhood of a kink, as will be discussed in section 6.3.

Another notable feature of equation (6.11) is that if the source is a periodic loop then its time-averaged gravitational field is a Newtonian one to first order [Tur84]. To see this, suppose that the motion of the string is periodic with period T. Then the time average of $h_{\mu\nu}$ over one oscillation is

$$\langle h_{\mu\nu}\rangle(\mathbf{x}) = -\frac{4\mu}{T}\int_0^T\int_0^L \frac{\Psi_{\mu\nu}(\tau,\sigma)}{|\mathbf{x}-\mathbf{r}(\tau,\sigma)|}[1-\mathbf{n}\cdot\mathbf{r}_\tau(\tau,\sigma)]^{-1}\,\mathrm{d}\sigma\,\mathrm{d}t \qquad (6.13)$$

where, in view of (6.12), $\mathrm{d}t = (1-\mathbf{n}\cdot\mathbf{r}_\tau)\,\mathrm{d}\tau$. Also, the retarded time τ clearly changes by an amount T as t varies from 0 to T. Hence, the time-averaged metric perturbation is

$$\langle h_{\mu\nu}\rangle(\mathbf{x}) = -\frac{4\mu}{T}\int_0^T\int_0^L \frac{\Psi_{\mu\nu}(\tau,\sigma)}{|\mathbf{x}-\mathbf{r}(\tau,\sigma)|}\,\mathrm{d}\sigma\,\mathrm{d}\tau. \qquad (6.14)$$

In the weak-field approximation a non-relativistic particle experiences a gravitational acceleration with spatial components

$$a^i = \frac{\partial}{\partial t}h_{it} - \frac{1}{2}\frac{\partial}{\partial x^i}h_{tt}. \qquad (6.15)$$

In view of the periodicity of the metric perturbations $h_{\mu\nu}$, the first term on the right of this expression vanishes after time-averaging, and the time-averaged acceleration becomes

$$\langle a^i\rangle = -\frac{1}{2}\frac{\partial}{\partial x^i}\langle h_{tt}\rangle = \frac{2\mu}{T}\frac{\partial}{\partial x^i}\int_0^T\int_0^L \frac{\Psi_{tt}(\tau,\sigma)}{|\mathbf{x}-\mathbf{r}(\tau,\sigma)|}\,\mathrm{d}\sigma\,\mathrm{d}\tau \qquad (6.16)$$

where, for a Nambu–Goto string, $\Psi_{tt} = \mathbf{r}_\tau^2$. Thus, the time-averaged acceleration at a fixed point in space is the same as that produced by a mass distribution confined to the surface $\mathbf{r} = \mathbf{r}(\tau, \sigma)$ traced out by the string, with local surface density $2\mu\mathbf{r}_\tau^2$. It was seen in section 3.3 that the period mean of $\mathbf{r}_\tau^2$ is equal to $\frac{1}{2}$ in the string's centre-of-momentum frame. The total mass of this surface is therefore just the mass μL of the string, and, in particular, the time-averaged gravitational force exerted by a string loop on a distant particle is the same as that due to a point particle with mass μL located at the loop's centre of mass.

The effect of the linearized gravitational field (6.11) on the motion of particles close to a string loop has been examined in numerical simulations run by Tanmay Vachaspati [Vac87]. Vachaspati numerically integrated the equations of motion corresponding to the acceleration vector (6.15) for a distribution of test particles around a string with the trajectory

$$\mathbf{r}(\tau, \sigma) = \frac{L}{4\pi}[-\sin(2\pi\sigma_-/L), \tfrac{1}{2}\sin(4\pi\sigma_+/L), \cos(2\pi\sigma_-/L)$$
$$+ \tfrac{1}{2}\cos(4\pi\sigma_+/L)] \tag{6.17}$$

where $\sigma_\pm = \tau \pm \sigma$ as before. This trajectory is a member of the family of non-planar p/q harmonic solutions described in section 4.4.2, with $p = 2, q = 1$ and $\psi = \pi/2$ (although the coordinate frame has been rotated $90°$ about the y-axis). It is non-intersecting, has period $L/2$ and supports two cusps which appear on the equatorial plane, one at $\mathbf{r} = \frac{L}{4\pi}[-1, \tfrac{1}{2}, 0]$ at $\tau = 3L/16$ and the second at the diametrically opposite point at $\tau = 5L/16$. The first cusp moves in the negative z-direction, and the second in the positive z-direction.

Vachaspati discovered three interesting features of the linearized field of this loop. The first is that there is a weak gravitational attraction to the surface traced out by the world sheet, which is not surprising. The second feature, which is more specific to cosmic strings, is a powerful repulsive gravitational force on those test particles which happen to pass immediately in front of the cusps. The third feature, which became evident towards the end of Vachaspati's simulation, is that there is an accumulation of test particles immediately behind the points where the cusps appear. The cusps therefore generate a highly anisotropic field, consisting of an intense but narrow repulsive beam in the forward direction and a strong attractive force (relative to other parts of the world sheet) elsewhere.

6.2 Cusps in the weak-field approximation

The behaviour of the metric perturbation $h_{\mu\nu}$ near a *generic* cusp is essentially no different from that observed by Vachaspati in his numerical simulation. To see this, suppose without loss of generality that the cusp lies at $\tau = \sigma = 0$. The position vector $\mathbf{r} = \frac{1}{2}(\mathbf{a} + \mathbf{b})$ of the source points near the cusp then has the parametric form:

$$\mathbf{r}(\tau, \sigma) \approx \mathbf{r}_c + \mathbf{v}_c\tau + \tfrac{1}{4}(\mathbf{a}_c''\sigma_+^2 + \mathbf{b}_c''\sigma_-^2) + \tfrac{1}{12}(\mathbf{a}_c'''\sigma_+^3 + \mathbf{b}_c'''\sigma_-^3) \tag{6.18}$$

where, as in section 3.6, $\mathbf{r}_c$ is the position of the cusp, $\mathbf{v}_c$ is its velocity $\mathbf{r}_\tau$, and $\mathbf{a}_c''$ and $\mathbf{b}_c''$ are the values of $\mathbf{a}''$ and $\mathbf{b}''$ at the cusp, and so forth. Recall that in view of the gauge conditions $|\mathbf{a}'| = |\mathbf{b}'| = 1$ the unit vector $\mathbf{v}_c$ is orthogonal to both $\mathbf{a}_c''$ and $\mathbf{b}_c''$, while $\mathbf{v}_c \cdot \mathbf{a}_c''' = -|\mathbf{a}_c''|^2$ and $\mathbf{v}_c \cdot \mathbf{b}_c''' = -|\mathbf{b}_c''|^2$.

Near the cusp, $\Psi_{\mu\nu} \approx q_\mu q_\nu$, where $q^\mu = [1, \mathbf{v}_c]$ is null. The *beam* of the cusp is the set of field points $x^\mu = [t, \mathbf{x}]$ with $t = |\mathbf{x} - \mathbf{r}_c|$ and $\mathbf{n} \equiv (\mathbf{x} - \mathbf{r}_c)/|\mathbf{x} - \mathbf{r}_c|$ equal to $\mathbf{v}_c$. Consider a field point just outside the beam, with

$$t = |\mathbf{x} - \mathbf{r}_c| + \varepsilon \qquad \text{and} \qquad \mathbf{x} - \mathbf{r}_c = |\mathbf{x} - \mathbf{r}_c|(\mathbf{v}_c + \delta\mathbf{n}) \qquad (6.19)$$

where ε is small, $\delta\mathbf{n}$ is orthogonal to $\mathbf{v}_c$ and $|\delta\mathbf{n}|$ is of order ε. Then the coordinates τ and σ of the source points near the cusp are both of order $\varepsilon^{1/3}$ and the equation (6.237) for τ reads, to leading order in ε,

$$|\mathbf{a}_c''|^2 \sigma_+^3 + |\mathbf{b}_c''|^2 \sigma_-^3 \approx 12\varepsilon \qquad (6.20)$$

while the beaming factor has the form

$$1 - \mathbf{n} \cdot \mathbf{r}_\tau \approx \tfrac{1}{4}[|\mathbf{a}_c''|^2 \sigma_+^2 + |\mathbf{b}_c''|^2 \sigma_-^2]. \qquad (6.21)$$

In both equations, it is understood that σ_+ and σ_- are restricted to values for which $\tau \le t$.

The metric perturbation $h_{\mu\nu}$ in this case is most conveniently expressed in terms of the rescaled coordinates

$$\bar{\sigma}_\pm = 12^{-1/3}|\varepsilon|^{-1/3} R_c^{-2/3} \sigma_\pm \qquad (6.22)$$

where

$$R_c = (|\mathbf{a}_c''|^2 + |\mathbf{b}_c''|^2)^{-1/2} \qquad (6.23)$$

is one of the cusp radii introduced in section 3.6, and is typically of the same order as the length L of the loop. Equation (6.11) then reads

$$h_{\mu\nu}(t, \mathbf{x}) \approx -\left(\frac{1024}{3}\right)^{1/3} \mu q_\mu q_\nu |\mathbf{x} - \mathbf{r}_c|^{-1} |\varepsilon|^{-1/3} R_c^{4/3} \int \frac{d\bar{\sigma}}{\bar{\sigma}_+^2 \sin^2 \chi + \bar{\sigma}_-^2 \cos^2 \chi} \qquad (6.24)$$

where the *cusp angle* $\chi \in [0, \pi/2]$ is defined by $\sin \chi = |\mathbf{a}_c''|/R_c$, and $\bar{\sigma}_+$ and $\bar{\sigma}_-$ are implicit functions of $\bar{\sigma} = \tfrac{1}{2}(\bar{\sigma}_+ - \bar{\sigma}_-)$ through the equation

$$\bar{\sigma}_+^3 \sin^2 \chi + \bar{\sigma}_-^3 \cos^2 \chi = 1. \qquad (6.25)$$

Provided that χ is not equal to 0 or $\pi/2$ (that is, neither $|\mathbf{a}_c''|$ nor $|\mathbf{b}_c''|$ is zero), the integral on the right of (6.24) is finite, irrespective of the limits of integration. It, therefore, follows that

$$h_{\mu\nu}(t, \mathbf{x}) \sim -\mu q_\mu q_\nu R_c^{4/3} r^{-1} |t - r|^{-1/3} \qquad (6.26)$$

where $r = |\mathbf{x} - \mathbf{r}_c|$ is the distance of the field point from the cusp. Since $q_t = 1$ and $q_r = -1$ it is evident from (6.15) that a non-relativistic test particle that passes through the beam of the cusp will experience a radial acceleration of the form

$$\ddot{r} \sim -\frac{\mu}{6} R_c^{4/3} r^{-1} (t - r)^{-1} |t - r|^{-1/3} \tag{6.27}$$

to leading order in $(t - r)^{-1}$.

Thus $\ddot{r}$ is positive before the particle enters the beam (for $t < r$) but reverses sign as soon as the particle leaves the beam (that is, for $t > r$). Although the radial acceleration is strictly antisymmetric about $t = r$ to this level of approximation, the fact that the particle is first driven outwards means that it ultimately experiences a weaker inward force, and so the net effect of the beam is to expel the particle. In fact, if the acceleration (6.27) is integrated from $t = 0$ to $t = r$ then the net change in r during the initial, repulsive phase is of order

$$\Delta r \sim \mu r^{-1/3} R_c^{4/3} \tag{6.28}$$

and so can be relatively large for particles close to the cusp.

The leading-order expression (6.26) for the potential $h_{\mu\nu}$ near the beam was first derived by Vachaspati [Vac87], and for an asymmetric loop suggests that the beaming of gravitational radiation from cusps would quickly accelerate the loop to relativistic velocities, a topic I will return to in section 6.11. At the level of the weak-field approximation gravitational beaming from cusps also accounts for a large fraction of the total gravitational energy radiated by loops, as will be seen later.

In addition to gravitational beaming, the weak-field approximation also predicts that a cusp exerts a strong attractive force at points on its forward light cone in directions away from its beam. In this case $r = |\mathbf{x} - \mathbf{r}_c|$ and $t \geq 0$ are both small but $\mathbf{n} \cdot \mathbf{v}_c < 0$. If r and t are both of order ε, then τ is of order ε and σ of order $\varepsilon^{1/2}$, so that equation (6.237) becomes

$$2(r\mathbf{n} \cdot \mathbf{v}_c - t)\tau \approx r^2 - t^2 - \tfrac{1}{2} r\mathbf{n} \cdot (\mathbf{a}_c'' + \mathbf{b}_c'')\sigma^2 + \tfrac{1}{16} |\mathbf{a}_c'' + \mathbf{b}_c''|^2 \sigma^4 \tag{6.29}$$

while $|\mathbf{x} - \mathbf{r}| \equiv t - \tau$. Hence, to leading order in ε the metric perturbation is

$$h_{\mu\nu}(t, \mathbf{x}) \approx -8\mu q_\mu q_\nu \frac{t - r\mathbf{n} \cdot \mathbf{v}_c}{1 - \mathbf{n} \cdot \mathbf{v}_c} \int \frac{d\sigma}{F(t, \mathbf{x}, \sigma)} \tag{6.30}$$

where

$$F(t, \mathbf{x}, \sigma) = t^2 + r^2 - 2\mathbf{n} \cdot \mathbf{v}_c rt - \tfrac{1}{2} r\mathbf{n} \cdot (\mathbf{a}_c'' + \mathbf{b}_c'')\sigma^2 + \tfrac{1}{16} |\mathbf{a}_c'' + \mathbf{b}_c''|^2 \sigma^4 \tag{6.31}$$

and the integral ranges over all values of σ for which $\tau \leq t$ or, equivalently, for which F is positive.

It is easily seen that F is positive definite if $t \geq 0$ and $\mathbf{n} \cdot \mathbf{v}_c < 0$, so on defining the rescaled coordinate

$$\bar{\sigma} = \tfrac{1}{2} \varpi^{-1/2} \rho_c^{-1/2} \sigma \tag{6.32}$$

with

$$\varpi = (t^2 + r^2 - 2\mathbf{n} \cdot \mathbf{v}_c rt)^{1/2} \quad \text{and} \quad \rho_c = |\mathbf{a}_c'' + \mathbf{b}_c''|^{-1} \tag{6.33}$$

the metric perturbation becomes

$$h_{\mu\nu}(t, \mathbf{x}) \approx -16\mu q_\mu q_\nu \frac{t - r\mathbf{n} \cdot \mathbf{v}_c}{1 - \mathbf{n} \cdot \mathbf{v}_c} \varpi^{-3/2} \rho_c^{1/2} \int \frac{\mathrm{d}\bar{\sigma}}{1 - 2\cos\beta\bar{\sigma}^2 + \bar{\sigma}^4} \tag{6.34}$$

where

$$\cos\beta = \varpi^{-1} r |\mathbf{a}_c'' + \mathbf{b}_c''|^{-1} \mathbf{n} \cdot (\mathbf{a}_c'' + \mathbf{b}_c''). \tag{6.35}$$

Since the integral converges and t and r are both of order ε, the divergence in $h_{\mu\nu}$ behind the cusp has the form

$$h_{\mu\nu}(t, \mathbf{x}) \sim -\mu q_\mu q_\nu \varepsilon^{-1/2} \rho_c^{1/2} \tag{6.36}$$

where the characteristic cusp dimension $\rho_c \geq R_c$ for this regime was examined in some detail in section 3.6, and is again typically of order L. Note that on the spacelike section $t = 0$ the variable ϖ is simply r, and the limiting behaviour of $h_{\mu\nu}$ is found by replacing ε in (6.36) with r. The potential, therefore, diverges as $r^{-1/2}$, and the cusp exerts an attractive force which falls off as $r^{-3/2}$. The weak-field approximation therefore breaks down not only near the beam but also inside a radius $r \sim \mu^2 \rho_c$ about the cusp (which would be of the order of 10^8 cm for a GUT string loop the size of a star cluster).

The result embodied in equation (6.36) can also be derived in a more heuristic fashion, as follows. If $\mathbf{r}$ denotes any point on the string near the cusp with $\tau = 0$ then

$$|\mathbf{r} - \mathbf{r}_c| \approx \tfrac{1}{4}\rho_c^{-1}\sigma^2. \tag{6.37}$$

Since μ is the rest mass per unit length of the string, and σ in the aligned standard gauge is a measure of the proper length of the string, the mass M_r inside a radius $|\mathbf{r} - \mathbf{r}_c| = r$ is

$$M_r \sim 2\mu|\sigma| \sim 4\mu(r\rho_c)^{1/2} \tag{6.38}$$

and hence

$$M_r/r \sim 4\mu(\rho_c/r)^{1/2} \tag{6.39}$$

as predicted by (6.36).

Furthermore, the mass M_c inside the strong-field region $r \leq \mu^2 \rho_c$ is

$$M_c \sim 4\mu^2 \rho_c \sim 4\mu M \tag{6.40}$$

where $M = \mu L \sim \mu \rho_c$ is the total mass of the string. Thus for a GUT string (that is, for $\mu \sim 10^{-6}$) about 10^{-6}–10^{-5} of the total mass of the string would be contained in the near-cusp region. Since the total mass of a string loop with length of order of the current horizon radius would be comparable to the mass of a cluster of galaxies, the cusp mass M_c is not necessarily negligible.

The breakdown of the weak-field approximation near a cusp probably indicates that something more complex than mere gravitational beaming occurs there. On the face of it, there would seem to be two alternative fates for a cusp on a cosmic string: either higher-order corrections to the Nambu–Goto action (2.10) suppress the formation of a full cusp, with the result that the gravitational field of the string departs only minimally from the weak-field approximation; or the cusp is unstable to strong-field effects, and fundamentally new features appear (including perhaps the collapse of the cusp to form a black hole).

Unfortunately, neither alternative can at present be ruled out, although the perturbative analysis of the Nielsen–Olesen vortex outlined at the end of section 1.5 strongly suggests that higher-order corrections do not in general suppress cusp formation. However, if field-theoretic effects *were* to act to limit the local Lorentz factor of the string to a maximum value λ then an analysis similar to that which led to equation (6.39) indicates that the potential at a distance r from a source point with Lorentz factor λ would be:

$$M/r \sim \mu(\rho_c/r)^{1/2}[1 - \lambda^{-1}(\rho_c/r)^{1/2}]. \tag{6.41}$$

According to (6.41), the weak-field approximation would still break down when $r \sim \mu^2 \rho_c$, provided that λ is larger than $\mu^{-1} \sim 10^6$.

6.3   Kinks in the weak-field approximation

At the level of the weak-field approximation kinks exhibit a beaming effect similar to that of a cusp, although the divergences are not as severe. Recall that a kink is a discontinuity in the spatial tangent vector $\mathbf{r}_\sigma$ which propagates around the string at the speed of light. Here, following David Garfinkle and Tanmay Vachaspati [GV88], I will consider a cuspless loop supporting a single kink which corresponds to a discontinuity in the mode function $\mathbf{b}$ at $\tau = \sigma$.

If $x^\mu = [t, \mathbf{x}]$ is a general field point, the kink crosses the past light cone of x^μ at $\tau = \sigma = \sigma_k$, where σ_k is the root of the equation

$$\sigma_k = t - |\mathbf{x} - \mathbf{r}(\sigma_k, \sigma_k)|. \tag{6.42}$$

The metric perturbation $h_{\mu\nu}$ is then given by

$$h_{\mu\nu}(t, \mathbf{x}) = -4\mu \left[\int_0^{\sigma_k^-} \frac{\Psi_{\mu\nu}(\tau, \sigma)}{|\mathbf{x} - \mathbf{r}|(1 - \mathbf{n} \cdot \mathbf{r}_\tau)} \, d\sigma + \int_{\sigma_k^+}^L \frac{\Psi_{\mu\nu}(\tau, \sigma)}{|\mathbf{x} - \mathbf{r}|(1 - \mathbf{n} \cdot \mathbf{r}_\tau)} \, d\sigma \right]. \tag{6.43}$$

Because the loop is cuspless, the integrand here is piecewise smooth for field points off the string, and so $h_{\mu\nu}$ is continuous. However, the spacetime derivatives of $h_{\mu\nu}$—which appear in the geodesic equation (6.15)—need not be finite.

In calculating the derivatives $h_{\mu\nu,\lambda}$ it is evident that differentiating the integrand in (6.43) will, at worst, produce terms that are piecewise smooth. Thus,

any singularity will stem from the spacetime derivatives of the integration limit σ_k. In fact, differentiation of (6.42) gives

$$\sigma_{k,\lambda} = (1 - \mathbf{n} \cdot \mathbf{v}_k)^{-1} k_\lambda \tag{6.44}$$

where $\mathbf{n}$ is the unit vector from the kink source point $\mathbf{r}_k = \mathbf{r}(\sigma_k, \sigma_k)$ to the field point $\mathbf{x}$, $c^\mu = [1, \mathbf{n}]$ and

$$\mathbf{v}_k = \frac{\partial \mathbf{r}_k}{\partial \sigma_k} \equiv \mathbf{a}'(2\sigma_k) \tag{6.45}$$

is the phase velocity of the kink, which in view of the gauge condition $|\mathbf{a}'| = 1$ is a unit vector (as was previously seen in section 2.7).

Hence, the divergent part of $h_{\mu\nu,\lambda}$ has the form

$$h_{\mu\nu,\lambda} \sim -4\mu(1 - \mathbf{n} \cdot \mathbf{v}_k)^{-1}|\mathbf{x} - \mathbf{r}_k|^{-1}\Delta_{\mu\nu}c_\lambda \tag{6.46}$$

where

$$\Delta_{\mu\nu} = \left[\frac{\Psi_{\mu\nu}(\tau, \sigma)}{(1 - \mathbf{n} \cdot \mathbf{r}_\tau)} \right]_{\tau=\sigma=\sigma_k^+}^{\tau=\sigma=\sigma_k^-}. \tag{6.47}$$

The presence of the factor $(1 - \mathbf{n} \cdot \mathbf{v}_k)^{-1}$ in $h_{\mu\nu,\lambda}$ indicates that the kink, like a cusp, emits a beam of gravitational radiation in the direction of its motion, as the acceleration on a test particle in the future light cone of any point on the locus of the kink with $\mathbf{n} = \mathbf{v}_k$ is instantaneously infinite. However, because the divergence appears in $h_{\mu\nu,\lambda}$ rather than $h_{\mu\nu}$ itself, the net effect of the beam on the motion of nearby particles is substantially weaker.

To obtain an estimate of the strength of the beam, let the source point be the point $\tau = \sigma = 0$ on the kink, and consider a field point x^μ just outside the beam of this point, with

$$t = |\mathbf{x} - \mathbf{r}_k| + \varepsilon \quad \text{and} \quad \mathbf{x} - \mathbf{r}_k = |\mathbf{x} - \mathbf{r}_k|(\mathbf{v}_k + \delta\mathbf{n}) \tag{6.48}$$

where $\delta\mathbf{n}$ is orthogonal to $\mathbf{v}_k$ and $|\delta\mathbf{n}|$ is again of order ε. Then the trajectory of the kink intersects the past light cone of x^μ at a point $\tau = \sigma = \sigma_k$ with σ_k of order $\varepsilon^{1/3}$. In fact, from the kink equation (6.42)

$$2|\mathbf{a}_k''|^2\sigma_k^3 \approx 3\varepsilon \tag{6.49}$$

while

$$1 - \mathbf{n} \cdot \mathbf{v}_k \approx |\mathbf{a}_k''|^2\sigma_k^2. \tag{6.50}$$

Hence, the divergent part of $h_{\mu\nu,\lambda}$ becomes

$$h_{\mu\nu,\lambda} \sim -(\tfrac{256}{9})^{1/3}\mu r^{-1}(t - r)^{-2/3} R_k^{2/3} \Delta_{\mu\nu}c_\lambda \tag{6.51}$$

where $r = |\mathbf{x} - \mathbf{r}_k|$ and $R_k = |\mathbf{a}_k''|^{-1}$ is a characteristic length scale associated with the kink point $\tau = \sigma = 0$, and is typically of order L.

The acceleration a^i experienced by a non-relativistic particle which passes through the beam, therefore, has the form

$$a^i \sim -(\tfrac{256}{9})^{1/3} \mu r^{-1} (t-r)^{-2/3} R_k^{2/3} (\Delta_{it} - \tfrac{1}{2}\Delta_{tt} c_i). \qquad (6.52)$$

Here, the components Δ_{it} and Δ_{tt} depend on the difference in the local velocity $\mathbf{r}_\tau$ of the string on the two sides of the kink, which bears no direct relation to $\mathbf{v}_k$. Hence, the acceleration vector a^i is, in general, not radial. Even the radial acceleration

$$\ddot{r} \sim -(32/9)^{1/3} \mu r^{-1} (t-r)^{-2/3} R_k^{2/3} (\Delta_{rt} + \tfrac{1}{2}\Delta_{tt}) \qquad (6.53)$$

need not be initially outwards but it does change sign as the particle emerges from the beam.

As in the cusp case, it is possible to integrate $\ddot{r}$ from $t=0$ to $t=r$ to get an order-of-magnitude estimate of the effect of the initial acceleration regime. The resulting change in the radial distance r is

$$|\Delta r| \sim \mu r^{1/3} R_k^{2/3} \qquad (6.54)$$

which for particles close to the kink is considerably smaller than the corresponding radial displacement $\Delta r \sim \mu r^{-1/3} R_c^{4/3}$ caused by the beam from a cusp.

Any string loop with one or more kinks has the potential to support microcusps (see section 3.6). The analysis of the gravitational field near a microcusp is no different from the treatment given in the previous section of the gravitational field near an ordinary cusp, save that the scale factors ρ_c and R_c are extremely small in comparison with L at a microcusp. It is, therefore, unlikely that the gravitational effects generated by a microcusp would be strong enough to be distinguished from the background field of the string.

6.4 Radiation of gravitational energy from a loop

Another property of the gravitational field of a string loop that has potentially important observational consequences is the rate at which the energy of the loop is radiated away. At a point $\mathbf{x}$ in the *wave zone*, where $r = |\mathbf{x}|$ is much larger than the characteristic size L of the loop, the power radiated per unit solid angle Ω is given by

$$\frac{\mathrm{d}P}{\mathrm{d}\Omega} = r^2 \sum_{j=1}^{3} n^j \mathfrak{T}^{jt} \qquad (6.55)$$

where $\mathbf{n} = \mathbf{x}/r$ as previously, and

$$\mathfrak{T}^{\mu\nu} = -\frac{1}{8\pi} \langle R^{\mu\nu} - \tfrac{1}{2}\eta^{\mu\nu} R \rangle \qquad (6.56)$$

is the gravitational stress–energy pseudo-tensor which needs to be inserted into the Einstein equation to balance the Ricci tensor $R^{\mu\nu}$ when the latter is evaluated to quadratic order in the metric perturbation $h_{\mu\nu}$. (Recall that in the weak-field approximation $R_{\mu\nu} = 0$ in vacuum to linear order only.) The angled brackets indicate that the stress–energy pseudo-tensor $\mathfrak{T}^{\mu\nu}$ is a coarse-grained average over many wavelengths of the radiation field.

If the source of the gravitational field is periodic with period T then its stress–energy tensor can be expressed as a harmonic series:

$$T^{\mu\nu}(t, \mathbf{x}) = \sum_{m=-\infty}^{\infty} T^{\mu\nu}(\omega_m, \mathbf{x}) e^{-i\omega_m t} \tag{6.57}$$

where $\omega_m = 2\pi m / T$ and

$$T^{\mu\nu}(\omega_m, \mathbf{x}) = T^{-1} \int_0^T T^{\mu\nu}(t, \mathbf{x}) e^{i\omega_m t} \, dt. \tag{6.58}$$

For $r = |\mathbf{x}| \gg |\mathbf{x}'|$ the source term on the right of equation (6.6) now becomes

$$S_{\mu\nu}(t', \mathbf{x}') = \sum_{m=-\infty}^{\infty} [T_{\mu\nu}(\omega_m, \mathbf{x}') - \tfrac{1}{2}\eta_{\mu\nu} T(\omega_m, \mathbf{x}')] e^{-i\omega_m t} e^{i\omega_m |\mathbf{x}-\mathbf{x}'|}$$

$$\approx \sum_{m=-\infty}^{\infty} [T_{\mu\nu}(\omega_m, \mathbf{x}') - \tfrac{1}{2}\eta_{\mu\nu} T(\omega_m, \mathbf{x}')] e^{i\omega_m (r-t)} e^{-i\omega_m \mathbf{n}\cdot\mathbf{x}'} \tag{6.59}$$

and so

$$h_{\mu\nu}(t, \mathbf{x}) \approx \sum_{m=-\infty}^{\infty} E_{\mu\nu}(\omega_m, \mathbf{x}) e^{-i\omega_m c_\lambda x^\lambda} \tag{6.60}$$

where $c^\mu = [1, \mathbf{n}]$ and

$$E_{\mu\nu}(\omega_m, \mathbf{x}) = -4r^{-1} \int [T_{\mu\nu}(\omega_m, \mathbf{x}') - \tfrac{1}{2}\eta_{\mu\nu} T(\omega_m, \mathbf{x}')] e^{-i\omega_m \mathbf{n}\cdot\mathbf{x}'} \, d^3 x'. \tag{6.61}$$

If the expression (6.60) for $h_{\mu\nu}$ is used to calculate the second-order Ricci tensor then, since all spatial derivatives of $E_{\mu\nu}$ are of order r^{-2} and can be neglected in the wave zone,

$$R^{\mu\nu} = -\tfrac{1}{2} \sum_{m=1}^{\infty} \omega_m^2 (E^{\kappa\lambda} E_{\kappa\lambda}^* - \tfrac{1}{2} E E^*) c^\mu c^\nu \tag{6.62}$$

(where $E = E_\lambda^\lambda$) plus cross terms proportional to $e^{-i\omega_{m+n} c_\lambda x^\lambda}$ with $m + n \neq 0$. On averaging $R^{\mu\nu}$ over a spacetime region with dimensions large compared to the characteristic wavelength of the gravitational radiation, these additional terms

disappear. The expression (6.55) for the power radiated per unit solid angle, therefore, becomes:

$$\frac{\mathrm{d}P}{\mathrm{d}\Omega} = \sum_{m=1}^{\infty} \frac{r^2 \omega_m^2}{16\pi} (E^{\mu\nu} E_{\mu\nu}^* - \tfrac{1}{2} E E^*) = \sum_{m=1}^{\infty} \frac{\omega_m^2}{\pi} [\bar{T}^{\mu\nu} \bar{T}_{\mu\nu}^* - \tfrac{1}{2} |\bar{T}_\mu^\mu|^2] \quad (6.63)$$

where

$$\bar{T}^{\mu\nu} \equiv \int T^{\mu\nu}(\omega_m, \mathbf{x}') e^{-i\omega_m \mathbf{n}\cdot\mathbf{x}'} \, \mathrm{d}^3 x'. \quad (6.64)$$

In the case of the string stress–energy tensor (6.7),

$$\bar{T}^{\mu\nu} = \frac{\mu}{T} \int \mathrm{d}^3 x' \int_0^T \mathrm{d}\tau \int_0^L \mathrm{d}\sigma \, (V^\mu V^\nu - N^\mu N^\nu) e^{i\omega_m(\tau - \mathbf{n}\cdot\mathbf{x}')} \delta^{(3)}(\mathbf{x}' - \mathbf{r}(\tau, \sigma))$$

$$= \frac{\mu}{T} \int_0^T \mathrm{d}\tau \int_0^L \mathrm{d}\sigma \, (V^\mu V^\nu - N^\mu N^\nu) e^{i\omega_m(\tau - \mathbf{n}\cdot\mathbf{r})} \quad (6.65)$$

where $V^\mu = [1, \mathbf{r}_\tau]$ and $N^\mu = [0, \mathbf{r}_\sigma]$ as before.

It was seen in chapter 3 that the trajectory of a string loop with invariant length L obeying the Nambu–Goto equations of motion is periodic with period $L/2$ in the centre-of-momentum frame, so $T = L/2$ and $\omega_m = 4\pi m/L$. Since the general solution to the equations of motion is $\mathbf{r}(\tau, \sigma) = \frac{1}{2}[\mathbf{a}(\sigma_+) + \mathbf{b}(\sigma_-)]$ where $\mathbf{a}$ and $\mathbf{b}$ are periodic functions with period L, the domain $[0, T] \times [0, L]$ in τ–σ space can be mapped to $[0, L] \times [0, L]$ in σ_+–σ_- space (as shown in figure 6.2). This allows the Fourier components (6.65) of $T^{\mu\nu}$ to be recast in the form

$$\bar{T}^{\mu\nu} = \frac{\mu}{L} \int_0^L e^{i\omega_m(\sigma_+ - \mathbf{n}\cdot\mathbf{a})/2} \, \mathrm{d}\sigma_+ \int_0^L e^{i\omega_m(\sigma_- - \mathbf{n}\cdot\mathbf{b})/2} \, \mathrm{d}\sigma_- \, a'^{(\mu} b'^{\nu)} \quad (6.66)$$
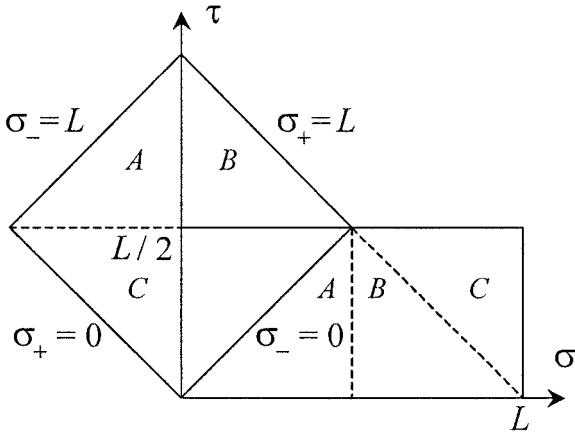
where $a'^\mu(\sigma_+) = [1, \mathbf{a}']$ and $b'^\nu(\sigma_-) = [1, \mathbf{b}']$ and the round brackets in $a'^{(\mu} b'^{\nu)}$ denote symmetrization.

One interesting feature of this formula is that the radiated power is proportional to the square of the mass per unit length μ (as would be expected) but is independent of the length L of the string. This is a generic property of far-zone gravitational radiation from a loop which obeys the Nambu–Goto equations of motion, as the total energy of the loop is proportional L but the frequency of oscillation is proportional to L^{-1}.

To see this explicitly, note that because of the gauge conditions $|\mathbf{a}'|^2 = |\mathbf{b}'|^2 = 1$, the vectors $\mathbf{a}$ and $\mathbf{b}$ in the centre-of-momentum frame have the general form

$$\mathbf{a}(\sigma_+) = \frac{L}{2\pi} \bar{\mathbf{a}}(2\pi\sigma_+/L) \qquad \text{and} \qquad \mathbf{b}(\sigma_-) = \frac{L}{2\pi} \bar{\mathbf{b}}(2\pi\sigma_-/L) \quad (6.67)$$

where $\bar{\mathbf{a}}$ and $\bar{\mathbf{b}}$ are periodic functions with period 2π, and satisfy the identity $|\bar{\mathbf{a}}'| = |\bar{\mathbf{b}}'| = 1$. If $\sigma_\pm$ is replaced with $\xi_\pm = 2\pi\sigma_\pm/L$ as the variable of integration

Figure 6.2. The fundamental domain in standard and light-cone coordinates.

in (6.66), then

$$\bar{T}^{\mu\nu} = \frac{\mu L}{4\pi^2} \int_0^{2\pi} e^{im(\xi_+ - \mathbf{n}\cdot\bar{\mathbf{a}})}\, d\xi_+ \int_0^{2\pi} e^{im(\xi_- - \mathbf{n}\cdot\bar{\mathbf{b}})}\, d\xi_- \, a'^{(\mu} b'^{\nu)} \qquad (6.68)$$

where now $a'^{\mu} = [1, \bar{\mathbf{a}}']$ and $b'^{\nu} = [1, \bar{\mathbf{b}}']$. Since the expression (6.63) for the radiated power is quadratic in both $\bar{T}^{\mu\nu}$ and $\omega_m = 4\pi m/L$, it has no dependence on L.

Note also that (6.68) can be expressed in the more compact form $\bar{T}^{\mu\nu} = \mu L A^{(\mu} B^{\nu)}$, where

$$A^{\mu} = \frac{1}{2\pi} \int_0^{2\pi} e^{im[\xi_+ - \mathbf{n}\cdot\bar{\mathbf{a}}(\xi_+)]} a'^{\mu}(\xi_+)\, d\xi_+ \qquad (6.69)$$

and

$$B^{\mu} = \frac{1}{2\pi} \int_0^{2\pi} e^{im[\xi_- - \mathbf{n}\cdot\bar{\mathbf{b}}(\xi_-)]} b'^{\mu}(\xi_-)\, d\xi_-. \qquad (6.70)$$

The radiated power per unit solid angle (6.63), therefore, reduces to

$$\frac{dP}{d\Omega} = 8\pi\mu^2 \sum_{m=1}^{\infty} m^2[(A^{\mu} A^*_{\mu})(B^{\nu} B^*_{\nu}) + |A^{\mu} B^*_{\mu}|^2 - |A^{\mu} B_{\mu}|^2]. \qquad (6.71)$$

Furthermore, integration of (6.69) by parts yields the identity

$$\frac{1}{2\pi} \int_0^{2\pi} e^{im[\xi_+ - \mathbf{n}\cdot\bar{\mathbf{a}}(\xi_+)]} \mathbf{n} \cdot \bar{\mathbf{a}}'\, d\xi_+ = \frac{1}{2\pi} \int_0^{2\pi} e^{im[\xi_+ - \mathbf{n}\cdot\bar{\mathbf{a}}(\xi_+)]}\, d\xi_+ \equiv A^t \qquad (6.72)$$

and consequently A^{μ} has only three independent components. Let $\mathbf{k}_1$, $\mathbf{k}_2$ and $\mathbf{k}_3$ be the unit vectors in the directions of the spatial (x, y and z) coordinate axes. If

$\mathbf{k}_3$ is chosen to be $\mathbf{n}$ then $A^3 = A^t$, and similarly $B^3 = B^t$. Substituting these identities into equation (6.71) generates the simple result

$$\frac{\mathrm{d}P}{\mathrm{d}\Omega} = 8\pi\mu^2 \sum_{m=1}^{\infty} m^2 [|A_m^1 B_m^1 - A_m^2 B_m^2|^2 + |A_m^1 B_m^2 + A_m^2 B_m^1|^2] \tag{6.73}$$

where the subscript m has been added to A^j and B^j to indicate that they depend explicitly on the wavenumber. Equation (6.73) is a restatement of the well-known result that only motion transverse to the line-of-sight contributes to the radiated energy.

Garfinkle and Vachaspati [GV87a] have used (6.73) to show that the power radiated per unit solid angle from a string loop is, in all cases, finite unless the unit vector $\mathbf{n}$ to the field point lies in the beaming direction of a cusp. To see this, it is necessary to consider only one of the terms in (6.73), for example

$$A_m^1 = \frac{1}{2\pi} \int_0^{2\pi} e^{im(\xi_+ - \mathbf{n}\cdot\overline{\mathbf{a}})} \mathbf{k}_1 \cdot \overline{\mathbf{a}}' \, \mathrm{d}\xi_+. \tag{6.74}$$

If ξ_+ is replaced by $u = \xi_+ - \mathbf{n} \cdot [\overline{\mathbf{a}}(\xi_+) - \overline{\mathbf{a}}(0)]$ then, since a change of 2π in ξ_+ corresponds to a change of 2π in u,

$$A_m^1 = \frac{1}{2\pi} e^{-im\mathbf{n}\cdot\overline{\mathbf{a}}(0)} \int_0^{2\pi} e^{imu} F(u) \, \mathrm{d}u \tag{6.75}$$

where $F = (1 - \mathbf{n} \cdot \overline{\mathbf{a}}')^{-1} \mathbf{k}_1 \cdot \overline{\mathbf{a}}'$.

Now, if the unit vector $\mathbf{n}$ to the field point is not equal to $\overline{\mathbf{a}}'$ at any point on the loop trajectory, and $\overline{\mathbf{a}}'$ is k times piecewise differentiable, then at worst $F^{(k+1)}$ contains one or more integrable singularities, and integrating (6.75) by parts $k + 1$ times demonstrates that A_m^1 goes to zero at least as rapidly as $m^{-(k+1)}$. In particular, if there is a kink in the $\mathbf{a}$ mode at $u = u_k$ then $\overline{\mathbf{a}}'$ is only piecewise continuous, and integrating (6.75) by parts once gives

$$A_m^1 = \frac{1}{2\pi mi} e^{-im\mathbf{n}\cdot\overline{\mathbf{a}}(0)} \left[e^{imu_k} \Delta F - \int_0^{2\pi} e^{imu} F'(u) \, \mathrm{d}u \right] \tag{6.76}$$

where ΔF is the change in F across the kink, and so A_m^1 falls off as m^{-1}.

However, if $\mathbf{n}$ is equal to $\overline{\mathbf{a}}'$ at some point on the loop (say $\xi_+ = 0$) and the mode function $\overline{\mathbf{a}}$ is at least three times differentiable at $\xi_+ = 0$ then, in a similar fashion to the near-cusp analysis of section 6.2,

$$\overline{\mathbf{a}}(\xi_+) \approx \overline{\mathbf{a}}(0) + \mathbf{n}\xi_+ + \tfrac{1}{2}\overline{\mathbf{a}}_0''\xi_+^2 + \tfrac{1}{6}\overline{\mathbf{a}}_0'''\xi_+^3 \tag{6.77}$$

where $\mathbf{n} \cdot \overline{\mathbf{a}}_0'' = 0$, $\mathbf{n} \cdot \overline{\mathbf{a}}_0''' = -|\overline{\mathbf{a}}_0''|^2$ and $\mathbf{k}_1 \cdot \mathbf{n} = 0$. Hence,

$$u \approx \tfrac{1}{6}|\overline{\mathbf{a}}_0''|^2\xi_+^3 \quad \text{and} \quad F \approx 2|\overline{\mathbf{a}}_0''|^{-2}\mathbf{k}_1 \cdot \overline{\mathbf{a}}_0''\xi_+^{-1}. \tag{6.78}$$

On defining $w = mu$, the integral across the discontinuity at $\xi_+ = 0$ in (6.75) gives

$$A_m^1 \approx \frac{1}{2\pi} e^{-im\mathbf{n}\cdot\bar{\mathbf{a}}(0)} (4/3)^{1/3} m^{-2/3} |\bar{\mathbf{a}}_0''|^{-4/3} \mathbf{k}_1 \cdot \bar{\mathbf{a}}_0'' \int e^{iw} w^{-1/3} \, dw \qquad (6.79)$$

and since the singularity is integrable, A_m^1 falls off as $m^{-2/3}$.

The expression (6.73) for the power per unit solid angle is quadratic in both A_m^j and B_m^j. It has been shown that A_m^j goes to zero at least as rapidly as m^{-1} if the vector $\mathbf{n}$ does not coincide with one of the beaming directions of the $\mathbf{a}$ mode, and like $m^{-2/3}$ if it does. A similar statement applies to B_m^j. Broadly speaking, then, there are three possibilities for the high-frequency contributions to $dP/d\Omega$:

(i)   If $\mathbf{n}$ is beamed by neither mode then at worst $dP/d\Omega \sim \sum m^{-2}$ and the sum converges.

(ii) If $\mathbf{n}$ is beamed by one of the modes but not both then at worst $dP/d\Omega \sim \sum m^{-4/3}$ and the sum again converges.

(iii) If $\mathbf{n}$ is beamed by both modes then $dP/d\Omega \sim \sum m^{-2/3}$ and the sum diverges.

Thus it is only in the third case that the power radiated per unit solid angle in the direction of the field point is infinite. In this case $\mathbf{n}$ is beamed by both modes and so there is a point on each mode where $\bar{\mathbf{a}}' = \bar{\mathbf{b}}' = \mathbf{n}$. In other words $dP/d\Omega$ diverges if and only if $\mathbf{n}$ is in the beaming direction of a cusp.

Some explicit calculations of the power radiated by a selection of kinked or cusped loops are examined in the following section, and the results are, in all cases, consistent with the analysis presented here. It should be noted that although $dP/d\Omega$ is always infinite in the beaming direction of a cusp (as expected), the total integrated power P is generally finite, except in certain pathological cases.

6.5   Calculations of radiated power

The importance of being able to estimate the power loss from a generic cosmic string loop is twofold, in that it gives a characteristic radiative lifetime for the network of loops that may have formed in the early Universe, and also an indication of the amplitude and frequency distribution of the radiative cosmological background that would have been produced by this network. It is not surprising, therefore, that a number of authors have published calculations of the power radiated by various families of loops.

Here I will examine three standard studies involving the following trajectories:

(i)   the degenerate kinked cuspless loop of section 4.2.3, which has the mode functions

$$\mathbf{a}(\sigma_+) = \begin{cases} (\sigma_+ - \frac{1}{4}L)\widehat{\mathbf{a}} & 0 \leq \sigma_+ \leq \frac{1}{2}L \\ (\frac{3}{4}L - \sigma_+)\widehat{\mathbf{a}} & \frac{1}{2}L \leq \sigma_+ \leq L \end{cases} \qquad (6.80)$$

and

$$\mathbf{b}(\sigma_-) = \begin{cases} (\sigma_- - \tfrac{1}{4}L)\widehat{\mathbf{b}} & 0 \le \sigma_- \le \tfrac{1}{2}L \\ (\tfrac{3}{4}L - \sigma_-)\widehat{\mathbf{b}} & \tfrac{1}{2}L \le \sigma_- \le L \end{cases} \tag{6.81}$$

where $\widehat{\mathbf{a}}$ and $\widehat{\mathbf{b}}$ are constant unit vectors, and has been treated in the weak-field approximation by David Garfinkle and Tanmay Vachaspati [GV87a];

(ii) the 3-harmonic Vachaspati–Vilenkin solutions introduced in section 4.4.3, for which

$$\mathbf{a}(\sigma_+) = \frac{L}{2\pi} \left[(1 - \alpha) \sin \xi_+, -(1 - \alpha) \cos \xi_+, \sqrt{\alpha - \alpha^2} \sin(2\xi_+) \right]$$
$$+ \frac{L}{2\pi} [-\tfrac{1}{3}\alpha \sin(3\xi_+), -\tfrac{1}{3}\alpha \cos(3\xi_+), 0] \tag{6.82}$$

and

$$\mathbf{b}(\sigma_-) = \frac{L}{2\pi} [\sin \xi_-, -\cos \psi \cos \xi_-, -\sin \psi \cos \xi_-] \tag{6.83}$$

(where $0 \le \alpha < 1$, $0 \le \psi \le \pi$ and $\xi_\pm = 2\pi\sigma_\pm/L$), which have been studied analytically in the case $\alpha = 0$ and numerically for other values of α by Tanmay Vachaspati and Alexander Vilenkin [VV85] and Ruth Durrer [Dur89]; and

(iii) the family of p/q harmonic solutions discussed in section 4.4.2, which have

$$\mathbf{a}(\sigma_+) = \frac{L}{2\pi p} [\cos(p\xi_+), \sin(p\xi_+), 0] \tag{6.84}$$

and

$$\mathbf{b}(\sigma_-) = \frac{L}{2\pi q} [\cos(q\xi_-), \cos \psi \sin(q\xi_-), \sin \psi \sin(q\xi_-)] \tag{6.85}$$

where ψ is a constant and p and q are positive integers, and have been analysed principally by Conrad Burden [Bur85].

I will also briefly mention other numerical estimates of radiated power involving trajectories for which there is no comparable analytic development.

6.5.1 Power from cuspless loops

The degenerate kinked cuspless loop is the easiest to examine analytically. If $n_1 = \widehat{\mathbf{a}} \cdot \mathbf{n}$ and $n_2 = \widehat{\mathbf{b}} \cdot \mathbf{n}$ then

$$\bar{T}^{\mu\nu} = \frac{16\mu}{L} \frac{(-1)^m \cos[m\pi(n_1 - n_2)/2] - \cos[m\pi(n_1 + n_2)/2]}{\omega_m^2 (1 - n_1^2)(1 - n_2^2)} M^{\mu\nu} \tag{6.86}$$

for $m \neq 0$, where

$$M^{\mu\nu} = \begin{pmatrix} 2n_1 n_2 & n_2\widehat{\mathbf{a}} + n_1\widehat{\mathbf{b}} \\ n_2\widehat{\mathbf{a}} + n_1\widehat{\mathbf{b}} & \widehat{\mathbf{a}} \otimes \widehat{\mathbf{b}} + \widehat{\mathbf{b}} \otimes \widehat{\mathbf{a}} \end{pmatrix}. \tag{6.87}$$

Since $M^{\mu\nu}M_{\mu\nu} - \frac{1}{2}(M_\mu^\mu)^2 = 2(1-n_1^2)(1-n_2^2)$ it follows that

$$\frac{dP}{d\Omega} = \frac{32\mu^2}{\pi^3} \sum_{m=1}^\infty \frac{[1-(-1)^m \cos(m\pi n_1)][1-(-1)^m \cos(m\pi n_2)]}{m^2(1-n_1^2)(1-n_2^2)}. \quad (6.88)$$

The series can summed explicitly by invoking the identity

$$\sum_{m=1}^\infty \frac{\cos(mu)\cos(mv)}{m^2} = \frac{1}{8}[(|u+v|-\pi)^2 + (|u-v|-\pi)^2] - \frac{\pi^2}{12} \quad (6.89)$$

for any u, v in $[-\pi, \pi]$, giving
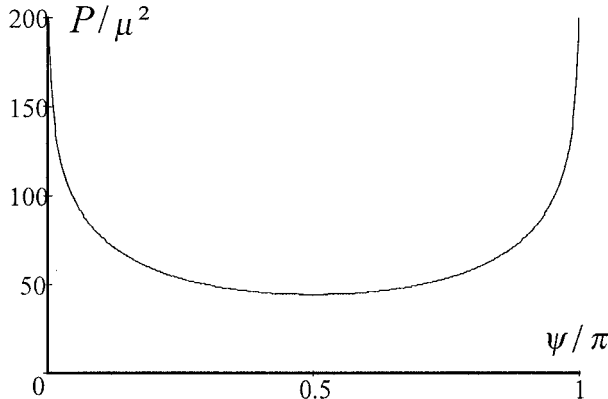
$$\frac{dP}{d\Omega} = \frac{16\mu^2}{\pi} \frac{1 - \frac{1}{2}(|n_1+n_2| + |n_1-n_2|)}{(1-n_1^2)(1-n_2^2)}. \quad (6.90)$$

Note here that as $n_1 \to 1$, the right-hand side of (6.90) tends to $8\mu^2\pi^{-1}(1-n_2^2)^{-1}$ and so the power radiated per solid angle remains finite in all directions. Furthermore, the angular integration can be performed to give an explicit formula for the total power of the loop. If the coordinates are aligned so that $\widehat{\mathbf{a}} = [\cos(\psi/2), \sin(\psi/2), 0]$ and $\widehat{\mathbf{b}} = [\cos(\psi/2), -\sin(\psi/2), 0]$, where $\cos\psi = \widehat{\mathbf{a}}\cdot\widehat{\mathbf{b}}$, then

$$P = \frac{128\mu^2}{\pi} \int_0^{\pi/2} d\phi \int_0^{\pi/2} d\theta$$
$$\times \frac{1 - \cos(\phi - \psi/2)\sin\theta}{[1 - \cos^2(\phi - \psi/2)\sin^2\theta][1 - \cos^2(\phi + \psi/2)\sin^2\theta]} \sin\theta$$
$$= \frac{32\mu^2}{\sin^2\psi}\{(1+\cos\psi)\ln[2/(1+\cos\psi)] + (1-\cos\psi)\ln[2/(1-\cos\psi)]\}. $$
$$(6.91)$$

The integrated power P is, of course, finite except in the limits $\psi \to 0$ and π (when the loop is effectively a line segment with permanent cusps), in which case it diverges logarithmically in $\sin\psi$ (see figure 6.3). The minimum value of the radiative efficiency $\gamma^0 \equiv P/\mu^2$ is $64(\ln 2) \approx 44.4$, and occurs when $\psi = \pi/2$.

Garfinkle and Vachaspati [GV87a] have published numerical estimates of the radiated power from two other families of cuspless loops, namely the 4-harmonic Garfinkle–Vachaspati solutions described by (4.95) and (4.96) in the specific case $p = 1$ (which is illustrated in figures 4.28 and 4.29), and a five-parameter family which is similar to the balloon strings of section 4.3, save that the mode functions are broken near the north pole in exactly the same manner as near the south pole, and the planes of the two mode functions need not be orthogonal. In the first case Garfinkle and Vachaspati find that $\gamma^0 \approx 65$ and in the second case that γ^0 is 'of the order of 100' (although unfortunately no parameter values are quoted in connection with this result). Later work by Bruce Allen and Paul Casper [AC94], using an improved numerical algorithm to be described in section 6.9, has confirmed the order of magnitude of this second estimate.

Figure 6.3. Radiated power P from a degenerate kinked cuspless loop as a function of the angle ψ.

6.5.2   Power from the Vachaspati–Vilenkin loops

The radiated power can also be evaluated explicitly for the Vachaspati–Vilenkin solutions of case (ii) in the 1-harmonic limit $\alpha = 0$, for which

$$\overline{\mathbf{a}}(\xi_+) = [\sin \xi_+, -\cos \xi_+, 0] \tag{6.92}$$

and

$$\overline{\mathbf{b}}(\xi_-) = [\sin \xi_-, -\cos \psi \cos \xi_-, -\sin \psi \cos \xi_-]. \tag{6.93}$$

For $0 < \psi < \pi$ these functions describe a loop in the shape of a doubled straight line parallel to $[0, \cos \psi + 1, \sin \psi]$ at time $\tau = 0$, which evolves to form an ellipse with axes in the directions of $[1, 0, 0]$ and $[0, \cos \psi - 1, \sin \psi]$ at time $\tau = L/4$. In the degenerate cases $\psi = 0$ and $\psi = \pi$ the trajectory describes a doubled rotating rod (section 4.2.2) and a collapsing circular loop (section 4.2.1), respectively.

If the coordinate system is rotated so that the ellipse lies in the x–z plane then

$$\overline{\mathbf{a}}(\xi_+) = [\sin(\psi/2) \sin \xi_+, -\cos(\psi/2) \sin \xi_+, -\cos \xi_+] \tag{6.94}$$

and

$$\overline{\mathbf{b}}(\xi_-) = [\sin(\psi/2) \sin \xi_-, \cos(\psi/2) \sin \xi_-, \cos \xi_-] \tag{6.95}$$

and the doubled line which forms at $\tau = 0$ now lies along the y-axis, with cusps at $y = \pm \cos(\psi/2)$ moving in the negative and positive z-directions respectively.

In this case, the Fourier transforms A^μ and B^μ defined by (6.69) and (6.70) can be evaluated by invoking the identity

$$\frac{1}{2\pi} \int_0^{2\pi} e^{i(p\xi - u \sin \xi - v \cos \xi)} \, d\xi = \left(\frac{u - iv}{w} \right)^p J_p(w) \tag{6.96}$$

for $p \in \mathbb{Z}$, where $w = (u^2 + v^2)^{1/2} \neq 0$ and J_p is the Bessel function of order p.

If the unit vector to the field point is $\mathbf{n} = [\cos\phi\sin\theta, \sin\phi\sin\theta, \cos\theta]$ then

$$A^\mu = [F_m^+, \mathbf{A}_m] \qquad \text{and} \qquad B^\mu = [F_m^-, \mathbf{B}_m] \tag{6.97}$$

where

$$\begin{aligned}
\mathbf{A}_m &= \tfrac{1}{2}[\mathrm{i}\sin(\psi/2), -\mathrm{i}\cos(\psi/2), 1]F_{m+1}^+ \\
&\quad + \tfrac{1}{2}[-\mathrm{i}\sin(\psi/2), \mathrm{i}\cos(\psi/2), 1]F_{m-1}^+ \tag{6.98}
\end{aligned}$$

$$\begin{aligned}
\mathbf{B}_m &= \tfrac{1}{2}[\mathrm{i}\sin(\psi/2), \mathrm{i}\cos(\psi/2), -1]F_{m+1}^- \\
&\quad + \tfrac{1}{2}[-\mathrm{i}\sin(\psi/2), -\mathrm{i}\cos(\psi/2), -1]F_{m-1}^- \tag{6.99}
\end{aligned}$$

and $F_k^\pm = \beta_\pm^k J_k(mr_\pm)$, with

$$\beta_\pm = \frac{\pm\cos\theta - \mathrm{i}\sin(\psi/2 \mp \phi)\sin\theta}{r_\pm} \tag{6.100}$$

and

$$r_\pm = [1 - \cos^2(\psi/2 \mp \phi)\sin^2\theta]^{1/2}. \tag{6.101}$$

Substituting $\bar{T}^{\mu\nu}$ into (6.63) gives the following formula for the power radiated per unit solid angle:

$$\begin{aligned}
\frac{\mathrm{d}P}{\mathrm{d}\Omega} &\equiv \sum_{m=1}^\infty \frac{\mathrm{d}P_m}{\mathrm{d}\Omega} \\
&= 8\pi\mu^2 \sum_{m=1}^\infty m^2[(J_m^{+\prime}J_m^{-\prime} + \lambda_+\lambda_- J_m^+ J_m^-)^2 + (\lambda_+ J_m^+ J_m^{-\prime} + \lambda_- J_m^- J_m^{+\prime})^2]
\end{aligned} \tag{6.102}$$

where now $J_m^\pm$ denotes $J_m(mr_\pm)$, $\lambda_\pm = (r_\pm^{-2} - 1)^{1/2}$ and $J_{m\pm1}(mr)$ has everywhere been replaced by $r^{-1}J_m \mp J_m'$.

This expression for the radiated power simplifies somewhat for field points on the equatorial plane or the x–z and y–z planes, where the distinction between r_+ and r_- disappears. In particular, when the field point is aligned with the $\pm z$-axis then $r_+ = r_- = 1$ and

$$\frac{\mathrm{d}P}{\mathrm{d}\Omega} = 8\pi\mu^2 \sum_{m=1}^\infty m^2[J_m'(m)]^4. \tag{6.103}$$

The same is true in the degenerate case $\psi = 0$ (the doubled rotating rod) for any field point in the plane of rotation of the rod and in the case $\psi = \pi$ (the circular loop) for any point in the plane of the loop. At a physical level, $r_+ = r_- = 1$ if and only if the field point lies in the beaming direction of a cusp.

Now, for large m, the asymptotic form of $J'_m(m)$ is $0.41m^{-2/3}$ and so the sum on the right of (6.103) diverges. Thus the power radiated per unit solid angle is singular in the beaming directions of the cusps, as anticipated. However, for r close to 1,

$$J_m(mr) \sim 0.45m^{-1/3} \quad \text{and} \quad J'_m(mr) \sim 0.41m^{-2/3} \quad (6.104)$$

only when $m \ll m_{\text{crit}} = 3[2(1-r)]^{-3/2}$, while $J_m(mr)$ and $J'_m(mr)$ both fall off like $\exp(-m/m_{\text{crit}})$ for $m \gg m_{\text{crit}}$. For field points near the z-axis ($\sin\theta \ll 1$),

$$\lambda_\pm \sim 2(1-r_\pm) \sim \sin^2\theta[\kappa_1\cos\phi \pm \kappa_2\sin\phi]^2 \quad (6.105)$$

where $\kappa_1 = \cos(\psi/2)$ and $\kappa_2 = \sin(\psi/2)$.

Hence the power radiated per unit solid angle (6.102) can be approximated by truncating the sums at $m = m_{\text{max}}$, where

$$m_{\text{max}} = 3\sin^{-3}\theta[\kappa_1|\cos\phi| + \kappa_2|\sin\phi|]^{-3}. \quad (6.106)$$

This gives

$$\frac{dP}{d\Omega} \sim \mu^2[m_{\text{max}}^{1/3} + (\lambda_+^2 + 4\lambda_+\lambda_- + \lambda_-^2)m_{\text{max}} + \lambda_+^2\lambda_-^2 m_{\text{max}}^{5/3}]$$

$$\sim \mu^2 m_{\text{max}}^{1/3} \sim \mu^2[\kappa_1|\cos\phi| + \kappa_2|\sin\phi|]^{-1}\frac{1}{\sin\theta}. \quad (6.107)$$

Since the function $1/\sin\theta$ is integrable on the unit sphere, the total power P radiated by the loop is finite unless either κ_1 or κ_2 is zero. In the latter circumstance (the degenerate cases $\psi = 0$ or π) the total power P diverges because $dP/d\Omega$ is singular on the circles $\sin\phi = 0$ or $\cos\phi = 0$ rather than at isolated points. A more detailed examination of the weak-field radiation from a collapsing circular loop is given in section 6.10.

A final feature of the 1-harmonic limit is that for a fixed wavenumber m, the power radiated per unit solid angle has peaks (centred on the two beaming directions $\theta = 0$ and $\theta = \pi$) with angular radii $\Delta\theta_x \sim m^{-1/3}\kappa_1^{-1}$ and $\Delta\theta_y \sim m^{-1/3}\kappa_2^{-1}$ in the directions of the circles $\sin\phi = 0$ and $\cos\phi = 0$ respectively, as is evident from (6.106). Since the power P_m radiated in the mth harmonic has an angular density

$$\frac{dP_m}{d\Omega} \sim \mu^2 m^{-2/3} \quad (6.108)$$

near the beaming directions, the integrated power scales as

$$P_n \sim \mu^2 m^{-2/3}\Delta\theta_x\Delta\theta_y \sim \mu^2(\sin\psi)^{-1}m^{-4/3}. \quad (6.109)$$

This estimate can be used to accelerate the convergence of the series $P = \sum P_m$, although it should be noted that it applies only when $\Delta\theta_x$ and $\Delta\theta_y$ are both small or, equivalently, when $m \gg (\sin\psi)^{-3}$.

Vachaspati and Vilenkin [VV85] have numerically integrated the total power P radiated by the Vachaspati–Vilenkin solutions for $\alpha = 0$ and 0.5. In both cases $P = \gamma^0 \mu^2$ with a coefficient of radiative efficiency $\gamma^0 \sim 50$ when $\psi = \pi/2$. (Note that the parameter ϕ used by Vachaspati and Vilenkin is just $\pi - \psi$.) With $\alpha = 0$, the efficiency γ^0 increases to about 100 at $\psi = \pi/4$ and about 60 at $\psi = 3\pi/4$, and, of course, diverges at $\psi = 0$ and π. With $\alpha = 0.5$, the value of γ^0 remains fairly constant at about 50, although numerical accuracy is poor near $\psi = 0$ and π. Durrer [Dur89] has obtained similar results for the case $\alpha = 0.5$ over the range $\pi/4 \leq \psi < 3\pi/4$, although when $\alpha = 0$ her estimates for γ^0 are 10–30% smaller than Vachaspati and Vilenkin's. Durrer has also considered the case $\alpha = 0.8$, and finds that γ^0 increases from 48.1 at $\psi = \pi/4$ to 75.1 at $\psi = 3\pi/4$. Vachaspati and Vilenkin's estimates of γ^0 in the 1-harmonic case $\alpha = 0$ have been independently confirmed by Burden [Bur85] and Allen and Casper [AC94].

However, Allen and Casper [AC94] have carefully reanalysed the radiative efficiencies from a sequence of Vachaspati–Vilenkin loops with $\alpha = 0.5$, using both the standard Fourier decomposition method (combined with a fast Fourier transform) and the piecewise-linear approximation algorithm to be described in section 6.9, and conclude that γ^0 is, in this case, always greater than about 75. For example, when $\psi = \pi/2$ Allen and Casper calculate the value of γ^0 to be 97.2 ± 0.2, in contrast to Vachaspati and Vilenkin's quoted value of 54.0 and Durrer's of 56.9. There seems to be little doubt that Allen and Casper's rigorous analysis is the more reliable and that the source of the errors in the earlier published values of γ^0 lies in mistaken estimates of the contribution of the tail of the series $\sum P_m$, which Vachaspati and Vilenkin truncate at $m = 30$ (and Durrer at $m = 50$). Vachaspati and Vilenkin claim, on the basis of their numerical results, that P_m falls off as m^{-3} for large m, whereas Allen and Casper find (more plausibly) that $P_m \sim m^{-1.25}$ for m between 100 and 300. Durrer seems to have included no correction for the tail contribution in her estimates at all.

Finally, mention should be made of the one published estimate of the radiative efficiency from a non-trivial member of the Turok class of 1–3/1 harmonic solutions, which are described by the mode functions (4.82) and (4.83). Vachaspati and Vilenkin [VV85] have considered the case $\alpha = 0.5$ and $\psi = \pi$, and conclude that γ^0 lies between 32.4 and 64.4. The lower bound is the value of $\sum P_m$ truncated at $m = 30$, without any correction for the contribution of the tail, while the upper bound includes a tail correction estimated on the basis of a numerical fit of the form $P_m \sim m^{-1.17}$ for large m.

6.5.3 Power from the p/q harmonic solutions

Burden's analysis of the power per unit solid angle radiated by the p/q harmonic solutions in [Bur85] is very similar to the above treatment of the 1-harmonic solutions (which, of course, are just p/q harmonic solutions with $p = q = 1$). As was seen in section 4.4.2, the parametrization of the p/q harmonic solutions

can always be adjusted so that p and q are relatively prime and the loops are self-intersecting unless either p or q is 1. However, in contrast to the conventions of section 4.4.2, where p and q can be either positive or negative and ψ ranges over $[0, \pi)$, it will here be more convenient to constrain p and q to be positive and allow ψ to range over $[0, 2\pi)$. The solutions of section 4.4.2 with $pq < 0$ are then mapped onto the interval $[\pi, 2\pi)$.

To facilitate comparison with the 1-harmonic solutions it is also convenient to rotate the coordinate axes so that the p/q mode functions take the form:

$$\overline{\mathbf{a}}(\xi_+) = p^{-1}[\sin(\psi/2)\sin(p\xi_+), \cos(\psi/2)\sin(p\xi_+), \cos(p\xi_+)] \qquad (6.110)$$

and

$$\overline{\mathbf{b}}(\xi_-) = q^{-1}[-\sin(\psi/2)\sin(q\xi_-), \cos(\psi/2)\sin(q\xi_-), \cos(q\xi_-)]. \qquad (6.111)$$

All members of the family with $0 < \psi < \pi$ or $\pi < \psi < 2\pi$ then support cusps with beaming directions aligned with the $\pm z$-axes. In the degenerate planar cases $\psi = 0$ and π the cusps are permanent and their beam directions fill out the y–z and x–z planes respectively[1].

The most important difference between the 1-harmonic case and the more general case is that the power radiated at a frequency $\omega_m = 4\pi m/L$ is zero unless m is an integer multiple of pq. At a physical level this is not surprising, as the trajectory of a p/q harmonic solution is periodic in the light-cone coordinates σ_+ and σ_- with periods L/p and L/q respectively. Mathematically, the result follows from the fact that the components of the Fourier transforms A^μ and B^ν defined by (6.69) and (6.70) are all of the form

$$I = \frac{1}{2\pi} \int_0^{2\pi} e^{i[(m+j)\xi - u\sin(c\xi) - v\cos(c\xi)]}\, d\xi \qquad (6.112)$$

with $c = p$ or q and $j = 0$ or $\pm c$. If $m + j$ is an integer multiple kc of c then $I = (\frac{u-iv}{w})^k J_k(w)$ where $w = (u^2 + v^2)^{1/2}$ but $I = 0$ otherwise. So at least one of the transforms A^μ and B^ν will vanish unless $m = n|pq|$ for some positive integer n.

In view of this property, the power radiated per unit solid angle by the p/q harmonic solutions turns out to be

$$\frac{dP}{d\Omega} = 8\pi(pq)^2\mu^2 \sum_{n=1}^{\infty} n^2[(J_n^{+\prime}J_n^{-\prime} + \lambda_+\lambda_- J_n^+ J_n^-)^2 + (\lambda_+ J_n^+ J_n^{-\prime} + \lambda_- J_n^- J_n^{+\prime})^2]$$

$$\qquad (6.113)$$

where $\lambda_\pm = (r_\pm^{-2} - 1)^{1/2}$ as before, and now

$$J_n^+ = J_{np}(npr_+) \qquad \text{and} \qquad J_n^- = J_{nq}(nqr_-) \qquad (6.114)$$

[1] Unfortunately, the gauge choices made for the p/q harmonic solutions and the Vachaspati–Vilenkin solutions with $\alpha = 0$ are slightly different, with the result that the expressions for the mode functions given in this section do not agree exactly when $p = q = 1$. However, the p/q solutions are easily converted to the Vachaspati–Vilenkin form by replacing τ with $\tau - \pi/2$ and σ with $\pi/2 - \sigma$.

with

$$r_\pm = [1 - \cos^2(\psi/2 \mp \phi) \sin^2 \theta]^{1/2} \qquad (6.115)$$

again defined in terms of the field direction $\mathbf{n} = [\cos\phi \sin\theta, \sin\phi \sin\theta, \cos\theta]$. In line with the previous results, $dP/d\Omega$ is finite everywhere except in the beaming directions, and the total power P is finite except in the degenerate cases $\psi = 0$ and π. Also, the power P_n in the nth harmonic scales as $\mu^2 n^{-4/3}$.

Numerical calculations of the total power P made by Burden in the cases $q = 1$ and $p = 1, 2, 3$ and 5 indicate that the coefficient of radiative efficiency γ^0 remains in the range 50–120 for ψ between $4\pi/3$ and $5\pi/3$, with γ^0 increasing monotonically with p. For $q = 1$, $p = 15$ and $\psi = 3\pi/2$, the radiative efficiency increases to $\gamma^0 \sim 150$. The cases $q = 1$ and $p = 3$ and 5 have also been examined by Jean Quashnock and David Spergel [QS90] and Allen and Casper [AC94], with good agreement with Burden in both instances. (In fact, all the quoted values of γ^0 agree to within 8%.)

Although the loop solutions examined in this section are all extremely idealized, it is encouraging to note that the radiative efficiencies inferred from more realistic simulations of the primordial cosmic string network lie in the same general range. For example, Bruce Allen and Paul Shellard [AS92] have numerically evolved a network of both long strings and string loops in an expanding Robertson–Walker metric and calculated that the mean value of γ^0 over the ensemble of loops remained in the approximate range 65–70 over a simulation time corresponding to an expansion of the horizon size by a factor of more than 60. Furthermore, as will be seen later, there are good theoretical reasons for believing that γ^0 can never fall below a minimum value $\gamma^0_{\text{min}} \approx 39$.

6.6   Power radiated by a helical string

The weak-field formalism can also be adapted to give an estimate of the power per unit length radiated by an infinite string. The case of a helical string of the type described in section 4.1.4 has been treated in detail by Maria Sakellariadou [Sak90]. The trajectory of a helical string has the form $X^\mu = [\tau, \frac{1}{2}(\mathbf{a} + \mathbf{b})]$, with

$$\mathbf{a}(\sigma_+) = [R \cos(k\sigma_+), R \sin(k\sigma_+), \sigma_+ \sin\alpha] \qquad (6.116)$$

and

$$\mathbf{b}(\sigma_-) = [R \cos(k\sigma_-), -R \sin(k\sigma_-), -\sigma_- \sin\alpha] \qquad (6.117)$$

where $k = R^{-1} \cos\alpha$ and α is the pitch angle of the helix at maximum extension. The trajectory is periodic in $t \equiv \tau$ with period $2\pi k^{-1}$, and is also periodic in z with period $2\pi k^{-1} \sin\alpha$. In the limit $\alpha \to \pi/2$ the trajectory degenerates into a straight line along the z-axis.

The wave zone in this case consists of field points $\mathbf{x} = [x, y, z]$ for which $\rho \gg R$, where ρ is the cylindrical radius $(x^2 + y^2)^{1/2}$. The power radiated by the

string per unit longitudinal angle ϕ and unit length in the z-direction is

$$\frac{\mathrm{d}P}{\mathrm{d}\phi\,\mathrm{d}z} = \rho \sum_{i=1}^{2} \widehat{q}^i\, \mathfrak{T}^{it} \tag{6.118}$$

where $\widehat{\mathbf{q}} = \mathbf{q}/\rho$ for $\mathbf{q} = [x, y, 0]$, and $\mathfrak{T}^{\mu\nu}$ is the gravitational stress–energy pseudo-tensor given by (6.56).

Because of the periodicity of the trajectory in z, the stress–energy tensor of the string can be decomposed as a Fourier series in both t and z:

$$T^{\mu\nu}(t, \mathbf{x}) = \sum_{m,n=-\infty}^{\infty} T^{\mu\nu}(\kappa_n, \omega_m, \mathbf{q})e^{\mathrm{i}\kappa_n z - \mathrm{i}\omega_m t} \tag{6.119}$$

where $\omega_m = mk$, $\kappa_n = nk/\sin\alpha$ and

$$T^{\mu\nu}(\kappa_n, \omega_m, \mathbf{x}) = \frac{k^2}{4\pi^2 \sin\alpha} \int_0^{2\pi k^{-1}} \mathrm{d}t \int_0^{2\pi k^{-1}\sin\alpha} \mathrm{d}z\, T^{\mu\nu}(t, \mathbf{x})e^{\mathrm{i}\omega_m t - \mathrm{i}\kappa_n z}. \tag{6.120}$$

The solution (6.6) for the metric perturbation $h_{\mu\nu}$ then becomes

$$\begin{aligned}
h_{\mu\nu}(t, \mathbf{x}) &= -4 \sum_{m,n=-\infty}^{\infty} \int \frac{S_{\mu\nu}(\kappa_n, \omega_m, \mathbf{q}')}{|\mathbf{x} - \mathbf{x}'|} e^{\mathrm{i}\kappa_n z' + \mathrm{i}\omega_m |\mathbf{x}-\mathbf{x}'|} e^{-\mathrm{i}\omega_m t}\, \mathrm{d}z'\, \mathrm{d}^2 q' \\
&= -4\mathrm{i}\pi \sum_{m,n=-\infty}^{\infty} e^{\mathrm{i}\kappa_n z - \mathrm{i}\omega_m t} \int S_{\mu\nu}(\kappa_n, \omega_m, \mathbf{q}') F_{mn}(\mathbf{q}, \mathbf{q}')\, \mathrm{d}^2 q'
\end{aligned} \tag{6.121}$$

where

$$F_{mn}(\mathbf{q}, \mathbf{q}') = H_0^{(1)}[(\omega_m^2 - \kappa_n^2)^{1/2}|\mathbf{q} - \mathbf{q}'|] \tag{6.122}$$

and $H_0^{(1)}$ is the Hankel function of order 0.

For values of $\rho = |\mathbf{q}|$ large compared to $|\mathbf{q}'| \le R$,

$$F_{mn}(\mathbf{q}, \mathbf{q}') \approx (2/\pi)^{1/2} e^{-\mathrm{i}\pi/4} \frac{e^{\mathrm{i}(\omega_m^2 - \kappa_n^2)^{1/2}(\rho - \widehat{\mathbf{q}}\cdot\mathbf{q}')}}{(\omega_m^2 - \kappa_n^2)^{1/4}\rho^{1/2}} \tag{6.123}$$

provided that $\omega_m^2 > \kappa_n^2$. If $\omega_m^2 < \kappa_n^2$ then F_{mn} falls off exponentially with ρ and can be ignored. Hence, the asymptotic form of the metric perturbation is

$$\begin{aligned}
h_{\mu\nu}(t, \mathbf{x}) \approx\ &-4(2\pi)^{1/2} e^{\mathrm{i}\pi/4} \sum_{\omega_m^2 > \kappa_n^2} \frac{e^{\mathrm{i}\kappa_n z - \mathrm{i}\omega_m t + \mathrm{i}(\omega_m^2 - \kappa_n^2)^{1/2}\rho}}{(\omega_m^2 - \kappa_n^2)^{1/4}\rho^{1/2}} \\
&\times \int S_{\mu\nu}(\kappa_n, \omega_m, \mathbf{q}')e^{-\mathrm{i}(\omega_m^2 - \kappa_n^2)^{1/2}\widehat{\mathbf{q}}\cdot\mathbf{q}'}\, \mathrm{d}^2 q'.
\end{aligned} \tag{6.124}$$

The important feature of this expression is that $h_{\mu\nu}$ has the generic form

$$h_{\mu\nu}(t, \mathbf{x}) \approx \sum_{\omega_m^2 > \kappa_n^2} E_{\mu\nu}(\kappa_n, \omega_m, \mathbf{q}) e^{-ic_\lambda x^\lambda} \tag{6.125}$$

where

$$c^\mu = [\omega_m, (\omega_m^2 - \kappa_n^2)^{1/2} \widehat{\mathbf{q}}, \kappa_n] \tag{6.126}$$

is null, and $E_{\mu\nu}$ can be read off from (6.124).

After averaging over a spacetime region with dimensions large compared with the characteristic wavelength of the gravitational field the second-order Ricci tensor takes the form

$$R^{\mu\nu} = \tfrac{1}{2} \sum_{m=1}^{\infty} \sum_{\kappa_n < \omega_m} (E^{\kappa\lambda} E_{\kappa\lambda}^* - \tfrac{1}{2} E E^*) c^\mu c^\nu \tag{6.127}$$

and the power radiated per unit ϕ and z is

$$\frac{\mathrm{d}P}{\mathrm{d}\phi \, \mathrm{d}z} = \sum_{m=1}^{\infty} \sum_{\kappa_n < \omega_m} \frac{\rho \omega_m (\omega_m^2 - \kappa_n^2)^{1/2}}{16\pi} (E^{\kappa\lambda} E_{\kappa\lambda}^* - \tfrac{1}{2} E E^*)$$

$$= 2 \sum_{m=1}^{\infty} \sum_{\kappa_n < \omega_m} \omega_m (\bar{T}^{\mu\nu} \bar{T}_{\mu\nu}^* - \tfrac{1}{2} |\bar{T}_\mu^\mu|^2) \tag{6.128}$$

where

$$\bar{T}^{\mu\nu} \equiv \int T^{\mu\nu}(\kappa_n, \omega_m, \mathbf{q}') e^{-i(\omega_m^2 - \kappa_n^2)^{1/2} \widehat{\mathbf{q}} \cdot \mathbf{q}'} \, \mathrm{d}^2 q'$$

$$= \frac{\mu k^2}{4\pi^2 \sin\alpha} \int_0^{2\pi/k} \mathrm{d}\tau \int_0^{2\pi/k} \mathrm{d}\sigma \, (V^\mu V^\nu - N^\mu N^\nu) e^{i\omega_m \tau - i\kappa_n z - i(\omega_m^2 - \kappa_n^2)^{1/2} \widehat{\mathbf{q}} \cdot \mathbf{r}}. \tag{6.129}$$

This integral can be simplified by transforming to reduced light-cone coordinates $\xi_\pm = k(\tau \pm \sigma)$. For this purpose it is convenient to integrate τ over two complete periods $2\pi k^{-1}$, as then ξ_+ and ξ_- both range over $[0, 4\pi]$. After inserting the trajectory $\mathbf{r}$ specific to the helical string (6.129) can be expressed in the form

$$\bar{T}^{\mu\nu} = \frac{\mu}{\sin\alpha} A^{(\mu} B^{\nu)} \tag{6.130}$$

where

$$A^\mu = \frac{1}{4\pi} \int_0^{4\pi} e^{i(m-n)\xi_+/2 - i\beta_{mn} \cos\alpha [\cos\phi \sin(\xi_+) - \sin\phi \cos(\xi_+)]/2} [1, \mathbf{a}'] \, \mathrm{d}\xi_+ \tag{6.131}$$

and

$$B^\nu = \frac{1}{4\pi} \int_0^{4\pi} e^{i(m+n)\xi_-/2 - i\beta_{mn}\cos\alpha[\cos\phi\sin(\xi_-) + \sin\phi\cos(\xi_-)]/2}[1, \mathbf{b}']\,d\xi_-$$
(6.132)

with $\beta_{mn} = (m^2 - n^2/\sin^2\alpha)^{1/2}$,

$$\mathbf{a}' = [-\cos\alpha\sin\xi_+, \cos\alpha\cos\xi_+, \sin\alpha]$$
(6.133)

and $\mathbf{b}'$ given by the corresponding expression with ξ_- in place of ξ_+.

In view of the earlier discussion of the Fourier integrals associated with the p/q harmonic solutions, it is clear that the integrals A^μ and B^ν appearing here will both vanish unless $m + n$ is an even integer. After a calculation similar to that given for the 1-harmonic solutions in the previous section the radiated power turns out to be

$$\frac{dP}{d\phi\,dz} = \frac{\mu^2 k\cos^4\alpha}{\sin^2\alpha} \sum_{m=1}^{\infty} m \sum_{0 \le n < m\sin\alpha}' [(J_a'^2 + \gamma_a J_a^2)(J_b'^2 + \gamma_b J_b^2) - 4\widehat{\gamma} J_a J_b J_a' J_b']$$
(6.134)

with $a = (m - n)/2$ and $b = (m + n)/2$, and

$$\gamma_c = \frac{4c^2}{\beta_{mn}^2 \cos^2\alpha} - 1 \qquad \widehat{\gamma} = \left(\frac{4ab}{\beta_{mn}^2} - 2\right)\sec^2\alpha + 1 \qquad J_c = J_c(\tfrac{1}{2}\beta_{mn}\cos\alpha).$$
(6.135)

The prime on the second summation sign in (6.134) indicates that only values of n for which $m + n$ is even should be included in the summation (and so strictly speaking the outer summation should begin at $m = 2$, as the modes with $m = 1$ make no contribution).

Since the right-hand side of (6.134) has no dependence on the longitudinal angle ϕ the total power radiated per unit length in the z-direction, dP/dz, is found by multiplying (6.134) by 2π. Also $J_c \sim \cos^c\alpha$ for α close to $\pi/2$, and all the Bessel functions appearing in (6.134) have $a, b \ge 1$, so in the limit as the trajectory tends to a static straight line the power falls off as $\cos^4\alpha$. In the opposite limit, $\alpha \to 0$, the winding number of the helix (the number of turns of the string per unit length in the z-direction) diverges, and the world sheet approaches that of a cylinder composed of a continuous sheet of collapsing circular strings centred on the z-axis. Since the restriction on the range of n ensures that the β_{mn} remain real and bounded as α tends to 0, the power per unit length in this limit diverges as α^{-2}. Sakellariadou [Sak90] has numerically evaluated the double summation in (6.134) and shown that it remains of order unity for all values of α.

The expression (6.134) can be broken naturally into two parts, one containing all the modes with even values of m and the other containing all the odd modes. In each part, the power radiated per mode turns out to be a monotonically decreasing function of the mode number m, but the power in each even mode ($m = 2j$) is in all cases greater than the power in the preceding odd mode ($m = 2j - 1$), with the

difference between the even and odd modes increasing as α increases. In the limit as $\alpha \to \pi/2$ almost all the power is emitted by the lowest even mode ($m = 2$).

6.7   Radiation from long strings

Sakellariadou's analysis of the gravitational radiation from a helical string has been extended to arbitrary periodic disturbances of an infinite straight string by Mark Hindmarsh [Hin90]. Without loss of generality, the spacelike cross sections of the string can be assumed to have infinite range in the z-direction. If the string's trajectory $\mathbf{r}(\tau, \sigma)$ is periodic in $\tau \equiv t$ with a period $2\pi k^{-1}$ for some constant k then the spacelike cross sections of $\mathbf{r}$ will be periodic in σ with the same period, save for a shift proportional to σ in the z-direction. For causal disturbances, the pattern length in the z-direction can be no greater than the period $2\pi k^{-1}$ and so will be written as $2\pi k^{-1} \sin\alpha$ for some α in $(0, \pi/2)$.

   This allows the notation of the previous section to be retained unchanged and, in particular, the Fourier transforms A^μ and B^ν appearing in the symmetrized product (6.130) now take the generalized forms

$$A^\mu = \frac{k}{4\pi} \int_0^{4\pi/k} e^{i\omega_m \sigma_+/2 - i\mathbf{c}\cdot\mathbf{a}(\sigma_+)/2}[1, \mathbf{a}'(\sigma_+)]\, d\sigma_+ \qquad (6.136)$$

and

$$B^\nu = \frac{k}{4\pi} \int_0^{4\pi/k} e^{i\omega_m \sigma_-/2 - i\mathbf{c}\cdot\mathbf{b}(\sigma_-)/2}[1, \mathbf{b}'(\sigma_-)]\, d\sigma_- \qquad (6.137)$$

with $\mathbf{c} = [(\omega_m^2 - \kappa_n^2)^{1/2}\widehat{\mathbf{q}}, \kappa_n]$, $\omega_m = mk$ and $\kappa_n = nk/\sin\alpha$. The expression (6.128) for the power radiated per unit ϕ and z can then be written in the reduced form

$$\frac{dP}{d\phi\, dz} = \frac{\mu^2}{\sin^2\alpha} \sum_{m=1}^{\infty} \sum_{\kappa_n < \omega_m} \omega_m(|A^\mu A^*_\mu||B^\nu B^*_\nu| + |A^\mu B^*_\mu|^2 - |A^\mu B_\mu|^2). \quad (6.138)$$

   For weak excitations of the string the transverse mode functions $\mathbf{a}'_\perp = [a'_x, a'_y, 0]$ and $\mathbf{b}'_\perp = [b'_x, b'_y, 0]$ are small compared to the corresponding longitudinal mode functions a'_z and b'_z. To second order in the transverse excitations the gauge conditions $|\mathbf{a}'|^2 = |\mathbf{b}'|^2 = 1$ therefore read:

$$a'_z \approx 1 - \tfrac{1}{2}|\mathbf{a}'_\perp|^2 \qquad \text{and} \qquad b'_z \approx -1 + \tfrac{1}{2}|\mathbf{b}'_\perp|^2 \qquad (6.139)$$

and, in particular, (since $a_z \approx \sigma_+$ and $b_z \approx -\sigma_-$ to leading order) it follows that $\sin\alpha \approx 1$.

   Furthermore,

$$e^{i\omega_m \sigma_+/2 - i\mathbf{c}\cdot\mathbf{a}(\sigma_+)/2} \approx e^{i(\omega_m - \kappa_n)\sigma_+/2}[1 - \tfrac{1}{2}i(\omega_m^2 - \kappa_n^2)^{1/2}\widehat{\mathbf{q}}\cdot\mathbf{a}_\perp] \qquad (6.140)$$

and so if A^μ is decomposed in the form $[A^t, \mathbf{A}_\perp, A^z]$ then $A^z \approx A^t$ where

$$A^t = \frac{k}{4\pi} \int_0^{4\pi/k} e^{i\omega_m\sigma_+/2 - i\mathbf{c}\cdot\mathbf{a}(\sigma_+)/2} \, d\sigma_+$$

$$\approx -\frac{ik}{8\pi}(\omega_m^2 - \kappa_n^2)^{1/2} \int_0^{4\pi/k} e^{i(\omega_m - \kappa_n)\sigma_+/2}\widehat{\mathbf{q}} \cdot \mathbf{a}_\perp \, d\sigma_+. \quad (6.141)$$

Similarly, after integrating by parts once,

$$\widehat{\mathbf{q}} \cdot \mathbf{A}_\perp \approx \frac{k}{4\pi} \int_0^{4\pi/k} e^{i(\omega_m - \kappa_n)\sigma_+/2}\widehat{\mathbf{q}} \cdot \mathbf{a}'_\perp \, d\sigma_+$$

$$= -\frac{ik}{8\pi}(\omega_m - \kappa_n) \int_0^{4\pi/k} e^{i(\omega_m - \kappa_n)\sigma_+/2}\widehat{\mathbf{q}} \cdot \mathbf{a}_\perp \, d\sigma_+. \quad (6.142)$$

and hence

$$A^t \approx \left(\frac{\omega_m + \kappa_n}{\omega_m - \kappa_n}\right)^{1/2} \widehat{\mathbf{q}} \cdot \mathbf{A}_\perp. \quad (6.143)$$

The corresponding calculations for the **b** mode give $B^z \approx -B^t$ and

$$B^t \approx \left(\frac{\omega_m - \kappa_n}{\omega_m + \kappa_n}\right)^{1/2} \widehat{\mathbf{q}} \cdot \mathbf{B}_\perp. \quad (6.144)$$

Thus the terms appearing in the expression (6.138) for the radiated power reduce to

$$|A^\mu A_\mu^*| \approx |\mathbf{A}_\perp|^2 \qquad |B^\nu B_\nu^*| \approx |\mathbf{B}_\perp|^2 \quad (6.145)$$

and

$$A^\mu B_\mu \approx 2(\widehat{\mathbf{q}} \cdot \mathbf{A}_\perp)(\widehat{\mathbf{q}} \cdot \mathbf{B}_\perp) - \mathbf{A}_\perp \cdot \mathbf{B}_\perp \quad (6.146)$$

(with an analogous identity for $A^\mu B_\mu^*$).

An important consequence of these relations is that a long string will not radiate gravitationally (to leading order in the transverse excitations at least) unless both $\mathbf{A}_\perp$ and $\mathbf{B}_\perp$ are non-zero or, equivalently, unless the string supports transverse modes propagating in both directions. This result is in accord with the behaviour of travelling-wave solutions, which are distinguished by the feature that either $\mathbf{a}'_\perp$ or $\mathbf{b}'_\perp$ is zero and are known to be self-consistent solutions of the *full* Einstein equations (see section 9.1) whatever the shape of the non-zero mode. Since the wave pattern in a travelling-wave solution propagates without distortion or dissipation it is clearly non-radiative, although the string still exerts a non-trivial gravitational field.

The expression (6.138) for the radiated power can be simplified further by integrating over the azimuthal angle ϕ. In view of the identity

$$\int_0^{2\pi} (\widehat{\mathbf{q}} \cdot \mathbf{A})(\widehat{\mathbf{q}} \cdot \mathbf{B}) \, d\phi = \pi\mathbf{A} \cdot \mathbf{B} \quad (6.147)$$

the power radiated per unit length of the string becomes

$$\frac{\mathrm{d}P}{\mathrm{d}z} \approx 2\pi\mu^2 k \sum_{m=1}^{\infty} \sum_{0 \leq n < m} m(|\mathbf{A}_\perp|^2|\mathbf{B}_\perp|^2 + |\mathbf{A}_\perp \cdot \mathbf{B}_\perp|^2 - |\mathbf{A}_\perp \cdot \mathbf{B}_\perp^*|^2) \quad (6.148)$$

where

$$\mathbf{A}_\perp \approx \frac{k}{4\pi} \int_0^{4\pi/k} \mathrm{e}^{\mathrm{i}(m-n)k\sigma_+/2} \mathbf{a}'_\perp \,\mathrm{d}\sigma_+ \quad (6.149)$$

and

$$\mathbf{B}_\perp \approx \frac{k}{4\pi} \int_0^{4\pi/k} \mathrm{e}^{\mathrm{i}(m+n)k\sigma_-/2} \mathbf{b}'_\perp \,\mathrm{d}\sigma_-. \quad (6.150)$$

Although the range of integration in (6.149) and (6.150) has for reasons mentioned in section 6.6 been fixed at $[0, 4\pi/k]$, the functions $\mathbf{a}'_\perp$ and $\mathbf{b}'_\perp$ separately have periods $2\pi/k$. The Fourier transforms $\mathbf{A}_\perp$ and $\mathbf{B}_\perp$ are thus both zero unless $m + n$ is an even integer, just as was the case for the helical string. It is therefore natural to replace m and n with $a = (m - n)/2$ and $b = (m + n)/2$, and to identify the corresponding Fourier modes as $\mathbf{A}_\perp^a$ and $\mathbf{B}_\perp^b$.

Now any individual Fourier mode, $\mathbf{A}_\perp^a$ say, can always be chosen to be real by suitably rezeroing σ_+, for if $\mathbf{A}_\perp^a = \mathrm{e}^{\mathrm{i}\theta}|\mathbf{A}_\perp^a|$ the phase factor θ will disappear after replacing σ_+ with $\tilde{\sigma}_+ = \sigma_+ - \theta/(ka)$. The contribution of $\mathbf{A}_\perp^a$ to the total radiated power per unit length (6.148) is then:

$$\frac{\mathrm{d}P_a}{\mathrm{d}z} \approx 2\pi\mu^2 k |\mathbf{A}_\perp^a|^2 \sum_{b=1}^{\infty} (a + b)|\mathbf{B}_\perp^b|^2. \quad (6.151)$$

Also, it was seen in section 3.3 that the energy of a segment of string with parametric length $\Delta\sigma$ is $\Delta E = \mu\Delta\sigma$. In view of the approximations (6.139) and the fact that

$$\frac{\mathrm{d}\sigma}{\mathrm{d}z} = 2(a'_z - b'_z)^{-1} \quad (6.152)$$

it follows that the total energy of a string segment with fundamental length $2\pi/k$ in the z-direction is

$$\Delta E \approx \mu \int_0^{2\pi/k} [1 + \tfrac{1}{4}|\mathbf{a}'_\perp|^2 + \tfrac{1}{4}|\mathbf{b}'_\perp|^2] \,\mathrm{d}z$$

$$= 2\pi\mu k^{-1} \left[1 + \tfrac{1}{2} \sum_{a=1}^{\infty} |\mathbf{A}_\perp^a|^2 + \tfrac{1}{2} \sum_{b=1}^{\infty} |\mathbf{B}_\perp^b|^2 \right] \quad (6.153)$$

as $\mathrm{d}z = \mathrm{d}\sigma_+ = -\mathrm{d}\sigma_-$ on surfaces of constant t.

Thus the averaged energy per unit length in the z-direction is

$$\bar{\mu} \approx \mu \left[1 + \tfrac{1}{2} \sum_{a=1}^{\infty} |\mathbf{A}_\perp^a|^2 + \tfrac{1}{2} \sum_{b=1}^{\infty} |\mathbf{B}_\perp^b|^2 \right] \quad (6.154)$$

and so it is possible, at this level of approximation, to associate an energy per unit length with each of the Fourier modes.

If it is assumed that the partial power P_a radiated by the Fourier mode $\mathbf{A}_\perp^a$ is extracted solely from the energy associated with that mode then equation (6.151) can be rewritten in the form

$$\frac{\mathrm{d}}{\mathrm{d}t}|\mathbf{A}_\perp^a|^2 \approx -4\pi\mu k|\mathbf{A}_\perp^a|^2(a+\overline{b})\sum_{b=1}^{\infty}|\mathbf{B}_\perp^b|^2 \qquad (6.155)$$

where $\overline{b}$ is an average wavenumber for the **b** modes, defined by

$$\overline{b} = \sum_{b=1}^{\infty}b|\mathbf{B}_\perp^b|^2 \Big/ \sum_{b=1}^{\infty}|\mathbf{B}_\perp^b|^2. \qquad (6.156)$$

Now, a number of simulations of realistic string networks [BB88, BB89, AS90] indicate that the average energy per unit length is typically of order $\bar{\mu} \sim 2\mu$, and so $\sum_{b=1}^{\infty}|\mathbf{B}_\perp^b|^2 \sim 1$. For high-frequency modes with $a \gg \overline{b}$ (6.155), therefore, predicts exponential decay of the mode energy with a characteristic decay time $\Delta t \sim (4\pi\mu ka)^{-1}$. The corresponding fundamental wavelength is $r = 2\pi/(ka)$, and so it follows that gravitational radiation will suppress high-frequency structure with a characteristic dimension r after a time

$$\Delta t \sim r/(8\pi^2\mu). \qquad (6.157)$$

Of course, the validity of this approximation depends critically on the assumption that the partial power P_a is extracted solely from the energy of the corresponding Fourier mode $\mathbf{A}_\perp^a$, but calculations incorporating the full back-reaction effects of linearized gravity, to be discussed later in section 6.11, suggest that (6.157) is indeed a reasonable order-of-magnitude estimate of the efficiency of radiative dampening.

6.8   Radiation of linear and angular momentum

6.8.1   Linear momentum

Although most analytic and numerical studies of the asymptotic gravitational field due to a cosmic string to date have focused on estimates of the radiated power, important information about the dynamics of a string can also be extracted from the rate at which the string radiates linear and angular momentum.

Calculating the flux of linear momentum is comparatively straightforward. A pulse of gravitational radiation with energy E also carries a momentum $\mathbf{p} = E\mathbf{n}$, where $\mathbf{n}$ is the unit vector in the direction of propagation, and so the total flux of momentum from a string loop is

$$\frac{\mathrm{d}\mathbf{p}}{\mathrm{d}t} = \int \frac{\mathrm{d}P}{\mathrm{d}\Omega}\mathbf{n}\,\mathrm{d}\Omega \qquad (6.158)$$

where $dP/d\Omega$ is the power loss per unit solid angle (6.63). Except in cases where it is clear from the symmetry of the string's trajectory that the total momentum flux is identically zero, the string typically emits a non-zero net flux and consequently accelerates in the opposite direction. This is the origin of the 'gravitational rocket effect'.

Of the trajectories examined in section 6.5 the kinked cuspless loop and the Turok solutions possess mirror symmetry and so do not radiate a net flux of momentum. The same is true of Burden's p/q harmonic solutions if p and q are both odd. However, the Vachaspati–Vilenkin solutions described by the mode functions (6.82) and (6.83) are asymmetric if $\alpha \neq 0$ or 1, and Vachaspati and Vilenkin [VV85] have calculated the momentum flux radiated by the loops with the parameter values $\alpha = 0.5$ and $\psi = \pi/4$, $\pi/2$ and $3\pi/4$. They find that $|d\mathbf{P}/dt| = \gamma_P \mu^2$ with the coefficient γ_P ranging from 5 to 12 (and, as was seen earlier, a radiative efficiency γ^0 in all three cases of the order of 50).

Vachaspati and Vilenkin go on to argue that the gravitational back-reaction on the loop will ultimately accelerate it to a speed of the order of $|d\mathbf{P}/dt|\Delta t/M$ (where M is the mass and Δt the radiative lifetime of the loop) or, equivalently, γ_P/γ^0. For the three trajectories they examined the inferred back-reaction speed γ_P/γ^0 lies between about 10% and 20% of the speed of light. However, this conclusion depends critically on the assumption that the torque on the loop induced by the radiation of angular momentum does not significantly rotate the direction of recoil. The validity of this assumption will be examined in more detail in section 6.11.

Durrer [Dur89] has also attempted to calculate the coefficient γ_P for a selection of Vachaspati–Vilenkin solutions with both $\alpha = 0.5$ and $\alpha = 0.8$. Her estimates in the case $\alpha = 0.5$ are comparable to Vachaspati and Vilenkin's for $\psi = \pi/4$ and $3\pi/4$ but differ substantially when $\psi = \pi/2$ (Durrer has $\gamma_P = 2.35$ whereas Vachaspati and Vilenkin have $\gamma_P = 12.0$). In the case $\alpha = 0.8$, with $\psi = \pi/4$, $\pi/2$ and $3\pi/4$ again, Durrer finds that the value of γ_P ranges from about 0.8 to 2.3. However, Allen *et al* [ACO95] have recalculated γ_P using the piecewise-linear numerical algorithm of section 6.9 in the cases $\alpha = 0.5$ and $\alpha = 0.8$, and conclude that the value of γ_P has a considerably larger range and wider variability than either Durrer's or Vachaspati and Vilenkin's results would suggest. In both cases Allen *et al* find that the maximum value of γ_P is about 20 ± 1 (at $\psi = \pi/2$ when $\alpha = 0.5$ and at $\psi = 2\pi/3$ when $\alpha = 0.8$), but that γ_P fluctuates dramatically before falling off to 0 as $\psi \to 0$ or π. The acceleration factor γ_P/γ^0 is, therefore, about 20% in the case $\alpha = 0.5$, $\psi = \pi/2$, but is negligibly small near $\psi = 0$ and π.

A further study by Casper and Allen [CA94] of an ensemble of 11 625 string loops—generated by evolving a large set of parent loops forward in time (in the absence of radiative effects) until only non-intersecting daughter loops remain—has found that most of the daughter loops radiate an insignificant fraction of their total linear momentum. The inferred back-reaction speed γ_P/γ^0 is, in most cases,

smaller than about 10% of the speed of light, whereas the bulk speed $|\mathbf{V}|$ of the loops is typically much larger.

6.8.2   Angular momentum

The net flux of angular momentum from a cosmic string can be evaluated using a procedure similar to that outlined in section 6.4 for the radiated power. In the wave zone, the rate at which the gravitational field carries off angular momentum $\mathbf{J}$ can be represented as a surface integral

$$P_{\mathbf{J}}^a = \int_{\partial\mathfrak{B}} r^3 \sum_{j,k,m=1}^{3} \varepsilon^{ajk} n^j n^m \mathfrak{T}^{mk} \, d\Omega \tag{6.159}$$

where $\mathfrak{B}$ is a sphere of radius r (much greater than the characteristic source size L), $\mathbf{n} = \mathbf{x}/r$ is the unit vector to the field point as before, $\mathfrak{T}^{\mu\nu}$ is the gravitational stress–energy pseudo-tensor defined by (6.56), and ε^{ajk} is the three-dimensional Levi-Cività symbol.

To calculate $P_{\mathbf{J}}^a$ for a periodic source, the metric perturbation $h_{\mu\nu}$ is again decomposed as a harmonic series

$$h_{\mu\nu}(t, \mathbf{x}) = \sum_{p=-\infty}^{\infty} E_{\mu\nu}(\omega_p, \mathbf{x}) e^{-i\omega_p c_\lambda x^\lambda} \tag{6.160}$$

where $\omega_p = 2\pi p/T$ and $c^\mu = [1, \mathbf{n}]$, and

$$E_{\mu\nu}(\omega_p, \mathbf{x}) = -4 \int |\mathbf{x} - \mathbf{x}'|^{-1} S_{\mu\nu}(\omega_p, \mathbf{x}') e^{i\omega_p(|\mathbf{x}-\mathbf{x}'|-r)} \, d^3 x' \tag{6.161}$$

with $S_{\mu\nu}(\omega_p, \mathbf{x}')$ the Fourier transform of the source function $S_{\mu\nu}(t', \mathbf{x}')$ defined by (6.8). The principal difference between the present case and the analysis of section 6.4 is that whereas it was necessary only to evaluate $h_{\mu\nu}$ and its derivatives to first order in r^{-1} (and so $\mathfrak{T}^{\mu\nu}$ to order r^{-2}) when calculating the radiated power, the sum appearing in the angular momentum flux integral (6.159) vanishes identically to this order. It is, therefore, necessary here to calculate $\mathfrak{T}^{\mu\nu}$ to order r^{-3}, which complicates the analysis considerably.

In terms of $E_{\mu\nu}$ the first and second derivatives of the metric perturbation read:

$$h_{\mu\nu,\lambda} = \sum_{p=-\infty}^{\infty} (E_{\mu\nu,\lambda} - i\omega_p k_\lambda E_{\mu\nu}) e^{-i\omega_p c_\sigma x^\sigma} \tag{6.162}$$

and

$$
\begin{aligned}
h_{\mu\nu,\kappa\lambda} = \sum_{p=-\infty}^{\infty} [& E_{\mu\nu,\kappa\lambda} - i\omega_p(c_\lambda E_{\mu\nu,\kappa} + c_\kappa E_{\mu\nu,\lambda}) \\
& - \omega_p^2 c_\kappa c_\lambda E_{\mu\nu} - i\omega_p c_{\kappa,\lambda} E_{\mu\nu}] e^{-i\omega_p c_\sigma x^\sigma}
\end{aligned} \tag{6.163}
$$

where each derivative of $E_{\mu\nu}$ introduces an extra multiplicative factor of r^{-1}. Since $\mathfrak{T}^{\mu\nu}$ is a quadratic functional of $h_{\mu\nu}$ and its derivatives, and $E_{\mu\nu}$ is itself of order r^{-1}, any term in $\mathfrak{T}^{\mu\nu}$ containing a second derivative or a product of first derivatives of $E_{\mu\nu}$ makes no contribution to order r^{-3} and can be discarded.

Also, the harmonic gauge conditions $h^{\lambda}_{\mu},_{\lambda} = \frac{1}{2}h,_{\mu}$ imply that

$$c_{\lambda}E^{\lambda}_{\mu} = \frac{1}{2}c_{\mu}E + i\omega_p^{-1}(\frac{1}{2}E,_{\mu} - E^{\lambda}_{\mu},_{\lambda}) \tag{6.164}$$

while

$$c_{\kappa},_{\lambda} = -r^{-1}\sum_{r,s=1}^{3} P^{rs}\delta^r_{\kappa}\delta^s_{\lambda} \tag{6.165}$$

where $P^{rs} \equiv \delta^{rs} - n^r n^s$ is the three-dimensional projection operator on the surface normal to the line of sight.

To leading order in r^{-1},

$$E_{\mu\nu} \approx -4r^{-1}(\bar{T}_{\mu\nu} - \frac{1}{2}\eta_{\mu\nu}\bar{T}) \tag{6.166}$$

and

$$E_{\mu\nu},_{\lambda} \approx 4r^{-2}\sum_{r=1}^{3} n^r\delta^r_{\lambda}(\bar{T}_{\mu\nu} - \frac{1}{2}\eta_{\mu\nu}\bar{T}) + 4r^{-2}i\omega_p\sum_{r,s=1}^{3} P^{rs}\delta^r_{\lambda}(\bar{T}^s_{\mu\nu} - \frac{1}{2}\eta_{\mu\nu}\bar{T}^s) \tag{6.167}$$

where the Fourier transform

$$\bar{T}_{\mu\nu} = T^{-1}\int_0^T\int T_{\mu\nu}(\omega_p, \mathbf{x}')e^{i\omega_p(t'-\mathbf{n}\cdot\mathbf{x}')}\, d^3x'\, dt' \tag{6.168}$$

was defined previously (albeit in two steps) in section 6.4, and now

$$\bar{T}^s_{\mu\nu} = T^{-1}\int_0^T\int T_{\mu\nu}(\omega_p, \mathbf{x}')x'^s e^{i\omega_p(t'-\mathbf{n}\cdot\mathbf{x}')}\, d^3x'\, dt'. \tag{6.169}$$

The symbols $\bar{T}$ and $\bar{T}^s$ denote the traces $\bar{T}^{\mu}_{\mu}$ and $\bar{T}^{\mu s}_{\mu}$ of $\bar{T}_{\mu\nu}$ and $\bar{T}^s_{\mu\nu}$ respectively. Also, in view of the conservation equation $T^{\lambda}_{\mu},_{\lambda} = 0$,

$$0 = \int T^{\lambda}_{\mu},_{\lambda}\, x^j e^{i\omega_p c_{\sigma}x^{\sigma}}\, d^4x = -\int T^{\lambda}_{\mu}(x^j e^{i\omega_p c_{\sigma}x^{\sigma}}),_{\lambda}\, d^4x \tag{6.170}$$

and so

$$c^{\lambda}\bar{T}^s_{\lambda\mu} = i\omega_p^{-1}\bar{T}^s_{\mu}. \tag{6.171}$$

Combining all these identities together and performing a coarse-grained averaging of $\mathfrak{T}^{mk}$ to eliminate any interference between modes of different

frequencies gives, after considerable manipulation,

$$
r^3 \sum_{j,k,m=1}^{3} \varepsilon^{ajk} n^j n^m \mathfrak{T}^{mk}
$$

$$
= \frac{1}{4\pi} \sum_{p=-\infty}^{\infty} \omega_p^2 \varepsilon^{ajk} n^j (\bar{T}^* \bar{T}^k - 2\bar{T}^{*\lambda\mu} \bar{T}_{\lambda\mu}^k + 4 P^{rs} \bar{T}^{\lambda k} \bar{T}_{\lambda}^{*rs}
$$

$$
- 4 P^{rs} \bar{T}^{*r\lambda} \bar{T}_{\lambda}^{ks}) + \frac{3}{\pi} i \sum_{p=-\infty}^{\infty} \omega_p \varepsilon^{ajk} n^j n^m \bar{T}_{\lambda}^{*m} \bar{T}^{k\lambda}. \tag{6.172}
$$

where summation over repeated superscripts in the right-hand expressions is understood.

As a final simplification, the timelike components of $\bar{T}_{\mu\nu}$ and $\bar{T}_{\mu\nu}^s$ can be eliminated in favour of their spacelike components by invoking the equations

$$
\bar{T}^{0\mu} = \sum_{r=1}^{3} n^r \bar{T}^{r\mu} \qquad \text{and} \qquad \bar{T}^{0\mu s} = \sum_{r=1}^{3} n^r \bar{T}^{r\mu s} + i\omega_p^{-1} \bar{T}^{\mu s} \tag{6.173}
$$

which follow directly from (6.171) and the identity $c^\lambda \bar{T}_{\lambda\mu} = 0$. The flux of angular momentum at infinity then satisfies

$$
\frac{dP_{\mathbf{J}}^a}{d\Omega} = \frac{1}{4\pi} \sum_{p=-\infty}^{\infty} \omega_p^2 \varepsilon^{ajk} n^j P^{rs} P^{pq} (\bar{T}^{*rs} \bar{T}^{pqk} - 2\bar{T}^{*pr} \bar{T}^{qsk}
$$

$$
- 4\bar{T}^{pk} \bar{T}^{*qrs} + 4\bar{T}^{*pr} \bar{T}^{kqs})
$$

$$
- \frac{3}{2\pi} i \sum_{p=-\infty}^{\infty} \omega_p \varepsilon^{ajk} n^j n^m P^{rs} (2\bar{T}^{*mr} \bar{T}^{ks} + \bar{T}^{*rs} \bar{T}^{mk}). \tag{6.174}
$$

This expression for the angular momentum flux from a periodic source was first derived by Ruth Durrer [Dur89]. However, it should be noted that Durrer's analysis proceeds from a slightly different initial point, as she calculates $\mathfrak{T}^{\mu\nu}$ on the basis of the weak-field limit of the Landau–Lifshitz gravitational stress–energy tensor [LL62] rather than from equation (6.56). The final results are, nonetheless, the same.

Now, it was shown in section 6.4 that for a string source with fundamental period $T = L/2$ and mode functions $\mathbf{a}(\sigma_+)$ and $\mathbf{b}(\sigma_-)$ the spacelike components of $\bar{T}^{\mu\nu}$ have the form

$$
\bar{T}^{jk} = \frac{1}{2}\mu L (A^j B^k + A^k B^j) \tag{6.175}
$$

where

$$
A^j = \frac{1}{2\pi} \int_0^{2\pi} e^{ip(\xi_+ - \mathbf{n}\cdot\mathbf{a})} \overline{a}'^j \, d\xi_+ \tag{6.176}
$$

and a similar definition applies to B^j.

Furthermore, the spacelike components of the moment tensor $\bar{T}^{\mu\nu s}$ are

$$\bar{T}^{jks} = \frac{1}{8\pi}\mu L^2(A^{js}B^k + A^{ks}B^j + A^jB^{ks} + A^kB^{js}) \tag{6.177}$$

where

$$A^{js} = \frac{1}{2\pi}\int_0^{2\pi} e^{ip(\xi_+ - \mathbf{n}\cdot\overline{\mathbf{a}})}\overline{a}'^j\overline{a}^s\,d\xi_+ \tag{6.178}$$

and there is an analogous definition for B^{js}.

If the spatial coordinates are again chosen so that $\mathbf{k}_3 = \mathbf{n}$ then (after adding the mode number p as a subscript on the various moment functions) the two non-trivial components of the angular momentum flux per unit solid angle (6.174) become:

$$\begin{aligned}
\frac{dP_{\mathbf{J}}^a}{d\Omega} = &-3i\mu^2 L\sum_{p=1}^{\infty} p(\mathbf{A}_p^* \times \mathbf{A}_p)^a(|B_p^1|^2 + |B_p^2|^2) \\
&+ 2\mu^2 L\sum_{p=1}^{\infty} p^2 \operatorname{Re}[A_p^+\widehat{A}_p^{*a} + A_p^-A_p^{*a} + (A_p^{1a}A_p^{*2} - A_p^{2a}A_p^{*1})] \\
&\times (|B_p^1|^2 + |B_p^2|^2) \\
&- 4\mu^2 L\sum_{p=1}^{\infty} p^2 \operatorname{Im}[A_p^+A_p^{*a} - A_p^-\widehat{A}_p^{*a} + (A_p^{1a}A_p^{*1} + A_p^{2a}A_p^{*2})] \\
&\times \operatorname{Im}(B_p^1 B_p^{2*}) \\
&+ 12\mu^2 L\sum_{p=1}^{\infty} p \operatorname{Re}(A_p^a A_p^{*3})\operatorname{Im}(B_p^1 B_p^{*2}) + \text{conj.} \tag{6.179}
\end{aligned}$$

for $a = 1$ and 2, where

$$A_p^+ = A_p^{11} + A_p^{22} \qquad \text{and} \qquad A_p^- = A_p^{12} - A_p^{21} \tag{6.180}$$

the components of $\widehat{A}_p^r$ are

$$\widehat{A}_p^1 = A_p^2 \qquad \text{and} \qquad \widehat{A}_p^2 = -A_p^1 \tag{6.181}$$

and 'conj.' denotes the same terms repeated with A and B everywhere interchanged. The component of the angular momentum flux in the direction of $\mathbf{n}$ is, of course, zero.

It was shown in section 6.4 that A_p^r goes to zero at least as rapidly as p^{-1} if the vector $\mathbf{n}$ does not coincide with one of the beaming directions of the $\mathbf{a}$ mode, and like $p^{-2/3}$ if it does. Similar statements apply to B_p^r, A_p^{rs} and B_p^{rs}, as the inclusion of a continuous vector function $\overline{a}^s$ in the moment integral (6.178) does

not alter the singularity in the integrand when **n** lies in a beaming direction. Just like the energy flux, therefore, the angular momentum flux per unit solid angle diverges in the beaming direction of a cusp but is finite elsewhere.

Durrer [Dur89] has examined the properties of the angular momentum flux from a number of simple string configurations. In particular, she has shown that if the mode functions **a** and **b** satisfy the relation $\mathbf{a}(\xi) = \mathbf{b}(-\xi)$ for all ξ in $[0, 2\pi]$ then the net flux of angular momentum from the string is zero. This condition on the mode functions might seem somewhat restrictive but, in fact, it is satisfied by any configuration which is initially stationary, as is evident from the discussion of the initial-value problem in section 3.4. Since the angular momentum of any segment of a stationary string configuration is zero, it is not surprising that the net flux of radiated angular momentum is also zero.

Durrer's result can be proved by noting that the contributions (6.179) to the total angular momentum flux $P_{\mathbf{J}}^a$ from each pair of antipodal points cancel exactly. To see this, let $\mathbf{k}_1$, $\mathbf{k}_2$ and $\mathbf{k}_3$ define the coordinate axes at a field point **n**, and choose a second set of coordinate axes at the antipodal point $-\mathbf{n}$ so that $\bar{\mathbf{k}}_1 = \mathbf{k}_1$, $\bar{\mathbf{k}}_2 = -\mathbf{k}_2$ and $\bar{\mathbf{k}}_3 = -\mathbf{k}_3$. Then if $\mathbf{a}(\xi) = \mathbf{b}(-\xi)$ the definitions (6.176) and (6.178) imply that

$$B_p^r(\mathbf{n}) = [-A_p^{*1}(-\mathbf{n}), \, A_p^{*2}(-\mathbf{n}), \, A_p^{*3}(-\mathbf{n})] \tag{6.182}$$

and

$$\begin{bmatrix} B_p^{11}(\mathbf{n}) & B_p^{12}(\mathbf{n}) \\ B_p^{21}(\mathbf{n}) & B_p^{22}(\mathbf{n}) \end{bmatrix} = \begin{bmatrix} -A_p^{*11}(-\mathbf{n}) & A_p^{*12}(-\mathbf{n}) \\ A_p^{*21}(-\mathbf{n}) & -A_p^{*22}(-\mathbf{n}) \end{bmatrix}. \tag{6.183}$$

The corresponding relationships with **n** and $-\mathbf{n}$ interchanged also hold. If the $a = 1$ component of $\mathrm{d}P_{\mathbf{J}}^a/\mathrm{d}\Omega$ is now evaluated at both **n** and $-\mathbf{n}$ it is readily seen that the two expressions cancel. The analogous result for the $a = 2$ component follows if the coordinate axes at $-\mathbf{n}$ are chosen so that $\bar{\mathbf{k}}_1 = -\mathbf{k}_1$, $\bar{\mathbf{k}}_2 = \mathbf{k}_2$ and $\bar{\mathbf{k}}_3 = -\mathbf{k}_3$.

Another family of trajectories with zero net angular momentum and no flux of radiated angular momentum are the degenerate kinked cuspless loops examined in section 6.5. Here, $\mathbf{a}'$ is parallel to $\mathbf{a}$ (and $\mathbf{b}'$ parallel to $\mathbf{b}$) everywhere except at the kinks, where $\mathbf{a}'$ (and $\mathbf{b}'$) has a step-function discontinuity. Hence, the expression (3.45) for the loop's angular momentum **J** is automatically zero.

As in the previous example, the fact that the total angular momentum flux $P_{\mathbf{J}}^a$ vanishes follows from the cancellation of the contributions of each pair of antipodal points. If the axes at the point $-\mathbf{n}$ are chosen so that $\bar{\mathbf{k}}_1 = \mathbf{k}_1$, $\bar{\mathbf{k}}_2 = -\mathbf{k}_2$ and $\bar{\mathbf{k}}_3 = -\mathbf{k}_3$ then a straightforward calculation shows that

$$A_p^r(-\mathbf{n}) = [-A_p^{*1}(\mathbf{n}), \, A_p^{*2}(\mathbf{n}), \, A_p^{*3}(\mathbf{n})] \tag{6.184}$$

and

$$\begin{bmatrix} A_p^{11}(-\mathbf{n}) & A_p^{12}(-\mathbf{n}) \\ A_p^{21}(-\mathbf{n}) & A_p^{22}(-\mathbf{n}) \end{bmatrix} = \begin{bmatrix} -A_p^{*11}(\mathbf{n}) & A_p^{*12}(\mathbf{n}) \\ A_p^{*21}(\mathbf{n}) & -A_p^{*22}(\mathbf{n}) \end{bmatrix} \tag{6.185}$$

with similar identities applying to B_p^r and B_p^{rs}. The contributions of **n** and $-\mathbf{n}$ to the $a = 1$ component of $P_{\mathbf{J}}^a$, therefore, cancel as before. A comparable argument disposes of the $a = 2$ component.

Durrer [Dur89] has also calculated the flux of angular momentum from the 3-harmonic Vachaspati–Vilenkin solutions discussed in sections 6.5 and 6.8.1. The net angular momentum of these solutions is

$$\mathbf{J} = \frac{\mu L^2}{8\pi}[0, -\sin\psi, 1 + \cos\psi + \tfrac{2}{3}\alpha^2 - 2\alpha]. \qquad (6.186)$$

In the case $\alpha = 0$ the integrals which appear in the expression (6.179) for the flux per unit solid angle can be evaluated explicitly in terms of Bessel functions but in all other cases the integrals need to be calculated numerically. Durrer has examined the angular momentum flux for $\alpha = 0, 0.5$ and 0.8 and a wide range of values of ψ. She finds that $|\mathbf{P_J}| = \gamma_J \mu L^2$ with an efficiency parameter γ_J which ranges between 3 and 6.

More surprisingly, Durrer's results also indicate that the angular momentum flux $\mathbf{P_J}$ is in all cases aligned with $\mathbf{J}$ (to within the limits of numerical accuracy). In the case $\alpha = 0$ this feature is relatively easy to explain, as the angular momentum flux should be dominated by the contributions of the two cusps at $\tau = 0, \sigma = 0$ and $L/2$. These cusps occur symmetrically about the centre-of-momentum of the loop, at the points

$$\mathbf{r_c} = \mp\frac{L}{4\pi}[0, 1 + \cos\psi, \sin\psi] \qquad (6.187)$$

while their velocities are $\mathbf{v_c} = \pm[1, 0, 0]$. Hence, both cusps should radiate angular momentum with helicity

$$\mathbf{r_c} \times \mathbf{v_c} = \frac{L}{4\pi}[0, -\sin\psi, 1 + \cos\psi] \qquad (6.188)$$

which is in the same direction as $\mathbf{J}$.

This argument does not account quite so neatly for the correlation when $\alpha \neq 0$ but it does suggest that the cusp helicities might play an important role in determining the direction of $\mathbf{P_J}$. For example, if $\alpha = 0.5$ and $\psi = \pi/2$ then the trajectory supports four cusps, at $(\tau/L, \sigma/L) = (0, \tfrac{1}{4})$, $(\tfrac{1}{4}, \tfrac{1}{2})$, $(\tfrac{1}{8}, \tfrac{7}{8})$ and $(\tfrac{3}{8}, \tfrac{1}{8})$. The first two cusps have helicities aligned with the negative y-axis, while the helicities of the last two cusps are:

$$\mathbf{r_c} \times \mathbf{v_c} = \frac{L}{2\pi}[\mp\tfrac{1}{3}, -\tfrac{1}{2}, 0] \qquad (6.189)$$

and, moreover, these cusps have identical structure. It is, therefore, to be expected that the net angular momentum flux from the four cusps would be anti-parallel to the y-axis.

By comparison, the total angular momentum of the loop is

$$\mathbf{J} = \frac{\mu L^2}{48\pi}[0, -6, 1].$$ (6.190)

If the angular momentum flux were directed along the cusps' overall helicity axis (rather than $\mathbf{J}$) then the cosine of the angle between $\mathbf{J}$ and $\mathbf{P_J}$ would be approximately 0.986. The difference between this number and 1 is of the same order as the numerical accuracy of Durrer's calculations.

6.9 Radiative efficiencies from piecewise-linear loops

6.9.1 The piecewise-linear approximation

The standard Fourier decomposition method for calculating the radiative efficiencies γ^0 and γ_P of a string loop, described in sections 6.4 and 6.8.1, suffers from the weakness that the rate of convergence of the sum over the wavenumbers m is either unknown or, in the rare cases where it can be determined analytically, very slow. By way of improvement, Allen and Casper [AC94] have developed— and Allen *et al* [ACO95] have elaborated—an algorithm that can relatively rapidly estimate γ^0 and γ_P to high accuracy by approximating the mode functions $\mathbf{a}(\sigma_+)$ and $\mathbf{b}(\sigma_-)$ as piecewise-linear functions of the gauge coordinates. Because the resulting series can, in all cases, be evaluated explicitly, the error in the approximation stems not from the truncation of a slowly-converging series but from the necessarily finite number of linear segments used to represent the mode functions.

All relevant information about the net power and momentum flux radiated by a string loop can be extracted from the 4-vector of radiative efficiencies

$$\gamma^\mu \equiv [\gamma^0, \gamma^j] = \mu^{-2} \int \frac{\mathrm{d}P}{\mathrm{d}\Omega}[1, \mathbf{n}]\, \mathrm{d}\Omega$$ (6.191)

where $\mathbf{n}$ is again the unit vector in the direction of integration and $\mathrm{d}P/\mathrm{d}\Omega$ is given by the infinite series (6.63). Note that the overall momentum coefficient γ_P is just the norm of the 3-vector γ^j.

If the expression (6.66) for the Fourier components $\bar{T}^{\mu\nu}$ of the string's stress–energy tensor is inserted into (6.63) then

$$\mu^{-2}\frac{\mathrm{d}P}{\mathrm{d}\Omega} = \sum_{m=-\infty}^{\infty} \frac{\omega_m^2}{4\pi L^2} \int_0^L \mathrm{d}u \int_0^L \mathrm{d}v \int_0^L \mathrm{d}\tilde{u} \int_0^L \mathrm{d}\tilde{v}\, \Psi(u, v, \tilde{u}, \tilde{v}) \mathrm{e}^{\mathrm{i}\omega_m(\Delta\tau - \mathbf{n}\cdot\Delta\mathbf{r})}$$ (6.192)

where $\omega_m = 4\pi m/L$ as before, $\Delta\tau = \frac{1}{2}(u + v - \tilde{u} - \tilde{v})$, $\Delta\mathbf{r} = \frac{1}{2}(\mathbf{a} + \mathbf{b} - \tilde{\mathbf{a}} - \tilde{\mathbf{b}})$ and

$$\Psi(u, v, \tilde{u}, \tilde{v}) = (1 - \mathbf{a}' \cdot \tilde{\mathbf{a}}')(1 - \mathbf{b}' \cdot \tilde{\mathbf{b}}') + (1 - \mathbf{a}' \cdot \tilde{\mathbf{b}}')(1 - \tilde{\mathbf{a}}' \cdot \mathbf{b}')$$
$$- (1 - \mathbf{a}' \cdot \mathbf{b}')(1 - \tilde{\mathbf{a}}' \cdot \tilde{\mathbf{b}}')$$ (6.193)

with $\mathbf{a} \equiv \mathbf{a}(u)$, $\mathbf{b} \equiv \mathbf{b}(v)$, $\tilde{\mathbf{a}} \equiv \mathbf{a}(\tilde{u})$ and $\tilde{\mathbf{b}} \equiv \mathbf{b}(\tilde{v})$. The manifest symmetry of $\Psi(u, v, \tilde{u}, \tilde{v})$ under the interchange $(u, v) \leftrightarrow (\tilde{u}, \tilde{v})$ allows the sum in (6.192) to range over $(-\infty, \infty)$ rather than from 1 to ∞ as previously.

Evaluation of the 4-vector γ^{μ}, therefore, involves angular integrals of the form $\int [1, \mathbf{n}] e^{i\omega_m(\Delta\tau - \mathbf{n}\cdot\Delta\mathbf{r})} \, d\Omega$. Now, in view of the identity $\int e^{i\mathbf{n}\cdot\mathbf{k}} \, d\Omega = 4\pi \sin(|\mathbf{k}|)/|\mathbf{k}|$, it follows that

$$\int e^{i\omega_m(\Delta\tau - \mathbf{n}\cdot\Delta\mathbf{r})} \, d\Omega = \frac{4\pi}{\omega_m|\Delta\mathbf{r}|} e^{i\omega_m\Delta\tau} \sin(\omega_m|\Delta\mathbf{r}|) \tag{6.194}$$

and so

$$\sum_{m=-\infty}^{\infty} \omega_m \int e^{i\omega_m(\Delta\tau - \mathbf{n}\cdot\Delta\mathbf{r})} \, d\Omega$$

$$= \frac{2\pi}{i|\Delta\mathbf{r}|} \sum_{m=-\infty}^{\infty} [e^{i\omega_m(\Delta\tau + |\Delta\mathbf{r}|)} - e^{i\omega_m(\Delta\tau - |\Delta\mathbf{r}|)}]$$

$$= \frac{4\pi^2}{i|\Delta\mathbf{r}|} \{\delta_p[4\pi(\Delta\tau + |\Delta\mathbf{r}|)/L] - \delta_p[4\pi(\Delta\tau - |\Delta\mathbf{r}|)/L]\} \tag{6.195}$$

as $\sum_{m=-\infty}^{\infty} e^{imx} = 2\pi\delta_p(x)$, where $\delta_p(x) \equiv \sum_{n=-\infty}^{\infty} \delta(x + 2\pi n)$ is the 2π-periodic delta-function.

On rescaling the delta functions by a factor of $4\pi/L$, this relation reads:

$$\sum_{m=-\infty}^{\infty} \omega_m \int e^{i\omega_m(\Delta\tau - \mathbf{n}\cdot\Delta\mathbf{r})} \, d\Omega$$

$$= \frac{\pi L}{i|\Delta\mathbf{r}|} \sum_{n=-\infty}^{\infty} \left[\delta\left(\Delta\tau + |\Delta\mathbf{r}| + \frac{L}{2}n\right) - \delta\left(\Delta\tau - |\Delta\mathbf{r}| + \frac{L}{2}n\right) \right]$$

$$= 2\pi i L \sum_{n=-\infty}^{\infty} \text{sgn}\left(\Delta\tau + \frac{L}{2}n\right) \delta\left[\left(\Delta\tau + \frac{L}{2}n\right)^2 - |\Delta\mathbf{r}|^2\right] \tag{6.196}$$

where the second line follows from the identity $\delta(x^2 - y^2) = \frac{1}{|x|+|y|}\delta(|x| - |y|)$.

Of course it is not the sum on the left of (6.196) that needs to be evaluated in calculating γ^{μ} but rather the 4-vector quantity

$$I^{\mu}(u, v, \bar{u}, \bar{v}) = \sum_{m=-\infty}^{\infty} \frac{\omega_m^2}{4\pi L^2} \int e^{i\omega_m(\Delta\tau - \mathbf{n}\cdot\Delta\mathbf{r})}[1, \mathbf{n}] \, d\Omega. \tag{6.197}$$

However, if it is possible to find a 4-vector operator $D^{\mu} = U^{\mu}\partial_u + V^{\mu}\partial_v - \tilde{U}^{\mu}\partial_{\tilde{u}} - \tilde{V}^{\mu}\partial_{\tilde{v}}$ (where U^{μ}, V^{μ}, $\tilde{U}^{\mu}$ and $\tilde{V}^{\mu}$ are all functions of u, v, $\tilde{u}$ and $\tilde{v}$) with the property that

$$D^{\mu} e^{i\omega_m(\Delta\tau - \mathbf{n}\cdot\Delta\mathbf{r})} = i\omega_m[1, \mathbf{n}] e^{i\omega_m(\Delta\tau - \mathbf{n}\cdot\Delta\mathbf{r})} \tag{6.198}$$

then

$$I^\mu(u, v, \tilde{u}, \tilde{v}) = D^\mu \sum_{m=-\infty}^{\infty} \frac{\omega_m}{4\pi i L^2} \int e^{i\omega_m(\Delta\tau - \mathbf{n}\cdot\Delta\mathbf{r})} \, d\Omega$$

$$= \frac{1}{2} D^\mu \sum_{n=-\infty}^{\infty} \text{sgn}\left(\Delta\tau + \frac{L}{2}n\right) \delta\left[\left(\Delta\tau + \frac{L}{2}n\right)^2 - |\Delta\mathbf{r}|^2\right].$$

$$(6.199)$$

The operator equation (6.198) defining D^μ decomposes into 16 linear equations for the 16 independent components of U^μ, V^μ, $\tilde{U}^\mu$ and $\tilde{V}^\mu$, namely

$$D^0\Delta\tau = 1 \qquad D^0\Delta\mathbf{r} = \mathbf{0} \qquad D^j\Delta\tau = 0 \qquad \text{and} \qquad D^j(\Delta\mathbf{r})^k = -\delta^{jk}.$$

$$(6.200)$$

The solution to these equations is:

$$U^\mu = [\mathbf{b}' \cdot (\tilde{\mathbf{a}}' \times \tilde{\mathbf{b}}'), \tilde{\mathbf{a}}' \times \tilde{\mathbf{b}}' + \mathbf{b}' \times (\tilde{\mathbf{a}}' - \tilde{\mathbf{b}}')]/Q \qquad (6.201)$$

and

$$V^\mu = -[\mathbf{a}' \cdot (\tilde{\mathbf{a}}' \times \bar{\mathbf{b}}'), \tilde{\mathbf{a}}' \times \tilde{\mathbf{b}}' + \mathbf{a}' \times (\tilde{\mathbf{a}}' - \tilde{\mathbf{b}}')]/Q \qquad (6.202)$$

with

$$Q = 2[(\mathbf{b}' - \mathbf{a}') \cdot (\tilde{\mathbf{a}}' \times \tilde{\mathbf{b}}') + (\tilde{\mathbf{b}}' - \tilde{\mathbf{a}}') \cdot (\mathbf{a}' \times \mathbf{b}')] \qquad (6.203)$$

while, in view of the obvious symmetries, $\tilde{U}^\mu(u, v, \tilde{u}, \tilde{v}) = U^\mu(\tilde{u}, \tilde{v}, u, v)$ and $\tilde{V}^\mu(u, v, \tilde{u}, \tilde{v}) = V^\mu(\tilde{u}, \tilde{v}, u, v)$.

Collecting together the results (6.199) and (6.192) gives

$$\gamma^\mu = \frac{1}{2L} \int_0^L du \int_0^L dv \int_0^L d\tilde{u} \int_0^L d\tilde{v} \, \Psi D^\mu$$

$$\times \sum_{n=-\infty}^{\infty} \text{sgn}\left(\Delta\tau + \frac{L}{2}n\right) \delta\left[\left(\Delta\tau + \frac{L}{2}n\right)^2 - |\Delta\mathbf{r}|^2\right]. \quad (6.204)$$

Furthermore, since Ψ and $\Delta\mathbf{r}$ are invariant under the transformation $\tilde{v} \to \tilde{v} - nL$ whereas $\Delta\tau \to \Delta\tau + \frac{1}{2}Ln$, the summation over n can be absorbed into the integral over $\tilde{v}$, giving

$$\gamma^\mu = \frac{1}{2L} \int_0^L du \int_0^L dv \int_0^L d\tilde{u} \int_{-\infty}^{\infty} d\tilde{v} \, \Psi D^\mu \{\text{sgn}(\Delta\tau)\delta[(\Delta\tau)^2 - |\Delta\mathbf{r}|^2]\}.$$

$$(6.205)$$

(Of course, the summation could just as easily be absorbed into the integral over v instead.) Further symmetry considerations can be invoked to show that the integrand in (6.205) has support on only a compact interval in $\tilde{v}$-space.

The value of the formula (6.205) lies in the fact that, if the mode functions **a** and **b** are assumed to be piecewise-linear functions of their arguments, then

the integral on the right of (6.205) can be evaluated explicitly. At a geometric level, such a piecewise-linear approximation involves replacing each of the curves traced out by $\mathbf{a}'$ and $\mathbf{b}'$ on the surface of the Kibble–Turok sphere with a series of points equally spaced in gauge space.

To be specific, if the mode function $\mathbf{a}$ is approximated by a function $\hat{\mathbf{a}}$ consisting of $N_{\mathbf{a}}$ linear segments then

$$\hat{\mathbf{a}}'(\sigma_+) = \mathbf{a}'_j \qquad \text{if } u_j < \sigma_+ < u_{j+1} \qquad (6.206)$$

where $u_j \equiv jL/N_{\mathbf{a}}$ and $\mathbf{a}'_j \equiv \mathbf{a}'(u_j)$. If $\mathbf{a}_j \equiv \mathbf{a}(u_j)$ then the mode function itself has the piecewise-linear form

$$\hat{\mathbf{a}}(\sigma_+) = \mathbf{a}_j + (\sigma_+ - u_j)\mathbf{a}'_j \qquad \text{if } u_j \leq \sigma_+ < u_{j+1}. \qquad (6.207)$$

Similarly, if $\mathbf{b}$ is approximated by a function $\hat{\mathbf{b}}$ consisting of $N_{\mathbf{b}}$ linear segments then

$$\hat{\mathbf{b}}'(\sigma_-) = \mathbf{b}'_k \qquad \text{if } v_k < \sigma_- < v_{k+1} \qquad (6.208)$$

while

$$\hat{\mathbf{b}}(\sigma_-) = \mathbf{b}_k + (\sigma_- - v_k)\mathbf{b}'_k \qquad \text{if } v_k \leq \sigma_- < v_{k+1} \qquad (6.209)$$

where $v_k \equiv kL/N_{\mathbf{b}}$, $\mathbf{b}'_k \equiv \mathbf{b}'(v_k)$ and $\mathbf{b}_k \equiv \mathbf{b}(v_k)$.

The domain of integration can, therefore, be broken up into a collection of rectangular 4-cells, each identified by the vector of indices (j, k, m, n) if $u \in I_j$, $v \in J_k$, $\tilde{u} \in I_m$ and $\tilde{v} \in J_n$, where $I_j = (u_j, u_{j+1})$ and $J_k = (v_k, v_{k+1})$. Since the functions Ψ, U, V, $\tilde{U}$ and $\tilde{V}$ are all constant, and $(\Delta\tau)^2 - |\Delta\mathbf{r}|^2$ is a second-degree polynomial in u, v, $\tilde{u}$ and $\tilde{v}$ (although not involving u^2, v^2, $\tilde{u}^2$ or $\tilde{v}^2$), on each 4-cell, the integral (6.205) reduces to the sum over j, k, m and n of four pairs of triple integrals of the form

$$\Psi_{jkmn} F_{jkmn} \int_0^{\Delta x} \mathrm{d}x \int_0^{\Delta y} \mathrm{d}y \int_0^{\Delta z} \mathrm{d}z \, H[C \pm (x + y - z)]\delta[p(x, y, z)] \quad (6.210)$$

where Ψ_{jkmn} is the value of Ψ on the 4-cell (j, k, m, n), F_{jkmn} is U_{jkmn}, V_{jkmn}, $-U_{jkmn}$ or $-V_{jkmn}$, the limits Δx, Δy and Δz on the integrals are each a cell length $L/N_{\mathbf{a}}$ or $L/N_{\mathbf{b}}$, H is the Heaviside step function, the constant C is a linear combination of the boundary values on the intervals I_j, J_k, I_m and J_n, and $p(x, y, z)$ is, in general, a second-degree polynomial in x, y and z that does not contains terms in x^2, y^2 or z^2.

Evaluation of these integrals is a straightforward task, although there are a number of different subcases that need to be considered, as is discussed fully in [AC94]. A simple example will be given shortly. The calculated values that Allen and Casper [AC94] obtain for the radiative efficiency γ^0 and Allen *et al* [ACO95] obtain for the momentum coefficient γ_P of various benchmark loops have already been mentioned in sections 6.5 and 6.8.1. In the case of the Vachaspati–Vilenkin solution in the 1-harmonic limit $\alpha = 0$, Allen and Casper estimate that the

dependence of the calculated value γ_N of γ^0 on the total number of segments $N = N_{\mathbf{a}} + N_{\mathbf{b}}$ over the range $60 \leq N \leq 256$ is

$$\gamma_N \approx 64.49 + 97.13N^{-1} \tag{6.211}$$

when $\psi = 69°$ and

$$\gamma_N \approx 52.01 + 181.64N^{-1} \tag{6.212}$$

when $\psi = 141°$. Allen *et al* [ACO94] conjecture that $\gamma^0 - \gamma_N$ is, in general, of order N^{-1}, except when one or both of the mode functions is itself piecewise linear and the rate of convergence is naturally much faster.

6.9.2 A minimum radiative efficiency?

In [ACO94] Allen, Casper and Ottewill also calculate explicit values of γ^0 for a large class of piecewise-linear loops with **a** consisting of two anti-parallel segments of length $\frac{1}{2}L$ aligned along the z-axis, so that

$$\mathbf{a}(\sigma_+) = \begin{cases} \sigma_+\widehat{\mathbf{z}} & \text{if } 0 \leq \sigma_+ < \frac{1}{2}L \\ (L - \sigma_+)\widehat{\mathbf{z}} & \text{if } \frac{1}{2}L \leq \sigma_+ < L \end{cases} \tag{6.213}$$

and **b** tracing out various figures in the x–y plane including regular polygons, isosceles triangles and connected N-grams. In particular, the value γ_N of γ^0 for the N-sided regular polygon converges like N^{-2} to $\gamma_\infty \approx 39.0025$ as $N \to \infty$ (and the polygon becomes a circle).

In general, when **a** has the form (6.213) and **b** is confined to the x–y plane, then $\Psi = 2(1 - \mathbf{b}' \cdot \tilde{\mathbf{b}}')$ if $(u, \tilde{u})$ lies in $R_1 \equiv [0, \frac{1}{2}L) \times [\frac{1}{2}L, L)$ or $R_2 \equiv [\frac{1}{2}L, L) \times [0, \frac{1}{2}L)$, and is zero otherwise. Also, $D^0 = \partial_u - \partial_{\tilde{u}}$ on $R_1 \cup R_2$, so the timelike component of (6.205) becomes

$$\gamma^0 = \frac{1}{2L} \int_0^L \mathrm{d}v \int_{-\infty}^\infty \mathrm{d}\tilde{v}\, \Psi \int \int_{\bar{R}_1 \cup \bar{R}_2} \mathrm{d}u\, \mathrm{d}\tilde{u}\, (\partial_u - \partial_{\tilde{u}})\{\mathrm{sgn}(\Delta\tau)\delta[(\Delta\tau)^2 - |\Delta\mathbf{r}|^2]\} \tag{6.214}$$

where $\Delta\mathbf{r} = \frac{1}{2}[\pm(u + \tilde{u} - L)\widehat{\mathbf{z}} + \mathbf{b}(v) - \mathbf{b}(\tilde{v})]$. Here, the exchange $u \leftrightarrow \tilde{u}$ transforms $\partial_{\tilde{u}}$ to ∂_u but leaves the region $\bar{R}_1 \cup \bar{R}_2$ invariant. As was mentioned following (6.205), the limits of integration for v and $\tilde{v}$ can be interchanged at will. If this is done in the term proportional to $\partial_{\tilde{u}}$ in (6.214) then the simultaneous exchange $u \leftrightarrow \tilde{u}$ and $v \leftrightarrow \tilde{v}$ leaves $|\Delta\mathbf{r}|^2$ and the domain of integration unchanged, but transforms $\Delta\tau = \frac{1}{2}(u - \tilde{u} + v - \tilde{v})$ to $-\Delta\tau$. Thus the operator $\partial_u - \partial_{\tilde{u}}$ in (6.214) can be replaced with $2\partial_u$.

A second interchange of the form $(u, \tilde{u}) \to (L - u, L - \tilde{u})$ and $v \leftrightarrow \tilde{v}$ maps $\bar{R}_2$ to $\bar{R}_1$ and transforms ∂_u to $-\partial_u$ and $\Delta\tau = -\Delta\tau$, and so reduces (6.214) to

$$\gamma^0 = 4L^{-1} \int_0^L \mathrm{d}v \int_{-\infty}^\infty \mathrm{d}\tilde{v}\, (1 - \mathbf{b}' \cdot \tilde{\mathbf{b}}')W(v, \tilde{v}) \tag{6.215}$$

where

$$W(v, \tilde{v}) = \int \int_{\bar{R}_1} d\tilde{u}\, \partial_u \{\text{sgn}(\Delta\tau)\delta[(\Delta\tau)^2 - |\Delta\mathbf{r}|^2]\}$$

$$= \int_{L/2}^{L} d\tilde{u}\, \{\text{sgn}(\Delta\tau)\delta[(\Delta\tau)^2 - |\Delta\mathbf{r}|^2]\}|_{u=0}^{u=L/2}. \qquad (6.216)$$

One last series of replacements $\tilde{u} \to \frac{3}{2}L - \tilde{u}$, $\tilde{v} \to v$ and $v \to \tilde{v} + L$ maps $\Delta\tau|_{u=0}$ to $-\Delta\tau|_{u=L/2}$ and $|\Delta\mathbf{r}|^2|_{u=0}$ to $|\Delta\mathbf{r}|^2|_{u=L/2}$. So the contributions of the two endpoints in (6.216) are equal and (with $u' = \tilde{u} - \frac{1}{2}L$ at the vertex $u = L/2$)

$$W(v, \tilde{v}) = \int_0^{L/2} du'\, \text{sgn}(-u' + v - \tilde{v})$$

$$\times \delta[-\tfrac{1}{2}u'(v - \tilde{v}) + \tfrac{1}{4}(v - \tilde{v})^2 - \tfrac{1}{4}|\mathbf{b} - \tilde{\mathbf{b}}|^2]$$

$$= 2\,\text{sgn}(-q + v - \tilde{v})H(q)H(\tfrac{1}{2}L - q)/|v - \tilde{v}| \qquad (6.217)$$

where $q = \frac{1}{2}[(v - \tilde{v})^2 - |\mathbf{b} - \tilde{\mathbf{b}}|^2]/(v - \tilde{v})$.

Now,

$$-q + v - \tilde{v} \equiv \tfrac{1}{2}[(v - \tilde{v})^2 + |\mathbf{b} - \tilde{\mathbf{b}}|^2]/(v - \tilde{v}) \qquad (6.218)$$

and so $\text{sgn}(-q + v - \tilde{v}) = \text{sgn}(v - \tilde{v})$. Also, since $\mathbf{b}'$ is a unit vector, the triangle inequality indicates that $|v - \tilde{v}| \geq |\mathbf{b} - \tilde{\mathbf{b}}|$, and so $H(q) = H(v - \tilde{v})$ and $v - \tilde{v}$ must be positive. Furthermore, because $\mathbf{b}$ is a periodic function with period L, it follows that $v - \tilde{v} - L \geq |\mathbf{b} - \tilde{\mathbf{b}}|$ whenever $v - \tilde{v} \geq L$. So it must be the case that $v - \tilde{v} \leq L$, as

$$\tfrac{1}{2}L - q \equiv \tfrac{1}{2}[\{L - (v - \tilde{v})\}(v - \tilde{v}) + |\mathbf{b} - \tilde{\mathbf{b}}|^2]/(v - \tilde{v}) \qquad (6.219)$$

is negative otherwise.

Collecting these results together gives

$$W(v, \tilde{v}) = 2H(v - \tilde{v})H[L - (v - \tilde{v})]/(v - \tilde{v}) \qquad (6.220)$$

and so

$$\gamma^0 = 16L^{-1} \int_0^L dv \int_{v-L}^v d\tilde{v}\, [1 - \mathbf{b}'(v) \cdot \mathbf{b}'(\tilde{v})]/(v - \tilde{v})$$

$$= 16L^{-1} \int_0^L dv \int_0^L d\bar{v}\, \bar{v}^{-1}[1 - \mathbf{b}'(v) \cdot \mathbf{b}'(v - \tilde{v})]. \qquad (6.221)$$

It is a straightforward matter to use (6.221) to calculate γ^0 for any string loop in the class under consideration, whether $\mathbf{b}$ is a smooth or piecewise linear function. In general, if $\mathbf{b}'$ has the Fourier decomposition

$$\mathbf{b}'(v) = \sum_{n=-\infty}^{\infty} (x_n\widehat{\mathbf{x}} + y_n\widehat{\mathbf{y}})e^{2n\pi i v/L} \qquad (6.222)$$

then because $\mathbf{b}'$ is real and $\mathbf{b}(L) = \mathbf{b}(0)$ the coefficients x_0 and y_0 are both zero, while $x_{-n} = x_n^*$ and $y_{-n} = y_n^*$. So

$$
\gamma^0 = 16L^{-1} \int_0^L d\bar{v}\, \bar{v}^{-1} \int_0^L dv \left[1 - \sum_{m,n}(x_m x_n + y_m y_n)e^{2(n+m)\pi i v/L}e^{-2m\pi i\bar{v}/L} \right]
$$

$$
= 16 \sum_n (|x_n|^2 + |y_n|^2) \int_0^L d\bar{v}\, \bar{v}^{-1}(1 - e^{2n\pi i\bar{v}/L}) \tag{6.223}
$$

where the last line follows from the constraint $2\sum_{n=1}^{\infty}(|x_n|^2 + |y_n|^2) = 1$, which, in turn, stems from the gauge condition $|\mathbf{b}'|^2 = 1$.

Hence,
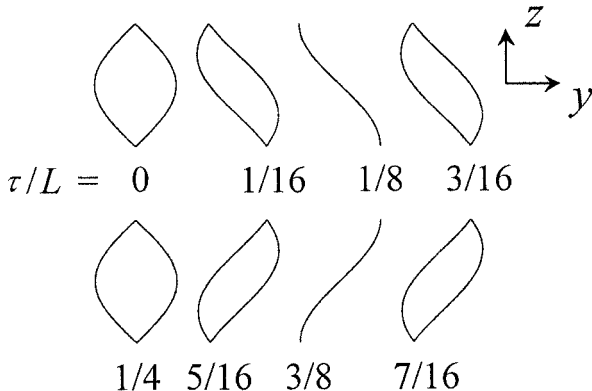
$$
\gamma^0 = 32 \sum_{n=1}^{\infty}(|x_n|^2 + |y_n|^2) \int_0^L d\bar{v}\, \bar{v}^{-1}[1 - \cos(2\pi n\bar{v}/L)]
$$

$$
= \sum_{n=1}^{\infty} 2\lambda_n(|x_n|^2 + |y_n|^2) \tag{6.224}
$$

where $\lambda_n = 16 \int_0^{2\pi n} w^{-1}\, dw\, (1 - \cos w)$. The sequence $\{\lambda_n\}_{n=1}^{\infty}$ is obviously positive and increasing, with $\lambda_1 \approx 39.0025$, $\lambda_2 \approx 49.8297$, $\lambda_3 \approx 56.2636$ and so forth. The minimum possible value of the radiative efficiency γ^0 for this class of loops is, therefore, $\gamma^0_{\min} \approx 39.0025$, and occurs when $|x_1|^2 + |y_1|^2 = \frac{1}{2}$ and $x_n = y_n = 0$ for $n \geq 2$. The only loop solutions consistent with the gauge condition $|\mathbf{b}'|^2 = 1$ then have $|x_1| = |y_1| = \frac{1}{2}$, with the phase angle between x_1 and y_1 equal to $\frac{1}{2}\pi$. That is, $\mathbf{b}'$ traces out an equatorial circle on the Kibble–Turok sphere, and if $x_1 = \frac{1}{2}$ and $y_1 = \frac{1}{2}i$ the mode function $\mathbf{b}$ takes on the simple form

$$
\mathbf{b}(\sigma_-) = \frac{L}{2\pi}[\cos(2\pi\sigma_-/L)\hat{\mathbf{x}} + \sin(2\pi\sigma_-/L)\hat{\mathbf{y}}]. \tag{6.225}
$$

The evolution of the corresponding loop is illustrated in figure 6.4, which shows the y–z projection of the loop at times $\tau = 0$, $L/16$, $L/8$ and $3L/16$ (top row) and $\tau = L/4$, $5L/16$, $3L/8$ and $7L/16$ (bottom row). The projections of the loop onto the x–y plane are just circles of radius $L/(4\pi)$. The loop is, in fact, rotating rigidly with a pattern speed $\omega = 4\pi/L$ and angular momentum $\mathbf{J} = \frac{1}{4\pi}\mu L^2\hat{\mathbf{z}}$, with the kinks visible at the top and bottom of the projections in figure 6.4 tracing out circles in the planes $z = 0$ and $z = L/4$ (and all other points tracing out identical circles with varying phase lags). It is, therefore, an example of the class of rigidly-rotating, non-planar kinked loops mentioned in section 4.5 as exceptions to Embacher's general analysis of stationary string solutions.

Because all points on this particular loop are travelling with the same constant speed $|\mathbf{r}_\tau|$, and the period mean of $\mathbf{r}_\tau^2$ for any string loop is $\frac{1}{2}$, the instantaneous speed of each segment of the loop is $|\mathbf{r}_\tau| = 1/\sqrt{2}$. Following

Figure 6.4. The *y–z* projection of the Allen–Casper–Ottewill loop with minimum radiative efficiency.

Casper and Allen [CA94], it is possible for any Nambu–Goto string loop to define the mean deviation s of the local squared loop velocity from $\frac{1}{2}$ through the formula

$$s^2 = L^{-2} \int_0^L \int_0^L (\mathbf{r}_\tau^2 - \tfrac{1}{2})^2 \, d\sigma_+ \, d\sigma_- = \tfrac{1}{4} L^{-2} \int_0^L \int_0^L [\mathbf{a}'(\sigma_+) \cdot \mathbf{b}'(\sigma_-)]^2 \, d\sigma_+ \, d\sigma_-.$$

(6.226)

Clearly s^2 is non-negative, and lies in the range $[0, \frac{1}{4}]$ (as $\mathbf{a}'$ and $\mathbf{b}'$ are unit vectors). It is also evident that $s^2 = 0$ if and only if $\mathbf{a}'$ and $\mathbf{b}'$ are orthogonal for all values of σ_+ and σ_-.

Casper and Allen [CA94] have plotted the radiative efficiency γ^0 against s^2 (both evaluated in the loop's centre-of-momentum frame) for the 11 625 non-intersecting daughter loops generated as part of the numerical study of radiation rates described in section 6.8.1. They found that for each value of s^2 there was a well-defined minimum radiative efficiency $\gamma^*(s^2)$, with γ^* increasing monotonically with s^2, from a value of about 40 at $s^2 = 0$ to about 50 at $s^2 = 0.15$ and about 100 at $s^2 = 0.25$. In fact, only six of the 11 625 loops studied had radiative efficiencies γ^0 less than 42 (and none at all had $\gamma^0 < 40$). All six of these loops, when examined more closely, were seen to have the same general shape as the loop shown in figure 6.4, whose radiative efficiency $\gamma^0 \approx 39.0025$ is the lowest known of any string loop. A second study by Casper and Allen involving another 12 830 loops yielded similar results. There thus seems to be a strict lower bound $\gamma^0_{\min} \approx 39.0025$ to the radiative efficiency of all possible cosmic string loops.

6.10   The field of a collapsing circular loop

It is evident from the analysis of the 1-harmonic solutions in section 6.4 that the weak-field formalism breaks down when applied to a string in the shape of

an oscillating circular loop. The total power radiated by a loop of this type is infinite, because the string periodically collapses to a singular point at which all parts of the string are instantaneously moving at the speed of light and hence combine to beam a circular pulse of gravitational radiation out along the plane of the loop. However, as will be seen in section 10.2, there are reasons for believing that a circular loop would collapse to form a black hole rather than collapse and re-expand indefinitely, and furthermore in collapsing would radiate only a finite fraction of its own rest energy in the form of gravitational waves.

David Garfinkle and Comer Duncan [GD94] have attempted to model this situation by calculating the linearized gravitational field produced by a circular loop of cosmic string which is held at rest until a particular time t_0, after which it is released to collapse freely to a point. The weak-field formalism again breaks down near the moment of collapse but the metric perturbation $h_{\mu\nu}$ and the radiated power per unit solid angle remain finite outside the future light cone of the collapse.

The string loop in this case has the trajectory $X^\mu = [\tau, \mathbf{r}]$, with

$$\mathbf{r}(\tau, \sigma) = \frac{L}{2\pi} \sin(2\pi\tau/L)[\cos(2\pi\sigma/L), \sin(2\pi\sigma/L), 0] \tag{6.227}$$

where τ is restricted to the range $[-L/4, 0]$. The loop is released at $t = -L/4$ and collapses to a point at $t = 0$.

In the harmonic gauge the metric perturbation $h_{\mu\nu}$ satisfies the usual inhomogeneous wave equation (6.5):

$$\Box h_{\mu\nu} = -16\pi S_{\mu\nu} \tag{6.228}$$

but to ensure a unique solution in this case it is necessary to specify $h_{\mu\nu}$ and $\partial h_{\mu\nu}/\partial t$ on the initial surface $t = -L/4$. Since the loop is assumed to be static until the moment of release, the natural choice of initial data is for $\partial h_{\mu\nu}/\partial t$ to be zero and $h_{\mu\nu}$ to satisfy the Poisson equation $\nabla^2 h_{\mu\nu} = 16\pi \Sigma_{\mu\nu}$, where
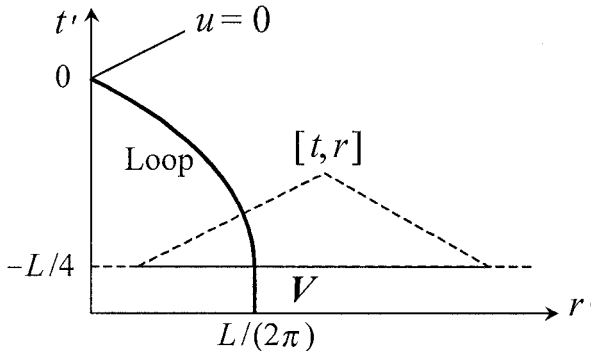
$$\Sigma_{\mu\nu}(\mathbf{x}) = S_{\mu\nu}(t, \mathbf{x})|_{t=-L/4}. \tag{6.229}$$

The analogue of the retarded solution (6.6) is then

$$h_{\mu\nu}(t, \mathbf{x}) = -4 \int \frac{S_{\mu\nu}(t', \mathbf{x}')}{|\mathbf{x} - \mathbf{x}'|} \, \mathrm{d}^3 x' - 4 \int_{\mathbb{R}^3 - \mathbf{V}} \frac{\Sigma_{\mu\nu}(\mathbf{x}')}{|\mathbf{x} - \mathbf{x}'|} \, \mathrm{d}^3 x' \tag{6.230}$$

where $\mathbf{V}$ is the interior of the intersection of the past light cone of the field point $x^\mu = [t, \mathbf{x}]$ with the initial surface (that is, a spherical ball in $\mathbb{R}^3$ with radius $t + L/4$ centred on $\mathbf{x}$) and the retarded time $t' = t - |\mathbf{x} - \mathbf{x}'|$ in the first integral, which ranges over the past light cone of x^μ, is constrained to be greater than $-L/4$.

The geometry of the solution is sketched in figure 6.5, which shows the projection of the spacetime onto the t'–r' plane, where $r' \equiv |\mathbf{x}'|$. The set $\mathbf{V}$ is

Figure 6.5. Equatorial projection of the domains of dependence for a collapsing circular loop.

represented by the line segment indicated, while the domain of the first integral in (6.230) projects onto the triangle bounded by **V** and the past light cone of the field point $[t, r]$.

Because the gravitational field of the loop has a non-trivial time dependence, the wave zone for this problem is the set of field points with t and $r \equiv |\mathbf{x}| \gg L$ but $u \equiv t - r$ finite. If $\mathbf{n}$ here denotes the unit vector $\mathbf{x}/r$, then in the wave zone

$$|\mathbf{x} - \mathbf{x}'| \sim r - \mathbf{n} \cdot \mathbf{x}' \qquad \text{and} \qquad t' \sim u + \mathbf{n} \cdot \mathbf{x}' \qquad (6.231)$$

for any point $\mathbf{x}'$ on the world sheet of the loop, while the boundary of **V** near the source is effectively a plane surface at a normal distance $|u + L/4|$ from the origin.

If the coordinates of the field point $\mathbf{x}$ are varied with u kept fixed the resulting change in $|\mathbf{x} - \mathbf{x}'|^{-1} \sim r^{-1}$ will be of order $r^{-2}\mathbf{n} \cdot \delta\mathbf{x}$ and the change in t' of order $r^{-1}(\mathbf{x}' - \mathbf{n} \cdot \mathbf{x}'\mathbf{n}) \cdot \delta\mathbf{x}$. Also the boundary of **V** near the source will be rotated by an angle of order $r^{-1}|\mathbf{n} \times \delta\mathbf{x}|$ about a line through its point of closest approach to the origin, and the fractional change in the volume common to both **V** and the source region will similarly be of order $r^{-1}|\mathbf{n} \times \delta\mathbf{x}|$. The corresponding change in $h_{\mu\nu}$ will, therefore, be of order $r^{-1}|\delta\mathbf{x}|h_{\mu\nu}$, and to leading order in r^{-1} the only derivatives of $h_{\mu\nu}$ which contribute to the gravitational stress–energy pseudo-tensor $\mathfrak{T}^{\mu\nu}$ defined by (6.56) are the derivatives with respect to u.

In fact, in the harmonic gauge,

$$\mathfrak{T}^{rt} \approx \frac{1}{32\pi} \langle -h^j_{k,u} h^k_{j,u} - 2h^j_k h^k_{j,uu} \rangle \qquad (6.232)$$

where the indices j and k range over the angular coordinates θ and ϕ of the unit vector $\mathbf{n} = [\cos\phi \sin\theta, \sin\phi \sin\theta, \cos\theta]$ only. The process of coarse-grained time-averaging entails integrating the second term in (6.232) by parts, and so the

power radiated per unit solid angle is

$$\frac{\mathrm{d}P}{\mathrm{d}\Omega} \equiv r^2 \mathfrak{T}^{rt} \approx \frac{r^2}{32\pi} (h^j_{k,u} \, h^k_{j,u}). \tag{6.233}$$

Also, because the loop is axisymmetric the metric cross-term $h_{\theta\phi}$ is zero, while the harmonic gauge condition $h^u_{u,u} = \frac{1}{2}h_{,u}$ implies that $h^\theta_{\theta,u} = -h^\phi_{\phi,u}$ to leading order in r^{-1}. Hence,

$$\frac{\mathrm{d}P}{\mathrm{d}\Omega} \approx \frac{r^2}{16\pi} (h^\phi_{\phi,u})^2 = \frac{1}{16\pi} \left(\frac{h_{\phi\phi,u}}{r \sin^2\theta} \right)^2. \tag{6.234}$$

If the source term $S_{\mu\nu}$ specific to a cosmic string given by (6.8) is inserted into (6.230) then

$$h_{\mu\nu}(t, \mathbf{x}) = -4\mu \int \beta^{-1} \Psi_{\mu\nu}(t', \sigma) \, \mathrm{d}\sigma - 4\mu \int \frac{\Psi_{\mu\nu}(-L/4, \sigma)}{|\mathbf{x} - \mathbf{r}|} \, \mathrm{d}\sigma \tag{6.235}$$

where it is understood that $t' > -L/4$ in the first integral and $\mathbf{r} \in \mathbb{R}^3 - \mathbf{V}$ in the second integral, and

$$\beta(t, \mathbf{x}; t', \mathbf{r}) = |\mathbf{x} - \mathbf{r}| - (\mathbf{x} - \mathbf{r}) \cdot \mathbf{r}_\tau \tag{6.236}$$

is a beaming factor.

In view of the equation (6.227) for $\mathbf{r}$, the retarded time t' for the collapsing loop in the wave zone is given implicitly by the equation

$$t' \approx u + \frac{L}{2\pi} \sin\theta \sin(2\pi t'/L) \cos\xi \tag{6.237}$$

where $\xi = 2\pi\sigma/L - \phi$, while

$$\beta \approx r[1 - \sin\theta \cos(2\pi t'/L) \cos\xi] \qquad \text{and} \qquad |\mathbf{x} - \mathbf{r}| \approx r. \tag{6.238}$$

Also, from (6.9) $\Psi_{\phi\phi} = r^2 \sin^2\theta \sin^2\xi$ for all values of t', and the source point $\mathbf{r}$ in the second integral in (6.235) will be in $\mathbb{R}^3 - \mathbf{V}$ if

$$u + L/4 \le \frac{L}{2\pi} \sin\theta \cos\xi. \tag{6.239}$$

If σ is now replaced by ξ as the variable of integration, (6.235) gives

$$\frac{h_{\phi\phi}(t, \mathbf{x})}{r \sin^2\theta} \approx -\frac{2L\mu}{\pi} \int_{\xi_1}^{\xi_2} \frac{\sin^2\xi}{1 - \sin\theta \cos(2\pi t'/L) \cos\xi} \, \mathrm{d}\xi - \frac{2L\mu}{\pi} \int_{\xi_2 - 2\pi}^{\xi_1} \sin^2\xi \, \mathrm{d}\xi \tag{6.240}$$

where $\xi_{1,2} \in (0, 2\pi)$ are the ordered roots of the equation

$$u + L/4 = \frac{L}{2\pi} \sin\theta \cos\xi_{1,2} \qquad \text{if } |u + L/4| < \frac{L}{2\pi} \sin\theta \tag{6.241}$$

and

$$\xi_1 = 0 \qquad \xi_2 = 2\pi \qquad \text{if } |u + L/4| \geq \frac{L}{2\pi} \sin\theta. \tag{6.242}$$

Note from (6.237) that in the first case $\xi = \xi_{1,2}$ corresponds to $t' = -L/4$, and so the partial derivatives of $h_{\phi\phi}$ with respect to both ξ_1 and ξ_2 are (by direct calculation) identically zero. The only contribution to $h_{\phi\phi,u}$, therefore, comes from the dependence of the first integrand on t' which, in turn, is a function of u and ξ through equation (6.237). Hence,

$$\frac{h_{\phi\phi,u}}{r\sin^2\theta} \approx 4\mu \int_{\xi_1}^{\xi_2} \frac{\sin\theta \sin(2\pi t'/L) \sin^2\xi \cos\xi}{[1 - \sin\theta \cos(2\pi t'/L)\cos\xi]^3} \, d\xi. \tag{6.243}$$

For computational purposes, it is more convenient to express this function as an integral over the rescaled time $\chi = 2\pi t'/L$. This gives a total power per unit solid angle

$$\frac{dP}{d\Omega} \approx \frac{4\mu^2}{\pi} K^2 \tag{6.244}$$

where

$$K(u, \theta) = \int \frac{(2\pi u/L - \chi)\sqrt{\sin^2\theta \sin^2\chi - (2\pi u/L - \chi)^2}}{\sin^2\theta[\sin\chi + (2\pi u/L - \chi)\cos\chi]^2} \, d\chi \tag{6.245}$$

and the range of χ is such that $\chi \in [-\frac{1}{2}\pi, 0]$ and the argument of the square root is non-negative.

Garfinkle and Duncan [GD94] have evaluated K numerically for a range of latitudes θ and u in the interval $[-L/4, 0]$. Recall that any gravitational radiation produced at the moment of collapse will propagate along the radial geodesics $u = 0$ (which are shown in equatorial projection in figure 6.5). It is not surprising then that Garfinkle and Duncan find that most of the power is emitted immediately before $u = 0$, and that $dP/d\Omega$ diverges as $u \to 0$ on the equatorial plane.

To examine the late-time behaviour of K in more detail, suppose that $2\pi u/L = -\varepsilon$ with $\varepsilon \ll 1$, and transform to the scaled variables $\bar\chi \equiv -\varepsilon^{-1/3}\chi$ and $\bar\theta = \varepsilon^{-1/3}(\frac{1}{2}\pi - \theta)$. Then, to leading order in ε,

$$K(u, \theta) \sim \varepsilon^{-2/3} \bar{K}(\bar\theta) \tag{6.246}$$

where

$$\bar{K}(\bar\theta) = \int_0^{\bar\chi_+} \frac{\bar\chi\sqrt{2\bar\chi - \bar\chi^2\bar\theta^2 - \bar\chi^4/3}}{(1 + \bar\chi^4/3)^2} \, d\bar\chi \tag{6.247}$$

and $\bar\chi_+$ is the positive root of the expression under the square root.

Since the element of solid angle is $d\Omega \sim \varepsilon^{1/3} d\bar\theta \, d\phi$, the total power P radiated by the loop for small values of u is

$$P \approx \frac{4\mu^2}{\pi}\varepsilon^{-1} \int \bar{K}^2(\bar\theta) \, d\bar\theta \, d\phi = 8\mu^2\varepsilon^{-1} \int_{-\infty}^{\infty} \bar{K}^2(\bar\theta) \, d\bar\theta \approx 7.86\mu^2\varepsilon^{-1} \tag{6.248}$$

and so the energy $\Delta E = \int P \, dt$ lost by the loop diverges logarithmically in $|u|$. Garfinkle and Duncan have calculated that when the loop collapses to 10 times its Schwarzschild radius μL the fraction of its initial rest energy that has been radiated away is approximately $|1.25\mu \ln(80\mu)|$, or about 10^{-5} for a GUT string with $\mu \sim 10^{-6}$.

6.11 The back-reaction problem

6.11.1 General features of the problem

Because strings are extended objects, a self-consistent treatment of the gravitational field of a string needs to correct for the dynamical effects at each point on the string of the gravitational force due to other segments of the string. At the level of the weak-field approximation it is straightforward enough to write down the equations governing the motion of a string in its own back-reaction field, although solving these equations can pose a computational problem of some complexity.

It was seen in section 2.3 that the string trajectory $x^\mu = X^\mu(\tau, \sigma)$ in the standard gauge in a general background spacetime satisfies the equation of motion

$$X^\mu{}_{;\tau\tau} = X^\mu{}_{;\sigma\sigma} \qquad (6.249)$$

where '$; \tau$' is shorthand for the projected covariant derivative $X^\nu_\tau D_\nu$, and a similar remark applies to '$; \sigma$'. In the weak-field approximation, this equation of motion reads:

$$X^\mu{}_{,\tau\tau} - X^\mu{}_{,\sigma\sigma} = -(h^\mu_{\kappa,\lambda} - \tfrac{1}{2}\eta^{\mu\nu}h_{\kappa\lambda,\nu})(V^\kappa V^\lambda - N^\kappa N^\lambda) \qquad (6.250)$$

where the metric perturbation $h_{\mu\nu}$ is given by equation (6.11), and $V^\mu = X^\mu_\tau$ and $N^\mu = X^\mu_\sigma$. For the moment the equation for $h_{\mu\nu}$ will be written as

$$h_{\mu\nu}(t, \mathbf{x}) = -4\mu \int [|\mathbf{x} - \mathbf{r}| - (\mathbf{x} - \mathbf{r}) \cdot \mathbf{r}_\tau]^{-1} \Psi_{\mu\nu} \, d\sigma \qquad (6.251)$$

where $\Psi_{\mu\nu}$ (defined in (6.9)), $\mathbf{r}$ and $\mathbf{r}_\tau$ are all functions of σ and the retarded time τ, which, in turn, is an implicit function of t, $\mathbf{x}$ and σ through the equation $\tau = t - |\mathbf{x} - \mathbf{r}(\tau, \sigma)|$.

Equations (6.250) and (6.251) together constitute the weak-field back-reaction problem for a cosmic string. These two equations are linked by the fact that the field point $x^\mu = [t, \mathbf{x}]$ in (6.251) is the point X^μ on the string at which (6.250) is locally being integrated. The problem is, therefore, a highly nonlinear one, and it seems unlikely that any exact solutions will ever be found— apart from the few exact fully relativistic solutions that are already known (such as the travelling-wave solutions of section 9.1).

An alternative, computer-based approach to the back-reaction problem is to start with an exact solution of the Nambu–Goto equations of motion, calculate

the spacetime derivatives of the corresponding metric perturbation $h_{\mu\nu}$ at each point on the string from (6.251), insert these into the right-hand side of the equation of motion (6.250) and then integrate the equation of motion over a single period of the string to give a new periodic trajectory X^μ. The entire procedure can then be iterated indefinitely, leading hopefully to an accurate picture of the secular evolution of the string's trajectory under the action of its own gravitational field. This is the approach adopted by Jean Quashnock and David Spergel in a pioneering paper on the back-reaction problem published in 1990 [QS90].

It turns out that the problem is somewhat simpler to analyse in the light-cone gauge than in the standard gauge. In terms of the light-cone coordinates $\sigma_\pm = \tau \pm \sigma$ the back-reaction equation (6.250) reads:

$$X^\mu,_{+-} = \tfrac{1}{4}\alpha^\mu(\sigma_+, \sigma_-) \tag{6.252}$$

where

$$\alpha^\mu = -2(h^\mu_{\kappa},_\lambda + h^\mu_{\lambda},_\kappa - \eta^{\mu\nu}h_{\kappa\lambda},_\nu)X^\kappa_+ X^\lambda_- \tag{6.253}$$

is the local acceleration 4-vector of the string.

If the initial state of the string is prescribed to be a Nambu–Goto solution with parametric period $T = L/2$ then, in principle, the acceleration vector α^μ can be evaluated at each point (σ_+, σ_-) in the fundamental domain $[0, L] \times [0, L]$ on the world sheet. The changes in the null tangent vectors X^μ_+ and X^μ_+ as a result of gravitational back-reaction over the course of a single period are then

$$\delta X^\mu_+(\sigma_+) = \tfrac{1}{4}\int_0^L \alpha^\mu(\sigma_+, \sigma_-)\, d\sigma_-$$
$$\delta X^\mu_-(\sigma_-) = \tfrac{1}{4}\int_0^L \alpha^\mu(\sigma_+, \sigma_-)\, d\sigma_+ \tag{6.254}$$

and a new, perturbed trajectory can be generated from the new tangent vectors $X^\mu_+ + \delta X^\mu_+$ and $X^\mu_- + \delta X^\mu_-$.

Note that δX^μ_+ and δX^μ_- are both periodic with period L (as α^μ is periodic on the fundamental domain), and that the perturbed solution remains spatially closed, as

$$\int_0^L \delta X^\mu,_\sigma\, d\sigma = \int_0^L \delta X^\mu_+\, d\sigma_+ - \int_0^L \delta X^\mu_-\, d\sigma_- = 0. \tag{6.255}$$

Also,

$$X_+ \cdot \delta X_+ = -\tfrac{1}{2}\int_0^L (h_{\mu\kappa},_\lambda + h_{\mu\lambda},_\kappa - h_{\kappa\lambda},_\mu)\, X^\kappa_+ X^\lambda_- X^\mu_+\, d\sigma_-$$
$$= -\tfrac{1}{2}X^\kappa_+ X^\mu_+[h_{\mu\kappa}]_{\sigma_-=0}^{\sigma_-=L} = 0 \tag{6.256}$$

and so (given that $X_- \cdot \delta X_- = 0$ as well) the light-cone gauge conditions $X_+^2 = X_-^2 = 0$ are preserved to linear order in the perturbations δX^μ_+ and δX^μ_-,

which for a GUT string would be of order $\mu \sim 10^{-6}$. Thus the new solution remains, to leading order, a Nambu–Goto solution in light-cone coordinates with period L.

However, the original coordinates $\sigma_{\pm}$ will not, in general, define an aligned gauge for the perturbed solution, as

$$t_{,\tau} = 1 + \delta X^0_+ + \delta X^0_- \neq 1. \qquad (6.257)$$

At a physical level the misalignment occurs because as the string radiates energy its invariant length falls below $L_{\min}$ and its fundamental period (in t) shrinks, causing a secular decrease in $t_{,\tau}$. In order to facilitate comparison between successive stages in the evolution of a given radiating solution, Quashnock and Spergel choose to realign the gauge coordinates σ_+ and σ_-, in the manner described in section 3.1, at the end of each period. Specifically, the realigned gauge coordinates $\bar{\sigma}_+$ and $\bar{\sigma}_-$ become:

$$\bar{\sigma}_+ = \sigma_+ + 2 \int_0^{\sigma_+} \delta X^0_+(u)\,\mathrm{d}u \qquad \text{and} \qquad \bar{\sigma}_- = \sigma_- + 2 \int_0^{\sigma_-} \delta X^0_-(v)\,\mathrm{d}v \qquad (6.258)$$

and the parametric period changes from L to $L + \delta L$, where

$$\delta L = \tfrac{1}{2} \int_0^L \int_0^L \alpha^0 \, \mathrm{d}\sigma_+ \, \mathrm{d}\sigma_-. \qquad (6.259)$$

One of the advantages of Quashnock and Spergel's approach is that the total energy and momentum lost by the string during the course of a single period can be calculated directly from a knowledge of α^μ. The 4-momentum of the string as measured on any constant-t hypersurface is:

$$P^\mu = \int T^{\mu 0} \, \mathrm{d}^3\mathbf{x} \qquad (6.260)$$

where

$$T^{\mu\nu} = \mu \int (X^\mu_+ X^\nu_- + X^\mu_- X^\nu_+)\delta^4(x - X) \, \mathrm{d}\sigma_+ \, \mathrm{d}\sigma_- \qquad (6.261)$$

is the standard string stress–energy tensor (6.1) in light-cone coordinates.

In view of Gauss's theorem, the time derivative of P^μ is

$$P^\mu{}_{,0} = \int T^{\mu 0}{}_{,0} \, \mathrm{d}^3\mathbf{x} = \int T^{\mu\nu}{}_{,\nu} \, \mathrm{d}^3\mathbf{x} \qquad (6.262)$$

and so the change in P^μ over a single period $T = L/2$ is

$$\delta P^\mu = \int_0^T \mathrm{d}t \int T^{\mu\nu}{}_{,\nu} \, \mathrm{d}^3\mathbf{x} = -\int_0^T \mathrm{d}t \int (\Gamma^\mu{}_{\lambda\nu} T^{\lambda\nu} + \Gamma^\nu{}_{\lambda\nu} T^{\mu\lambda}) \, \mathrm{d}^3\mathbf{x} \qquad (6.263)$$

where the right-hand expression follows from the stress–energy conservation equation $T^{\mu\nu}{}_{;\nu} = 0$. Substitution of (6.261) into this expression gives

$$\delta P^\mu = -2\mu \int_0^L \int_0^L \Gamma^\mu{}_{\lambda\nu} X_+^\lambda X_-^\nu \, d\sigma_+ \, d\sigma_-$$

$$- \mu \int_0^L \int_0^L \Gamma^\nu{}_{\lambda\nu} (X_+^\mu X_-^\lambda + X_-^\mu X_+^\lambda) \, d\sigma_+ \, d\sigma_-. \qquad (6.264)$$

In the weak-field approximation $\Gamma^\mu{}_{\lambda\nu} = \frac{1}{2}(h^\mu_{\lambda,\nu} + h^\mu_{\nu,\lambda} - \eta^{\mu\kappa} h_{\lambda\nu,\kappa})$ and, in particular, $\Gamma^\nu{}_{\lambda\nu} = \frac{1}{2} h^\nu_{\nu,\lambda}$. The second term on the right of (6.264) vanishes because h^ν_ν is periodic on the fundamental domain. Thus in view of (6.253) the change in P^μ over a single period is

$$\delta P^\mu = \frac{1}{2}\mu \int_0^L \int_0^L \alpha^\mu \, d\sigma_+ \, d\sigma_-. \qquad (6.265)$$

Equation (6.265) allows the changes in the string's energy and momentum in passing from one perturbation solution to the next to be tracked with relative ease.

Quashnock and Spergel [QS90] have also shown, after a lengthy calculation, that the loss of energy $\delta P^0 \equiv \mu \delta L$ over a single period exactly balances the energy flux TP at infinity calculated on the basis of the weak-field formalism outlined in section 6.4. To be specific, they show that $\delta P^0 = -\delta E$, where

$$\delta E = 2 \int_0^\infty \omega^2 \, d\omega \int d\Omega \, (\tau^{\mu\nu} \tau^*_{\mu\nu} - \frac{1}{2}|\tau^\mu_\mu|^2) \qquad (6.266)$$
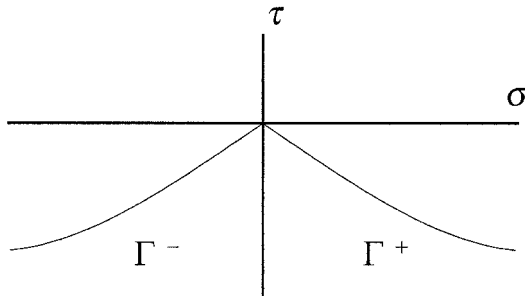
is the energy flux TP expanded as a functional of the Fourier transform

$$\tau^{\mu\nu} = \frac{1}{2\pi} \int_{-\infty}^\infty dt' \int d^3x' \, T^{\mu\nu}(t', \mathbf{x}') e^{i\omega(t' - \mathbf{n} \cdot \mathbf{x}')} \qquad (6.267)$$

of the stress–energy tensor. Since the integral (6.266) and the corresponding series for TP generated by (6.63) are identical when the source is periodic, the radiative flux calculations examined earlier and the back-reaction calculations to be described later treat complementary aspects of the same problem.

6.11.2 Self-acceleration of a cosmic string

All that remains to complete the specification of the back-reaction formalism is to explain how the acceleration term α^μ is evaluated. In view of (6.253), α^μ is a linear combination of the spacetime derivatives of the metric perturbations $h_{\mu\nu}$, which are, in turn, given by the world-sheet line integral (6.251). Suppose for the moment that the field point $[t, \mathbf{x}]$ at which $h_{\mu\nu}$ is evaluated lies at $\tau = \sigma = 0$. The integration contour $\Gamma = \{\tau = t - |\mathbf{x} - \mathbf{r}(\tau, \sigma)|\}$ in (6.251), which is the intersection of the backwards light cone of the field point $[t, \mathbf{x}]$ with the world

Figure 6.6. The two branches of the projection of the backwards light cone at $(\tau, \sigma) = (0, 0)$.

sheet **T**, and will then have the general shape indicated in figure 6.6 (although it need not be symmetric about $\sigma = 0$). Note, in particular, that the two branches of Γ are asymptotically null (and thus intersect at a right angle) at the field point.

As previously mentioned, at each step in the iterative evolution of a radiating string the trajectory will satisfy the Nambu–Goto equations to order μ. So provided that the field point is not a cusp or a kink the retarded time τ for source points close to the field point is given by $\tau \approx -|\sigma|$, while

$$\mathbf{x} - \mathbf{r} \approx |\sigma| \times \begin{cases} \mathbf{a}_0' & \text{if } \sigma < 0 \\ \mathbf{b}_0' & \text{if } \sigma > 0 \end{cases} \tag{6.268}$$

where $\mathbf{a}_0'$ and $\mathbf{b}_0'$ are the derivatives of the mode functions $\mathbf{a}$ and $\mathbf{b}$ at $\tau = \sigma = 0$.

Thus the beaming factor in (6.251) has the small-distance dependence

$$|\mathbf{x} - \mathbf{r}| - (\mathbf{x} - \mathbf{r}) \cdot \mathbf{r}_\tau \approx \lambda^{-2} |\sigma| \tag{6.269}$$

where $\lambda = [\frac{1}{2}(1 - \mathbf{a}_0' \cdot \mathbf{b}_0')]^{-1/2}$ is the local Lorentz factor of the string. The contribution of the points near $[t, \mathbf{x}]$ to $h_{\mu\nu}$, therefore, has the approximate form

$$h_{\mu\nu} \approx -4\mu\lambda^2 \Psi_{\mu\nu} \int \frac{d\sigma}{|\sigma|} \tag{6.270}$$

where $\Psi_{\mu\nu}$ is evaluated at $\tau = \sigma = 0$.

On the face of it, then, the metric perturbation $h_{\mu\nu}$ contains a logarithmic divergence, and the self-energy of each of the points on the string is infinite. However, this divergence is pure gauge and vanishes when the spacetime derivatives $h_{\mu\nu,\kappa}$ are calculated. As previously, the short-distance behaviour of the integrands from which α^μ is constructed is most conveniently studied in the light-cone gauge rather than the standard gauge. For source points near the field point $[t, \mathbf{x}]$ the integration contour Γ in figure 6.6 divides naturally into two parts: the segment Γ^- to the left of the field point, where $\sigma < 0$, $\sigma_+ < 0$ and $\sigma_- \approx 0$;

and the segment Γ^+ to the right of the field point, where $\sigma > 0$, $\sigma_- < 0$ and $\sigma_+ \approx 0$.

For source points on Γ^- the most convenient choice of integration variable is σ_+. Since the Jacobian of the transformation from σ to σ_+ on Γ is given by

$$[|\mathbf{x} - \mathbf{r}| - (\mathbf{x} - \mathbf{r}) \cdot \mathbf{r}_\tau]^{-1} \, d\sigma = [|\mathbf{x} - \mathbf{r}| - 2(\mathbf{x} - \mathbf{r}) \cdot \mathbf{r}_-]^{-1} \, d\sigma_+ \qquad (6.271)$$

it follows that the contribution of Γ^- to $h_{\mu\nu,\kappa}$ is

$$h^-_{\mu\nu,\kappa} = -4\mu \int_{\Gamma^-} \frac{\partial}{\partial x^\kappa} \{[|\mathbf{x} - \mathbf{r}| - 2(\mathbf{x} - \mathbf{r}) \cdot \mathbf{r}_-]^{-1} \Psi_{\mu\nu}\} \, d\sigma_+ \qquad (6.272)$$

where, now, $\Psi_{\mu\nu} = 2(V^+_\mu V^-_\nu + V^-_\mu V^+_\nu - \eta_{\mu\nu} V^+ \cdot V^-)$, with $V^\pm_\mu = \partial X_\mu / \partial \sigma_\pm$.

Also, taking the spacetime derivatives of the equation $\tau = t - |\mathbf{x} - \mathbf{r}|$ for Γ with σ_+ fixed gives

$$\sigma_{-,\kappa} = (\Delta X \cdot V^-)^{-1} \Delta X_\kappa \qquad (6.273)$$

where $\Delta X^\kappa = [t - \tau, \mathbf{x} - \mathbf{r}]$ is the separation of the source point from the field point and

$$\Delta X \cdot V^- = \tfrac{1}{2}(t - \tau) - (\mathbf{x} - \mathbf{r}) \cdot \mathbf{r}_-. \qquad (6.274)$$

Hence,

$$\frac{\partial}{\partial x^\kappa} \{[|\mathbf{x} - \mathbf{r}| - 2(\mathbf{x} - \mathbf{r}) \cdot \mathbf{r}_-]^{-1} \Psi_{\mu\nu}\}$$
$$= \tfrac{1}{2}(\Delta X \cdot V^-)^{-1} \Delta X_\kappa \frac{\partial}{\partial \sigma_-}[(\Delta X \cdot V^-)^{-1} \Psi_{\mu\nu}] - \tfrac{1}{2}(\Delta X \cdot V^-)^{-2} V^-_\kappa \Psi_{\mu\nu}$$
$$(6.275)$$

where $V^-_\kappa = [\tfrac{1}{2}, -\mathbf{r}_-]$, and the partial derivative $\partial/\partial\sigma_-$ is understood to be taken off-shell (that is, with t, $\mathbf{x}$ and σ_+ constant).

In view of the fact that $(\partial/\partial\sigma_-)\Delta X_\kappa = -V^-_\kappa$, therefore,

$$h^-_{\mu\nu,\kappa} = -2\mu \int_{\Gamma^-} (\Delta X \cdot V^-)^{-1} \frac{\partial}{\partial \sigma_-}[(\Delta X \cdot V^-)^{-1} \Psi_{\mu\nu} \Delta X_\kappa] \, d\sigma_+ \qquad (6.276)$$

and so the contribution of Γ^- to the acceleration vector α^μ in the weak-field approximation is

$$\alpha^{-\mu} = 4\mu \int_{\Gamma^-} (\Delta X \cdot V^-)^{-1} \frac{\partial}{\partial \sigma_-}[Q^\mu_{(+-)} + Q^\mu_{(-+)} - R^\mu] \, d\sigma_+ \qquad (6.277)$$

where

$$Q^\mu_{(+-)} = (\Delta X \cdot V^-)^{-1} \Psi^\mu_\kappa V^{+\kappa}_0 \Delta X \cdot V^-_0$$
$$Q^\mu_{(-+)} = (\Delta X \cdot V^-)^{-1} \Psi^\mu_\kappa V^{-\kappa}_0 \Delta X \cdot V^+_0 \qquad (6.278)$$

and

$$R^\mu = (\Delta X \cdot V^-)^{-1} \Psi_{\kappa\lambda} V^{+\kappa}_0 V^{-\lambda}_0 \Delta X^\mu \qquad (6.279)$$

and $V_0^{\pm\kappa}$ are the limiting values of $V^{\pm\kappa}$ at the field point $\sigma_+ = \sigma_- = 0$.

An immediate consequence of (6.277) is that a long string in the shape of a travelling wave experiences no self-acceleration. It has already been mentioned that travelling-wave solutions are known to satisfy the full Einstein equations and so it should come as no surprise that α^μ is identically zero for a travelling wave. The defining feature of a travelling-wave solution is that either $V^{+\mu}$ or $V^{-\mu}$ is a constant vector. In the first case $V^{+\mu} = V_0^{+\mu}$ everywhere, and so $\Psi_\kappa^\mu V_0^{+\kappa} \equiv 0$.

If the origin of the spatial coordinates is chosen so that $\mathbf{x} = \mathbf{0}$, the equation for the integration curve Γ becomes

$$\sigma_+ + \sigma_- = -|\mathbf{a}_0'\sigma_+ + \mathbf{b}(\sigma_-)| \tag{6.280}$$

where $\mathbf{a}_0'$ is a constant unit vector and $\mathbf{b}(0) = \mathbf{0}$. The curve Γ^- is, therefore, simply the null segment $\sigma_- = 0$, and $V^{-\mu} = V_0^{-\mu}$ at all points on Γ^-. It follows that $\Psi_\kappa^\mu V_0^{-\kappa} \equiv 0$ as well, and so $\alpha^{-\mu}$ is identically zero. However, if $V^{-\mu}$ is constant then $\Psi_\kappa^\mu V_0^{-\kappa} \equiv 0$, and the only terms in (6.277) which depend on σ_- are $\Delta X \cdot V^-$ and $\Delta X \cdot V_0^-$, whose σ_- derivatives are both $-(V_0^-)^2 = 0$. Thus $\alpha^{-\mu}$ vanishes again. By symmetry, the contribution to α^μ of Γ^+ also vanishes, irrespective of whether $V^{+\mu}$ or $V^{-\mu}$ is constant.

In the case of a more general string configuration, ΔX^κ can be expanded in the standard form

$$\Delta X^\kappa \approx -\tfrac{1}{2}[\sigma_+ + \sigma_-, \mathbf{a}_0'\sigma_+ + \mathbf{b}_0'\sigma_- + \tfrac{1}{2}(\mathbf{a}_0''\sigma_+^2 + \mathbf{b}_0''\sigma_-^2) + \tfrac{1}{6}(\mathbf{a}_0'''\sigma_+^3 + \mathbf{b}_0'''\sigma_-^3)]. \tag{6.281}$$

and so the beaming factor in (6.277) becomes

$$\begin{aligned}
\Delta X \cdot V^- \approx -\tfrac{1}{4}(2\lambda^{-2}\sigma_+ &- \mathbf{a}_0' \cdot \mathbf{b}_0''\sigma_+\sigma_- - \tfrac{1}{2}\mathbf{a}_0' \cdot \mathbf{b}_0'''\sigma_+\sigma_-^2 - \tfrac{1}{2}\mathbf{b}_0' \cdot \mathbf{a}_0''\sigma_+^2 \\
&- \tfrac{1}{6}\mathbf{b}_0' \cdot \mathbf{a}_0'''\sigma_+^3 + \tfrac{1}{6}|\mathbf{b}_0''|^2\sigma_-^3 - \tfrac{1}{2}\mathbf{a}_0'' \cdot \mathbf{b}_0''\sigma_+^2\sigma_-).
\end{aligned} \tag{6.282}$$

Also, the equation $(\Delta X)^2 = 0$ for the integration contour Γ reads:

$$\begin{aligned}
0 \approx \lambda^{-2}\sigma_+\sigma_- &- \tfrac{1}{4}(\mathbf{b}_0' \cdot \mathbf{a}_0''\sigma_+ + \mathbf{a}_0' \cdot \mathbf{b}_0''\sigma_-)\sigma_+\sigma_- + \tfrac{1}{48}(|\mathbf{a}_0''|^2\sigma_+^4 + |\mathbf{b}_0''|^2\sigma_-^4) \\
&- \tfrac{1}{4}(\tfrac{1}{3}\mathbf{b}_0' \cdot \mathbf{a}_0'''\sigma_+^2 + \tfrac{1}{2}\mathbf{a}_0'' \cdot \mathbf{b}_0''\sigma_+\sigma_- + \tfrac{1}{3}\mathbf{a}_0' \cdot \mathbf{b}_0'''\sigma_-^2)\sigma_+\sigma_- \tag{6.283}
\end{aligned}$$

and so to leading order in σ_+ the segment Γ^- has the equation

$$\sigma_- \approx -\tfrac{1}{48}|\mathbf{a}_0''|^2\sigma_+^3. \tag{6.284}$$

Expanding the integrands in (6.277) in σ_+ and σ_- is a tedious process best performed with a computer algebra system and, in general, it is necessary to retain all terms up to and including $\mathbf{a}_0^{(4)}$ and $\mathbf{b}_0^{(4)}$. Once σ_- has been eliminated in favour of σ_+ through (6.284), it turns out that, to second order in σ_+,

$$\frac{\partial}{\partial\sigma_-}R^\mu \approx \tfrac{1}{8}\{\lambda^2(\mathbf{a}_0' \cdot \mathbf{b}_0'')(\mathbf{b}_0' \cdot \mathbf{a}_0'') + 2\mathbf{a}_0'' \cdot \mathbf{b}_0''\}[1, \mathbf{a}_0']\sigma_+$$

$$+ \tfrac{1}{32}\{\lambda^2(\mathbf{a}_0' \cdot \mathbf{b}_0'')(\mathbf{b}_0' \cdot \mathbf{a}_0'') + 2\mathbf{a}_0'' \cdot \mathbf{b}_0''\}$$

$$\times \{\lambda^2(\mathbf{b}_0' \cdot \mathbf{a}_0'')[1, \mathbf{a}_0'] + 2[0, \mathbf{a}_0'']\}\sigma_+^2$$

$$+ \tfrac{1}{16}\{2\mathbf{b}_0'' \cdot \mathbf{a}_0''' + \lambda^2(\mathbf{a}_0' \cdot \mathbf{b}_0'')(\mathbf{b}_0' \cdot \mathbf{a}_0''')\}[1, \mathbf{a}_0']\sigma_+^2 \qquad (6.285)$$

$$\frac{\partial}{\partial\sigma_-}Q^\mu_{(+-)} \approx \frac{\partial}{\partial\sigma_-}R^\mu + \tfrac{1}{16}|\mathbf{a}_0''|^2\{\lambda^2(\mathbf{a}_0' \cdot \mathbf{b}_0'')[1, \mathbf{b}_0'] + 2[0, \mathbf{b}_0'']\}\sigma_+^2 \quad (6.286)$$

and

$$\frac{\partial}{\partial\sigma_-}Q^\mu_{(-+)} \approx \tfrac{1}{96}|\mathbf{a}_0''|^2\{\lambda^2(\mathbf{a}_0' \cdot \mathbf{b}_0'')[1, \mathbf{b}_0'] + 2[0, \mathbf{b}_0'']\}\sigma_+^2. \qquad (6.287)$$

Since $(\Delta X \cdot V^-)^{-1} \approx -2\lambda^2\sigma_+^{-1}$ to leading order, the contribution of Γ^- to the self-acceleration of the string, for source points near to the field point, is [QS90]:

$$\alpha^{-\mu} \approx -\tfrac{7}{12}\mu\lambda^2|\mathbf{a}_0''|^2\{\lambda^2(\mathbf{a}_0' \cdot \mathbf{b}_0'')[1, \mathbf{b}_0'] + 2[0, \mathbf{b}_0'']\}\int_{\Gamma^-}\sigma_+\,d\sigma_+ \qquad (6.288)$$

and is clearly free of short-distance divergences. The contribution of Γ^+ is found by replacing σ_+ with σ_- in this expression and interchanging $\mathbf{a}_0'$ with $\mathbf{b}_0'$ (and $\mathbf{a}_0''$ with $\mathbf{b}_0''$) throughout.

The one obvious case in which this analysis breaks down occurs when the field point is located at a cusp, as then the local Lorentz factor λ is undefined. At a cusp, the separation vector ΔX^κ has the standard expansion

$$\Delta X^\kappa \approx -\tfrac{1}{2}[\sigma_+ + \sigma_-, \mathbf{v}_c(\sigma_+ + \sigma_-) + \tfrac{1}{2}(\mathbf{a}_c''\sigma_+^2 + \mathbf{b}_c''\sigma_-^2) + \tfrac{1}{6}(\mathbf{a}_c'''\sigma_+^3 + \mathbf{b}_c'''\sigma_-^3)] \qquad (6.289)$$

where $\mathbf{v}_c$ is a unit vector orthogonal to both $\mathbf{a}_c''$ and $\mathbf{b}_c''$, while $\mathbf{v}_c \cdot \mathbf{a}_c''' = -|\mathbf{a}_c''|^2$ and $\mathbf{v}_c \cdot \mathbf{b}_c''' = -|\mathbf{b}_c''|^2$. The integration contour Γ in this case has the same basic form as in figure 6.6, except that the angle between the two branches of Γ at the field point is, in general, greater than $\pi/2$.

In fact the equation $(\Delta X)^2 = 0$ for Γ reads:

$$0 \approx \tfrac{1}{48}|\mathbf{a}_c''|^2(\sigma_+ + 4\sigma_-)\sigma_+^3 + \tfrac{1}{48}|\mathbf{b}_c''|^2(\sigma_- + 4\sigma_+)\sigma_-^3 - \tfrac{1}{8}(\mathbf{a}_c'' \cdot \mathbf{b}_c'')\sigma_+^2\sigma_-^2 \quad (6.290)$$

and so $\sigma_- \approx k\sigma_+$ where k is a root of the quartic equation

$$f(k) \equiv |\mathbf{a}_c''|^2(1 + 4k) - 6(\mathbf{a}_c'' \cdot \mathbf{b}_c'')k^2 + |\mathbf{b}_c''|^2(4k^3 + k^4) = 0. \qquad (6.291)$$

On Γ^-, where τ and σ are both negative, k must lie in $(-1, 1)$. Since $f(0) = |\mathbf{a}_c''|^2$ and $f(-1) = -3|\mathbf{a}_c'' + \mathbf{b}_c''|^2$ there is a least one root in $[-1, 0]$. It is easily seen that none of the roots is positive, and that the root in $[-1, 0]$ is unique (save for multiplicities when $k = -1$ or 0). For present purposes the extreme cases $k = 0$ (which occurs, for example, at a cusp on a travelling wave) and $k = -1$ (which occurs only when $\mathbf{b}_c'' = -\mathbf{a}_c''$, so that the cusp is degenerate and the bridging vector $\mathbf{s}_c = \tfrac{1}{2}(\mathbf{a}_c''' - \mathbf{b}_c''')$ is orthogonal to the cusp velocity $\mathbf{v}_c$) will be ignored.

The fact that σ_- is proportional to σ_+ near the field point simplifies the calculation of the short-distance divergence in $\alpha^{-\mu}$ considerably. The beaming factor

$$\Delta X \cdot V^- \approx -[\tfrac{1}{24}|\mathbf{a}_c''|^2\sigma_+^3 + \tfrac{1}{24}|\mathbf{b}_c''|^2(\sigma_- + 3\sigma_+)\sigma_-^2 - \tfrac{1}{8}(\mathbf{a}_c'' \cdot \mathbf{b}_c'')\sigma_+^2\sigma_-] \quad (6.292)$$

is of order σ_+^3, and so

$$\begin{aligned}
\frac{\partial}{\partial\sigma_-}Q_{(+-)}^\mu &\equiv \frac{\partial}{\partial\sigma_-}Q_{(-+)}^\mu \\
&\approx \tfrac{1}{4}(\mathbf{a}_c'' \cdot \mathbf{b}_c'')\{|\mathbf{a}_c''|^4 + |\mathbf{a}_c''|^2|\mathbf{b}_c''|^2(2k^3 - 3k^2) \\
&\quad + |\mathbf{b}_c''|^4(k^6 + 6k^5) - 9(\mathbf{a}_c'' \cdot \mathbf{b}_c'')|\mathbf{b}_c''|^2k^4\} \\
&\quad \times \{[|\mathbf{a}_c''|^2 + |\mathbf{b}_c''|^2(3k^2 + k^3) - 3(\mathbf{a}_c'' \cdot \mathbf{b}_c'')k]^2\}^{-1} \\
&\quad \times [1, \mathbf{v}_c]\sigma_+
\end{aligned} \quad (6.293)$$

while

$$\begin{aligned}
\frac{\partial}{\partial\sigma_-}R^\mu &\approx \frac{3}{4}|\mathbf{a}_c''|^2|\mathbf{b}_c''|^2 \frac{|\mathbf{a}_c''|^2(2 + 3k) - (\mathbf{a}_c'' \cdot \mathbf{b}_c'')(3k + 6k^2) + 2|\mathbf{b}_c''|^2k^3}{[|\mathbf{a}_c''|^2 + |\mathbf{b}_c''|^2(3k^2 + k^3) - 3(\mathbf{a}_c'' \cdot \mathbf{b}_c'')k]^2} \\
&\quad \times [1, \mathbf{v}_c]\sigma_+.
\end{aligned} \quad (6.294)$$

Thus, for source points in the neighbourhood of a field point located at a cusp, the expression (6.277) for $\alpha^{-\mu}$ contains a short-distance divergence of the form $\int_{\Gamma-} \sigma_+^{-2}\,d\sigma_+$ which is proportional to the cusp 4-velocity $[1, \mathbf{v}_c]$. A similar statement is true of $\alpha^{+\mu}$. Although the nature of the gravitational beaming from a cusp (discussed in section 6.2) suggests very strongly that the divergent contribution to the cusp's self-acceleration should be directed anti-parallel to $\mathbf{v}_c$, the multiplicative factor appearing outside $[1, \mathbf{v}_c]$ in $\alpha^{-\mu}$ turns out to be neither negative nor positive definite.

In fact, if the available two-dimensional parameter space is described in terms of the cusp angles χ and ψ, where
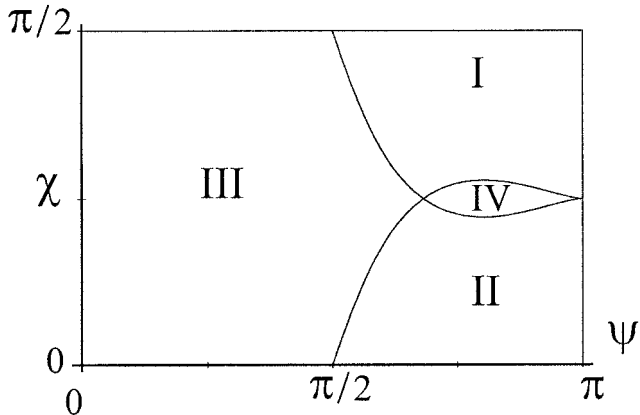
$$\tan\chi = |\mathbf{a}_c''|/|\mathbf{b}_c''| \qquad \text{and} \qquad \cos\psi = \mathbf{a}_c'' \cdot \mathbf{b}_c''/(|\mathbf{a}_c''||\mathbf{b}_c''|) \quad (6.295)$$

then to leading order

$$\begin{aligned}
\alpha^{-\mu} &\approx 32k\frac{(k^{10} + 4k^9)\rho^6 - (6k^7 + 3k^6)\rho^4 + (12k^4 + 18k^3)\rho^2 - 8k - 2}{[(k^4 + 2k^3)\rho^2 - 2k - 1]^3} \\
&\quad \times [1, \mathbf{v}_c]\int\sigma_+^{-2}\,d\sigma_+
\end{aligned} \quad (6.296)$$

with $\rho = \cot\chi$ and k the root of the quartic equation $1 + 4k - 6k^2\rho\cos\psi + (4k^3 + k^4)\rho^2 = 0$ lying in $(-1, 0)$.

The corresponding equation for $\alpha^{+\mu}$ is found by reading ρ as $\tan\chi$ and replacing σ_+ with σ_-. (Note that the quartic equation for k generally has two real

Figure 6.7. Orientations of the divergent contributions to the self-acceleration near a cusp.

roots, one in $(-1, 0)$ and one less than -1. Under the transformation $\rho \to \rho^{-1}$ the new roots are just the reciprocals of the old ones, $k \to k^{-1}$. So the value of k used when calculating $\alpha^{+\mu}$ is just the reciprocal of the root in $(-\infty, -1)$ of the original quartic.)

Figure 6.7 divides the $\chi-\psi$ parameter space into four regions determined by the orientations of the short-distance divergences in $\alpha^{-\mu}$ and $\alpha^{+\mu}$. In region I $\alpha^{-\mu}$ is parallel to $[1, \mathbf{v}_c]$ but $\alpha^{+\mu}$ is anti-parallel to $[1, \mathbf{v}_c]$; in region II the reverse is true; in region III both $\alpha^{-\mu}$ and $\alpha^{+\mu}$ are anti-parallel to $[1, \mathbf{v}_c]$; and in region IV both are parallel to $[1, \mathbf{v}_c]$. It therefore seems possible, in principle, for gravitational back-reaction to accelerate a cusp forwards rather than backwards, although only in cases where the angle between $\mathbf{a}_c''$ and $\mathbf{b}_c''$ is greater than $\pi/2$ (that is, in regions I, II and IV).

6.11.3 Back-reaction and cusp displacement

Of course, a cusp is not a physical point on the string but a structural feature of the string's trajectory. Once the perturbed mode functions δX_+^μ and δX_-^μ have been calculated the effect of the perturbation on the position of a cusp can be determined directly. Suppose as before that the cusp initially appears at $(\sigma_+, \sigma_-) = (0, 0)$, with $X_+^\mu(0) = X_-^\mu(0) = \frac{1}{2}[1, \mathbf{v}_c]$. After a single period of oscillation the cusp will typically appear at a new gauge position $(\sigma_+, \sigma_-) = (\delta\sigma_+, \delta\sigma_-)$, where $\delta\sigma_+$ and $\delta\sigma_-$ are small compared to the parametric period L.

In view of the realignment conditions (6.258) the new aligned gauge coordinates are

$$\bar{\sigma}_+ \approx [1 + 2\delta X_+^0(0)]\sigma_+ \qquad \text{and} \qquad \bar{\sigma}_- \approx [1 + 2\delta X_-^0(0)]\sigma_- \qquad (6.297)$$

in the neighbourhood of $(\sigma_+, \sigma_-) = (0, 0)$. The equation $X_+^\mu + \delta X_+^\mu = X_-^\mu + \delta X_-^\mu$

for a cusp (in the barred gauge, of course), therefore, reduces to

$$-\mathbf{v}_c \delta X^0_+(0) + \tfrac{1}{2}\mathbf{a}''_c \delta\sigma_+ + \delta\mathbf{r}_+(0) \approx -\mathbf{v}_c \delta X^0_-(0) + \tfrac{1}{2}\mathbf{b}''_c \delta\sigma_- + \delta\mathbf{r}_-(0) \quad (6.298)$$

where $\delta\mathbf{r}$ denotes the spacelike components of δX^μ.

Given that $\delta X^0_\pm(0) = \mathbf{v}_c \cdot \delta\mathbf{r}_\pm(0)$ by virtue of (6.256), and $\mathbf{a}''_c$ and $\mathbf{b}''_c$ are orthogonal to $\mathbf{v}_c$, this equation can be solved by projection to give

$$\tfrac{1}{2}\delta\sigma_+ = \mathbf{\Delta} \cdot [|\mathbf{b}''_c|^2 \mathbf{a}''_c - (\mathbf{a}''_c \cdot \mathbf{b}''_c)\mathbf{b}''_c]/|\mathbf{a}''_c \times \mathbf{b}''_c|^2 \quad (6.299)$$

and

$$\tfrac{1}{2}\delta\sigma_- = \mathbf{\Delta} \cdot [|\mathbf{a}''_c|^2 \mathbf{b}''_c - (\mathbf{a}''_c \cdot \mathbf{b}''_c)\mathbf{a}''_c]/|\mathbf{a}''_c \times \mathbf{b}''_c|^2 \quad (6.300)$$

where $\mathbf{\Delta} = \delta\mathbf{r}_-(0) - \delta\mathbf{r}_+(0)$. Thus, the spatial position of the perturbed cusp will be

$$(\mathbf{r} + \delta\mathbf{r})|_{(\delta\sigma_+, \delta\sigma_-)} \approx \mathbf{r}_c + \delta\mathbf{r}(0, 0) + \mathbf{v}_c \delta\tau \quad (6.301)$$

where $\delta\tau = \tfrac{1}{2}(\delta\sigma_+ + \delta\sigma_-)$ and $\mathbf{r}_c = \mathbf{r}(0, 0)$ is its unperturbed position.

If, for the sake of computational convenience, the perturbation δX^μ is generated by integrating away from the point $(\sigma_+, \sigma_-) = (0, 0)$ then

$$\delta X^\mu(\sigma_+, \sigma_-) = \tfrac{1}{4} \int_0^{\sigma_+} \int_0^L \alpha^\mu(u, \sigma_-)\, \mathrm{d}\sigma_-\, \mathrm{d}u + \tfrac{1}{4} \int_0^{\sigma_-} \int_0^L \alpha^\mu(\sigma_+, v)\, \mathrm{d}\sigma_+\, \mathrm{d}v$$
$$(6.302)$$

and, in particular, $\delta\mathbf{r}(0, 0) = \mathbf{0}$. However, a valid comparison of the positions of the cusp before and after the perturbation is possible only after subtracting the centre-of-mass of the loop in the two cases.

Initially, the centre-of-mass of the loop has the trajectory

$$\bar{\mathbf{r}}(t) = \bar{\mathbf{r}}_0 + t\mathbf{V} \quad (6.303)$$

where t is the time since the beginning of the oscillation, $\mathbf{V}$ is the initial bulk 3-velocity of the loop and

$$\bar{\mathbf{r}}_0 = L^{-1} \int_0^L \mathbf{r}|_{\tau=0}\, \mathrm{d}\sigma \quad (6.304)$$

is the centre-of-mass along the constant-time slice $t = 0$ corresponding to the unperturbed position of the cusp.

In order to calculate the centre-of-mass along the constant-time slice of the perturbed position of the cusp it is necessary to first convert to the realigned coordinates $(\bar{\sigma}_+, \bar{\sigma}_-)$ and then find the mean value of $\mathbf{r} + \delta\mathbf{r}$ along the slice $\bar{\tau} = \delta\tau$, which in terms of the original standard gauge coordinates has the parametric form $\tau(\sigma) \approx \delta\tau - \delta X^0|_{\tau=0}$, with $\mathrm{d}\bar{\sigma} \approx (1 + X^0_{,\tau}|_{\tau=0})\, \mathrm{d}\sigma$.

To leading order in the perturbation the result is:

$$\overline{\mathbf{r} + \delta\mathbf{r}}|_{\bar{\tau}=\delta\tau} = \bar{\mathbf{r}}_0 + \overline{\delta\mathbf{r}}_0 + \mathbf{V}\delta\tau - \frac{\delta L}{L}\bar{\mathbf{r}}_0 + L^{-1} \int_0^L [\mathbf{r}\delta X^0_{,\tau} - \mathbf{r}_{,\tau}\,\delta X^0]|_{\tau=0}\, \mathrm{d}\sigma$$
$$(6.305)$$

where δL is given by (6.259) and

$$\overline{\delta \mathbf{r}_0} = L^{-1} \int_0^L \delta \mathbf{r}|_{\tau=0} \, d\sigma. \tag{6.306}$$

Thus the displacement of the perturbed position of the cusp from the perturbed centre-of-mass is

$$(\mathbf{r} + \delta \mathbf{r})|_{(\delta \sigma_+, \delta \sigma_-)} - \overline{\mathbf{r} + \delta \mathbf{r}}|_{\bar{\tau} = \delta \tau} = \mathbf{r}_c - \bar{\mathbf{r}}_0 + \delta \mathbf{r}_c \tag{6.307}$$

where

$$\delta \mathbf{r}_c \approx \mathbf{v}_c \delta \tau - \mathbf{V} \delta \tau - \overline{\delta \mathbf{r}_0} + \frac{\delta L}{L} \bar{\mathbf{r}}_0 - L^{-1} \int_0^L [\mathbf{r} \delta X^0,_\tau - \mathbf{r},_\tau \, \delta X^0]|_{\tau=0} \, d\sigma. \tag{6.308}$$
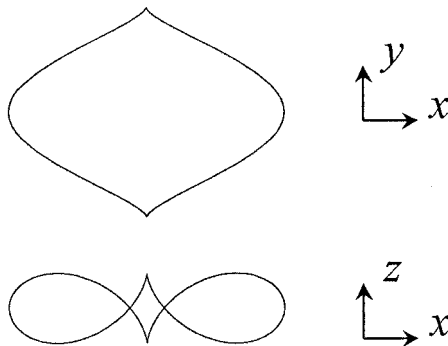
Here, the first two contributions to $\delta \mathbf{r}_c$ represent the drift of the cusp and the centre-of-mass, respectively, over the delay time $\delta \tau$, and the last three terms reflect displacements due to the non-local effects of the perturbation. Unfortunately, there is no direct relationship between the last three terms and the two drift terms, so the naive expectation that (in the centre-of-momentum frame) cusps will simply precess about the loop under the action of their self-acceleration has only limited theoretical support. However, as will be seen in the next section, the two features of cusp displacement most evident in numerical simulations are precession due to the first (cusp drift) term and self-similar shrinkage of the loop, which is included in the last three terms.

6.11.4   Numerical results
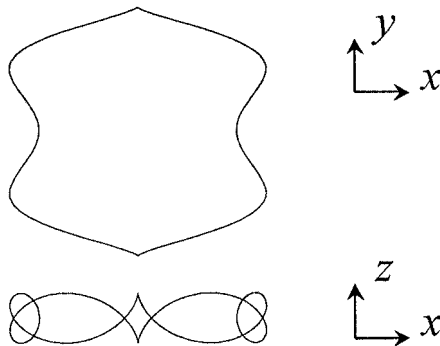
Quashnock and Spergel [QS90] have used the back-reaction formalism outlined here to numerically simulate the evolution of three classes of radiating string loops. The time-step between successive perturbation solutions was chosen to represent the cumulative effect of $10^{-3}/\mu$ oscillations (of period $L/2$) of the loop, and at each step the acceleration vector α^μ was evaluated at a grid of equally-spaced points on the fundamental domain $[0, L] \times [0, L]$. In the faster version of their code Quashnock and Spergel approximated the world sheet as a piecewise-plane surface.

In the first series of simulations, the loop was initially configured to be one of the p/q harmonic solutions described by equations (6.84) and (6.85), with $\psi = \pi/2$, $p = 1$ and $q = 3$ or 5. The $1/3$ harmonic string supports two cusps over its fundamental period $T = L/6$, at $(\tau, \sigma) = (0, \pm L/4)$. The cusps lie at $\mathbf{r}_c = \pm \frac{L}{2\pi}[0, \frac{1}{2}, \frac{1}{6}]$, and have velocities $\mathbf{v}_c = \mp[1, 0, 0]$. The $1/5$ harmonic string also supports two cusps over its fundamental period $T = L/10$, at $(\tau, \sigma) = (L/20, L/5)$ and $(\tau, \sigma) = (L/20, -3L/10)$. In this case the cusps lie at $\mathbf{r}_c = \pm \frac{L}{2\pi}[0, \frac{1}{2}, \frac{1}{10}]$, and have velocities $\mathbf{v}_c = \mp[1, 0, 0]$.

The two loops at the moment of cusp formation are shown in figures 6.8 and 6.9. In both cases the cusp velocities are directed anticlockwise and the cusps lie
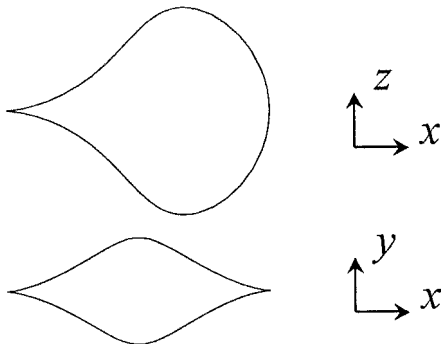
Figure 6.8. The 1/3 harmonic loop at the moment of cusp formation.

Figure 6.9. The 1/5 harmonic loop at the moment of cusp formation.

in region III of figure 6.7, so that the divergent component of the self-acceleration of each cusp is anti-parallel to its velocity.

Quashnock and Spergel found that both loops evolved in an essentially self-similar manner, with the loop patterns shrinking in response to the radiative energy loss and consequent reduction in the invariant length L, and the cusps slowly precessing around the loops. Unfortunately, it is not clear from the presentation of their results whether the precession was in the same direction as, or counter to, the velocities of the cusps. The authors state (in reference to one of the cusps on the 1/3 loop) that 'the cusp survives the back reaction, but is deformed and delayed'; and the accompanying figures support the claim of a 'delay' (that is, precession in the same direction as $\mathbf{v}_c$) in the case $q = 3$. However, later diagrams depicting an asymmetric Vachaspati–Vilenkin solution clearly indicate an inversion of the horizontal (x)-axis. If the x-axis is similarly inverted in the earlier figures, then the precession is counter to $\mathbf{v}_c$, as would be expected if the cusp drift term in (6.308) with a parametric shrinkage $\delta\tau < 0$ were dominant.

Figure 6.10. The $\alpha = \frac{1}{2}$, $\psi = \frac{1}{2}\pi$ Vachaspati–Vilenkin loop at a moment of cusp formation.

In any case, the cusps were not destroyed by back-reaction effects, as the topological arguments of section 3.6 anticipated. The energy loss δP^0 at each step in the simulations was effectively constant, a result consistent with the prediction of section 6.4 that the radiative power is independent of the loop size L. The radiative efficiency γ^0 of the $1/5$ loop was found to lie between 90 and 100 over the 10 steps of the simulation.

In their second series of simulations, Quashnock and Spergel tracked the evolution of three Vachaspati–Vilenkin solutions of the form (6.82) and (6.83), with the parameter choices $(\alpha, \psi) = (\frac{1}{4}, \pi/2)$, $(\frac{1}{4}, 3\pi/4)$ and $(\frac{1}{2}, \pi/2)$. In each case the loop supported a total of four cusps distributed non-symmetrically about its centre-of-momentum, and Quashnock and Spergel examined the solutions primarily to test the effectiveness of cusps in boosting an asymmetric loop to relativistic velocities (the 'gravitational rocket effect'). They found that all three solutions were rapidly accelerated to speeds between about 6% and 14% of the speed of light, much as predicted by Vachaspati and Vilenkin (see section 6.8.1).

The solution with $\alpha = \frac{1}{2}$ and $\psi = \pi/2$ was discussed briefly at the end of section 6.8.2. Its cusps occur at $(\tau/L, \sigma/L) = (0, \frac{1}{4})$, $(\frac{1}{4}, \frac{1}{2})$, $(\frac{1}{8}, \frac{7}{8})$ and $(\frac{3}{8}, \frac{1}{8})$, with velocities $\mathbf{v}_c = [0, 0, -1]$ in the first two cases, and $\mathbf{v}_c = [0, 0, 1]$ in the other two. The second cusp, at $(\tau/L, \sigma/L) = (\frac{1}{4}, \frac{1}{2})$, is the furthest from the loop and presumably exerts the greatest torque (although the net torque of the cusps is directed along the y-axis irrespective of the strength of the individual cusps: see section 6.8.2). The loop is depicted, at the moment of formation of this cusp, in figure 6.10.

Quashnock and Spergel found that the rocket effect accelerated this particular loop to a maximum velocity of about 9% of the speed of light in the negative z-direction, plus smaller components in the x- and y-directions. Given that there is no obvious asymmetry in the cusp velocities, the magnitude and direction of the acceleration is somewhat of a mystery. However, if A^-

denotes the scaling factor outside $[1, \mathbf{v}_c] \int \sigma_+^{-2} \, d\sigma_+$ in the formula (6.296) for the divergent component of the self-acceleration $\alpha^{-\mu}$, and A^+ the corresponding factor for $\alpha^{+\mu}$, then the cusps at $(\tau/L, \sigma/L) = (\frac{1}{8}, \frac{7}{8})$ and $(\frac{3}{8}, \frac{1}{8})$, which have $\mathbf{v}_c = [0, 0, 1]$, lie in region III of figure 6.7 with $(A^+, A^-) = (-23.0, -4.9)$. The cusp at $(\tau/L, \sigma/L) = (\frac{1}{4}, \frac{1}{2})$ also lies in region III with $(A^+, A^-) = (-13.9, -11.7)$, but the remaining cusp, at $(\tau/L, \sigma/L) = (0, \frac{1}{4})$ has $(A^+, A^-) = (-155.7, 83.4)$ and lies in region I. Thus the self-acceleration of the first pair of cusps is consistently directed in the negative z-direction, whereas the self-acceleration of the second pair has contributions in both directions, although this may be a fortuitous coincidence.

Further acceleration of the asymmetric loops beyond about 10–15% of the speed of light seems to have limited by two factors. The first was the precession of the cusps, which had the effect of rotating the beaming directions of the cusps away from the original boost axis. The cusp precession apparently developed in the same direction as the cusp velocities, as was earlier seen to be the case with the 1/3 and 1/5 harmonic solutions. However, the published diagrams corresponding to the top frame of figure 6.10 show the cusp to the right rather than the left, and so there is good reason to suspect an inversion of the x-axis (which would reverse the precession).

The second factor inhibiting acceleration was the suppression of the asymmetric structure by the preferential radiation of energy from the higher-order harmonics of the $\mathbf{a}$ mode. Thus as the loops evolved they not only shrank in response to the overall energy loss, but began increasingly to resemble the corresponding 1-harmonic solutions (which have $\alpha = 0$).

The last of Quashnock and Spergel's back-reaction simulations involved a family of kinked loops constructed by superimposing a sawtooth wave with N equally-spaced kinks on an initially circular string. The resulting configurations resembled cog wheels with $N/2$ teeth, although unfortunately the authors did not provide sufficient information to allow an explicit reconstruction of the unperturbed trajectories. Quashnock and Spergel followed the evolution of three trajectories, with $N = 8$, 16 and 32 kinks. In each case the loop slowly shrank in size, with the kink amplitudes decaying more rapidly than the radius of the loop.

Due to the decay of the kinks the ratio of the loop's energy to its mean radius decreased from iteration to iteration, and the decay time Δt for the kinks was defined to be the time taken for this ratio to fall halfway to its asymptotic value. On the basis of the results for the three test loops, Quashnock and Spergel estimated that for kinks with a characteristic size $r = 2\pi R/N$ (where R is the initial radius of the loop)

$$\Delta t \sim r/(50\mu). \qquad (6.309)$$

This result is gratifyingly close to the estimate $\Delta t \sim r/(8\pi^2\mu)$ for the decay time of kinks obtained from purely theoretical considerations at the end of section 6.7.

Chapter 7

The gravitational field of an infinite straight string

7.1 The metric due to an infinite straight string

The metric due to an infinite straight cosmic string *in vacuo* is, in its distributional form, arguably the simplest non-empty solution of the Einstein field equations. The weak-field version (which is virtually identical to the full solution) was first derived by Alexander Vilenkin in 1981 [Vil81b]. The full metric was independently discovered in 1985 by J Richard Gott [Got85] and William Hiscock [His85], who matched a vacuum exterior solution to a simple interior solution containing fluid with the equation of state $T_t^t = T_z^z = \varepsilon_0$ (a constant) and then let the radius of the interior solution go to zero. Gott's work followed directly from a study of the gravitational field of point particles in $2 + 1$ dimensions [GA84]. A more general class of interior solutions was subsequently constructed by Bernard Linet [Lin85].

The Gott–Hiscock solution is constructed by first assuming a static, cylindrically-symmetric line element with the general form:

$$ds^2 = e^{2\chi}\, dt^2 - e^{2\psi}(dr^2 + dz^2) - e^{2\omega}\, d\phi^2 \tag{7.1}$$

where χ, ψ and ω are functions of r alone, and r and ϕ are standard polar coordinates on $\mathbb{R}^2$. The metric has Killing fields ∂_t, ∂_z and ∂_ϕ.

The non-zero components of the Einstein tensor $G_\nu^\mu = R_\nu^\mu - \frac{1}{2}R\delta_\nu^\mu$ are:

$$G_t^t = [\psi'' + \omega'' + (\omega')^2]e^{-2\psi} \tag{7.2}$$

$$G_z^z = [\chi'' + (\chi')^2 + \omega'' + (\omega')^2 + \chi'\omega' - \psi'\chi' - \psi'\omega']e^{-2\psi} \tag{7.3}$$

$$G_r^r = (\psi'\chi' + \psi'\omega' + \chi'\omega')e^{-2\psi} \tag{7.4}$$

and

$$G_\phi^\phi = [\chi'' + (\chi')^2 + \psi'']e^{-2\psi}. \tag{7.5}$$

The metric is generated by solving the Einstein equations $G_\nu^\mu = -8\pi T_\nu^\mu$. In the wire approximation, the world sheet of the string is the 2-surface $r = 0$. If the world-sheet parameters ζ^0 and ζ^1 are identified with the spacetime coordinates t and z respectively, then the distributional stress–energy tensor (6.1) has only two non-zero components:

$$T_t^t = T_z^z = \mu e^{-\chi-2\psi-\omega}\delta^{(2)}(r) \tag{7.6}$$

where $\delta^{(2)}(r)$ is the standard unit distribution with support localized at the origin in $\mathbb{R}^2$. It is, therefore, natural to postulate that the interior solution has a stress–energy tensor of the form

$$T_t^t = T_z^z \equiv \varepsilon \qquad T_r^r = T_\phi^\phi = 0 \tag{7.7}$$

where the energy density and longitudinal tension ε is a function of r only.

The identities $T_{\mu;\nu}^\nu = 0$ then give rise to the conservation equation:

$$\delta_r^\mu T_{\mu;\nu}^\nu = -(\chi' + \psi')\varepsilon = 0. \tag{7.8}$$

which, in turn, implies that $\chi'' + \psi'' = 0$ and hence, since $G_\phi^\phi = 0$, that χ' and ψ' separately vanish. The functions χ and ψ are therefore constants and can be set to zero by suitably rescaling t, z and r, so that

$$ds^2 = dt^2 - dz^2 - dr^2 - e^{2\omega}\,d\phi^2. \tag{7.9}$$

The Einstein equations then reduce to the single equation

$$\omega'' + (\omega')^2 = -8\pi\varepsilon \tag{7.10}$$

or, equivalently,

$$(e^\omega)'' + 8\pi\varepsilon e^\omega = 0. \tag{7.11}$$

Equation (7.11) can be used to solve for the metric function ω once ε has been prescribed as a function of r or, alternatively, to solve for ε if ω is given. The only constraints are that ε should be positive and that the solution should be regular on the axis $r = 0$, so that $e^\omega \sim r$ for small r. Gott [Got85] and Hiscock [His85] both assumed ε to be a constant ε_0, in which case

$$e^\omega = r_* \sin(r/r_*) \tag{7.12}$$

where $r_* = (8\pi\varepsilon_0)^{-1/2}$. The more general situation where ε is varying has been discussed by Linet [Lin85].

The exterior metric is a solution of the vacuum Einstein equations $G_\nu^\mu = 0$ and is most easily derived by rearranging the equations in the form

$$e^{\chi+2\psi+\omega}(\tfrac{1}{2}G - G_t^t) = (\chi'e^{\chi+\omega})' = 0 \tag{7.13}$$

$$e^{\chi+2\psi+\omega}(\tfrac{1}{2}G - G_z^z) = (\psi'e^{\chi+\omega})' = 0 \tag{7.14}$$

$$e^{\chi+2\psi+\omega}(\tfrac{1}{2}G - G_\phi^\phi) = (\omega'e^{\chi+\omega})' = 0 \tag{7.15}$$

and

$$e^{2\psi} G_r^r = \psi'\chi' + \psi'\omega' + \chi'\omega' = 0. \tag{7.16}$$

The general solution to this system of equations is:

$$\chi = m \ln|r + K| + C_1 \tag{7.17}$$
$$\psi = m(m - 1) \ln|r + K| + C_2 \tag{7.18}$$

and

$$\omega = (1 - m) \ln|r + K| + C_3 \tag{7.19}$$

where m, K, C_1, C_2 and C_3 are all integration constants. After eliminating K by re-zeroing the radial coordinate r, the line element becomes

$$ds^2 = r^{2m} c^2 \, dt^2 - r^{2m(m-1)} b^2 (dz^2 + dr^2) - r^{2(1-m)} a_0^2 \, d\phi^2 \tag{7.20}$$

where a_0, b and c are constants. Equation (7.20) describes the most general static, cylindrically-symmetric vacuum line element, and was first discovered by Tullio Levi-Cività in 1917. It is always possible to set b and c to 1 by suitably rescaling t, z and r, but for present purposes it is more convenient to retain them as arbitrary integration constants.

The interior and exterior solutions can be matched at any nominated value r_0 of r in the interior solution. Since the coordinates r appearing in the two line elements (7.9) and (7.20) will typically have different scalings, the boundary radius in the exterior solution will be denoted R_0. The boundary 3-surface is spanned by the orthonormal triad

$$\{t_{(i)}^\mu\} = \{e^{-\chi} \delta_t^\mu, e^{-\psi} \delta_z^\mu, e^{-\omega} \delta_\phi^\mu\} \tag{7.21}$$

and has unit normal

$$n_\mu = e^\psi \delta_\mu^r. \tag{7.22}$$

The extrinsic curvature of the surface is, therefore,

$$K_{ij} = -t_{(i)}^\mu t_{(j)}^\nu n_{\mu;\nu} = e^{-\psi} \operatorname{diag}(\chi', -\psi', -\omega'). \tag{7.23}$$

The two solutions can be matched without inducing a boundary layer on the surface by requiring that both K_{ij} and the metric intrinsic to the surface be continuous. This, in turn, means that e^χ, e^ψ, e^ω, χ', ψ' and ω' must be continuous across the surface. Since χ and ψ are constants in the interior solution, the continuity of χ' and ψ' requires that $m/R_0 = m(m - 1)/R_0 = 0$, and so $m = 0$. Similarly, the continuity of e^χ and e^ψ implies that $b = c = 1$.

Now, integration of the Einstein equation (7.11) across the interior solution gives

$$[\omega' e^\omega]_0^{r_0} = -8\pi \int_0^{r_0} \varepsilon e^\omega \, dr \tag{7.24}$$

where $\mathrm{e}^\omega \sim r$ for small r and so $\omega' \mathrm{e}^\omega \to 1$ as $r \to 0$. Since $\omega' \mathrm{e}^\omega = a_0$ in the exterior solution, matching $\omega' \mathrm{e}^\omega$ across the boundary gives

$$a_0 = 1 - 8\pi \int_0^{r_0} \varepsilon \mathrm{e}^\omega \, \mathrm{d}r. \tag{7.25}$$

This last identity can be expressed in a more compact form by noting that the total mass per unit length μ on each surface of constant t and z in the interior solution is:

$$\mu = \int_0^{2\pi} \int_0^{r_0} \varepsilon \mathrm{e}^\omega \, \mathrm{d}r \, \mathrm{d}\phi = 2\pi \int_0^{r_0} \varepsilon \mathrm{e}^\omega \, \mathrm{d}r \tag{7.26}$$

and so

$$a_0 = 1 - 4\mu. \tag{7.27}$$

Also, the function e^ω will itself be continuous if $R_0 = 1/\omega'(r_0)$.

In the particular case of the Gott [Got85] and Hiscock [His85] $\varepsilon = \varepsilon_0$ interior solution given by (7.9) and (7.12), $R_0 = \sec(r_0/r_*)$ and $\mu = 2\pi \varepsilon_0 r_*^2 [1 - \cos(r_0/r_*)]$. The exterior boundary radius R_0 will, therefore, be positive if $r_0 < \pi r_*/2$, in which case $\mu < 2\pi \varepsilon_0 r_*^2 = \frac{1}{4}$ and $0 < a_0 < 1$.
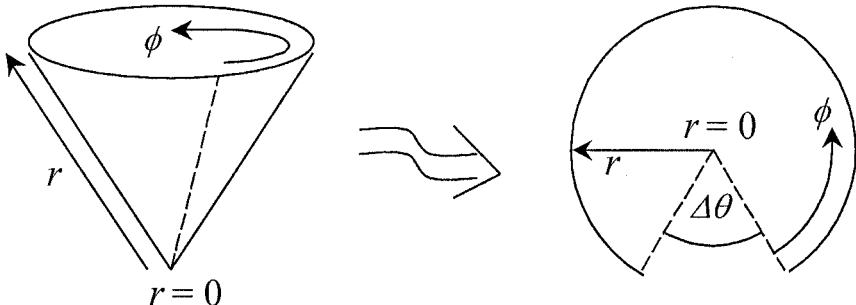
In summary, the exterior solution is simply

$$\mathrm{d}s^2 = \mathrm{d}t^2 - \mathrm{d}z^2 - \mathrm{d}r^2 - (1 - 4\mu)^2 r^2 \, \mathrm{d}\phi^2 \qquad \text{for } r \geq R_0 \tag{7.28}$$

and there is a large class of interior solutions with the simple equation of state $T_t^t = T_z^z = \varepsilon$ that can be matched to (7.28) at $r = R_0$.

The metric outside a straight zero-thickness string is now generated by letting the boundary radius R_0 go to zero while keeping the mass per unit length μ constant, so that the range of the line element (7.28) extends to $r = 0$. The resulting spacetime is empty and flat everywhere except on the 2-surface $r = 0$, where the metric is singular. Strictly speaking, the surface $r = 0$ is, therefore, a singular boundary and is not part of the spacetime at all. However, it is still possible to associate with the metric a distributional stress–energy tensor of the form (7.6), in a sense that will be defined more formally in section 7.5.

It should also be noted that the parameter μ appearing in this derivation plays two essentially independent roles: one as a measure of the strength of the gravitational field in the exterior metric (7.28) and a second one as the integrated mass per unit length of the interior solution as defined by equation (7.26). The identity of these two quantities is a non-trivial consequence of the simple equation of state $T_t^t = T_z^z = \varepsilon$ and $T_r^r = T_\phi^\phi = 0$ assumed for the interior fluid. As will be seen in section 7.4, it is possible to endow the interior solution with an equation of state more general than that considered by Gott, Hiscock and Linet [Got85, His85, Lin85] while preserving the form (7.28) of the exterior metric. The mass per unit length in the interior solution is then typically not equal to the metric parameter $\frac{1}{4}(1 - a_0)$. For this reason the symbol μ will be reserved for the quantity $\frac{1}{4}(1 - a_0)$, and—since it reflects a geometric property of the exterior metric only—will be referred to as the *gravitational mass per unit length* of the spacetime.

Figure 7.1. The constant t, z slices of the conical spacetime (7.28).

7.2 Properties of the straight-string metric

The line element (7.28) has a very simple geometric interpretation. If the angular coordinate ϕ is replaced by $\theta = (1 - 4\mu)\phi$ then (7.28) reduces to the Minkowski line element

$$ds^2 = dt^2 - dz^2 - dr^2 - r^2\, d\theta^2 \tag{7.29}$$

with the exception that θ ranges from 0 to $2\pi(1 - 4\mu)$ rather than from 0 to 2π. The metric, therefore, describes Minkowski spacetime with a wedge of angular extent $\Delta\theta = 8\pi\mu$ removed from each of the surfaces of constant t and z, as shown in figure 7.1. The apex of each wedge lies on the axial plane $r = 0$, and the sides of the wedge are 'glued' together, forming what is sometimes referred to as *conical spacetime*.

The fact that the metric (7.28) is locally Minkowskian implies that the Riemann tensor is zero everywhere outside the axial plane, and therefore that a test particle moving through the metric would experience no tidal forces. In particular, such a particle would not be accelerated towards the string. This curious feature is due to the special nature of the equation of state $T_t^t = T_z^z$, which—as was first noted by Vilenkin [Vil81b]—is invariant under boosts along the z-axis. A local observer should, therefore, be unable to distinguish a preferred velocity in the z-direction; whereas any gravitational force in the radial direction would destroy this symmetry. When combined with the other symmetries of the metric, this property forbids gravitational acceleration in any direction.

An alternative version of the metric which is more useful for studying the structure of the singularity on the axial plane $r = 0$ can be found by replacing r and ϕ with the new coordinates

$$x = \rho(r)\cos\phi \qquad \text{and} \qquad y = \rho(r)\sin\phi \tag{7.30}$$

where

$$\rho(r) \equiv (x^2 + y^2)^{1/2} = [(1 - 4\mu)r]^{1/(1-4\mu)}. \tag{7.31}$$

The line element (7.28) then becomes

$$ds^2 = dt^2 - \rho^{-8\mu}(dx^2 + dy^2) - dz^2 \tag{7.32}$$

which is often referred to as the *isotropic form* of the straight-string metric.

An even more compact version of this line element can be constructed by introducing the complex coordinate $w = x + iy$. In terms of w and its conjugate w^* the line element is

$$ds^2 = dt^2 - dz^2 - (ww^*)^{-4\mu} dw\, dw^* \tag{7.33}$$

which demonstrates explicitly that the metric is locally flat, as it reduces to the Minkowski line element under a complex transformation $w \to W(w) = (1 - 4\mu)^{-1} w^{1-4\mu}$ which is analytic everywhere except at $w = 0$.

The simple geometry of the straight-string metric (7.28) allows the geodesics to be easily constructed. In the locally-Minkowskian coordinate system (t, r, z, θ) the geodesics are straight lines, and so in the original (t, r, z, ϕ) coordinates have the parametric form

$$t(s) = \gamma_p s + t_p \tag{7.34}$$
$$r(s) = r_p[1 + (1 - 4\mu)^2 \omega_p^2 s^2]^{1/2} \tag{7.35}$$
$$z(s) = V_p s + z_p \tag{7.36}$$

and

$$\phi(s) = \phi_p + (1 - 4\mu)^{-1} \tan^{-1}[(1 - 4\mu)\omega_p s] \tag{7.37}$$

where a subscripted p denotes the value of the variable at the point of closest approach to the string, which has been chosen as the zero point for the proper time s, while γ is shorthand for dt/ds, ω for $d\phi/ds$ and V for dz/ds.

In isotropic coordinates, the projection of the geodesic onto the x–y plane traces out the curve

$$x(s) = \rho(s) \cos \theta_p \qquad \text{and} \qquad y(s) = \rho(s) \sin \theta_p \tag{7.38}$$

where
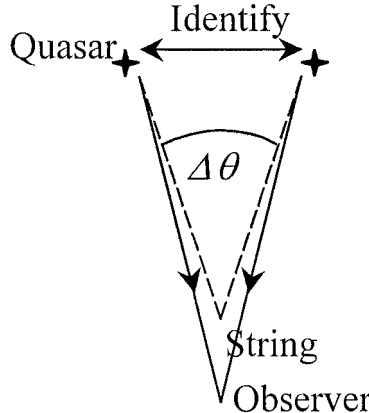
$$\rho(s) = \rho_p[1 + (1 - 4\mu)^2 \omega_p^2 s^2]^{1/(2 - 8\mu)}. \tag{7.39}$$

One of the few ways that an observer would be able to detect the presence of an infinite straight cosmic string is through gravitational lensing. Consider two geodesics originating from the same azimuthal direction $\phi = \phi_0$ and passing symmetrically on opposite sides of the string. The angular coordinates of the two geodesics then satisfy

$$\phi_+(s) = \phi_0 + (1 - 4\mu)^{-1} \left\{ \tan^{-1}[(1 - 4\mu)\omega_p s] + \frac{\pi}{2} \right\} \tag{7.40}$$

and

$$\phi_-(s) = \phi_0 - (1 - 4\mu)^{-1} \left\{ \tan^{-1}[(1 - 4\mu)\omega_p s] + \frac{\pi}{2} \right\}. \tag{7.41}$$

Figure 7.2. Gravitational lensing of the light from a distant quasar by an intervening string.

In particular, the asymptotic directions of the two geodesics in the limit as $s \to \infty$ are not the same, as

$$\phi_+ \to \phi_0 + \frac{\pi}{1 - 4\mu} \tag{7.42}$$

while

$$\phi_- \to \phi_0 - \frac{\pi}{1 - 4\mu}. \tag{7.43}$$

The angular difference between the geodesics after the transit is, therefore,

$$\Delta\phi = \frac{2\pi}{1 - 4\mu} - 2\pi = \frac{8\pi\mu}{1 - 4\mu} \tag{7.44}$$

which when measured as a physical angle is just the angle deficit $\Delta\theta = 8\pi\mu$.

An observer situated at a sufficiently large distance from a straight cosmic string would see two images of any point source lying behind the string, as illustrated in figure 7.2. If the line of sight from the observer to the source is perpendicular to the string, the angular separation between the two images is $8\pi\mu$. For GUT strings (which have $\mu \approx 10^{-6}$), this corresponds to a separation of the order of 1 arcsecond, which is detectable with a modern telescope.

Incidentally, Mark Hindmarsh and Andrew Wray [HW90] have shown, by detailed analysis of the geodesics in a general Levi-Civita spacetime (7.20), that gravitational lensing with a well-defined angular separation between the images is possible only in the specialized string case $m = 0$.

7.3   The Geroch–Traschen critique

The claim that the conical metric (7.28) would adequately represent the gravitational field outside a realistic cosmic string is founded on the critical

assumption that it is possible to give a meaningful distributional interpretation to the stress–energy content of the singular boundary at $r = 0$. This assumption was first systematically questioned on a number of grounds by Robert Geroch and Jennie Traschen [GT87] in 1987. Their concerns were wide-ranging but it is possible to group them into four main categories:

(1) *The absence of a suitable distributional formalism in general relativity.* Since the Einstein equations are nonlinear in the metric tensor $g_{\mu\nu}$ and its first and second derivatives, it is not, in general, meaningful to treat them as equations on distributions (that is, continuous linear functionals). In particular, the Riemann tensor

$$R_{\kappa\lambda\mu\nu} = \tfrac{1}{2}(g_{\kappa\mu,\lambda\nu} + g_{\lambda\nu,\kappa\mu} - g_{\kappa\nu,\lambda\mu} - g_{\lambda\mu,\kappa\nu}) + g_{\rho\sigma}(\Gamma^{\rho}_{\kappa\mu}\Gamma^{\sigma}_{\lambda\nu} - \Gamma^{\rho}_{\kappa\nu}\Gamma^{\sigma}_{\lambda\mu})$$
$$(7.45)$$

is quadratic in the Christoffel symbol $\Gamma^{\rho}_{\kappa\mu}$ and so may not be expressible as a distribution if the Christoffel symbol is itself a singular distribution. In order to ensure that each of the terms on the right-hand side of (7.45) is separately no worse than distributional, Geroch and Traschen defined a class of what they called *regular metrics*, which are characterized by the following properties:

   (i)   the inverse metric tensor $g^{\mu\nu}$ exists everywhere;
   (ii) both $g_{\mu\nu}$ and $g^{\mu\nu}$ are locally bounded; and
   (iii) the weak derivative of $g_{\mu\nu}$ (the distributional analogue of $g_{\mu\nu,\lambda}$) is locally square integrable.

One objection levelled by Geroch and Traschen against the use of the distributional approximation to model cosmic strings is that the isotropic form (7.32) of the metric is not regular, as the weak first derivative of $g_{\mu\nu}$ is not locally square integrable. In fact, it can be shown that any metric with distributional curvature concentrated on a submanifold of co-dimension 2, like the world sheet of a zero-thickness cosmic string, must be non-regular. The problem of whether a suitable distributional formalism can be constructed for non-regular metrics remains an open one, and will be discussed in more detail in sections 7.5 and 10.4.4.

(2) *The uncertain physical interpretation of distributional solutions.* Geroch and Traschen rightly stressed that a given distributional string solution is nothing more than a mathematical curiosity unless it can be shown to be the zero-thickness limit of a family of solutions containing energy and matter fields that are physically reasonable and in some sense smooth. Unfortunately, imposing this as a general requirement would destroy much of the rationale behind the distributional approximation, which is to avoid having to solve the full Einstein–Yang–Mills–Higgs field equations. In the case of the Nielsen–Olesen vortex string [NO73], which is the canonical Abelian Higgs model for an infinite straight string (see section 1.3), David Garfinkle [Gar85] has shown that the metric at large distances tends asymptotically to the conical

line element (7.28), which would therefore be recovered in the limit as the core radius of the string goes to zero. It is usually taken for granted that limiting sequences of smooth solutions exist for more complicated distributional string metrics but so far this has been demonstrated only in a few special cases, most notably the travelling-wave solutions (see section 9.1).

(3) *The possibility that the large-scale structure of the conical metric is unstable to perturbations in the equation of state.* As was seen in section 7.1, the most general static vacuum metric with cylindrical symmetry has the Levi-Cività form (7.20), which is flat (both asymptotically and locally) only in the special case $m = 0$. One way of singling out the choice $m = 0$ is to match the metric to an interior solution with the canonical equation of state $T_t^t = T_z^z = \varepsilon$ and $T_r^r = T_\phi^\phi = 0$. However, there is a multitude of other equations of state that could plausibly be prescribed for the interior solution and those that match smoothly onto an exterior spacetime with $m = 0$ form a subset of measure zero. This suggests that a tiny change in the equation of state of the putative interior fluid could, in principle, lead to a completely different (that is, non-flat) large-scale structure. Geroch and Traschen regarded this as a potentially serious problem for the theory of cosmic strings, attributable ultimately to the simplifying assumption that straight strings have infinite length and therefore infinite mass–energy. Geroch and Traschen also suggested that a similar breakdown might occur outside a curved string or in the presence of another gravitating object, as the symmetry in $T^{\mu\nu}$ would then be destroyed. The particulars of this argument, and its resolution, will be examined in sections 7.4.

(4) *The lack of any clear relationship between the mass per unit length of a cosmic string and its near gravitational field.* It was mentioned earlier that the simple correspondence between the gravitational mass per unit length μ (or, equivalently, the angle deficit $\Delta\theta = 8\pi\mu$) in the exterior metric (7.28) and the mass per unit length of the interior solution (7.9) is a consequence of the specific equation of state assumed for the interior fluid. Given any other equation of state consistent with the $m = 0$ subfamily of the Levi-Cività metrics (7.20), it turns out the mass per unit length in the fluid is strictly smaller than the value that would be inferred from the geometry of the exterior solution (see section 7.4). This feature is simply a reflection of the self-gravity of the fluid, and has been explored most extensively in the case of the Nielsen–Olesen vortex by Garfinkle and Laguna [GL89]. Geroch and Traschen expressed some disquiet at the absence of a direct relationship between the angle deficit and mass–energy content of a straight string, but it should be borne in mind that a similar indeterminacy exists in relation to the gravitational field of a static fluid sphere, where the active mass defining the exterior (Schwarzschild) solution is not, in general, equal to the physical mass of the sphere. More problematic perhaps is Geroch and Traschen's

concern that an analogous relationship between source and field is not possible even, in principle, in the case of a curved string, as the rotational and translational Killing vectors used respectively to define the angle deficit and mass-energy of a straight string are no longer available. Analysis of the near gravitational field outside a general curved string suggests a way of circumventing this problem, which will be considered in more detail in section 10.4.1.

Of the four concerns listed here, all but the second would cast considerable doubt on the suitability of the wire approximation if substantiated. However, the concerns were posed by Geroch and Traschen as open questions only, and the following sections will show that all have simple resolutions in the case of an infinite straight string. It is not at present possible to make similar statements about the value of the wire approximation in more complicated situations where curvature of the string or the presence of another gravitating object destroys the high degree of symmetry evident in the straight-string metric (7.28) but such doubts as persist are due primarily to the fact that very few exact non-straight solutions are available for analysis. So far no compelling reason has been found for believing that the wire approximation creates insuperable problems of either a physical or a mathematical nature, regardless of the string geometry. This lends qualified support to the claim that the distributional stress–energy tensor (6.1) defines a class of solutions to the Einstein equations which is rich and physically interesting, whatever the final verdict on the existence of cosmic strings in the Universe at large.

7.4 Is the straight-string metric unstable to changes in the equation of state?

To examine in detail the possibility that the large-scale geometry outside an infinite straight string could be sensitive to changes in the equation of state of the putative source fluid, recall from section 7.1 that if the general static line element with cylindrical symmetry is written in the form (7.1) then the components of the Einstein tensor satisfy the identities

$$[\chi'(e^{\chi+\omega})]' = \tfrac{1}{2}(-G_t^t + G_r^r + G_z^z + G_\phi^\phi)e^{\chi+2\psi+\omega} \tag{7.46}$$

$$[\psi'(e^{\chi+\omega})]' = \tfrac{1}{2}(G_t^t + G_r^r - G_z^z + G_\phi^\phi)e^{\chi+2\psi+\omega} \tag{7.47}$$

$$[\omega'(e^{\chi+\omega})]' = \tfrac{1}{2}(G_t^t + G_r^r + G_z^z - G_\phi^\phi)e^{\chi+2\psi+\omega} \tag{7.48}$$

and

$$G_r^r = (\chi'\psi' + \chi'\omega' + \psi'\omega')e^{-2\psi}. \tag{7.49}$$

As was done in the case of the restricted equation of state considered by Gott and Hiscock, I will divide the metric into an interior solution with a non-zero stress–energy tensor and a vacuum exterior solution. The exterior line element

then has the Levi-Cività form (7.20). In particular, the continuity of the three metric functions χ, ψ and ω across the boundary between the two solutions requires that

$$a_0 R_0^{1-m} = e^{\omega_0} \qquad b R_0^{m(m-1)} = e^{\psi_0} \qquad \text{and} \qquad c R_0^m = e^{\chi_0} \qquad (7.50)$$

where $r = R_0$ is the equation of the boundary in the exterior solution, and a subscripted zero denotes the value of the corresponding metric function on the boundary of the interior solution.

Similarly, the matching of the extrinsic curvature tensor on the two sides of the boundary gives the conditions

$$b^{-1} m R_0^{-(m^2-m+1)} = e^{-\psi_0} \chi_0' \qquad (7.51)$$

$$b^{-1} m (m-1) R_0^{-(m^2-m+1)} = e^{-\psi_0} \psi_0' \qquad (7.52)$$

and

$$b^{-1}(1-m) R_0^{-(m^2-m+1)} = e^{-\psi_0} \omega_0' \qquad (7.53)$$

where χ_0' denotes the boundary value of the radial derivative of χ, and similar remarks apply to the other metric functions.

The continuity of the normal derivatives across the boundary, combined with the fact that G_r^r vanishes in the exterior solution, implies that $\chi_0' \psi_0' + \chi_0' \omega_0' + \psi_0' \omega_0' = 0$. (In physical terms, this means that the radial pressure T_r^r must be zero on the boundary of the cylinder.) The constants b and c fix the relative scalings of t, r and z. Solving for the remaining three constants gives

$$m = (\chi_0' + \omega_0')^{-1} \chi_0' \qquad R_0 = (\chi_0' + \omega_0')^{-1} \qquad \text{and} \qquad a_0 = R_0^{m-1} e^{\omega_0}. \quad (7.54)$$

The scaling of the interior metric can be fixed by requiring that $e^\chi = 1$ and $e^\psi = 1$ at $r = 0$. The cylinder is then regular on the axis if $e^\omega \sim r$ for small values of r, and the functions χ' and ψ' remain bounded as $r \to 0$. In view of the Einstein equations $G_\nu^\mu = -8\pi T_\nu^\mu$, equations (7.46)–(7.48) can then be integrated from the axis out to the boundary to give

$$\chi_0' = 2e^{-\psi_0-\omega_0}(S_t^t - S_r^r - S_z^z - S_\phi^\phi) \qquad (7.55)$$

$$\psi_0' = 2e^{-\psi_0-\omega_0}(-S_t^t - S_r^r + S_z^z - S_\phi^\phi) \qquad (7.56)$$

and

$$\omega_0' = 2e^{-\psi_0-\omega_0}(-S_t^t - S_r^r - S_z^z + S_\phi^\phi + \tfrac{1}{2}) \qquad (7.57)$$

where

$$S_\nu^\mu = 2\pi \int_0^{r_0} T_\nu^\mu e^{\chi+2\psi+\omega} \, dr \qquad (7.58)$$

is the total integrated stress–energy of the cylinder per unit t and z.

Comparison of equations (7.54) with (7.55)–(7.57) indicates that

$$m = 2\frac{(S_t^t - S_z^z) - (S_r^r + S_\phi^\phi)}{1 - 4S_z^z - 4S_r^r} \tag{7.59}$$

and

$$R_0 = e^{\psi_0 + \omega_0}(1 - 4S_t^t - 4S_r^r)^{-1} \tag{7.60}$$

while the hydrostatic boundary condition $\chi_0'\psi_0' + \chi_0'\omega_0' + \psi_0'\omega_0' = 0$ is equivalent to the equation

$$(S_r^r + S_\phi^\phi)(2S_t^t + 2S_z^z + 3S_r^r - S_\phi^\phi - 1) - (S_t^t - S_z^z)^2 = 0. \tag{7.61}$$

In view of (7.59), the exterior solution reduces to the Gott–Hiscock metric (7.28) if

$$S_t^t = S_z^z + S_r^r + S_\phi^\phi \tag{7.62}$$

as then $m = 0$.

Recall that the solutions considered by Gott [Got85], Hiscock [His85] and Linet [Lin85] are all characterized by the equation of state

$$T_r^r = T_\phi^\phi = 0 \qquad T_t^t = T_z^z > 0 \tag{7.63}$$

which clearly implies (7.62), and, therefore, that $m = 0$. By contrast, the Nielsen–Olesen vortex described in chapter 1 has the equation of state $T_t^t = T_z^z$, but there is no direct relationship between T_r^r and T_ϕ^ϕ. David Garfinkle [Gar85] has written down the field equations for the line element (7.1) in the more realistic case of a coupled Higgs and Yang–Mills source, and has integrated these equations numerically to develop a fully general relativistic version of the Nielsen–Olesen vortex solution[1].

If Garfinkle's solution were to be truncated at a finite radius (with T_r^r adjusted so that it goes to zero at the boundary) then from equations (7.55) and (7.56) $\chi_0' = \psi_0'$. Equations (7.51) and (7.52) then indicate that $m(m - 1) = m$ and so m could, in principle, be either 0 or 2. (This result was first obtained by Vilenkin [Vil81b] in 1981.) In fact, as Garfinkle has shown, the vortex solution does tend asymptotically to the bare straight-string metric (7.28).

However, it is evident from (7.59) that the class of interior stress–energy tensors consistent with a flat exterior solution (that is, with the choice $m = 0$) forms a set of measure zero in the parameter space spanned by the integrated stress–energy components S_t^t, S_z^z, S_r^r and S_ϕ^ϕ. On the face of it, therefore, it would seem that Geroch and Traschen are justified in claiming that a small change in the structure of the interior solution—provided that it was consistent with the

---

[1] A more general family of solutions describing cylindrically symmetric Einstein–Higgs–Yang–Mills strings has been constructed by Dyer and Marleau [DM95], under less stringent assumptions about the regularity of the solution on the symmetry axis.

hydrostatic constraint (7.61)—could conceivably lead to an exterior solution with $m \neq 0$.

What undermines this claim is the fact that the tensor S_ν^μ has no real physical significance: it is the total stress–energy inside a section of the cylinder of unit *coordinate* length in the t- and z-directions. It might seem like a trivial matter to posit a small change in the components of S_ν^μ and so perturb the exterior metric away from the canonical value $m = 0$ but in all cases such a change will have drastic consequences for the overall energy and tension of the cylinder.

To see this, note from (7.2) that the energy per unit proper length of the cylinder is

$$\langle T_t^t \rangle = 2\pi \int_0^{r_0} e^{\psi + \omega} T_t^t \, dr = -\tfrac{1}{4} \int_0^{r_0} (\psi'' + \omega'' + \omega'^2) e^{\omega - \psi} \, dr. \qquad (7.64)$$

If the first two terms in brackets on the right are integrated by parts and the appropriate boundary conditions imposed at $r = 0$ and $r = r_0$ then

$$\langle T_t^t \rangle = -\tfrac{1}{4} [e^{\omega - \psi} (\psi' + \omega')]_0^{r_0} - \tfrac{1}{4} \int_0^{r_0} e^{\omega - \psi} \psi'^2 \, dr$$

$$= \tfrac{1}{4} [1 - a_0 b^{-1} (1 - m)^2 R_0^{-m^2}] - \tfrac{1}{4} \int_0^{r_0} e^{\omega - \chi} \psi'^2 \, dr. \qquad (7.65)$$

Similarly, the net tension of the cylinder is

$$\langle T_z^z \rangle = 2\pi \int_0^{r_0} e^{\psi + \omega} T_z^z \, dr = -\tfrac{1}{4} \int_0^{r_0} [e^{\omega - \psi} (\chi' + \omega')]' \, dr - \tfrac{1}{4} \int_0^{r_0} e^{\omega - \chi} \chi'^2 \, dr$$

$$= \tfrac{1}{4} (1 - ab^{-1} R_0^{-m^2}) - \tfrac{1}{4} \int_0^{r_0} e^{\omega - \chi} \chi'^2 \, dr. \qquad (7.66)$$

Note here that both the energy per unit proper length and the tension are bounded above by quantities which depend only on the properties of the exterior metric:

$$\langle T_t^t \rangle \leq \tfrac{1}{4} [1 - a_0 b^{-1} (1 - m)^2 R_0^{-m^2}] \qquad \text{and} \qquad \langle T_z^z \rangle \leq \tfrac{1}{4} (1 - a_0 b^{-1} R_0^{-m^2}). \qquad (7.67)$$

Consider now a continuous family of exterior metrics with the same values of a_0, b, c and m but different boundary radii R_0. As R_0 tends to zero, the net tension $\langle T_z^z \rangle$ inevitably diverges to $-\infty$ unless $m = 0$ (as $a_0 b^{-1}$ is by assumption positive). The same is true of the energy per unit length $\langle T_t^t \rangle$, except in the special case $m = 1$. However, the circumference $2\pi a_0 R_0^{1-m}$ of the interior solution remains bounded as $R_0 \to 0$ if $m = 1$, and so this case (which is conjugate to the case $m = 0$ in the sense that the roles of t and ϕ are interchanged) supports no zero-thickness limit at all.

These observations lead to the following important conclusion: Of all the Levi-Cività metrics (7.4), only the Gott–Hiscock spacetime ($m = 0$) can represent the zero-thickness limit of a family of static cylinders with *bounded* tension and

energy per unit length. Moreover, if the weak energy condition $T_t^t \geq 0$ is imposed on the material composing the cylinder, the boundary radius R_0 cannot be smaller than a minimum value $R_{\min} = [a_0 b^{-1}(1 - m)^2]^{1/m^2}$. This leads to a non-trivial lower bound on the circumference of the interior solution for every member of the family of Levi-Città metrics (7.4) except those with $m = 0$ and $a_0 b^{-1} < 1$.

In the case $m = 0$, the equations for the energy per unit length and the tension read:

$$\langle T_t^t \rangle = \mu - \tfrac{1}{4} \int_0^{r_0} e^{\omega - \psi}\, \psi'^2 \, \mathrm{d}r \qquad \text{and} \qquad \langle T_z^z \rangle = \mu - \tfrac{1}{4} \int_0^{r_0} e^{\omega - \psi}\, \chi'^2 \, \mathrm{d}r \tag{7.68}$$

where $\mu = \tfrac{1}{4}(1 - a_0 b^{-1})$. Thus, the simple relationship $\langle T_t^t \rangle = \langle T_z^z \rangle = \mu$, which is characteristic of Linet's solutions [Lin85], holds only if both χ' and ψ' are everywhere zero. This, in turn, is true only if $T_t^t = T_z^z$ and $T_r^r = T_\phi^\phi = 0$ everywhere (see (7.2)–(7.5)), a result first discovered by Werner Israel [Isr77]. Otherwise, μ is strictly greater than $\langle T_t^t \rangle$ and $\langle T_z^z \rangle$. The deviation of μ from the energy per unit length in the case of the Nielsen–Olesen vortex string has been calculated as a function of the gauge-to-scalar mass ratio for the constituent fields by David Garfinkle and Pablo Laguna [GL89].

To summarize, the straight-string metric (7.28) is the only possible spacetime exterior to a family of static cylinders with bounded energy per unit length in the limit of zero thickness. This result goes some way towards establishing that $m = 0$ is the only physically viable choice for the metric outside a bare straight cosmic string, but does not meet objection (3) completely. A realistic cosmic string would have a small but non-zero thickness, and there is no *a priori* reason why the exterior metric should not have $m \neq 0$, provided that the value of $|m|$ is small enough to avoid a negative energy per unit proper length.

However, the fully time-dependent Einstein equations for the metric exterior to a non-static (but non-rotating) fluid cylinder have been examined in some detail in [And99a]. There it is shown that a transition from the straight-string metric (7.28) to another member of the Levi-Città class (7.20) requires the injection of an infinite amount of Thorne's C-energy or, equivalently, an infinite amount of physical energy per unit proper length. Thus static exterior solutions with $m = 0$ and $m \neq 0$ may be close together in parameter space, but a transition from $m = 0$ to $m \neq 0$ is energetically forbidden. This does not in itself imply that a given static interior solution with $m = 0$ is guaranteed to be stable, but it does mean that any instability will not have the drastic consequences for the large-scale geometry of the solution postulated by Geroch and Traschen.

7.5   A distributional description of the straight-string metric

The singularity along the axial plane of the straight-string metric (7.28) has been the cause of much controversy since the early 1980s. In Newtonian gravity there is a linear relationship between source and field, embodied in the Poisson equation,

and it is relatively easy to accommodate distributional matter sources concentrated on points, lines or thin shells. Under what circumstances singular solutions of the Einstein equations can be described analogously in terms of distributional stress–energy sources remains an open question.

It has long been known that stress–energy sources concentrated on hypersurfaces (that is, thin shells, reversing layers and shock waves) in general relativity can be treated as conventional distributions [Isr66] but sources concentrated on lower-dimensional surfaces are more problematic. In 1968 Yvonne Choquet-Bruhat [CB68] claimed that 'except perhaps in very special cases of spacetime symmetry' the Ricci tensor on a given spacetime will not admit a satisfactory distributional interpretation unless the Christoffel components $\Gamma^{\mu}_{\kappa\lambda}$ and their pairwise products are defined almost everywhere and are locally integrable. Stephen Hawking and George Ellis made a similar statement in *The Large-Scale Structure of Space-Time* [HE73], writing that '[the field equations] can be defined in a distributional sense if the metric coordinate components g_{ab} and g^{ab} are continuous and have locally square integrable first derivatives with respect to the local co-ordinates'.

The Geroch–Traschen definition of metric regularity, given in section 7.3, differs only in detail from the prescriptions offered by Choquet-Bruhat and Hawking and Ellis. All three were motivated by the concern that the Riemann tensor can have a distributional interpretation only if all the terms on the right-hand side of (7.45) are separately distributions. However, Geroch and Traschen went further in demonstrating that the singularities in a regular metric must be concentrated on a submanifold with co-dimension no greater than 1. Thus the straight-string metric (7.28) cannot be regular, no matter what local coordinates are used. This is clear in the case of the isotropic line element (7.32), as the metric tensor is not locally bounded but other choices of coordinates can obscure the result. For example, if the local coordinates are $\overline{x} = r \cos \phi$ and $\overline{y} = r \sin \phi$ then the metric components $g_{\overline{x}\overline{x}}$, $g_{\overline{x}\overline{y}}$ and $g_{\overline{y}\overline{y}}$ and the corresponding inverse components are all locally bounded, but their derivatives diverge as r^{-1} and so (just) fail to be square integrable [GT87].

Before proceeding, it is useful to first define a distributional tensor field. A distribution on a manifold **M** is a continuous linear functional acting on the set of smooth functions with compact support on **M**. If (**M**, g) is a smooth spacetime then Geroch and Traschen define the distributional action of a smooth tensor field t to be

$$\widehat{t}^{\beta...\delta}{}_{\alpha...\gamma}(\psi^{\alpha...\gamma}{}_{\beta...\delta}) = \int_{\mathbf{M}} t^{\beta...\delta}{}_{\alpha...\gamma}\, \psi^{\alpha...\gamma}{}_{\beta...\delta}\, \mathrm{d}^4x \qquad (7.69)$$

for all smooth tensor densities ψ of weight -1 with compact support on **M** and the appropriate index structure.

For reasons of simplicity I will here choose to regard the corresponding density $\sqrt{g}t$ as a distribution rather than the tensor field t, and take the action

to be

$$\widehat{\sqrt{g}t}^{\beta...\delta}{}_{\alpha...\gamma}(\psi) = \int_{\mathbf{M}} \sqrt{g}t^{\beta...\delta}{}_{\alpha...\gamma}\psi\,\mathrm{d}^4x \tag{7.70}$$

where ψ is any smooth scalar field with compact support. The differences between (7.70) and (7.69) are for present purposes very minor.

In the case of a singular spacetime $(\mathbf{M}, g)$, it is necessary first of all to replace $\mathbf{M}$ with an extended manifold $\widetilde{\mathbf{M}}$ constructed by adding a set of boundary points to $\mathbf{M}$. Exactly how the boundary points are generated will depend on the spacetime but in the case of the isotropic line element (7.32) the natural choice is to take the boundary $\rho = 0$ to be a two-dimensional surface with the topology of $\mathbb{R}^2$. In local coordinates x^μ on $\widetilde{\mathbf{M}}$ a smoothing operator is any smooth function h with compact support on $\widetilde{\mathbf{M}}$ normalized so that

$$\int_{\widetilde{\mathbf{M}}} h\,\mathrm{d}^4x = 1. \tag{7.71}$$

Then for any $\varepsilon > 0$ the function $h_\varepsilon(x^\lambda) = \varepsilon^{-4}h(x^\lambda/\varepsilon)$ is also a smoothing operator.

The singular metric tensor $g_{\mu\nu}$, if locally integrable on $\mathbf{M}$, can now be used to generate a family of smooth metrics on $\widetilde{\mathbf{M}}$ by defining

$$g^\varepsilon_{\mu\nu}(x) = \int_{\widetilde{\mathbf{M}}} g_{\mu\nu}(y)h_\varepsilon(y-x)\,\mathrm{d}^4y. \tag{7.72}$$

(Here, the spacetime indices on x and y have been suppressed.) Note that $g^\varepsilon_{\mu\nu} \to g_{\mu\nu}$ pointwise on $\mathbf{M}$ as $\varepsilon \to 0$. Also, because $g^\varepsilon_{\mu\nu}$ is smooth and (in the case considered here) invertible if $h \geq 0$ everywhere, the corresponding Riemann tensor $R^\varepsilon_{\kappa\lambda\mu\nu}$ and all its products and contractions with $g^\varepsilon_{\mu\nu}$ are defined at all points on $\widetilde{\mathbf{M}}$.

In particular, if $T^{(\varepsilon)\mu}_\nu$ is the stress–energy tensor induced by $g^\varepsilon_{\mu\nu}$ then it is possible to associate with the original metric $g_{\mu\nu}$ a distributional stress–energy density $\widehat{\sqrt{g}T^\mu_\nu}$ on $\widetilde{\mathbf{M}}$ if, for every test function ψ,

$$\lim_{\varepsilon\to 0} \widehat{\sqrt{g^\varepsilon}T^{(\varepsilon)\mu}_\nu}(\psi) = \widehat{\sqrt{g}T^\mu_\nu}(\psi) \tag{7.73}$$

independently of the choice of smoothing operator h.

Now, in the case of the isotropic form (7.32) of the straight-string metric the metric tensor is $g_{\mu\nu} = \mathrm{diag}(1, -\rho^{-8\mu}, -\rho^{-8\mu}, -1)$, where $\rho = (x^2 + y^2)^{1/2}$. So irrespective of the choice of h the smoothed metric tensor has the general structure $g^\varepsilon_{\mu\nu} = \mathrm{diag}(1, -F^\varepsilon, -F^\varepsilon, -1)$, where from (7.72) $F^\varepsilon = \varepsilon^{-8\mu}f(\frac{x}{\varepsilon}, \frac{y}{\varepsilon})$ for some smooth function f, and, in particular, $F^\varepsilon \approx \rho^{-8\mu}$ for large ρ. The corresponding smoothed Riemann tensor has only one non-zero component (modulo symmetries):

$$R^\varepsilon_{xyxy} = -\tfrac{1}{2}F^\varepsilon[(\ln F^\varepsilon)_{,xx} + (\ln F^\varepsilon)_{,yy}] \tag{7.74}$$

and the smoothed stress–energy density has only two non-zero components:

$$\sqrt{g^\varepsilon}\,T_t^{(\varepsilon)t} = \sqrt{g^\varepsilon}\,T_z^{(\varepsilon)z} = -\frac{1}{16\pi}[(\ln F^\varepsilon)_{,xx} + (\ln F^\varepsilon)_{,yy}]. \tag{7.75}$$

If ψ is any smooth function with compact support in $\mathbb{R}^4$ then, on any surface of constant t and z, the mean-value theorem implies that

$$\int_{\mathbb{R}^2} \sqrt{g^\varepsilon}\,T_t^{(\varepsilon)t}\psi \, dx \, dy = \psi(t,0,0,z)\int_K \sqrt{g^\varepsilon}\,T_t^{(\varepsilon)t}\,dx\,dy$$
$$+ \int_K \sqrt{g^\varepsilon}\,T_t^{(\varepsilon)t}\rho\psi_{,\rho}\,(t,\xi x,\xi y,z)\,dx\,dy \tag{7.76}$$

where the parameter ξ is a (position-dependent) number in $[0,1]$, and K is any disc centred on the origin in $\mathbb{R}^2$ with $\mathrm{supp}\psi \subset K$. In view of (7.75) and the fact that $\lim_{\varepsilon\to 0} F^\varepsilon = \rho^{-8\mu}$ is smooth on ∂K,

$$\lim_{\varepsilon\to 0}\int_K \sqrt{g^\varepsilon}\,T_t^{(\varepsilon)t}\,dx\,dy = -\frac{1}{16\pi}\lim_{\varepsilon\to 0}\oint_{\partial K}\nabla(\ln F^\varepsilon)\cdot d\mathbf{x} = \mu. \tag{7.77}$$

Also, $\sqrt{g^\varepsilon}\,T_t^{(\varepsilon)t} = \varepsilon^{-2}H(\frac{x}{\varepsilon},\frac{y}{\varepsilon})$ for some smooth function H, and $\sqrt{g^\varepsilon}\,T_t^{(\varepsilon)t}$ falls off at least as rapidly as ρ^{-2} for large ρ. Let C be the supremum of $|\rho^2 H(x,y)|$ on $\mathbb{R}^2$. Then $|\sqrt{g^\varepsilon}\,T_t^{(\varepsilon)t}\rho| = |\frac{\rho^2}{\varepsilon^2}H(\frac{x}{\varepsilon},\frac{y}{\varepsilon})\rho^{-1}| \leq C\rho^{-1}$ for all ε, and since ρ^{-1} is locally integrable on $\mathbb{R}^2$ and $\lim_{\varepsilon\to 0}\sqrt{g^\varepsilon}\,T_t^{(\varepsilon)t} = 0$ almost everywhere,

$$\lim_{\varepsilon\to 0}\int_K \sqrt{g^\varepsilon}\,T_t^{(\varepsilon)t}\rho\psi_{,\rho}\,(t,\xi x,\xi y,z)\,dx\,dy = 0 \tag{7.78}$$

by virtue of the dominated convergence theorem.

The two results (7.77) and (7.78) are independent of the choice of smoothing operator h, and so

$$\widehat{\sqrt{g}T_t^t}(\psi) = \widehat{\sqrt{g}T_z^z}(\psi) = \mu\int_{\mathbb{R}^2}\psi(t,0,0,z)\,dt\,dz \tag{7.79}$$

while all other components of the stress–energy density map to the zero distribution. In terms of the two-dimensional Dirac distribution $\delta^{(2)}$ this means that

$$\widehat{\sqrt{g}T_\nu^\mu} = \mu\,\delta^{(2)}(x,y)(\delta_t^\mu\delta_\nu^t + \delta_z^\mu\delta_\nu^z). \tag{7.80}$$

It should be noted that (7.80) holds not only in the isotropic coordinate system (t,x,y,z) but can be shown by similar methods to hold in any coordinate system of the form $(t,\overline{x},\overline{y},z)$, where $\overline{x} = r^k\cos\phi$ and $\overline{y} = r^k\sin\phi$ for some $k > 0$. This includes, in particular, the $k = 1$ coordinate system preferred by Geroch and Traschen.

The distributional identity (7.80) has been derived with differing degrees of rigour by many authors over the years, including Sokolov and Starobinskii [SS77], Taub [Tau80], Linet [Lin85] and, most recently, by Clarke *et al* [CVW96]. The zero-thickness straight-string metric (7.28) is the clearest example of a non-regular spacetime admitting a well-defined distributional stress–energy tensor. It is often countered that the high degree of symmetry present in the metric qualifies it as one of Choquet-Bruhat's 'very special cases', with little predictive value for the structure of more general string-generated spacetimes. While it is true that this derivation of (7.80) relies heavily on the simple form of the isotropic line element (7.32), it will be seen in section 10.4.4 that a distributional stress–energy density, in the sense defined here, can be associated with a wide class of string metrics.

7.6   The self-force on a massive particle near a straight string

Although the conical spacetime described by (7.28) is everywhere locally flat and thus free of tidal forces, it turns out that a particle of mass m at rest in the spacetime does experience a gravitational self-force of order m^2 directed towards the singularity at $r = 0$. At a heuristic level, this self-force can be attributed to the 'refraction' about the conical singularity of the gravitational lines of force centred on the particle, which thus mimic the presence of an image particle lying directly behind the string. The phenomenon is not peculiar to the gravitational force alone. A charged particle at rest in the spacetime experiences a repulsive self-force [Lin86], while fluctuations of the quantum vacuum near a straight string have a non-zero stress–energy tensor and can induce a range of interesting effects [HK86, Dow87, DS88].

In the weak-field approximation, the gravitational field due to a particle of mass m at rest at a distance a from a straight string is most conveniently calculated by transforming to the Minkowski form (7.29) of the metric and fixing the coordinates so that the particle lies at $z = 0$ and $\theta = \theta_0 \equiv \pi(1 - 4\mu)$. Note here that θ ranges over $[0, 2\theta_0)$. The weak-field gravitational potential $\Phi(r, z, \theta)$ then satisfies the Poisson equation

$$\nabla^2 \Phi = -4\pi G m a^{-1} \delta(r - a)\delta(z)\delta(\theta - \theta_0) \tag{7.81}$$

subject to the conical boundary conditions

$$\Phi(z, r, 2\theta_0) = \Phi(z, r, 0) \qquad \text{and} \qquad \frac{\partial}{\partial \theta}\Phi(z, r, 2\theta_0) = \frac{\partial}{\partial \theta}\Phi(z, r, 0) = 0. \tag{7.82}$$

The most general harmonic expansion consistent with the boundary conditions and the obvious reflection symmetry about $z = 0$ is:

$$\Phi(z, r, \theta) = \sum_{n=-\infty}^{\infty} \cos(n\pi\theta/\theta_0) \int_0^{\infty} \Phi_{nk}(r)\cos(kz)\,\mathrm{d}k \tag{7.83}$$

where $\Phi_{(-n)k} = \Phi_{nk}$ for all n. In view of (7.81), Φ_{nk} satisfies the modified Bessel equation

$$r^2 \Phi_{nk}'' + r \Phi_{nk}' - (k^2 r^2 + n^2 \pi^2 / \theta_0^2) \Phi_{nk} = 0 \tag{7.84}$$

for $r \neq a$, and so

$$\Phi_{nk}(r) = \begin{cases} A_{nk} I_{|n|\pi/\theta_0}(kr) & \text{for } r < a \\ B_{nk} K_{|n|\pi/\theta_0}(kr) & \text{for } r > a \end{cases} \tag{7.85}$$

where I_ν and K_ν are modified Bessel functions of the first and second kind, respectively, and A_{nk} and B_{nk} are constants to be determined.

Requiring Φ_{nk} to be continuous at $r = a$ implies that

$$A_{nk} = C_{nk} K_{|n|\pi/\theta_0}(ka) \qquad \text{and} \qquad B_{nk} = C_{nk} I_{|n|\pi/\theta_0}(ka) \tag{7.86}$$

for some constant C_{nk}, which, in turn, indicates that the jump in Φ_{nk}' at $r = a$ is

$$\Delta \Phi_{nk}' = k C_{nk} [K_{|n|\pi/\theta_0}'(ka) I_{|n|\pi/\theta_0}(ka) - I_{|n|\pi/\theta_0}'(ka) K_{|n|\pi/\theta_0}(ka)] = -C_{nk}/a. \tag{7.87}$$

Given the identities

$$\delta(z) = \frac{1}{\pi} \int_0^\infty \cos kz \, dk \qquad \text{and} \qquad \delta(\theta - \theta_0) = \frac{1}{2\theta_0} \sum_{n=-\infty}^{\infty} (-1)^n \cos(n\pi\theta/\theta_0) \tag{7.88}$$

it follows that (7.81) is satisfied completely if $C_{nk} = 2(-1)^n Gm/\theta_0$.

Hence, the potential Φ is formally given by

$$\Phi(z, r, \theta) = \frac{2Gm}{\theta_0} \sum_{n=-\infty}^{\infty} (-1)^n \cos(n\pi\theta/\theta_0)$$
$$\times \begin{cases} \int_0^\infty K_{|n|\pi/\theta_0}(ka) I_{|n|\pi/\theta_0}(kr) \cos(kz) \, dk & \text{for } r < a \\ \int_0^\infty I_{|n|\pi/\theta_0}(ka) K_{|n|\pi/\theta_0}(kr) \cos(kz) \, dk & \text{for } r > a. \end{cases} \tag{7.89}$$

Furthermore, in view of the identity

$$\int_0^\infty K_\nu(ka) I_\nu(kr) \cos(kz) \, dk = \frac{1}{2(2ar)^{1/2}} \int_\eta^\infty \frac{e^{-\nu u}}{(\cosh u - \cosh \eta)^{1/2}} \, du \tag{7.90}$$

where $\cosh \eta = (a^2 + r^2 + z^2)/(2ar)$, this expression for Φ reduces to:

$$\Phi(z, r, \theta) = \frac{Gm}{(2ar)^{1/2}\theta_0} \int_\eta^\infty \frac{\sum_{n=-\infty}^{\infty} (-1)^n \cos(n\pi\theta/\theta_0) e^{-|n|\pi u/\theta_0}}{(\cosh u - \cosh \eta)^{1/2}} \, du. \tag{7.91}$$

Finally, given that

$$\sum_{n=-\infty}^{\infty} w^{|n|} \cos(nx) = \frac{1 - w^2}{1 - 2w \cos x + w^2} \tag{7.92}$$

it follows that

$$\Phi(r, z, \theta) = \frac{Gm}{(2ar)^{1/2}\theta_0}$$
$$\times \int_\eta^\infty \frac{\sinh(\pi u/\theta_0)}{[\cosh(\pi u/\theta_0) + \cos(\pi\theta/\theta_0)](\cosh u - \cosh \eta)^{1/2}} \, du.$$
$$(7.93)$$

The gradient of Φ gives the gravitational acceleration induced by the particle at any point in the spacetime. In particular, since

$$\Phi \approx \frac{Gm\pi/\theta_0}{(a^2 + z^2)^{1/2}} - \frac{2Gm/\theta_0}{(a^2 + z^2)^{1/2+\pi/\theta_0}}(ar)^{\pi/\theta_0}$$
$$\times \cos(\pi\theta/\theta_0) \int_0^1 x^{\pi/\theta_0} \frac{dx}{(x - x^2)^{1/2}} + O(r^{2+\pi/\theta_0}) \qquad (7.94)$$

for small r, and $\pi/\theta_0 = (1 - 4\mu)^{-1} > 1$, the string itself experiences a gravitational acceleration

$$\mathbf{a} = -\frac{Gm\pi/\theta_0}{(a^2 + z^2)^{3/2}} z\hat{\mathbf{z}} \qquad (7.95)$$

which has no radial component whatsoever. This surprising result is due to the fact, mentioned in section 5.3, that an initially straight string placed in the gravitational field of a particle of mass m will be distorted by a periastron bending angle of the order of m^2. Thus a radial component of acceleration is absent at the level of the weak-field approximation, which retains only terms linear in m.

To generate a meaningful expression for the self-force on the particle, it is necessary to first renormalize Φ by subtracting from

$$\Phi(a, 0, \theta_0) = \frac{Gm}{\sqrt{2}\theta_0 a} \int_0^\infty \frac{\sinh(\pi u/\theta_0)}{[\cosh(\pi u/\theta_0) - 1](\cosh u - 1)^{1/2}} \, du \qquad (7.96)$$
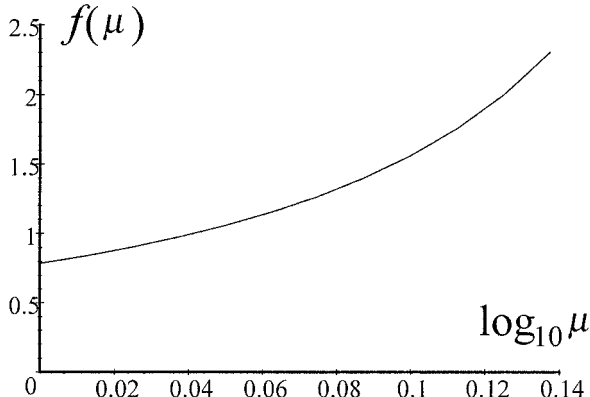
the value that Φ would take at the locus of the particle in the absence of the string, which is found by replacing θ_0 with π in (7.93) and taking the limit as $\theta \to \pi$. The resulting renormalized potential is

$$\Phi_R = \frac{Gm}{\sqrt{2}\pi a} \int_0^\infty \left[\frac{\sinh(\pi u/\theta_0)\pi/\theta_0}{\cosh(\pi u/\theta_0) - 1} - \frac{\sinh u}{\cosh u - 1} \right] \frac{du}{(\cosh u - 1)^{1/2}}. \qquad (7.97)$$

The self-force on the particle is, therefore, $\mathbf{F} = \frac{1}{2}m\frac{\partial}{\partial a}\Phi_R\hat{\mathbf{r}}$, where

$$\frac{\partial}{\partial a}\Phi_R = -\frac{Gm}{2\pi a^2} \int_0^\infty \left[\frac{\sinh(\pi u/\theta_0)\pi/\theta_0}{\cosh(\pi u/\theta_0) - 1} - \frac{\sinh u}{\cosh u - 1} \right] \frac{du}{\sinh(u/2)}. \qquad (7.98)$$

This formula for the gravitational self-force was first derived by Dmitri Gal'tsov in 1990 [Gal90], although the electrostatic case, which is formally

Figure 7.3. The scaling factor f as a function of the string's mass per unit length μ.

identical, was analysed by Bernard Linet four years earlier [Lin86]. Following Gal'tsov, it is instructive to write the self-force in the form

$$\mathbf{F} = -\frac{Gm^2\mu}{a^2} f(\mu)\hat{\mathbf{r}} \tag{7.99}$$

where

$$f(\mu) = \frac{1}{4\pi\mu} \int_0^\infty \left[\frac{\sinh(\pi u/\theta_0)\pi/\theta_0}{\cosh(\pi u/\theta_0) - 1} - \frac{\sinh u}{\cosh u - 1} \right] \frac{\mathrm{d}u}{\sinh(u/2)}. \tag{7.100}$$

In particular

$$\lim_{\mu\to 0} f(\mu) = \frac{1}{\pi} \int_0^\infty \frac{\sinh u - u}{\cosh u - 1} \frac{\mathrm{d}u}{\sinh(u/2)} = \pi/4 \tag{7.101}$$

while $f(\frac{1}{8}) = 2$. A plot of $f(\mu)$ against $\log_{10}\mu$ is shown in figure 7.3. It should be noted that the parameter b used by Gal'tsov in [Gal90] is just $1 - 4\mu$ and his function $\beta(b)$ is $f(\mu)/2$. For some reason, the values for β quoted by Gal'tsov are all too small by between 10 and 15%. Incidentally, Linet [Lin86] estimated the value of $\lim_{\mu\to 0} f(\mu)$ as $2.5/\pi$, which is only 1% too large. It seems that the exact value of $\pi/4$ was first given by Vachaspati *et al* [VHR90].

The fact that the self-force $\mathbf{F}$ is central has given rise to the common misapprehension that bound circular orbits exist for massive particles in the neighbourhood of a straight cosmic string. It is true that if (7.99) were to continue to hold for a moving particle, then circular orbits would exist with the standard Newtonian dependence of the orbital speed

$$v_{\mathrm{circ}} = \sqrt{\frac{Gm\mu f(\mu)}{a}}. \tag{7.102}$$

Thus, for example, a body with $m = 7 \times 10^{22}$ kg (roughly equal to the mass of the Moon) could orbit a GUT string with $\mu = 10^{-6}$ at a distance $a = 4 \times 10^8$ m (the mean Earth–Moon distance) if $v_{\text{circ}} \approx 0.1$ m s^{-1}, which is about 1/10 000th of the Moon's actual orbital speed around the Earth.

However, the assumption that the self-force $\mathbf{F}$ remains central is valid only in the slow-motion limit. A massive particle orbiting a straight string at relativistic speeds would generate a weak-field gravitational potential substantially different from (7.93), with non-radial corrections to the self-force $\mathbf{F}$ which a rough analysis suggests would be of order $\omega^3 \ln \omega$, where $\omega = v_{\text{circ}}/c$. Whether closed bound orbits are still possible in this situation remains an open question.

7.7 The straight-string metric in 'asymptotically-flat' form

The metric (7.28) due to an infinite straight cosmic string is clearly not asymptotically flat, as the defect on the world sheet extends to spacelike infinity along the axis $r = 0$. (For future reference, a spacetime which at spacelike infinity has the same global geometry as (7.28) does at spacelike infinity will be said to be *asymptotically flat**.) However, Jiri Bičák has constructed a coordinate transformation, singular on the world sheet, which reduces the line element to that of an asymptotically-flat spacetime with axial symmetry [Bi90]. The result may be little more than a mathematical curiosity, but it does provide an alternative insight into the geometry of the bare straight-string metric.

The line element describing a general asymptotically-flat vacuum spacetime with axial symmetry can be written in the form:

$$ds^2 = g_{uu}\, du^2 + 2g_{u\rho}\, du\, d\rho + 2g_{u\theta}\, du\, d\theta - \rho^2(e^{2\alpha}\, d\theta^2 + e^{-2\alpha}\sin^2\theta\, d\phi^2)$$

$$(7.103)$$

where u is a retarded time coordinate, θ and ϕ are polar angles along outgoing null geodesics, and ρ is the luminosity distance [BvdBM62].

The constraint of asymptotic flatness requires that the various metric functions appearing in (7.103) fall off appropriately for large values of ρ and, in particular, that

$$g_{uu} = 1 - 2M\rho^{-1} + O(\rho^{-2}) \tag{7.104}$$

and

$$\alpha = c\rho^{-1} + O(\rho^{-2}). \tag{7.105}$$

Here, the functions $M(u, \theta)$ and $c(u, \theta)$ are the 'mass' and 'news function' of the metric, respectively. The asymptotic expansions for the other two metric functions can be found by imposing the vacuum Einstein equations, which according to [BvdBM62] give

$$g_{u\rho} = 1 - \tfrac{1}{2}c^2\rho^{-2} + O(\rho^{-3}) \tag{7.106}$$

and

$$g_{u\theta} = c_{,\theta} + 2c\cot\theta + O(\rho^{-1}). \tag{7.107}$$

The straight-string metric (7.28) can be rewritten in the axisymmetric form (7.103) by first replacing (t, r, z) with an interim set of coordinates $(U, R, \overline{\theta})$ defined via the equations

$$r = R \sin \overline{\theta} \qquad z = R \cos \overline{\theta} \qquad \text{and} \qquad t = U + R. \qquad (7.108)$$

The line element then becomes:

$$ds^2 = dU^2 + 2dU\, dR - R^2\, d\overline{\theta}^2 - (1 - 4\mu)^2 R^2 \sin^2 \overline{\theta}\, d\phi^2. \qquad (7.109)$$

Note that, because of the presence of the multiplier $1 - 4\mu$, this expression is still asymptotically flat* rather than strictly asymptotically flat.

To reduce (7.109) to the asymptotically-flat form (7.103) requires a rather complicated transformation of coordinates which is only known in its asymptotic form. The general structure of the transformation is:

$$U = uw(\eta, \theta) \qquad R = \rho x(\eta, \theta) \qquad \text{and} \qquad \overline{\theta} = y(\eta, \theta) \qquad (7.110)$$

where $\eta = u/\rho$.

If the constraints $g_{\rho\rho} = g_{\rho\theta} = 0$ are imposed, the expressions for g_{uu}, $g_{u\rho}$ and $g_{u\theta}$ quickly reduce to

$$g_{uu} = w^2 + 2\eta ww_{,\eta} + 2wx_{,\eta} + 2xw_{,\eta} \qquad (7.111)$$

$$g_{u\rho} = -\eta^2 ww_{,\eta} + wx - \eta wx_{,\eta} - \eta xw_{,\eta} \qquad (7.112)$$

and

$$g_{u\theta} = \rho(\eta ww_{,\theta} + wx_{,\theta} + xw_{,\theta}) \qquad (7.113)$$

or, in terms of the potential $\Psi \equiv w^2 + 2\eta^{-1}wx$,

$$g_{uu} = (\eta\Psi)_{,\eta} \qquad g_{u\rho} = -\tfrac{1}{2}\eta^2\Psi_{,\eta} \qquad \text{and} \qquad g_{u\theta} = \tfrac{1}{2}u\Psi_{,\theta}. \qquad (7.114)$$

The functions $M(u, \theta)$ and $c(u, \theta)$ can now be calculated by assuming an asymptotic expansion for Ψ of the form

$$\Psi = A(\theta)\eta^{-1} + B(\theta) + C(\theta)\eta + O(\eta^2) \qquad (7.115)$$

and comparing the expansions of (7.114) with (7.104)–(7.107). The result is

$$A(\theta) = 2 \qquad B(\theta) = 1 \qquad \text{and} \qquad C(\theta) = -M/u = c^2/u^2 \qquad (7.116)$$

where

$$c_{,\theta} + 2c \cot\theta = \tfrac{1}{2}B_{,\theta}\, u \equiv 0. \qquad (7.117)$$

Hence,

$$c(u, \theta) = Ku \operatorname{cosec}^2\theta \qquad (7.118)$$

and

$$M(u, \theta) = -K^2 u \operatorname{cosec}^4\theta \qquad (7.119)$$

where K is a constant of integration.

A particular value for K is fixed by the requirement that

$$(1 - 4\mu)^2 x^2 \sin^2 y = \sin^2 \theta + O(\eta) \tag{7.120}$$

as then $g_{\phi\phi} \approx -\rho^2$ for large values of ρ, and the transformed line element is strictly asymptotically flat. However, in order to solve for K it is necessary to concurrently solve the constraint equations $g_{\rho\rho} = 0$ and $g_{\rho\theta} = 0$ to leading order in η.

Explicitly, the constraint equations read:

$$x^2(y_{,\eta})^2 + 2xw_{,\eta} - 2\eta w_{,\eta} x_{,\eta} - \eta^2(w_{,\eta})^2 = 0 \tag{7.121}$$

and

$$xw_{,\theta} + x^2 y_{,\eta} y_{,\theta} - \eta x_{,\eta} w_{,\theta} - \eta w_{,\eta} x_{,\theta} - \eta^2 w_{,\eta} w_{,\theta} = 0 \tag{7.122}$$

respectively. If w, x and y are expanded to linear order in η then the solution which simultaneously satisfies (7.120), (7.121) and (7.122) has the limiting form

$$w = \psi' - \frac{(\psi'')^2}{2\psi'}\eta + O(\eta^2) \tag{7.123}$$

$$x = (\psi')^{-1} + \frac{1}{2\psi'}\{(\psi''/\psi')^2 - (\psi')^2 + 1\}\eta + O(\eta^2) \tag{7.124}$$

and

$$y = \psi - \psi''\eta + O(\eta^2) \tag{7.125}$$

where

$$\psi(\theta) = 2\tan^{-1}(|\tan\theta/2|^{1-4\mu}). \tag{7.126}$$

At this point, the simplest way to calculate K is to substitute these formulae into the equation for $g_{\theta\theta}$, which reads:

$$x^2(y_{,\theta})^2 - 2\eta w_{,\theta} x_{,\theta} - \eta^2(w_{,\theta})^2 \approx e^{2c\rho^{-1}} = 1 + 2\eta K \operatorname{cosec}^2 \theta + O(\eta^2). \tag{7.127}$$

Then

$$K = \frac{\sin^2 \theta}{2(\psi')^2}[(\psi')^2 + 3(\psi'')^2 - (\psi')^4 - 2\psi'\psi'''] \equiv -4\mu(1 - 2\mu). \tag{7.128}$$

and the news and mass functions for the bare straight-string metric are

$$c(u, \theta) = -4\mu(1 - 2\mu)u \operatorname{cosec}^2 \theta \tag{7.129}$$

and

$$M(u, \theta) = -16\mu^2(1 - 2\mu)^2 u \operatorname{cosec}^4 \theta. \tag{7.130}$$

Note that, even to leading order in η, the coordinate transformation from $(U, \bar{r}, \bar{\theta})$ to (u, ρ, θ) is singular on the axis, as $\psi \sim 2(\theta/2)^{1-4\mu}$ for small θ, and so the Jacobian determinant of the transformation is

$$
\begin{aligned}
|J(U, \bar{r}, \bar{\theta}; u, \rho, \theta)| &= \psi' + (\psi'')^2/\psi' + O(\eta) \\
&\approx 2^{4\mu} 16\mu^2 (1 - 4\mu)\theta^{-2-4\mu}.
\end{aligned} \tag{7.131}
$$

This is, of course, unavoidable, given that the mass and news functions (7.118) and (7.119) are both singular on the axis.

Chapter 8

Multiple straight strings and closed timelike curves

8.1 Straight strings and 2 + 1 gravity

Because of its invariance under boosts in the z-direction, the metric (7.28) due to an infinite straight string in vacuum is closely connected with the gravitational field of an isolated point mass in $2 + 1$ dimensions. In fact, if the z coordinate is suppressed, the resulting line element

$$ds^2 = dt^2 - dr^2 - (1 - 4\mu)^2 r^2 \, d\phi^2 \tag{8.1}$$

completely characterizes a (spinless) point source of mass μ in $2 + 1$ gravity [Sta63, DJtH84, GA84].

This formal correspondence motivates yet another explanation of the locally-flat nature of the string metric (7.28). In $2 + 1$ dimensions both the Ricci tensor and the Riemann tensor have only six algebraically-independent components (in contrast to the situation in $3 + 1$ gravity, where the Ricci tensor has 10 algebraically-independent components and the Riemann tensor 20). Thus, whenever the Ricci tensor vanishes the Riemann tensor automatically vanishes as well. In other words, spacetime is locally flat in any vacuum region in $2 + 1$ dimensions. This property is inherited also by the string metric (7.28).

The analogy between relativistic strings and point masses in $2+1$ dimensions is not an exact one, of course. Strings have an extra dimensional degree of freedom, can bend and can radiate and interact with gravitational waves (which do not exist in $2+1$ gravity). The full theory of the gravitational field of a relativistic string is, therefore, much richer than an analysis of $2 + 1$ gravity would suggest. However, $2 + 1$ gravity does provide a full description of the gravitational field due to any number of *parallel* straight strings (whether static or moving) in the absence of gravitational radiation. In particular, the metric due to such a system of multiple strings is locally flat everywhere (except on the strings themselves).

The simplest extension of the single-string metric (7.28) is the metric due to N parallel static strings, which was first derived by Patricio Letelier in 1987 [Let87]. The metric is most easily understood as a modification of the isotropic line element (7.32)

$$ds^2 = dt^2 - dz^2 - \rho^{-8\mu}(dx^2 + dy^2) \tag{8.2}$$

which describes a single string passing through the origin in the x–y plane. If there are N strings of mass per unit length μ, each located at $x = x_k$, $y = y_k$ (where the index k runs from 1 to N), then the corresponding line element is:

$$ds^2 = dt^2 - dz^2 - \left(\prod_{k=1}^{N} \rho_k^{-8\mu} \right)(dx^2 + dy^2) \tag{8.3}$$

where

$$\rho_k = [(x - x_k)^2 + (y - y_k)^2]^{1/2}. \tag{8.4}$$

To see that (8.3) does indeed satisfy the vacuum Einstein equations everywhere except at the locations of the N strings, note that a naive calculation of the Riemann tensor gives

$$R_{xyxy} = 4\mu \left(\prod_{k=1}^{N} \rho_k^{-8\mu} \right) \sum_{j=1}^{N} \nabla^2(\ln \rho_j)$$

$$= 8\pi\mu \left(\prod_{k=1}^{N} \rho_k^{-8\mu} \right) \sum_{j=1}^{N} \delta^{(2)}(x - x_j, y - y_j) \tag{8.5}$$

and all other components zero. Since $\prod_{k=1}^{N} \rho_k^{-8\mu} = \sqrt{g}$, a more rigorous treatment along the lines of section 7.5 indicates that the stress–energy density has the non-zero distributional components

$$\widehat{\sqrt{g}T_t^t} = \widehat{\sqrt{g}T_z^z} = \mu \sum_{j=1}^{N} \delta^{(2)}(x - x_j, y - y_j) \tag{8.6}$$

as required.

The physical interpretation of the multiple string metric (8.3) is straightforward. Each string marks the location of a conical singularity with angle deficit $\Delta\theta = 8\pi\mu$; elsewhere the metric is locally flat. At large distances from the string system, $\prod_{k=1}^{N} \rho_k^{-8\mu} \sim \rho^{-8N\mu}$ and so the combined effect of the strings is similar to that of a single string with mass per unit length $N\mu$. The spacetime is open (that is, the total angle deficit is less than 2π) if $N\mu < 1/4$. Generalization to the case of N parallel static strings with differing masses per unit length $\mu_1, \ldots, \mu_N$ is accomplished by simply replacing $\rho_k^{-8\mu}$ with $\rho_k^{-8\mu_k}$ in the product term in the line element (8.3).

8.2   Boosts and rotations of systems of straight strings

Spacetimes containing straight strings which are either boosted or rotated relative to one another can be generated by making use of a construction due originally to J Richard Gott [Got91]. Since the multiple string metric (8.3) is locally flat, it contains three-dimensional hypersurfaces—generated by the t- and z-translates of any geodesic in the x–y plane which does not intersect one of the strings—with zero intrinsic and extrinsic curvature. These hypersurfaces are simply copies of the three-dimensional Minkowski spacetime $\mathbb{M}^3$, and so there exists on them a three-parameter isometry group of boosts and rotations. It is therefore possible to split the metric (8.3) along one of the hypersurfaces and then boost and/or rotate one of the fragments relative to the other before rejoining them. Since the junction surface has zero extrinsic and extrinsic curvature, the relativistic matching conditions are automatically satisfied, and the resulting metric is a locally-flat solution to the Einstein equations.

This procedure can, in principle, be repeated indefinitely to produce ever more complicated systems of straight strings in relative motion, but it is typically harder after each iteration to find a three-dimensional flat hypersurface which does not intersect one of the strings. If only boosts orthogonal to the z-axis are used, it is always possible to set all N strings independently into motion. The resulting metric (with the z coordinate suppressed) then describes the motion of N point masses in $2+1$ gravity.

However, despite claims to the contrary (see section 8.5) no solution has yet been found describing three or more *non-parallel* strings in relative motion, apart from the simple case where the static N-string spacetime (8.3) is split along a single flat three-dimensional hypersurface and one of the fragments is boosted and rotated relative to the other, leaving M parallel, co-moving strings in the first fragment and $N - M$ parallel, co-moving strings in the other. Indeed, it remains an open question whether three or more mutually non-parallel straight strings can be set into motion without radiating gravitational energy.

Gal'tsov *et al* [GGL93] have examined the gravitational interaction of N straight strings, with arbitrary velocities and orientations, in the weak-field approximation and have reported that if $N = 2$ the flux of emitted gravitational radiation vanishes exactly at second, post-linear order (as would be expected). But no such cancellation is evident in the general case of three or more strings.

Gal'tsov *et al* have also offered a simple physical argument to explain why a system of two non-parallel strings (or two non-parallel groups of parallel strings) will not radiate gravitational energy. Consider two non-parallel strings S_1 and S_2 in relative motion. In the rest frame of S_1, with S_1 aligned along the z-axis and the 3-velocity of S_2 parallel to the y–z plane, the world sheets of the two strings can be represented parametrically in the form

$$X_1^\mu(\tau, \sigma) = [\tau, 0, 0, \sigma] \tag{8.7}$$

and

$$X_2^\mu(\tau, \sigma) = [\tau, b, \sigma\gamma^{-1}\sin\theta + \tau v\cos\theta, \sigma\gamma^{-1}\cos\theta - \tau v\sin\theta] \qquad (8.8)$$

where v is the speed of S_2, $\gamma = (1 - v^2)^{-1/2}$ the corresponding Lorentz factor, θ the angle between S_2 and the z-axis, and b the normal distance between the strings.

As viewed from a second reference frame moving along the z-axis with speed $\bar{v}$, the equation for S_1 becomes

$$\bar{X}_1^\mu = [\bar{\gamma}(\tau - \bar{v}\sigma), 0, 0, \bar{\gamma}(\sigma - \bar{v}\tau)] \equiv [\bar{\tau}, 0, 0, \bar{\sigma}] \qquad (8.9)$$

where $\bar{\gamma} = (1 - \bar{v}^2)^{-1/2}$, while the equation for S_2 is

$$\begin{aligned} \bar{X}_2^\mu &= [\kappa_1\tau - \bar{v}\lambda\sigma, b, \sigma\gamma^{-1}\sin\theta + \tau v\cos\theta, \lambda\sigma - \kappa_2\tau] \\ &= [\bar{\tau}, b, \Delta^{-1}(\bar{\sigma}\gamma^{-1}\kappa_3 + \bar{\tau}\kappa_4\cos\theta), \Delta^{-1}(\bar{\sigma}\gamma^{-1}\cos\theta - \bar{\tau}\kappa_3\kappa_4)] \end{aligned} \qquad (8.10)$$

with $\kappa_1 = \bar{\gamma}(1 + \bar{v}v\sin\theta)$, $\kappa_2 = \bar{\gamma}(\bar{v} + v\sin\theta)$, $\kappa_3 = \bar{\gamma}(\bar{v}v + \sin\theta)$, $\kappa_4 = \bar{\gamma}(v + \bar{v}\sin\theta)$, $\lambda = \bar{\gamma}\gamma^{-1}\cos\theta$ and $\Delta = \kappa_1^2 - \bar{v}^2\lambda^2$. In the case of S_2, the new aligned standard-gauge coordinates are $\bar{\tau} = \kappa_1\tau - \bar{v}\lambda\sigma$ and $\bar{\sigma} = \kappa_1\sigma - \bar{v}\lambda\tau$.

As can be seen, the trajectory of S_1 is unaffected by the boost, whereas if $|v| > \sin\theta$ the spatial projections of S_2 will appear to be parallel to the z-axis to an observer with boost velocity $\bar{v} = -\sin\theta/v$, as then $\kappa_3 = 0$ and

$$\bar{X}_2^\mu = [\bar{\tau}, b, \bar{\tau}(v^2 - \sin^2\theta)^{1/2}\sec\theta, \bar{\sigma}\gamma^{-1}\sec\theta] \qquad (8.11)$$

so that $\partial\bar{X}_2^\mu/\partial\bar{\sigma}$ has a z-component only. However, if $|v| < \sin\theta$ then to an observer with boost velocity $\bar{v} = -v/\sin\theta$ the string S_2 will appear to be static, as $\kappa_4 = 0$,

$$\bar{X}_2^\mu = [\bar{\tau}, b, \bar{\sigma}\gamma(\sin^2\theta - v^2)^{1/2}, \bar{\sigma}\gamma\cos\theta] \qquad (8.12)$$

and $\partial\bar{X}_2^\mu/\partial\bar{\tau}$ has a t-component only.

Thus, except in the marginal case $|v| = \sin\theta$, it is always possible to find an inertial frame in which the two strings are parallel (reducing the problem to one of point particles in $2 + 1$ gravity) or are both static. In neither case will the strings radiate gravitational energy. (And if $|v| = \sin\theta$ it is still possible to find a *null* reference frame in which the two strings are both parallel and static.)

8.3   The Gott construction

Returning now to Gott's construction itself, the simplest examples of boosted or rotated multiple string metrics can be generated by applying the construction to a spacetime containing only two straight strings. If the strings are located at $(x, y) = (0, a)$ and $(x, y) = (0, -a)$ respectively, then the line element (8.3) becomes:

$$ds^2 = dt^2 - dz^2 - [x^2 + (y - a)^2]^{-4\mu}[x^2 + (y + a)^2]^{-4\mu}(dx^2 + dy^2). \qquad (8.13)$$

The hypersurface $y = 0$ is flat (both intrinsically and extrinsically), and has Minkowski coordinates t, z and X, where

$$X = \Psi(x) \equiv \int_0^x (u^2 + a^2)^{-4\mu} \, du. \tag{8.14}$$

If the spacelike coordinates z and X are replaced by a second pair of coordinates $\overline{z}$ and $\overline{X}$ generated by rotating through an angle $\alpha/2$ if $y > 0$ and an angle $-\alpha/2$ if $y < 0$, the resulting metric has the form

$$ds^2 = dt^2 - [\cos^2(\alpha/2) + F \sin^2(\alpha/2)] \, d\overline{z}^2 - (F - 1) \sin\alpha \, \text{sgn}(y) \, d\overline{X} \, d\overline{z}$$
$$- [F \cos^2(\alpha/2) + \sin^2(\alpha/2)] \, d\overline{X}^2 - (x^2 + a^2)^{-8\mu} F \, dy^2 \tag{8.15}$$

where

$$F(x, y) = (x^2 + a^2)^{8\mu}[x^2 + (y - a)^2]^{-4\mu}[x^2 + (y + a)^2]^{-4\mu} \tag{8.16}$$

and

$$x = \Psi^{-1}[\overline{X} \cos(\alpha/2) + \text{sgn}(y)\overline{z} \sin(\alpha/2)]. \tag{8.17}$$

However, if instead of a rotation in the X–z plane the hypersurface $y = 0$ is mapped onto itself through a boost in the X–t plane, the metric becomes

$$ds^2 = [\cosh^2(\beta/2) - F \sinh^2(\beta/2)] \, d\overline{t}^2 - (F - 1) \sinh\beta \, \text{sgn}(y) \, d\overline{X} \, d\overline{t}$$
$$- [F \cosh^2(\beta/2) - \sinh^2(\beta/2)] \, d\overline{X}^2 - (x^2 + a^2)^{-8\mu} F \, dy^2 - dz^2 \tag{8.18}$$
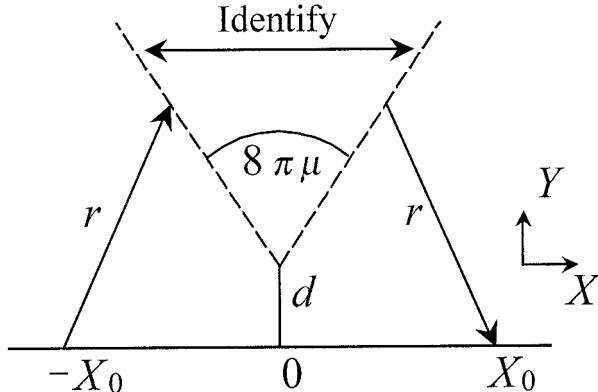
where $F(x, y)$ is as defined in equation (8.16) but now

$$x = \Psi^{-1}[\overline{X} \cosh(\beta/2) + \text{sgn}(y)\overline{t} \sinh(\beta/2)]. \tag{8.19}$$

The constant β is the rapidity of the boost, so that the relative speed of the two strings is $v = \tanh\beta$.

One of the most surprising features of the boosted two-string metric (8.18) is that it can support closed timelike curves (CTCs). The crucial factor is the behaviour of the function F. Its value is 1 on the hypersurface $y = 0$ and it diverges in the neighbourhood of the two strings but for values of $|y| \gg a$ it can be substantially smaller than 1. The coordinate $\overline{t}$ is timelike near the hypersurface $y = 0$, but its orientation can be reversed in any region where $F < \tanh^2(\beta/2)$, as $\overline{X}$ is then timelike.

It is, therefore, possible to construct future-directed timelike curves through the region $y > 0$ which start at some point $\overline{t} = 0$, $\overline{X} < 0$ on the hypersurface $y = 0$ and end at a second point $\overline{t} = 0$, $\overline{X} > 0$ on the same hypersurface. (To accomplish this, the orientation of $\overline{t}$ needs to be reversed twice in the region $F < \tanh^2(\beta/2)$.) Such a curve can be made to close (while remaining timelike) by continuing it along its mirror image in the region $y < 0$.

Figure 8.1. Construction of a closed timelike curve in a boosted 2-string spacetime.

It turns out that the most efficient way of constructing CTCs is by making them piecewise geodesic, and since the geodesic formalism is relatively unwieldy in isotropic coordinates (see section 7.2) it is more convenient to follow Gott [Got91] and work with Cartesian coordinates in the rest frame of one of the strings. In figure 8.1 the locally-flat 2-surface normal to the world sheet of the string in the fragment $y > 0$ is shown. As was seen in the previous chapter, it is a Euclidean plane with a wedge of angular extent $8\pi\mu$ projecting from the string removed and the two sides of the excision identified. Let X and Y be Cartesian coordinates on the surface, with the axis $Y = 0$ corresponding to the boundary $y = 0$. The projections of geodesics are represented by straight lines, and the normal distance from the junction hypersurface $Y = 0$ to the string is:

$$d = \int_0^a (a^2 - y^2)^{-4\mu}\, \mathrm{d}y. \tag{8.20}$$

Consider a general curve confined to the surface $z = 0$ which starts at the point $(t = -t_0, X = -X_0)$ on the hypersurface $Y = 0$, strikes the left-hand side of the excision at time $t = 0$, and then continues back to $Y = 0$ along its mirror image about the line $X = 0$, as shown. Provided that $X_0 \geq d\cot(4\pi\mu)$, the length r of each of the two segments of the curve is bounded below by the normal distance $r_{\min}$ from $(X = -X_0, Y = 0)$ to the wedge:

$$r \geq r_{\min} = X_0 \cos(4\pi\mu) + d\sin(4\pi\mu). \tag{8.21}$$

If the curve is timelike, it follows that $t_0 > r_{\min}$.

The second string is boosted with respect to the first by a velocity $\tanh\beta$ in the X-direction. In the rest frame of the second string, therefore, the point $(t = t_0, X = X_0)$ on the hypersurface $Y = 0$ has the coordinates

$$t' = t_0 \cosh\beta - X_0 \sinh\beta \tag{8.22}$$

and

$$X' = X_0 \cosh \beta - t_0 \sinh \beta. \tag{8.23}$$

If the parameter t_0 is chosen to have the value $X_0 \tanh(\beta/2)$ then $t' = -t_0$ and $X' = X_0$, and so if the curve is continued along its mirror image through the hypersurface $y = 0$ it ultimately closes at the point $(t' = t_0, X' = -X_0)$.

The resulting curve is timelike everywhere if

$$X_0 \tanh(\beta/2) > X_0 \cos(4\pi\mu) + d \sin(4\pi\mu). \tag{8.24}$$

In particular, if $X_0 \gg d$ it is always possible to construct a CTC enclosing the two strings provided that

$$\tanh(\beta/2) > \cos(4\pi\mu). \tag{8.25}$$

Representing the boosted two-string spacetime (8.18) by the Euclidean projection in figure 8.1 has the added advantage of giving a direct physical explanation for the existence of CTCs. From the vantage point of an observer in front of the string, the points where the curve intersects the boundary of the excised wedge, although identified, appear to be spacelike-separated. By boosting in the X-direction, the observer can make any particle crossing the wedge appear to jump backwards in time; and since r_{min} can always be chosen to be smaller than X_0, it is then possible to refract the particle around the second string into its own past lightcone. The feasiblity of the technique depends on the magnitude of the boost and the size of the wedge, as summarized by equation (8.25).

The properties of CTCs in the boosted two-string metric (8.18) have been examined in greater detail by Amos Ori [Ori91] and Curt Cutler [Cut92]. Ori has shown that CTCs intersect every constant-time hypersurface in the centre-of-momentum frame of the two strings, and so the closed timelike curves are in some sense 'eternal' (that is, they do not spontaneously appear in what was previously a causal spacetime). Using a construction very similar to the one sketched earlier, Ori has generated CTCs which cross the junction hypersurface $Y = 0$ at arbitrary values of the time coordinate t_{cm} in the centre-of-momentum frame of the two strings (whereas the curves in figure 7.1 all cross $Y = 0$ at the moment of closest approach $t_{cm} = 0$). Again, a necessary and sufficient condition for the existence of CTCs at each value of t_{cm} is given by (8.25).

As part of a more extensive analysis, Cutler [Cut92] has demonstrated that there exist closed null curves which are geodesic everywhere except at one point and encircle the strings an arbitrary number of times, that the boundary of the region containing the CTCs is a null hypersurface with topology $\mathbb{S}^1 \times \mathbb{R}^2$, and that the spacetime contains complete spacelike, edgeless, achronal[1] hypersurfaces which do not intersect any of the CTCs (despite the fact that the latter extend to spacelike infinity and to all values of t_{cm}, as was seen earlier).

---

[1] A set S is said to be achronal if no two points in S can be joined with a timelike curve.

8.4   String holonomy and closed timelike curves

When Gott first published the boosted two-string spacetime in 1991 [Got91], it caused a brief flurry of speculation. Current cosmological theories envisaged an early Universe filled with a network of cosmic strings moving at relativistic velocities and the possibility (however remote) that such a network might support closed timelike curves had dramatic ramifications. Although the CTCs appearing in Gott's spacetime are pre-existing and eternal, this does not mean that it is not possible to create CTCs by, for example, causing one cosmic string to break into two fragments moving apart with a high relative velocity. In fact, the latter process turns out to be energetically impossible, as the momentum of a single straight string is always timelike, whereas the total momentum (to be defined shortly) of any two-string spacetime containing CTCs is spacelike, even though both strings are moving at subluminal speed. Nonetheless, there remains an endless number of spacetimes containing three or more moving strings that could conceivably support CTCs and yet have a timelike total momentum.

   The early history of this particular problem is somewhat murky. In a 1984 paper Deser *et al* [DJtH84] claimed (without proof) that CTCs could not be created by spinless point particles in $2 + 1$ gravity—a contention apparently contradicted by Gott's two-string solution. In 1992, Deser *et al* [DJtH91] and Carroll *et al* [CFG92] simultaneously pointed out that the Gott spacetime has spacelike total momentum and, therefore, cannot be created by simply rearranging a timelike system of strings. Deser *et al* also qualified their 1984 claim by explicitly excluding spacetimes without 'physically acceptable global structure', a proviso which somewhat begs the question of whether it is possible to construct a spacelike subsystem of strings inside a spacetime with timelike total momentum. In fact, in a *closed* universe (which results when the total angle deficit of the constituent strings is greater than 2π) a spacelike subsystem can be created from static initial conditions, but Gerard 't Hooft [tH92] has shown that such a universe shrinks to zero volume before any CTCs appear. The definitive proof that CTCs cannot arise in an open string spacetime with timelike total momentum was given by Carroll *et al* in 1994 [CFGO94].

   The overall effect of a system of moving parallel cosmic strings is most compactly characterized by the system's holonomy—that is to say, the net rotation experienced by an orthonormal tetrad after it has been parallel transported around a closed curve enclosing the strings. In what follows, the z-axis will always be taken to be parallel to the strings. If in some local Lorentz frame L the components of the tetrad are $(\widehat{t}, \widehat{x}, \widehat{y}, \widehat{z})$ then the unimodular representation of the tetrad is:

$$S = \begin{pmatrix} \widehat{t} + \widehat{z} & \widehat{x} - \mathrm{i}\widehat{y} \\ \widehat{x} + \mathrm{i}\widehat{y} & \widehat{t} - \widehat{z} \end{pmatrix}. \tag{8.26}$$

   After being parallel transported around a single string with angle deficit

$\Delta\theta = 8\pi\mu$ at rest relative to the frame L, the tetrad is transformed into

$$S' = R^\dagger S R \tag{8.27}$$

where

$$R(\mu) = \begin{pmatrix} e^{-4\pi\mu i} & 0 \\ 0 & e^{4\pi\mu i} \end{pmatrix}. \tag{8.28}$$

If the string is moving with a speed $\tanh\beta$ at a longitudinal angle ϕ in the $x-y$ plane of L, parallel transport around the string is equivalent to first boosting the tetrad into the rest frame of the string, rotating by the deficit angle $\Delta\theta$, then boosting back to L. The net effect is to transform S into

$$S' = T^\dagger S T \tag{8.29}$$

where

$$T = BRB^{-1} \tag{8.30}$$

with the boost matrix B given by:

$$B(\beta, \phi) = \begin{pmatrix} \cosh(\beta/2) & e^{-i\phi}\sinh(\beta/2) \\ e^{i\phi}\sinh(\beta/2) & \cosh(\beta/2) \end{pmatrix}. \tag{8.31}$$

For a system of N strings, any path around the entire system can always be deformed into a sequence of loops around the individual strings. Hence, parallel transport around the system transforms S into

$$S' = T^\dagger S T \tag{8.32}$$

where now

$$T = T_N T_{N-1} \ldots T_1 \qquad (T_k = B_k R_k B_k^{-1}) \tag{8.33}$$

for any ordering of the strings. Thus, every system of parallel strings has associated with it a 2×2 complex unimodular matrix T, its 'holonomy matrix'.

The set of all possible holonomy matrices forms a group [in fact $SU(1, 1)$] with general element

$$T = \begin{pmatrix} e^{i\chi}\cosh\zeta & e^{i\psi}\sinh\zeta \\ e^{-i\psi}\sinh\zeta & e^{-i\chi}\cosh\zeta \end{pmatrix} \tag{8.34}$$

where ζ, χ and ψ are real parameters, with $\zeta \geq 0$. Each holonomy matrix has two real eigendirections, one of which is always the z-direction. The other eigendirection can be either spacelike, timelike or null; the string system is then said to have spacelike, timelike or null total *momentum*, respectively.

For the general matrix (8.34), the second eigendirection has tangent vector

$$(t, x, y, z) = (\cosh\zeta\sin\chi, \sinh\zeta\sin\psi, \sinh\zeta\cos\psi, 0) \tag{8.35}$$

and so is timelike if $\cosh^2 \zeta \cos^2 \chi < 1$ and spacelike if $\cosh^2 \zeta \cos^2 \chi > 1$. Since $\mathrm{Tr}(T) = 2 \cosh \zeta \cos \chi$, it is not necessary to find the eigenvectors of the holonomy matrix to classify the total momentum of the corresponding system of strings. A system has timelike total momentum if and only if

$$\tfrac{1}{2}| \mathrm{Tr}(T)| < 1. \tag{8.36}$$

A system consisting of only one string (whether static or moving) is always timelike, as

$$\tfrac{1}{2} \mathrm{Tr}(T) = \cos(4\pi \mu). \tag{8.37}$$

However, a system containing two equal-mass strings moving in opposite directions with speed $\tanh(\beta/2)$ (that is, the Gott case as viewed from the centre-of-momentum frame) has

$$\begin{aligned} \tfrac{1}{2} \mathrm{Tr}(T) &= \cos^2(4\pi \mu) - \cosh \beta \sin^2(4\pi \mu) \\ &\equiv 2 \cosh^2(\beta/2)[\cos^2(4\pi \mu) - \tanh^2(\beta/2)] - 1. \end{aligned} \tag{8.38}$$

The value of the expression on the right-hand side lies between 1 and -1 if $\tanh^2(\beta/2) < \cos^2(4\pi \mu)$, and is less than -1 if $\tanh^2(\beta/2) > \cos^2(4\pi \mu)$. In view of condition (8.25), the Gott spacetime admits closed timelike curves if and only if the total momentum is spacelike[2]. In fact, it is easily seen that a closed curve encircling any system of parallel strings can be timelike only if the total momentum of the system is spacelike, for if the momentum is timelike it is always possible to boost into a reference frame in which T is indistinguishable from the holonomy matrix of a single static string.

Any conservative interaction (for example, decay, merger or scattering) that takes place in an isolated system of strings will not affect a path enclosing the system, and so the holonomy matrix T will be conserved. In particular, if T is initially timelike, no CTCs will ever develop that encircle the entire system. Thus the only way that a CTC can occur in an isolated system of strings with timelike total momentum is if it contains a spacelike subsystem. The proof that, in fact, this never occurs in an open universe, due to Carroll *et al* [CFGO94], proceeds as follows.
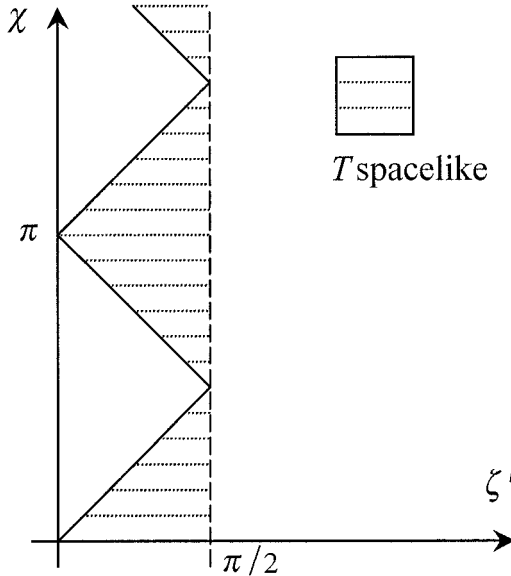
The three-dimensional parameter space of holonomy matrices (8.34) can be given a metric structure by the defining the line element

$$\mathrm{d}s^2 = \det(\mathrm{d}T) = \cosh^2 \zeta \, \mathrm{d}\chi^2 - \mathrm{d}\zeta^2 - \sinh^2 \zeta \, \mathrm{d}\psi^2. \tag{8.39}$$

The parameter space can further be compactified by replacing ζ with

$$\zeta' = 2 \tan^{-1}(e^\zeta) - \frac{\pi}{2} \tag{8.40}$$

---

[2] The derivation of (8.25) implicitly assumes that the mass per unit length $\mu < 1/8$ so that $\cos(4\pi \mu)$ is positive. If this is not the case, the right-hand side of (8.25) should read as $| \cos(4\pi \mu)|$ and the equivalence of the two conditions is preserved.

Figure 8.2. The metrized parameter space for an arbitrary system of parallel cosmic strings.

so that the line element becomes

$$ds^2 = \sec^2 \zeta' (d\chi^2 - d\zeta'^2 - \sin^2 \zeta' \, d\psi^2) \tag{8.41}$$

with ζ' in the range $[0, \pi/2)$.

The conformal diagram of (8.41) is illustrated in figure 8.2, with the coordinate ψ suppressed. The boundary between the timelike and the spacelike matrices is the line $\cos^2 \chi = \cos^2 \zeta'$.

Suppose now that the holonomy matrix (8.34) is modified to include an extra string with infinitesimal mass per unit length $d\mu$ moving at a speed $\tanh \beta$ with polar angle ϕ. The net effect is to pre-multiply (8.34) by BRB^{-1}, where the matrices R and B are defined by (8.28) and (8.31), with μ replaced by $d\mu$. It is easily verified that the infinitesimal changes in ζ, χ and ψ are then

$$d\zeta = -4\pi \sinh \beta \sin(\phi + \chi + \psi) \, d\mu \tag{8.42}$$

$$d\chi = 4\pi [\cosh \beta - \sinh \beta \tanh \zeta \cos(\phi + \chi + \psi)] \, d\mu \tag{8.43}$$

and

$$d\psi = 4\pi [\cosh \beta - \sinh \beta \coth \zeta \cos(\phi + \chi + \psi)] \, d\mu. \tag{8.44}$$

Hence, $d\chi > 0$ and $ds^2 = (4\pi \, d\mu)^2 > 0$. Consequently, the effect of adding an extra string to a pre-existing string system is to shift the holonomy matrix along

some future-directed timelike path in the three-dimensional metrised parameter space (8.41).

Suppose now that a string system with holonomy matrix T_{tot} has timelike total momentum but that some subsystem with matrix T_{sub} is spacelike. If the reference frame L is chosen to be the centre-of-momentum frame of the total system, then T_{tot} is the holonomy matrix of a single static string with mass per unit length μ_{tot}, and so $\chi_{\text{tot}} = 4\pi\mu_{\text{tot}}$ and $\zeta'_{\text{tot}} = 0$. Since T_{sub} is a product of single-string holonomy matrices, and is spacelike, it must lie in one of the shaded regions to the timelike future of the origin in figure 8.2 (as the origin corresponds to the identity matrix). Also, since T_{tot} can be generated by pre-multiplying T_{sub} with single-string holonomy matrices, it must lie to the timelike future of T_{sub}. From figure 8.2, it is clear that this is possible only if $\chi_{\text{tot}} > \pi$; hence, the total angle deficit of the system is $\Delta\theta = 8\pi\mu_{\text{tot}} > 2\pi$, and the universe must be closed.

Thus, an open universe containing straight parallel strings—no matter what their relative velocities—cannot support closed timelike curves if its total momentum is timelike. However, this conclusion is not without its critics. In particular, Gott and Matthew Headrick [HG94] have called into question the legitimacy of defining the 'total momentum' of a system of point particles in $2 + 1$ gravity in terms of the holonomy of the system. They point out that in $2 + 1$ dimensions only empty spacetime is asymptotically flat (provided that negative-mass particles are excluded), and that the standard definitions of energy and momentum in $3 + 1$ gravity, which rely on asymptotic flatness, do not apply. Furthermore, they claim that in the absence of a careful analysis of systems of particles in $2 + 1$ gravity there is no guarantee that the total holonomy matrix T of such a system is uniquely defined.

There is much force to these objections but the logical conclusion of this line of argument is that almost nothing is known about the physical properties of $2 + 1$ spacetimes and, therefore, any configuration of particles is as acceptable as any other. While such pessimism might be justified, it is certainly not an argument in favour of the claim that realistic $3 + 1$ systems of cosmic strings could support closed timelike curves. If anything, it undermines the appeal of the simplest models of string-supported CTCs by highlighting the dubious physical status of the spacetimes in which they occur.

8.5   The Letelier–Gal'tsov spacetime

As mentioned earlier, no exact solution is known which describes the gravitational field of three or more non-parallel straight strings in relative motion. This claim might seem to be contradicted by the existence of what appears to be a completely general multi-string spacetime, published by Patricio Letelier and Dmitri Gal'tsov [LG93] in 1993. The Letelier–Gal'tsov spacetime is locally flat and non-radiating, and although not the general string spacetime a first perusal suggests it to be, it is

nonetheless mathematically very intriguing.

The starting point for the Letelier–Gal'tsov spacetime is the line element (8.3) corresponding to N parallel straight strings. If the strings are assumed to have differing masses per unit length $\mu_1, \ldots, \mu_N$ the line element reads:

$$ds^2 = dt^2 - dz^2 - \left(\prod_{k=1}^{N} \rho_k^{-8\mu_k} \right)(dx^2 + dy^2) \tag{8.45}$$

where

$$\rho_k = [(x - x_k)^2 + (y - y_k)^2]^{1/2} \tag{8.46}$$

as before.

Just as the single-string metric (7.32) can be reduced locally to the Minkowski metric by introducing the complex coordinate $w = x + iy$, the local flatness of the line element (8.45) is evident under a transformation of the form $(x, y) \rightarrow (W, W^*)$, where

$$W(x, y) = \int_{\zeta_0}^{x+iy} \prod_{k=1}^{N} (\zeta - \zeta_k)^{-4\mu_k} \, d\zeta \tag{8.47}$$

and $\zeta_k = x_k + y_k$, with ζ_0 a fixed point in the complex plane. For the line integral in (8.47) to be well defined, the curve from ζ_0 to $x + iy$ should be chosen so that it avoids the N poles $\zeta = \zeta_k$ and should also be a continuous functional of $x + iy$. The second condition cannot, of course, be imposed globally, as a line integral of the form (8.47) around any closed contour enclosing one or more of the poles $\zeta = \zeta_k$ is, in general, non-zero. This, in turn, is due to the presence of conical singularities at the poles: the surface of a cone can be mapped conformally to a plane locally but not globally.

Nonetheless, the complex mapping (8.47) is analytic everywhere except at the locations of the N strings and transforms the line element locally into the line element of Minkowski spacetime:

$$ds^2 = dt^2 - dz^2 - dW \, dW^*. \tag{8.48}$$

The Letelier–Gal'tsov spacetime is constructed by taking this line element and using (8.47) to re-express it in terms of x and y, with the important difference that the positions ζ_k are now to be regarded as arbitrary functions of the coordinates t and z.

The resulting line element is

$$ds^2 = dt^2 - dz^2 - \left(\prod_{k=1}^{N} \rho_k^{-8\mu_k} \right)[(dx + F_1 \, dt + G_1 \, dz)^2 + (dy + F_2 \, dt + G_2 \, dz)^2] \tag{8.49}$$

where

$$F \equiv F_1 + iF_2 = \prod_{j=1}^{N} (w - \zeta_j)^{4\mu_j} \int_{\zeta_0}^{x+iy} \prod_{k=1}^{N} (\zeta - \zeta_k)^{-4\mu_k} \sum_{m=1}^{N} \frac{4\mu_m \dot{\zeta}_m}{\zeta - \zeta_m} \, d\zeta \quad (8.50)$$

and

$$G \equiv G_1 + iG_2 = \prod_{j=1}^{N} (w - \zeta_j)^{4\mu_j} \int_{\zeta_0}^{x+iy} \prod_{k=1}^{N} (\zeta - \zeta_k)^{-4\mu_k} \sum_{m=1}^{N} \frac{4\mu_m \zeta'_m}{\zeta - \zeta_m} \, d\zeta. \quad (8.51)$$

Here, an overdot denotes $\partial/\partial t$ and a prime $\partial/\partial z$.

The multi-string line element (8.49) is clearly isometric to Minkowski spacetime everywhere outside the trajectories $\{w = \zeta_k(t, z)\}$. If it is assumed that $|\zeta_0| \to \infty$, so that the value of ζ_0 contributes no boundary terms to the derivatives of W, then F and G are regular functions of $w = x + iy$ with

$$\lim_{w \to \zeta_k} F(w) = -\dot{\zeta}_k \quad \text{and} \quad \lim_{w \to \zeta_k} G(w) = -\zeta'_k \quad (8.52)$$

for all k. Hence, near the trajectory of the nth string the line element has the limiting form

$$ds^2 \approx dt^2 - dz^2 - A^2 \rho_n^{-8\mu_n} [(dx - \dot{x}_n \, dt - x'_n \, dz)^2 + (dy - \dot{y}_n \, dt - y'_n \, dz)^2] \quad (8.53)$$

where $A^2 = \prod_{k \neq n} |\zeta_n - \zeta_k|^{-8\mu_k}$.

On defining $\bar{x} = x - x_n$ and $\bar{y} = y - y_n$, this expression becomes

$$ds^2 \approx dt^2 - dz^2 - A^2 \rho^{-8\mu_n} (d\bar{x}^2 + d\bar{y}^2)^2 \quad (8.54)$$

where now $\rho = (\bar{x}^2 + \bar{y}^2)^{1/2}$. Apart from the conformal factor A^2 this is just the isotropic line element (7.32) due to a single straight string.

On the face of it, then, the Letelier–Gal'tsov metric (8.49) seems capable of describing an arbitrary number of open strings with essentially arbitrary shapes, and in arbitrary states of relative motion. This interpretation is at odds with both the dynamical picture of cosmic strings in flat spacetime presented in chapters 2 and 3 (as string motion in flat space is constrained by the Nambu–Goto action) and the gravitational theory of curved strings outlined in chapters 6 and 10 (as bent or accelerating strings should radiate). It also suggests something that was perhaps evident from the start, namely that (8.49) is just the static parallel-string metric (8.3) written in an obscure coordinate system.

To see this, note first that the geodesic structure of the Letelier–Gal'tsov spacetime is fixed by the original Minkowski spacetime (8.48). Provided that it does not pass through the trajectory of one of the strings, a curve $x^\mu(\lambda)$ is a geodesic if and only if t, z, W and W^* can be expressed as linear functions of an affine parameter. In particular, the geodesic distance between two points (x_1, y_1) and (x_2, y_2) on the same surface of constant t and z is $|W(x_1, y_1) - W(x_2, y_2)|$.

Consider now the 2-surface defined by $w = \zeta_n(t, z) + \varepsilon$, where ζ_n is the position function of the nth string, and ε is a non-zero constant. As t and z vary across this surface, the corresponding changes in W are given by

$$dW = \left(\prod_{k=1}^{N} \rho_k^{-4\mu_k} \right) [(\dot{\zeta}_n + F)\, dt + (\zeta_n' + G)\, dz)]. \tag{8.55}$$

Here, to leading order in ε,

$$\prod_{k=1}^{N} \rho_k^{-4\mu_k} \approx \varepsilon^{-4\mu_n} \prod_{k \neq n} (\zeta_n - \zeta_k)^{-4\mu_k} \tag{8.56}$$

while, from the definitions of F and G,

$$F \approx -\dot{\zeta}_n - \varepsilon \frac{4}{1 - 4\mu_n} \sum_{j \neq n} \frac{\mu_j (\dot{\zeta}_n - \dot{\zeta}_j)}{\zeta_n - \zeta_j} \tag{8.57}$$

and

$$G \approx -\zeta_n' - \varepsilon \frac{4}{1 - 4\mu_n} \sum_{j \neq n} \frac{\mu_j (\zeta_n' - \zeta_j')}{\zeta_n - \zeta_j}. \tag{8.58}$$

Thus, in the limit as $\varepsilon \to 0$ and the 2-surface approaches the trajectory of the nth string, the change dW goes to zero like $\varepsilon^{1-4\mu}$. The same is true of all the other strings and, therefore, the geodesic distance between any two strings is the same on each constant t, z slice, as is the geodesic distance between any string and a general point W in the spacetime. In other words, the strings are all straight and parallel, no matter what choice is made for the functions $\{\zeta_k\}$.

Chapter 9

Other exact string metrics

Numerical simulations of the dynamics of (non-gravitating) cosmic string networks strongly suggest that realistic cosmic strings—if present at all in the early Universe—would have had structure on all sizes down to a length scale determined by the dissipative effects of gravitational radiation [BB91]. In addition, it is thought that the vast bulk of the energy of the network would have quickly been channeled into a system of small, high-velocity loops, with perhaps one long (horizon-sized) string per horizon volume. The metric (7.28) due to an infinite straight cosmic string in vacuum is, therefore, unlikely to be of direct cosmological interest.

Unfortunately, it is difficult to generate exact string metrics in the absence of the high degree of symmetry evident in the straight-string metric (7.28), even with the simplifications afforded by the wire approximation. In particular, no exact solution has to date been found describing a closed string loop. In this chapter I will present a compendium of most of the known exact string metrics. These are all of necessity highly symmetric and thus, although they provide important clues to the gravitational effects of more general string configurations, are probably not directly relevant to the study of realistic cosmic strings. Nonetheless, the solutions are of considerable mathematical interest and in some cases shed unexpected light on other areas of mathematical relativity.

9.1 Strings and travelling waves

The simplest generalization of the bare straight-string metric (7.28) is the family of *travelling-wave* solutions first published by David Garfinkle [Gar90] in 1990. The corresponding weak-field solutions were discovered by Tanmay Vachaspati [Vac86] in 1986. Although the solutions examined here will be presented in the wire approximation only, it should be noted that there exist exact families of solutions of the full Einstein–Higgs–Yang–Mills field equations with the same geometric structure [VV90, GV90], which generalize Garfinkle's gravitating

Nielsen–Olesen vortex solution [Gar85]. The travelling-wave solutions are the only known cosmic string metrics with exact field-theoretic analogues of this type.

Following Valeri Frolov and David Garfinkle [FG90], the most direct way of generating cosmic string travelling-wave solutions is to note that if $\bar{g}_{\mu\nu}$ is a metric tensor admitting a covariantly constant null vector field k_μ then any spacetime with a metric tensor of the form

$$g_{\mu\nu} = \bar{g}_{\mu\nu} + F k_\mu k_\nu \tag{9.1}$$

where $k^\mu F,_\mu = 0$ and $\bar{D}^\mu F,_\mu = 0$ (with $\bar{D}_\mu$ the covariant derivative operator induced by $\bar{g}_{\mu\nu}$) differs from the initial spacetime only by the addition of plane-fronted gravitational radiation propagating in the direction of k_μ.

To see this explicitly, note first that because k_μ is null

$$g^{\mu\nu} = \bar{g}^{\mu\nu} - F k^\mu k^\nu \tag{9.2}$$

where the index on k_μ can be raised or lowered interchangeably by $g_{\mu\nu}$ or $\bar{g}_{\mu\nu}$. Hence, if ω_μ is any vector field the covariant derivative operators generated by $g_{\mu\nu}$ and $\bar{g}_{\mu\nu}$ satisfy

$$D_\mu \omega_\nu = \bar{D}_\mu \omega_\nu - \Lambda^\lambda_{\mu\nu} \omega_\lambda \tag{9.3}$$

where, in view of the constancy condition $\bar{D}_\mu k_\nu = 0$,

$$\Lambda^\lambda_{\mu\nu} = F,_{(\mu} k_{\nu)} k^\lambda - \tfrac{1}{2} \bar{g}^{\lambda\kappa} F,_\kappa k_\mu k_\nu. \tag{9.4}$$

The Riemann tensor corresponding to $g_{\mu\nu}$ can now be generated from the identity $R_{\kappa\lambda\mu\nu}\omega^\nu = 2D_{[\lambda}D_{\kappa]}\omega_\mu$ and is given by

$$R_{\kappa\lambda\mu\nu} = \bar{R}_{\kappa\lambda\mu\nu} + 2k_{[\lambda}\bar{D}_{\kappa]}F,_{[\mu} k_{\nu]} \tag{9.5}$$

where $\bar{R}_{\kappa\lambda\mu\nu}$ is the Riemann tensor of the initial spacetime. In particular, the Ricci tensor of the new spacetime is:

$$R_{\lambda\nu} = \bar{R}_{\lambda\nu} + \tfrac{1}{2}(\bar{D}^\mu F,_\mu) k_\lambda k_\nu \tag{9.6}$$

and so if $\bar{D}^\mu F,_\mu = 0$ the two spacetimes have the same stress–energy content. However, as is evident from (9.5), the two Riemann tensors are not, in general, equal. The new spacetime thus differs from the old only through the addition of gravitational radiation whose Riemann tensor has a covariantly constant null eigenvector and is thus plane-fronted.

If plane-fronted gravitational waves are added to the bare straight-string metric in its isotropic form (7.32) then the initial line element has the form

$$d\bar{s}^2 = dt^2 - dz^2 - \rho^{-8\mu}(dx^2 + dy^2) \tag{9.7}$$

with $\rho = (x^2 + y^2)^{1/2}$ and μ the mass per unit length of the string. There are two possible choices of covariantly constant null vector field for this spacetime:

$$k^+_\mu = \delta^t_\mu + \delta^z_\mu \qquad \text{or} \qquad k^-_\mu = \delta^t_\mu - \delta^z_\mu \tag{9.8}$$

and the function F is, therefore, constrained by the conditions:

$$k^{+\mu} F_{,\mu} \equiv F_{,t} - F_{,z} = 0 \qquad \text{or} \qquad k^{-\mu} F_{,\mu} \equiv F_{,t} + F_{,z} = 0 \qquad (9.9)$$

and

$$\bar{D}^{\mu} F_{,\mu} \equiv F_{,tt} - F_{,zz} - \rho^{8\mu}(F_{,xx} + F_{,yy}) = 0. \qquad (9.10)$$

Hence, the most general solution for F is

$$F(t, x, y, z) = \sum_i M_i(t \pm z) H_i(x, y) \qquad (9.11)$$

where the H_i are linearly independent harmonic functions of x and y, and the M_i are arbitrary twice differentiable functions of $t + z$ (if $k_\mu = k_\mu^+$) or $t - z$ (if $k_\mu = k_\mu^-$). The corresponding travelling-wave line element reads:

$$ds^2 = (1 + F)\,dt^2 - (1 - F)\,dz^2 \pm 2F\,dt\,dz - \rho^{-8\mu}(dx^2 + dy^2). \qquad (9.12)$$

As can be seen, travelling waves on cosmic strings exist in either left- or right-moving modes, with the parity fixed by the choice of k_μ. Once the mode functions H_i and M_i have been fixed, the travelling wave propagates along the string with a constant structure, and the spacetime (9.12) remains stationary and non-dissipative. The nonlinearity of the Einstein equations prevents the two types of modes from being superposed in a non-dissipative manner. Thus, although the family of solutions (9.12) exhibits a considerable degree of parametric freedom, it is far from being the most general vacuum spacetime outside an infinite cosmic string.

Incidentally, this construction could equally well be applied to any *non-vacuum* metric tensor $\bar{g}_{\mu\nu}$ that admits a covariantly constant null vector field. A simple example is the constant-ε_0 interior solution examined in section 7.1, which has the line element

$$ds^2 = dt^2 - dz^2 - dr^2 - e^{2\omega}\,d\phi^2 \qquad (9.13)$$

where $e^\omega = r_* \sin(r/r_*)$, and also admits the constant null vector fields $k_\mu^\pm = \delta_\mu^t \pm \delta_\mu^z$. The corresponding travelling-wave metrics $g_{\mu\nu} = \bar{g}_{\mu\nu} + F k_\mu k_\nu$ also describe interior solutions with constant density and tension ε_0 and are generated in the same way as before, with the only difference being that F satisfies the equation

$$F_{,tt} - F_{,zz} - e^{-\omega}(e^\omega F_{,r})_{,r} - e^{-2\omega} F_{,\phi\phi} = 0. \qquad (9.14)$$

The travelling-wave analogues of the Nielsen–Olesen vortex solutions discussed in [VV90] and [GV90] are straightforward extensions of this type of solution.

In view of the fact that the bare straight-string spacetime (9.7) is locally flat, and

$$D_\mu F_{,\nu} = F_{,\mu\nu} + 4\mu\rho^{-2}(x F_{,x} - y F_{,y})(\delta_\mu^x \delta_\nu^x - \delta_\mu^y \delta_\nu^y)$$
$$+ 4\mu\rho^{-2}(x F_{,x} + y F_{,y})(\delta_\mu^x \delta_\nu^y + \delta_\mu^y \delta_\nu^x) \qquad (9.15)$$

the Riemann tensor (9.5) corresponding to a generic cosmic string travelling wave has only three algebraically independent components (for $\rho \neq 0$):

$$k^{\mp\lambda}k^{\mp\nu}R_{x\lambda x\nu} = 2[F_{,xx} + 4\mu\rho^{-2}(xF_{,x} - yF_{,y})] \tag{9.16}$$

$$k^{\mp\lambda}k^{\mp\nu}R_{x\lambda y\nu} = 2[F_{,xy} + 4\mu\rho^{-2}(xF_{,x} + yF_{,y})] \tag{9.17}$$

and

$$k^{\mp\lambda}k^{\mp\nu}R_{y\lambda y\nu} = 2[F_{,yy} + 4\mu\rho^{-2}(yF_{,y} - xF_{,x})]. \tag{9.18}$$

In particular, if the travelling wave contains only linear harmonics in x and y, so that

$$F = 2x\,A''(t \pm z) + 2y\,B''(t \pm z) \tag{9.19}$$

where A and B are arbitrary four-times differentiable functions, then

$$R_{\kappa\lambda\mu\nu} = 16\mu\rho^{-1}k_{[\lambda}C_{\kappa][\mu}k_{\nu]} \tag{9.20}$$

with

$$C_{\kappa\mu} = (A''\cos\phi - B''\sin\phi)(\delta_\kappa^x\delta_\mu^x - \delta_\kappa^y\delta_\mu^y) + (A''\cos\phi + B''\sin\phi)(\delta_\kappa^x\delta_\mu^y + \delta_\kappa^y\delta_\mu^x) \tag{9.21}$$

where ϕ is the polar angle defined by $\rho e^{i\phi} = x + iy$.

The form of the Riemann tensor (9.20) illustrates an important feature of linear travelling waves. In a Minkowski background ($\mu = 0$) linear travelling waves have no tidal effects whatsoever, and it can be shown that the corresponding metric (9.12) is just Minkowski spacetime in non-standard coordinates [KSHM80]. In a cosmic string background, by contrast, linear travelling waves induce a non-zero Riemann tensor. The spacetime (9.12) with (9.19) is, therefore, entirely new and, unlike all higher harmonic solutions, has no non-flat analogue in the limit as $\mu \to 0$. This suggests that a linear travelling wave is somehow intrinsic to the underlying cosmic string and that, in the words of Frolov and Garfinkle [FG90], 'we can regard the [linear] traveling-wave metric as the gravitational field of the moving string'.

Support for this interpretation can be bolstered by noting that the transformation

$$x = \bar{x} - A \qquad y = \bar{y} - B \tag{9.22}$$

$$t = \bar{t} - \bar{x}A' - \bar{y}B' + \tfrac{1}{2}\int_0^{\bar{t}\pm\bar{z}} [A'^2(u) + B'^2(u)]\,du \tag{9.23}$$

and

$$z = \bar{z} - \bar{x}A' - \bar{y}B' + \tfrac{1}{2}\int_0^{\bar{t}\pm\bar{z}} [A'^2(u) + B'^2(u)]\,du \tag{9.24}$$

recasts the line element (9.12) with (9.19) in the form

$$ds^2 = d\bar{t}^2 - d\bar{z}^2 + 2(\rho^{-8\mu} - 1)(A'\,d\bar{x} + B'\,d\bar{y})(d\bar{t} \pm d\bar{z})$$
$$- (\rho^{-8\mu} - 1)(A'^2 + B'^2)(d\bar{t} \pm d\bar{z})^2 - \rho^{-8\mu}(d\bar{x}^2 + d\bar{y}^2) \tag{9.25}$$

where now $\rho = [(\bar{x} - A)^2 + (\bar{y} - B)^2]^{1/2}$. (Note that A and B are interchangeably functions of $t \pm z$ or $\bar{t} \pm \bar{z}$, as this is an invariant of the transformation.) Thus it can be argued that a linear travelling-wave solution is simply the metric induced by a non-straight string moving along the world sheet $\bar{x} = A(\bar{t} \pm \bar{z})$ and $\bar{y} = B(\bar{t} \pm \bar{z})$.

Nonetheless, the fact that the gravitational radiation content of the linear travelling-wave metric (9.25) occurs in the form of collective oscillations of the entire spacetime, rather than as localized disturbances which propagate outwards from the world sheet, argues strongly that (9.25) does not represent the response of an otherwise empty spacetime to waves on a cosmic string. Instead it is more natural to regard the linear travelling waves as an exotic form of plane-fronted gravitational waves catalysed by the non-trivial holonomy of the spacetime around a single straight string. In support of this view, the construction outlined earlier can also be used to superimpose travelling waves on the multiple straight-string spacetime (8.3), but all the strings then 'oscillate' in exactly the same manner.

One critic of the belief that (9.25) describes a cosmic string at all is Patricio Letelier, who claims that the linear travelling-wave solution 'represents a "rod" rather than a string' [Let92]. In defence of this statement, he cites the fact that the physical components of the Riemann tensor (9.20) diverge as $\rho^{8\mu - 1}$ as ρ tends to zero, and, therefore, that the linear travelling-wave spacetime describes 'an object more singular than a cosmic string'. As further evidence, Letelier also notes that a freely-falling observer will measure a tidal force that diverges as s^{-2}, where s is the proper time to the locus of the string.

Now, while it is true that the divergence of the physical components of the Riemann tensor (9.20) contrasts strongly with the benign nature of the Riemann tensor outside the bare straight string (9.7), the singularity in (9.20) remains an integrable one. If $\hat{R}$ is any of the physical components of (9.20) then the integral $\int \hat{R} \sqrt{g} \, d^4x$ involves terms no worse than $\int \rho^{-2} x \, dx \, dy$ and $\int \rho^{-2} y \, dx \, dy$. Furthermore, as will be seen in section 10.4.4, the inclusion of travelling waves has no effect on the distributional stress–energy density (7.80) characteristic of the world sheet of a bare straight cosmic string. Finally, the fact that metrics of the form (9.12) with (9.19) are the zero-thickness limits of known exact vortex solutions of the Einstein–Higgs–Yang–Mills field equations argues strongly in favour of the position that they do describe cosmic strings at the level of the wire approximation.

Letelier [Let91] has also investigated a more general family of travelling-wave string metrics of the form (9.12), in which F is not constrained to be a harmonic function of x and y (although the coordinate system he uses makes direct comparison with (9.12) rather complicated). The effect of relaxing this constraint is to admit a non-zero stress–energy tensor $T_{\mu\nu}$ proportional to $k_\mu k_\nu$, which, therefore, describes electromagnetic radiation propagating along the string in the same direction as the travelling waves.

As a final remark, it should be noted that travelling waves containing only

second-order harmonics have the generating function

$$F = (x^2 - y^2) P''(t \pm z) + 2xy Q''(t \pm z) \tag{9.26}$$

where P and Q are arbitrary four-times differentiable functions. In this case the physical components of the Riemann tensor go to zero as $\rho^{8\mu}$. More generally, in terms of the proper distance $r \propto \rho^{1-4\mu}$ from the world sheet each nth-order harmonic travelling wave contributes terms of order $r^{n/(1-4\mu)}$ to the metric tensor and terms of order $r^{(8\mu+n-2)/(1-4\mu)}$ to the physical components of the Riemann tensor. Also, with the gauge choice $\tau = t$ and $\sigma = z$ the 2-metric of the world sheet in (9.12) has the form $\gamma_{AB} = \mathrm{diag}(1, -1)$, and so the world sheet is flat. In chapter 10, near-field behaviour of this type will be regarded as the signature of travelling waves in more general cosmic string spacetimes.

9.2   Strings from axisymmetric spacetimes

Another method of generating cosmic string solutions is to take an axisymmetric spacetime, excise a wedge of fixed angular extent from around the symmetry axis, and then glue the exposed faces together, in much the same way as the bare straight-string metric can be conjured from Minkowski spacetime (see section 7.2). In fact, James Vickers [Vic87, Vic90] has developed a general formalism which can be applied to any spacetime $(\mathbf{M}, g)$ that admits an isometry f^λ with a fixed point set $\mathbf{T} = \{x^\mu : f^\lambda(x^\mu) = x^\lambda\}$. A conical singularity can be inserted into the spacetime by removing the fixed point set $\mathbf{T}$ from $\mathbf{M}$, identifying all points x^μ and y^λ with $y^\lambda = f^\lambda(x^\mu)$ in the universal covering space, and if necessary deleting some points to restore Hausdorff topology to the resulting spacetime $(\mathbf{M}', g')$.

Vickers [Vic87, Vic90] notes the following important properties of the construction outlined here:

(1) The fixed point set $\mathbf{T}$ is a totally geodesic submanifold of $\mathbf{M}$ (that is, geodesics initially tangent to $\mathbf{T}$ remain tangent to $\mathbf{T}$).
(2) The Riemann tensor on $(\mathbf{M}', g')$ is everywhere the same as the Riemann tensor on $(\mathbf{M} \setminus \mathbf{T}, g)$.
(3) If $(\mathbf{M}, g)$ is an axisymmetric spacetime with $\mathbf{T}$ the symmetry axis then in a neighbourhood of any point x_0^μ on $\mathbf{T}$ it is possible to introduce *geodesic cylindrical* coordinates (t, r, θ, z), where δ_μ^θ is the rotational Killing vector, θ has range $[0, 2\pi)$, $\mathbf{T}$ is the set $r = 0$, and curves of the form $t = z = 0$ and $\theta = $ constant are geodesics with affine parameter r terminating at x_0^μ and orthogonal to $\mathbf{T}$. If the spacetime $(\mathbf{M}', g')$ is now generated by identifying θ and $\theta + 2\pi - \Delta\theta$ in the universal covering space (with $\Delta\theta$ some constant) then the Riemann component $R^r_{\theta r\theta}$ on $\mathbf{M}'$ supports a distributional singularity at $r = 0$, in the sense that

$$\lim_{\varepsilon \to 0} \int_0^\varepsilon \int_0^{2\pi - \Delta\theta} R^r_{\theta r\theta} r \, \mathrm{d}r \, \mathrm{d}\theta = \Delta\theta. \tag{9.27}$$

In line with the corresponding treatment of the bare straight-string metric in section 7.2, it is possible to infer that $(\mathbf{M}', g')$ has a distributional stress–energy density with non-zero components

$$\widehat{\sqrt{g}T_t^t} = \widehat{\sqrt{g}T_z^z} = \mu\delta^{(2)}(r) \qquad (9.28)$$

where $\mu = \frac{1}{8\pi}\Delta\theta$ and $\delta^{(2)}(r)$ is the unit distribution in $\mathbb{R}^2$.

(4) Conversely, an axisymmetric spacetime $(\mathbf{M}', g')$ with distributional stress–energy of the form (9.28) and a Riemann tensor whose components in a parallel-propagated frame tend to well-defined limits along all curves ending at the singularity can be completed by the addition of a singular boundary $\mathbf{T}$ which is a totally geodesic submanifold of $\mathbf{M}' \cup \mathbf{T}$.

Vickers chooses to call any spacetime $(\mathbf{M}', g')$ constructed in this way a 'generalized cosmic string', to distinguish it from the bare straight-string metric (7.28). However, it should be noted that Vickers' class of 'generalized' cosmic strings does not encompass all metrics with cosmic string sources in the sense of section 7.2. In particular, as was seen earlier, the linear travelling-wave solution (9.12) with (9.19) has a Riemann tensor whose physical components are unbounded near the singularity, and, therefore, cannot be generated by excising a conical wedge from any non-singular spacetime $(\mathbf{M}, g)$.

Given the plethora of known axisymmetric solutions to the Einstein equations, it is possible here to explore only a small sample of 'generalized' cosmic string metrics. The examples given here show the effect of embedding a straight string in two of the most important astrophysical spacetimes: the Robertson–Walker and Schwarzschild metrics. A third class of solutions, which describe a straight string coupled to a cosmological constant, will also be examined briefly.

9.2.1   Strings in a Robertson–Walker universe

The line element for the class of Robertson–Walker spacetimes was given in (5.3). Because the spacelike slices are maximally symmetric, any spacelike geodesic with $\eta = $ constant delineates an axis of rotational symmetry. It is always possible to rotate the coordinates so that this line becomes the polar axis. If a cosmic string with mass per unit length μ is embedded along this axis then the line element reads:

$$\mathrm{d}s^2 = a^2(\eta)\left[\mathrm{d}\eta^2 - \frac{\mathrm{d}R^2}{1 - kR^2} - R^2\mathrm{d}\theta^2 - (1 - 4\mu)^2 r^2 \sin^2\theta\,\mathrm{d}\phi^2\right] \qquad (9.29)$$

where $k = 0$ or ± 1 as before and R, θ and ϕ are standard spherical polar coordinates. A more detailed derivation of this line element in the flat case ($k = 0$) can be found in [Gre89].

As mentioned earlier, the presence of the cosmic string does not affect the value of the Riemann tensor away from the axis, and so the only algebraically

independent components of the Riemann and stress–energy tensors for $r \sin \theta \neq 0$ are:

$$R^{\eta r}{}_{\eta r} = R^{\eta \theta}{}_{\eta \theta} = R^{\eta \phi}{}_{\eta \phi} = a^{-4}(a\ddot{a} - \dot{a}^2) \tag{9.30}$$

$$R^{r\theta}{}_{r\theta} = R^{r\phi}{}_{r\phi} = R^{\theta \phi}{}_{\theta \phi} = a^{-4}(\dot{a}^2 + ka^2) \tag{9.31}$$

and

$$T^\eta_\eta = \frac{3}{8\pi} a^{-4}(\dot{a}^2 + ka^2) \qquad T^r_r = T^\theta_\theta = T^\phi_\phi = \frac{1}{8\pi} a^{-4}(2a\ddot{a} - \dot{a}^2 + ka^2) \tag{9.32}$$

where an overdot denotes $d/d\eta$.

Incidentally, the closed ($k = 1$) Robertson–Walker spacetime has the interesting feature that it can be recast in a simple form which allows the direct insertion of two orthogonal cosmic strings. If $k = 1$ and $\mu = 0$ the spatial cross sections of (9.29) are 3-spheres with line element proportional to

$$-(d\varpi^2 + \sin^2 \varpi \, d\chi^2 + \sin^2 \varpi \sin^2 \chi \, d\phi^2) \tag{9.33}$$

where the coordinate $\varpi = \sin^{-1} R$ has range $[0, \pi)$. Transforming from (ϖ, θ) to coordinates (β, ψ) defined by

$$\sin \beta = \sin \varpi \sin \theta \qquad \text{and} \qquad \tan \psi = \tan \varpi \cos \theta \tag{9.34}$$

then reduces this line element to the form

$$-(d\beta^2 + \cos^2 \beta \, d\psi^2 + \sin^2 \beta \, d\phi^2) \tag{9.35}$$

where β and ψ both range from 0 to π (with the endpoints identified).

The 3-spherical line element (9.35) clearly has symmetry axes along the lines $\beta = 0$ and $\beta = \pi/2$, which are the fixed points of the isometries generated by the Killing vectors δ^ϕ_μ and δ^ψ_μ respectively. It is, therefore, possible to embed cosmic strings along each of these axes in a general closed Robertson–Walker spacetime by writing

$$ds^2 = a^2(\eta)[d\eta^2 - d\beta^2 - (1 - 4\mu_1)^2 \cos^2 \beta \, d\psi^2 - (1 - 4\mu_2)^2 \sin^2 \beta \, d\phi^2] \tag{9.36}$$

where the masses per unit length μ_1 and μ_2 need not be equal. The line element (9.36) describes the simplest known non-static universe containing two cosmic strings, although it should be recalled from chapter 7 that there is no difficulty in embedding two (or more) straight cosmic strings in Minkowski spacetime.

Strictly speaking, the general Robertson–Walker string solution (9.29) should not be interpreted as the metric exterior to a straight cosmic string in a homogeneous, isotropic universe unless it can be shown to be the zero-thickness limit of a family of non-singular spacetimes containing a cylindrical distribution of stress–energy embedded in a cosmological background, as was seen to be the case for a Minkowski string in section 7.4. To date, no smooth cylindrical interior

solution has been published which matches onto (9.29) at a finite radial distance $r \equiv R \sin\theta = r_0(\eta)$. Nor, if such solutions do exist, is it known whether the exterior metric (9.29) would be energetically favoured over other cylindrically-symmetric spacetimes containing cosmological fluid with the same equation of state.

However, Ruth Gregory [Gre89] has pointed out that if the radius r_S of the string core is small compared to the Hubble radius $a/\dot{a}$ then a Nielsen–Olesen vortex can be embedded in a flat Robertson–Walker spacetime by assuming a line element with the approximate form

$$ds^2 = a^2(\eta)[e^{2\chi_M(ar)}\,d\eta^2 - e^{2\psi_M(ar)}(dr^2 + dz^2)] - e^{2\omega_M(ar)}\,d\phi^2 \qquad (9.37)$$

where $\chi_M(r)$, $\psi_M(r)$ and $\omega_M(r)$ are the corresponding metric functions for a Nielsen–Olesen vortex in a flat background, which, in principle, can be read from Garfinkle's solution [Gar85]. If $r \gg r_S$ then $\chi_M(r)$ and $\psi_M(r)$ are negligibly small while $e^{\omega_M(r)} \approx (1 - 4\mu)r$, and Gregory's line element (9.37) tends asymptotically to the flat version of (9.29).

Near the string core, however, the detailed form of the line element depends on the behaviour of χ_M, ψ_M and ω_M, for which no explicit solutions are known. However, the argument leading to (9.37) is applicable no matter what stress–energy content is assumed for the string, so a toy model of the embedding can be constructed by assuming a constant-density interior, which (from section 7.1) has $T^t_t = T^z_z = \varepsilon_0$, $\chi(r) = \psi(r) = 0$ and $e^{\omega(r)} = r_* \sin(r/r_*)$ where $r_* = (8\pi\varepsilon_0)^{-1/2}$.

In a dust-filled universe, $a(\eta) = \lambda\eta^2$ for some constant λ and the stress–energy tensor corresponding to (9.37) has the non-zero components

$$T^t_t = \varepsilon_0 + \tfrac{1}{3}\varepsilon_c(\eta)(1 + 2\bar{r}\cot\bar{r}) \qquad T^z_z = \varepsilon_0(1 - 4r^2/\eta^2) - \tfrac{1}{6}\varepsilon_c(\eta)(1 - \bar{r}\cot\bar{r}) \qquad (9.38)$$

$$T^r_r = -4\varepsilon_0 r^2/\eta^2 - \tfrac{1}{6}\varepsilon_c(\eta)(1 - \bar{r}\cot\bar{r}) \qquad \text{and} \qquad T^t_r = -T^r_t = 2\varepsilon_0 r/\eta \qquad (9.39)$$

where $\varepsilon_c(\eta) = 96\pi/(\lambda^2\eta^6)$ is the energy density of the dust, and $\bar{r} = \lambda\eta^2 r/r_*$.

The assumption that the core radius is small compared to the Hubble radius is equivalent to the condition $r_S \sim \lambda\eta^2 r \ll \eta$, while the mass per unit length $\mu \sim \tfrac{1}{4}(1 - \cos\bar{r})$ of the string will be of GUT size if $\bar{r} \ll 1$. Thus $\varepsilon_0 r^2/\eta^2 \ll \varepsilon_c(\eta)$ and the stress–energy tensor has the approximate form $T^t_t = \varepsilon_0 + \varepsilon_c(\eta)$, $T^z_z = \varepsilon_0$ as expected. Similarly, although the constant-density interior cannot be matched exactly to the cosmological exterior (9.29) across a boundary surface $r = r_0(\eta)$ (an indication that the string radiates energy, at a rate proportional to r_S^2/η^2, as the universe expands), the mismatch between the extrinsic curvatures vanishes in the zero-thickness limit.

Bill Unruh [Unr92] and Jaime Stein-Schabes and Adrian Burd [SSB88] have also addressed this particular problem, using slightly different approaches. Unruh

added an *ad hoc* correction to the standard Robertson–Walker line element to model the presence of a cosmic string near the axis, showed that the correction required a string source whose equation of state deviated slightly from the naive choice $T_t^t = T_z^z$, and concluded that this deviation would have negligible effect on the external spacetime. Stein-Schabes and Burd integrated the Higgs–Yang–Mills equations numerically to generate a vortex solution in a fixed flat Robertson–Walker background, and similarly concluded that the stress–energy tensor of the vortex fields was unlikely to satisfy the relation $T_t^t = T_z^z$.

A related but somewhat different question has been raised by Dyer *et al* [DOS88], who examined whether an *evacuated* cylinder containing a zero-thickness cosmic string on axis can be embedded inside a Robertson–Walker background of the form (9.29). The purpose of such a construction was to attempt to justify the standard vacuum calculations of the gravitational lensing effects of a straight string, in the spirit of the 'Swiss cheese' model for spherical inhomogeneities in an expanding universe.

Dyer *et al* argued that the bare straight-string spacetime (7.28) cannot be embedded in a flat ($k = 0$) Robertson–Walker exterior, and after a much more thorough analysis Eric Shaver and Kayll Lake came to the same conclusion [SL89]. However—as Unruh [Unr92] has pointed out—this result is obvious, as the conical spacetime (7.28) is invariant under boosts in the z-direction, whereas a Robertson–Walker spacetime with an excised cylinder is not. A more interesting question is whether a radiating vacuum cylinder containing a cosmic string can be embedded in a Robertson–Walker background.

To examine this problem in more detail, it is convenient to rewrite the Robertson–Walker exterior (9.29) in the cylindrical form

$$ds^2 = a^2(\eta)[d\eta^2 - dr^2 - K^2(r)\,dz^2 - (1 - 4\mu)^2 S^2(r)\,d\phi^2] \qquad (9.40)$$

where $S(r) = \sin r$, r or $\sinh r$ and $K(r) = \cos r$, 1 or $\cosh r$ as $k = 1$, 0 or -1. The transformation from (R, θ) to (r, z) is accomplished by defining $S(r) = R \sin\theta$ and $T(z) = (1 - kR^2)^{-1/2} R \cos\theta$, with $T(z) = \tan z$, z or $\tanh z$ when $k = 1$, 0 or -1. The problem is then to match the line element (9.40) to the metric of a cylindrical radiating vacuum across some boundary surface $r = r_0(\eta)$.

As will be demonstrated later, in section 9.3.1, a (non-static) cylindrical vacuum spacetime with z-reflection symmetry can always be described by a line element of the form

$$ds^2 = e^{2C - 2\psi}(dt^2 - dr^2) - e^{2\psi}\,dz^2 - e^{-2\psi} r^2\,d\phi^2 \qquad (9.41)$$

where C and ψ are functions of t and r alone, with $\ddot\psi = \psi'' + r^{-1}\psi'$, $\dot C = 2r\dot\psi\psi'$ and $C' = r(\dot\psi^2 + \psi'^2)$. To distinguish between the interior and exterior versions of the radial coordinate r, the exterior coordinate will henceforth be relabelled ϖ.

The two line elements (9.40) and (9.41) will be isometric at the junction surface $\varpi = \varpi_0(\eta)$ and $r = r_0(t)$ if

$$(1 - 4\mu)a S_0 = r_0 e^{-\psi_0} \qquad a K_0 = e^{\psi_0} \qquad (9.42)$$

and

$$a(1 - \dot{\varpi}_0^2)^{1/2}\,\mathrm{d}\eta = \mathrm{e}^{C_0 - \psi_0}(1 - \dot{r}_0^2)^{1/2}\,\mathrm{d}t \qquad (9.43)$$

where a subscripted 0 indicates that the corresponding metric function is evaluated at the boundary.

Furthermore, the extrinsic curvature tensors of the boundary surfaces will match only if

$$(1 - \dot{\varpi}_0^2)^{-1}(G_{\varpi}^{\varpi} - 2\dot{\varpi}_0 G_{\varpi}^{\eta} - \dot{\varpi}_0^2 G_{\eta}^{\eta}) = (1 - \dot{r}_0^2)^{-1}(G_r^r - 2\dot{r}_0 G_r^t - \dot{r}_0^2 G_t^t) \quad (9.44)$$

and

$$(1 - \dot{\varpi}_0^2)^{-1}[\dot{\varpi}_0(G_{\eta}^{\eta} - G_{\varpi}^{\varpi}) + (1 + \dot{\varpi}_0^2)G_{\varpi}^{\eta}] = (1 - \dot{r}_0^2)^{-1}[\dot{r}_0(G_t^t - G_r^r) + (1 + \dot{r}_0^2)G_r^t]$$
$$(9.45)$$

on the boundary [And99a], and since $G_{\nu}^{\mu} = 0$ identically in the interior vacuum solution, while $G_{\varpi}^{\eta} = 0$, $G_{\eta}^{\eta} \neq 0$ and $G_{\varpi}^{\varpi} = -a^{-4}(2a\ddot{a} - \dot{a}^2 + ka^2)$ in the Robertson–Walker exterior, it follows that $\dot{\varpi}_0 = 0$ and the exterior spacetime must be pressure-free ($2a\ddot{a} - \dot{a}^2 + ka^2 = 0$).

The latter condition gives rise to the standard Robertson–Walker dust solution:

$$a(\eta) = 2\lambda(1 - \cos\eta), \ \lambda\eta^2 \text{ or } 2\lambda(\cosh\eta - 1) \qquad \text{as } k = 1, 0 \text{ or } -1 \quad (9.46)$$

where λ is a scaling constant. In addition, the matching of the extrinsic curvature tensors generates two further boundary conditions:

$$a^{-1}K_0^{-1}K_0' = \mathrm{e}^{\psi_0 - C_0}(1 - \dot{r}_0^2)^{-1/2}(\psi_0' + \dot{r}_0\dot{\psi}_0) \qquad (9.47)$$

and

$$a^{-1}(KS)_0^{-1}(KS)_0' = \mathrm{e}^{\psi_0 - C_0}(1 - \dot{r}_0^2)^{-1/2}r_0^{-1}. \qquad (9.48)$$

The conversion from the exterior variables η and ϖ_0 to the interior variables t and r_0 is given implicitly by

$$t = (1 - 4\mu)(KS)_0' \int_0^{\eta} a^2(u)\,\mathrm{d}u \qquad \text{and} \qquad r_0(t) = (1 - 4\mu)K_0 S_0 a^2(\eta)$$
$$(9.49)$$

and, in particular, $\dot{r}_0 = \beta a^{-1}\dot{a}$ with $\beta = 2K_0 S_0/(KS)_0'$. By taking the time derivative of $\mathrm{e}^{\psi_0} = aK_0$ along the boundary, then solving separately for $\dot{\psi}_0$, ψ_0' and e^{C_0}, the boundary conditions can be re-expressed in the form

$$\mathrm{e}^{\psi_0} = aK_0 \qquad \dot{\psi}_0 = (\tfrac{1}{2} - \gamma)(1 - \dot{r}_0^2)^{-1}r_0^{-1}\dot{r}_0 \qquad \psi_0' = (\gamma - \tfrac{1}{2}\dot{r}_0^2)(1 - \dot{r}_0^2)^{-1}r_0^{-1}$$
$$(9.50)$$

and

$$\mathrm{e}^{C_0} = (1 - 4\mu)^{-1}K_0[(KS)_0']^{-1}(1 - \dot{r}_0^2)^{-1/2} \qquad (9.51)$$

where $\gamma = K_0' S_0/(KS)_0'$. To fully specify the vacuum interior it is necessary, therefore, to solve the wave equation $\ddot{\psi} = \psi'' + r^{-1}\psi'$ plus one of the equations

for C on $0 \leq r \leq r_0(t)$, subject to the boundary conditions (9.50) and (9.51) at $r = r_0$.

Note that no matching interior solution is possible at early times ($\eta \ll 1$), as then $\dot{r}_0 \approx 2\beta\eta^{-1}$ and the boundary is receding superluminally ($\dot{r}_0 > 1$) and so lies outside the Hubble radius of the string. The same is true when $\eta \approx 2\pi$ in the case of a closed universe ($k = 1$). However, the matching procedure is of interest only when the boundary radius is small compared to the Hubble radius, which occurs at late times η in the flat ($k = 0$) and open ($k = -1$) cases.

In the case $k = -1$ the late-time solution has $r_0 \approx \beta t$ with $\beta = \tanh(2\varpi_0) < 1$, plus $e^{\psi_0} \approx t^{1/2}$ and $e^{C_0} \approx (1 - 4\mu)^{-1} \cosh(\varpi_0)$. The interior solution satisfying these boundary conditions is

$$
\begin{aligned}
e^{\psi(r,t)} &= \frac{1}{\sqrt{2}(1 - 4\mu)^{1/2}} [t + (t^2 - r^2)^{1/2}]^{1/2} \\
e^{C(r,t)} &= \frac{1}{\sqrt{2}(1 - 4\mu)} \frac{[t + (t^2 - r^2)^{1/2}]^{1/2}}{(t^2 - r^2)^{1/4}}
\end{aligned}
\tag{9.52}
$$

and the corresponding metric (9.41) is just a patch of the bare straight-string spacetime (7.28) in a coordinate system tailored to the Robertson–Walker exterior. Thus a 'Swiss cheese' embedding is possible in an open universe in the late-time limit, and the interior is, in this case, non-radiating.

The flat ($k = 0$) case at late times has $r_0 \sim t^{4/5}$, $e^{\psi_0} \sim t^{2/5}$ and e^{C_0} asymptotically constant, with $\psi'_0/\dot{\psi}_0 = -\dot{r}_0$. Unfortunately, no explicit interior solution matching these boundary conditions has yet been found, although the initial-value problem is well posed and a solution undoubtedly exists. Unruh [Unr92] has attempted to generate an approximate solution by assuming that the time derivatives of ψ are negligible in comparison with the radial derivatives. If the known open solution (9.52) is any guide this assumption is a poor one, and it is not surprising that Unruh's approximate interior solution induces a non-zero stress–energy tensor which diverges on the axis $r = 0$.
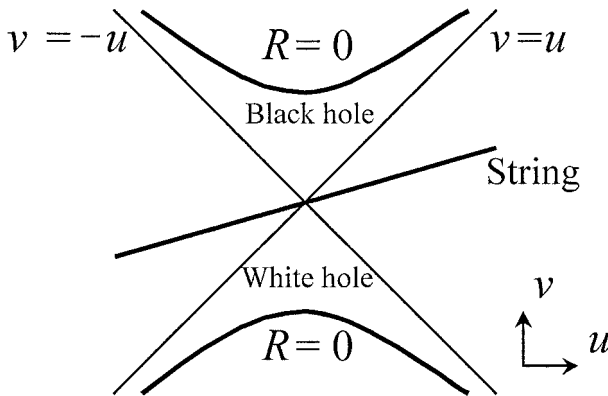
9.2.2 A string through a Schwarzschild black hole

The second simple example of a 'generalized' string metric is the Aryal–Ford–Vilenkin solution [AFV86], which describes a cosmic string passing through a black hole. The line element is

$$
ds^2 = (1 - 2m/R)\,dt^2 - (1 - 2m/R)^{-1}\,dR^2 - R^2\,d\theta^2 - (1 - 4\mu)^2 R^2 \sin^2\theta\,d\phi^2
\tag{9.53}
$$

and can be constructed by removing a wedge of angular extent $8\pi\mu$ from along any axis of the Schwarzschild metric. When $R\sin\theta \neq 0$ the Riemann tensor is, of course, identical to that of the Schwarzschild metric, and so (modulo symmetries):

$$
R^{tr}{}_{tr} = R^{\theta\phi}{}_{\theta\phi} = 2m/R^3
\tag{9.54}
$$

Figure 9.1. Kruskal diagram for a cosmic string through a Schwarzschild black hole.

and

$$R^{t\theta}{}_{t\theta} = R^{t\phi}{}_{t\phi} = R^{r\theta}{}_{r\theta} = R^{r\phi}{}_{r\phi} = -m/R^3 \qquad (9.55)$$

while the stress–energy tensor is zero.

To an external observer, it would appear that the string passes directly through the hole, piercing the horizon $R = 2m$ at the north and south poles. However, the horizon is a null surface and the spacelike sections of the string do not physically extend across it. As with the Schwarzschild metric, the full geometry of the Aryal–Ford–Vilenkin solution is best appreciated by replacing t and r with the Kruskal–Szekeres null coordinates u and v, which are defined by

$$2m(u^2 - v^2) = (R - 2m)e^{r/(2m)} \qquad (9.56)$$

and

$$t = \begin{cases} 4m \tanh^{-1}(v/u) & \text{if } |v| < |u| \\ 4m \tanh^{-1}(u/v) & \text{if } |v| > |u|. \end{cases} \qquad (9.57)$$

It is then apparent that the spacetime consists of four regions—one containing a past spacelike singularity (the 'white hole'), one containing a future spacelike singularity (the 'black hole') and two asymptotically-flat* exterior universes— separated by the horizons $v = \pm u$.

Any constant-t slice of the string world sheet which starts in one of the exterior universes will not enter the black hole or white hole regions but instead extends to the wormhole 'throat' at $u = v = 0$. From there it can be continued into the second exterior universe as shown in figure 9.1, which depicts the u–v plane with either $\theta = 0$ or $\theta = \pi$. Because the minimum value of R along the slice is $2m > 0$, the northern ($\theta = 0$) and southern ($\theta = \pi$) halves of the string are, in fact, disconnected.

However, this is not to imply that the string is undetectable inside the singular regions. There is still a conical singularity on the axis when $R < 2m$, even

though R is a timelike coordinate inside the horizon. An observer falling into the black hole would not be able to examine both the northern and southern halves of the string in the time left between crossing the horizon and plunging into the singularity but he or she would, in principle, be able to measure the circumference and radius of a small ($\sin\theta \ll R/m$) circle centred on the axis and deduce that there was an angle deficit $8\pi\mu$ there.

A straight string can be embedded in a similar fashion in any of the other standard black hole solutions, namely the Kerr, Reissner–Nordström and Kerr–Newman metrics—which describe rotating, charged and charged and rotating black holes respectively. The only proviso is that the string must lie along the rotation axis if the black hole is rotating.

Aryal *et al* [AFV86] have also constructed a solution which describes two Schwarzschild black holes held apart by a system of cosmic strings by generalizing a solution, due to Bach and Weyl, that dates back to 1922. The relevant line element is

$$ds^2 = e^{2\chi}\,dt^2 - e^{-2\chi}[e^{2\psi}(dr^2 + dz^2) + r^2\,d\phi^2] \tag{9.58}$$

where

$$e^{2\chi} = \left(\frac{\rho_{1+} + \rho_{1-} - 2m_1}{\rho_{1+} + \rho_{1-} + 2m_1}\right)\left(\frac{\rho_{2+} + \rho_{2-} - 2m_2}{\rho_{2+} + \rho_{2-} + 2m_2}\right) \tag{9.59}$$

and

$$e^{2\psi} = K^2\left[\frac{(\rho_{1+} + \rho_{1-})^2 - 4m_1^2}{4\rho_{1+}\rho_{1-}}\right]\left[\frac{(\rho_{2+} + \rho_{2-})^2 - 4m_2^2}{4\rho_{2+}\rho_{2-}}\right]$$
$$\times \left[\frac{(m_2 + d)\rho_{1+} + (m_1 + m_2 + d)\rho_{1-} - m_1\rho_{2-}}{d\rho_{1+} + (m_1 + d)\rho_{1-} - m_1\rho_{2+}}\right]^2 \tag{9.60}$$

with $\rho_{j\pm} = [r^2 + (z - c_{j\pm})^2]^{1/2}$ for $j = 1$ or 2, and the constants $c_{1-} < c_{1+} < c_{2-} < c_{2+}$ satisfy the conditions

$$c_{2+} - c_{2-} = 2m_2 \qquad c_{2-} - c_{1+} = 2d \qquad \text{and} \qquad c_{1+} - c_{1-} = 2m_1. \tag{9.61}$$

The metric (9.58) is vacuum at all points away from the axis $r = 0$, and describes two black holes with masses m_1 and m_2 located on the axis at $z = c_{1+} - m_1$ and $z = c_{2-} + m_2$ respectively, and so separated by a z-coordinate distance $2d$. The black holes are held in place by conical singularities along the axial segments $z > c_{2+}$, $c_{2-} > z > c_{1+}$ and $z < c_{1-}$. The effective mass per unit length μ of any of the conical segments depends only on the limiting value of the metric function ψ on the axis:

$$1 - 4\mu = \lim_{r\to 0} e^{-\psi}. \tag{9.62}$$

Thus, on the segments $z > c_{2+}$ and $z < c_{1-}$ joining the black hole horizons to infinity

$$1 - 4\mu_{\text{ext}} = K^{-1}\frac{d}{m_1 + d} \tag{9.63}$$

while on the segment $c_{1+} < z < c_{2-}$ linking the two horizons

$$1 - 4\mu_{\text{int}} = K^{-1} \frac{m_2 + d}{m_1 + m_2 + d}. \tag{9.64}$$

Clearly $\mu_{\text{ext}} > \mu_{\text{int}}$ for all positive values of m_1, m_2 and d. In the original Bach–Weyl solution the mass per unit length μ_{ext} of the exterior segments was assumed to be zero, and so K was fixed at $\frac{d}{m_1 + d}$. This forces μ_{int} to be negative, and the interior Bach–Weyl segment is normally characterized as a 'strut' rather than a string. However, all three segments will have non-negative masses per unit length if $K \geq \frac{m_2 + d}{m_1 + m_2 + d}$. In the particular case $K = \frac{m_2 + d}{m_1 + m_2 + d}$ the interior segment vanishes and the two black holes are suspended from infinity, their attractive gravitational force exactly balanced by the tension of the strings.

However, no matter what values are assumed for μ_{ext} and μ_{int}, this system of strings and black holes is manifestly unstable, as any perturbation in the distance between the black holes will enhance or dampen their mutual attraction while the tension in each conical segment remains constant. If the black holes have equal mass m and their initial separation is larger than the equilibrium distance, they will both be accelerated off to infinity by the string tension. This situation is described by a variant of the Kinnersley–Walker metric [KW70]:

$$ds^2 = A^{-2}(x + y)^{-2}[F(y)\,dt^2 - dx^2/G(x) - dy^2/F(y) - \kappa^2 G(x)\,d\phi^2] \tag{9.65}$$

where A and κ are positive constants, and $F(y) = y^2 - 1 - 2mAy^3$ and $G(x) = 1 - x^2 - 2mAx^3$.

Here, if $mA < 1/\sqrt{27}$ the three roots of G are real and distinct and will be denoted by $x_1 < x_2 < x_3$. The coordinate patch $\{x_2 < x < x_3, -x_2 < y < -x_1\}$ then has F and G both positive, and covers the exterior region of one of the black holes out to its acceleration horizon at $y = -x_2$. The event horizon of the black hole lies at $y = -x_1$ while the remaining boundaries $x = x_2$ and $x = x_3$ correspond to segments of the symmetry axis (the axis joining the two black holes) north and south of the event horizon.

Near the first segment, $x = x_2 + r^2$ where r is small, and the line element (9.65) has the approximate form

$$ds^2 \approx A^{-2}(x_2 + y)^{-2}[F(y)\,dt^2 - 4\,dr^2/G'(x_2) - dy^2/F(y) - \kappa^2 G'(x_2)r^2\,d\phi^2] \tag{9.66}$$

indicating that the segment has an effective mass per unit length μ given by

$$1 - 4\mu = \tfrac{1}{2}\kappa G'(x_2) \equiv -\kappa x_2(1 + 3mAx_2). \tag{9.67}$$

The mass per unit length of the second segment is given by a similar expression, with x_3 replacing x_2 and an overall change in sign, but can always be set to zero by choosing $\kappa = -2/G'(x_3)$.

In the flat-space limit $m \ll A^{-1}$ the line element (9.65) reduces to Rindler spacetime (that is, Minkowski spacetime in an accelerating reference frame) with

a conical singularity on axis:

$$ds^2 = z^2 \, dt^2 - dr^2 - dz^2 - \kappa^2 r^2 \, d\phi^2 \tag{9.68}$$

where $r = A^{-1}(x + y)^{-1}(1 - x^2)^{1/2}$ and $z = A^{-1}(x + y)^{-1}(y^2 - 1)^{1/2}$. Since $x_1 \approx -1/(2mA)$, $x_2 \approx -1 - mA$ and $x_3 \approx 1 - mA$ in this limit, the event horizon corresponds to the surface $\{z \approx A^{-1}, \ r \approx 2m\}$ while $\mu = \frac{1}{4}[1 + G'(x_2)/G'(x_3)] \approx mA$.

Thus, if the segment of length $2A^{-1}$ between the horizons were to be replaced by a piece of the string, it would have the same mass, $2m$, as the black holes. This fact lends support to the idea that (9.65) is the metric that would result if a straight cosmic string were to split into two through spontaneous black hole pair production [GH95], although the quantum probability of such an event has been shown to be infinitesimally small [HR95, EHKT95].

Achucarro *et al* [AGK95] have discussed in detail the possibility of embedding a Nielsen–Olesen vortex solution in a Schwarzschild spacetime so as to give a metric which reduces to the Aryal–Ford–Vilenkin metric (9.53) in the zero-thickness limit. They have shown that when the core radius of the string is much smaller than the black hole's radius the vortex fields deviate minimally from their flat-space analogues (as was shown in the previous section to be the case in a flat Robertson–Walker background), although as seen by an external observer the vortex terminates on the event horizon. Ruth Gregory and Mark Hindmarsh [GH95] have extended this analysis to include the coupling of a Nielsen–Olesen vortex to a pair of static or accelerating black holes, so as to obtain field-theoretic realizations of the Bach–Weyl and Kinnersley–Walker solutions, with similar results.

9.2.3 Strings coupled to a cosmological constant

A spacetime with a non-zero cosmological constant Λ, but no other matter content, is described by a stress–energy tensor $T_{\mu\nu} = \frac{1}{8\pi}\Lambda g_{\mu\nu}$. The most famous spacetimes of this type are the homogeneous de Sitter universes, for which $\Lambda > 0$ and

$$ds^2 = \frac{3}{\Lambda^2 S^2(\eta)}[d\eta^2 - d\varpi^2 - K^2(\varpi)\,dz^2 - S^2(\varpi)\,d\phi^2] \tag{9.69}$$

where $S(\eta) = \sin\eta$, η or $\sinh\eta$ and $K(\varpi) = \sin\varpi$, ϖ or $\sinh\varpi$ as $k = 1, 0$ or -1; and the anti-de Sitter metric, which has $\Lambda < 0$ and

$$ds^2 = \frac{3}{\Lambda^2 z^2}(d\eta^2 - dz^2 - dr^2 - r^2\,d\phi^2). \tag{9.70}$$

The flat ($k = 0$) de Sitter universe and the anti-de Sitter metric are possibly better known in their 'spherical null' form:

$$ds^2 = [1 + \tfrac{1}{12}\Lambda(r^2 + z^2 - t^2)]^{-2}(dt^2 - dr^2 - dz^2 - r^2\,d\phi^2) \tag{9.71}$$

in which Λ can be either positive or negative[1].

In addition, Qingjun Tian [Tia86] has constructed two spacetimes with constant Λ which are neither homogeneous nor conformally flat, namely

$$ds^2 = \cos^{4/3}(\lambda r)(dt^2 - dz^2) - dr^2 - \lambda^{-2} \sin^2(\lambda r) / \cos^{2/3}(\lambda r) \, d\phi^2 \quad (9.72)$$

where $\lambda = (3\Lambda)^{1/2}/2$, $0 \le \lambda r \le \pi/2$ and $\Lambda > 0$, and

$$ds^2 = \cosh^{4/3}(\lambda r)(dt^2 - dz^2) - dr^2 - \lambda^{-2} \sinh^2(\lambda r) / \cosh^{2/3}(\lambda r) \, d\phi^2 \quad (9.73)$$

where $\lambda = (3|\Lambda|)^{1/2}/2$ and $\Lambda < 0$.

All of these solutions are axisymmetric, with the axis $r = 0$ as a fixed-point set. It is, therefore, possible to introduce a cosmic string with mass per unit length μ along the axis of any of these spacetimes by replacing $d\phi^2$ with $(1 - 4\mu)^2 \, d\phi^2$ in the usual way. The only notable feature of these solutions is that Tian [Tia86] has managed to find smooth interior solutions that join the string analogues of (9.72) or (9.73) at a finite radius $r = r_0$. Thus, apart from the bare straight-string metric (7.28) and its travelling-wave extensions (9.12), the string analogues of Tian's solutions are the only well-behaved string spacetimes for which explicit interior solutions are known.

The interior solution matching the string analogue of the first of Tian's solutions (9.72) at $r = r_0$ has the form

$$ds^2 = [A + B \cos(\kappa R)]^{4/3}(dt^2 - dz^2) - dR^2$$
$$- C^2 \sin^2(\lambda R)/[A + B \cos(\kappa R)]^{2/3} d\phi^2 \quad (9.74)$$

where $C\lambda(A + B)^{-1/3} = 1$ to guarantee regularity on the axis $R = 0$, and the metric functions and their normal derivatives will be continuous across the junction surface $R = R_0$ matching $r = r_0$ if

$$\cos(\lambda r_0) = A + B \cos(\kappa R_0) \qquad \lambda^{-1}(1 - 4\mu) \sin(\lambda r_0) = C \sin(\lambda R_0)$$
$$(9.75)$$

$$\lambda \sin(\lambda r_0) = B\kappa \sin(\kappa R_0) \qquad \text{and} \qquad (1 - 4\mu) \cos(\lambda r_0) = C\lambda \cos(\lambda R_0).$$
$$(9.76)$$

Thus, if λ and r_0 are fixed there are five equations for the five interior parameters A, B, C, R_0 and κ.

In particular, if $R_0 = r_0$ then $C = \lambda^{-1}(1 - 4\mu)$, $A = (1 - 4\mu)^3 - B$ and $B = (\lambda r_0) \sin(\lambda r_0)/[(\kappa r_0) \sin(\kappa r_0)]$, where κr_0 is the smallest positive root x of the equation

$$(1 - \cos x)/(x \sin x) = [(1 - 4\mu)^3 - \cos(\lambda r_0)]/[(\lambda r_0) \sin(\lambda r_0)] \quad (9.77)$$

---

[1] The transformation from the $k = 0$ form of (9.69) to (9.71) is accomplished by letting $t = 2K^{-1/2}[1 - K(\eta^2 - \mathbf{x}^2)]F(\eta, \mathbf{x})$ and $\bar{\mathbf{x}} = 4\mathbf{x}F(\eta, \mathbf{x})$, where $K = \frac{1}{3}\Lambda$, $\mathbf{x} = (\varpi \cos \phi, \varpi \sin \phi, z)$, $\bar{\mathbf{x}} = (r \cos \phi, r \sin \phi, \bar{z})$ and $F(\eta, \mathbf{x}) = \frac{1 + K(\eta^2 - \mathbf{x}^2) - 2\sqrt{K}\eta}{[1 + K(\eta^2 - \mathbf{x}^2)]^2 - 4K\eta^2}$, then dropping the overbar on z. The transformation from the anti-de Sitter metric (9.70) to (9.71) is similar, with the roles of η and z (and t and $\bar{z}$) interchanged.

provided that $\cos(\lambda r_0) \neq (1-4\mu)^3$. For example, if $\mu \ll \sin(\lambda r_0)[\lambda r_0 - \sin(\lambda r_0)]$ then

$$\kappa r_0 \approx \lambda r_0 \left\{ 1 - 12\mu \frac{1 + \cos(\lambda r_0)}{\sin(\lambda r_0)[\lambda r_0 - \sin(\lambda r_0)]} \right\}. \qquad (9.78)$$

In this limit, because $\kappa r_0 < \lambda r_0 < \pi/2$ and $A + B \cos(\kappa r_0) = \cos(\lambda r_0) > 0$, the interior solution will be singularity-free. However, there is a range of values of μ and λr_0 for which $A + B \cos(\kappa R) = 0$, and the interior solution is singular, at some radius $R < r_0$.

The stress–energy tensor of the interior solution has non-zero components:

$$T_t^t = T_z^z = \frac{1}{8\pi} \left[\lambda^2 + \frac{B\kappa^2/3}{A + B \cos(\kappa R)} \right] \qquad (9.79)$$

$$T_R^R = \frac{1}{6\pi} \frac{B\kappa\lambda \sin(\kappa R) \cot(\lambda R)}{A + B \cos(\kappa R)} \qquad \text{and} \qquad T_\phi^\phi = \frac{1}{6\pi} \frac{B\kappa^2 \cos(\kappa R)}{A + B \cos(\kappa R)}. \qquad (9.80)$$

A non-zero radial pressure T_R^R is unavoidable here, as hydrostatic equilibrium requires that $T_R^R = T_r^r$ on the boundary surface, and $T_r^r = \frac{1}{8\pi}\Lambda \neq 0$ in the exterior solution.

The smooth interior solution matching the string analogue of the second of Tian's solutions (9.73) is similar to (9.74), with the trigonometric functions replaced by the corresponding hyperbolic functions.

9.3 Strings in radiating cylindrical spacetimes

9.3.1 The cylindrical formalism

Such is the complexity of the Einstein equations that even radiating vacuum solutions are difficult to construct unless a high degree of symmetry is assumed. For the purposes of studying gravitational radiation one of the most convenient and mathematically tractable devices is to impose cylindrical symmetry and the properties of radiating cylindrical spacetimes have been extensively studied since the 1930s. Although the resulting solutions obviously bear little geometrical resemblance to the actual Universe, and are often dismissed as inconsequential on this account, they are ideally suited for modelling the interaction of gravitational waves with an infinite straight cosmic string. Indeed, the theory of cosmic strings has provided the study of cylindrical waves with a physical context that was previously conspicuously lacking.

The most general (non-static) line element with cylindrical symmetry has the form [KSHM80]

$$ds^2 = e^{2\chi}(dt^2 - dr^2) - e^{2\psi}(dz + \alpha\, d\phi)^2 - e^{2\omega}\, d\phi^2 \qquad (9.81)$$

where χ, ψ, ω and α are functions of t and r only, r has range $[0, \infty)$, and ϕ is an angular coordinate with range $[0, 2\pi)$. In vacuum, an immediate simplification is afforded by noting that

$$0 = G_t^t + G_r^r = [(e^{\psi+\omega})'' - (e^{\psi+\omega})^{\cdot\cdot}]e^{-2\chi-\psi-\omega} \tag{9.82}$$

where a prime denotes $\partial/\partial r$ and an overdot $\partial/\partial t$. It is, therefore, possible to make the gauge choice $e^{\psi+\omega} = r$ and reduce the line element to

$$ds^2 = e^{2\chi}(dt^2 - dr^2) - e^{2\psi}(dz + \alpha\, d\phi)^2 - e^{-2\psi}r^2\, d\phi^2. \tag{9.83}$$

The vacuum field equations $G_r^r = 0$, $G_r^t = 0$, $G_\phi^\phi = 0$ and $G_z^z - G_\phi^\phi = 0$ then read, respectively,

$$C' = r(\dot{\psi}^2 + \psi'^2) + \tfrac{1}{4}r^{-1}e^{4\psi}(\dot{\alpha}^2 + \alpha'^2) \tag{9.84}$$

$$\dot{C} = 2r\dot{\psi}\psi' + \tfrac{1}{2}r^{-1}e^{4\psi}\dot{\alpha}\alpha' \tag{9.85}$$

and

$$\ddot{C} - C'' + \dot{\psi}^2 - \psi'^2 + \tfrac{1}{4}r^{-2}e^{4\psi}(\alpha'^2 - \dot{\alpha}^2)$$
$$= \tfrac{1}{2}r^{-2}e^{4\psi}\alpha(\alpha'' - \ddot{\alpha} - r^{-1}\alpha' + 4\alpha'\psi' - 4\dot{\alpha}\dot{\psi})$$
$$= \ddot{\psi} - r^{-1}\psi' - \psi'' + \tfrac{1}{2}r^{-2}e^{4\psi}(\alpha'^2 - \dot{\alpha}^2) \tag{9.86}$$

where the function $C = \chi + \psi$ (known as *Thorne's C-energy* [Tho65]) provides a measure of the gravitational energy per unit length out to a radius r at a given time t.

It is evident from the first two equations that $C' \geq 0$ everywhere, and if $u = t + r$ and $v = t - r$ are advanced and retarded radial null coordinates then $C_{,u} \geq 0$ and $C_{,v} \leq 0$. The function $C_{,u}$ is a measure of the inward flux of C-energy at any point, and $C_{,v}$ a measure of the outward flux.

If the radial derivative of (9.85) is subtracted from the time derivative of (9.84) and the result inserted into (9.86), the latter breaks up into two simpler equations [PSS85]:

$$\ddot{\psi} - r^{-1}\psi' - \psi'' = \tfrac{1}{2}r^{-2}e^{4\psi}(\dot{\alpha}^2 - \alpha'^2) \tag{9.87}$$

and

$$\ddot{\alpha} + r^{-1}\alpha' - \alpha'' = 4(\alpha'\psi' - \dot{\alpha}\dot{\psi}). \tag{9.88}$$

In the special case where $\alpha = 0$ the metric function ψ satisfies the standard cylindrical wave equation $\ddot{\psi} - r^{-1}\psi' - \psi'' = 0$, and the corresponding solutions are called *Einstein–Rosen metrics*. More generally, the functions ψ and α represent the two independent degrees of freedom of the gravitational field, with ψ describing the $+$ mode and α the $\times$ mode. Moreover, the C-energy fluxes $C_{,u}$

and $C_{,v}$ can then be broken up into two parts attributable separately to the $+$ and $\times$ gravitational modes:

$$C_{,u} = C_u^+ + C_u^\times \equiv 2r\psi_{,u}^2 + \tfrac{1}{2}r^{-1}e^{4\psi}\alpha_{,u}^2 \tag{9.89}$$

and

$$C_{,v} = C_v^+ + C_v^\times \equiv -2r\psi_{,v}^2 - \tfrac{1}{2}r^{-1}e^{4\psi}\alpha_{,v}^2 . \tag{9.90}$$

The cylindrical line element (9.83) will include a zero-thickness cosmic string along the axis $r = 0$ if it supports a conical singularity there. Any axial singularity will be, at worst, conical if the limits $\chi_0(t) = \lim_{r\to 0} \chi(r,t)$ and $\psi_0(t) = \lim_{r\to 0} \psi(r,t)$ are well defined, and the metric component $-g_{\phi\phi}$ has the limiting form $a_0^2(t)\rho^2$ where $\rho \approx e^{\chi_0}r$ is the physical radius. The last condition requires that

$$a_0^2(t) = e^{-2\psi_0 - 2\chi_0} + e^{2\psi_0 - 2\chi_0} \lim_{r\to 0} \frac{\alpha^2}{r^2} \tag{9.91}$$

also be well defined, and, in particular, that α goes to zero at least as rapidly as r. The gravitational mass per unit length μ of the axial string is then given by $1 - 4\mu = a_0(t)$. In particular, if $\lim_{r\to 0}\alpha^2/r^2 = 0$ then $\mu = \tfrac{1}{4}(1 - e^{-C_0})$, where C_0 is the axial value of the C-energy.

Furthermore, as is evident from (9.86), if $\alpha = 0$ and ψ is regular on the axis (which is true for almost all the solutions examined in this chapter) then $\dot{C}_0 = 0$ and μ is constant. However, this result does not extend to *finite-thickness* strings embedded in an Einstein–Rosen spacetime, as the gravitational mass per unit length of these can vary [And99a], although if the spacetime is asymptotically flat* and there is no inward flux of C-energy at infinity then any change $\Delta\mu$ in μ must be negative.

9.3.2 Separable solutions

The simplest way to generate solutions to the cylindrical wave equations (9.84) to (9.86) is to assume that the metric functions are separable in t and r, in the sense that $\chi = \chi_1(t) + \chi_2(r)$, $\psi = \psi_1(t) + \psi_2(r)$ and $\alpha = \alpha_1(t)\alpha_2(r)$. A selection of solutions of this type are briefly described here. It should be mentioned that all are 'generalized' string solutions, constructible by excising an angular wedge from along the axis of a pre-existing vacuum solution, and none has an acceptable physical interpretation.

It is readily seen that if $\alpha = 0$ then the only separable solutions are of the form:

$$ds^2 = e^{2kt + k^2 r^2}(dt^2 - dr^2) - a_0^{-2}e^{-2kt}\,dz^2 - a_0^2 e^{2kt}r^2\,d\phi^2 \tag{9.92}$$

where k and $0 < a_0 < 1$ are constants. The corresponding mass per unit length is $\mu = \tfrac{1}{4}(1 - a_0)$, while the C-energy is $C = \tfrac{1}{2}k^2 r^2 - \ln a_0$. The bare straight-string metric (7.28) is recovered when $k = 0$. Although the solutions are all non-singular

for finite values of t and r, there is a curvature singularity at timelike infinity if $k \neq 0$, as the Kretschmann scalar $\mathcal{K} \equiv R_{\mu\nu\kappa\lambda}R^{\mu\nu\kappa\lambda} = 16k^4(3-k^2r^2)\mathrm{e}^{-4kt-2k^2r^2}$ diverges there.

Unfortunately no work to date has been done on separable solutions with $\alpha \neq 0$. However, it should be remembered that the field equations (9.84) to (9.86) are predicated on a particular gauge choice $\mathrm{e}^{\psi+\omega} = r$, and solutions that are separable in one gauge are not necessarily separable in another. If the metric functions are assumed to be separable in t and r before the gauge is chosen, the wave equation (9.82) has a number of possible solutions which (after suitably rescaling and rezeroing the coordinates t, r and z) can be represented in one of the forms $\mathrm{e}^{\psi+\omega} = 1, t, r, tr, \sin t \sin r$ or $(p\sinh t + q\cosh t)(k\cosh r + \sinh r)$. The first two forms are inconsistent with the presence of a conical singularity on the axis (which requires that $\mathrm{e}^{\psi+\omega} \sim r$ for small r), as is the last unless $k = 0$ but the remaining choices can all be used to construct separable solutions containing axial strings.

A limited version of this problem was first considered by Jaime Stein-Schabes [SS86], who set $\alpha = 0$ and attempted to construct separable solutions describing both the exterior and interior of a finite-thickness axial string. Of the three classes of exterior solutions he generated, two turn out to be just the bare straight-string metric (7.28) in unusual coordinates, while the third is reducible to the line element

$$\mathrm{d}s^2 = (1+\cosh t)^2[\mathrm{d}t^2 - \mathrm{d}r^2 - a_0^2\sinh^2(r)\,\mathrm{d}\phi^2] - \frac{\sinh^2 t}{(1+\cosh t)^2}\,\mathrm{d}z^2 \quad (9.93)$$

with $a_0 = 1 - 4\mu$ as before.

The Stein-Schabes line element (9.93) can be converted to the canonical form (9.83) by making the coordinate transformation

$$T + R = a_0\cosh(t+r) \qquad \text{and} \qquad T - R = a_0\cosh(t-r). \quad (9.94)$$

The metric components are somewhat complicated functions of the canonical coordinates (T, R), and the only advantage of the transformation is that it allows the C-energy to be computed as a function of t and r:

$$\mathrm{e}^{2C} = \frac{\sinh^2 t}{a_0^2\sinh(t+r)\sinh(t-r)}. \quad (9.95)$$

As can be seen, the C-energy diverges at the singular points of the coordinate transformation (the null surfaces $t + r = 0$ and $t - r = 0$), and the solution in canonical form cannnot cover the region $T^2 - R^2 < a_0^2$. However, the solution has no obvious curvature singularities (the Kretschmann scalar is $\mathcal{K} = 48(1 + \cosh t)^{-6}$ and the physical components of the Riemann tensor are all bounded) and its physical interpretation remains uncertain.

The problem of constructing separable solutions (again with $\alpha = 0$) has since been reanalysed by Eric Shaver and Kayll Lake [SL89], although they devoted

most of their efforts to fully classifying the class of interior string solutions (that is, solutions with the non-zero stress–energy components $T_t^t = T_z^z$). In addition to the vacuum solution (9.92) generated by the gauge choice $e^{\psi+\omega} = r$, there is a plethora of possible exterior string metrics that are separable in other gauges.

For example, the unique separable string solution corresponding to the gauge choice $e^{\psi+\omega} = tr$ is:

$$ds^2 = t^4(dt^2 - dr^2 - a_0^2 r^2 \, d\phi^2) - t^{-2} \, dz^2 \tag{9.96}$$

and has C-energy given by $e^{2C} = a_0^{-2} t^2/(t^2 - r^2)$ and Kretschmann scalar $\mathcal{K} = 192t^{-12}$. The solution has an initial singularity, and the transformation to canonical coordinates $R = tr$ and $T = \frac{1}{2}(t^2 + r^2)$ is again degenerate on the null surfaces $t \pm r = 0$.

By contrast, the gauge choice $e^{\psi+\omega} = \sin t \sin r$ leads to four different types of string solution, including the one generated from the Stein-Schabes metric (9.93) by replacing $\sinh t$ with $\sin t$ and $\cosh t$ with $\cos t$. All four types contain curvature singularities that are periodic in either r or t (although this need not be an insuperable problem: see section 9.3.3 below).

The family of separable solutions with $e^{\psi+\omega} = (p \sinh t + q \cosh t) \sinh r$ is even larger, containing as it does the hyperbolic analogues of the four types of sinusoidal solutions plus a number of others. The particular choice $e^{\psi+\omega} = e^t \sinh r$ generates a one-parameter class of solutions with the line element

$$ds^2 = e^{2(1-k)t}(1 + \cosh r)^{4k^2-2k}(dt^2 - dr^2) - e^{2kt}(1 + \cosh r)^{2k} dz^2$$
$$- 2^{4k^2} a_0^2 e^{2(1-k)t}(1 + \cosh r)^{-2k} \sinh^2(r) \, d\phi^2 \tag{9.97}$$

for which $e^{2C} = a_0^{-2}(\frac{1}{2} + \frac{1}{2}\cosh r)^{4k^2}$ and

$$\mathcal{K} = -16(2k-1)^2 k^2 e^{4(k-1)t}(1 + \cosh r)^{-2(4k^2-2k+1)}$$
$$\times [(2k^2 - k - 1)(-1 + \cosh r) + 2k - 1]. \tag{9.98}$$

If $k = 0$ or $k = \frac{1}{2}$ the metric is flat, and if $k = 1$ it is non-flat but singularity-free. However, in common with all the other solutions mentioned in this section, it is not possible to extend the canonical version of the metric to spacelike infinity ($R^2 - T^2 \to \infty$), as the transformation to canonical coordinates is $T \pm R = a_0 e^{t \pm r}$.

9.3.3 Strings in closed universes

In 1989 Robert Gowdy and Sandeep Chaube published a radiating string spacetime which describes two orthogonal cosmic strings in a closed universe [GC89]. Gowdy and Chaube assumed a line element of the general cylindrical form (9.81), set α to zero, and effectively made the vacuum gauge choice $e^{\psi+\omega} = \sin t \sin r$. With the ranges of t and r restricted to $(0, \pi)$, the spacetime

is radially compact, and if a periodic identification is imposed on the z-coordinate then it is most naturally characterized as a 'closed universe', although it must be remembered that the closure is caused not by an overdensity of stress–energy, as in the closed Robertson–Walker spacetimes, but rather by gravitational radiation.

In the chosen gauge, the analogue of the cylindrical wave equation (9.87) for the metric function ψ reads:

$$\ddot{\psi} + \cot(t)\dot{\psi} - \psi'' - \cot(r)\psi' = 0 \qquad (9.99)$$

and admits series solutions of the form

$$\psi(t, r) = \sum_{n=0}^{\infty} [A_n P_n(\cos t) + B_n Q_n(\cos t)]P_n(\cos r) \qquad (9.100)$$

where P_n and Q_n are Legendre functions of the first and second kind, respectively, and A_n and B_n are undetermined constants. (Here, all terms proportional to $Q_n(\cos r)$ have been omitted from ψ because $Q_n(x)$ diverges as $x \to \pm 1$, and the presence of such terms would induce a curvature singularity at $r = 0$.)

Once ψ has been specified, the remaining metric function χ is found by integrating the analogues of (9.84) and (9.85), which can be rearranged to read:

$$(\cos^2 r - \cos^2 t)\dot{C} = \sin r \sin t[2\cos r \sin t \dot{\psi}\psi' - \cos t \sin r(\dot{\psi}^2 + \psi'^2)] + \cos t \sin t \qquad (9.101)$$

and

$$(\cos^2 r - \cos^2 t)C' = \sin r \sin t[\cos r \sin t(\dot{\psi}^2 + \psi'^2) - 2\cos t \sin r \dot{\psi}\psi']$$
$$- \cos r \sin r \qquad (9.102)$$

where $C = \chi + \psi$. Clearly, all points on the null surfaces $t = r$ and $t = \pi - r$ (where $\cos^2 r = \cos^2 t$) are singular points of this system of equations, and χ will be singular on these surfaces unless the right-hand sides of (9.101) and (9.102) also vanish there.

For example, if ψ contains only zeroth-order Legendre functions, so that

$$\psi = A_0 + \tfrac{1}{2}B_0 \ln\left(\frac{1 + \cos t}{1 - \cos t}\right) \qquad (9.103)$$

then the general solution for χ is

$$\chi = \chi_0 - \tfrac{1}{2}(B_0^2 - 1)\ln(\cos^2 r - \cos^2 t) + (B_0^2 + B_0)\ln(\sin t) - B_0 \ln(1 + \cos t) \qquad (9.104)$$

where χ_0 is an integration constant.

The metric is, therefore, singular on the surfaces $t = r$ and $t = \pi - r$ unless $B_0 = \pm 1$. The choice $B_0 = -1$ reduces the metric (after rescaling) to the sinusoidal version of the hyperbolic Stein-Schabes solution (9.93):

$$ds^2 = (1 + \cos t)^2[dt^2 - dr^2 - a_0^2 \sin^2(r) \, d\phi^2] - \frac{\sin^2 t}{(1 + \cos t)^2} \, dz^2 \qquad (9.105)$$

while the choice $B_0 = 1$ gives another of the separable sinusoidal solutions:

$$ds^2 = (1+\cos t)^{-2} \sin^4 t \, [dt^2 - dr^2 - a_0^2 \sin^2(r) \, d\phi^2] - \frac{(1+\cos t)^2}{\sin^2 t} \, dz^2. \quad (9.106)$$

With r restricted to the range $(0, \pi)$, both solutions describe spacetimes whose spacelike sections are either radially compact or (if z is recast as an angular coordinate) topological 3-spheres. Each universe emerges from an initial singularity at $t = 0$, is terminated by a second singularity at $t = \pi$ and supports conical singularities along the axes $r = 0$ and $r = \pi$. However, the initial and final singularities have fundamentally different characters, as is evident from the Kretschmann scalars of the two solutions:

$$\mathcal{K} = 48(1 + \cos t)^{-6} \quad \text{and} \quad \mathcal{K} = 48(1 - \cos t)^{-6} \quad (9.107)$$

respectively. In the first solution (9.105) only the final singularity is a curvature singularity, whereas the initial singularity is conical. The reverse is true of the second solution.

The solution developed by Gowdy and Chaube [GC89] is similar in structure but proceeds from a slightly different decomposition of ψ. Gowdy and Chaube first introduced a supplementary metric function λ defined by $e^{2\psi} = (1 + \cos t)(1 + \cos r)e^{2\lambda}$. Then because $\hat{\psi} \equiv \frac{1}{2} \ln(1 + \cos t) + \frac{1}{2} \ln(1 + \cos r)$ is a particular solution of the wave equation (9.99) for ψ, the function λ also satisfies (9.99) and can be decomposed as a series of Legendre functions as per (9.100). However, $\hat{\psi}$ cannot be expressed as a finite series of Legendre functions, and so the long-wavelength (or small mode number n) limit is not the same for λ as it is for ψ.

In particular, it turns out that if λ contains only zeroth-order Legendre functions then a singularity in χ on the null surfaces $t = r$ and $t = \pi - r$ is unavoidable. Gowdy and Chaube, therefore, chose λ to be a mixture of zeroth- and first-order modes:

$$\lambda = B_0 \ln \left(\frac{1 + \cos t}{\sin t} \right) + B_1 \left[\cos(t) \ln \left(\frac{1 + \cos t}{\sin t} \right) - 1 \right] \cos r. \quad (9.108)$$

Equations (9.101) and (9.102) then integrate to give:

$$\begin{aligned}
\chi = {} & \chi_0 + \tfrac{1}{2} B_1^2 (Q_0^2 \sin^2 t + 2Q_0 \cos t - 1) \sin^2 r - B_1(1 + 2B_0)Q_0 \cos r \\
& - B_1 Q_0 \cos t + (B_0^2 + B_0 + B_1^2 - B_1) \ln(\sin t) \\
& + C_+ \ln(\cos r + \cos t) + C_- \ln(\cos r - \cos t)
\end{aligned} \quad (9.109)$$

where $Q_0 = \ln((1 + \cos t)/\sin t)$ and

$$C_+ = (B_1 - B_0)[1 - \tfrac{1}{2}(B_1 - B_0)] \quad \text{and} \quad C_- = \tfrac{1}{2}[1 - (B_0 + B_1)^2]. \quad (9.110)$$

The function χ will remain regular on the interior of the null surfaces $t = r$ and $t = \pi - r$ if C_+ and C_- are both zero, which, in turn, requires that $(B_0, B_1) = \pm(\frac{1}{2}, \frac{1}{2})$, $(-\frac{1}{2}, \frac{3}{2})$ or $(-\frac{3}{2}, \frac{1}{2})$.

The resulting line elements are clearly very complicated but their limiting forms near the singular surfaces $r = 0$ and $r = \pi$ are relatively straightforward. For small values of r,

$$\mathrm{d}s^2 \approx 2\mathrm{e}^{2\chi_0 - 2\psi_0(t) - 2B_1} \sin^2(t)(\mathrm{d}t^2 - \mathrm{d}r^2) - \mathrm{e}^{2\psi_0(t)} \,\mathrm{d}z^2 - \mathrm{e}^{-2\psi_0(t)} \sin^2(t) r^2 \,\mathrm{d}\phi^2 \tag{9.111}$$

where

$$\mathrm{e}^{2\psi_0(t)} = 2(1 + \cos t) \left(\frac{1 + \cos t}{\sin t} \right)^{2B_0} \mathrm{e}^{2B_1[\cos(t)Q_0 - 1]}.$$

The axis $r = 0$, therefore, supports a conical singularity with deficit parameter $a_0^2 = \frac{1}{2}\mathrm{e}^{2B_1 - 2\chi_0}$.

Similarly, it turns out that Gowdy and Chaube's inclusion of a factor of $1 + \cos r$ in the definition of λ induces a conical singularity at $r = \pi$. For small values of $\bar{r} = \pi - r$,

$$\mathrm{d}s^2 \approx 2\mathrm{e}^{2\chi_0 + 2\psi_\pi(t) - 2B_1}(\mathrm{d}t^2 - \mathrm{d}\bar{r}^2) - \mathrm{e}^{2\psi_\pi(t)} \bar{r}^2 \,\mathrm{d}z^2 - \mathrm{e}^{-2\psi_\pi(t)} \sin^2(t) \,\mathrm{d}\phi^2 \tag{9.112}$$

where now

$$\mathrm{e}^{2\psi_\pi(t)} = \frac{1}{2}(1 + \cos t) \left(\frac{1 + \cos t}{\sin t} \right)^{2B_0} \mathrm{e}^{-2B_1[\cos(t)Q_0 - 1]}.$$

At $r = \pi$, therefore, the z-dimension collapses to a point, and if the natural interpretation of the spacetime as describing a closed universe is imposed by treating z as an angular coordinate with period 2π, the axis $r = \pi$ coincides with a second conical singularity with the same deficit parameter $a_0^2 = \frac{1}{2}\mathrm{e}^{2B_1 - 2\chi_0}$. Thus the universe contains two orthogonal straight cosmic strings with equal masses per unit length (although these can be independently varied simply by altering the period of z and/or ϕ), much like the closed Robertson–Walker spacetime (9.36).

Gowdy and Chaube regarded the minimal effect of the two strings as surprising, because 'it seems to contradict the usual argument that long straight strings would quickly come to dominate an initially radiation-dominated universe' [GC89]. However, the closed Robertson–Walker spacetime (9.36) is a much simpler and cosmologically more germane example supporting this claim and in both cases the solutions, exploiting as they do the highly symmetric nature of the underlying spacetimes, are too idealized to be relevant to the evolution of a general string network in a closed universe.

9.3.4   Radiating strings from axisymmetric spacetimes

It has long been known that cylindrical solutions of the Einstein equations can, in principle, be generated by applying a simple complex substitution to known stationary axisymmetric solutions. A general stationary axisymmetric line element can always be written in the form

$$\mathrm{d}s^2 = \mathrm{e}^{2\psi} (\mathrm{d}t + \alpha \,\mathrm{d}\phi)^2 - \mathrm{e}^{2\chi} (\mathrm{d}r^2 + \mathrm{d}z^2) - \mathrm{e}^{2\omega} \,\mathrm{d}\phi^2 \tag{9.113}$$

where ψ, χ, ω and α are functions of r and z alone. The substitution $t \to iz$, $z \to it$ and $\alpha \to i\alpha$ then transforms this into the general cylindrical line element (9.81), although there is no guarantee that the metric functions ψ, χ, ω and α will remain real once z has been replaced by it.

In 1986 Basilis Xanthopoulos [Xan86a, Xan86b] applied a similar transformation to the Kerr metric and constructed a simple regular solution describing the interaction of a straight cosmic string with cylindrical waves. Recall that in Boyer–Lindquist coordinates the Kerr metric has the form

$$ds^2 = \rho^{-2}[(R^2 - 2mR + a^2\cos^2\theta)\,dT^2 + 4maR\sin^2\theta\,dT\,d\phi - \Sigma^2\sin^2\theta\,d\phi^2]$$
$$- \Delta^{-1}\rho^2\,dR^2 - \rho^2\,d\theta^2 \tag{9.114}$$

where

$$\rho^2 = R^2 + a^2\cos^2\theta \qquad \Delta = R^2 - 2mR + a^2 \tag{9.115}$$

and

$$\Sigma^2 = (R^2 + a^2)^2 - a^2\Delta\sin^2\theta. \tag{9.116}$$

If the angular coordinate θ is everywhere replaced by $i\theta$ then (because $\cos^2\theta \to \cosh^2\theta$ and $\sin^2\theta \to -\sinh^2\theta$) the resulting line element has signature $+2$ rather than the conventional -2, with R now playing the role of the timelike coordinate.

Without loss of generality it can be assumed that $m = 1$. If it is further assumed that $j \equiv a/m > 1$ and the coordinates are relabelled as follows:

$$T \to z \qquad R \to 1 + (j^2 - 1)^{1/2}\sinh t \qquad \theta \to r \qquad \text{and} \qquad \phi \to a_0\phi \tag{9.117}$$

then after reversing the signs of all the metric components the line element takes on the manifestly cylindrical form

$$ds^2 = \rho^2(dt^2 - dr^2) - \kappa^2\rho^{-2}(dz + \alpha\,d\phi)^2 - a_0^2\rho^2\kappa^{-2}(j^2 - 1)\sinh^2 r\cosh^2 t\,d\phi^2 \tag{9.118}$$

where now

$$\rho^2 = [1 + (j^2 - 1)^{1/2}\sinh t]^2 + j^2\cosh^2 r \tag{9.119}$$
$$\kappa^2 = (j^2 - 1)\sinh^2 t + j^2\cosh^2 r - 1 \tag{9.120}$$

and

$$\alpha = -2ja_0\kappa^{-2}[1 + (j^2 - 1)^{1/2}\sinh t]\sinh^2 r. \tag{9.121}$$

The Xanthopoulos line element (9.118) can be further reduced to the canonical form (9.83) by making the transformation to a new set of coordinates (T, R) defined by

$$T \pm R = a_0(j^2 - 1)^{1/2}\sinh(t \pm r) \tag{9.122}$$

but the value of this change is limited. One benefit is that the C-energy can be read off directly as

$$e^{2C} = \frac{(j^2 - 1)\sinh^2 t + j^2\cosh^2 r - 1}{a_0^2(j^2 - 1)(\sinh^2 t + \cosh^2 r)}. \tag{9.123}$$

Also, for small values of R, the line element becomes:

$$ds^2 \approx \rho_0^2(dt^2 - dr^2) - \kappa_0^2\rho_0^{-2}(dz + \beta r^2 d\phi)^2 - a_0^2\rho_0^2 r^2 d\phi^2 \qquad (9.124)$$

where $\rho_0^2(t)$ and $\kappa_0^2(t)$ are the values of ρ^2 and κ^2 on the axis, and $\beta(t) = -2ja_0\kappa_0^{-2}[1+(j^2-1)^{1/2}\sinh t]$. The solution, therefore, supports an axial string with mass per unit length μ given by the standard formula $1 - 4\mu = a_0$.

Another regime of interest is spacelike infinity, where $R \gg |T|$ or, equivalently, $r \gg |t|$. In this limit $\rho^2 \approx \kappa^2 \approx j^2\cosh^2 r \approx j^2 a_0^{-2}(j^2-1)^{-1}R^2$ and $\alpha \approx -2a_0 j^{-1}$, and so

$$ds^2 \approx j^2 a_0^{-2}(j^2-1)^{-1}(dT^2 - dR^2) - (dz - 2a_0 j^{-1}d\phi)^2 - R^2 d\phi^2. \quad (9.125)$$

On replacing z with $Z = z - 2a_0 j^{-1}\phi$ it is evident that the spacetime is asymptotically flat*, with an effective mass per unit length μ_{eff} (defined in terms of the angle deficit on circles of radius R) given by

$$1 - 4\mu_{\text{eff}} = j^{-1}(j^2-1)^{1/2}a_0. \qquad (9.126)$$

The difference between the mass per unit length of the string and the mass per unit length of the spacetime

$$\mu_{\text{eff}} - \mu = \tfrac{1}{4}j^{-1}[j - (j^2-1)^{1/2}]a_0 \qquad (9.127)$$

(which incidentally is equal to $\tfrac{1}{4}(e^{-C_0} - e^{-C_\infty})$) is attributable to the energy of the gravitational waves filling the spacetime.

In terms of the rescaled null coordinates $u = \sinh(t+r)$ and $v = \sinh(t-r)$ the C-energy is:

$$e^{2C} = a_0^{-2}(j^2-1)^{-1}\left[j^2 - \frac{1}{2} - \frac{1}{2}\frac{uv+1}{(u^2+1)^{1/2}(v^2+1)^{1/2}}\right] \qquad (9.128)$$

and so

$$C_{,v} \approx -\frac{1}{2(v^2+1)[(2j^2-1)(v^2+1)^{1/2} - v]} \qquad (9.129)$$

for large u and there is an outward flux of C-energy at future null infinity. (Xanthopoulos [Xan86b] mistakenly claimed that $C_{,v}$ falls off as u^{-3} for large u and so regarded the solution as non-radiating.) Similarly,

$$C_{,u} \approx \frac{1}{2(u^2+1)[(2j^2-1)(u^2+1)^{1/2} + u]} \qquad (9.130)$$

at past null infinity ($v \to -\infty$) and thus the ingoing and outgoing pulses of C-energy have the same profiles (one being the time reverse of the other). In particular, $C_{,u}$ falls off as $|u|^{-3}$ as $|u| \to \infty$ and $C_{,v}$ as $-|v|^{-3}$ as $|v| \to \infty$ at past and future null infinity respectively.

Furthermore, the energy fluxes in the individual $+$ and $\times$ gravitational modes at future null infinity are

$$C_v^+ = -\tfrac{1}{2}(j^2 - 1)\frac{[2(j^2 - 1)v^2 - 2j^2 - 1 + 2v(j^2 - 1)(v^2 + 1)^{1/2}]^2}{(v^2 + 1)[(v^2 + 1)^{1/2} + v][(2j^2 - 1)(v^2 + 1)^{1/2} - v]^4}$$

(9.131)

and

$$\begin{aligned} C_v^\times = -\tfrac{1}{2}j^2\{[(v^2 + 1)^{1/2} - v]^2[6(j^2 - 1)v^2 + 2j^2 - 3 \\ + 6v(j^2 - 1)(v^2 + 1)^{1/2}]^2\}\{(v^2 + 1)[(v^2 + 1)^{1/2} + v] \\ \times [(2j^2 - 1)(v^2 + 1)^{1/2} - v]^4\}^{-1}. \end{aligned}$$

(9.132)

Hence, at early times at future null infinity (that is, when $v \to -\infty$),

$$C_v^+ \approx -\tfrac{9}{16}j^{-4}(j^2 - 1)|v|^{-5} \qquad \text{and} \qquad C_v^\times \approx -\tfrac{1}{4}j^{-2}|v|^{-3} \qquad (9.133)$$

and the $\times$ mode dominates the outgoing radiation flux, while at late times (when $v \to \infty$),

$$C_v^+ \approx -\tfrac{1}{4}(j^2 - 1)^{-1}v^{-3} \qquad \text{and} \qquad C_v^\times \approx -\tfrac{9}{16}(j^2 - 1)^{-2}j^2v^{-5} \qquad (9.134)$$

and the $+$ mode dominates. At past null infinity, of course, the asymptotic behaviour of the two modes is the same, except in time-reversed order.

Xanthopoulos [Xan86b] describes the metric (9.118) as a 'rotating cosmic string', presumably because $\alpha \neq 0$. However, a non-zero α is an indication only of the presence of $\times$ mode gravitational waves, not that the axial string is spinning. The canonical metric describing a zero-thickness cosmic string with angular momentum per unit length J, which was first constructed by Pawel Mazur [Maz86], has the form

$$ds^2 = (dt + 4J \, d\phi)^2 - dr^2 - dz^2 - (1 - 4\mu)^2 r^2 \, d\phi^2 \qquad (9.135)$$

and is stationary axisymmetric rather than cylindrically symmetric. It also suffers from the defect that any horizontal circle centred on the axis with radius $r < 4J(1 - 4\mu)^{-1/2}$ forms a closed timelike curve. The spinning string metric, therefore, violates causality and is unlikely to be of physical importance.

Xanthopoulos [Xan87] has also extended the complex transformation described here to the Kerr–Newman metric (which describes a spinning black hole with electric charge), to generate a family of radiating solutions describing a string immersed in a parallel electric field.

Furthermore, the Kerr metric (9.114) is the simplest member of a one-parameter family of stationary axisymmetric vacuum solutions discovered by Tomimatsu and Sato in 1972. It should not be surprising, therefore, that the transformations used by Xanthopoulos can be applied to other Tomimatsu–Sato solutions to generate well-behaved radiating string spacetimes.

To see this directly, consider again the canonical cylindrical metric (9.83). The field equation (9.88) can be formally integrated by introducing a potential function $\Phi(t, r)$ with the property that

$$r^{-1}e^{4\psi}\dot{\alpha} = \Phi' \quad \text{and} \quad r^{-1}e^{4\psi}\alpha' = \dot{\Phi}. \tag{9.136}$$

The integrability condition for α then becomes

$$(re^{-4\psi}\dot{\Phi})^{\cdot} = (re^{-4\psi}\Phi')' \tag{9.137}$$

and the two field equations (9.87) and (9.137) are just the real and imaginary components of a single equation

$$\text{Re}(E)(\ddot{E} - r^{-1}E' - E'') = \dot{E}^2 - E'^2 \tag{9.138}$$

for the complex potential $E = e^{2\psi} + i\Phi$.

On defining $\xi = \frac{E-1}{E+1}$ or, equivalently, $E = \frac{1+\xi}{1-\xi}$, the equation for E reduces to the cylindrical Ernst equation:

$$(1 - |\xi|^2)(\ddot{\xi} - r^{-1}\xi' - \xi'') = 2\xi^*(\dot{\xi}^2 - \xi'^2). \tag{9.139}$$

In terms of ξ, the components of E are $e^{2\psi} = \frac{1-|\xi|^2}{|1-\xi|^2}$ and $i\Phi = \frac{\xi - \xi^*}{|1-\xi|^2}$. A final transformation from the canonical coordinates t and r to prolate coordinates $x \in \mathbb{R}$ and $y \geq 1$ defined by $t = xy$ and $r = (x^2 + 1)^{1/2}(y^2 - 1)^{1/2}$ results in the equation

$$(|\xi|^2 - 1)\{[(x^2 + 1)\xi_{,x}]_{,x} - [(y^2 - 1)\xi_{,y}]_{,y}\} = 2\xi^*[(x^2 + 1)\xi_{,x}^2 - (y^2 - 1)\xi_{,y}^2]. \tag{9.140}$$

The analogue of this equation in the case of a stationary axisymmetric spacetime is recovered by replacing x with ix. The Tomimatsu–Sato (TS) metrics are generated from rational polynomial solutions ξ of the analogue equation. For example, the Kerr metric (the $\delta = 1$ TS solution) has $\xi = (px - iqy)^{-1}$, where p and q are real constants satisfying $p^2 + q^2 = 1$, while the $\delta = 2$ solution has

$$\xi = \frac{2px(x^2 - 1) - 2iqy(1 - y^2)}{p^2(x^4 - 1) - q^2(1 - y^4) - 2ipqxy(x^2 - y^2)} \tag{9.141}$$

(again with $p^2 + q^2 = 1$).

The Tomimatsu–Sato solutions are asymptotically flat but all except the Kerr metric contain naked curvature singularities. Xanthopolous and Demetrios Papadopoulos [PX90] have transformed the $\delta = 2$ TS metric into a non-singular radiating string solution by making the replacements $x \to ix$ and $p \to ip$ in the complex potential (9.141). The resulting formula for the metric function ψ is:

$$\begin{aligned}
e^{2\psi} = \{&(y^2 - 1)^4 + 2(y^2 - 1)(x^2 + y^2)[2x^4 + x^2y^2 + 3x^2 \\
&+ (y^2 - 1)^2 + y^2 + 1]p^2 + (x^2 + y^2)^4p^4\} \\
&\times \{[p^2(x^4 - 1) + q^2(1 - y^4) + 2px(x^2 + 1)]^2 \\
&+ 4q^2y^2[px(x^2 + y^2) + y^2 - 1]^2\}^{-1}
\end{aligned} \tag{9.142}$$

where now $q^2 - p^2 = 1$.

The remaining metric components $e^{2\chi}$ and α can be calculated by integrating (9.84)–(9.85) and (9.136) respectively. Papadopoulos and Xanthopoulos find that

$$e^{2\chi} = a_0^{-2}\{[p^2(x^4 - 1) + q^2(1 - y^4) + 2px(x^2 + 1)]^2 \\ + 4q^2y^2[px(x^2 + y^2) + y^2 - 1]^2\}\{p^4(x^2 + y^2)^4\}^{-1} \quad (9.143)$$

(where a_0 is an integration constant) and

$$\alpha = -4p^{-1}q(y^2 - 1)\{xp^3(x^2 + y^2)[2x^4 + y^4 - x^2(y^2 - 1) - 3y^2] \\ + p^2(x^2 + y^2)[x^2(4x^2 + 5 - y^2) + (y^2 - 1)(y^2 - 2)] \\ + (y^2 - 1)^3(px + 1)\}\{(y^2 - 1)^4 + 2(y^2 - 1)(x^2 + y^2)[2x^4 + x^2y^2 \\ + 3x^2 + (y^2 - 1)^2 + y^2 + 1]p^2 + (x^2 + y^2)^4 p^4\}^{-1}. \quad (9.144)$$

Near the axis of symmetry (where $r = 0$), $x \approx t - \frac{1}{2}\frac{t}{1+t^2}r^2$ and $y \approx 1 + \frac{1}{2}\frac{1}{1+t^2}r^2$, and so

$$a_0^2 e^{2\chi} \approx e^{-2\psi} \approx \frac{p^2(t^2 + 1)^2 + 4pt(t^2 - 1) + 8t^2}{p^2(1 + t^2)^2} \quad (9.145)$$

while

$$\alpha \approx -8p^{-3}qt\frac{p(t^2 - 1) + 2t}{(t^2 + 1)^3}r^2. \quad (9.146)$$

The axis, therefore, defines a conical singularity with the usual mass per unit length $\mu = \frac{1}{4}(1 - a_0)$.

Near spacelike infinity ($r \gg |t|$), however, $x \approx t/r + \frac{1}{2}t(t^2 - 1)/r^3$ and $y \approx r - \frac{1}{2}(t^2 - 1)/r$, and so

$$e^{2\psi} \approx 1 - 8q^{-2}r^{-2} \qquad a_0^2 e^{2\chi} \approx p^{-4}q^4 + 4p^{-4}q^2r^{-2} \quad (9.147)$$

and

$$\alpha \approx -4p^{-1}q^{-1} - 4q^{-1}t/r. \quad (9.148)$$

The metric is, therefore, asymptotically flat* with a constant C-energy $C_\infty = a_0^{-2}p^{-4}q^4$ at infinity, with the difference $C_\infty - C_0 = a_0^{-2}p^{-4}(p^2 + q^2)$ again attributable to the energy of the cylindrical gravitational waves filling the spacetime.

Examination of the expressions for $e^{2\psi}$, $e^{2\chi}$ and α confirms that the metric components are all finite if $p \neq 0$ and $y > 1$ (that is, away from the axis). The denominators in (9.143) and (9.144) are clearly positive definite, while the second squared term in the denominator of (9.142) can vanish only if $px < 0$ and $y^2 = (1 - px^3)/(1 + px)$, which condition forces the first squared term to be positive definite. Furthermore, the determinant of the metric tensor $g = -r^2 e^{4\chi}$ is non-zero if $r \neq 0$. Thus the solution describes an asymptotically-flat* radiating

string spacetime which, like the Xanthopoulos solution, is free of curvature singularities. Indeed, in the words of Papadopoulos and Xanthopoulos [PX90], 'it appears that the correct place of TS solutions is in the description of cylindrically symmetric spacetimes, as opposed to stationary axisymmetric spacetimes...'.

9.3.5 Einstein–Rosen soliton waves

The relatively simple form of the equations (9.87) and (9.88) for the metric functions ψ and α appearing in the canonical line element (9.83) has invited the application of a wide variety of mathematical techniques. One that has proved to be particularly fruitful is the inverse scattering transform method, developed by Belinsky and Zakharov in the late 1970s.

To apply the Belinsky–Zakharov method, the equations for ψ and α are first rewritten as a 2×2 system of nonlinear wave equations:

$$[r(h^{-1})^{ac}\dot{h}_{cb}]^{\cdot} = [r(h^{-1})^{ac}h'_{cb}]' \tag{9.149}$$

for the matrix components

$$h_{ab} = \begin{bmatrix} e^{2\psi} & \alpha e^{2\psi} \\ \alpha e^{2\psi} & r^2 e^{-2\psi} + \alpha^2 e^{2\psi} \end{bmatrix}. \tag{9.150}$$

The wave equations (9.149) are then used to generate a system of Schrödinger-like equations

$$\dot{\Phi}_{ab} - \frac{2\lambda^2}{\lambda^2 - r^2}\Phi_{ab,\lambda} = -\frac{r}{\lambda^2 - r^2}(h^{-1})^{cd}(r\dot{h}_{ca} + \lambda h'_{ca})\Phi_{db} \tag{9.151}$$

and

$$\Phi'_{ab} - \frac{2\lambda r}{\lambda^2 - r^2}\Phi_{ab,\lambda} = -\frac{r}{\lambda^2 - r^2}(h^{-1})^{cd}(\lambda\dot{h}_{ca} + r h'_{ca})\Phi_{db} \tag{9.152}$$

for a 'wavefunction' Φ_{ab} which depends on a complex parameter λ as well as the coordinates r and t, and satisfies the initial condition $\lim_{\lambda \to 0} \Phi_{ab} = h_{ab}$.

The power of the Belinsky–Zakharov method lies in the fact that new solutions $\bar{\Phi}_{ab}$ of (9.151) and (9.152) can be generated by applying a series of algebraic operations to any known solution Φ_{ab}. It is, therefore, possible to construct new metric solutions h_{ab} by making a simple initial choice for h_{ab}, solving for the corresponding wave equation Φ_{ab}, then transforming Φ_{ab} algebraically and taking the limit $\lambda \to 0$.

The simplest choice of seed solution is the Minkowski metric $g_{\mu\nu} = \text{diag}(1, -1, -1, -r^2)$, which has $h_{ab} = \text{diag}(1, r^2)$ and $\Phi_{ab} = \text{diag}(1, r^2 + 2t\lambda + \lambda^2)$, although the more general Levi-Città seed

$$ds^2 = r^{2(q^2-q)}(dt^2 - dr^2) - r^{2q}\,dz^2 - r^{2(1-q)}d\phi^2 \tag{9.153}$$

for which

$$\Phi_{ab} = \mathrm{diag}((r^2 + 2t\lambda + \lambda^2)^q, (r^2 + 2t\lambda + \lambda^2)^{1-q}) \tag{9.154}$$

is also commonly used[2].

By extending earlier work by Cespedes and Verdaguer [CV87] on plane-symmetric Kasner solutions, Jaume Garriga and Enric Verdaguer [GV87b] have identified two general classes of Einstein–Rosen ($\alpha = 0$) solutions containing a total of N solitons superimposed on a Levi-Cività seed, which they describe as 'generalized soliton solutions'.

The first class of solutions has

$$\mathrm{e}^{2\psi} = r^{2q} \prod_{j=1}^{N} p_j(t, r)^{k_j} \tag{9.155}$$

where k_j are real constants and

$$p_j(t, r) = P_j + (P_j^2 - 1)^{1/2} \tag{9.156}$$

with

$$P_j = r^{-2}[(t - b_j)^2 + w_j^2] + \{1 + r^{-4}[(t - b_j)^2 + w_j^2]^2 - 2r^{-2}[(t - b_j)^2 - w_j^2]\}^{1/2} \tag{9.157}$$

and b_j and w_j also real constants.

With the same definition of p_j, the second class of solutions has

$$\mathrm{e}^{2\psi} = r^{2q} \prod_{j=1}^{N} \mathrm{e}^{k_j \gamma_j(t,r)} \tag{9.158}$$

where

$$\gamma_j(t, r) = \cos^{-1}[2r^{-1}(t - b_j)p_j^{1/2}(1 + p_j)^{-1}]. \tag{9.159}$$

The corresponding metric functions χ can be constructed either by integrating the field equations (9.84) and (9.85) or by direct use of the inverse scattering formalism. In either case, the general expression for χ is too complicated to reproduce here.

The family of one-soliton solutions belonging to the first class (9.155) with $k_1 = 1$ and $b_1 = 0$ were first examined by Verdaguer and Xavier Fustero [FV86], and with $k_1 \neq 1$ by Garriga and Verdaguer [GV87b]. The full line element is:

$$\mathrm{d}s^2 = a_0^{-2} r^{2(q^2 - q - k^2)} \frac{p^{k(2k+2q-1)}}{(1 - p)^{2k^2} H^{k^2}} (\mathrm{d}t^2 - \mathrm{d}r^2) - r^{2q} p^k \, \mathrm{d}z^2 - r^{2(1-q)} p^{-k} \, \mathrm{d}\phi^2 \tag{9.160}$$

---

[2] Despite appearances to the contrary, the line element (9.153) given here for the Levi-Cività solution is isometric to the alternative form (7.20) used in chapter 7. This can be seen by replacing r in (9.153) with $\bar{r} = r^{(q-1)^2}$, defining $m = q/(q - 1)$ and then dropping the overbar. The asymptotically-flat* subcase corresponds interchangeably to $m = 0$ or $q = 0$.

where a_0 is an integration constant and

$$H = (1 - p)^2 + 16w^2 r^{-2} p^2 (1 - p)^{-2} \qquad (9.161)$$

with $k \equiv k_1$, $w \equiv w_1$ and $p \equiv p_1$.

In principle, the solution contains four adjustable parameters (A, k, q and w) but one of these can be eliminated by requiring the singularity on the symmetry axis $r = 0$ to be conical. For small values of r, $p \approx 4r^{-2}(t^2 + w^2)$ and $H \approx 16r^{-4}(t^2 + w^2)^2$, and so

$$\begin{aligned}
e^{2\chi} &\approx a_0^{-2}[4(t^2 + w^2)]^{k(2q-1-2k)} r^{2(q-k)(q-k-1)} \\
&\text{and} \qquad e^{2\psi} \approx [4(t^2 + w^2)]^k r^{2(q-k)}.
\end{aligned} \qquad (9.162)$$

Thus $e^{2C} \equiv e^{2(\chi+\psi)} \propto r^{2(q-k)^2}$ and the solution supports a cosmic string at $r = 0$, with the usual strength a_0, if and only if $k = q$. In addition, there is a curvature singularity at timelike infinity ($|t| \gg r$) unless either $k(2q-1-2k) \geq 0$ (if $k \neq q$) or $k = q \leq 1$.

At spacelike infinity, however, $p \approx 1 + 2|w|r^{-1}$ and $H \approx 4 + 8|w|r^{-1}$, and so with $k = q$

$$e^{2\chi} \approx a_0^{-2}(4w)^{-2q^2} r^{2(q^2-q)} \qquad \text{and} \qquad e^{2\psi} \approx r^{2q}. \qquad (9.163)$$

Apart from the scaling factor $a_0^{-2}(4w)^{-2q^2}$, therefore, the solution has the same asymptotic structure as the Levi-Città seed solution (9.153). In particular, the C-energy diverges as $q^2 \ln r$, and the solution cannot be asymptotically flat* unless $q = 0$. Of course, if $q = 0$ then the bare straight-string metric (7.28) is recovered.

Garriga and Verdaguer [GV87b] claim that, with $v = t - r$, the rate of change of the C-energy at future null infinity in the general one-soliton solution (9.160) is $C_{,v} \approx -\frac{1}{2}w^{-1}k^2$, and so there is a net outward flux of gravitational energy unless $k = 0$. Strictly speaking, however, this expression is valid only for $|v| \ll w$. For general values of v, it turns out that

$$C_{,v} \approx -\tfrac{1}{2}k^2 \frac{2v(v^2 + w^2)^{1/2} + 2v^2 + w^2}{(v^2 + w^2)^{1/2}[v^2 + w^2 + v(v^2 + w^2)^{1/2}]}. \qquad (9.164)$$

Here, and in all other soliton solutions in this section, the corresponding rate of change of C-energy at past null infinity, $C_{,u}$, is found by multiplying $C_{,v}$ by -1 and replacing v everywhere with $-u$.

The two-soliton solutions belonging to class (9.155) with $k_1 = -k_2 \equiv k$ have the line element

$$\begin{aligned}
ds^2 = a_0^{-2} r^{2(q^2-q-4k^2)} F \frac{(p_1/p_2)^{k(2q-1)}}{(1-p_1)^{2k^2}(1-p_2)^{2k^2} H_1^{k^2} H_2^{k^2}}(dt^2 - dr^2) \\
- r^{2q}(p_1/p_2)^k dz^2 - r^{2(1-q)}(p_1/p_2)^{-k} d\phi^2
\end{aligned} \qquad (9.165)$$

where H_j is generated by reading p as p_j and w as w_j in the expression (9.161) for H, and

$$F = \left\{\left[(1 + p_1 p_2)r^2 - \frac{8(t - b_1)(t - b_2)p_1 p_2}{(1 + p_1)(1 + p_2)}\right]^2 - \frac{64 w_1^2 w_2^2 p_1^2 p_2^2}{(1 - p_1)^2 (1 - p_2)^2}\right\}^{2k^2}. \tag{9.166}$$

These solutions were first studied with $k = 1$ and $b_1 = b_2 = 0$ by Fustero and Verdaguer [FV86], and in full generality by Garriga and Verdaguer [GV87b].

For small values of r,

$$e^{2\chi} \approx a_0^{-2} r^{2(q^2 - q)} [(t_1^2 + w_1^2)/(t_2^2 + w_2^2)]^{k(2q-1)} \tag{9.167}$$

and

$$e^{2\psi} \approx r^{2q} [(t_1^2 + w_1^2)/(t_2^2 + w_2^2)]^k \tag{9.168}$$

where $t_j \equiv t - b_j$, and so the axis supports a conical singularity if and only if $q = 0$.

In addition, for large values of r the line element tends asymptotically to the Levi-Cività seed solution (9.153), save for a constant scaling factor in $e^{2\chi}$ (this is easily seen to be a general feature of all soliton solutions of class (9.155)). Thus the two-soliton solution describes a cosmic string on axis and is asymptotically flat* if $q = 0$, in which case $e^{2C_0} = a_0^{-2}$ and

$$e^{2C_\infty} = a_0^{-2} (4 w_1 w_2)^{-2k^2} [(w_1 + w_2)^2 + (b_1 - b_2)^2]^{2k^2} \geq a_0^{-2}. \tag{9.169}$$

Equality holds on the right-hand side if and only if $w_1 = w_2$ and $b_1 = b_2$, in which case the bare straight-string metric is recovered.

As in the one-soliton solutions, the rates of change $C_{,u}$ and $C_{,v}$ of C-energy in (9.165) are finite and non-zero at past and future null infinity respectively. Also, near timelike infinity ($|t| \gg r$) the two-soliton line element tends asymptotically to that of the Levi-Cività seed solution, as does the Riemann tensor. The two-soliton solution with $q = 0$ is, therefore, most naturally interpreted as the superposition of an incoming and an outgoing pulse of C-energy outside an otherwise bare zero-thickness cosmic string.

The one-soliton solutions of the second type (9.158), which were first analysed by Garriga and Verdaguer, have $e^{2\psi} = r^{2q} e^{k\gamma}$ and

$$e^{2\chi} = a_0^{-2} r^{2(q^2 - q) - k - k^2} e^{k(2q-1)\gamma} \frac{[(t^2 - w^2 - r^2)^2 + 4w^2 t^2]^{k(k+1)/4} p^{k(k+1)/2}}{(1 - p)^{k^2/2} H^{k(k+2)/4}} \tag{9.170}$$

where p, k and w are again shorthand for p_1, k_1 and w_1, the constant b_1 has been set to zero, and $\gamma = \cos^{-1}[2r^{-1}tp^{1/2}(1 + p)^{-1}]$. For small values of r, $\gamma \approx \cos^{-1}[t/(t^2 + w^2)^{1/2}] \equiv \gamma_0(t)$ and so

$$e^{2\chi} \approx a_0^{-2} r^{2(q^2 - q)} e^{k(2q-1)\gamma_0(t)} \qquad \text{and} \qquad e^{2\psi} \approx r^{2q} e^{k\gamma_0(t)}. \tag{9.171}$$

That is, the radial dependence of the Levi-Cività seed solution is preserved, and there is a conical singularity on the axis if and only if $q = 0$.

However, near spacelike infinity $\gamma \approx \frac{1}{2}\pi - t/r$ and

$$e^{2\chi} \approx a_0^{-2} 2^{-k^2-k} e^{k(2q-1)\pi/2} w^{-k^2/2} r^{2(q^2-q)+k^2/2} \quad \text{and} \quad e^{2\psi} \approx r^{2q} e^{k\pi/2}$$
(9.172)

and so the solutions are asymptotically flat* if and only if $2q^2 + k^2/2 = 0$ or, equivalently, $k = q = 0$ (in which case the metric once more reduces to the bare straight-string metric). Unlike the previous family of one-soliton solutions, these solutions are free of curvature singularities at timelike infinity for all values of k and q. The rate of radiation of C-energy at future null infinity is

$$C_{,v} \approx -\tfrac{1}{8}k^2 \frac{w^2}{(v^2 + w^2)^{1/2}[v^2 + w^2 + v(v^2 + w^2)^{1/2}]}$$
(9.173)

indicating again that there is a non-zero outward flux of gravitational radiation there.

Although the family of one-soliton solutions of this class cannot generate a non-trivial, asymptotically-flat* string spacetime, the family of two-soliton solutions with $k_1 = -k_2 \equiv k$ can. In this case, $e^{2\psi} = r^{2q} e^{k(\gamma_1 - \gamma_2)}$, while

$$e^{2\chi} = a_0^{-2} r^{2(q^2-q-k-k^2)} e^{k(2q-1)(\gamma_1-\gamma_2)}$$
$$\times G \frac{4^{k(k+1)}(p_1 p_2)^{k(k+1)/2}}{(1 - p_1)^{k^2/2}(1 - p_2)^{k^2/2} H_1^{k(k+2)/4} H_2^{k(k+2)/4}}$$
(9.174)

where

$$G = \{[(t_1^2 - w_1^2 - r^2)^2 + 4w_1^2 t_1^2][(t_2^2 - w_2^2 - r^2)^2 + 4w_2^2 t_2^2]\}^{k(k+1)/4} \left(\frac{A_-}{A_+}\right)^{k^2/2}$$
(9.175)

with

$$A_\pm = (1 + p_1 p_2)(1 - p_1^2)(1 - p_2^2)r^2 - 8 p_1 p_2[t_1 t_2(1 - p_1)(1 - p_2)$$
$$\mp |w_1 w_2|(1 + p_1)(1 + p_2).$$
(9.176)

Garriga and Verdaguer [GV87b] have shown that these solutions are both conical on the axis $r = 0$ and asymptotically flat* if and only if $q = 0$, in which case $e^{2C_0} = a_0^{-2}$ as usual, while

$$e^{2C_\infty} = a_0^{-2}(4w_1 w_2)^{-k^2/2}[(w_1 + w_2)^2 + (b_1 - b_2)^2]^{k^2/2} \geq a_0^{-2}.$$
(9.177)

As in the first class of two-soliton solutions, the rates $C_{,u}$ and $C_{,v}$ of radiation of C-energy at past and future null infinity are non-zero, and the line element (and Riemann tensor) reduces to that of the Levi-Cività seed solution at timelike

infinity. Thus the natural interpretation of the subclass of solutions with $q = 0$ is again as the superposition of an incoming and an outgoing pulse of C-energy on an otherwise bare straight-string metric.

More elaborate solutions of this type describing cosmic strings embedded in radiating asymptotically-flat* spacetimes can be constructed in the obvious way, namely by taking the metric function ψ appropriate to either a class 1 (9.155) or class 2 (9.158) solution with $q = 0$ and $N = 2M$ solitons paired in such a way that $k_{2j-1} = -k_{2j}$ for all $1 \leq j \leq M$. Formulae for the corresponding metric functions χ can be found in [GV87b].

9.3.6   Two-mode soliton solutions

One restrictive feature of the soliton solutions considered in the previous section is that they contain only $+$ mode gravitational waves. In 1988 Athanasios Economou and Dimitri Tsoubelis [ET88a, ET88b] constructed a four-parameter solution describing a bare straight string interacting with both $+$ and $\times$ mode gravitational radiation by superimposing two soliton waves on a Minkowski ($q = 0$) seed metric.

The corresponding metric functions are given by:

$$e^{2\chi} = A^2 |q_1 q_2|^{-1} (q_1^2 - 1)^{-1} (q_2^2 - 1)^{-1} |Z_1| \tag{9.178}$$

$$e^{2\psi} = |q_1 q_2| Z_2 / Z_1 \quad \text{and} \quad \alpha = 2|q_1 q_2|(b_2 - b_1) Z_3 / Z_2 \tag{9.179}$$

where A is a real constant,

$$Z_1 = (1 + c_1 c_2 q_1 q_2)^2 (q_1 - q_2)^2 + (c_1 q_1 - c_2 q_2)^2 (q_1 q_2 - 1)^2 \tag{9.180}$$

$$Z_2 = (1 + c_1 c_2)^2 (q_1 - q_2)^2 + (c_1 - c_2)^2 (q_1 q_2 - 1)^2 \tag{9.181}$$

and

$$Z_3 = (1 + c_1 c_2)(c_1 q_1^2 - c_2 q_2^2) - (c_1 - c_2)(1 + c_1 c_2 q_1^2 q_2^2) \tag{9.182}$$

with $q_j = (b_j - t)r^{-1} + [(b_j - t)^2 r^{-2} - 1]^{1/2}$ for $j = 1$ or 2.

Here, b_1, b_2, c_1 and c_2 are complex constants constrained by the requirement that the metric components be real but are otherwise arbitrary. One way to guarantee the reality of the metric components is to choose $b_2^* = b_1 \equiv b$ and $c_2^* = c_1 \equiv c$, in which case $q_2^* = q_1$ as well. If b is real then $\alpha = 0$ and the $\times$ mode gravitational waves are absent. However, if b is complex $\text{Re}(b)$ can always to set to zero by rezeroing t and $\text{Im}(b)$ set to 1 by rescaling t and r. So without loss of generality the two-mode solutions can be studied by setting $b = i$.

If the branch of the square root is chosen so that q_j is of order r for small values of r, the line element near the symmetry axis then becomes

$$ds^2 \approx 4A^2 K(t)(dt^2 - dr^2) - c_1^2 K(t)^{-1}(dz + 2c_1^{-1} d\phi)^2 - r^2 c_1^{-2} K(t) d\phi^2 \tag{9.183}$$

where

$$K(t) = (t^2 + 1)^{-1}[(c_{\mathrm{I}}t + c_{\mathrm{R}})^2 + 1] \tag{9.184}$$

and $c_{\mathrm{R}} = \mathrm{Re}(c)$ and $c_{\mathrm{I}} = \mathrm{Im}(c)$. This metric supports a conical singularity on the axis, as is evident on replacing z with $\bar{z} = z + 2c_{\mathrm{I}}^{-1}\phi$ and α with $\bar{\alpha} = \alpha - 2c_{\mathrm{I}}^{-1} = O(r^2)$. The value of the C-energy on the axis is, therefore, given by $\mathrm{e}^{2C_0} = 4A^2 c_{\mathrm{I}}^2 \equiv a_0^{-2}$. The solution is free of curvature singularities at timelike infinity.

Near spacelike infinity, the line element has the form

$$\mathrm{d}s^2 \approx A^2(|c|^2 + 1)^2(\mathrm{d}t - \mathrm{d}r)^2 - \left[\mathrm{d}\bar{z} + \left(\frac{4c_{\mathrm{I}}}{|c|^2 + 1} - \frac{2}{c_{\mathrm{I}}}\right)\mathrm{d}\phi\right]^2 - r^2\,\mathrm{d}\phi^2 \tag{9.185}$$

with the succeeding terms in χ, ψ and α all of order r^{-1}. Thus, as in the Xanthopoulos solution (9.118), the solution is asymptotically flat* in a rotated coordinate system with $\bar{z}$ replaced by $Z = \bar{z} + (\frac{4c_{\mathrm{I}}}{|c|^2+1} - \frac{2}{c_{\mathrm{I}}})\phi$. The C-energy at spacelike infinity satisfies $\mathrm{e}^{2C_\infty} = A^2(|c|^2 + 1)^2 \geq 4A^2 c_{\mathrm{I}}^2$, with equality occurring here if and only if $c = \pm \mathrm{i}$, in which case the bare straight-string metric with $a_0^2 = \frac{1}{4}A^{-2}$ is recovered in the $\bar{z}$-coordinate system.

At future null infinity, the rate of radiation of C-energy is

$$C_{,v} = -\frac{1}{2}\frac{(|c|^2 + 1)^2 - 4c_{\mathrm{I}}^2}{(v^2 + 1)\{(|c|^2 + 1)^2[(v^2 + 1)^{1/2} - v] + 4c_{\mathrm{I}}^2[(v^2 + 1)^{1/2} + v]\}} \tag{9.186}$$

which exactly matches the inward flux $C_{,u}$ of C-energy at past null infinity (again found by multiplying $C_{,v}$ by -1 and replacing v everywhere with $-u$). The $+$ and $\times$ mode energy fluxes C_v^+ and $C_v^\times$ are briefly discussed by Economou and Tsoubelis [ET88b] but no explicit formulae have been published.

The close relationship between the two-mode soliton solution described here and the Xanthopoulos metric (9.118) can be brought out by again transforming to prolate coordinates $x \in \mathbb{R}$ and $y \geq 1$ defined by $t = xy$ and $r = (x^2 + 1)^{1/2}(y^2 - 1)^{1/2}$, in terms of which $q_1 = -(y - 1)(x + \mathrm{i})(x^2 + 1)^{-1/2}(y^2 - 1)^{-1/2}$. Then

$$g_{xx} = A^2\frac{4(c_{\mathrm{R}} + c_{\mathrm{I}}x)^2 + [(|c|^2 + 1)y + 1 - |c|^2]^2}{x^2 + 1}$$

$$g_{yy} = -A^2\frac{4(c_{\mathrm{R}} + c_{\mathrm{I}}x)^2 + [(|c|^2 + 1)y + 1 - |c|^2]^2}{y^2 - 1} \tag{9.187}$$

$$\mathrm{e}^{2\psi} = \frac{4c_{\mathrm{I}}^2(x^2 + 1) + (|c|^2 + 1)^2(y^2 - 1)}{4(c_{\mathrm{R}} + c_{\mathrm{I}}x)^2 + [(|c|^2 + 1)y + 1 - |c|^2]^2} \tag{9.188}$$

and

$$\bar{\alpha} = -4\frac{c_{\mathrm{I}}(|c|^2 - 1)y(x^2 + 1) + (|c|^2 + 1)[c_{\mathrm{R}}x(y^2 - 1) - c_{\mathrm{I}}(x^2 + y^2)]}{4c_{\mathrm{I}}^2(x^2 + 1) + (|c|^2 + 1)^2(y^2 - 1)} - \frac{2}{c_{\mathrm{I}}}. \tag{9.189}$$

The Xanthopoulos metric with $x = \sinh T$, $y = \cosh R$ and $\bar{z} = z$ is recovered (up to a constant rescaling of the coordinates T and R) by setting $c_R = j^{-1}$ and $c_I = (1 - j^{-2})^{1/2}$. In fact, the Economou–Tsoubelis solution with general values of c can be generated by applying a complex transformation to a two-parameter family of stationary axisymmetric solutions (the Kerr–Newman–Unti–Tamburino family) which generalizes the Kerr metric.

Another simple solution which has been investigated in some detail by Economou and Tsoubelis [ET88a] occurs when $c_R = 0$. The metric components in the prolate coordinate system are then

$$g_{xx} = A^2 \frac{4\delta^2 x^2 + [(\delta^2 + 1)y + 1 - \delta^2]^2}{x^2 + 1}$$

$$g_{yy} = -A^2 \frac{4\delta^2 x^2 + [(\delta^2 + 1)y + 1 - \delta^2]^2}{y^2 - 1} \tag{9.190}$$

$$e^{2\psi} = \frac{4\delta^2(x^2 + 1) + (\delta^2 + 1)^2(y^2 - 1)}{4\delta^2 x^2 + [(\delta^2 + 1)y + 1 - \delta^2]^2}$$

$$\bar{\alpha} = -2 \frac{(\delta^2 - 1)[2\delta^2 x^2 - (\delta^2 + 1)y + \delta^2 - 1](y - 1)}{[4\delta^2(x^2 + 1) + (\delta^2 + 1)^2(y^2 - 1)]\delta} \tag{9.191}$$

with $\delta \equiv c_I$.

The corresponding C-energy (as measured in the canonical t–r coordinate system) is given by

$$e^{2C} = A^2 \frac{4\delta^2(x^2 + 1) + (\delta^2 + 1)^2(y^2 - 1)}{x^2 + y^2}$$

$$= \frac{1}{8\delta^2} a_0^{-2} \left[\delta^4 + 6\delta^2 + 1 - (\delta^2 - 1)^2 \frac{uv + 1}{(u^2 + 1)^{1/2}(v^2 + 1)^{1/2}} \right] \tag{9.192}$$

where $u = t + r$ and $v = t - r$. In particular, the net energy of the gravitational field outside the string is $\frac{1}{4}(e^{-C_0} - e^{-C_\infty}) = \frac{1}{4}a_0(\delta^2 - 1)^2/(\delta^2 + 1)^2$.

The inward and outward fluxes of C-energy at past and future null infinity are, of course, non-zero, as was previously seen from (9.186), with $C_{,u}$ falling off as $|u|^{-3}$ as $|u| \to \infty$ and $C_{,v}$ as $-|v|^{-3}$ as $|v| \to \infty$ at past and future null infinity respectively. The energy fluxes in the individual $+$ and $\times$ gravitational modes at future null infinity are

$$C_v^+ = -\frac{1}{2}\{(\delta^4 - 1)^2\{2(\delta^2 + 1)^2[v^2 - v(1 + v^2)^{1/2}] + \delta^4 - 10\delta^2 + 1\}^2\}$$
$$\times \{(1 + v^2)[(1 + v^2)^{1/2} - v]\{(\delta^2 + 1)^2[(v^2 + 1)^{1/2} - v]$$
$$+ 4\delta^2[(v^2 + 1)^{1/2} + v]\}^4\}^{-1} \tag{9.193}$$

and

$$C_v^\times = -2\{(\delta^2 - 1)^2\delta^2[(3\delta^4 + 2\delta^2 + 3)(1 + v^2)^{1/2} - (\delta^2 + 3)(3\delta^2 + 1)v]^2\}$$

$$\times \{(1 + v^2)[(1 + v^2)^{1/2} - v]\{(\delta^2 + 1)^2[(v^2 + 1)^{1/2} - v]$$
$$+ 4\delta^2[(v^2 + 1)^{1/2} + v]\}^4\}^{-1}. \tag{9.194}$$

At early times at future null infinity,

$$C_v^+ \approx -\frac{1}{4}\frac{(\delta^2 - 1)^2}{(\delta^2 + 1)^2}|v|^{-3} \qquad \text{and} \qquad C_v^\times \approx -\frac{9}{256}\delta^{-4}(\delta^4 - 1)^2|v|^{-5} \tag{9.195}$$

and the $+$ mode dominates the outgoing radiation flux, while at late times,

$$C_v^+ \approx -\frac{9}{4}\frac{\delta^2(\delta^2 - 1)^2}{(\delta^2 + 1)^4}v^{-5} \qquad \text{and} \qquad C_v^\times \approx -\frac{1}{16}\delta^{-2}(\delta^2 - 1)^2v^{-3} \tag{9.196}$$

and the $\times$ mode dominates. (This is the opposite of the behaviour observed earlier for the Xanthopoulos metric (9.118).) As in the Xanthopoulos solution, the asymptotic behaviour of the two modes at past null infinity is the same but in time-reversed order.

9.4 Snapping cosmic strings

9.4.1 Snapping strings in flat spacetimes

The last class of exact string solutions to be considered here comprises metrics that result when a straight string (or pair of strings) spontaneously 'snaps', leaving two bare ends which recede from one another at the speed of light. The situation described here differs from the case, mentioned briefly in section 9.2.2, where a string breaks into two after black hole pair production, as snapping strings are bounded by null particles rather than accelerating black holes, and generate an impulsive gravitational shock wave as they snap. The act of snapping is, strictly speaking, not consistent with either the Einstein equations or the zero-thickness limit of any classical field-theoretic representation of a cosmic string, and the value of the solutions lies foremost in the structure of the shock wave that appears in the wake of the receding ends.

The simplest solution of this type begins with Minkowski spacetime in cylindrical coordinates:

$$ds^2 = dt^2 - dz^2 - dr^2 - r^2 d\theta^2. \tag{9.197}$$

Let ξ denote the complex coordinate $re^{i\theta}$ and u and v the null coordinates $t + z$ and $t - z$ respectively.

Then if $0 < a_0 \leq 1$ is a constant and $\varepsilon = -1, 0$ or 1, the transformation to a new set of coordinates (Z, U, V) defined by

$$u = a_0^{-1}|Z|^{1+a_0}\{\kappa^{-1}V - \tfrac{1}{4}[(1 + a_0)^2|Z|^{-2} + \varepsilon(1 - a_0)^2]U\} \tag{9.198}$$
$$v = a_0^{-1}|Z|^{1-a_0}\{\kappa^{-1}V - \tfrac{1}{4}[(1 - a_0)^2|Z|^{-2} + \varepsilon(1 + a_0)^2]U\} \tag{9.199}$$

and

$$\xi = a_0^{-1} Z^{a_0} [\kappa^{-1} |Z|^{1-a_0} V - \tfrac{1}{4}\kappa(1 - a_0^2)|Z|^{-1-a_0} U] \tag{9.200}$$

with $\kappa = 1 + \varepsilon |Z|^2$, results in the locally-flat line element

$$\mathrm{d}s^2 = \varepsilon\,\mathrm{d}U^2 - \mathrm{d}U\,\mathrm{d}V - |\kappa^{-1} V\,\mathrm{d}Z + \tfrac{1}{4}\kappa(1 - a_0^2)U Z^{*-2}\,\mathrm{d}Z^*|^2. \tag{9.201}$$

An important feature of the transformation $(u, v, \xi) \rightarrow (U, V, Z)$ is that $\arg(\xi) = a_0 \arg(Z)$, and so if $a_0 < 1$ the inverse image of the transformed spacetime is not the whole Minkowski spacetime but rather the conical spacetime covering $0 \le \arg(\xi) \le 2\pi a_0$, with $\arg(\xi) = 0$ and $\arg(\xi) = 2\pi a_0$ identified. In other words, the transformed spacetime is isometric to the spacetime outside a bare straight cosmic string with mass per unit length $\mu = \tfrac{1}{4}(1 - a_0)$. The string itself lies along the axis $\xi = 0$, which in the transformed coordinate system corresponds to the surface $\kappa^{-2}|Z|^2 = \tfrac{1}{4}(1 - a_0^2)U/V$.

In the special case $a_0 = 1$, the line element (9.201) reduces to

$$\mathrm{d}s^2 = \varepsilon\,\mathrm{d}U^2 - \mathrm{d}U\,\mathrm{d}V - \kappa^{-2}V^2\,\mathrm{d}Z\,\mathrm{d}Z^* \tag{9.202}$$

and the spacetime is isometric to the original Minkowski spacetime (with the axis $\xi = 0$ mapped to $Z = 0$). The parameter ε in this instance measures the Gaussian curvature of the 2-surfaces of constant U and V, which are respectively hyperboloids with $t^2 - r^2$ and z constant (if $\varepsilon = -1$), paraboloids with $t^2 - z^2 - r^2$ and $t - z$ constant (if $\varepsilon = 0$) or spheres with $z^2 + r^2$ and t constant (if $\varepsilon = 1$)[3].

Comparison of (9.201) with (9.202) indicates that the Minkowski metric ($a_0 = 1$) can be continuously matched to a string metric ($a_0 < 1$) across the surface $U = 0$ by letting

$$\mathrm{d}s^2 = \varepsilon\,\mathrm{d}U^2 - \mathrm{d}U\,\mathrm{d}V - |\kappa^{-1} V\,\mathrm{d}Z + \tfrac{1}{4}\kappa(1 - a_0^2)H(U)U Z^{*-2}\,\mathrm{d}Z^*|^2 \tag{9.203}$$

where H is the Heaviside step function. The spacetime is then empty for $U < 0$ but contains a cosmic string on axis for $U > 0$. Since $t^2 - z^2 - r^2 \equiv uv - |\xi|^2 = -U(V - \varepsilon U)$ independently of the value of a_0, the surface $U = 0$ corresponds to at least some part of the spherical null surface $t^2 = z^2 + r^2$ in both coordinate patches. This null surface is smooth everywhere except where it intersects the axis $\xi = 0$ in the string patch, as the string spacetime has a conical singularity there. Furthermore, the mean extrinsic curvature κ of the surface, as defined in [BI91], is $4\kappa V^{-1}$ in both patches. The junction surface $U = 0$ is therefore free of stress–energy at all points except possibly where $|t| - z = r = 0$.

By suitably restricting the ranges of U, V and Z in the two coordinate patches, therefore, it seems possible, in principle, to use the metric (9.203) to describe a straight cosmic string on the axis $r = 0$ which is static for $t < 0$ then

---

[3] Strictly speaking, the line element (9.201) is isometric to some patch of the Minkowski or string spacetimes for any value of ε. However, if ε is not 0 or ± 1 it can always be rescaled to ± 1 by making the supplementary transformation to $\bar{U} = |\varepsilon|^{1/2}U$, $\bar{V} = |\varepsilon|^{-1/2}V$ and $\bar{Z} = |\varepsilon|^{1/2}Z$, then dropping the overbars.

splits in two at $t = z = 0$, leaving behind a patch of Minkowski spacetime inside an expanding spherical wave front on the null surface $t = \sqrt{z^2 + r^2}$. The two free ends of the string would presumably inherit some stress–energy content as a result of the split, becoming 'monopoles', and recede from one another at the speed of light along the null lines $t - |z| = r = 0$.

This construction was first developed by Reinaldo Gleiser and Jorge Pullin [GP89] for the case $\varepsilon = 0$ in a slightly different coordinate system[4], then with varying degrees of generality by Peter Hogan [Hog93, Hog94] and Jiri Podolský and Jerry Griffiths [PG00]. However, the construction is complicated by the fact that the transformation $(u, v, \xi) \rightarrow (U, V, Z)$ is not bijective, and the image of the null spherical surface $t = \sqrt{z^2 + r^2}$ includes the surface $V - \varepsilon U = 0$ as well as the junction surface $U = 0$.
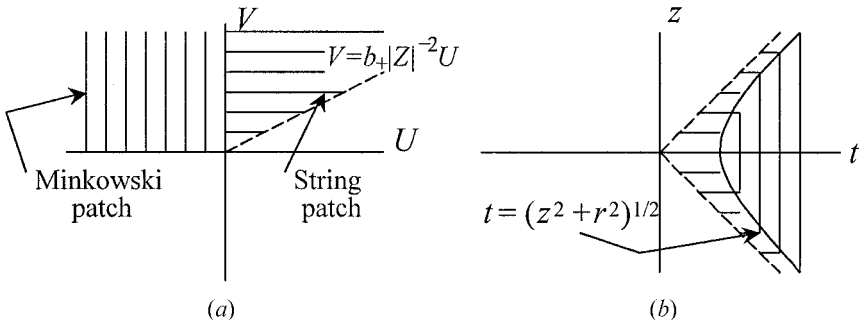
This does not pose a serious problem in the case $\varepsilon = 0$. The interior $t > \sqrt{z^2 + r^2}$ of the gravitational shock wave does map bijectively onto the quarter space $\{(U, V, Z) : U < 0, V > 0\}$ and the boundary $V = 0$ corresponds (for $U < 0$) to the null line $t = z > 0$ and $r = 0$, which is the trajectory of one of the free ends of the string. Also, the subset $|z| < t < \sqrt{z^2 + r^2}$ maps bijectively onto the subset $\{(U, V, Z) : U > 0, V > b_+|Z|^{-2}U\}$, where $b_\pm$ is shorthand for $\frac{1}{4}(1 \pm a_0)^2$. The boundary $U = 0$ (with $V > 0$) is, of course, the image of the spherical null surface $t = \sqrt{z^2 + r^2}$, while the other boundary $V = b_+|Z|^{-2}U$ is the image of the surface $t = -z > 0$. The remaining boundary in the original coordinate system, $t = z > 0$ (which includes, in particular, the null line $t = z > 0$ and $r = 0$), is recovered by taking suitably controlled limits with $|Z| \rightarrow \infty$.

Thus, the Minkowski patch defined by $U < 0$ and $V > 0$ and the string patch defined by $U > 0$ and $V > \frac{1}{4}(1+a)^2|Z|^{-2}U$ combine to give a continuous metric which describes the interior of the gravitational wave front $t = \sqrt{z^2 + r^2}$ plus its exterior out to $t = |z|$, as shown schematically in figure 9.2. The spacetime can be completed by extending the string patch (in the original coordinates) to the region $t < |z|$.

The situation in the case $\varepsilon = 1$ is broadly similar. The set $t > \sqrt{z^2 + r^2}$ again maps bijectively onto the quarter space $\{(U, V, Z) : U < 0, V > 0\}$, while the surface $V - U = 0$ lies outside this quarter space and can safely be ignored. (The boundary $V = 0$ corresponds to the spacelike line $z = r = 0$ only.) However, the restrictions on the string patch ($U > 0$) are a bit more elaborate. If $|Z| > 1$ then the patch $\{(U, V, Z) : U > 0, V > (b_-|Z|^{-2} + b_+)\kappa U\}$ maps bijectively onto the upper half ($z > 0$) of the subset $|z| < t < \sqrt{z^2 + r^2}$, while if $0 < |Z| < 1$ the patch $\{(U, V, Z) : U > 0, V > (b_+|Z|^{-2} + b_-)\kappa U\}$ maps bijectively onto the lower half ($z < 0$).

By contrast, the construction breaks down when $\varepsilon = -1$, as the only region of U–V–Z space with $U < 0$ that maps bijectively onto $t > \sqrt{z^2 + r^2}$ is the

---

[4] A time-symmetric version of this solution was independently discovered by Jiri Bičák and Bernhard Schmidt [BS89].

Figure 9.2. (a) The U–V coordinates and (b) the t–z coordinates.

set $\{(U, V, Z) : U < 0, V > -U, |Z| < 1\}$. Thus the Minkowski patch must be bounded by the surface $V = -U > 0$, $|Z| < 1$ (which is the image of $t = \sqrt{z^2 + r^2}$ with $z > 0$) as well as by $U = 0$, $V > 0$, $|Z| < 1$ (which covers the $z < 0$ half of the boundary only). The simple matching proposed in (9.203) is, therefore, incomplete if $\varepsilon = -1$ and needs to be replaced by a more intricate system of coordinate patches.

Subject to the coordinate restrictions mentioned earlier, the metric (9.203) describes a snapping cosmic string when $\varepsilon = 0$ or 1. One useful feature of the construction is that the geometric effect of the shock wave can be calculated directly. A given point (V, Z) on the junction surface $U = 0$ is the image of both a point (u_S, v_S, ξ_S) in the original string spacetime, and a point (u_M, v_M, ξ_M) in the remnant Minkowski spacetime. In particular, since $a_0|\xi| = \kappa^{-1}|Z|V$ when $U = 0$, the horizontal radius r of any point on the shock front satisfies $r_M = a_0 r_S < r_S$. That is, each spacetime point discontinuously 'jumps' towards the string axis as the shock wave passes.
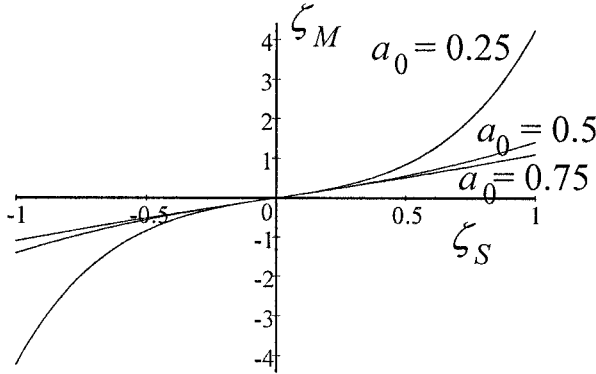
Similarly, since $u/v = |Z|^{2a_0}$ when $U = 0$, it follows that $u_M/v_M = (u_S/v_S)^{1/(2a_0)}$. In terms of r and the height z above the equatorial plane, this relation reads:

$$(z_M^2/r_M^2 + 1)^{1/2} + z_M/r_M = [(z_S^2/r_S^2 + 1)^{1/2} + z_S/r_S]^{1/a_0} \qquad (9.204)$$

and (since $r_M = a_0 r_S$) is easily solved to give $\zeta_M \equiv z_M/r_S$ as a function of $\zeta_S \equiv z_S/r_S$.

Figure 9.3 illustrates the dependence of ζ_M on ζ_S in the cases $a_0 = 0.25$, 0.5 and 0.75. As can be seen, z_M is, in all instances, larger than z_S. Thus the effect of the shock wave is to dilate the spacetime vertically while compressing it horizontally.

Given that the U–V–Z coordinate systems with $\varepsilon = 0$ and $\varepsilon = 1$ cover the same patches of the Minkowski and string spacetimes and the geometry of the shock front is the same in both cases, it is natural to ask what difference there is between the two transformations. The answer lies in the nature of the 'particles'

Figure 9.3. Scaled vertical displacements before (ζ_S) and after (ζ_M) the passage of the shock wave.

that appear at the free ends of the string, on the null lines $t - |z| = r = 0$, where the shock front fails to be smooth.

The only non-zero physical components of the Riemann tensor (modulo symmetries) are:

$$R^V{}_{ZU}{}^{Z^*} = (R^V{}_{Z^*U}{}^Z)^* = -\tfrac{1}{8}g^{-1/2}(1-a_0^2)V|Z|^{-4}Z^{*2}[2H'(U) + UH''(U)] \tag{9.205}$$

and

$$R^V{}_{ZU}{}^Z = R^V{}_{Z^*U}{}^{Z^*} = \tfrac{1}{32}g^{-1/2}(1-a_0^2)^2\kappa^2|Z|^{-4}UH(U)[2H'(U) + UH''(U)] \tag{9.206}$$

where the volume factor in U–V–Z coordinates is

$$g^{1/2} = \tfrac{1}{4}\kappa^{-2}|V^2 - \tfrac{1}{16}(1-a_0^2)^2\kappa^4|Z|^{-4}U^2H(U)|. \tag{9.207}$$

In terms of the Dirac δ-distribution, $2H'(U) + UH''(U) = \delta(U)$ and (it is often loosely asserted, although there is no formal justification in distribution theory) $H(U)\delta(U) = \tfrac{1}{2}\delta(U)$.

The physical components of the Riemann tensor are, therefore, non-zero only on the junction surface $U = 0$. On this surface $g^{1/2} = \tfrac{1}{4}\kappa^{-2}V^2$ and it would appear (as Hogan [Hog94] and Podolský and Griffiths [PG00] claim) that the Riemann tensor has a physical singularity on the wave front at $V = 0$. However, this is not a physical singularity but a coordinate singularity induced by the vanishing volume factor $g^{1/2}$. Indeed, in view of the distributional nature of the Riemann components, what is important is not the behaviour of the bare components themselves, but the convergence of integrals of the form $\int g^{1/2}R^\mu{}_{\kappa\lambda}{}^\nu \, \mathrm{d}^4x$ on appropriate subsets of U–V–Z space.

When $\varepsilon = 0$, the null line $t + z = r = 0$ (the 'south pole' of the shock front) corresponds to the limit $|Z| \to 0$, $U \sim |Z|^{1+a_0} \to 0$ and

$V \sim |Z|^{a_0-1} \rightarrow \infty$ in the string patch, and thus $V|Z|^{-4}Z^{*2}$ and $\kappa^2|Z|^{-4}U$ diverge as $|Z|^{a_0-3}$. Integrating $g^{1/2}R^V{}_{ZU}{}^{Z^*}$ or $g^{1/2}R^V{}_{ZU}{}^{Z}$ over the 'south pole' is, therefore, problematic. However, the null line $t - z = r = 0$ (the 'north pole') corresponds to the limit $V \rightarrow 0$ together with $U \rightarrow -2z$ in the Minkowski patch or $U \rightarrow \infty$ in the string patch. Thus $g^{1/2}R^V{}_{ZU}{}^{Z^*}$ and $g^{1/2}R^V{}_{ZU}{}^{Z}$ are free of singularities over the 'north pole', except perhaps when $z = 0$. This indicates that there is a fundamental asymmetry between the two ends of the string when $\varepsilon = 0$, which, in turn, is attributable to the basic asymmetry between the $z > 0$ and $z < 0$ half-spaces under the transformation $(u, v, \xi) \rightarrow (U, V, Z)$.

By contrast, when $\varepsilon = 1$ there is a manifest symmetry between the north and south ends of the string, as the isometry $z \rightarrow -z$ in the original coordinates corresponds to the mapping $Z \rightarrow W \equiv Z^{*-1}$, and the metric (9.203) is invariant under this additional transformation. The 'south pole' of the shock front corresponds to the limit $|Z| \rightarrow 0$, $U \sim |Z|^{1+a_0} \rightarrow 0$ and $V \sim |Z|^{a_0-1} \rightarrow \infty$ in the string patch, and $V|Z|^{-4}Z^{*2}$ and $\kappa^2|Z|^{-4}U$ again diverge as $|Z|^{a_0-3}$. An identical statement applies to the 'north pole', with Z everywhere replaced by W^*. Thus, the $\varepsilon = 1$ transformation is to be preferred unless there are strong reasons for wanting to break the symmetry between the two ends of the string.

Incidentally, not only is the Riemann tensor singular on the shock front, but so also is the Einstein tensor $G_{\mu\nu}$, which has a single non-zero mixed component:

$$G^V_U = -2R^V{}_{ZU}{}^{Z}. \tag{9.208}$$

Given that $R^V{}_{ZU}{}^{Z} = 0$ everywhere except at the free ends of the string, this fact is consistent with the interpretation that the free ends are, in some sense, null 'particles' with non-zero stress–energy.

9.4.2 Other spacetimes containing snapping strings

There exists an extensive, if somewhat specialized, literature on snapping strings, and the previous discussion gives some idea of the complexities involved. One straightforward extension of the snapping-string metric (9.203) is to add a cosmological constant Λ, so that the template spacetime is either the flat de Sitter ($\Lambda > 0$) or anti-de Sitter ($\Lambda < 0$) space with 'spherical null' line element (9.71). Applying the transformations (9.198)–(9.200) and joining together two patches with differing values of a_0 gives a spacetime

$$ds^2 = [1 + \tfrac{1}{12}\Lambda U(V - \varepsilon U)]^{-2} \, ds^2_{\mathrm{M}} \tag{9.209}$$

(where ds^2_{M} is the line element of (9.203)), which describes a snapping string in a de Sitter or anti-de Sitter background. This construction was first investigated by Hogan [Hog92].

Hogan [Hog93] and Podolský and Griffiths [PG00] have also developed a generalization of the transformations (9.198)–(9.200) which depends on a single

generating function $h(Z)$ and can be used to construct a large class of metrics of the form

$$\mathrm{d}s^2 = \varepsilon\,\mathrm{d}U^2 - \mathrm{d}U\,\mathrm{d}V - |\kappa^{-1}V\,\mathrm{d}Z + \kappa\,\bar{F}(Z)H(U)U\,\mathrm{d}Z^*|^2 \qquad (9.210)$$

where $F(Z) = \frac{1}{2}[(h'''/h') - \frac{3}{2}(h''/h')^2]$. For $U < 0$ the metric (9.210) describes a patch of Minkowski spacetime as before. Its interpretation when $U > 0$ is determined by the analytic properties of the function $h(Z)$. In the case of the single straight-string spacetime analysed in the previous section, $h(Z) = Z^{a_0}$ and $F(Z) = \frac{1}{4}(1 - a_0^2)Z^{-2}$. Spacetimes containing two or more strings can be accommodated by choosing more complicated generating functions.

Podolský and Griffiths [PG00], for example, have constructed a solution describing two orthogonal cosmic strings, which are initially at rest and snap at their crossover point $z = r = 0$ at time $t = 0$, by taking $h(Z) = [(iZ^{a_1} - 1)/(Z^{a_1} - i)]^{a_2}$, where $\mu_1 = \frac{1}{4}(1 - a_1)$ and $\mu_2 = \frac{1}{4}(1 - a_2)$ are the masses per unit length of the two strings. The corresponding metric function F is

$$F(Z) = \frac{1}{4}(1 - a_1^2)Z^{-2} - a_1^2(1 - a_2^2)(Z^{2a_1} + 1)^{-2}Z^{2(a_1 - 1)}. \qquad (9.211)$$

More complicated solutions which describe snapping strings in relative motion are also known [PG00]. Podolský and Griffiths [PG99] have shown that the general class of metrics (9.210) is equivalent to certain impulsive limits of type-N Robinson–Trautman solutions, and Griffiths and Docherty [GD02] have used this fact to construct a solution containing a single straight string that 'disintegrates' (meaning that $\mu \to 0$ continuously) instead of snapping.

Finally, mention should be made of an unusual solution which Sean Hayward [Hay89b] has interpreted as a snapping string metric. It involves strings in a Schwarzschild background, and is based on a metric due to Ulvi Yurtsever [Yur88]:

$$\mathrm{d}s^2 = 2(1 + S)^2\,\mathrm{d}U\,\mathrm{d}V - C_+^{-2}(1 - S)^2\,\mathrm{d}x^2 - C_-^2(1 + S)^2\,\mathrm{d}y^2 \qquad (9.212)$$

where $S = \sin[pUH(U) + qVH(V)]$ and $C_\pm = \cos[pUH(U) \pm qVH(V)]$, with p and q positive constants and H again the Heaviside step function.

The Yurtsever solution (9.212) is the metric formed by the collision of two gravitational waves in a vacuum spacetime. It is flat in the region $U, V < 0$, and supports impulsive gravitational shock waves on the null surfaces $U = 0$ and $V = 0$. Most importantly, the region $U, V > 0$ is isometric to a portion of the Schwarzschild metric (with or without a string on axis).

This can be seen by casting y as an angular coordinate with period $2\pi a_0 m$ and making the substitutions

$$\begin{aligned} t = x \qquad & R = m[1 + \sin(pU + qV)] \\ \theta = pU - qV - \pi/2 \quad & \text{and} \quad \phi = y/(a_0 m) \end{aligned} \qquad (9.213)$$

where $m = (2pq)^{-1/2}$. The Yurtsever line element (9.212) then reduces to the Aryal–Ford–Vilenkin line element (9.53) with $1 - 4\mu = a_0$, with the patch

$pU + qV < \pi/2$ mapping bijectively onto some subset of the black hole patch $m < R < 2m$.

Here, the boundary $pU + qV = \pi/2$ corresponds to the black hole horizon $R = 2m$, and by extending the solution across this boundary in the Kruskal–Szekeres coordinate system (9.56)–(9.57) it can be joined smoothly to the white hole and asymptotically-flat* exterior regions of figure 9.1. The other boundaries of the Yurtsever patch, $\{0 < pU < \pi/2, V = 0\}$ and $\{0 < qV < \pi/2, U = 0\}$, describe impulsive gravitational shock waves which propagate *inside* the black hole region of figure 9.1, along the null curves $\{R = m(1 + \cos\theta), 0 < \theta < \pi/2\}$ and $\{R = m(1 - \cos\theta), \pi/2 < \theta < \pi\}$ respectively. The shock waves first appear at the wormhole 'throat' $u = v = 0$ at the antipodal points $\theta = 0$ and $\theta = \pi$, then fall inwards and eventually collide on the equatorial plane ($\theta = \pi/2$) at $R = m$, at the image of the Yurtsever crossover point $U = V = 0$.

The spacetime interior to the shock waves is described by the Yurtsever metric with $0 < pU < \pi/2$ and $V < 0$ (in the northern hemisphere) or $0 < qV < \pi/2$ and $U < 0$ (in the southern hemisphere). Beyond the collision point $U = V = 0$ the spacetime is flat:

$$\mathrm{d}s^2 = 2\,\mathrm{d}U\,\mathrm{d}V - \mathrm{d}x^2 - \mathrm{d}y^2 \tag{9.214}$$

although the coordinate y is compactified with period $2\pi a_0 m$. Thus the full solution seems to describe the snapping of two (north and south) strings at the wormhole 'throat' of an Aryal–Ford–Vilenkin spacetime, the propagation and collision of the resulting shock waves and the formation of a relic compactified flat spacetime.

Of course, the entire process takes place inside the black hole horizon and so would be hidden from an external observer, although anyone who fell into the black hole would cross one of the shock waves before reaching $R = m$. However, the presence of the strings is inessential to the structure of the solution, as the effect of a non-zero μ is simply to rescale the compactification radius of y. The fact that shock waves can appear at the 'throat', collide and evaporate to leave behind a compactified space even in the absence of strings suggests strongly that the strings snap only incidentally, if at all.

Hayward has developed similar solutions describing the disappearance of strings in a Kerr–Newman spacetime [Hay89a] and in a Bertotti–Robinson electromagnetic universe [Hay89b].

Chapter 10

Strong-field effects of zero-thickness strings

As was seen in chapter 9, all known exact self-gravitating string solutions describe infinite strings in a spacetime with a high degree of symmetry. Although solutions of this type do have some heuristic value, their dynamics are, in general, not very interesting. More valuable from the point of view of understanding the gravitational properties of cosmic strings would be a solution with non-trivial (that is, dissipative) time evolution of the world sheet. Especially revealing would be a solution supporting the formation of a cusp. Unfortunately, it seems unlikely that an exact solution of this type—analytic or numerical—will ever be developed using current techniques.

Any exact solution showing non-trivial time evolution would almost certainly need to possess a high degree of spatial symmetry. If the world sheet is assumed to possess a spacelike Killing vector then (in a spacetime which is otherwise empty) the number of candidates immediately reduces to two: the circular loop (see section 4.2.1) and the helical breather (see section 4.1.4). Not surprisingly, most research in this area to date has concentrated on the circular loop. A summary of the known strong-field gravitational effects outside a circular loop is given in sections 10.1 and 10.2.

An alternative approach to the problem of the gravitational field outside a non-straight string has been to examine the near-field (small distance) limit of the vacuum Einstein equations. This method, which is the subject of sections 10.3 and 10.4, is limited by the fact that it is rarely possible to demonstrate that a given near-field solution can be matched to a physically acceptable far-field metric. Nonetheless, one clear result of the near-field approach is that the tidal force (as measured by the physical components of the Riemann tensor) is generally non-zero outside a non-straight string in the wire approximation and may even diverge in the small-distance limit [UHIM89], so that the world sheet marks the location of a curvature singularity rather than just a conical one.

This property, which contrasts strongly with the locally-flat nature of the bare straight-string metric (7.28), has prompted claims that divergent near-field behaviour is the signature of a fundamentally different type of two-dimensional

object [Let92], or conversely that cosmic strings cannot bend [CEV90]. However, as was mentioned in section 9.1, the fact that the travelling-wave metrics (which do support divergent tidal forces) are the zero-thickness limits of known exact vortex solutions of the Einstein–Higgs–Yang–Mills field equations demonstrates that the Riemann tensor can indeed be divergent outside a zero-thickness cosmic string.

A second feature of the near-field expansion of the metric tensor outside a general string world sheet $\mathbf{T}$ is that the extrinsic curvature of the surfaces of constant distance r from $\mathbf{T}$ (which will be defined more precisely in section 10.4.1) vanishes in the limit as $r \to 0$. This means that it is always possible to find a geodesically-generated 2-surface with given proper area which stays arbitrarily close to $\mathbf{T}$, and thus any nearby observer would measure $\mathbf{T}$ to be flat.

This is the second sense in which it is sometimes claimed that *all* zero-thickness cosmic strings are 'straight' [UHIM89]. The effect is similar to the rotational frame-dragging that occurs inside the ergosphere of a Kerr black hole, in that the world sheet 'drags' nearby geodesics so strongly that they are almost parallel to the string. However, the effect would be measurable only at extremely small distances from the world sheet, at distances which in the case of a realistic GUT string would lie well inside the string core, where the wire approximation breaks down.

Nonetheless, the fact that the world sheet of a zero-thickness cosmic string is extrinsically flat begs the question of what is actually meant by a 'non-straight' string. As will be seen in section 10.4.3, two fundamentally different types of gravitational disturbance are possible in the neighbourhood of a zero-thickness string, which I have previously called 'travelling waves' and 'curvature waves' [And99b]. Disturbances of the first type are decoupled from the intrinsic scalar curvature $^{(2)}R$ of the world sheet but can induce a singularity in the Riemann tensor, while disturbances of the second type typically occur only if $^{(2)}R \neq 0$ but are not generally associated with a curvature singularity.

The travelling-wave metrics of section 9.1 support travelling waves only, whereas all other solutions discussed in chapter 9 support curvature waves only. It is more natural to regard the travelling-wave metrics as describing the interaction of pp gravitational waves with straight strings rather than intrinsically non-straight strings, while all the other solutions clearly involve straight strings. The connection between the two types of disturbance and the 'straightness' of the embedded string therefore remains relatively unexplored, although the gravitational response to linearized perturbations about the constant-ε_0 interior solution defined by (7.9) plus (7.12) has recently been analysed in [NII00] and [NI01].

Finally, in section 10.4.4 I show that the near-field expansions developed here are consistent with the distributional stress–energy content that was argued earlier, in chapters 6 and 7, to be one of the defining features of a zero-thickness cosmic string.

10.1 Spatial geometry outside a stationary loop

A weak-field treatment of the collapse of a circular loop has already been discussed in chapter 6. In this section I will examine the structure of the spatial 3-geometry outside a circular loop at a moment of time symmetry, closely following an analysis of the problem published by Valeri Frolov *et al* in 1989 [FIU89].

If the metric due to a circular cosmic string is written in the ADM form

$$ds^2 = N^2\,dt^2 + g_{ab}(dx^a + N^a\,dt)(dx^b + N^b\,dt) \tag{10.1}$$

where lower-case indices run from 1 to 3 and N and N^a are the lapse and shift functions respectively, then a moment of time symmetry is a surface **S** of constant t with the property that the line element (10.1) is locally invariant with respect to time inversion through **S**. This means that

$$\frac{\partial N}{\partial t} = \frac{\partial g_{ab}}{\partial t} = 0 \qquad \text{and} \qquad N^a = 0 \tag{10.2}$$

on **S**. At a physical level, **S** is the instant in time at which an initially expanding loop reaches its maximum radius before beginning to recollapse.

When projected onto an arbitrary surface of constant t, the components of the Einstein equation take the Gauss–Codazzi form

$$^{(3)}R = 16\pi T_{\mu\nu}n^\mu n^\nu + K_{\mu\nu}K^{\mu\nu} - K^2 \tag{10.3}$$

and

$$\nabla_\nu(K^{\mu\nu} - Kh^{\mu\nu}) = 8\pi T_{\lambda\nu}n^\lambda h^{\mu\nu} \tag{10.4}$$

where $n_\mu = N\delta^t_\mu$ is the unit normal to the 3-surface,

$$h^{\mu\nu} = g^{\mu\nu} - n^\mu n^\nu \tag{10.5}$$

is the projection operator on the surface,

$$K_{\mu\nu} = h^\kappa_{(\mu}h^\lambda_{\nu)}D_\kappa n_\lambda \tag{10.6}$$

is the surface's extrinsic curvature, ∇_μ is the covariant derivative operator on the surface and $^{(3)}R$ is the Ricci scalar associated with ∇_μ.

On the time-symmetric surface **S** the extrinsic curvature tensor

$$K^{ab} = -\tfrac{1}{2}N^{-1}g^{ac}g^{bd}\left(\nabla_c N_d + \nabla_c N_c - \frac{\partial}{\partial t}g_{cd}\right) \tag{10.7}$$

and its spatial derivatives are zero, and so the constraint equations (10.3) and (10.4) reduce to

$$^{(3)}R = 16\pi T_{\mu\nu}n^\mu n^\nu \tag{10.8}$$

and

$$T_{\lambda\nu}n^\lambda h^{\mu\nu} = 0. \tag{10.9}$$

The second of these simply states that any sources of stress–energy must be stationary on **S**, while the first is the relativistic analogue of Poisson's equation. Equation (10.8) can, in principle, be used to construct the gravitational field outside any momentarily stationary string configuration but for the present it will be specialized to the case of a circular loop.

If cylindrical coordinates (r, ϕ, z) are chosen on **S** then the most general axisymmetric line element has the form

$$g_{ab}\, dx^a\, dx^b = -e^{2(\chi - \psi)}(dr^2 + dz^2) - r^2 e^{-2\psi}\, d\phi^2 \qquad (10.10)$$

where $r \geq 0$, ϕ lies in $[0, 2\pi)$ and χ and ψ are functions of r and z only. The corresponding Ricci scalar is

$$^{(3)}R = 2e^{2(\psi - \chi)}(2\psi_{,rr} + 2\rho^{-1}\psi_{,r} + 2\psi_{,zz} - \psi_{,r}^2 - \psi_{,z}^2 - \chi_{,rr} - \chi_{,zz}) \quad (10.11)$$

and so the constraint equation (10.8) becomes

$$\psi_{,rr} + r^{-1}\psi_{,r} + \psi_{,zz} - \tfrac{1}{2}(\psi_{,r}^2 + \psi_{,z}^2 + \chi_{,rr} + \chi_{,zz}) = 4\pi e^{2(\chi - \psi)} T_{\mu\nu} n^\mu n^\nu. \tag{10.12}$$

The right-hand side of this equation will, of course, be zero everywhere except at the position of the loop.

The residual gauge freedom in the line element (10.10) can be eliminated by requiring that $\chi = O(R^{-2})$ and $\psi \sim -M/R$ for large values of $R = (r^2 + z^2)^{1/2}$, where M is a positive constant. The 3-surface **S** is then asymptotically flat, and M is the instantaneous gravitational mass of the loop. Also, if the string loop lies on the equatorial circle $\{r = a, z = 0\}$ then, in analogy with the isotropic form (7.32) of the bare straight-string metric, it is expected that for small values of $\rho = [(r - a)^2 + z^2]^{1/2}$ the metric function ψ will tend to a finite value ψ_0, while $e^{2(\chi - \psi)} \sim c\rho^{-8\mu}$, where μ is the mass per unit length of the string and c is a positive constant.

The line element (10.10) near the string then becomes

$$g_{ab}\, dx^a\, dx^b \sim -c\rho^{-8\mu}(dr^2 + dz^2) - a^2 e^{-2\psi_0}\, d\phi^2 \qquad (10.13)$$

and so the proper length of the loop is $L = 2\pi a e^{-\psi_0}$. Also, substituting the asymptotic expansion

$$\chi \sim -4\mu \ln \rho \qquad (\rho \ll a) \qquad (10.14)$$

into the equation (10.12) for the stress–energy tensor of the source gives

$$T_{\mu\nu} n^\mu n^\nu = \mu c^{-1} \rho^{8\mu} \delta^{(2)}(r - a, z). \qquad (10.15)$$

Now, if equation (10.12) is integrated over the volume bounded on the outside by a sphere S_1 with R large and on the inside by a torus T_1 with ρ small,

using the Euclidean volume element $dV = r\,dr\,d\phi\,dz$, then

$$\tfrac{1}{2}\int (\psi,_\rho^2 +\psi,_z^2)\,dV = \int_{S_1}(\nabla\psi - \tfrac{1}{2}\nabla\chi)\cdot d\mathbf{S} - \int_{T_1}(\nabla\psi - \tfrac{1}{2}\nabla\chi)\cdot d\mathbf{S}$$
$$+ \pi\int_{S_1}\chi\,dz - \pi\int_{T_1}\chi\,dz \tag{10.16}$$

where ∇ is the standard cylindrical gradient operator.

In view of the boundary conditions in the limit as $R \to \infty$ and $\rho \to 0$, this equation reduces to

$$\tfrac{1}{2}\int (\psi,_r^2 +\psi,_z^2)\,dV = 4\pi M - 8\pi^2\mu a. \tag{10.17}$$

Thus, the gravitational mass M of the loop is related to its local properties and the field ψ by

$$M = \mu L e^{\psi_0} + (8\pi)^{-1}\int (\psi,_r^2 +\psi,_z^2)\,dV. \tag{10.18}$$

The second term on the right of (10.18) reflects the contribution of free gravitational radiation to the total mass of the loop as measured by a distant observer. Because the constraint equation (10.12) contains two independent fields χ and ψ there is a limitless range of possible solutions even when the source parameters μ and L are fixed, each corresponding to a different axisymmetric distribution of gravitational radiation on $\mathbf{S}$. It might be thought that one way to resolve this ambiguity would be to require that $\mathbf{S}$ be free of gravitational radiation, in the sense that the gravitational mass M take the smallest possible value for given values of μ and L. However, Frolov *et al* [FIU89] have shown that there exist sequences of solutions in which μ and L are fixed but M can be chosen to be arbitrarily close to zero. Thus there is no direct relationship between the properties of the near-field and far-field solutions.

In the absence of any obvious physical criteria for singling out a particular class of solutions, Frolov *et al* have instead investigated two families of solutions notable for their mathematical tractability. Both families are most compactly described in terms of toroidal coordinates (ξ, η), defined implicitly by
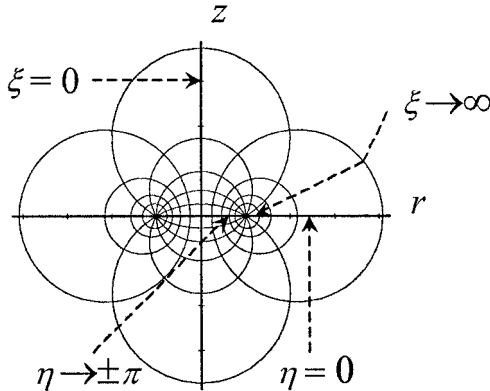
$$r = a(\cosh\xi - \cos\eta)^{-1}\sinh\xi \tag{10.19}$$

and

$$z = a(\cosh\xi - \cos\eta)^{-1}\sin\eta \tag{10.20}$$

with $\eta \in (-\pi, \pi]$ and $\mathrm{sgn}(\eta) = \mathrm{sgn}(z)$.

The equatorial plane corresponds to $\eta = 0$ (for $r > a$) and $\eta \to \pm\pi$ (for $r < a$ with $z \to 0^\pm$ respectively), while the axis of rotational symmetry is $\xi = 0$ (see figure 10.1). Each surface of constant ξ is a torus enclosing the equatorial circle $r = a$, with the circle itself corresponding to the limit $\xi \to \infty$. Near the

Figure 10.1. The toroidal coordinate system.

circle, $\rho \sim 2a e^{-\xi}$, and so the near-field geometry will be string-like if $\chi \sim 4\mu\xi$ for large ξ.

The first of the two classes of solutions constructed by Frolov *et al* is chosen to have

$$\chi = \begin{cases} 4\mu(\xi - \xi_0) & \xi > \xi_0 \\ 0 & \xi < \xi_0 \end{cases} \tag{10.21}$$

where ξ_0 is an arbitrary positive constant. Hence,

$$\begin{aligned} \chi_{,rr} + \chi_{,zz} &= a^{-2}(\cosh\xi - \cos\eta)^2(\chi_{,\sigma\sigma} + \chi_{,\eta\eta}) \\ &= 4\mu a^{-2}(\cosh\xi - \cos\eta)^2 \delta(\xi - \xi_0) \end{aligned} \tag{10.22}$$
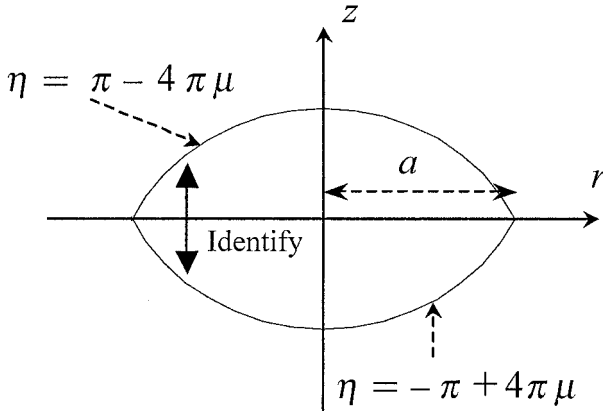
and so the solution is characterized by an impulsive gravitational wavefront on the toroidal surface $\xi = \xi_0$.

The remaining metric function, ψ, is fixed by the constraint equation (10.12) and can be expressed as an infinite series of toroidal harmonics [FIU89]. It turns out that ψ is well defined if ξ_0 is smaller than a critical value ξ_{crit} which depends only on the mass per unit length μ of the string. One interesting feature of the solutions, alluded to earlier, is that as $\xi_0 \to \xi_{\text{crit}}$ the ratio $M/(\mu L)$ of the gravitational mass of the string to its local mass tends to zero. Thus, the effect of the impulsive toroidal wavefront is, in some sense, to mask the far gravitational field of the string.

The second class of solutions has a more geometrical flavour. Starting with the metric of a conformally-flat 3-surface in toroidal coordinates

$$ds_{\text{cf}}^2 = -a^2\omega^4(d\xi^2 + d\eta^2 + \sinh^2\xi \, d\phi^2) \tag{10.23}$$

with a conformal factor $\omega(\xi, \eta)$, Frolov *et al* excised the discus-shaped wedge bounded above by the surface $\eta = \pi - 4\pi\mu$ and below by the surface $\eta = -\pi + 4\pi\mu$, and then glued the exposed faces together, as shown in figure 10.2.

Figure 10.2. Excising the wedge $-\pi + 4\pi\mu < \eta < \pi - 4\pi\mu$.

The extrinsic curvature of the exposed faces has components

$$K_{\xi\xi} = 2a\omega\omega_{,\eta} \qquad \text{and} \qquad K_{\phi\phi} = 2a\omega\omega_{,\eta} \sinh^2 \xi \qquad (10.24)$$

and so the faces have a matching extrinsic geometry if $\omega_{,\eta} = 0$ at $\eta = \pm(\pi - 4\pi\mu)$. This, in turn, is guaranteed if the conformal factor ω is a smooth, periodic and even function of the rescaled angular coordinate

$$\eta_* = (1 - 4\mu)^{-1}\eta \qquad (10.25)$$

which ranges over $(-\pi, \pi]$.

Because the metric of a *flat* 3-surface in toroidal coordinates has $\omega = (\cosh\xi - \cos\eta)^{-1/2}$, the conformally-flat metric (10.23) will be locally isometric to the spatial section of the straight-string metric (7.28) in the neighbourhood of the string if

$$\omega \sim (\cosh\xi - \cos\eta_*)^{-1/2} \qquad (10.26)$$

for large values of ξ. In addition, ω must satisfy the constraint equation
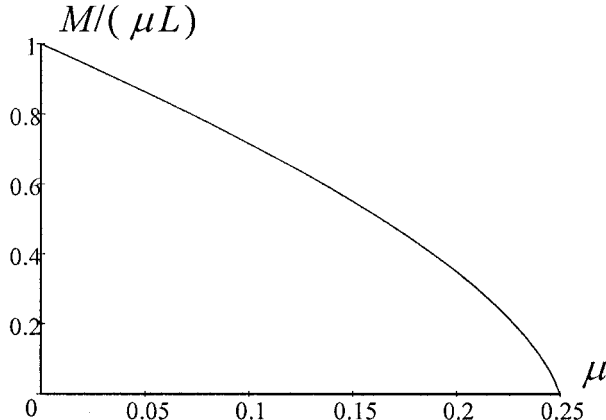
$$^{(3)}R = -2a^{-2}\omega^{-4}[1 + 4\omega^{-1}(\omega_{,\xi\xi} + \coth\xi\,\omega_{,\xi} + \lambda^2\omega_{,\eta_*\eta_*})] = 0 \qquad (10.27)$$

where $\lambda \equiv (1 - 4\mu)^{-1}$. The required solution has been constructed by Frolov *et al*, and is most conveniently written in the form

$$\omega(\xi, \eta_*) = \pi^{-1} \int_\xi^\infty \frac{d\tau}{(\cosh\tau - \cosh\xi)^{1/2}} \frac{\sinh\lambda\tau}{\cosh\lambda\tau - \cos\eta_*}. \qquad (10.28)$$

Note here that in the limit $\lambda \to 1$ the metric is flat, and so the integral in (10.28) reduces to $(\cosh\xi - \cos\eta)^{-1/2}$ when $\lambda = 1$. Furthermore, for large values of the spherical radius R,

$$(\xi^2 + \eta^2)^{1/2} \sim 2a\,R^{-1} \qquad (10.29)$$

Figure 10.3. The ratio $M/(\mu L)$ as a function of μ.

and so spacelike infinity corresponds to the limit ξ, $\eta_* \to 0$. From equation (10.28) it is easily verified that in this limit

$$\omega \sim \lambda^{-1}(\cosh \xi - \cos \eta)^{-1/2} + 2^{1/2}\pi^{-1}\lambda^{-1}I(\lambda) \qquad (10.30)$$

where

$$I(\lambda) = \int_0^\infty \operatorname{cosech} x\,(\lambda \coth \lambda x - \coth x)\,\mathrm{d}x. \qquad (10.31)$$

Now, in terms of the original cylindrical coordinates r and z, the line element at spacelike infinity reads:

$$\begin{aligned}
\mathrm{d}s_{\mathrm{cf}}^2 &= -\omega^4(\cosh \xi - \cos \eta)^2(\mathrm{d}r^2 + \mathrm{d}z^2 + r^2\,\mathrm{d}\phi^2) \\
&\approx -\lambda^{-4}[1 + 8a\pi^{-1}I(\lambda)/R](\mathrm{d}r^2 + \mathrm{d}z^2 + r^2\,\mathrm{d}\phi^2) \qquad (10.32)
\end{aligned}$$

and so the proper asymptotic distance from the origin is $R_{\mathrm{prop}} = \lambda^{-2}R$, while the gravitational mass M is

$$M = 4a\pi^{-1}\lambda^{-2}I(\lambda). \qquad (10.33)$$

Also, the local mass of the string is $\mu L = 2\pi \mu a \equiv \frac{1}{2}\pi a\lambda^{-1}(\lambda - 1)$, and so the ratio of gravitational-to-local mass is

$$M/(\mu L) = 8\pi^{-2}\lambda^{-1}(\lambda - 1)^{-1}I(\lambda). \qquad (10.34)$$

As $\lambda \to 1$ (the weak-field limit) the mass ratio goes to 1, as would be expected. However, as λ increases the mass ratio declines monotonically, and tends to zero like $4\pi^{-1}\lambda^{-1}\ln \lambda$ as $\lambda \to \infty$ (which corresponds to the critical angle deficit limit $\Delta\theta \equiv 8\pi \mu = 2\pi$). The dependence of $M/(\mu L)$ on the bare string mass per unit length μ is shown in figure 10.3.

10.2   Black-hole formation from a collapsing loop

Given the degree of complexity evident even in the construction of the 3-surface outside a circular cosmic string at a moment of time symmetry, it is unlikely that an exact solution for a collapsing loop will ever be developed. This is a great pity, given the interesting and—almost certainly—pathological behaviour that is expected of a string loop as it collapses to a point.

The trajectory of a circular loop in Minkowski spacetime was discussed in chapter 3, and the equation of the world sheet in the aligned standard gauge was seen to be

$$X^{\mu}(\tau, \sigma) = R_0[\tau, \cos\tau\cos\sigma, \cos\tau\sin\sigma, 0] \qquad (10.35)$$

where R_0 is the initial radius of the loop, and σ ranges from 0 to 2π. The loop collapses to a point at the origin at $\tau = \pi/2$, and the 4-velocity of the string as measured by a local observer

$$V^{\mu} = R_0^{-1}X^{\mu}{}_{,\tau} = [1, -\sin\tau\cos\sigma, -\sin\tau\cos\sigma, 0] \qquad (10.36)$$

is asymptotically null, as $V^2 = \cos^2\tau$.

The likely fate of a realistic (that is, self-gravitating and quantum-mechanical) loop when it collapses to a point was the subject of sustained if minor interest throughout the 1980s. The possibilities included the naive view that the string would pass through itself and re-expand, that it would unwind and dissipate, and that it would trigger the formation of an event horizon and ultimately a black hole. The question was finally resolved by Stephen Hawking in 1990, who used a simple geometric analysis of the problem to argue that a circular loop would form an event horizon after radiating away at most 29% of its original energy [Haw90].

If $\mathbf{T}$ again denotes the world sheet of the loop, then in the neighbourhood of the collapse event $\mathbf{T}$ will be effectively null. Furthermore, in the absence of other sources of stress–energy or gravitational radiation the spacetime $\mathbf{M}$ will be flat outside the future $J^+(\mathbf{T})$ of $\mathbf{T}$. If a cylindrical coordinate system $x^{\mu} = (t, r, \phi, z)$ is used to describe the flat region $\mathbf{M} - J^+(\mathbf{T})$, with the collapse event at $t = 0$, then near the moment of collapse $\mathbf{T}$ will trace out the null 2-surface $\{r = -t, z = 0\}$, with $t < 0$.

Let $v = t + r$ be a null coordinate which is zero on $\mathbf{T}$. Then $n_{\mu} = v_{,\mu}$ is a null vector tangent to $\mathbf{T}$, and the stress–energy tensor of the string loop has the form

$$T_{\mu\nu} = sn_{\mu}n_{\nu}\delta(v)\delta(z) \qquad (10.37)$$

where s is a scalar field. The energy conservation equation $D^{\nu}T_{\mu\nu} = 0$, therefore, reduces to

$$s_{,r} + r^{-1}s = 0 \qquad (10.38)$$

and so $s = k/r$ for some constant k, a result which is any case evident from the geometry of the problem.

Consider now the collapsing null spherical shell **N** inscribed by **T**, which in spherical coordinates (t, R, ϕ, θ) has the equation $R = -t$, again with $t < 0$. According to the well-known singularity theorems of Penrose and Hawking [HE73], the string loop will collapse to form a singularity if a trapped surface appears. A trapped surface is a closed 2-surface with the property that both the ingoing and outgoing families of normal null geodesics are non-diverging. Let **C** be the closed 2-surface formed by the intersection of the spherical shell **N** with a general smooth surface $R = h(\theta)$, where h is symmetric about the equatorial plane $(\theta = \pi/2)$, and $h(\pi/2) = r_0$ for some fixed constant r_0. The equatorial cross section of **C** is then the position of the string at time $t = -r_0$.

The 2-surface **C** is spanned by the unit vectors

$$\tau^\mu = R^{-1}h_{,\theta}\,(\delta_t^\mu - \delta_R^\mu) - R^{-1}\delta_\theta^\mu \qquad \text{and} \qquad \sigma^\mu = (R\sin\theta)^{-1}\delta_\phi^\mu \quad (10.39)$$

and so to within a scale factor the vector tangent to the outward null geodesics orthogonal to **C** is:

$$q^\mu = \tfrac{1}{2}(1 + R^{-2}h_{,\theta}^2)\delta_t^\mu + \tfrac{1}{2}(1 - r^{-2}h_{,\theta}^2)\delta_R^\mu - R^{-2}h_{,\theta}\,\delta_\theta^\mu. \quad (10.40)$$

The corresponding geodesic expansion Θ is:

$$\Theta = -(\tau^\mu\tau^\nu + \sigma^\mu\sigma^\nu)D_\mu q_\nu = \tfrac{1}{2}R^{-1} - R^{-2}h_{,\theta\theta} + \tfrac{3}{2}R^{-3}h_{,\theta}^2. \quad (10.41)$$

In general Θ will be positive and of order R^{-1} but the stress–energy of the string loop will cause any geodesics passing through it to reconverge, with the net effect on Θ given by Raychaudhuri's equation:

$$q^\mu\Theta_{,\mu} = -\tfrac{1}{2}\Theta^2 + 2\omega^2 - 2\sigma^2 - 8\pi T_{\mu\nu}q^\mu q^\nu \quad (10.42)$$

where ω is the rotation and σ the shear of the geodesic congruence. Because **C** is axisymmetric the congruence is actually shear-free but for the purposes of the analysis it is necessary only that Θ, ω and σ be bounded on **C**.

If equation (10.42) is integrated an infinitesimal distance forward across **C** then because $\delta_R^\mu = \delta_r^\mu$ on the equatorial plane and $q^t + q^R = 1$, the expression $q^\mu\Theta_{,\mu}$ is equivalent to $d\Theta/dv$ for equatorial geodesics. Furthermore, since $n^\mu q_\mu = 1$,

$$T_{\mu\nu}q^\mu q^\nu = k\delta(v)\delta(z)/r_0 \quad (10.43)$$

on **C**, and so the net change in Θ in crossing **C** is

$$\Delta\Theta = -8\pi k\delta(z)/r_0. \quad (10.44)$$

Suppose now that the function h defining **C** is smoothly deformed to give a sequence of functions which converge pointwise to

$$h_0(\theta) = r_0(1 + |\cos\theta|)^{-1}. \quad (10.45)$$

The closed 2-surface $\mathbf{C}_0$ corresponding to h_0 is the intersection of the spherical shell $\mathbf{N}$ with the two null hyperplanes satisfying the equation $-t + |z| = r_0$. Geometrically, $\mathbf{C}_0$ consists of two paraboloid caps glued together on the equatorial circle $r = -t = r_0$, where the hyperplanes cross.

Since $\mathbf{C}_0$ is constructed from sections of hyperplanes, it is clear that $\Theta = 0$ everywhere on $\mathbf{C}_0$ except possibly the equatorial plane. (Alternatively, this can be verified by substituting h_0 into equation (10.41) above.) Also, $h_{0,\theta}$ has the values r_0 just above the equatorial plane and $-r_0$ just below it. From equation (10.41) therefore, the geodesic expansion on $\mathbf{C}_0$ is:

$$\Theta = 2r_0^{-1}\delta(\theta - \pi/2) = 2\delta(z). \tag{10.46}$$

The net expansion $\Theta + \Delta\Theta$ will, therefore, be zero and the surface $\mathbf{C}_0$ marginally trapped, if $r_0 = 4\pi k^1$.

The physical significance of this result is that if $\mu \sim 10^{-6}$ is the mass per unit length of the string (in Planck units) and r_l is a characteristic dimension of the loop—for example, its radius at maximum expansion—then a trapped surface will form about the loop when it has shrunk to a radius $r = 4\pi\mu r_l \sim 10^{-5}r_l$. Furthermore, if the hypothesis of Cosmic Censorship holds then an event horizon will form about the loop, whose final state according to the No-Hair Theorem will be a Schwarzschild black hole. By the Second Law of Black Hole Thermodynamics, the area of this black hole will be bounded below by the area of the trapped surface $\mathbf{C}_0$, which is

$$A(\mathbf{C}_0) = 2\pi \int r|\mathrm{d}t^2 - \mathrm{d}r^2 - \mathrm{d}z^2|^{1/2} = 4\pi \int_0^{r_0} r\,\mathrm{d}r = 2\pi r_0^2 \tag{10.47}$$

where the line element on $\mathbf{C}_0$ reduces to $\mathrm{d}r$ because $-t + |z| = \rho_0$ and so $\mathrm{d}t^2 = \mathrm{d}z^2$.

The mass of the final black hole, therefore, satisfies

$$M_f \geq \sqrt{A(\mathbf{C}_0)/16\pi} = r_0/\sqrt{8}. \tag{10.48}$$

By contrast, the mass of the string loop at large radius is

$$M_i = 2\pi \int T_t^t r\,\mathrm{d}r\,\mathrm{d}z = 2\pi k = r_0/2 \tag{10.49}$$

---

[1] This argument, which effectively depends on the cancellation of two distributional quantities, Θ and $\Delta\Theta$, can be made more rigorous by smearing out the string's stress–energy tensor along $\mathbf{C}$. For example, if equation (10.37) is replaced with

$$T_{\mu\nu} = sn_\mu n_\nu \delta(t+r)\varepsilon^{-1}\Phi(\varepsilon^{-1}z)$$

where Φ is any even smooth function with support on $[-1, 1]$ and ε is a positive constant, then in the limit as $\varepsilon \to 0$ the value of $\Delta\Theta$ integrated over z along $\mathbf{C}$ tends to $-8\pi k/r_0$. Similarly, from (10.41) the integrated expansion Θ in the limit as $h \to h_0$ is 2.

and so the maximum energy that can be radiated away in the form of gravitational waves during the course of the collapse is

$$M_i - M_f \leq (1 - 1/\sqrt{2})M_i \tag{10.50}$$

or 29.3% of the initial mass.

Claude Barrabès [Bar91] has generalized this result to include loops with a 'stadium' geometry (that is, in the shape of a pair of semi-circles connected by straight-line segments) which are collapsing at the speed of light. The maximum energy that can be radiated away is then about 33% of the initial mass but this bound is little more than a mathematical curiosity, as no cosmic string with stadium geometry obeying the Nambu–Goto equations of motion would collapse to a singular line in the manner envisaged by Barrabès.

10.3   Properties of the near gravitational field of a cosmic string

Another line of approach to the problem of understanding the gravitational properties of a string loop is to analyse the gravitational field in the vicinity of the world sheet. This was first done in detail by Unruh *et al* in 1989 [UHIM89], although some preliminary versions of their results were developed by Sokolov and Starobinskii [SS77] and Clarke *et al* [CEV90].

As usual, let the world sheet of a general string configuration be a two-dimensional manifold $\mathbf{T}$. Following Unruh *et al* it is assumed that $\mathbf{T}$ is equipped with a smooth metric tensor γ_{AB} (where A, B ... range from 0 to 1). Let Γ be a fixed timelike geodesic on $\mathbf{T}$ and t the proper distance along Γ from an arbitrary reference point. If z is chosen to be the proper distance from Γ along the family of spacelike geodesics on $\mathbf{T}$ which intersect Γ orthogonally, then with $\zeta^A = (t, z)$ the intrinsic metric in the neighbourhood of any point $\mathfrak{p}$ on Γ has the form $\gamma_{AB} = \text{diag}(1, -1)$ plus terms of order z^2.

In order to construct a full four-dimensional coordinate system in the neighbourhood of $\mathfrak{p}$ Unruh *et al* appealed to the existence of a family of geodesically-generated spacelike 2-surfaces $\{\mathbf{N_q}\}$ with the properties that

(i)   each surface $\mathbf{N_q}$ intersects the world sheet at a point $\mathfrak{q} = (t, z)$ on $\mathbf{T}$; and
(ii) if a general point on $\mathbf{N_q}$ is identified by the coordinates $x^\mu = (t, z, r, \phi)$, where r is the geodesic distance along $\mathbf{N_q}$ from $\mathfrak{q}$ and $\phi \in [0, 2\pi)$ is a suitably-chosen angular coordinate, then near $\mathfrak{p}$ the line element reads:

$$ds^2 \approx dt^2 - dz^2 - dr^2 - a_0^2 r^2 \, d\phi^2 \tag{10.51}$$

where $a_0 < 1$ is a constant.

The asymptotic form (10.51) of the line element is, of course, modelled on the metric (7.28) outside an infinite straight string. Unruh *et al* envisaged the

surfaces $\mathbf{N_q}$ being generated by spacelike geodesics which intersect the world sheet $\mathbf{T}$ 'orthogonally' but since the line element (10.51) has a conical singularity and, therefore, no well-defined tangent space at $\mathbf{T}$ the definition of an 'orthogonal' geodesic is somewhat problematic. For the moment $\mathbf{N_q}$ will be restricted only by the requirement that the $dr \, d\zeta^A$ and $d\phi \, d\zeta^A$ cross terms that would appear at higher order in (10.51) go to zero sufficiently rapidly that they can be ignored as $r \to 0$. As will be seen in section 10.4.1—where the assumptions made here are given a more rigorous justification—this means in practice that the cross terms should be of order r^2.

In parallel with the analysis of section 7.2, the metric near $\mathfrak{p}$ can be reduced to a more convenient form by replacing the geodesic radius r with the isotropic radius $\rho = (a_0 \, r)^{1/a_0}$. The near-field line element (10.51) then becomes:

$$ds^2 \approx dt^2 - dz^2 - \rho^{-8\mu}(dx^2 + dy^2) \tag{10.52}$$

where $x = \rho \cos\phi$, $y = \rho \sin\phi$ and $\mu = \frac{1}{4}(1 - a_0)$. In what follows, I will abbreviate (x, y) as x^i, where the indices $i, j, \ldots$ range from 2 to 3.

The structure of the Riemann tensor near the world sheet is, of course, determined by terms of higher order than those appearing in (10.52). In order to calculate the effect of such terms, the full metric will be taken to have the ADM form (10.1), with the important proviso that the shift function N^a is assumed to be small enough that it can be ignored to leading order. Following the notation of section 10.1, the acceleration of the unit vector $n_\mu = N\delta_\mu^t$ normal to the surfaces of constant t is

$$a_\mu \equiv n^\lambda D_\lambda n_\mu = N^{-1}(n^\lambda N_{,\lambda} \, n_\mu - N_{,\mu}). \tag{10.53}$$

Because n_μ is tangent to the world-sheet geodesic Γ the only non-zero components of the acceleration vector in the limit $r \to 0$ (with z small) will be a_x and a_y.

Now, the components R_{atbt} of the Riemann tensor can be decomposed in the form

$$h_\rho^\kappa h_\sigma^\mu R_{\kappa\lambda\mu\nu} n^\lambda n^\nu = h_\rho^\kappa h_\sigma^\lambda n^\mu D_\mu K_{\kappa\lambda} + a_\rho a_\sigma - \nabla_\rho a_\sigma + K_\rho^\mu K_{\mu\sigma} \tag{10.54}$$

where $h_{\mu\nu}$ is the projection operator and $K_{\mu\nu}$ the extrinsic curvature tensor on the surfaces of constant t, as before. If it is assumed that $K_{\mu\nu}$ and a_μ are differentiable functions of t, z and the coordinates x^i spanning the surfaces $\mathbf{N_q}$, then the only singular term on the right of (10.54) is $-\nabla_\rho a_\sigma$. Using the connection generated by the near-field line element (10.52), it is easily seen that the only divergent components of R_{atbt} are

$$R_{itjt} \sim -\nabla_i a_j \sim -4\mu\rho^{-2}(\delta_{ik} x^k \bar{a}_j + \delta_{jk} x^k \bar{a}_i - \bar{a}_k x^k \delta_{ij}) \tag{10.55}$$

where $\bar{a}_i$ denotes the value of $a_i = (a_x, a_y)$ in the limit $r \to 0$.

If the foregoing analysis is now repeated with Γ chosen to be the spacelike geodesic parametrized by z which passes through $\mathfrak{p}$ and the roles of the coordinates t and z reversed, then in exactly the same way the tidal components R_{azbz} can be shown to include the divergent terms

$$R_{izjz} \sim -\nabla_i b_j \sim -4\mu\rho^{-2}(\delta_{ik}x^k\bar{b}_j + \delta_{jk}x^k\bar{b}_i - \bar{b}_k x^k \delta_{ij}) \tag{10.56}$$

where b_μ is the acceleration of the unit vector normal to the surfaces of constant z, and $\bar{b}_i$ is the limiting value of b_i. Thus, R_{itjt} and R_{izjz} both diverge as $\rho^{-1} \sim r^{-1/a_0}$, and their physical components diverge as $\rho^{8\mu-1} \sim r^{-2+1/a_0}$. Despite this divergence, however, the Ricci components R_{tt} and R_{zz} remain finite as $r \to 0$, as the contractions of the expressions on the right of (10.55) and (10.56) with $g^{ij} = -\rho^{8\mu}\delta^{ij}$ are identically zero[2].

The divergent terms $\nabla_i a_j$ and $\nabla_i b_j$ also contribute to the Ricci components R_{ij}. The projection of the Ricci tensor tangent to the surfaces of constant t can be written in the Gauss–Codazzi form

$$h^\kappa_\rho h^\lambda_\sigma R_{\kappa\lambda} = {}^{(3)}R_{\rho\sigma} + h^\kappa_\rho h^\lambda_\sigma n^\mu D_\mu K_{\kappa\lambda} + a_\rho a_\sigma - \nabla_\rho a_\sigma + K K_{\rho\sigma} \tag{10.57}$$

and if $K_{\mu\nu}$ and a_μ are again assumed to be differentiable functions of t, z and x^i then the only divergent terms on the right of (10.57) are ${}^{(3)}R_{\rho\sigma}$ and $-\nabla_\rho a_\sigma$. The asymptotic form of ${}^{(3)}R_{\rho\sigma}$ could, in principle, be calculated directly but a more elegant method is to again reverse the roles of t and z and note that the analogue of (10.57) contains $\nabla_\rho b_\sigma$ in place of $-\nabla_\rho a_\sigma$.

Thus,

$$R_{ij} \sim \nabla_i b_j - \nabla_i a_j \sim 4\mu\rho^{-2}[\delta_{ik}x^k(\bar{b}_j - \bar{a}_j) + \delta_{jk}x^k(\bar{b}_i - \bar{a}_i) - (\bar{b}_k - \bar{a}_k)x^k\delta_{ij}] \tag{10.58}$$

and the stress–energy tensor will remain bounded near the string only if $\bar{b}_i = \bar{a}_i$. Indeed, the physical components of R_{ij} will remain bounded only if $b_i - a_i$ goes to zero at least as rapidly as $\rho^{1-8\mu} \sim r^{2-1/a_0}$.

The constraint $\bar{b}_i = \bar{a}_i$ is an expression of the fact that the world sheet **T** must have zero mean curvature[3], which was earlier (in section 2.2) seen to be a consequence of the equation of motion in the absence of gravitational back-reaction. In terms of the metric components the equation (10.53) for the acceleration vector a_μ and its analogue for b_μ indicate that

$$g_{tt} \sim 1 - 2\bar{a}_i x^i \qquad \text{and} \qquad g_{zz} \sim -(1 + 2\bar{b}_i x^i) \tag{10.59}$$

[2] The divergence of the Riemann tensor near a general string world sheet was discovered independently by Clarke *et al* [CEV90], although they assumed that the tidal tensor must remain bounded near a string and, as a result, claimed that strings could not bend on anything smaller than a cosmological scale.

[3] Or more accurately that the mean curvature scalars $K_{(i)} = p^{\lambda\nu}D_\lambda n_{(i)\nu}$ of the surfaces of constant r must go to zero as r tends to zero, where $n^\nu_{(i)} \approx \rho^{4\mu}\delta^\nu_i$ ($i = 2, 3$) are the unit vectors normal to the surfaces and $p^{\lambda\nu} \approx g^{\lambda\nu} + \delta^{ij}n^\lambda_{(i)}n^\nu_{(j)}$ is the projection operator along the surfaces. Near the world sheet, $K_{(i)} \approx \rho^{4\mu}(\bar{b}_i - \bar{a}_i)$ and the result follows.

for small r, and so (since $\bar{b}_i = \bar{a}_i$) neighbouring spacelike-separated surfaces $\mathbf{N_q}$ diverge with increasing distance from the world sheet if $\bar{a}_i > 0$ and converge if $\bar{a}_i < 0$.

Another interesting property is that the magnitudes a and b of the acceleration vectors a_i and b_i tend to zero as $\rho^{4\mu}$ (or faster):

$$a \sim b \sim \rho^{4\mu}(\delta^{ij}\bar{a}_i\bar{a}_j)^{1/2} \qquad (10.60)$$

which, in turn, means that all spacelike and timelike geodesics on the world sheet $\mathbf{T}$ are also geodesics of the full four-dimensional spacetime $\mathbf{M}$. The world sheet is, therefore, a totally-geodesic submanifold of $\mathbf{M}$, a fact which led Unruh *et al* [UHIM89] to declare that all string loops are necessarily straight. In physical terms, there exists a family of geodesics in the neighbourhood of $\mathbf{T}$ which trace the contours of the world sheet and so at the level of geodesic structure (although not of the tidal forces) the world sheet is indistinguishable from a flat manifold. However, this effect would not be observable near a realistic cosmic string, because with $\mu \sim 10^{-6}$ the conformal factor $\rho^{4\mu}$ appearing in (10.60) would remain of order unity until well inside the string core.

The analysis given here of the near gravitational field of a string has been predicated on a number of assumptions, not the least of which is that the acceleration vectors normal to the surfaces of constant t and z are differentiable functions of the coordinates x^i. This assumption might seem somewhat strong but, in fact, all the exact solutions with conical singularities examined in chapter 9 satisfy these assumptions (in many cases with $\bar{a}_i = \bar{b}_i = 0$). So too does the metric on the conformally-flat 3-surface described in section 10.1, where the analogue of the world-sheet coordinate z is the angular coordinate ϕ. The crucial feature of the analysis is not the arbitrary nature of the assumptions (which, in fact, could be taken to be *defining* properties of a general string metric) but that they are consistent with the vacuum Einstein equations $R_{\mu\nu} = 0$. The assumptions are extended and given a more rigorous foundation in the next section.

10.4   A 3 + 1 split of the metric near a cosmic string

10.4.1   General formalism

So far no formal definition has been offered of a general zero-thickness cosmic string metric. Clearly, any proposed definition must be narrow enough to apply only to spacetimes containing a two-dimensional submanifold with distributional stress–energy tensor of the form (6.1) but broad enough to encompass all known exact solutions which have been identified as string metrics. It should be noted that the first requirement specifically excludes metrics containing 'spinning' cosmic strings of the type first introduced by [Maz86], which are endowed with angular momentum and are sheathed by congruences of closed timelike curves (see section 9.3.4).

In this section a general (zero-thickness) cosmic string will be defined to be a line singularity with certain restrictive features. The concept of a line singularity was first given a formal justification in 1977 by Werner Israel [Isr77], who defined a line singularity to be a singular boundary **T** of spacetime with the following properties:

(i)   Each point q in a neighbourhood of **T** can be connected to **T** with a spacelike curve of finite proper length. The spacelike geodesic which extremises the distance from q to **T** will be referred to as a 'radial geodesic', and the distance r from q to **T** along this curve as the 'geodesic distance' to q.

(ii) The surfaces $r =$ constant are 3-cylinders with topology $\mathbb{S} \times \mathbb{R}^2$ (outside an infinite string, for example) or $\mathbb{S} \times \mathbb{S} \times \mathbb{R}$ (outside a string loop).

(iii) Each 3-surface $r =$ constant is surrounded by a congruence of simple, non-reducible closed spacelike curves Γ whose circumference tends to zero as they are Lie-transported inwards to **T** along radial geodesics.

As was done in section 10.3, a natural coordinate system can be erected in a neighbourhood of **T** by labelling each point $\mathfrak{p}$ on **T** with coordinates (t, z) and parametrizing the family of radial geodesics which terminate at $\mathfrak{p}$ with a continuous variable η which ranges from 0 to 2π and is chosen so that each closed curve Γ stipulated by (iii) is a parametric curve of η. Thus, a radial geodesic can be identified by a triple of coordinates $x^a = (t, z, \eta)$, and the coordinates of a point at a geodesic distance r from **T** will be written as $x^\mu = (r, t, z, \eta)$. This coordinate system uniquely identifies spacetime points out to the local radius of curvature of **T**, where neighbouring radial geodesics first begin to cross.

The difference between this coordinatization and the more primitive version used in the previous section is the fact that the radial geodesics are stipulated to extremize the proper distance from **T**. Because r measures the proper distance along a family of spacelike geodesics, the metric tensor $g_{\mu\nu}$ satisfies:

$$g_{rr} = -1 \qquad \text{and} \qquad g_{ar,r} = 0. \tag{10.61}$$

Furthermore, if $x^\mu(r) = (r, x_0^a + \varepsilon \zeta^a(r))$ denotes an arbitrary perturbation of any of the radial geodesics then the distance along this curve to **T** is

$$s(r) = r - g_{ar}(x_0^b)\varepsilon \zeta^a(0) + O(\varepsilon^2) \tag{10.62}$$

and so because the radial geodesics extremise the proper distance to **T**,

$$g_{ar} = 0. \tag{10.63}$$

Thus, instead of the less stringent ADM form (10.1), the line element decomposes into the $3 + 1$ Gaussian normal form:

$$ds^2 = -dr^2 + g_{AB}\,d\zeta^A\,d\zeta^B + 2g_{\eta A}\,d\zeta^A\,d\eta + g_{\eta\eta}\,d\eta^2 \tag{10.64}$$

where again $\zeta^A = (t, z)$ and $A, B \ldots$ range from 0 to 1.

Also, according to property (iii) $g_{\eta\eta} < 0$ and the proper length of each closed curve with r, t and z constant tends to zero as $r \to 0$, so that $\lim_{r\to 0} g_{\eta\eta} = 0$.

The spacelike surface generated by all the radial geodesics which terminate at a given point $\mathfrak{p}$ on the singularity will be denoted $\mathbf{N_p}$, and is spanned by the vectors δ_r^μ and δ_η^μ. In the absence of Killing vectors, the 2-surfaces $\mathbf{N_p}$ provide a natural mechanism for developing an invariant characterization of the angle deficit around $\mathbf{T}$. If $\mathbf{N}$ is any geodesically-generated spacelike surface through a point $\mathfrak{p}$ on $\mathbf{T}$ then the angle deficit $\Delta\theta$ on $\mathbf{N}$ is defined by the Gauss–Bonnet formula

$$\Delta\theta = 2\pi - \lim_{\varepsilon\to 0} \oint_{\gamma_\varepsilon} \kappa_g \, ds \tag{10.65}$$

where $\{\gamma_\varepsilon\}$ is a continuous family of smooth closed curves with winding number 1 on $\mathbf{N}$ which shrink to $\mathfrak{p}$ as $\varepsilon \to 0$, and κ_g is the geodesic curvature of γ_ε.

In the case of the bare straight-string metric (7.28) the surfaces $\mathbf{N_p}$ are just the surfaces of constant t and z, and the angle deficit on each of these surfaces is $\Delta\theta = 8\pi\mu$. As a natural generalization of this result, I will define a spinless cosmic string to be a line singularity $\mathbf{T}$ with the following additional properties:

(iv) On each surface $\mathbf{N_p}$ the angle deficit $\Delta\theta$ has the value $8\pi\mu$, where $\mu \in (0, \frac{1}{4})$ is a fixed constant.

(v) It is possible to choose the coordinates t and z so that the metric components g_{AB} and g^{AB} tend to well-defined, non-degenerate, η-independent limits γ_{AB} and γ^{AB} as $r \to 0$, with γ^{AB} the inverse of γ_{AB}.

(vi) The stress–energy tensor $T^{\mu\nu}$ in any (deleted) neighbourhood of $\mathbf{T}$ is locally finite, in the sense that if E is any of the physical components of $T^{\mu\nu}$ then the limit

$$\lim_{\varepsilon\to 0} \int_\varepsilon^r E\sqrt{g} \, dr \tag{10.66}$$

is well defined for all $r > 0$.

Property (vi) ensures that the string is surrounded by vacuum or material with a finite total stress–energy but places no intrinsic constraint on the string itself.

Since $\kappa_g = |g_{\eta\eta}|^{-1/2}(|g_{\eta\eta}|^{1/2})_{,r}$ on each surface $\mathbf{N_p}$, property (iv) ensures that

$$\Delta\theta \equiv 8\pi\mu = 2\pi - \lim_{r\to 0} \int_0^{2\pi} (|g_{\eta\eta}|^{1/2})_{,r} \, d\eta \tag{10.67}$$

and so

$$\lim_{r\to 0} (|g_{\eta\eta}|^{1/2})_{,r} = (1 - 4\mu)G(t, z, \eta) \tag{10.68}$$

where G is some function (periodic in η) satisfying the normalization condition $\int_0^{2\pi} G \, d\eta = 2\pi$.

If the radial geodesics are now reparametrized with an angular coordinate $\phi(t, z, \eta)$ defined by

$$\frac{d\phi}{d\eta} = G(t, z, \eta) \qquad \text{and} \qquad \phi(t, z, 0) = 0 \tag{10.69}$$

then $g_{\phi r} = 0$, ϕ ranges over $[0, 2\pi)$ on each surface $\mathbf{N_p}$, and $\lim_{r \to 0}(|g_{\phi\phi}|^{1/2})_{,r} = 1 - 4\mu$. Thus

$$g_{\phi\phi} \approx -a_0^2 r^2 \tag{10.70}$$

for small values of r, where again $a_0 = 1 - 4\mu$.

Finally, property (v) endows the singularity $\mathbf{T}$ with a 2-metric γ_{AB}, which allows $\mathbf{T}$ to be treated as a geometrical object—the world sheet of the string—in its own right. In the vicinity of $\mathbf{T}$, given that γ^{AB} is the inverse of $\gamma_{AB} \equiv \lim_{r \to 0} g_{AB}$,

$$g^{AB} \approx (-\gamma^{AB} g_{\phi\phi} - \gamma^{-1} \varepsilon^{AC} \varepsilon^{BD} g_{C\phi} g_{D\phi})(-g_{\phi\phi} + \gamma^{EF} g_{E\phi} g_{F\phi})^{-1} \tag{10.71}$$

where $\gamma = -\det(\gamma_{AB})$ and ε^{AC} is the flat-space alternating tensor (with $\varepsilon^{12} = -\varepsilon^{21} = 1$ and $\varepsilon^{11} = -\varepsilon^{22} = 0$). Taking the inner product of (10.71) with γ_{AB} and requiring that $\lim_{r \to 0} g^{AB} = \gamma^{AB}$ forces $\gamma^{EF} g_{E\phi} g_{F\phi}$ to go to zero more rapidly than r^2. This fact, combined with (10.71), indicates that the components $g_{A\phi}$ must go to zero more rapidly than r.

In summary, therefore, the line element (10.64) has the limiting form

$$ds^2 \approx \gamma_{AB} \, d\zeta^A \, d\zeta^B + 2g_{\phi A} \, d\zeta^A \, d\phi - dr^2 - a_0^2 r^2 \, d\phi^2 \tag{10.72}$$

where the indefinite 2-metric tensor γ_{AB} is a function of $\zeta^A = (t, z)$ only and $\lim_{r \to 0} g_{\phi A}/r = 0$.

Incidentally, Israel in his general characterization of line sources [Isr77] assumed in place of properties (iv) and (v) that the limits $C_\nu^\mu \equiv \frac{1}{2} \lim_{r \to 0} \sqrt{g} g^{\mu\lambda} g_{\lambda\nu, r}$ are well defined and that

$$C_\nu^\mu{}_{,\eta} = 0 \qquad \text{and} \qquad C_t^\eta = C_z^\eta = 0. \tag{10.73}$$

Israel imposed the second condition in order to exclude line singularities with intrinsic angular momentum but, unfortunately, it also disallows cylindrical metrics supporting $\times$ mode gravitational waves, such as the Xanthopoulos solution (9.118), which has $C_z^\phi = -\beta\kappa_0^2\rho_0^{-4}$. In fact, it turns out that in the more fully developed near-field expansions of section 10.4.3 all components of C_ν^μ except C_t^ϕ and C_z^ϕ are zero, whereas the reverse is true of Israel's class of line sources. Thus, the two characterizations are quite different.

10.4.2   Some sample near-field expansions

Before proceeding to examine the vacuum Einstein equations in the near-field limit, it is instructive to transform some of the string solutions discussed in chapter 9 into the $3 + 1$ form (10.64). Indeed, it is useful to first of all compare (10.64) with the Minkowski metric rewritten in terms of coordinates (ζ^A, r, ϕ) expanded about an arbitrary smooth indefinite surface $\mathbf{S}' = \{x^\mu = X^\mu(\zeta^0, \zeta^1)\}$,

in the same way that (10.64) is tailored to the geometry of the normal surfaces $\mathbf{N}_\mathfrak{p}$. In these coordinates the Minkowski line element becomes:

$$ds^2 = (\gamma_{AB} + 2x^i K_{(i)AB} + x^i x^j \gamma^{CD} K_{(i)AC} K_{(j)BD} - r^2 \omega_A \omega_B) d\zeta^A d\zeta^B$$
$$+ 2r^2 \omega_A d\zeta^A d\phi - dr^2 - r^2 d\phi^2 \tag{10.74}$$

where $\gamma_{AB} = X_{,A} \cdot X_{,B}$ is the 2-metric induced on $\mathbf{S}'$, $x^i = [r\cos\phi, r\sin\phi]$, and $K_{(i)AB}$ and ω_A are the extrinsic curvature tensors and twist vector of the surface $\mathbf{S}'$, respectively. (This expansion is just the cylindrically-symmetric version of the tailored line element (1.82).)

The similarities between (10.74) and the limiting form (10.72) of the general string metric are clear and indicate that the latter presumes only a minimal departure from the geometry around surfaces in flat space. In particular, it is expected that the short-distance behaviour of the metric components $g_{A\phi}$ should encode information about the twist of the world sheet $\mathbf{T}$, while the first-order terms in g_{AB} should be related to the extrinsic curvature of $\mathbf{T}$.

Turning now to the explicit string solutions of chapter 9, it is evident that the general travelling-wave metric (9.12) can be recast in the $3 + 1$ form (10.64) by defining $r = a_0^{-1} \rho^{a_0}$ and $\tan\phi = y/x$. Then $g_{A\phi} = 0$, $g_{\phi\phi} = -a_0^2 r^2$ and

$$g_{AB} = \gamma_{AB} + \begin{bmatrix} F & \pm F \\ \pm F & F \end{bmatrix}_{AB} \tag{10.75}$$

where $\gamma_{AB} = \mathrm{diag}(1, -1)$ and

$$F(t, r, \phi, z) = \sum_{n=1}^{\infty} r^{n/a_0} [\cos(n\phi) A_n''(t \pm z) + \sin(n\phi) B_n''(t \pm z)] \tag{10.76}$$

for arbitrary four-times differentiable functions A_n and B_n.

Continuing the analogy with (10.74), it can be seen that the world sheet of the string is twist-free, and that the first-order (r^{1/a_0}) terms in g_{AB} suggest that the surfaces of constant r have extrinsic curvature tensors $K_{(i)AB}$ proportional to $r^{-1+1/a_0} A_n''(t \pm z)$ and $r^{-1+1/a_0} B_n''(t \pm z)$, which since $r^{-1+1/a_0} = r^{4\mu/(1-4\mu)}$ vanish in the limit as $r \to 0$. This behaviour is, of course, consistent with the general analysis of section 10.3.

Rewriting the Robertson–Walker string metric (9.29) in $3 + 1$ form is more intricate. It is necessary first of all to integrate the geodesics of the 3-metric

$$ds^2 = a^2(\eta)[d\eta^2 - (1 - kR^2)^{-1} dR^2 - R^2 d\theta^2] \tag{10.77}$$

out from the axis $\theta = 0$ with $d\eta/ds = dR/ds = 0$ initially, then identify r with the proper distance s, t with the initial value η_0 of the cosmic time η, and z with the initial value R_0 of R.

The resulting transformation from (η, R, θ) to (t, r, z) is defined by the equations

$$R \sin \theta = \left(\frac{R^2 - z^2}{1 - kz^2} \right)^{1/2} \qquad r = \left| \int_t^\eta [a^2(t) - a^2(u)]^{-1/2} a^2(u)\, du \right| \quad (10.78)$$

and

$$\int_z^R (1 - ku^2)^{-1/2} (u^2 - z^2)^{-1/2} u\, du = a(t) \left| \int_t^\eta [a^2(t) - a^2(u)]^{-1/2}\, du \right| \quad (10.79)$$

where $\eta > t$ if $\dot{a}(t) > 0$ and $\eta < t$ if $\dot{a}(t) < 0$.

For small values of the geodesic distance r, this transformation reads:

$$\eta = t - \tfrac{1}{2} a(t)^{-3} \dot{a}(t) r^2 \qquad R = z + \tfrac{1}{2} z^{-1} a(t)^{-2} (1 - kz^2) r^2 \qquad (10.80)$$

(plus terms of order r^4 in both cases) and

$$\theta = z^{-1} a(t)^{-1} r + \tfrac{1}{3} z^{-3} a(t)^{-5} [z^2 \dot{a}(t)^2 - a(t)^2 (1 - kz^2)] r^3 + O(r^5). \quad (10.81)$$

The corresponding line element has $g_{A\phi} = 0$,

$$g_{tt} \approx a(t)^2 + [a(t)^{-1} \dot{a}(t)]\dot{}\, r^2 \qquad (10.82)$$

$$g_{zz} \approx -(1 - kz^2)^{-1} \{ a(t)^2 - a(t)^{-2} [\dot{a}(t)^2 + ka(t)^2] r^2 \} \qquad (10.83)$$

and

$$g_{\phi\phi} \approx -a_0^2 r^2 \{ 1 - \tfrac{1}{3} a(t)^{-4} [\dot{a}(t)^2 + ka(t)^2] r^2 \}. \qquad (10.84)$$

Note that, in contrast with the travelling-wave solutions, the metric tensor appearing here expands as a power series in r^2 rather than in r^{1/a_0}. The near-field behaviour of the string spacetime (9.29) is, therefore, qualitatively different from that of a travelling wave. Furthermore, with the gauge choice

$$\tau = t \qquad \text{and} \qquad \sigma = \int (1 - kz^2)^{-1/2}\, dz \qquad (10.85)$$

the world sheet **T** has the 2-metric $\gamma_{AB} = a^2(\tau) \operatorname{diag}(1, -1)$, and so **T** has non-zero intrinsic curvature if $\dot{a} \neq 0$. It is evident from the near-field expansion that the terms in the metric proportional to r^2 are all dependent on the presence of non-zero spatial curvature ($k \neq 0$) or non-zero world-sheet curvature ($\dot{a} \neq 0$).

The Aryal–Ford–Vilenkin metric (9.53) can be treated in a similar way. The $3 + 1$ form is found by defining r and z implicitly by the equations

$$r = \pm \int_z^R \left[\left(1 - \frac{2m}{u} \right) \left(1 - \frac{z^2}{u^2} \right) \right]^{-1/2} du$$

$$\theta = \pm z \int_z^R \left[\left(1 - \frac{2m}{u} \right) \left(1 - \frac{z^2}{u^2} \right) \right]^{-1/2} u^{-2}\, du \qquad (10.86)$$

where the positive branch applies outside the event horizon ($R > 2m$) and the negative branch inside the event horizon ($R < 2m$). For small values of r the line element has the limiting form:

$$ds^2 \approx \left(1 - \frac{2m}{z}\right)\left(1 + \frac{m}{z^3}r^2\right) dt^2 - \left(1 - \frac{2m}{z}\right)^{-1}\left(1 + \frac{m}{z^3}r^2\right) dz^2$$

$$- a_0^2 r^2 \left(1 - \frac{2m}{3z^3}r^2\right) d\phi^2 - dr^2. \tag{10.87}$$

Again the near-field expansion proceeds in powers of r^2 rather than powers of r^{1/a_0} and the second-order terms are dependent on the existence of non-zero world-sheet curvature, as they are all proportional to the tidal term m/z^3 while the 2-metric on the world sheet

$$\gamma_{tt} = 1 - \frac{2m}{z} \qquad \gamma_{zz} = -\left(1 - \frac{2m}{z}\right)^{-1} \tag{10.88}$$

has an associated scalar curvature $^{(2)}R = 4m/z^3$.

As a final example, this time involving a non-zero twist term, consider the canonical cylindrically-symmetric line element (9.83). Provided that the metric functions χ, ψ and α can be expanded as powers of r^2 (which is true of all the solutions in section 9.3 except those Levi-Cività-seeded soliton solutions which fail to be conical on axis) and α is of order at least r^2, the line element in $3 + 1$ form has:

$$g_{tt} \approx e^{2\chi_0} + (2\dot\chi_0 + \dot\chi_0^2 - \ddot\chi_0 - \tfrac{1}{2}\dot\chi_0\chi_0'')r^2 \tag{10.89}$$

$$g_{zz} \approx -e^{2\psi_0} - e^{2(\psi_0-\chi_0)}(2\dot\psi_0 - \tfrac{1}{2}\dot\chi_0\psi_0'')r^2 \tag{10.90}$$

$$g_{\phi\phi} \approx -e^{-2(\chi_0+\psi_0)}r^2 - e^{2\psi_0}\alpha^2$$
$$- \tfrac{1}{3}e^{-2(2\chi_0+\psi_0)}(\dot\chi_0^2 - 2\ddot\chi_0 + \tfrac{1}{2}\dot\chi_0\chi_0'' - 6\dot\psi_0 + \tfrac{3}{2}\dot\chi_0\psi_0'')r^4 \tag{10.91}$$

and $g_{z\phi} \approx -e^{2\psi_0}\alpha$, with g_{tz} and $g_{t\phi}$ of order r^4 or smaller. (Here, a subscripted 0 denotes the value of the corresponding function at $r = 0$, so that χ_0, ψ_0 and the subscripted derivatives are all functions of t only.) The twist term $g_{z\phi}$ is, therefore, dependent directly on the presence of $\times$ mode gravitational waves.

10.4.3   Series solutions of the near-field vacuum Einstein equations

The class of solutions to the Einstein equations containing a zero-thickness cosmic string as defined in section 10.4.1 is presumably very broad, if only because the stress–energy tensor outside the string is only weakly constrained by condition (vi). The properties of such a string can be studied in isolation from the effects of any surrounding matter or radiation fields by making the more restrictive assumption that the string lies in a vacuum exterior, so that the Einstein equations reduce to $R_{\mu\nu} = 0$ away from the world sheet **T**.

Furthermore, all the exact string solutions examined so far admit near-field series expansions of the $3 + 1$ metric tensor in powers of either r^{1/a_0} (where $0 < a_0 < 1$) or r^2. Expansions of the first type are characteristic of the travelling-wave metrics (9.25), while expansions of the second type seem to be associated with non-zero world-sheet or metric curvature. It is for this reason that I chose in [And99b] to refer to the two types of disturbances as 'travelling waves' and 'curvature waves' respectively.

These considerations suggest that one avenue of approach to studying the near gravitational field outside a general cosmic string is to expand the $3 + 1$ metric tensor in undetermined powers of the geodesic distance r and then impose the vacuum Einstein equations. Before this is done, note first that the coordinates $\zeta^A = (t, z)$ on **T** can always be chosen so that the 2-metric γ_{AB} is conformally flat:

$$\gamma_{AB} = \kappa(t, z)\eta_{AB} \tag{10.92}$$

where $\eta_{AB} = \text{diag}(1, -1)$, in which case the scalar curvature of the world sheet is

$$^{(2)}R = \kappa^{-1}\eta^{AB}(\ln \kappa),_{AB}. \tag{10.93}$$

Then the general series expansion of the $3 + 1$ metric tensor has the form

$$g_{AB} = \kappa\left(\eta_{AB} + \sum_{n=1}^{\infty} P_{AB}^{(n)}r^{j_n}\right) \qquad g_{A\phi} = \sum_{n=1}^{\infty} Q_A^{(n)}r^{k_n} \tag{10.94}$$

and

$$g_{\phi\phi} = -a_0^2 r^2\left(1 - \sum_{n=1}^{\infty} \beta^{(n)}r^{l_n}\right) \tag{10.95}$$

where $P_{AB}^{(n)}$, $Q_A^{(n)}$ and $\beta^{(n)}$ are all functions of t, z and ϕ, and the sequences of exponents $\{j_n\}$, $\{k_n\}$ and $\{l_n\}$ are positive and ascending, with $k_1 > 1$ as required by property (v).

Generating the corresponding power-series expansions of the Riemann and Ricci tensors is a tedious process whose first steps have been outlined in [And99b]. For instance,

$$R_{A\phi} = \tfrac{1}{2}k_1(2 - k_1)Q_A^{(1)}r^{k_1-2} + o(r^0) \tag{10.96}$$

and so the assumption of a vacuum exterior entails that $k_1 \geq 2$. Similarly,

$$R_{AB} = -\tfrac{1}{2}\kappa a_0^{-2}(P_{AB}^{(1)},_{\phi\phi} + j_1^2 a_0^2 P_{AB}^{(1)})r^{j_1-2} + O(r^0) \tag{10.97}$$

and so either $j_1 \geq 2$ or $P_{AB}^{(1)},_{\phi\phi} + j_1^2 a_0^2 P_{AB}^{(1)} = 0$. In the second case, a non-trivial solution $P_{AB}^{(1)}$ exists if and only if j_1 is an integer multiple of $1/a_0$. If $j_1 = 1/a_0$ then

$$P_{AB}^{(1)} = L_{AB}\cos\phi + M_{AB}\sin\phi \tag{10.98}$$

where the coefficient matrices L_{AB} and M_{AB} are functions of t and z only. In addition, the leading-order term in the expansion of $R_{r\phi}$ imposes the trace constraints $\eta^{AB}L_{AB} = \eta^{AB}M_{AB} = 0$.

Continuing in this way gradually builds up a multinomial expansion for the metric tensor in powers of r^{1/a_0} and r^2. If it is assumed that $\mu < 1/8$ (so that $1 < 1/a_0 < 2$) and the smallest possible power of r is chosen at each step then

$$g_{AB} = \kappa[\eta_{AB} + (L_{AB}\cos\phi + M_{AB}\sin\phi)r^{1/a_0}$$
$$+ (\tfrac{1}{4}\,^{(2)}R\eta_{AB} - \kappa^{-1}a_0^{-2}\omega_A\omega_B)r^2] + O(r^{2+1/a_0}) \tag{10.99}$$

$$g_{A\phi} = r^2\omega_A + (2a_0+1)^{-1}[\omega^B(L_{BA}\cos\phi + M_{BA}\sin\phi)$$
$$+ a_0^2\kappa^{-1}(\kappa L_A^B)_{,B}\sin\phi - a_0^2\kappa^{-1}(\kappa M_A^B)_{,B}\cos\phi]r^{2+1/a_0} + O(r^4) \tag{10.100}$$

and

$$g_{\phi\phi} = -a_0^2 r^2(1 - \tfrac{1}{6}\,^{(2)}Rr^2) + O(r^{4+1/a_0}) \tag{10.101}$$

where the twist vector ω_A, the symmetric travelling-wave potentials L_{AB} and M_{AB} and the scalar curvature $^{(2)}R$ are all functions of t and z, and the world-sheet indices A, B ... are raised and lowered using the flat 2-metric η_{AB}.

It has already been mentioned that the potentials L_{AB} and M_{AB} must be trace-free. Further conditions on L_{AB} and M_{AB} appear at higher orders in the expansion. For example, the Ricci components R_{AB} vanish at order r^{2/a_0} only if $L_{tz}/L_{tt} = M_{tz}/M_{tt} = \pm 1$, while if $g_{A\phi}$ vanishes to order r^{2+1/a_0} then κL_{AB} and κM_{AB} are functions of $t \pm z$ only, and the leading-order ($n = 1$) terms in the generating function (10.76) for a travelling-wave metric are completely specified.

Moreover, if $R_{AB} = 0$ at order r^{2/a_0} then g_{AB} contains a term of the form

$$\kappa(\bar{L}_{AB}\cos 2\phi + \bar{M}_{AB}\sin 2\phi)r^{2/a_0} \tag{10.102}$$

where $\bar{L}_{AB}$ and $\bar{M}_{AB}$ must be trace-free if $R_{\phi r} = 0$ at order r^{2/a_0}, while $\bar{L}_{tz}/\bar{L}_{tt} = \bar{M}_{tz}/\bar{M}_{tt} = L_{tz}/L_{tt}$ if $R_{AB} = 0$ at order r^{3/a_0}. Thus, the full travelling-wave metric term (10.75) appears piece by piece at successive orders in the expansion, provided that $g_{A\phi}$ is identically zero.

The corresponding series expansion of the Riemann tensor contains only three terms (modulo symmetries) whose physical components diverge near the world sheet, namely

$$R_{ArBr} \sim \tfrac{1}{2}a_0^{-1}(a_0^{-1} - 1)\kappa P_{AB}^{(1)}r^{1/a_0-2} \tag{10.103}$$

$$R_{ArB\phi} \sim \tfrac{1}{2}(a_0^{-1} - 1)\kappa P_{AB,\phi}^{(1)}\, r^{1/a_0-1} \tag{10.104}$$

and

$$R_{A\phi B\phi} \sim \tfrac{1}{2}(a_0 - 1)\kappa P_{AB}^{(1)}r^{1/a_0}. \tag{10.105}$$

The physical components of all three of these terms diverge as $(1/a_0 - 1)r^{1/a_0-2} \sim \mu r^{4\mu-1}$ (for small μ), which is again in agreement with the analysis

of section 10.3. As can be seen, the divergence in the Riemann tensor is due solely to the contribution of the leading-order ($n = 1$) travelling waves. The remaining physical components of R_{abcd} all tend to zero as r^{1/a_0-1}, except for those of $R_{r\phi r\phi}$ and R_{ABCD}, which tend to finite, generally non-zero limits on the world sheet.

In summary, there seems to be no obstacle to developing a series solution for the $3 + 1$ metric tensor outside the world sheet **T** of a zero-thickness cosmic string, with the scalar curvature $^{(2)}R$ of **T**, the twist vector ω_A and the full set of travelling-wave potentials as boundary data, although there is a complicated nonlinear coupling between the $\times$ mode gravitational waves (represented by ω_A) and the travelling waves. The physical properties of such a solution are consistent with the general description of the metric near **T** offered in the previous sections, although there is no guarantee that the near-field solution in any particular case can be extended to give an acceptable global solution.

One outstanding problem that has yet to be resolved is the connection between the general relativistic description of a zero-thickness string, which hints at a complex set of dynamical modes coupled to various types of gravitational radiation, and the conventional flat-space description, in which the string motion is constrained by the Nambu–Goto action. The two regimes appear to have points of contact in the weak-field approximation, particularly in the context of the back-reaction problem (where radiative effects contribute a secular correction to the Nambu–Goto motion) but these contacts remain very tenuous. Of course, the world sheet of a zero-thickness gravitating string is a totally geodesic submanifold, and so there is a sense in which it not only satisfies the Nambu–Goto equations but is, in fact, 'straight'. However, this effect is merely a mathematical curiosity and would not be detectable by a distant observer. Whether the motion of a gravitating string can ever be approximated by a Nambu–Goto string in an otherwise flat spacetime remains an unanswered question.

10.4.4   Distributional stress–energy of the world sheet

One final property of the near-field metric expansions (10.99) to (10.101) that deserves special mention is that they induce a distributional stress–energy density with $\widehat{\sqrt{g}T_t^t} = \widehat{\sqrt{g}T_z^z} = \mu\delta^{(2)}(r)$ and all other components zero, just as the bare straight-string metric does. A stress–energy density of this form is, of course, implied by the general expression for the stress–energy tensor (6.1) of a Nambu–Goto string, and is here assumed to be one of the defining features of a zero-thickness cosmic string.

The proof of this claim is similar to the corresponding proof in section 7.5. In isotropic coordinates $x^i \equiv (x, y) = (\rho\cos\phi, \rho\sin\phi)$, the leading-order terms in the near-field expansions of the $3 + 1$ metric components become:

$$g_{AB} = \kappa\eta_{AB} + a_0^{-1/a_0}\kappa(L_{AB}x + M_{AB}y) + O(\rho^{2a_0}) \qquad (10.106)$$

$$g_{Ax} = -a_0^{-2}\omega_A\rho^{-8\mu}y + O(\rho^{2a_0}) \qquad \text{and} \qquad g_{Ay} = a_0^{-2}\omega_A\rho^{-8\mu}x + O(\rho^{2a_0})$$
$$(10.107)$$

and

$$g_{ij} = -\rho^{-8\mu}\delta_{ij} + O(\rho^{4a_0-2}). \tag{10.108}$$

In what follows, it will be assumed that the full expansions converge at all points inside a fixed deleted neighbourhood **S** of the world sheet **T**. The isotropic coordinate system maps **S** to the neighbourhood of a plane (the image of **T**) in $\mathbb{R}^4$. Let $\mathfrak{p}_0$ be a point on the world sheet, with coordinates $(\zeta^A, x^i) = (\zeta_0^A, \mathbf{0}) \equiv x_0^\mu$, and define $D(\mathfrak{p}_0)$ to be the minimum Euclidean distance from $\mathfrak{p}_0$ to the boundary of **S**. Let h be a smoothing operator with support that lies entirely within the 4-sphere of radius $\frac{1}{2}D(\mathfrak{p}_0)$ centred on the origin in $\mathbb{R}^4$. Define $\mathbf{S}_{\mathfrak{p}_0}$ to be interior of the sphere of radius $\frac{1}{2}D(\mathfrak{p}_0)$ centred on $\mathfrak{p}_0$ in $\mathbb{R}^4$.

Then if x^μ is any point in $\mathbf{S}_{\mathfrak{p}_0}$, $\Delta x^\mu = x^\mu - x_0^\mu$ and $h_\varepsilon(x^\lambda) = \varepsilon^{-4}h(x^\lambda/\varepsilon)$ for any ε in $(0, 1]$, the smoothed metric components $g_{\mu\nu}^\varepsilon$ in $\mathbf{S}_{\mathfrak{p}_0}$ are defined in analogy with (7.72) by

$$g_{\mu\nu}^\varepsilon(x) = \int_{\mathbb{R}^4} g_{\mu\nu}(x_0 + y)h_\varepsilon(y - \Delta x)\,\mathrm{d}^4y. \tag{10.109}$$

(Note that the restrictions on x and the support of h ensure that the integrand is non-zero only if the point $x_0 + y$ lies within **S**.)

In particular,

$$g_{AB}^\varepsilon = \kappa^\varepsilon(\zeta^C)\eta_{AB} + \varepsilon N_{AB}^\varepsilon\left(\zeta^C, \frac{x}{\varepsilon}, \frac{y}{\varepsilon}\right) + O^*(\varepsilon^{2a_0}) \tag{10.110}$$

$$g_{Ax} = -\varepsilon^{1-8\mu}W_A^\varepsilon\left(\zeta^C, \frac{y}{\varepsilon}, \frac{x}{\varepsilon}\right) + O^*(\varepsilon^{2a_0})$$

$$g_{Ay} = \varepsilon^{1-8\mu}W_A^\varepsilon\left(\zeta^C, \frac{x}{\varepsilon}, \frac{y}{\varepsilon}\right) + O^*(\varepsilon^{2a_0}) \tag{10.111}$$

and

$$g_{ij} = -\varepsilon^{-8\mu}f\left(\frac{x}{\varepsilon}, \frac{y}{\varepsilon}\right)\delta_{ij} + O^*(\varepsilon^{4a_0-2}) \tag{10.112}$$

where κ^ε, N_{AB}^ε, W_A^ε and f are smooth functions of their arguments (including ε), and a function is said to be $O^*(\varepsilon^k)$ if it has the general form $\varepsilon^k G^\varepsilon$ where G^ε is a smooth function of ζ^A and x^i/ε and a continuous function of ε, with the property that $\lim_{\varepsilon\to 0}^* G^\varepsilon$ is also a smooth function of ζ^A and x^i/ε (where $\lim^*$ denotes that the limit is taken with x^i/ε fixed) of order $(\rho/\varepsilon)^k$ when ρ/ε is large.

The smoothed stress–energy tensor $T_\nu^{(\varepsilon)\mu}$ induced by $g_{\mu\nu}^\varepsilon$ can be expanded in powers of ε by noting that the x or y derivatives of any of the previous smooth functions is just ε^{-1} times another smooth function. It turns out that

$$\sqrt{g^\varepsilon}T_t^{(\varepsilon)t} = \varepsilon^{-2}H\left(\frac{x}{\varepsilon}, \frac{y}{\varepsilon}\right) + O^*(\varepsilon^{-1}) \tag{10.113}$$

and

$$\sqrt{g^\varepsilon}T_z^{(\varepsilon)z} = \varepsilon^{-2}H\left(\frac{x}{\varepsilon}, \frac{y}{\varepsilon}\right) + O^*(\varepsilon^{-1}) \tag{10.114}$$

where H is the function defined in a similar context in section (7.5), namely

$$H = -\frac{\varepsilon^2}{16\pi}[(\ln f),_{xx} + (\ln f),_{yy}] \tag{10.115}$$

and the remaining components of $\sqrt{g^\varepsilon}T_\nu^{(\varepsilon)\mu}$ are all $O^*(\varepsilon^{-1-8\mu})$ or smaller.

Now let $K \subset \mathbf{S}(\mathfrak{p}_0)$ be a closed ball centred on $\mathfrak{p}_0$. The action of $\sqrt{g^\varepsilon}T_t^{(\varepsilon)t}$ on an arbitrary smooth function ψ with compact support lying inside K is, therefore,

$$\int_K \sqrt{g^\varepsilon}T_t^{(\varepsilon)t}\psi \, d^4x = \varepsilon^{-2}\int_K H\psi \, d^4x + \varepsilon^{-1}\int_K G^\varepsilon\psi \, d^4x \tag{10.116}$$

where G^ε is a smooth function of ζ^A and x^i/ε, with $\lim^*_{\varepsilon\to 0} G^\varepsilon$ also a smooth function of ζ^A and x^i/ε, of order $(\rho/\varepsilon)^{-1}$ when ρ/ε is large. It was shown in section (7.5) that in the limit as $\varepsilon \to 0$ the first integral on the right tends to

$$\mu \int_K \psi(\zeta^A, \mathbf{0}) \, d^2\zeta. \tag{10.117}$$

Let $\bar{G}$ be the function $\frac{\rho}{\varepsilon}G^\varepsilon$, and $\mathbf{T}^*$ the compact two-dimensional set $K \cap \mathbf{T}$. Viewed as a function of the five parameters x^μ and ε, $\bar{G}$ is continuous on $K \times (0, 1]$, and, in particular, is zero on $\mathbf{T}^* \times (0, 1]$ as $\rho = 0$ there. By construction $\lim_{\varepsilon\to 0}\varepsilon^{-1}G^\varepsilon = 0$ pointwise on $K - \mathbf{T}^*$, as $T_\nu^\mu = 0$ there, so $\bar{G}$ can be extended to a continuous function on $K \times [0, 1] - (\mathbf{T}^* \times \{0\})$ by defining it to be zero on $(K - \mathbf{T}^*) \times \{0\}$. Finally, since taking $\lim^*_{\varepsilon\to 0}$ is the same as taking $\lim_{\varepsilon\to 0}$ with $x^i = \kappa^i\varepsilon$ where κ^i and ζ^A are constant, and $\lim^*_{\varepsilon\to 0}\frac{\rho}{\varepsilon}G^\varepsilon$ is a continuous and bounded function of $x^i/\varepsilon \equiv \kappa^i$, the set of limiting values of $\bar{G}$ along any curve of the form $x^i = \kappa^i\varepsilon$ and ζ^A constant as $\varepsilon \to 0$ is bounded, as it is along any curve with $\varepsilon \equiv 0$ (on which $\bar{G} \equiv 0$) terminating at the same point on $\mathbf{T}^* \times \{0\}$.

This means that $\bar{G}$ must be bounded in some neighbourhood of each point on $\mathbf{T}^* \times \{0\}$ (with trivial adjustments to this statement necessary for points in the boundary $(\partial K \cap \mathbf{T}^*) \times \{0\}$) and so $\bar{G}$ is bounded throughout $K \times [0, 1]$. Hence, the function $|\frac{\rho}{\varepsilon}G^\varepsilon|$ has a supremum C for all ε in $(0, 1]$ and $|\varepsilon^{-1}G^\varepsilon|$ is uniformly bounded above by $C\rho^{-1}$ on K. Since ρ^{-1} is locally integrable on $\mathbb{R}^2$ the dominated convergence theorem implies that

$$\lim_{\varepsilon\to 0}\varepsilon^{-1}\int_K G^\varepsilon\psi \, d^4x = 0.$$

A similar argument disposes of the remainder terms in the other components of $\sqrt{g^\varepsilon}T_\nu^{(\varepsilon)\mu}$, as they are all of the form $\varepsilon^{-k}G^\varepsilon$ where $k < 2$ (provided that

$8\mu < 1$ as assumed earlier)[4]. So $|\varepsilon^{-k} G^\varepsilon|$ is uniformly bounded above by $C\rho^{-k}$ for some constant C on K, and since ρ^{-k} is locally integrable on $\mathbb{R}^2$ when $k < 2$, the integral of $\varepsilon^{-k} G^\varepsilon \psi$ over K vanishes in the limit as $\varepsilon \to 0$.

The original metric $g_{\mu\nu}$, therefore, induces a distributional stress–energy density $\widehat{\sqrt{g}T_\nu^\mu}$ with

$$\widehat{\sqrt{g}T_t^t}(\psi) = \widehat{\sqrt{g}T_z^z}(\psi) = \mu \int_K \psi(\zeta^A, \mathbf{0}) \, d^2\zeta \qquad (10.118)$$

and all other components zero. Thus, provided that the expansions (10.99) to (10.101) converge in some deleted neighbourhood of the world sheet $\mathbf{T}$ to tensor fields which can be extended to give a globally acceptable $3 + 1$ vacuum metric tensor, a distributional stress–energy density can be ascribed to $\mathbf{T}$, and it has the same form

$$\widehat{\sqrt{g}T_\nu^\mu} = \mu\delta^{(2)}(x, y)(\delta_t^\mu \delta_\nu^t + \delta_z^\mu \delta_\nu^z) \qquad (10.119)$$

as the stress–energy density of the bare straight-string metric (7.28).

---

[4] A slight adjustment to the proof is necessary if $k < 0$, as then $(\frac{\rho}{\varepsilon})^k G^\varepsilon$ is no longer a continuous function on $K \times (0, 1]$. But in this case it is easily seen that G^ε itself is uniformly bounded on K.

Bibliography

[AB93]   Ahmed M and Biswas E U 1993 Cosmic string in the NUT–Kerr–Newman
            spacetime *Int. J. Theoret. Phys.* **32** 813

[ABGS97]   Anderson M, Bonjour F, Gregory R and Stewart J 1997 Effective action and
            motion of a cosmic string *Phys. Rev.* D **56** 8014

[AC94]   Allen B and Casper P 1994 Closed-form expression for the gravitational
            radiation rate from cosmic strings *Phys. Rev.* D **50** 2496

[ACO94]   Allen B, Casper P and Ottewill A 1994 Analytic results for the gravitational
            radiation from a class of cosmic string loops *Phys. Rev.* D **50** 3703

[ACO95]   Allen B, Casper P and Ottewill A 1995 Closed-form expression for the
            momentum radiated from cosmic string loops *Phys. Rev.* D **51** 1546

[AFV86]   Aryal M, Ford L H and Vilenkin A 1986 Cosmic strings and black holes
            Phys. Rev. D **34** 2263

[AGK95]   Achucarro A, Gregory R and Kuijken K 1995 Abelian Higgs hair for black
            holes *Phys. Rev.* D **52** 5729

[And90]   Anderson M R 1990 Invariant length of a cosmic string *Phys. Rev.* D **41** 3612

[And95]   Anderson M R 1995 Leading-order corrections to the Nambu action *Phys.
            Rev.* D **51** 2863

[And99a]   Anderson M R 1999 An energy principle for relativistic fluid cylinders *Class.
            Quantum Grav.* **16** 2845

[And99b]   Anderson M R 1999 Near-field expansion of the gravitational field due to a
            cosmic string *J. Austral. Math. Soc.* B **41** 180

[AS90]   Allen B and Shellard E P S 1990 Cosmic-string evolution: A numerical
            solution *Phys. Rev. Lett.* **64** 119

[AS92]   Allen B and Shellard E P S 1992 Gravitational radiation from cosmic strings
            Phys. Rev. D **45** 1898

[AY88]   Albrecht A and York T 1988 Kinky structure on strings *Phys. Rev.* D **38** 2958

[Bar91]   Barrabès C 1991 Prolate collapse of string loops and domain walls *Class.
            Quantum Grav.* **8** L199

[BB88]   Bennett D P and Bouchet F R 1988 Evidence for a scaling solution in cosmic-
            string evolution *Phys. Rev. Lett.* **60** 257

[BB89]   Bennett D P and Bouchet F R 1989 Cosmic-string evolution *Phys. Rev. Lett.*
            63 2776

[BB91]   Bennett D P and Bouchet F R 1991 Constraints on the gravity-wave
            background generated by cosmic strings *Phys. Rev.* D **43** 2733

[BD89]   Brown R W and DeLaney D B 1989 Product representation for the harmonic
            series of a unit vector: A string application *Phys. Rev. Lett.* **63** 474

[Bi90]   Bičàk J 1990 Is there a news function for an infinite cosmic string? *Astronomische Nachrichten* **311** 189

[BI91]   Barrabès C and Israel W 1991 Thin shells in general relativity and cosmology: The lightlike limit *Phys. Rev.* D **43** 1129

[Bog76]   Bogomol'nyi E 1976 The stability of classical solutions. *Sov. J. Nucl. Phys.* **24** 449

[BPO99]   Blanco-Pillado J J and Olum K D 1999 The form of cosmic string cusps *Phys. Rev.* **59** 063508

[Bra87]   Brandenburger R H 1987 On the decay of cosmic string loops *Nucl. Phys.* B **293** 812

[BRT91]   Brown R R, Rains E M and Taylor C C 1991 Harmonic analysis of the relativistic string in spinorial coordinates *Class. Quantum Grav.* **8** 1245

[BS89]   Bičàk J and Schmidt B 1989 On the asymptotic structure of axisymmetric radiative spacetimes *Class. Quantum Grav.* **6** 1547

[BT84]   Burden C J and Tassie L J 1984 Additional rigidly rotating solutions to the string model of hadrons *Austral. J. Phys.* **37** 1

[Bur85]   Burden C J 1985 Gravitational radiation from a particular class of cosmic strings *Phys. Lett.* B **164** 277

[BvdBM62]   Bondi H, van der Burg M and Metzner A W K 1962 Gravitational waves in general relativity VII *Proc. R. Soc.* A **269** 21

[CA94]   Casper P and Allen B 1994 Gravitational radiation from realistic cosmic string loops *Phys. Rev.* D **50** 2496

[Car77]   Carter B 1977 Killing tensor quantum numbers and conserved currents in curved space *Phys. Rev.* D **16** 3414

[CB68]   Choquet-Bruhat Y 1968 Espaces-temps einsteiniens généraux, chocs gravitationnels *Ann. Inst. Henri Poincaré* **VIII** 327

[CC96]   Caldwell R R and Casper P 1996 Formation of black holes from collapsed cosmic string loops *Phys. Rev.* D **53** 3002

[CDH88]   Chen A L, DiCarlo D A and Hotes S A 1988 Self-intersections in a three-parameter space of cosmic strings *Phys. Rev.* D **37** 863

[CEV90]   Clarke C J S, Ellis G F R and Vickers J A 1990 The large-scale bending of cosmic strings *Class. Quantum Grav.* **7** 1

[CF89]   Carter B and Frolov V P 1989 Separability of string equilibrium equations in a generalised Kerr–de Sitter background *Class. Quantum Grav.* **6** 569

[CFG92]   Carroll S, Farhi E and Guth A H 1992 An obstacle to building a time machine *Phys. Rev. Lett.* **68** 263

[CFGO94]   Carroll S, Farhi E, Guth A H and Olum K D 1994 Energy–momentum restrictions on the creation of Gott time machines *Phys. Rev.* D **50** 6190

[CGZ86]   Curtwight T L, Ghandour G I and Zachos C K 1986 Classical dynamics of strings with rigidity *Phys. Rev.* D **34** 3811

[CT86]   Copeland E and Turok N 1986 The stability of cosmic string loops *Phys. Lett.* B **173** 129

[Cut92]   Cutler C 1992 Global structure of Gott's two-string spacetime *Phys. Rev.* D **45** 487

[CV87]   Cespedes J and Verdaguer E 1987 Cosmological Einstein–Rosen metrics and generalized soliton solutions *Class. Quantum Grav.* **4** L7

[CVW96]   Clarke C J S, Vickers J A and Wilson J P 1996 Generalised functions and distributional curvature of cosmic strings *Class. Quantum Grav.* **13** 2485

[DES90]   DeLaney D, Engle K and Scheick X 1990 General two-harmonic cosmic string *Phys. Rev.* D **41** 1775

[DJtH84]   Deser S, Jackiw R and 't Hooft G 1984 Three-dimensional Einstein gravity—dynamics of flat space *Ann. Phys.* **152** 220

[DJtH91]   Deser S, Jackiw R and 't Hooft G 1991 Physical cosmic strings do not generate closed time-like times *Phys. Rev. Lett.* **68** 267

[DM95]   Dyer C C and Marleau F R 1995 Complete model of a self-gravitating cosmic string: A new class of exact solutions *Phys. Rev.* D **52** 5588

[DOS88]   Dyer C C, Oattes L M and Starkman G D 1988 Vacuum strings in FRW models *Gen. Rel. Grav.* **20** 71

[Dow87]   Dowker J S 1987 Casimir effect around a cone *Phys. Rev.* D **36** 3095

[DS88]   Davies P C W and Sahni V 1988 Quantum gravitational effects near cosmic strings *Class. Quantum Grav.* **5** 1

[Dur89]   Durrer R 1989 Gravitational angular momentum radiation of cosmic strings *Nucl. Phys.* B **328** 238

[dVE94]   de Vega H J and Egusquiza I L 1994 Strings in cosmological and black hole backgrounds: Ring solutions *Phys. Rev.* D **49** 763

[dVS93]   de Vega H J and Sanchez N 1993 Exact integrability of strings in *D*-dimensional de Sitter spacetime *Phys. Rev.* D **47** 3394

[EHKT95]   Eardley D, Horowitz G, Kastor D and Traschen. J 1995 Breaking cosmic strings without monopoles *Phys. Rev. Lett.* **75** 3390

[Eis40]   Eisenhart L P 1940 *An Introduction to Differential Geometry* (Princeton, NJ: Princeton University Press)

[Emb92]   Embacher F 1992 Rigidly rotating cosmic strings *Phys. Rev.* D **46** 3659

[ET88a]   Economou A and Tsoubelis D 1988 Interaction of cosmic strings with gravitational waves: A new class of exact solutions *Phys. Rev. Lett.* D **61** 2046

[ET88b]   Economou A and Tsoubelis D 1988 Rotating cosmic strings and gravitational soliton waves *Phys. Rev.* D **38** 498

[FG90]   Frolov V P and Garfinkle D 1990 Interaction of cosmic strings with gravitational waves *Phys. Rev.* D **42** 3980

[FIU89]   Frolov V P, Israel W and Unruh W G 1989 Gravitational fields of straight and circular cosmic strings *Phys. Rev.* D **39** 1084

[FL99]   Frolov A V and Larsen A L 1999 Chaotic scattering and capture of strings by black hole *Class. Quantum Grav.* **16** 3717

[För74]   Förster D 1974 Dynamics of relativistic vortex lines and their relation to dual theory *Nucl. Phys.* B **81** 84

[FSZH89]   Frolov V P, Skarzhinsky V D, Zelnikov A I and Heinrich O 1989 Equilibrium configurations of a cosmic string near a rotating black hole *Phys. Lett.* B **224** 255

[FV86]   Fustero X and Verdaguer E 1986 Einstein–Rosen metrics generated by the inverse scattering transform *Gen. Rel. Grav.* **18** 1141

[GA84]   Gott J R and Alpert M 1984 General relativity in $(2 + 1)$-dimensional spacetime *Gen. Rel. Grav.* **16** 243

[Gal90]   Gal'tsov D V 1990 Are cosmic strings gravitationally sterile? *Fortschrift Physik* **38** 945

[Gar85]   Garfinkle D 1985 General relativistic strings *Phys. Rev.* D **32** 1323

[Gar88]   Garfinkle D 1988 Cusps, kinks and all that *Cosmic Strings: the Current*

Status Proc. Yale Cosmic String Workshop, May 1988, ed F S Acetta and L M Kraus (Singapore: World Scientific) p 99

[Gar90]   Garfinkle D 1990 Traveling waves in strongly gravitating cosmic strings *Phys. Rev.* D **41** 1112

[GC89]   Gowdy R H and Chaube S N 1989 Exact solutions for cosmic strings in closed universes *Phys. Rev.* D **40** 1854

[GD94]   Garfinkle D and Duncan G C 1994 Collapse of a circular loop of cosmic string *Phys. Rev.* D **49** 2752

[GD02]   Griffiths J B and Docherty P 2002 A disintegrating cosmic string *Class. Quantum Grav.* **19** L109

[GGL93]   Gal'tsov D V, Grats Y V and Letelier P S 1993 Post-linear formalism for gravitating strings: crossed straight strings collision *Ann. Phys.* **224** 90

[GGRT73]   Goddard P, Goldstone J, Rebbi C and Thorn C B 1973 Quantum dynamics of a massless relativistic string *Nucl. Phys.* B **56** 109

[GH95]   Gregory R and Hindmarsh M 1995 Smooth metrics for snapping strings *Phys. Rev.* D **52** 5598

[GL89]   Garfinkle D and Laguna P 1989 Contribution of gravitational self-interaction to $\Delta\phi$ and μ for a cosmic string *Phys. Rev.* D **39** 1552

[Got71]   Goto T 1971 Relativistic quantum mechanics of a one-dimensional mechanical continuum and subsidiary condition of dual resonance model *Prog. Theoret. Phys.* **46** 1560

[Got85]   Gott J R 1985 Gravitational lensing effects of vacuum string: exact results *Astrophys. J.* **288** 422

[Got91]   Gott J R 1991 Closed timelike curves produced by pairs of moving cosmic strings—exact solutions *Phys. Rev. Lett.* **66** 1126

[GP89]   Gleiser R and Pullin J 1989 Are cosmic strings gravitationally stable topological defects? *Class. Quantum Grav.* **6** L141

[Gre89]   Gregory R 1989 Cosmological cosmic strings *Phys. Rev.* D **39** 2108

[GT87]   Geroch R and Traschen J 1987 Strings and other distributional sources in general relativity *Phys. Rev.* D **36** 1017

[GV87a]   Garfinkle D and Vachaspati T 1987 Radiation from kinky, cuspless cosmic loops *Phys. Rev.* D **36** 2229

[GV87b]   Garriga J and Verdaguer E 1987 Cosmic strings and Einstein–Rosen soliton waves *Phys. Rev.* D **36** 2250

[GV88]   Garfinkle D and Vachaspati T 1988 Fields due to kinky, cuspless, cosmic loops *Phys. Rev.* D **37** 257

[GV90]   Garfinkle D and Vachaspati T 1990 Cosmic-string traveling waves. *Phys. Rev.* D **42** 1960

[Haw90]   Hawking S W 1990 Gravitational radiation from collapsing cosmic string loops *Phys. Lett.* B **246** 36

[Hay89a]   Hayward S A 1989 Colliding waves and black holes *Class. Quantum Grav.* **6** 1021

[Hay89b]   Hayward S A 1989 Snapping of cosmic strings *Class. Quantum Grav.* **6** L179

[HCL00]   Hansen R N, Christensen M and Larsen A L 2000 Cosmic string loops collapsing to black holes *Int. J. Mod. Phys.* A **15** 4433

[HE73]   Hawking S W and Ellis G F R 1973 *The Large Scale Structure of Space-Time* (Cambridge: Cambridge University Press)

[HG94]   Headrick M P and Gott J R 1994 $(2 + 1)$-dimensional spacetimes containing timelike curves *Phys. Rev.* D **50** 7244

[Hin90]   Hindmarsh M 1990 Gravitational radiation from kinky infinite strings *Phys. Lett.* **251** 28

[His85]   Hiscock W A 1985 Exact gravitational field of a string *Phys. Rev.* D **31** 3288

[HK86]   Helliwell T M and Konkowski D A 1986 Vacuum fluctuations outside cosmic strings *Phys. Rev.* D **34** 1918

[Hog92]   Hogan P A 1992 A spherical gravitational wave in the de Sitter universe *Phys. Lett.* A **171** 20

[Hog93]   Hogan P A 1993 A spherical impulse gravity wave *Phys. Rev. Lett.* **70** 117

[Hog94]   Hogan P A 1994 Lorentz group and spherical impulse gravity waves *Phys. Rev.* **49** 6521

[HR95]   Hawking S W and Ross S F 1995 Pair production of black holes on cosmic strings *Phys. Rev. Lett.* **75** 3382

[HS88]   Hughston L P and Shaw W T 1988 Constraint-free analysis of relativistic strings *Class. Quantum Grav.* **5** L69

[HS90]   Horowitz G T and Steif A R 1990 Strings in strong gravitational fields *Phys. Rev.* D **42** 1950

[HW90]   Hindmarsh M and Wray A 1990 Gravitational effects of line sources and the zero-width limit *Phys. Lett.* B **251** 498

[Isr66]   Israel W 1966 Singular hypersurfaces and thin shells in general relativity *Nuovo Cimento* B **44** 1

[Isr77]   Israel W 1977 Line sources in general relativity *Phys. Rev.* D **15** 935

[Kib85]   Kibble T 1985 Evolution of a system of cosmic strings *Nucl. Phys.* B **252** 227

[KSHM80]   Kramer D, Stephani H, Herlt E and MacCallum M 1980 *Exact Solutions of Einstein's Field Equations* (Cambridge: Cambridge University Press)

[KT82]   Kibble T W B and Turok N 1982 Self-intersection of cosmic strings *Phys. Lett.* B **116** 141

[KW70]   Kinnersley W and Walker M 1970 Uniformly accelerating charged mass in general relativity *Phys. Rev.* D **2** 1359

[Let87]   Letelier P S 1987 Multiple cosmic strings *Class. Quantum Grav.* **4** L75

[Let91]   Letelier P S 1991 Nontrivial interactions of gravitational and electromagnetic waves with cosmic strings *Phys. Rev. Lett.* **66** 268

[Let92]   Letelier P S 1992 On the interaction of cosmic strings with gravitational waves *Class. Quantum Grav.* **9** 1707

[LG93]   Letelier P S and Gal'tsov D V 1993 Multiple moving crossed cosmic strings *Class. Quantum Grav.* **10** L101

[Lin85]   Linet B 1985 The static metrics with cylindrical symmetry describing a model of cosmic strings *Gen. Rel. Grav.* **17** 1109

[Lin86]   Linet B 1986 Force on a charge in the space-time of a cosmic string *Phys. Rev.* D **33** 1833

[LL62]   Landau L D and Lifshitz E M 1962 *The Classical Theory of Fields* (Oxford: Pergamon)

[LM88]   Lonsdale S and Moss I 1988 The motion of cosmic strings under gravity *Nucl. Phys.* B **298** 693

[LRvN87]   Lindström U, Rocek M and van Nieuwenhuizen P 1987 A Weyl-invariant rigid string *Phys. Lett.* B **199** 219

[Maz86]   Mazur P O 1986 Spinning cosmic strings and quantization of energy *Phys. Rev. Lett.* **57** 929

[MM88]   Matzner R and McCracken J 1988 Probability of interconnection of cosmic strings *Cosmic Strings: the Current Status* Proc. Yale Cosmic String Workshop, May 1988, ed F S Acetta and L M Kraus (Singapore: World Scientific) p 32

[MMR88a]   Moriarty K, Myers E and Rebbi C 1988 Dynamical interactions of cosmic strings and flux vortices in superconductors *Phys. Lett.* B **207** 411

[MMR88b]   Moriarty K, Myers E and Rebbi C 1988 Interactions of cosmic strings *Cosmic Strings: the Current Status* Proc. Yale Cosmic String Workshop, May 1988, ed F S Acetta and L M Kraus (Singapore: World Scientific) p 11

[MTW73]   Misner C W, Thorne K and Wheeler J 1973 *Gravitation* (San Francisco, CA: Freeman)

[Mue90]   Mueller M 1990 Rolling radii and a time-dependent dilaton *Nucl. Phys.* B **337** 37

[Mye87]   Myers R 1987 New dimensions for old strings *Phys. Lett.* B **199** 371

[Nam71]   Nambu Y 1971 Electromagnetic currents in dual hadrodynamics *Phys. Rev.* D **4** 1193

[NI01]   Nakamura K and Ishihara H 2001 Dynamics of a string coupled to gravitational waves II *Phys. Rev.* D **63** 127501

[NII00]   Nakamura K, Ishibashi A and Ishihara H 2000 Dynamics of a string coupled to gravitational waves *Phys. Rev.* D **62** 101502

[NO73]   Nielsen H B and Olesen P 1973 Vortex-line models for dual strings *Nucl. Phys.* B **61** 45

[OBP99]   Olum K D and Blanco-Pillado J J 1999 Field theory simulation of Abelian–Higgs cosmic string cusps *Phys. Rev.* D **60** 023503

[Ori91]   Ori A 1991 Rapidly moving cosmic strings and cosmology protection *Phys. Rev.* D **44** R2214

[Pag98]   Page D N 1998 Gravitational capture and scattering of straight test strings with large impact parameters *Phys. Rev.* D **58** 105026

[PG99]   Podolský J and Griffiths J B 1999 Expanding impulsive gravitational waves *Class. Quantum Grav.* **16** 2937

[PG00]   Podolský J and Griffiths J B 2000 The collision and snapping of cosmic strings generating spherical impulsive gravitational waves *Class. Quantum Grav.* **17** 1401

[Pol86]   Polyakov A M 1986 Fine structure of strings *Nucl. Phys.* B **268** 406

[PSS85]   Piran T, Safier P and Stark R 1985 General numerical simulation of cylindrical gravitational waves *Phys. Rev.* D **32** 3101

[PX90]   Papadopoulos D and Xanthopoulos B C 1990 Tomimatsu–Sato solutions describe cosmic strings interacting with gravitational waves *Phys. Rev.* D **41** 2512

[PZ91]   Polnarev A and Zembowicz R 1991 Formation of primordial black holes by cosmic strings *Phys. Rev.* D **43** 1106

[QS90]   Quashnock J M and Spergel D N 1990 Gravitational self-interaction of cosmic strings *Phys. Rev.* D **42** 2505

[Rub88]   Ruback P J 1988 Vortex string motion in the Abelian Higgs model *Nucl. Phys.* B **296** 669

[Sak90] Sakellariadou M 1990 Gravitational waves emitted from infinite strings *Phys. Rev.* D **42** 354

[She87] Shellard E P S 1987 Vortex scattering in two dimensions *Nucl. Phys.* B **283** 624

[She88] Shellard E P S 1988 Understanding intercommuting *Cosmic Strings: the Current Status* Proc. Yale Cosmic String Workshop, May 1988, ed F S Acetta and L M Kraus (Singapore: World Scientific) p 25

[SL89] Shaver E and Lake K 1989 Non-stationary general relativistic 'strings' *Phys. Rev.* D **40** 3287

[SQSP90] Scherrer R J, Quashnock J M, Spergel D N and Press W H 1990 Properties of realistic cosmic-string loops *Phys. Rev.* D **42** 1908

[SR88] Shellard E P S and Ruback P J 1988 Vortex scattering in two dimensions *Phys. Lett.* B **209** 262

[SS77] Sokolov D D and Starobinskii A A 1977 The structure of the curvature tensor at conical singularities *Sov. Phys. Dokl.* **22** 312

[SS86] Stein-Schabes J A 1986 Nonstatic vacuum strings: Exterior and interior solutions *Phys. Rev.* D **33** 3545

[SSB88] Stein-Schabes J A and Burd A B 1988 Cosmic strings in an expanding spacetime *Phys. Rev.* D **37** 1401

[Sta63] Staruskiewicz A 1963 Gravitation theory in three-dimensional space *Acta Phys. Polon.* **24** 735

[Sto89] Stoker J J 1989 *Differential Geometry* (New York: Wiley–Interscience)

[Tau80] Taub A H 1980 Space-times with distribution valued curvature tensors *J. Math. Phys.* **21** 1423

[tH92] 't Hooft G 1992 Causality in $(2 + 1)$-dimensional gravity *Class. Quantum Grav.* **9** 1335

[Tho65] Thorne K 1965 Energy of infinitely long, cylindrically symmetric systems in general relativity *Phys. Rev.* B **138** 251

[Tho88] Thompson C 1988 Dynamics of cosmic string *Phys. Rev.* D **37** 283

[Tia86] Tian Q 1986 Cosmic strings with cosmological constant *Phys. Rev.* D **33** 3549

[Tur84] Turok N 1984 Grand unified strings and galaxy formation *Nucl. Phys.* B **242** 520

[UHIM89] Unruh W G, Hayward G, Israel W and McManus D 1989 Cosmic-string loops are straight *Phys. Rev. Lett.* **62** 2897

[Unr92] Unruh W G 1992 Straight strings and Friedmann–Robertson–Walker spacetimes *Phys. Rev.* D **46** 3265

[Vac86] Vachaspati T 1986 Gravitational effects of cosmic strings *Nucl. Phys.* B **277** 593

[Vac87] Vachaspati T 1987 Gravity of cosmic loops *Phys. Rev.* D **35** 1767

[VF98a] De Villiers J-P and Frolov V 1998 Gravitational capture of cosmic strings by a black hole *Int. J. Mod. Phys.* **7** 957

[VF98b] De Villiers J-P and Frolov V 1998 Scattering of straight cosmic strings by black holes: Weak-field approximation *Phys. Rev.* D **58** 105018

[VF99] De Villiers J-P and Frolov V 1999 Gravitational scattering of cosmic strings by non-rotating black holes *Class. Quantum Grav.* **16** 2403

[VHR90] Vachaspati T, Hogan C J and Rees M 1990 Effects of the image universe on cosmic strings *Phys. Lett.* B **242** 29

[Vic87]   Vickers J A G 1987 Generalised cosmic strings *Class. Quantum Grav.* **4** 1

[Vic90]   Vickers J A G 1990 Quasi-regular singularities and cosmic strings *Class. Quantum Grav.* **7** 731

[Vil81a]   Vilenkin A 1981 Cosmic strings *Phys. Rev.* D **24** 2082

[Vil81b]   Vilenkin A 1981 Gravitational field of vacuum domain walls and strings *Phys. Rev.* D **23** 852

[Vil85]   Vilenkin A 1985 Cosmic strings and domain walls *Phys. Rep.* **121** 263

[VV85]   Vachaspati T and Vilenkin A 1985 Gravitational radiation from cosmic strings *Phys. Rev.* D **31** 3052

[VV90]   Vachaspati and Vachaspati. T 1990 Travelling waves on domain walls and cosmic strings *Phys. Lett.* B **238** 41

[Wei72]   Weinberg S 1972 *Gravitation* (New York: Wiley)

[Xan86a]   Xanthopoulos B 1986 Cylindrical waves and cosmic strings of Petrov type D *Phys. Rev.* D **34** 3608

[Xan86b]   Xanthopoulos B 1986 A rotating cosmic string *Phys. Lett.* B **178** 163

[Xan87]   Xanthopoulos B 1987 Cosmic strings coupled with gravitational and electromagnetic waves *Phys. Rev.* D **35** 3713

[Yur88]   Yurtsever U 1988 New family of exact solutions for colliding plane gravitational waves *Phys. Rev.* D **37** 2790

Index